APPLICATIONS OF STATISTICS IN THE SPECTRAL ANALYSIS OF TIME-VARYING SYSTEMS.

January 1975.

Author : P.W.DAVALL

Phd. thesis submitted to the UNIVERSITY OF WARWICK.

Department of Engineering.

ACKNOWLEDGEMENTS

I am most sincerely grateful to Professor J. L. Douce, who was most generous in his guidance, advice and encouragement throughout my years as a student. I also wish to thank Dr. F. Sherratt for his collaboration in research on metal fatigue, Dr. J. Gill for his help in research on human operator response, and Mr. A. Hulme for his never-ending patience with computer programming problems. Lastly, I am indebted to my wife for typing this thesis despite my poor handwriting.

This work was supported by a Science Research Council grant, computer facilities being provided by the Inter-University Institute of Engineering Control.

SUMMARY

Recent advances in the theory of evolutionary spectral analysis of time-varying systems has led to a resurgence in the popularity of frequency domain analysis techniques. Policies for adaptive control of time-varying systems based on state-space and Liaponov techniques require an accurate measurement of the system phase variables. Under inherently noisy conditions, access to the complete system state is seldom possible, and frequency domain analysis requiring only input/output measurements has an obvious appeal. The sampling properties of short-term spectral estimates are of central importance both in system tracking and in choosing suitable control policies.

Goodman (1957) developed some of the sampling properties associated with spectral estimates of complex bivariate Gaussian processes. Akaike (1962-66) extended Goodman's results to multi input/output linear systems with Gaussian input forcing functions. Both these authors considered the case where the data sequences were stationary.

This thesis reviews and extends the research of these two authors with respect to single input/output linear systems.

It is shown that the sampling distributions associated with spectral estimates of stationary open-loop systems are approximately valid for a restricted class of non-stationary systems. Two examples of non-stationary systems are investigated and an adaptive control technique using input compensation in the frequency domain is developed on a hydraulic fatigue loading rig. It is shown that statistical tests developed earlier can successfully identify system

variations when estimates are measured in a noisy environment.

The sampling distributions associated with spectral estimates of closed-loop systems are developed and the results are applied to the modelling and tracking of the human operator response in a tracking task situation, for various input signals.

With regard to future research, it remains to extend the results for closed-loop systems to the time-varying multi input/output case. In its full complexity this problem remains intractable, but by considering uncorrelated Gaussian inputs it reduces to determining the distributions associated with multi-variate complex Gaussian sequences.

CONTENTS

TITLE		PAGE
Chapter 1	INTRODUCTION	1
Chapter 2	SPECTRAL ANALYSIS OF OPEN-LOOP SYSTEMS . . .	6
	2.1) Introduction	10
	2.2) Choice of sampling parameters.	12
	2.3) Bias errors	13
	2.4) Sampling errors associated with :-	
	i) Auto-spectral estimates.	20
	ii) Cross-spectral estimates	22
	iii) Frequency Response estimates	25
	iv) Noise spectrum estimates	28
	2.5) Stationarity test for Open-loop systems. . .	31
	2.6) Extension to time varying situation.	34
	2.7) Statistics of overlapped time segments . . .	48
	2.8) Simulation results	56
	2.9) Applications	68
Chapter 3	SPECTRAL ANALYSIS OF CLOSED-LOOP SYSTEMS . .	73
	3.1) Introduction	76
	3.2) Sampling errors associated with :-	
	i) Cross-spectral estimates	80
	ii) Overall closed-loop response	84
	3.3) Stationarity testing	85
	3.4) Distribution of Forward-path frequency response estimates.	87

page.

3.5) Distribution of Feedback-path frequency response estimates. 99

3.6) Simulation results 99

3.7) Noise estimates in closed-loop systems . . . 107

3.8) Conclusions. 111

Chapter 4 . . . . SPECTRAL ANALYSIS OF SPEECH. 113

4.1) Introduction 115

4.2) Speech analysis and voice pitch detection. . 117

4.3) Statistical testing of speech. 120

4.4) Categorisation of vowel phonemes 122

4.5) Example of phonemic recognition. 137

4.6) Application to compressed speech 147

4.7) Conclusions 149

Chapter 5 . . . . APPLICATIONS TO FATIGUE ANALYSIS 158

5.1) Introduction 160

5.2) Generation of signals with specified statistics 160

5.3) Fatigue rig control. 174

5.4) Detection of fatigue cracks in Aluminium and Steel rods 187

5.5) Appendices 197

Chapter 6 . . . . APPLICATIONS TO HUMAN OPERATOR TRACKING TASKS- A COMPARISON OF AUDIO AND VISUAL DISPLAYS 208

6.1) Introduction 209

6.2) Comparison of Human Operator's performance using audio and visual displays. 211

page.

6.3) Justification of assumption of stationarity . 215

6.4) Investigation of transients in the Operator's frequency response with step changes in the frequency characteristics of the input signal. 222

6.5) Some extensions to two-dimensional and multi-dimensional displays. 236

6.6) Conclusions 239

6.7) Appendix. 244

Chapter 7 . . . .CONCLUSIONS & SOME SUGGESTIONS FOR FUTURE RESEARCH 273

APPENDIX . . . .COMPUTER PROGRAM LISTINGS. 285

CHAPTER 1

INTRODUCTION

Spectral techniques have been widely used in the analysis of stochastic processes. However, due to physical limitations regarding data acquisition, all such estimates are subject to random and bias errors accountable to short-term estimation in a noisy environment. To reduce these errors, estimates are usually averaged over a period of time: this requires the data to be stationary. Strict stationarity is seldom realised and hence averaging over time can produce bias errors. In 1965, Priestley introduced the concept of evolutionary spectral analysis and further work by Tong (1972) has developed this concept to include bivariate oscillatory processes. The physical interpretation is preserved in that we now consider energy distributions in the frequency domain which are local in nature. In estimating such distributions, we are confronted by what has been termed the frequency / time domain uncertainty principle. It is impossible to estimate the frequency content of a signal exactly from a finite time record of a random process. There is a trade-off between frequency resolution and record duration. In stationary situations it is often possible to choose the record length so that bias errors due to finite frequency resolution are acceptable. By averaging over many such record lengths, the random error may then be reduced. In time-varying situations, the physical nature of the variation often determines the record length regardless of the frequency content of the signal. Estimates can no longer be smoothed over time to reduce random error. Thus, even though estimates may be unbiased, it may be

impossible to detect small variations in time, due to the underlying distribution associated with the random error. Even when changes are detected, they are only significant in the statistical sense if the probability of obtaining such variations is unlikely given the parent distribution.

Adaptive stochastic control based on noisy system estimates is a relatively recent area of research. Criteria for optimal control can only be stated in the expected sense and often stability cannot be guaranteed. Current research has favoured the use of State-space methods using Liaponov functions to give stability. Recent extensions of spectral analysis to time-varying systems may lead to a resurgence in the use of frequency domain techniques. Clearly a knowledge of the sampling distributions associated with short-term spectral estimates is a prerequisite.

In the study of the distributions of short-term spectral estimates, much attention has been given to bivariate Gaussian processes. The reason for this is threefold. Firstly, the distributions derived from bivariate complex Gaussian systems can be determined analytically, using well-known statistical function theory, and yield reasonably simple results. Secondly, short-term Fourier estimates obtained from random non-Gaussian sequences are themselves often approximately Gaussian: this result may be predicted using the central-limit theorem. Thirdly, the resulting variance terms are often conservative in nature, the true distribution being more compact about the mean value.

In Chapter 2 some previous results of Goodman and Akaike are rephrased in terms of the parameters of an open-loop linear system

subject to noise. Some extensions to the results of these authors are derived and a simple stationarity test is included for estimates of the frequency response function. A brief consideration of the time-varying case shows that the distributions derived for stationary systems may be simply modified (by introducing time-varying mean and variance terms) to include slowly-varying processes, without serious loss of accuracy.

In Chapter 3 attention is drawn to the closed-loop stationary situation where there is noise both in the forward and feedback paths. The distributions associated with estimates of the forward loop frequency response and feedback loop frequency response functions are derived, and simulation results are presented. It is shown that the distribution of open-loop frequency response estimates is a particular case of the closed-loop distribution. An extension of the open-loop stationarity test to test for overall stationarity in the closed-loop case is included.

A major criticism of distribution theory as presented for short-term spectral estimation is that it is seldom used for more than a theoretical consideration of errors. As has been mentioned however the distribution of spectral estimates plays a central role in determining time-varying characteristics. Chapters 4, 5 and 6 examine three practical applications of some of the results of Chapters 2 and 3. The subjects chosen are research topics in their own right. Chapters 4 and 5 give examples of two forms of time-varying open-loop systems, while Chapter 6 examines a time-dependent closed-loop situation.

In Chapter 4 we consider the identification of step changes in open-loop system parameters with specific reference to speech. Each

phoneme is considered as an approximately stationary event with step changes at the boundaries. Such an assumption can only be partially justified, but it is shown that the vowel phonemes can be successfully identified using a throat microphone to access the input to the vocal tract and a crystal microphone to monitor the speech output. Application of statistical sectioning of speech to the production of compressed speech is included to show that the techniques can be extended to non-vowel sounds.

In Chapter 5 we consider the problem of identifying small parameter variations in a noisy environment. The identification of the onset of fatigue cracking in steel and aluminium rods is a good example of such a process. It is well known that little visible change in response can be detected during fatigue, and current methods of crack detection involve halting the test and removing the specimen.

In addition to the identification of fatigue, it is shown how short-term spectral estimation can be used to control a potentially time-varying system, using input compensation techniques. The method is applied to the control of a servo-hydraulic fatigue rig. Lastly, a method of producing signals with specified statistics is presented. The three topics together represent a unified approach to fatigue testing, taking into consideration the generation of the loading signal, the control of the fatigue rig, and the identification of the onset of failure.

Chapters 4 and 5 are concerned with open-loop systems. In Chapter 6 we consider the human operator in a tracking task environment as an example of a closed-loop time-varying system.

It is shown how a stationary linear model of the operator for stationary input dynamics can be justified in terms of the distributions derived in Chapter 3. Variations in the model parameters for step changes in the input dynamics are tracked and by use of a stationarity test for closed-loop systems, it is shown that these variations are due to actual changes in the operator's mode of response, rather than short-term measurement errors. Comparisons are made for different forms of audio and visual displays. Appendix A to Chapter 6 reports some preliminary findings on the comparison of displays.

CHAPTER 2.

SPECTRAL ANALYSIS OF OPEN-LOOP SYSTEMS

LIST OF SYMBOLS USED

$x(t)$: system input signal normally distributed with variance $\sigma_x^2(t)$. The dependence on t is sometimes dropped for stationary systems.

$y(t)$: system output signal, normally distributed with variance $\sigma_y^2(t)$

$n(t)$: A Gaussian noise input contaminating $y(t)$. Variance $\sigma_n^2(t)$.

(All these inputs have zero mean levels)

$x_t(i)$: the i^{th} sample of $x(t)$ in a block of N samples (similarly for $y_t(i)$)

$h(t,\tau)$: the time-dependent system impulse response. For stationary systems the dependence on t is dropped.

$H(z,u)$: the Fourier transform of $h(t, \tau)$ with respect to t,τ

$\phi_{xx}(t,w)$: the time-dependent power spectrum density of $x(t)$. Time dependence is dropped for stationary systems

$\phi_{xy}(t,w)$: the time-dependent cross-power spectrum density between $x(t)$ and $y(t)$

$\phi_{yy}(t,w)$: the time-dependent output spectrum density of $y(t)$

$\phi_{nn}(t,w)$: the time-dependent noise spectrum density of $n(t)$

$X(t,w)$: the time-dependent input signal generation source

$X(w)$: the Fourier transform of $x(t)$

$Y(w)$: the Fourier transform of $y(t)$

$N(w)$: the Fourier transform of $n(t)$

N : the number of independent samples per time block. Used as a parameter in the discrete transform.

f_s : the sampling frequency for $x(t)$, $y(t)$

T : ($= N/f_s$) : block time period, or in the continuous case, period of measurement over which spectral estimates are to be calculated.

$L(t)$: a weighting function by which $x(t)$, $y(t)$ are multiplied before the Fourier transform is carried out

$L(u)$: the Fourier transform of $L(t)$

$L(i)$: the i^{th} weight by which $x_t(i)$, $y_t(i)$ must be multiplied before estimating their discrete Fourier transform ($0 \leqslant i \leqslant N-1$)

w_0 : the effective bandwidth of the filter $L(u)$, when $L(t)$ is just the rectangular window over a period T, $w_0 = 2\pi/T$

$\hat{X}(kw_0)$: the complex Fourier coefficient of $L(i).x_t(i)$ ($i = 1,N$) at frequency kw_0 , $0 \leqslant k \leqslant N/2$.

$\hat{Y}(kw_0)$: the complex Fourier coefficient of $L(i).y_t(i)$ at frequency kw_0

$\hat{N}(kw_0)$: the complex Fourier coefficient of $L(i).n_t(i)$

$\hat{A}$: the estimate of a variable A obtained over an interval $t \in T$

$\bar{A}$: the average value of A taken over L independent estimates $\hat{A}$.

$\hat{\phi}_{xx}(kw_0)$: ($= \hat{X}(kw_0)^{*}.\hat{X}(kw_0)$) , * denotes complex conjugate.

The estimate of the power in $\phi_{xx}(w)$ over a frequency range $kw_0 \pm w_0/2$. Note that to obtain the estimate of the power spectral density function, $\hat{\phi}_{xx}(kw_0)$ must be normalised by the factor $1/w_0$, the bandwidth of L(u). Similar relationships describe $\hat{\phi}_{xy}(kw_0)$, $\hat{\phi}_{yy}(kw_0)$, $\hat{\phi}_{nn}(kw_0)$.

$\hat{\hat{\phi}}_{nn}(kw_0)$: the best obtainable estimate of $\phi_{nn}(kw_0)$ the noise spectrum, allowing for the fact that the noise is measured indirectly. $\hat{\phi}_{nn}(kw_0)$ is the estimate of the noise spectrum obtained if we can measure the noise source directly.

$N(\mu, \sigma^2)$: Gaussian distribution with mean μ and varinace σ^2

$Sx^2(t)$: half the power in $\phi_{xx}(t,w)$ over the frequency band $w_1 \pm w_0/2$. The dependence of Sx^2 upon w_1 is omitted and the dependence on t is dropped in the stationary case.

$Sn^2(t)$: half the power in $\phi_{nn}(t,w)$ over the frequency band $w_1 \pm w_0/2$

$Sy^2(t)$: half the power in $\phi_{yy}(t,w)$ over the frequency band $w_1 \pm w_0/2$

I_A : imaginary part of A

R_A : real part of A, A complex

$p_A(A)$: the probability distribution associated with a variable A

$p_A(A:B)$: the conditional probabiltiy distribution of a variable

A given B

$f_A(w)$: characteristic function of $P_A(A)$

μA : mean value of A

1) INTRODUCTION

This chapter outlines spectral techniques used in the analysis of linear open-loop systems (see Figure 1). It is shown that error analysis results as determined when the system is stationary are also approximately applicable to certain time-varying cases. Section 2 defines the system parameters and briefly describes time domain windowing, time domain smoothing and frequency smoothing. Section 3 investigates the bias terms encountered in short-term spectral estimates (for stationary systems) and shows that by a suitable choice of sampling frequency and frequency resolution, these terms can be suppressed, leaving random error as the major source of inaccuracy. Random errors are discussed in Sections 4, 5 and 7.

Fourier techniques have been used in time-varying situations for speech analysis (see references, Chapter 2, and Chapter 4) and in the analysis of non-stationary spacecraft vibration data (reference 24). Page (1950) first introduced the concept of instantaneous power spectra and since then Priestley, Tong and Subba-Rao have extended the classical Wiener-Kolmogorov theory to include non-stationary bivariate oscillatory systems. Section 6 shows how under restricted conditions the classical error analysis for complex bivariate Gaussian systems can be extended to include non-stationary data. The Gaussian case is chosen for two reasons: firstly the distribution of any variable formed from a linear transformation involving N independent variables will tend to the Gaussian distribution for large N. Thus the discrete Fourier coefficients formed from a linear transformation of N time sample points will be approximately

normally distributed. Secondly, frequency domain techniques are often used for system identification when the system input signals are band-limited white noise. Under these conditions the distribution of short-term discrete Fourier coefficients of the system input and output will be approximately Gaussian even when the original signals were non-Gaussian. A typical example is studied in Section 8.

The technique of overlapping time blocks to obtain better tracking characteristics has been used for speech analysis. The advantage of this form of analysis is that it presents better interpolation of the system parameters between adjacent block time periods. Section 7 develops some statistics for overlapped auto-spectral estimates. Lastly, Section 8 presents simulation results verifying some of the statistics derived in Sections 4,5 and 7. An example of a time-varying second-order system is studied and it is shown that under restricted conditions the coherency between input and output is approximately time-invariant. This result justifies the application of the error analysis results to time-varying systems in Chapters 4 and 5 and demonstrates that some simple extensions of stationary error analysis to the time-varying situation are not unreasonable.

2(i) CHOICE OF PARAMETERS IN THE ANALYSIS OF LINEAR OPEN-LOOP SYSTEMS

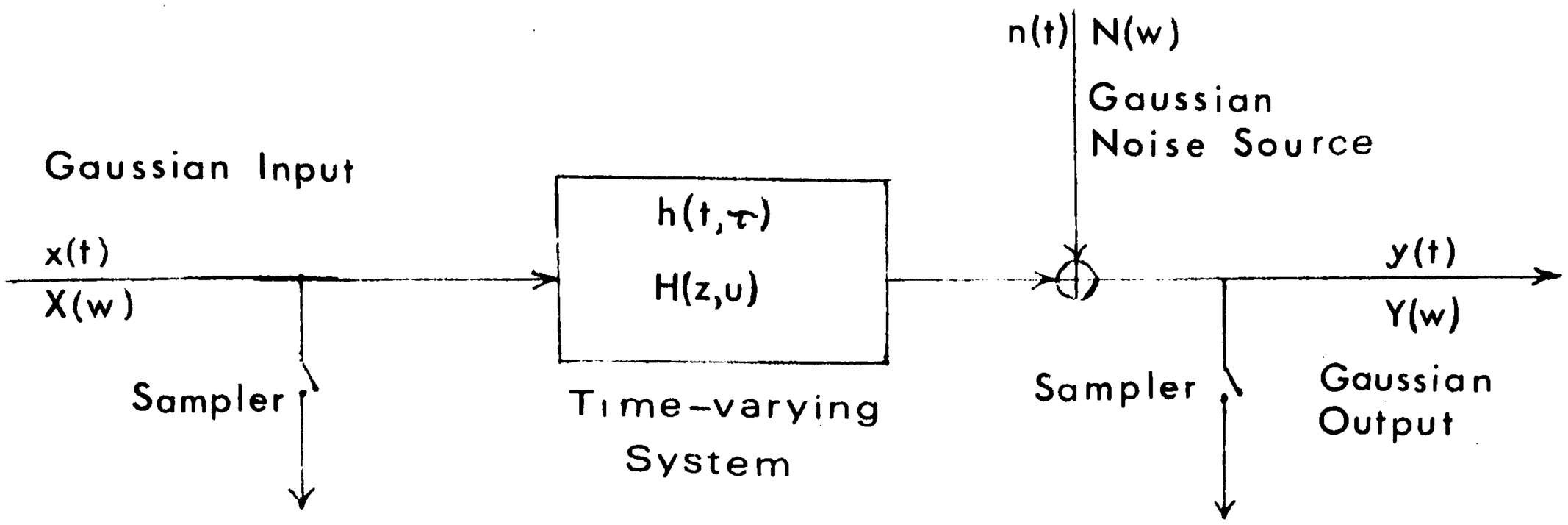

FIGURE 1 : SHOWS THE OPEN-LOOP SYSTEM CONFIGURATION

In Figure 1 $x(t)$, $n(t)$ are uncorrelated Gaussian random processes where the variable t may be considered as time. For the cases examined in this chapter $x(t)$ and $n(t)$ are considered real variables but they may be complex.

$$p\ (\ x(t)\ ) \quad = \quad N\ (\ 0,\ \sigma x^2\ )$$

$$p\ (\ n(t)\ ) \quad = \quad N\ (\ 0,\ \sigma n^2\ )$$

when the processes $x(t)$, $n(t)$ are 'stationary'

$$E\ (\ x(t),\ x(t-\tau\ )\ ) \quad = \quad Cxx\ (\ \tau)$$

$$E\ (\ n(t),\ n(t-\tau\ )\ ) \quad = \quad Cnn\ (\ \tau\ )$$

where $Cxx\ (\ \tau\ )$, $Cnn\ (\tau\ )$ are not functions of t. ($E \equiv$ expectation operator).

In short-term spectral analysis we are concerned with a realisation of $x(t)$, $y(t)$ (the two signals available) over a period $t_1 \leqslant t \leqslant t_2$. This realisation may take the form of continuous measurement or sampling at discrete intervals in t. Section 3 derives the expected

values for stationary systems from continuous measurement over t. The translation of results obtained to the discrete case is in general straightforward. Section 4 discusses random errors encountered in sampled data systems, as in practice the discrete fast Fourier transform is used to form spectral estimates of $\phi_{xx}(w)$, $\phi_{xy}(w)$ etc. Section 6 reverts to the continuous case to encompass the time-varying situation. Thus in general results are presented in whichever domain provides the simplest form and the domain in which the results might most commonly be applied.

The system $h(\tau)$ is a continuous function in τ such that $|h(\tau)| < \infty$ and tends to zero as $\tau \rightarrow \infty$. Also $h(\tau) = 0$ for $\tau < 0$ and is not a function of x(t), n(t), y(t). The Fourier transforms of x(t), $h(\tau)$ are given by:

$$X(w) = \int_{-\infty}^{\infty} x(t).\exp(-jwt)\, dt \quad \ldots\ldots\ldots\ldots\ldots 2.1$$

$$H(w) = \int_{-\infty}^{\infty} h(\tau).\exp(-jw\tau)\, d\tau \quad \ldots\ldots\ldots\ldots\ldots 2.2$$

where X(w), H(w) are in general complex functions in w (w is equated with frequency). In general $|X(w)|, |H(w)| \rightarrow 0$ as $|w| \rightarrow \infty$.

For y(t) to remain finite we let:

$$\int_{w-\partial}^{w+\partial} |H(w)|\, dw < \infty, \forall\ \partial > 0$$

Similar transform expressions can be written for N(w), Y(w) with identical conditions imposed on the finite magnitudes of these as funtions in w.

Short-term estimates of $\hat{X}(w)$, $\hat{Y}(w)$ over the interval $t_1 \leq t \leq t_2$ ($t_2 - t_1 = T$, $t = 0$ at $(t1+t2/2)$ will in general be biased due to

* (Eqn 2.1 is only defined if the integral of $|x(t)|^2$ is finite. In practise this is true as we consider a finite time interval)

finite frequency resolution $(w_0 \simeq \frac{2\pi}{T})$ and contain random errors due to short-term cross-correlation between x(t) and n(t). In the case where x(t), y(t) are sampled on the time interval T at a frequency f_s (= N/T) the Fourier transforms $\hat{X}(w)$, $\hat{Y}(w)$ become discrete Fourier series of the form:

$$\hat{X}(kw_0) = \sum_{i=0}^{N-1} L(i) . x_t(i) . \exp(j\frac{w_0 ki}{N})$$

$$, 0 \leqslant k \leqslant N/2, \quad w_0 = 2\pi / T$$

where $\sum_{i=0}^{N-1} |L(i)| = 1$ (the time domain window) ,

$$\hat{X}((N/2 + k) . w_0) = \hat{X}^* ((N/2 - k) . w_0)$$

for k = 0, 1, 2 . . . . N/2 - 1

and $I(\hat{X}(0)) = I(\hat{X}(N . w_0/2)) = 0$

* denotes the complex conjugate.

Thus for short-term estimates, when x(t), y(t) are continuous functions in t, we choose T, the measurement period; B_T, the frequency resolution; and the shape of the filter with bandwidth B_T. In the sampled data case we choose f_s, the sampling frequency; N, the number of samples per block; L(i), the time domain weighting function; and the desired smoothing of estimates in the frequency domain to reduce random errors. We note that $T = N/f_s$ and there is an equivalence between B_T and the filter shape in the continuous case, and the choice of L(i) and the frequency domain smoothing in the discrete case. In general the choices are made to satisfy the following criteria: -

T : sufficiently long such that 1/T, the frequency resolution, is substantially narrower than any spectral peak encountered in X(w), Y(w). This ensures that bias errors are reduced.

$\underline{f_s}$: this must be chosen such that $f_s > 2.$ fmax, where fmax is chosen such that components in X(w), Y(w) above this frequency can be neglected.

$\underline{L(i),\ (i = 0,\ N - 1)\ \text{and frequency domain smoothing}}$: these are chosen to optimise the filter characteristics in terms of side-band leakage and effective bandwidth without introducing unwanted bias in the final estimate. The form taken by any frequency smoothing is also dependent on the initial choice of T.

2(ii) DATA SMOOTHING IN THE FREQUENCY AND TIME DOMAINS

a) Time Domain Windows

The short-term estimate $\hat{X}(w)$ obtained from a realisation of x(t), $t \in T$, can be viewed as the Fourier transform of a process x(t).L(t) where $L(t) = 0$ for $t < t_1$, $t > t_2$. Letting $t_1 = -T/2$, $t_2 = T/2$, we choose L(t) such that:

$$\int_{-T/2}^{T/2} |L(t)|\ dt = 1 \quad \text{and} \quad |L(t)| < \infty, \forall\ t.$$

Typical examples of such windows are the rectangular window ($L(t) = 1/T\ ,\ t \in T$), the triangular window decaying to zero as $|t| \to T/2$, the Hanning and Hamming cosine bell windows. Each window L(t) has associated with it a frequency window L(u):

$$\hat{X}(w) = X(w - u) * L(u) \quad \ldots\ldots\ldots\ldots\ldots\ldots\ 2.3$$

where * denotes convolution.

Ideally L(u) should be rectangular with no sidebands and zero phase shift $\forall$ u. For L(u) to be real, L(t) must be an even function in t (this is not necessarily a restriction, but convoluting X(w) with a complex function leads to a complicated relationship between

$X(w)$ and $\hat{X}(w)$. For $L(u)$ to be exactly rectangular the function $L(t)$ is non-zero as t becomes large (in fact $L(t)$ is of the form $\sin \alpha t / \alpha t$ and T must be large to achieve an approximately rectangular window.)

Thus all time weighting functions compromise between the time period T becoming large and the frequency window $L(u)$ containing significant sidebands. In general, $L(u)$ is chosen so that sidebands are minimised while the bandwidth of the central peak about $(u = 0)$ is sufficiently narrow not to introduce bias errors in $\hat{X}(w)$ due to narrow peaks in $\phi_{xx}(w)$; and similarly for $\hat{Y}(w)$. In many real-time estimation problems the presence of noise in the output $y(t)$ is a far more serious restriction limiting the accuracy of estimates of $H(w)$ than errors due to sideband leakage in the frequency window $L(u)$. Wellstead (1971) and Blackman and Tukey (1959) have described the advantages of different time data windows in detail.

The effective bandwidth of the rectangular window, w_0, is $2\pi / T$. If the Hanning window is used, the bandwidth $L(u)$ increases as the proportion of time data 'Hanned' increases. In the discrete case where estimates of $\hat{X}(kw_0)$, $\hat{Y}(kw_0)$ are evaluated at frequency intervals of $2\pi/T$, Tukey has shown that adjacent estimates are essentially independent when $L(i)$ is the rectangular window (i.e. $L(i) = 1/N$), but that these points become correlated when a Hanning window is used. The error analysis in Sections 3 and 4 assumes the use of a rectangular data window.

b) Frequency Domain Smoothing

When $x(t)$ and $y(t)$ are sampled data sequences, blocks of N sample points are used to find $\hat{X}(kw_0)$, $\hat{Y}(kw_0)$, $0 \leqslant k \leqslant N/2$. To reduce random errors, the spectral estimates are computed from many such

blocks. The usual parameters of interest are:

$$\bar{\Phi}_{xx}(kw_0) = \frac{1}{L}\sum_{i=1}^{L} \hat{\Phi}^{i}_{xx}(kw_0) = \frac{1}{L}\sum_{i=1}^{L} \hat{X}^{*}_{i}(kw_0) \cdot \hat{X}_{i}(kw_0) \quad \ldots 2.4(a)$$

$$\bar{\Phi}_{yy}(kw_0) = \frac{1}{L}\sum_{i=1}^{L} \hat{\Phi}^{i}_{yy}(kw_0) \quad \ldots 2.4(b)$$

$$\bar{\Phi}_{xy}(kw_0) = \frac{1}{L}\sum_{i=1}^{L} \hat{X}^{*}_{i}(kw_0)\, \hat{Y}_{i}(kw_0) \quad \ldots 2.4(c)$$

$$\bar{H}(kw_0) = \bar{\Phi}_{xy}(kw_0) \;/\; \bar{\Phi}_{xx}(kw_0) \quad \ldots 2.4(d)$$

$$\bar{C}_{xy}^{2}(kw_0) = \frac{|\bar{\Phi}_{xy}^{2}(kw_0)|}{\bar{\Phi}_{xx}(kw_0)\cdot\bar{\Phi}_{yy}(kw_0)} \quad \ldots 2.4(e)$$

for $w_0 = 2\pi/T$, $0 \leqslant k \leqslant N/2$. (* denotes the complex conjugate)

Occasional other parameters used are estimates of the noise spectrum, $\bar{\Phi}_{\hat{n}\hat{n}}$, and estimates of the signal-to-noise ratio. Note that these estimates must be normalised by a factor $1/w_0$ to obtain the spectral density functions.

Statistical accuracy is increased as L becomes large. This is termed smoothing the spectral estimates in time. An alternative is to let T (and hence N) become large - typically L times as long to achieve similar accuracy - and then to smooth the resulting spectral estimates over neighbouring frequency points. This method has the advantage of interpolating the spectral estimates over frequency without recourse to function fitting. However, the two methods are approximately identical as a means of gaining stat-

istical accuracy. The method of time-domain smoothing is perhaps computationally simpler as it is dealing with smaller blocks of data. Physical limitations on core-size available are often the limiting criteria for the computer programmer.

3) BIAS ERRORS FOR STATIONARY SYSTEMS

Let the short-term Fourier transform of $x(t)$ be denoted by:

$$\hat{X}_{t_0}(w) = \int_{-\infty}^{\infty} L_{t_0}(t).\ x(t)\ \exp(-jwt)\ dt$$

where $L_{t_0}(t) = 1/T, \quad |t - t_0| \leqslant T/2$

and $L_{t_0}(t) = 0 \quad , \quad |t - t_0| > T/2$

To find the expected value of the spectral estimates we take the mean over all t_0. Normalizing by the bandwidth, B_T, of $L(u)$ to obtain the 'density' function:

$$\hat{\phi}_{xx}(w) = \frac{\hat{X}^*(w) \cdot \hat{X}(w)}{B_T}$$

Taking the expected value over all t:

$$E(\hat{\phi}_{xx}(w)) = \frac{1}{B_T} \int_{-\infty}^{\infty} |L(u)|^2 .\ X^*(w-u) \cdot X(w-u)\ du \quad \ldots\ldots 2.5$$

Expanding $X(w-u)$ as a truncated Taylor series about $X(w)$ and ignoring terms in u^3 and higher:

$$X(w-u) \simeq X(w) - u.\frac{\partial X(w)}{\partial w} + \frac{u^2}{2} \cdot \frac{\partial^2 X(w)}{\partial w^2}$$

Substituting in equation 2.5:

$$E(\hat{\phi}_{xx}(w)) \simeq \frac{1}{B_T}\int_{-\infty}^{\infty} \phi_{xx}(w) \cdot |L(u)|^2\ du$$

$$+ \frac{1}{B_T}\int_{-\infty}^{\infty} \frac{\partial^2 \phi_{xx}(w)}{\partial w^2} \cdot u^2 \cdot |L(u)|^2 .du + (\text{higher order terms in } u^4). \quad \ldots\ldots 2.6$$

Terms involving $u \cdot |L(u)|^2$ integrate to zero as $|L(u)|$ is an even function in u. When $L(t) = 1/T$ for $|t - t_0| \leq T/2$:

$$L(u) = \sin\left(\frac{UT}{2}\right) \Big/ \left(\frac{UT}{2}\right)$$

and $$\int_{-\infty}^{\infty} |L(u)|^2 \cdot du = \frac{2\pi}{T} = B_T$$

the characteristic width of the filter L(u) specified by the half power points. Also:

$$\int_{-\infty}^{\infty} u^2 \cdot |L(u)|^2 \cdot du = \frac{8\pi}{T^3} = \frac{B_T{}^3}{\pi^2}$$

Thus substituting back in equation 2.6:

$$E(\hat{\phi}_{xx}(w)) \simeq \phi_{xx}(w) + \frac{B_T{}^2}{\pi^2} \cdot \frac{\partial^2 \phi_{xx}(w)}{\partial w^2} \quad \ldots\ldots\ldots 2.7$$

The bias term is a function of $B_T{}^2$. As the filter bandwidth of $L(u) \rightarrow 0$, bias $(\hat{\phi}_{xx}(w)) \rightarrow 0$ as a function of $B_T{}^2$. Note that the result of equation 2.7 compares with:

$$E(\hat{\phi}_{xx}(w)) = \phi_{xx}(w) + \frac{B_T{}^2}{24} \cdot \frac{\partial^2 \phi_{xx}(w)}{\partial w^2} \quad \ldots\ldots 2.8$$

as quoted by Bendat and Piersol when L(u) is the ideal rectangular bandpass filter. This would indicate that the choice of time data window does not greatly affect the bias term.

Following a similar process we now derive the bias in the output spectrum density, $\hat{\phi}_{yy}(w)$, in terms of the input spectrum, the system, and the noise spectrum. Again considering a time function y(t) multiplied by a rectangular window function L(t) (where L(t) is defined as before)

$$E(\hat{\phi}_{yy}(w)) = \int_{-\infty}^{\infty} |L(u)|^2 \cdot \phi_{yy}(w - u) \, du$$

$\phi_{yy}(w - u)$ is expanded as a Taylor series about w and a bias term similar to that for $\hat{\phi}_{xx}(w)$ is obtained:

$$E(\hat{\phi}_{yy}(w)) = \phi_{yy}(w) + \frac{B_T^2}{\pi^2} \cdot \frac{\partial^2 \phi_{yy}(w)}{\partial w^2} \quad \ldots\ldots\ldots 2.9$$

where $\phi_{yy}(w) = |H^2(w)| . \phi_{xx}(w) + \phi_{nn}(w)$

(the terms involving $\phi_{xn}(w) = 0$ as x(t) and n(t) are uncorrelated)

Lastly we are interested in the expected value of the cross-spectrum density, $\hat{\phi}_{xy}(w)$. Again approximating $\phi_{xy}(w - u)$ by a three-term Taylor series expansion:

$$E(\hat{\phi}_{xy}(w)) = \phi_{xy}(w) + \frac{B_T^2}{\pi^2} \cdot \frac{\partial^2 \phi_{xy}(w)}{\partial w^2} \quad \ldots\ldots\ldots 2.10$$

where $\phi_{xy}(w) = H(w) . \phi_{xx}(w)$

In the derivations of the expected values of $\hat{\phi}_{yy}(w)$, $\hat{\phi}_{xy}(w)$, it has been assumed that T is sufficiently long for the transient effects of the filter to be negligible. (That is, $h(\tau) \rightarrow 0$ for $\tau \leqslant \varepsilon . T$, $\varepsilon << 1$) In practice T can be chosen so that the bias terms involving B_T^2 are minimal. Under these conditions more serious sources of error are random errors due to short-term sampling.

4) RANDOM ERRORS

4(i) DISTRIBUTION OF AUTO-SPECTRAL ESTIMATES

The previous section studied the case where x(t), y(t) are continuous random variables over a period $t_1 \rightarrow t_2$ such that $t_2 - t_1 = T$. As the analysis programs implemented use a discrete Fourier transform algorithm taking blocks of sampled data, this section and Section 4 develop the statistics of stationary open-loop linear systems in terms of the discrete transform.

$$\hat{X}(kw_0) = \frac{1}{N}\sum_{i=0}^{N-1} x_t(i).\ \exp\ (-j\ \frac{2\pi\ ki}{N})$$

$$0 \leqslant k \leqslant N/2.$$

where $w_0 = \frac{2\pi}{T}$, $T = N/f_s$

$\hat{Y}(kw_0)$ is defined in a similar way.

Let each $x_t(i)$ be a sample from a parent population with a probability distribution function given by:

$$p(\ x(t)\ ) = N\ (\ 0\ ,\sigma_x^{\ 2}\ )$$

where x(t) is band-limited white noise with zero mean and variance $\sigma_x^{\ 2}$. The restriction to zero mean only affects the D.C. component.

Again a similar condition is applied to $n_t(i)$ and $y_t(i)$. Goodman (1957) has shown that:

$$p(\hat{X}(kw_0)\ ) = N_{\text{complex}}\ (0,\ Sx^2) \quad \ldots\ldots\ldots\ldots\ldots\ldots\ 2.11$$

$$p(\hat{N}(kw_0)\ ) = N_{\text{complex}}\ (0,\ Sn^2) \quad \ldots\ldots\ldots\ldots\ldots\ldots\ 2.12$$

where Sx^2, Sn^2 are the half powers in x(t), n(t) respectively in the frequency band $kw_0 \pm w_0/2$. The total power over the frequency band $kw_0 \pm w_0/2$ is divided equally between the real and imaginary Fourier coefficients at frequency kw_0. Thus the variance term for $\hat{Rx}$, $\hat{Ix}$ is given by $\frac{\phi_{xx}(kw_0).\ w_0}{2}$ and for $\hat{Rn}$, $\hat{In}$ by $\frac{\phi_{nn}(kw_0).w_0}{2}$

It is assumed that bias errors have been reduced to negligible proportions by a suitable choice of T.

The dependence on frequency is now assumed except in cases of ambiguity. The sampling distributions are presented for a particular frequency kw_0. For the discrete transform:

$$\hat{\phi}_{xx} = (\hat{R}x^2 + \hat{I}x^2)$$

where $\hat{R}x$ and $\hat{I}x$ are the independent real and imaginary parts of $X(kw_0)$. Thus, referring to equation 2.11, ϕ_{xx} is Chi-square distributed with 2 degrees of freedom where:

$$VAR (\hat{\phi}_{xx}) \simeq 2Sx^2 \quad , \quad E(\hat{\phi}_{xx}) = 2Sx^2$$

If L such independent estimates are used to form $\bar{\phi}_{xx}$, the average value, then:

$$p(\bar{\phi}_{xx}) = \frac{(L)^L .(\bar{\phi}_{xx})^{L-1} . \exp.(-L.\bar{\phi}_{xx} / 2Sx^2)}{2^L . S_x{}^{2L} . \Gamma(L)} \quad . . . . 2.13$$

$$VAR (\bar{\phi}_{xx}) \simeq 2Sx^2/L \ , \ E(\bar{\phi}_{xx}) \simeq 2.S_x{}^2 \ , \ \Gamma(L) = (L-1)!$$

The distribution of the output auto-spectrum $\bar{\phi}_{yy}$ is likewise Chi-square distributed with 2L degrees of freedom. Note that to obtain a power spectrum density function, $\bar{\phi}_{xx}$ must be normalised to the resolution bandwidth w_0.

4(ii) DISTRIBUTION OF CROSS-SPECTRAL ESTIMATES, $\bar{\phi}_{xy}$

The cross-spectrum function is given as:

$$\hat{\phi}_{xy} = \hat{X}^* . \hat{Y} \quad . . . . . 2.14$$

For linear systems H, when the output is contaminated by a noise term N, we find that:

$$\hat{Y} \simeq H.\hat{X} + \hat{N} \quad . . . . . 2.15$$

The relationship again assumes T to be much longer than the transient response time of the filter H. Substituting for Y in the equation 2.14:

$$\hat{\phi}_{xy} \simeq H.\hat{\phi}_{xx} + \hat{\phi}_{xn} \quad \ldots\ldots\ldots\ldots\ldots 2.16$$

where in the short term $\hat{\phi}_{xn}$ is non-zero. When there is no noise in the system ($Sn^2 = 0$) the distribution of $\hat{\phi}_{xy}$ is just a constant times a Chi-square as $\hat{\phi}_{xx}$ is Chi-square distributed with 2 degrees of freedom. However for $Sn^2 \neq 0$:

$$Rxy = Rx(R_H\, Rx + Rn) + Ix(R_H\, Ix - In) \quad \ldots\ldots\ldots 2.17(a)$$

$$\hat{I}xy = \hat{R}x(I_H\, \hat{R}x + \hat{I}n) + \hat{I}x(I_H\, \hat{I}x - \hat{R}n) \quad \ldots\ldots\ldots 2.17(b)$$

Both $\hat{R}xy$ and $\hat{I}xy$ are distributed in a similar manner about $R_H.\phi_{xx}$ and $I_H.\phi_{xx}$ respectively. Thus a unified approach is given by studying the distribution of:

$$\hat{z} = \hat{X}_R(H\,\hat{X}_R + \hat{N}_R) + \hat{X}_I(H\,\hat{X}_I - \hat{N}_I) \quad \ldots\ldots\ldots 2.18$$

$$\text{with } \bar{z} = \sum_{i=1}^{L} \hat{z}_i \;/\; H.Sx^2 \quad \ldots\ldots\ldots 2.19$$

Letting $H = R_H, I_H$ in equation 2.18, we obtain expressions for Rxy and $\hat{I}xy$ respectively. $\bar{z}$ is <u>not</u> normalised by the factor L to find the mean values. This is a trivial step. In equation 2.18, $\hat{X}_R$, $\hat{N}_R$, $\hat{X}_I$, $\hat{N}_I$ are mutually independent and each estimate $\hat{z}_i$ is independent of $\hat{z}_j$ for $i \neq j$. Considering the distributions of two variables $\hat{X}_R(H.\hat{X}_R + \hat{N}_R)$ and $\hat{X}_I(H.\hat{X}_I + \hat{N}_I)$ it is seen that they are independent with identical distributions. Let:

$$\hat{S} = H\,\hat{X}_R + \hat{N}_R$$

$$\hat{t} = \hat{X}_R \;/\; H.Sx^2$$

and $$\hat{V} = \hat{t}\,.\,\hat{S}$$

$\hat{V}$ is a function of two variables so:

$$P_V(\hat{V}) = \int_{-\infty}^{\infty} \frac{1}{|\hat{t}|}\,.\,Pt(\hat{t})\,.\,Ps(\hat{V}/\hat{t} : \hat{t})\,dt \quad \ldots\ldots\ldots 2.19$$

where $Pt(\hat{t}) = N(0, {}^{1}/H.Sx^2)$

and $p_s(\hat{s} : \hat{t}) = N(H.Sx^2 . \hat{t}, Sn^2)$

Sn^2 = noise variance at frequency kw_0.

Substituting for $p_t(\hat{t})$ and $P_s(\hat{s})$: $\hat{t}$ in equation 2.19 and integrating:

$$p_V(\hat{V}) = \frac{H.Sx}{Sn} . \exp (H^2.Sx^2.\hat{V} / Sn^2) .$$

$$. K_0 \left\{ \frac{H.Sx}{Sn} . | \hat{V} | . \left(1 + \frac{H^2 Sx^2}{Sn^2}\right)^{\frac{1}{2}} \right\} \quad . . 2.20$$

where $K_\nu(x)$ is the modified Bessel function of order ν and $\hat{V}$ is considered positive in the sense of H positive.

Each $\hat{z}$ (equation 2.18) is the sum of two independent variables whose distribution is given by equation 2.20. Thus $\bar{z}$ is the sum of 2L such variables. Taking the Fourier transform of equation 2.20, the characteristic function $f_V(w)$ is given by:

$$f_V(w) = \alpha / (\alpha^2.(1 + \alpha^2) - (\alpha 2 - jw)^2)^{\frac{1}{2}} \quad . . . . . 2.21$$

where $\alpha = \frac{H.Sx}{Sn}$. The characteristic function of $P_z(\bar{z})$ is thus given by:

$$fz(w) = \alpha^{2L} / (\alpha^2.(1 + \alpha^2) - (\alpha^2 - jw)^2)^L \quad . . . . 2.22$$

Taking the inverse transform:

$$p_z(\bar{z}) = \frac{\alpha^{2L} . |\bar{z}|^{L-\frac{1}{2}} . \exp (\alpha^2.\bar{z})}{\sqrt{\pi} .\Gamma(L). (2\alpha.(1 + \alpha^2)^{\frac{1}{2}})^{L-\frac{1}{2}}} . K_{L-\frac{1}{2}} (\alpha(1 + \alpha^2)^{\frac{1}{2}}.| \bar{z}|)$$

$$. . . . . 2.23$$

in the range $-\infty \leqslant \bar{z} \leqslant \infty$

where $\Gamma(L)$ = Gamma integral = $(L-1)!$

Now reverting to $\bar{R}xy$ and $\bar{I}xy$ we find, letting $H = R_H$:

$$\bar{z} = L. \bar{R}xy / Rxy$$

and letting $H = I_H$:

$$\bar{z} = L. \bar{I}xy / Ixy$$

where Rxy and Ixy are the expected values of the real and imaginary

parts of ϕ_{xy}. Taking the first and second moments of equation 2.23:

$$\mu_z = \sum_{i=0}^{L-1} \frac{\alpha^{2L}}{2^{L+1}} \frac{(L-1+i)!\,(L+1-i)!\,(L-1)}{(L-1)!\,i!\,D^{L+i}} \cdot \frac{(D+\alpha^2)^{L+1-i} + (D-\alpha^2)^{L+1-i}}{(D^2-\alpha^4)^{L+2-i}} \quad \ldots\ldots 2.24(a)$$

and

$$VAR(\bar{z}) = \sum_{i=0}^{L-1} \frac{\alpha^{2L}}{2^{L+1}} \frac{(L-1+i)!\,(L+1-i)!\,(L-i)}{(L-1)!\,i!\,D^{L+i}} \cdot \frac{(D+\alpha^2)^{L+2-i} + (D-\alpha^2)^{L+2-i}}{(D^2-\alpha^4)^{L+2-i}} - \mu_z^2 \quad \ldots\ldots 2.24(b)$$

where $D = \alpha(1+\alpha^2)^{\frac{1}{2}}$.

Although the expressions for the mean and variance as given above are cumbersome it is easily shown that if $\alpha >> 1$ then:

$$\mu_z \rightarrow 2L \quad \text{and} \quad VAR(\bar{z}) \rightarrow 4L$$

The result is that expected of a Chi-square distribution with 2 L degrees of freedom. α becomes large as Sn^2 (the noise variance) tends to zero. In the limit equation 2.23 collapses to a Chi-square distribution as expected.

4(iii) <u>DISTRIBUTION OF FREQUENCY RESPONSE ESTIMATES, $\bar{H}$</u>

In the absence of noise, and for short memory systems, the frequency response can in theory be estimated extremely accurately. In practice the accuracy of short-term estimates is limited by transient effects associated with the initial conditions. The use of a suitable time data window can minimise the effects of these

transients at the expense of loss of frequency resolution. In general the noise term is finite leading to non-zero short-term correlation errors between the input signal and the noise.

Goodman (1957) and Akaike (1965) have derived the distribution associated with frequency response estimates of bivariate complex Gaussian systems. An outline of the general approach is given here, rephrasing the distribution parameters in terms of those encountered in open-loop systems (Figure 1). This procedure is useful in that some interim results lead to a simple stationarity test for open-loop systems and some fundamental relationships are introduced which are used extensively in the next chapter on closed-loop systems.

$$\bar{H} = \bar{\phi}_{xy} / \bar{\phi}_{xx} \simeq H + \bar{\phi}_{xn} / \bar{\phi}_{xx} \quad \ldots\ldots 2.25$$

where again $\hat{Y} \simeq H.\hat{X} + \hat{N}$. Defining the error in $\bar{H}$:

$$\bar{E}_H = \bar{\phi}_{xn} / \bar{\phi}_{xx} = \bar{M}_E . \exp(j\theta_E) \quad \ldots\ldots 2.26$$

where $\bar{\phi}_{xx} = \bar{M}x^2$, $\bar{\phi}_{xn} = \frac{1}{L}\sum_{i=1}^{L} \hat{M}x.\hat{M}n.\exp(j(\hat{\theta}n - \hat{\theta}x))$

Now: $$p(\hat{M}x, \hat{\theta}x) = \frac{\hat{M}x . \exp(-\hat{M}x^2 / 2.Sx^2)}{2\pi . S_x^2}$$

$$\ldots\ldots\ldots 0 \leqslant Mx \leqslant \infty$$

$$p(\hat{\theta}x) = 1/2\pi \quad , \quad 0 \leqslant \theta x \leqslant 2\pi$$

and similarly for $p(\hat{M}n, \hat{\theta}n)$ substituting Sn^2 for Sx^2. The above distribution is a transformation of the jointly normal distribution of $\hat{R}x$, $\hat{I}x$ to $\hat{M}x$, $\hat{\theta}x$ using:

$$\hat{M}x = \sqrt{(\hat{R}x^2 + \hat{I}x^2)} \quad , \quad \hat{\theta}x = \tan^{-1}(\hat{I}x / \hat{R}x)$$

We now consider the distribution of $\hat{M}xn.\exp(j\hat{\theta}_{xn})$ given $\hat{M}x$. From the definition of $\hat{\phi}_{xn}$ above:

$$\hat{M}xn = \hat{M}x.\hat{M}n \quad , \quad \hat{\theta}xn = \hat{\theta}_n - \hat{\theta}_x$$

The Jacobian of the transformation is given by:

$$J(\hat{M}xn, \hat{\theta}xn) = \begin{vmatrix} \frac{\partial \hat{M}xn}{\partial Mn} & \frac{\partial \hat{M}xn}{\partial \theta n} \\ \frac{\partial \hat{\theta}xn}{\partial Mn} & \frac{\partial \hat{\theta}xn}{\partial \theta x} \end{vmatrix} = \hat{M}x$$

$$\text{and } p(\hat{M}xn, \hat{\theta}xn : \hat{M}x) = \int_0^{2\pi} \frac{p_{Mn,\theta n}\left(\frac{\hat{M}xn}{\hat{M}x}, (\hat{\theta}xn + \hat{\theta}x) : \hat{M}x\right) d\hat{\theta}_x}{J(\hat{M}xn, \hat{\theta}_{xn})}$$

Integrating with respect to $\hat{\theta}x$:

$$p(\hat{M}xn, \hat{\theta}xn : \hat{M}x) = \frac{\hat{M}xn \,.\exp\left(-\hat{M}xn^2 / 2.Sn^2.\hat{M}x^2\right)}{2\pi.Sn^2.\hat{M}x^2}$$

Thus by specifying just the magnitude of $\hat{X}$ and not the phase, $\hat{\phi}xn$ is a jointly normally distributed variable with independent real and imaginary parts. On averaging $\bar{\phi}_{xy}$, $\bar{\phi}_{xx}$ over L independent estimates the distribution of $\bar{\phi}_{xn}$ is given by:

$$p(\bar{M}xn, \bar{\theta}xn : \bar{\phi}_{xx}) = \frac{L.\bar{M}xn.\exp\left(-\bar{M}xn^2.L / 2.Sn^2.\bar{\phi}_{xx}\right)}{2\pi.Sn^2.\bar{\phi}xx}$$

$$\text{but } \bar{E}_H = \bar{\phi}_{xn} / \bar{\phi}_{xx} \,. \quad \text{So:}$$

$$p(\bar{M}_E, \bar{\theta}_E : \bar{\phi}xx) = \frac{L.\bar{\phi}xx.\bar{M}_E.\exp\left(-\bar{M}_E^2.\bar{\phi}xx.L / 2.Sn^2\right)}{2\pi.Sn^2} \qquad \ldots\ldots\ldots\ldots 2.27$$

This is the conditional distribution of errors in $\bar{H}$ given the input spectrum $\bar{\phi}_{xx}$. This is just the bivariate Gaussian distribution with zero mean and variance $(Sn^2 / L.\bar{\phi}_{xx})$.

$$p(\bar{E}_H) = p(\bar{M}_E, \bar{\theta}_E) = \int_0^{\infty} p(\bar{M}_E, \bar{\theta}_E : \bar{\phi}_{xx}) \,.p(\bar{\phi}_{xx})\, d\bar{\phi}_{xx}$$

where $p(\bar{\phi}_{xx})$ is the Chi-square distribution with 2 L degrees of freedom. Performing the integration:

$$P(M_E, \theta_E) = \frac{L \cdot Sx \cdot M_E}{Sn\pi\left(1 + \frac{Sx^2}{Sn^2} \cdot M_E^2\right)^{L+1}} \quad \ldots\ldots\ldots\ldots 2.28$$

Equation 2.28 shows that the error in the frequency response estimate is approximately independent of the system H. The variance of the estimate is a function of the ratio Sx^2 (the input signal power) to Sn^2 (the noise power) and L, the number of independent estimates used. The distribution as presented differs from that of Jenkins and Akaike (see references 4,3) in that it is not a function of the sampled coherency estimate between input and output.

Thus the distribution of a variable $\overline{SN}$ (estimates of Sx^2/Sn^2) is investigated in preference to that of coherency as this ratio has a more direct bearing on the variance of the frequency response estimate.

4(iv) NOISE IN OPEN-LOOP SYSTEMS

A conventional method of gaining information on the accuracy of the frequency response estimate is to calculate the coherency between x(t) and y(t).

$$Cxy^2 = \frac{|\phi xy|^2}{\phi xx \cdot \phi yy}$$

Again substituting for $\hat{Y}$ in terms of H, $\hat{X}$ and $\hat{N}$:

$$Cxy^2 = \frac{1}{1 + \frac{\phi nn}{|H|^2 \cdot \phi_{xx}}} \qquad \text{in the range } 0 \leqslant Cxy^2 \leqslant 1$$

However, when investigating the accuracy of $\bar{H}$, we wish to know the value of SN (= ϕ_{xx} / ϕ_{nn}). The coherency function does <u>not</u> give this.

The best obtainable estimate of $\bar{\phi}_{nn}$ is given by:

$$\bar{\hat{\phi}}_{\hat{n}\hat{n}} = \bar{\phi}_{yy} - |\bar{H}|^2 . \bar{\phi}_{xx} \quad \ldots\ldots\ldots\ldots 2.29$$

($\hat{n}$ denotes the best estimate of n).

Substituting for Y in equation 2.29:

$$\bar{\hat{\phi}}_{\hat{n}\hat{n}} \simeq \bar{\phi}_{nn} - \frac{|\bar{\phi}_{xn}|^2}{\bar{\phi}_{xx}} \quad \ldots\ldots\ldots\ldots 2.30$$

Adopting Akaike's[ref 6] distribution for sampled coherency to the case when the two signals are uncorrelated:

$$p_{C_{xn}}(\bar{C}_{xn}) = 2(L-1).\bar{C}_{xn}.(1-\bar{C}_{xn}^2)^{L-2} \quad \ldots\ldots\ldots 2.31$$

where $\bar{C}_{xn}$ is defined in the same manner as $\bar{C}_{xy}$. (L= no. of blocks)

The coherency estimate between the input signal and the noise is independent of the input and noise auto-spectral estimates. The variance term in eqn. 2.31 is a function of L only. Simulation results estimating the joint probability distribution $p(\bar{C}_{xn}, \phi_{xx}, \phi_{nn})$ show that:

$$p(\bar{C}_{xn}, \bar{\phi}_{xx}, \bar{\phi}_{nn}) = p(\bar{C}_{xn}).\, p(\bar{\phi}_{xx}) \,.\, p(\bar{\phi}_{nn})$$

when x(t) and n(t) are Gaussian and uncorrelated. Thus equation 2.31 can be used directly to find $p(|\bar{\phi}_{xn}|^2 ; \bar{\phi}_{xx}, \bar{\phi}_{nn})$. Substituting for $\bar{C}_{xn}$ in terms of $\bar{\phi}_{xx}$, $\bar{\phi}_{nn}$ and $\bar{\phi}_{xn}$ and performing the variable transformation:

$$p(|\bar{\phi}_{xn}|^2 ; \bar{\phi}_{xx}, \bar{\phi}_{nn}) = \frac{(L-1).(\bar{\phi}_{xx}.\bar{\phi}_{nn} - |\bar{\phi}_{xn}|^2)^{L-2}}{(\bar{\phi}_{xx}.\bar{\phi}_{nn})^{L-1}} \quad \ldots. 2.32$$

The distribution of a variable $\bar{z}$ ($=|\bar{\phi}_{xn}|^2 / \bar{\phi}_{xx}$) is obtained from equation 2.32:

$$p(\bar{z} ; \bar{\phi}_{xx}, \bar{\phi}_{nn}) = \frac{(L-1).(\bar{\phi}_{nn} - \bar{z})^{L-2}}{\bar{\phi}_{nn}^{L-1}} \quad \ldots\ldots\ldots\ldots 2.33$$

in the range $0 \leqslant \bar{z} \leqslant \bar{\phi}_{nn}$

From equation 2.30 the best obtainable estimate of $\bar{\phi}_{nn}$ is given by:

$$\bar{\phi}\hat{\hat{nn}} = \bar{\phi}nn - \bar{z}$$

Furthermore, both $\bar{\phi}nn$ and $\bar{z}$ are independent of $\bar{\phi}xx$. The distribution of $\bar{\phi}\hat{\hat{nn}}$ is thus given by:

$$p(\bar{\phi}\hat{\hat{nn}}) = \int_0^\infty p_{\bar{\phi}\hat{\hat{nn}}}(\bar{\phi}\hat{\hat{nn}} + \bar{z}) \cdot p(\bar{z} : \bar{\phi}nn) \cdot d\bar{z}$$

Substituting the Chi-square distribution with 2L degrees of freedom for $p(\bar{\phi}nn)$ and integrating:

$$p(\bar{\phi}\hat{\hat{nn}}) = \frac{L^{L-1} \cdot \bar{\phi}\hat{\hat{nn}}^{L-2} \cdot \exp(-\bar{\phi}\hat{\hat{nn}} / 2Sn^2)}{2^{L-1} \cdot \Gamma(L-1) \cdot Sn^{2(L-1)}} \quad \ldots\ldots 2.34$$

This is just the Chi-square distribution with 2L -2 degrees of freedom.

Thus if L=1, $\bar{\phi}nn$ is constrained to be zero. The best estimate of Sn^2 is given by:

$$\hat{Sn}^2 = \frac{L}{2(L-1)} \cdot \bar{\phi}\hat{\hat{nn}}$$

and the signal-to-noise ratio estimate is given by;

$$\overline{SN} = (L-1) \cdot \bar{\phi}xx / L \cdot \bar{\phi}nn \quad \ldots\ldots 2.35$$

As $\bar{\phi}xx$ and $\bar{\phi}nn$ are independent the distribution of $\overline{SN}$ is given by:

$$p(\overline{SN}) = \int_0^\infty \bar{\phi}xx \cdot p_{\bar{\phi}xx}(\bar{\phi}xx) \cdot p_{\bar{\phi}nn}\left(\frac{(L-1)\cdot\bar{\phi}xx}{L \cdot \overline{SN}}\right) \cdot d\bar{\phi}xx$$

Substituting for the respective distributions and integrating:

$$p(\overline{SN}) = \frac{\left[\frac{L}{L-1}\right]^L \cdot \Gamma(2L-1) \cdot \overline{SN}}{\frac{Sx^2}{Sn^2}^L \cdot \Gamma(L-1) \cdot \left[1 + \frac{LSn^2 \cdot \overline{SN}}{(L-1) \cdot Sx^2}\right]^{2L-1}} \quad \ldots\ldots 2.36$$

in the range $0 \leqslant \overline{SN} \leqslant \infty$ and for $L \geqslant 2$.

The variable $F = \overline{SN} \cdot \frac{L}{(L-1)} \cdot \frac{Sn^2}{Sx^2}$ is 'Fisher' distributed with

2L , 2L -2 degrees of freedom. The expressions for the mean and variance

of equation 2.34 are easily found from those of the Fisher distribution.

The SN value is not intended as a replacement for coherency, but rather as a supplementary estimate. Its usefulness is that it gives direct information on the likely variance of the frequency response estimate.

5) STATIONARITY TESTING OF OPEN-LOOP SYSTEMS

Previous authors (Priestley, Tong, Bendat and Piersol) have suggested non-parametric tests for the stationarity of bivariate complex systems. The test put forward here has the advantage of simplicity.

Considering Figure 1 we are interested in variations of three parameters, the input spectrum Φxx, the system H, and the noise spectrum Φnn.

Ideally, we would like to test each independently. This is not possible, as it demands prior knowledge of at least one of these parameters, which in general is not available.

Auto-spectral estimates are most easily tested by forming a new variable, $F = \bar{\phi}^1_{xx} / \bar{\phi}^2_{xx}$ (where $\bar{\phi}^1_{xx}$ and $\bar{\phi}^2_{xx}$ are two independent estimates) with F Fisher distributed with $2L_1$, $2L_2$ degrees of freedom. This test has been discussed in detail by Bendat and Piersol and is not pursued here.

A test for changes in H can be derived using equation 2.27. This distribution gives the conditional probability of obtaining an error $\bar{E}_H$ given an estimate of the input spectrum. Thus variations in the input are allowed for by using the best estimate, $\bar{\Phi}xx$, as a parameter in the distribution.

Consider two independent frequency response estimates $\bar{H}_1$, $\bar{H}_2$ taken over L_1, L_2 independent sets of time data respectively. Let E_1, E_2 be the errors in $\bar{H}_1$, $\bar{H}_2$. Then:

$$p(E_1 : \bar{\phi}^{-1}_{xx}) = \underset{\text{complex}}{N} (0, Sn_1^2 / L_1 . \bar{\phi}^{-1}_{xx})$$

and:

$$p(E_2 : \bar{\phi}^{-2}_{xx}) = \underset{\text{complex}}{N} (0, Sn_2^2 / \bar{\phi}^{-2}_{xx}. L_2)$$

Let $\bar{D} = \bar{H}_1 - \bar{H}_2 = (H_1 - H_2) + (E_1 - E_2)$

Then:

$$p(\bar{D} : \bar{\phi}^{-1}_{xx}, \bar{\phi}^{-2}_{xx}) = \underset{\text{complex}}{N} \left(H_1 - H_2 , \left[\frac{Sn_1^2}{L_1 . \bar{\phi}^{-1}_{xx}} + \frac{Sn_2^2}{L_2 . \bar{\phi}^{-2}_{xx}} \right] \right) \quad ..2.37$$

Assuming the system to be stationary, $H_1 = H_2$, and the distribution of $\bar{D}$ is the bivariate normal distribution with independent real and imaginary coefficients. Thus $|\bar{D}|^2$ is Chi-square distributed with 2 degrees of freedom and variance:

$$VAR(\bar{D}^2) = \left[\frac{Sn_1^2}{L_1 . \bar{\phi}^{-1}_{xx}} + \frac{Sn_2^2}{L_2 . \bar{\phi}^{-2}_{xx}} \right] \quad ..... 2.38$$

If the noise source is known to be stationary the best estimate of Sn^2 can be used instead of Sn_1^2, Sn_2^2. This is given by:

$$\hat{Sn}^2 \simeq \frac{L_1 . \bar{\phi}^{-1}_{\hat{n}\hat{n}} + L_2 . \bar{\phi}^{-2}_{\hat{n}\hat{n}}}{2(L_1 + L_2 - 1)}$$

Substituting for Sn_1^2, Sn_2^2 in equation 2.38:

$$\widehat{VAR(|\bar{D}|^2)} \simeq \frac{(L_1 . \bar{\phi}^{-1}_{\hat{n}\hat{n}} + L_2 . \bar{\phi}^{-2}_{\hat{n}\hat{n}})}{2(L_1 + L_2 - 1)} \left[\frac{1}{L_1 . \bar{\phi}^{-1}_{xx}} + \frac{1}{L_2 . \bar{\phi}^{-2}_{xx}} \right]$$

However in general when the noise is known to be time-varying:

$$\widehat{VAR}(\bar{D}^2) \simeq \frac{1}{2.L_1.\overline{SN}_1} + \frac{1}{2.L_2.\overline{SN}_2} \quad \ldots\ldots 2.39$$

$\widehat{\ }$ denotes the best obtainable estimate of $VAR(\bar{D}^2)$. This approximation becomes better as L_1, L_2 become large. The test is only valid for L_1, $L_2 \geq 2$ as estimates of $\hat{\phi}\hat{\hat{n}}\hat{n} = 0$ for L=1.

By relating the noise spectrum estimate to the error in the frequency response it is found that:

$$\bar{\phi}\hat{\hat{n}}\hat{n} = \bar{\phi}nn - |E_H|^2 \bar{\phi}xx$$

Hence:

$$\overline{SN} = \frac{(L-1)}{L} \cdot \left[\frac{1}{\frac{\bar{\phi}_{nn}}{\bar{\phi}_{xx}} - |E_H|^2} \right] \quad \ldots\ldots 2.40$$

If $|E_H|^2$ is only slightly less than $\bar{\phi}nn / \bar{\phi}xx$, then $\overline{SN}$ will tend to overestimate SN , and $VAR(\bar{D}^2)$ will tend to underestimate the true variance. This tendency is allowed for by the normalisation factor in equation 2.40 of (L-1) / L. However when L is small there is a greater chance of seriously underestimating the variance of $\bar{D}^2$ and hence predicting that a change has occurred in H. In many instances we are interested in detecting changes in H over a wide frequency band. The variable $Si \{= \bar{D}i^2 / \widehat{VAR}(\bar{D}i^2)\}$ is approximately Chi-square distributed with unit variance: i denotes the i^{th} frequency point. As adjacent frequency points are approximately independent the variable $\bar{S}$ given by :

$$\bar{S} = \sum_{i=I_1}^{I_2} Si \quad \ldots\ldots 2.41$$

will be Chi-square distributed with 2M degrees of freedom, where $M = (I_2 - I_1 + 1)$. Thus the stationarity confidence interval

satisfied by $\bar{S}$ is given by:

$$p(\chi^2, \{ \chi^2 \leqslant \bar{S} \}) = \int_0^{\bar{S}} p_{2M} (\chi^2) \, d \chi^2 \quad \ldots\ldots 2.42$$

The system may be considered stationary over the frequency range $I_1 w_0 \leqslant w \leqslant I_2 w_0$ if this confidence level is less than some preset level α. Typically α might be chosen as 0.95. Chapters 4 and 5 make use of this test for identifying changes in the speech waveform and the onset of fatigue cracking respectively.

The distributions developed are for stationary systems. To justify their use in time-varying situations we now investigate some properties of short-term Fourier transforms when applied to time-varying systems.

6) SOME EXTENSIONS OF FOURIER TECHNIQUES TO TIME-VARYING SIGNALS

With reference to Figure 1, let $\phi xx(w)$, $\phi nn(w)$ and $H(w)$ all be functions of time. In particular we limit ourselves to considering functions which vary slowly over some finite period T. For meaningful results T must be sufficiently long so that any short-term Fourier analysis of $x(t)$, $y(t)$ for $t \in T$ does not lead to undue bias errors in estimates of $\phi xx(w)$, $\phi yy(w)$ etc, due to insufficient frequency resolution. Thus by slowly varying we mean with respect to the process $x(t)$, $y(t)$, $t \in T$.

In the interval $t \in T$ let $\phi xx(t,w)$, $H(t,w)$ be continuous and differentiable functions of time and frequency such that

$$| F (t,w) | < \infty \quad \forall \; t \in T$$

$\frac{\partial^{\alpha} F(t,w)}{\partial w^{\alpha}}$ is continuous for finite α

where $F(t,w)$ is either of the functions $\phi xx(t,w)$, $H(t,w)$. Consideration of an additional noise term $\phi nn(t,w)$ at the output of the system is not necessary for developing the Fourier relationships between $y(t)$ and $x(t)$. We need only show that a time-dependent frequency response can be defined in the interval $t \in T$ using short-term Fourier transform techniques. Let:

$$H(t, \tau) = \int_{-\infty}^{\infty} H(t,u) \cdot \exp(ju\tau) \, du \quad \ldots\ldots\ldots 2.43$$

such that a) $|H(t,\tau)| < \infty \quad t \in T$ and $\forall \tau$

b) $|H(t,\tau)| \simeq 0$ for $\tau > \tau max \quad t \in T$.

c) $|H(t,\tau)| = 0$ for $\tau \leqslant 0$

Let the input signal $x(t)$ be the output from a time-dependent generator function:

$$x(t) = \int_{-\infty}^{\infty} X_t(\Omega) \cdot \exp(+j\Omega t) \, d\Omega \quad \ldots\ldots\ldots 2.44$$

Writing the time-dependent convolution equation relating the input $x(t)$ to the output $y(t)$ we obtain:

$$y(t) = \int_{0}^{\tau} H(t,\tau) \cdot x(t-\tau) \, d\tau \quad \ldots\ldots\ldots 2.45$$

Substituting for $H(t,\tau)$, $x(t-\tau)$:

$$y(t) = \int_{0}^{\tau max} \int_{-\infty}^{\infty} H(t,u).\exp(+ju\tau) \, du. \int_{-\infty}^{\infty} X(t-\tau)(\Omega).\exp(+j\Omega(t-\tau)) \, d\Omega \, d\tau \quad \ldots\ldots 2.46$$

Let $Y_T(w)$ be the Fourier transform of $y(t)$, $t \in T$. We assume

y(t), x(t) are continuous processes over a short time record T. Arbitrarily, we let T be centred about t=0. Taking the Fourier transform of equation 2.46:

$$Y_T(w) = \frac{1}{T} \int_{-T/2}^{T/2} \int_{0}^{\tau max} \iint_{-\infty}^{\infty} H(t,u).X_{(t-\tau)}(\Omega).\exp\ (j(u-\Omega)\ \tau).$$

$$.\exp\ (j(\Omega-w)\ t).\ du\ d\Omega\ d\tau\ dt \quad .... \quad 2.47$$

In the interval T let H(t,u) be closely approximated by a truncated Taylor series expansion about t=0. We first consider the case when $X(t,\Omega) \equiv X(\Omega)$, that is, stationary input.

$$H(t,u) \simeq H_0(u) + t.\frac{\partial H(t,u)}{\partial t}\Bigg|_{t=0} + \frac{t^2}{2}.\ \frac{\partial^2 H(t,u)}{\partial t^2}\Bigg|_{t=0}$$

(+ higher order terms in t^3 which are small.) 2.48

Substituting for H(t,u) in equation 2.47:

$$Y_T(w) \simeq \frac{1}{T} \int_{-T/2}^{T/2} \int_{0}^{\tau max} \iint_{-\infty}^{\infty} \{\ H_0(u) + \frac{\partial H_0(u).}{\partial \tau}\ t$$

$$+ \frac{\partial^2 H_0(w).}{\partial \tau^2}\ \frac{t^2}{2}\ \}\ .\ X(\Omega)\ .\exp\ (j(u-\Omega)\ \tau).\ \exp\ (j(\Omega-w)\ t)\cdot$$

$$.\ du\ d\Omega\ d\tau\ dt \quad ..... \quad 2.49$$

The limits of the integral with respect to τ may be extended to $\pm\infty$, remembering $H(t,\tau) = 0$ for $\tau \leqslant 0$, $\tau \geqslant \tau max$. Thus integrating with respect to τ :

$$Y_T(w) = \frac{1}{T} \int_{-T/2}^{T/2} \iint_{-\infty}^{\infty} \{\ H_0(u) + t.\frac{\partial H_0(u)}{\partial t} + \frac{t^2}{2}.\ \frac{\partial^2 H_0(\ )}{\partial t^2}\ \}\ X(\Omega)$$

$$\delta_0(u-\Omega)\ .\ \exp(j(\Omega-w)\ t)\cdot du\ \ d\Omega\ dt \quad ..... \quad 2.50$$

where δ_0 is the dirac delta function at $u - \Omega = 0$. The extension

of the limits of integration in τ to $\pm \infty$ is not straightforward when $X(\Omega)$ is also a function of t. Integrating equation 2.50 with respect to u:

$$Y_T(w) = \frac{1}{T}\int_{-T/2}^{T/2}\int_{-\infty}^{\infty}\{ H_0(\Omega) + t.\frac{\partial H_0(\Omega)}{\partial t} + \frac{t^2}{2}.\frac{\partial^2 H_0(\Omega)}{\partial t^2}\}.$$

$$X(\Omega) . \exp (+ j(\Omega-w) t). d\Omega\ dt \quad \ldots\ldots\ldots\ldots\ldots 2.51$$

We split this integral into two constituent parts, the main part and a bias term. Considering the main part:

$$A = \frac{1}{T}\int_{-T/2}^{T/2}\int_{-\infty}^{\infty} H_0(\Omega) . X(\Omega) . \exp (+ j(\Omega-w) t) . d\Omega\, dt \ldots 2.52$$

Integrating with respect to t we obtain the classical relationship between $Y_T(w)$ and $X(w)$ for stationary systems modified over the interval T by a data window L(t) of the form:

$$L(t) = \frac{1}{T} , | t | \leqslant T/2$$

$$L(t) = 0 , | t | > T/2 \qquad \text{Thus:}$$

$$A = \int_{-\infty}^{\infty} H_0(\Omega)\, X(\Omega) . \frac{\sin \frac{(\Omega-w) T}{2}}{\left(\frac{(\Omega-w) T}{2}\right)} \quad d\Omega \quad \ldots\ldots 2.53$$

The use of, for example, a Hanning window for L(t) will result in a correspondingly different window in equation 2.53 and may be advantageous in reducing the bias terms given by:

$$B = \frac{1}{T}\int_{-T/2}^{T/2}\int_{-\infty}^{\infty}\{ t.\frac{\partial H_0(\Omega)}{\partial t} + \frac{t^2}{2}.\frac{\partial^2 H_0(\Omega)}{\partial t^2}\}.X(\Omega).\exp (j(\Omega-w) t).$$

$$d\Omega\ dt \quad \ldots\ldots\ldots\ldots 2.54$$

We now investigate the behaviour of B in the limit $T \rightarrow 0$. Considering the term involving $\frac{\partial H_0(\Omega)}{\partial t}$:

$$I_1 = \frac{1}{T}\int_{-T/2}^{T/2}\int_{-\infty}^{\infty} t.\exp\ (j(\Omega-w)\ t).\frac{\partial H_0(\Omega)}{\partial t}\ .X(\Omega).\ d\Omega\ \ dt\ \ .\ .\ .\ 2.55(a)$$

Integrating by parts with respect to t:

$$I_1 = \int_{-\infty}^{\infty} \frac{\partial H_0(\Omega)}{\partial t}\ .\ X(\Omega).\Big(\ j.\frac{2.\sin\ \frac{(\Omega-w)\ T}{2}}{T.\ (\Omega-w)^2}\ -\ j.\frac{\cos\ \frac{(\Omega-w)\ T}{2}}{(\Omega-w)}\ \Big).\ d\Omega\ .\ .\ 2.55(b$$

Letting $T \rightarrow 0$ and expanding the sine and cosine terms in a power series:

$$I_1 \underset{\lim\ T\rightarrow 0}{\simeq} \int_{-\infty}^{\infty} \frac{\partial H_0(\Omega)}{\partial t}\ .\ X(\Omega)\ .\Big(\ -j\ .\ \frac{(\Omega-w)\ T^2}{24}\ \Big).\ d\Omega$$

$$\rightarrow 0 \quad \text{as a function in } T^2 \qquad .\ .\ .\ .\ .\ .\ .\ .\ .\ .\ .\ .\ .\ 2.56$$

Investigating the bounds of I_1 as a function of T:

$$|I_1| \leqslant \frac{1}{T}\int_{-T/2}^{T/2}\int_{-\infty}^{\infty} \left|\ \frac{\partial H_0(\Omega)}{\partial t}\ \right|\ .\ |X(\Omega)|\ .\ |t|\ .\ dt\ \ d\Omega\ \ .\ .\ 2.57$$

$$= \frac{T}{4}\int_{-\infty}^{\infty} \left|\frac{\partial H_0(\Omega)}{\partial t}\right|\ .\ |\ X(\Omega)\ |\ .\ d\Omega\ \ .\ .\ .\ .\ .\ .\ .\ .\ .\ .\ 2.58$$

Tong and Priestley have considered the time-varying case when $X(t,\Omega)$, $H(t,\Omega)$ can be represented in the form:

$$X(t,\Omega) = \int_{-\infty}^{\infty} X(s,\Omega)\ \exp\ (jst)\ \ ds\ \ .\ .\ .\ .\ .\ .\ .\ .\ .\ 2.59$$

$$\text{and}\quad H(t,u) = \int_{-\infty}^{\infty} H(z,u)\ \exp\ (jzt)\ \ dz\ \ .\ .\ .\ .\ .\ .\ .\ .\ .\ 2.60$$

where $|X(s,\Omega)| \simeq 0$ for $|s| >$ Smax and

$|H(z,u)| \simeq 0$ for $|z| >$ Zmax such that Smax, Zmax are $<<$ Ωmax, Umax. Ωmax, Umax are defined in a similar manner to Smax and Zmax.

If $H(t,\Omega)$ belongs to this class of oscillatory functions then we can derive maximum values for $\frac{\partial H_0(\Omega)}{\partial t}$ in terms of Zmax.

$$\frac{\partial H_0(\Omega)}{\partial t} = \int_{-Zmax}^{Zmax} - j \cdot z \cdot H(z,\Omega) \cdot dz \quad \ldots\ldots\ldots 2.61$$

Using this relationship in equation 2.58 and integrating with respect to Ω:

$$| I_1 | \leq \frac{I}{4} . | H_0(\Omega) |_{max} . \quad \sigma x . Zmax^2 \quad \ldots\ldots\ldots 2.62(a)$$

If the system is slowly varying with respect to x(t) we can choose T such that $Zmax << 2\pi / T$, that is $Zmax = \alpha / T$ such that $\alpha << 1$. The strict inequality of equation 2.62(a) is more realistically represented by:

$$| I_1 | \leq \frac{I}{2} \left| \frac{\partial H_0(\Omega)}{\partial t} \right| . \quad w_0 \cdot |X(\Omega)| \quad \ldots\ldots\ldots 2.62(b)$$

where $\left|\frac{\partial H_0(\Omega)}{\partial t}\right|$ and $|X(\Omega)|$ are taken as the maximum values in the frequency range $w - w_0 \leq \Omega \leq w + w_0$. On considering equation 2.55(b) it can be seen that $X(\Omega)$, $\frac{\partial H_0(\Omega)}{\partial t}$ are in fact viewed through a bandpass filter with an effective bandwidth less than $\frac{4\pi}{T}$ $(2w_0)$ about w. The frequency response of this filter is however a complex function in $(\Omega - w)$ and no longer of the simple $\sin \alpha / \alpha$ form of part A. (equation 2.53) .

Considering terms involving $\frac{\partial^2 H_0(\Omega)}{\partial t^2}$ from equation 2.54:

$$I_2 = \frac{1}{T} \int_{-T/2}^{T/2} \frac{t^2}{2} . \frac{\partial^2 H_0(\Omega)}{\partial t^2} . X(\Omega) . \exp (j(\Omega - w) t) . d\Omega \; dt \quad \ldots 2.63$$

Integrating with respect to t:

$$I_2 = \int_{-\infty}^{\infty} \frac{\partial^2 H_0(\Omega)}{\partial t^2} . X(\Omega) . \left\{ \frac{I \sin \frac{(\Omega - w) I}{2}}{4 (\Omega - w)} + \frac{\cos \frac{(\Omega - w) I}{2}}{(\Omega - w)^2} - \frac{2 \sin \frac{(\Omega - w) I}{2}}{I (\Omega - w)^3} \right\} d\Omega$$

$\ldots\ldots$ 2.64

Expanding the sine and cosine terms as a power series and taking the limit as $T \rightarrow 0$:

$$I_2 \underset{\lim T\rightarrow 0}{\simeq} \int_{-\infty}^{\infty} \frac{\partial^2 H_0(\Omega)}{\partial t^2} \cdot X(\Omega) \cdot \left\{ \frac{T^2}{24} - \frac{(\Omega-w)^2 T^4}{192} \right\} .d\Omega \quad \ldots \quad 2.65(a)$$

which again goes to zero as a function of T^2. Also $|I_2|$ is bounded by:

$$|I_2| \leq \frac{1}{T} \int_{-T/2}^{T/2} \int_{-\infty}^{\infty} \left|\frac{t}{2}^2\right| \cdot \left| \frac{\partial^2 H_0(\Omega)}{\partial t^2} \right| \cdot |X(\Omega)| \, .dt \; d\Omega$$

$$= \frac{T^2}{24} \int_{-\infty}^{\infty} \left| \frac{\partial^2 H_0(\Omega)}{\partial t^2} \right| \cdot |X(\Omega)| \, .d\Omega \quad \ldots\ldots\ldots\ldots 2.65(b)$$

If $H(t,u)$ is restricted to the class of oscillatory functions, we find that:

$$|I_2| \leq \frac{T^2}{24} \cdot \sigma_x \cdot |H_0(\Omega)|_{\max_\Omega} \cdot \frac{Zmax^3}{3} \quad \ldots\ldots 2.66$$

Again on considering equation 2.64 the function $X(\Omega) \cdot \frac{\partial H_0(\Omega)}{\partial t^2}$ is viewed through a complex bandpass filter with centre frequency w and bandwidth $< 2w_0$. Thus the bound on $|I_2|$ is perhaps more accurately given by:

$$|I_2| \leq \frac{T^2}{12} \cdot \left| \frac{\partial^2 H_0(\Omega)}{\partial t^2} \right| \cdot w_0 \cdot |X(\Omega)| \quad \ldots\ldots 2.67$$

where $\frac{\partial^2 H_0(\Omega)}{\partial t^2}$ and $X(\Omega)$ are taken as the maximum values in the frequency range $w-w_0 < \Omega < w+w_0$.

Now if $|H(t,u) - H_0(u)| < \varepsilon$ for $t \in T$ and the Taylor series expansion of $H(t,u)$ is a good representation over the interval T then:

$$|\varepsilon| \simeq \frac{T}{2} \cdot \left| \frac{\partial H_0(u)}{\partial t} \right| + \frac{T^2}{8} \cdot \left| \frac{\partial H_0(u)}{\partial t^2} \right| \quad \ldots\ldots 2.68$$

and on substituting $B = I_1 + I_2$ we see:

$$Y_T(w) \simeq H_0(\Omega) \cdot X(\Omega) * L(\Omega-w) + I_1 + I_2 \quad , \quad * \text{ denotes convolution}$$

where $L(\Omega-w)$ is the bandpass filter found from the Fourier transform of $L(t)$, and $I_1 + I_2$ are approximately bounded by:

$$|I_1 + I_2| \underset{\text{approx}}{\leqslant} |\varepsilon| \cdot \max_{w-w_0 \leqslant \Omega \leqslant w+w_0} |X(\Omega)| \cdot w_0 \qquad \ldots . \; 2.69$$

This is arrived at by rewriting the expressions for $|I_1|$ and $|I_2|$ as given by equations 2.62 and 2.67 in terms of $|\varepsilon|$ as given by equation 2.68. It must be emphasised that linking the bounds on the bias term, B, to changes in the frequency response over the interval T in this manner is intended to show only the logical links and is <u>not</u> intended as a mathematical proof. For oscillatory systems, Tong has shown the relationship indicated by equation 2.69 to be valid.

We have shown that as $T \rightarrow 0$ the relationship between $Y_T(w)$ and $X(w)$ approaches that of the stationary case with a residual term which is a function of T^2. Further we have indicated that the residual term is bounded by the magnitude of changes in $H(t,u)$ over the interval T in the region of $u = w$.

We now extend the analysis to include a time-varying input $X(t,\Omega)$. In the interval $t \in T$ let $X(t,\Omega)$ be approximated by a truncated Taylor series expansion about $T = 0$.

$$X(t,\Omega) \simeq X_0(\Omega) + t.\frac{\partial X(t,\Omega)}{\partial t}\Bigg|_{t=0} + \frac{t^2}{2} \cdot \frac{\partial^2 X(t,\Omega)}{\partial t^2}\Bigg|_{t=0}$$

(+ higher order terms which can be neglected.)

Rewriting equation 2.49 we get:

$$Y_T(jw) \approx \frac{1}{T}\int_{-T/2}^{T/2}\int_{0}^{\tau max}\iint_{\infty}^{\infty}\left\{H_0(u) + \frac{\partial H_0(u)}{\partial t}\cdot t + \frac{\partial^2 H_0(u)}{\partial t^2}\cdot\frac{t^2}{2}\right\}$$

$$\cdot\left\{X_0(\Omega) + (t-\tau)\cdot\frac{\partial X(0,\Omega)}{\partial t} + (t-\tau)^2\cdot\frac{\partial^2 X(0,\Omega)}{\partial t^2}\right\}.$$

$$\cdot \exp\ (j(u-\Omega)\ \tau)\ .\ \exp\ (j(\Omega-w)\ t)\ .\ du\ \ d\Omega\ \ d\tau\ \ dt\ \ .\ .\ .\ 2.70$$

We have already shown that terms involving $H(t,u)$ and $X_0(\Omega)$ involve a bias term B $(= I_1 + I_2)$ which tends to zero as $T \rightarrow 0$. If we restrict $X(t,\Omega)$ to be slowly varying over the interval $t \in T$ we may neglect terms involving $\frac{\partial H_0(u)}{\partial t}\cdot\frac{\partial X_0(\Omega)}{\partial t}$ and higher as these will in general be an order of magnitude smaller than terms like $H_0(u)\cdot\frac{\partial X_0(\Omega)}{\partial t}$. We note in passing that these second order terms tend to zero as $T = 0$ as they always involve functions in t^n for $n \geq 1$.

Thus we are chiefly concerned with bias terms already investigated for the stationary case (I_1, I_2) plus terms involving $H_0(u)\cdot\frac{\partial X_0(\Omega)}{\partial t}$ and $H_0(u)\cdot\frac{\partial^2 X(0,\Omega)}{\partial t^2}$. Taking the first:

$$I_3 = \frac{1}{T}\int_{-T/2}^{T/2}\int_{0}^{\tau max}\iint_{\infty}^{\infty} H_0(u).(t-\tau)\cdot\frac{\partial X_0(\Omega)}{\partial t}.\exp\ (j(u-\Omega)\tau)\ .$$

$$\cdot\ \exp\ (j(\Omega-w)\,t).du\ \ d\Omega\ \ d\tau\ \ dt\ \ .\ .\ .\ .\ .\ .\ .\ .\ .\ .\ .\ .\ .\ .\ .\ 2.71$$

Splitting this up into two integrals:

$$I_3 = \frac{1}{T}\int_{-T/2}^{T/2}\int_{0}^{\tau max}\iint_{-\infty}^{\infty}\left[\left\{H_0(u).\frac{\partial X_0(\Omega)}{\partial t}\cdot\exp(j(u-\Omega)\tau).\right.\right.$$

$$\left.\left.\exp(j(\Omega-w)t)\right\}.t - \left\{H_0(u)\cdot\frac{\partial X_0(\Omega)}{\partial t}.\ \exp(j(u-\Omega)\tau)\ .\right.\right.$$

$$\left.\left.\exp(j(\Omega-w)t)\right\}.\tau\right]\ \partial u\ \partial\Omega\ \partial\tau\ \partial t\ \ .\ .\ .\ .\ .\ .\ .\ .2.72$$

Note that when $X(\Omega)$ is time-varying the expansion of $X_{t-\tau}(\Omega)$ is only strictly applicable when $|t-\tau| \leqslant T/2$. If the filter impulse response dies to zero for $|\tau| \ll T$ we may only integrate with respect to τ in the limits $|\tau| < \tau max$. In general we are only interested in the possible bounds of I_3 so:

$$|I_3| \leqslant \frac{1}{T} \int_{-T/2}^{T/2} \int_{0}^{\tau max} \iint_{-\infty}^{\infty} |H_0(u)| . \left| \frac{\partial X_0(\Omega)}{\partial t} \right| . |t| . \partial u \, \partial\Omega \, \partial\tau \, \partial t$$

$$+\frac{1}{T} \int_{-T/2}^{T/2} \int_{0}^{\tau max} \iint_{-\infty}^{\infty} |H_0(u)| . \left| \frac{\partial X_0(\Omega)}{\partial t} \right| . |\tau| . \partial u \, \partial\Omega \, \partial\tau \, \partial t$$

$$= \frac{\tau max . T}{4} \iint_{-\infty}^{\infty} |H_0(u)| . du . \left| \frac{\partial X_0(\Omega)}{\partial t} \right| . \partial\Omega$$

$$+ \frac{\tau max^2}{2} \iint_{-\infty}^{\infty} |H_0(u)| . du . \left| \frac{\partial X_0(\Omega)}{\partial t} \right| . d\Omega$$

In the limit as $T \to 0$ $|I_3| \to 0$ iff the restriction $\tau max \ll T$ is complied with. Clearly for physically realisable systems which in general display phase characteristics (i.e. not just pure gain systems) this is not reasonable. However in general we will choose $T \gg \tau max$ and the second term may be neglected. Letting:

$$\sigma_{H_0} = \int_{-\infty}^{\infty} |H_0(u)| . du \qquad < \infty$$

and again defining $X(t,\Omega)$ to belong to the class of slowly varying oscillatory functions such that:

$$X(t,\Omega) = \int_{-Smax}^{Smax} X(s,\Omega) . \exp(jst) . ds \qquad \text{....then:}$$

$$|I_3| \leqslant \frac{\tau max \, T}{4} . \sigma_{H_0} . \sigma x_0 . \frac{Smax^2}{2} \qquad \text{. . . . . 2.73}$$

where we try to choose T so that $Smax \ll \frac{2\pi}{T}$ and $\frac{2\pi}{T} <$ bandwidth of narrowest peak in $H(t,u)$, $X(t,\Omega)$ for $t \in T$.

Lastly we look at terms involving $H_0(u).\ \frac{\partial^2 X_0(\Omega)}{\partial t^2}$ in equation 2.70:

$$I_4 = \frac{1}{T}\int_{-T/2}^{T/2}\int_{o}^{\tau max}\iint_{-\infty}^{\infty} H_0(u).\ \frac{\partial^2 X_0(\Omega)}{\partial t^2}\ .\ (t-\tau)^2\ .\ \exp\left(j(u-\Omega)\tau\right).$$

$$.\exp\ \left(j(\Omega-w)\ t\right)\ .du\ d\Omega\ d\tau\ dt\ .\ .\ .\ .\ 2.74$$

$$|I_4| \leqslant \frac{1}{T}\int_{-T/2}^{T/2}\int_{o}^{\tau max}\iint_{-\infty}^{\infty}|H_0(u)|\left|\frac{\partial^2 X_0(\Omega)}{\partial t^2}\right|\ .(t-\tau)^2.du\ d\Omega\ d\tau\ dt\ .\ 2.75$$

Integrating with respect to t and τ we find:

$$|I_4| \leqslant \iint_{-\infty}^{\infty}|H_0(u)|.\left|\frac{\partial^2 X_0(\Omega)}{\partial t^2}\right|\ .\ du\ d\Omega\ .$$

$$.\left\{\frac{T^2\ \tau max}{12} - \frac{T\ \tau max^2}{4} + \frac{\tau max^3}{3}\right\}\ .\ .\ .\ .\ .\ 2.76(a)$$

Again if $\tau max << T$ we can neglect terms in τmax^2, τmax^3 and obtain:

$$|I_4| \leqslant \frac{T^2\ \tau max}{12}\ .\ \ \ \sigma_{H_o}\ .\ \sigma x_o\ \frac{Smax^3}{3}\ .\ .\ .\ .\ .\ .\ .\ 2.76(b)$$

This term is generally $< |I_3|$ if $Smax << \frac{2\pi}{T.}$

We have now shown that when both the input signal characteristics and the system are time-varying we may estimate a time-dependent frequency response between x(t), y(t) in the interval $t \in T$, which approximates the value $H_0^{\ T}(jw)$ obtained if the system were stationary. The time variations introduce bias and variance terms whose bounded absolute values are given by equations 2.62, 2.66, 2.73 and 2.76.

Equations 2.73 and 2.76 involve τ max, the effective period of influence of $H(t,\tau)$. This is in general much less than T and hence the bias due to these terms may be an order of magnitude less than the terms given by equations 2.62 and 2.66. Thus:

$$Y_T(w) \simeq \int_{-\infty}^{\infty} H_0(\Omega)\ .X_0(\Omega)\ .L(\Omega-w)\ .d\Omega \pm (\ |I_1|\ +\ |I_2|\ )\ .\ .\ .\ .\ 2.77$$

where $|I_1| + -|I_2|$ are approximately bounded by $\varepsilon.|X_T(w)|$,

$\{ \varepsilon = |H(t,u) - H_0(u)| \quad , t \in T \}$ where ε is taken as the modulus of the maximum change in $H(t,u)$ in the frequency range $w - w_0 \leqslant \Omega \leqslant w+w_0$. w_0 is the effective bandwidth of the frequency filter $L(u)$ and $X_T(w)$ is the short-term Fourier transform of $x(t)$ on the interval $t \in T$.

Reverting to the sampled data case when we calculate the discrete transforms of $\hat{X}(Kw_0)$, $\hat{Y}(Kw_0)$ we note that:

1) $x_t(i)$, $y_t(i)$ are normally-distributed variables with zero means and time-dependent variance terms.

2) When the systems $X(t,\Omega)$ and $H(t,u)$ are slowly varying with respect to $x(t)$, $y(t)$, then it is often possible to choose T such that:

$$VAR(\hat{X}_T(Kw_0)) \simeq Sx_0^2 \quad \text{and}$$

$$VAR(\hat{Y}_T(Kw_0)) \simeq \{|H_0(Kw_0)|^2 . Sx_0^2 + Sn_0^2\}$$

$$\text{for} \quad 0 \leqslant K \leqslant N/2.$$

where $\phi nn(t,w)$ is an additive Gaussian noise term at the output of the system. Sn_0^2, Sx_0^2 are the powers in $x(t)$, $n(t)$ respectively in the frequency band $Kw_0 \pm w_0/2$, evaluated at time $t=0$.

When the complete system is stationary adjacent frequency points are approximately independent when a rectangular 'do-nothing' time window is used. For slowly-varying oscillatory systems this independence is maintained. Consider:

$$x(t) = \int_{-Smax}^{Smax} x(s,t).\exp(+jst)\, ds$$

Taking the Fourier transform:

$$X(w) = \int_{-\infty}^{\infty}\int_{-Smax}^{Smax} x(s,t) \cdot \exp\ (-j(w-s)\ t) \cdot ds\ dt$$

$$= \int_{-Smax}^{Smax} X(s,\ w-s) \cdot ds \qquad \ldots\ldots\ldots\ldots\ldots\ldots\ 2.78$$

FIGURE 2. **Illustrates the convolution integral given by eqn. 2.73 for a real function X.**

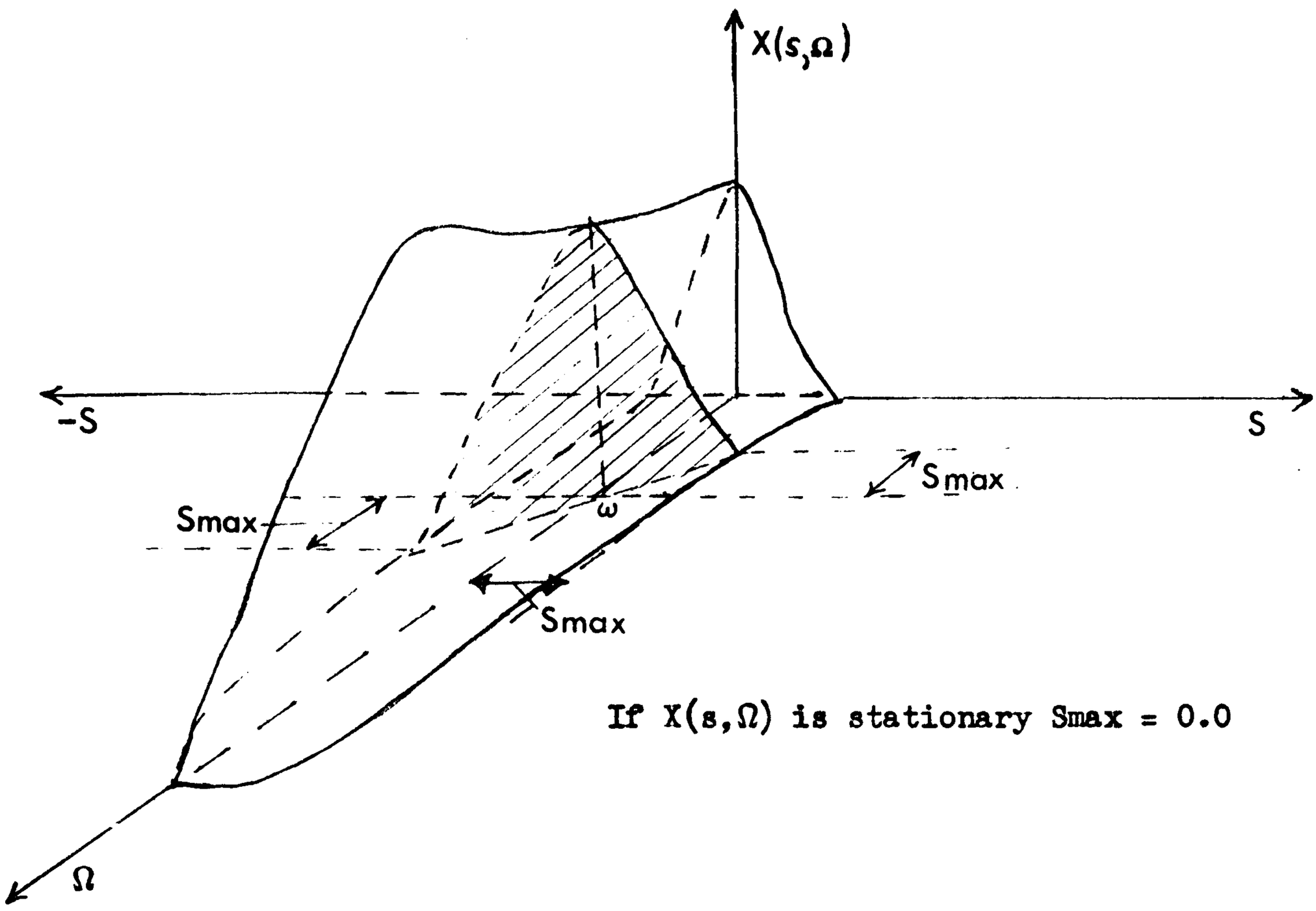

If X(s,Ω) is stationary Smax = 0.0

In the interval T centred about t=0, $X_T(w)$ is given by:

$$\hat{X}_T(Kw_0) = \int_{-\infty}^{\infty} X(w-u) \cdot L(u) \cdot du$$

where X(w) is given by equation 2.78 and $L(u) = \sin(\frac{UT}{2}) / (\frac{UT}{2})$.

To track time changes in $\phi xx(t,w)$ accurately $w_0 (\leq 2\pi/T) >>$ Smax. Under these conditions the blurring of X(w) with components in $X(w \pm s), (s \leq Smax)$ will be of secondary importance to the components introduced by the finite bandwidth of L(u). More exactly,

$X(Kw_0 + w_0 / 2)$ contains components in X from neighbouring frequencies $\pm$ Smax with Smax << w_0. Thus $\hat{X}(Kw_0)$ will only have marginal components in common with $\hat{X}((K-1).w_0)$ and $\hat{X}((K+1).w_0)$ and the independence of adjacent frequency points is still approximately maintained. If T is chosen so that Smax $\simeq \frac{(2\pi)}{T}$ then adjacent frequency points become correlated as is the case if a Hanning time data window is used. Indeed time changes in $\phi xx(w)$ can be regarded as a modulation of a stationary process.

Similarly if H(t,u) is an oscillatory process:

$$Y(w) = \int_{-\infty}^{\infty} y(t) . \exp(-jwt) . dt$$

$$\text{where } y(t) = \int_{-\infty}^{\infty} \int_{-Zmax}^{Zmax} H(z,\tau) . \int_{-Smax}^{Smax} X(s,t-\tau) . \exp(jzt) .$$

$$. \exp(js(t-\tau)) \, d\tau \, dz \, ds$$

$$\text{Hence: } Y(w) = \iint_{-\infty}^{\infty} \int_{-Zmax}^{Zmax} \int_{-Smax}^{Smax} H(z,\tau) . X(s,t-\tau) . \exp(jzt) .$$

$$. \exp(js(t-\tau)) \; . \exp(-jwt) . d\tau \, dz \, ds \, dt$$

Letting $V = t-\tau$ and substituting for t:

$$Y(w) = \iint_{-\infty}^{\infty} \int_{-Smax}^{Smax} \int_{-Zmax}^{Zmax} H(z,\tau) . X(s,v) . \exp(-j(w-z-s)\, v) .$$

$$. \exp(-j(w-z)\tau) . \, d\tau \, ds \, dz \, dv$$

$$= \int_{-Smax}^{Smax} \int_{-Zmax}^{Zmax} H(z,w-z) \; X(w-z-s) \, ds \, dz \quad \ldots\ldots 2.79$$

Y(w) contains components of $X(\Omega)$ in the range w-Zmax-Smax<Ω< w+Zmax+Smax. Again by choosing T such that $\frac{2\pi}{T}$ >> (Zmax + Smax), adjacent frequency points in $\hat{Y}(Kw_0)$ remain approximately independent. The approximation is not as good as that for $\hat{X}(Kw_0)$ as further frequency spreading has

occurred due to time variations in the system.

We have shown that for slowly varying functions, $\phi xx(t,\Omega)$, $H(t,u)$ where T can be chosen so that bias terms may be disregarded, a simple extension of stationary random error analysis, letting variance terms be time-dependent, is not unreasonable. The extension is valid for any system whose variations in time are continuous over an interval T, permitting a Taylor series approximation to the function about $t=0$, $t \in T$. When the system parameters are slowly varying oscillatory functions, we have shown that adjacent discrete frequency estimates $\hat{X}(Kw_0)$, $\hat{Y}(Kw_0)$ remain approximately independent if Smax, Zmax $<< \frac{2\pi}{T}$. This independence is lost as Smax, Zmax get larger (Smax and Zmax are defined as before).

7) <u>SOME STATISTICS OF SPECTRAL ESTIMATES OBTAINED FROM OVERLAPPING TIME SEGMENTS</u>

To track time-varying systems it is sometimes useful to obtain spectral estimates from overlapping time segments. This leads to:

a) Better system tracking for a fixed frequency resolution.

b) When the data contains information on the transient response of the system, the beginning and end points can be more accurately determined (e.g. Whittle: analysis of transient effects in jet engine noise).

We develop the joint distribution of 2 auto-spectral estimates $\hat{\phi}xx(w)$, $\hat{\phi}yy(w)$ obtained from short-term records of x(t), y(t) respectively, and then show how this distribution can be applied to overlapped spectral estimates obtained from the same signal x(t).

Let x(t), n(t) again be Gaussian band-limited white noise processes; y(t) is the output of a linear system whose input is x(t). The output is contaminated by noise n(t). (n(t) and x(t) are uncorrelated). As in Sections 3 and 4 we compute the input and output auto-spectral estimates as the average of L independent estimates obtained from L blocks of N sample points. If the system frequency response is denoted by H:

$$\bar{\phi}yy \simeq |H|^2 . \bar{\phi}xx + 2\,R\,L\,(H^*.\,\bar{\phi}xn) + \bar{\phi}nn \quad \ldots\ldots 2.80$$

* denotes the complex conjugate (frequency w is omitted).

Rewriting equation 2.80 in terms of the real and imaginary coefficients of $\hat{X}$, $\hat{N}$ we find:

$$\bar{\phi}yy = \frac{1}{L}\sum_{i=1}^{L} (R_H^2 + I_H^2).(\hat{R}_x^{i\,2} + \hat{I}_x^{i\,2}) + \hat{R}_n^{i\,2} + \hat{I}_n^{i\,2} +$$

$$2.R_H(\hat{R}_x^i.\,\hat{R}_n^i + \hat{I}_x^i.\hat{I}_n^i) - 2.I_H(\hat{R}_x^i.\hat{I}_n^i - \hat{I}_x^i.\hat{R}_n^i) \quad \ldots\ldots 2.81$$

Rearranging:

$$\bar{\phi}yy \simeq \frac{1}{L}\sum_{i=1}^{L} \hat{R}_n^{i\,2} + 2.\hat{R}n.\hat{\delta}_1^i + \hat{I}_n^{i\,2} + 2.\hat{I}_n^i.\hat{\delta}_2^i$$

$$+ (\hat{R}_H^2 + \hat{I}_H^2).(\hat{R}_x^{i\,2} + \hat{I}_x^{i\,2}) \quad \ldots\ldots 2.82$$

where $\hat{\delta}_1^i = R_H.\hat{R}_x^i + I_H.\hat{I}_x^i$, $\hat{\delta}_2^i = R_H.\hat{I}_x^i - I_H.\hat{R}_x^i$

and $(\hat{\delta}_1^{i2} + \hat{\delta}_2^{i\,2}) = (|H|^2 . \bar{\phi}_{xx}^{\,i})$

We now define 2 new variables:

$$\hat{Z}_R^i = \hat{R}_n^{i\,2} + 2\,\hat{R}_n^i.\,\hat{\delta}_1^i, \quad \hat{Z}_I^i = \hat{I}_n^{i\,2} + 2\,\hat{I}_n^i.\,\hat{\delta}_2^i$$

With $\hat{\delta}_1^i$ $\hat{\delta}_2^i$ fixed, $\hat{Z}_R^i$ and $\hat{Z}_I^i$ are not dependent on $\hat{R}_x^i$, $\hat{I}_x^i$ as n(t) and x(t) are uncorrelated. The distribution of $\hat{R}_n^i$, $\hat{I}_n^i$ is given by:

$$p(\hat{R}_n^i, \hat{I}_n^i) = \underset{\text{complex}}{N} (0, Sn^2)$$

with $\hat{R}n$, $\hat{I}n$ independent. Thus performing the variable transformation to find the conditioned distribution of $\hat{Z}_R^i$ given $\hat{\delta}_1^i$ we find:

$$p(\hat{Z}_R^i : \hat{\delta}_1^i) = \frac{\exp(-(\hat{\delta}_1^{i2}.V_R^i)/2.Sn^2).\cosh(\hat{\delta}_1^i\sqrt{V_R^i}/Sn^2)}{\sqrt{2\pi}.Sn.\sqrt{V_R^i}} \quad \ldots 2.83$$

where $V_R^i = \hat{\delta}_1^{i2} + \hat{Z}_R^i$

A similar transformation gives the conditional distribution of $\hat{Z}_I^i$ given $\hat{\delta}_2^i$. However, the spectrum estimate $\bar{\phi}yy$ is now given by:

$$\bar{\phi}yy = \frac{1}{L}\sum_{i=1}^{L} (\hat{Z}_R^i + \hat{\delta}_1^{i2} + \hat{Z}_I^i + \hat{\delta}_2^{i2}) \quad \ldots\ldots\ldots 2.84$$

Forming 2 more variables V_R^i, V_I^i given by:

$$V_R^i = \hat{Z}_R^i + \hat{\delta}_1^{i2}, \quad V_I^i = \hat{Z}_I^i + \hat{\delta}_2^{i2}$$

we find:

$$p(V_R^i : \hat{\delta}_1^i) = \frac{\exp(-(\hat{\delta}_1^{i2} + V_R^i)/2Sn^2).\cosh(\hat{\delta}_1^i.\sqrt{V_R^i}/Sn^2)}{\sqrt{2\pi}.Sn.\sqrt{V_R^1}} \quad \ldots 2.85$$

and similarly for V_I^i replacing $\hat{\delta}_1^i$ by $\hat{\delta}_2^i$ in equation 2.85. Taking the Fourier transform of equation 2.85 to give the characteristic function of $p(V_R^i : \hat{\delta}_1^i)$ we find:

$$f_{V_R}(w) = \frac{K_1 \cdot \exp\left\{\frac{\nu_1^2}{4.(\mu + jw)}\right\}}{(\mu + jw)^{\frac{1}{2}}} \quad \ldots\ldots\ldots\ldots 2.86$$

where $K_1 = \frac{\exp(-\hat{\delta}_1^{i2} / 2.Sn^2)}{\sqrt{2\pi} \cdot Sn}$, $\nu_1 = \frac{\hat{\delta}_1^i}{Sn^2}$, $\mu = \frac{1}{2.Sn^2}$

and again taking the Fourier transform of $p(V_I^i : \hat{\delta}_2^i)$ we obtain:

$$f_{V_I}(w) = \frac{K_2 \cdot \exp\left\{\frac{\nu_2^2}{4.(\mu + jw)}\right\}}{(\mu + jw)^{\frac{1}{2}}} \quad \ldots\ldots\ldots\ldots 2.87$$

The variables V_R^i , V_I^i are independent if $\hat{\delta}_1^i$ and $\hat{\delta}_2^i$ remain fixed. Also:

$$\hat{\phi}_{yy}^i = V_R^i + V_I^i$$

Thus the characteristic function of $p(\hat{\phi}_{yy}^i : \hat{\delta}_1^i , \hat{\delta}_2^i)$ is given by:

$$f_{\hat{\phi}yy}(w) = f_{V_R}(w) \cdot f_{V_I}(w) \quad \ldots\ldots\ldots\ldots 2.88$$

and in general when $(L.\bar{\phi}_{yy})$ is the sum of L independent estimates, $\hat{\phi}_{yy}^i$, the characteristic function of $p(L.\bar{\phi}yy : \hat{\delta}_1^i , \hat{\delta}_2^i \{i=1,L\})$ is given by:

$$f_{L.\bar{\phi}yy}(w) = \left\{ f_{V_R^i}(w) \cdot f_{V_I^i}(w) \right\}^L \quad \ldots\ldots\ldots\ldots 2.89$$

Substituting equations 2.86 and 2.87 for $f_{V_R^i}(w)$ and $f_{V_I^i}(w)$ respectively and remembering that $\hat{\delta}_1^{i2} + \hat{\delta}_2^{i2} = |H|^2 . \hat{\phi}_{xx}^i$ we find:

$$f_{L.\bar{\phi}yy}(w) = \frac{\exp(-(|H|^2.\bar{\phi}_{xx}.L)/ 2.Sn^2).L. (\bar{\phi}_{yy})^{\frac{L-1}{2}} \cdot}{2 . Sn^2 . (|H|^2.\bar{\phi}_{xx})^{\frac{L-1}{2}}}$$

$$\cdot I_{L-1}\left\{ \frac{L. |H|}{Sn^2} \cdot \sqrt{(\bar{\phi}_{yy} \cdot \bar{\phi}_{xx})} \right\} \quad \ldots\ldots 2.90$$

Taking the inverse transform of equation 2.90 (see reference 14) and normalising by the factor 1/L to find $p(\bar{\phi}_{yy}; \bar{\phi}_{xx})$:

$$p(\bar{\phi}_{yy}; \bar{\phi}_{xx}) = \frac{L.\ \bar{\phi}_{yy}^{(L-1)/2}\ .\ \exp\left(-\ |H|^2.\ L(\bar{\phi}_{xx} + \bar{\phi}_{yy})\ /2\ Sn^2\right)}{2.Sn^2.(\ |H|^2\ .\ \bar{\phi}_{xx})^{L-1/2}}$$

$$.I_{L-1}\left\{\frac{L.\ |H|\ .\ \bar{\phi}_{yy}.\ \bar{\phi}_{xx}}{Sn^2}\right\} \quad \ldots\ldots\ldots 2.91$$

We could equally well have written equation 2.91 in terms of the coherency between x(t) and y(t). Substituting:

$$Cxy^2 = \frac{1}{\left\{1 + \frac{Sn^2}{|H|^2.Sx^2}\right\}}$$

and letting $Sy^2 = |H|^2.Sx^2 + Sn^2$ we obtain:

$$p(\bar{\phi}_{yy}; \bar{\phi}_{xx}) = \frac{L.\ \bar{\phi}_{yy}^{(L-1)/2}\ .\ \exp\left(-\ |H|^2.L.(\bar{\phi}_{xx} + \bar{\phi}_{yy})\ /\ 2Sy^2(1-Cxy^2)\right)}{2.Sy^2.(1 - Cxy^2).\ (\ |H|^2.\ \bar{\phi}_{xx})^{L-1/2}}$$

$$.I_{L-1}\left\{\frac{L.\ |H|\ \bar{\phi}_{xx}.\ \bar{\phi}_{yy}}{Sy^2\ (1 - Cxy^2)}\right\} \quad \ldots\ldots\ldots 2.92$$

where I_{L-1} is the modified Bessel function of order (L-1).

In the general case the conditional distribution of the output spectrum in terms of the input spectrum estimate is not easily applied in practice as it requires prior knowledge of $|H|$ and Sn^2 (i.e. the system gain and the noise variance). However, when y(t) is no longer the output of a linear system but just a delayed version of x(t), equation 2.92 reduces to manageable form.

Consider the following situation:

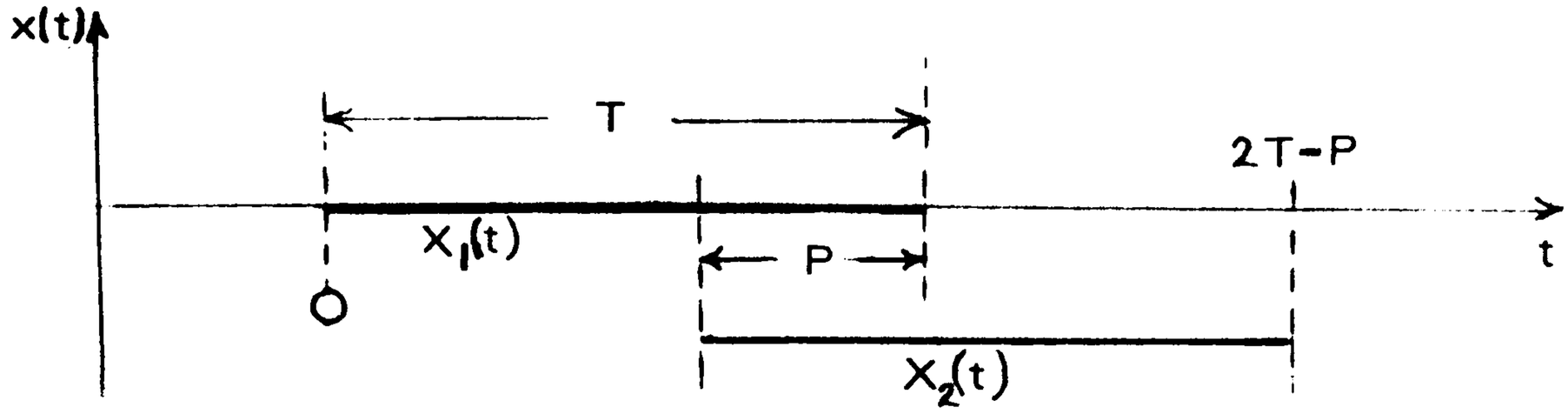

FIGURE 3. $x_1(t)$ and $x_2(t)$ are short-term realisations of x(t) on the interval $0 \leqslant t \leqslant T$, $T-p \leqslant t \leqslant 2T-p$ respectively.

We wish to find the correlation between $x_1(t)$ and $x_2(t)$ where the 2 time records are overlapped by an amount p, $(p \leqslant T)$. Let x(t) be Gaussian band-limited white noise.

We could equally well have considered the two concurrent time data records given by:

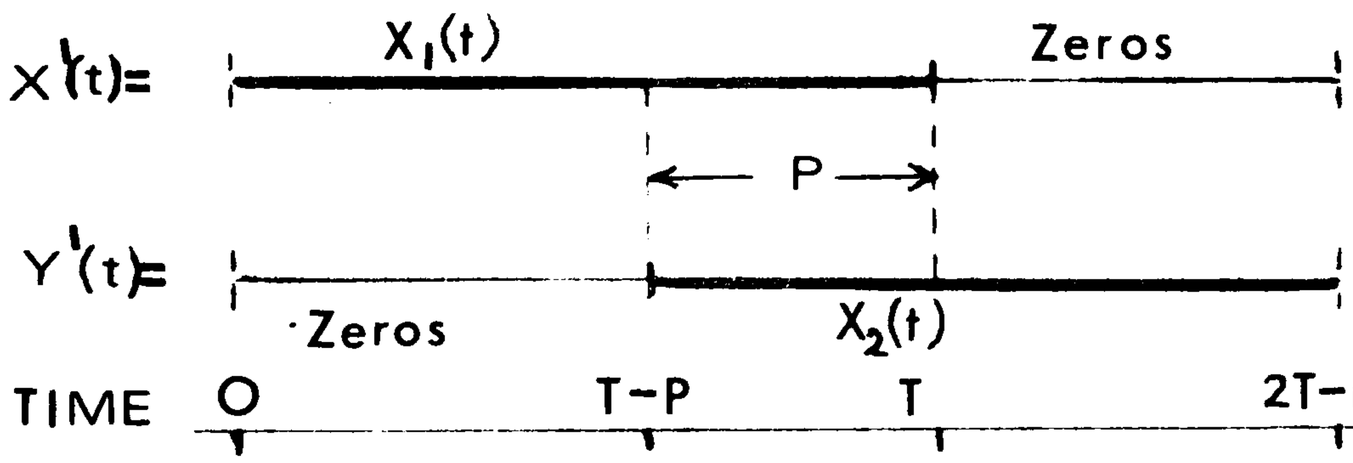

$x_1(t)$ and $x_2(t)$ are augmented by zeros

Calculating the short-term correlation functions for x'(t), y'(t) we find:

a) For $\tau > 0$

$$Cx'x'(\tau) = \frac{1}{2T-p-\tau} \cdot \int_0^{2T-p-\tau} x'(t).\, x'(t-\tau)\, dt$$

$$= \frac{1}{2T-p-\tau} \cdot \int_0^{T-\tau} x(t)\ .x(t-\tau)\, dt$$

$$Cy'y'(\tau) = \frac{1}{2T-p-\tau} \cdot \int_{T-p}^{2T-p-\tau} x(t)\ .x(t-\tau)\, dt$$

and:

$$Cx'y'(\tau) \quad = \quad \frac{1}{2T-p-\tau} \cdot \int_{T-p-\tau}^{T} x(t) \cdot x(t+\tau)\, dt$$

But $Cx'x'(\tau)$, $Cy'y'(\tau)$ and $Cx'y'(\tau)$ are biased estimates of $Cx_1x_1(\tau)$, $Cx_2x_2(\tau)$ and $Cx_1x_2(\tau)$. The bias factor, introduced by augmenting $x_1(t)$ and $x_2(t)$ with zeros is given by:

$$B \quad = \quad \frac{2T-p-\tau}{(T-\tau)}$$

Taking the expected values of $Cx'x'(\tau)$, $Cy'y'(\tau)$ and $Cx'y'(\tau)$ over an ensemble of similar processes we find:

$$E(Cx'x'(\tau)\ ) \quad = \quad \frac{T-\tau}{2T-p-\tau} \quad . \quad Cxx(\tau) \quad \ldots\ldots\ldots\ldots 2.93$$

$$E(Cy'y'(\tau)\ ) \quad = \quad \frac{T-\tau}{2T-p-\tau} \quad . \quad Cxx(\tau) \quad \ldots\ldots\ldots\ldots 2.94$$

and $$E(Cx'y'(\tau)\ ) \quad = \quad \frac{(p+\tau)}{2T-p-\tau} \quad . \quad Cxx(\tau) \quad \ldots\ldots\ldots\ldots 2.95$$

Normalising by the bias factor B shown above we find:

$$E(Cx_1x_1(\tau)\ ) \quad = \quad E(Cx_2x_2(\tau)\ ) \quad = \quad Cxx(\tau)$$

$$E(Cx_1x_2(\tau)\ ) \quad = \quad \frac{p+\tau}{T-\tau} \quad . \quad Cxx(\tau)$$

if $x(t)$ is a stationary process.

Performing the same steps for negative τ we find the expected values of $Cx_1x_1(\tau)$, $Cx_2x_2(\tau)$ are as shown above for τ positive, while:

$$E(Cx_1x_2(\tau)\ ) \quad = \quad \frac{p-|\tau|}{T-|\tau|} \quad . \quad Cxx(\tau) \text{ for } \tau \leqslant 0 \quad \ldots\ldots 2.96$$

Taking the Fourier transforms of equations 2.93 to 2.96 and recalling that if $x(t)$ is a white noise Gaussian process then $Cxx(\tau) = 0$ for $|\tau| << T$:

$$E(\phi x_1x_1(w)) \quad \simeq \quad \phi xx(w) \quad \ldots\ldots\ldots\ldots 2.97$$

$$E(\phi x_2x_2(w)) \quad \simeq \quad \phi xx(w) \quad \ldots\ldots\ldots\ldots 2.98$$

$$E(\phi x_1x_2(w)) \quad \simeq \quad \frac{P}{T} \cdot \phi xx(w) + j\,\frac{\partial \phi xx(w)}{\partial w} \quad \ldots\ldots\ldots 2.99$$

Strictly speaking, $E(\phi x_1 x_2(w)$ should include a factor exp $(-jw(T-P))$ to account for the shifting of $x_2(t)$ with respect to $x_1(t)$ in $y'(t)$. However as we are only interested in the magnitude of $\phi x_1 x_2(w)$ to find the coherency between $x_1(t)$ and $x_2(t)$ this factor may be omitted. Recalling that the coherency is given by the ratio:

$$\bar{C}x_1x_2{}^2 = \frac{|\bar{\phi}x_1x_2|^2}{\bar{\phi}x_1x_1 \cdot \bar{\phi}x_2x_2}$$

where $\bar{}$ denotes the mean value. We note that:

$$E(\bar{C}x_1x_2{}^2) \neq E\left(\frac{|\bar{\phi}x_1x_2|^2}{\bar{\phi}x_1x_1 \cdot \bar{\phi}x_2x_2}\right)$$

but is given by the ratio of the expected values of each of the terms individually.

Thus substituting equations 2.97, 2.98 and 2.99 we find:

$$Cx_1x_2{}^2 = \frac{P^2}{T^2} + \frac{1}{T^2} \cdot \frac{(\partial\phi xx(w) / \partial w)^2}{\phi xx(w)^2} \quad \ldots\ldots 2.100$$

If $x(t)$ is a white noise process then $\partial\phi xx(w) / \partial w = 0$ and the coherency is given by the ratio P/T. On substituting P^2/T^2 for Cxy^2, Sx^2 for Sy^2 and 1 for $|H|$ in equation 2.92 we obtain the conditional distribution of ϕx_2x_2 given ϕx_1x_1 assuming the system to be stationary. When $x(t)$ is not a band-limited white noise process, the coherency between $x_1(t)$ and $x_2(t)$ is greater than P/T and the variance of the distribution given by equation 2.92 decreases. Considering $x(t)$ as a white noise Gaussian signal gives a conservative estimate for the distribution of ϕx_2x_2 given ϕx_1x_1.

8) SIMULATION RESULTS

Many of the results presented in this chapter serve as a resume of previous work. The statistical distributions associated with auto-spectral and frequency response estimates are well known and are not verified here. Likewise a study of bias errors is unnecessary. Of more interest are the distributions associated with cross-spectral estimates and signal-to-noise (SN) estimates. These two distributions are verified and some typical comparisons of predicted and measured distributions are presented.

Section 2.7 develops the joint distribution of two auto-spectral estimates obtained from overlapping data blocks. This relationship is verified experimentally and the results presented.

Time variations in the system response or input signal characteristics are shown (Section 2.6) to introduce additional error terms in the spectral estimates. It is shown that if the system is slowly varying over a measurement interval, T, then these additional terms are of secondary importance compared with errors due to short-term sampling.

In this section a time-varying second-order system with light damping is considered. It is shown that the system response is approximately unbiased (with coherency between input and output remaining approximately constant) if the period of oscillation of w_0, the natural frequency of the system, is much greater than the data block interval, T. As the period of oscillation, w_0, decreases with respect to T, the coherency in the frequency band about w_0 decreases.

It is well known that when $x(t)$ is a Gaussian random variable with zero mean, the distribution of short-term Fourier coefficients obtained from sampling $x(t)$ on the interval T is just the bivariate Gaussian distribution with variance Sx^2 and independent real and imaginary terms. A reason for studying the Gaussian distribution is that even when $x(t)$ is non-Gaussian the distribution of $\hat{X}(Kw_0)$ ($0 \leqslant K \leqslant N/2$) will still be approximately normal for large N. This is demonstrated for the case where:

$$p(x(t)) = \tfrac{1}{2}, \quad |x(t)| \leqslant 1$$

$$p(x(t)) = 0, \quad |x(t)| > 1$$

and $\phi xx(w) \simeq 0.03, \quad 0 \leqslant w \leqslant 62.8$ rads/sec.

This signal was generated using the method outlined in Chapter 5 of this thesis. $x(t)$ was sampled 50 times per second and Fourier transformed using block sizes of 16, 32 and 64. The distribution of $\hat{X}_N(Kw_0) / \sqrt{w_0}$ was computed for K = 3 and N = 16, 32, 64 over 1000 independent estimates. Figure 4 shows the distribution of the real part of $\hat{X}_N(3w_0) / \sqrt{w_0}$ for the three block sizes :-

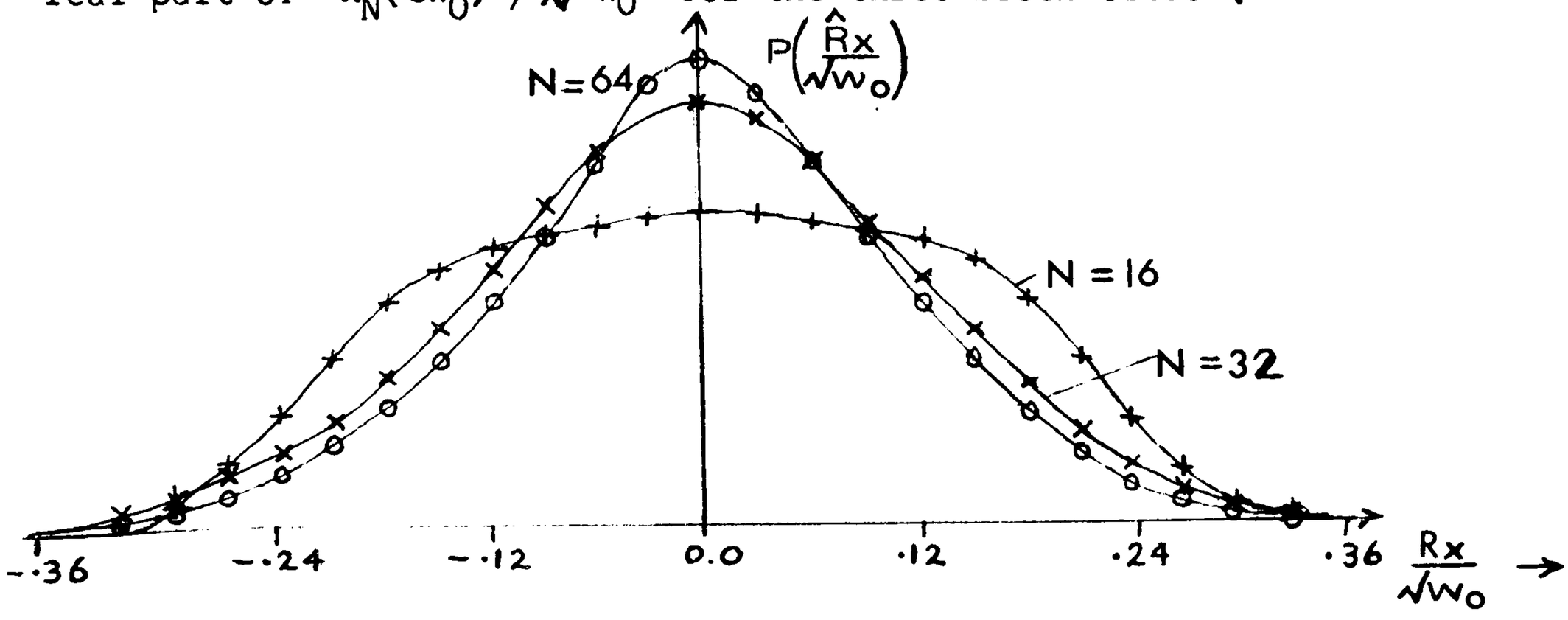

FIGURE 4 : Shows the measured distributions of $\hat{R}x/\sqrt{w_0}$ for N= 16, 32 and 64. $w_0 = 2\pi f_s / N$

Normalisation by the factor $1 / \sqrt{w_0}$, the frequency resolution, ensures that estimates of the power spectrum density function obtained for the 3 block sizes are consistent. It can be seen that as N increases, the distribution of $\hat{R}x / \sqrt{w_0}$ tends towards the Gaussian distribution with zero mean and variance $\simeq 0.015$ as expected. The distributions of the imaginary terms were in all cases similar to those shown above.

To reduce computing time the discrete Fourier coefficients $\hat{X}$, $\hat{N}$ were formed by taking 4 independent samples of a white noise Gaussian process $\zeta(t)$. Thus, referring to Figure 1:

$$\hat{X} = X_1 + j X_2$$

$$\hat{N} = (X_3 + j X_4).\alpha$$

where $X_1 \ldots . X_4$ are 4 independent samples of $\zeta(t)$ and $\hat{X}$, $\hat{N}$ are the discrete Fourier coefficients of $x(t)$, $n(t)$ at some general frequency (Kw_0), as measured on an interval T. Using this method for forming $\hat{X}$, $\hat{N}$, the signal-to-noise ratio can be controlled by varying α. The distributions of the various spectral estimates can be measured accurately without resorting to long computer simulations involving the use of an F.F.T. algorithm on many blocks of data.

Simulation results were compared with the predicted results for:

a) The distributions of cross-spectra $(L.\ \bar{\phi}xy)$ as given by equation 2.23

The Chi-square distribution does not predict a finite probability of obtaining negative estimates of $\bar{\phi}xy$. When the ratio Sx/Sn is large the discrepancy between the measured distribution and that predicted by a Chi-square distribution is less marked.

FIGURE 5 : Shows the distribution of $(L.\bar{R}xy / R_H Sx^2)$ for L=5, R_H=1.0

$Sx^2 = Sn^2 = 1.0$

a) As predicted by equation 2.23 (- - - - - -)

b) As predicted by a classical Chi-square distribution with 2L degrees of freedom (——————)

c) As measured from simulation results (- · - · - · -)

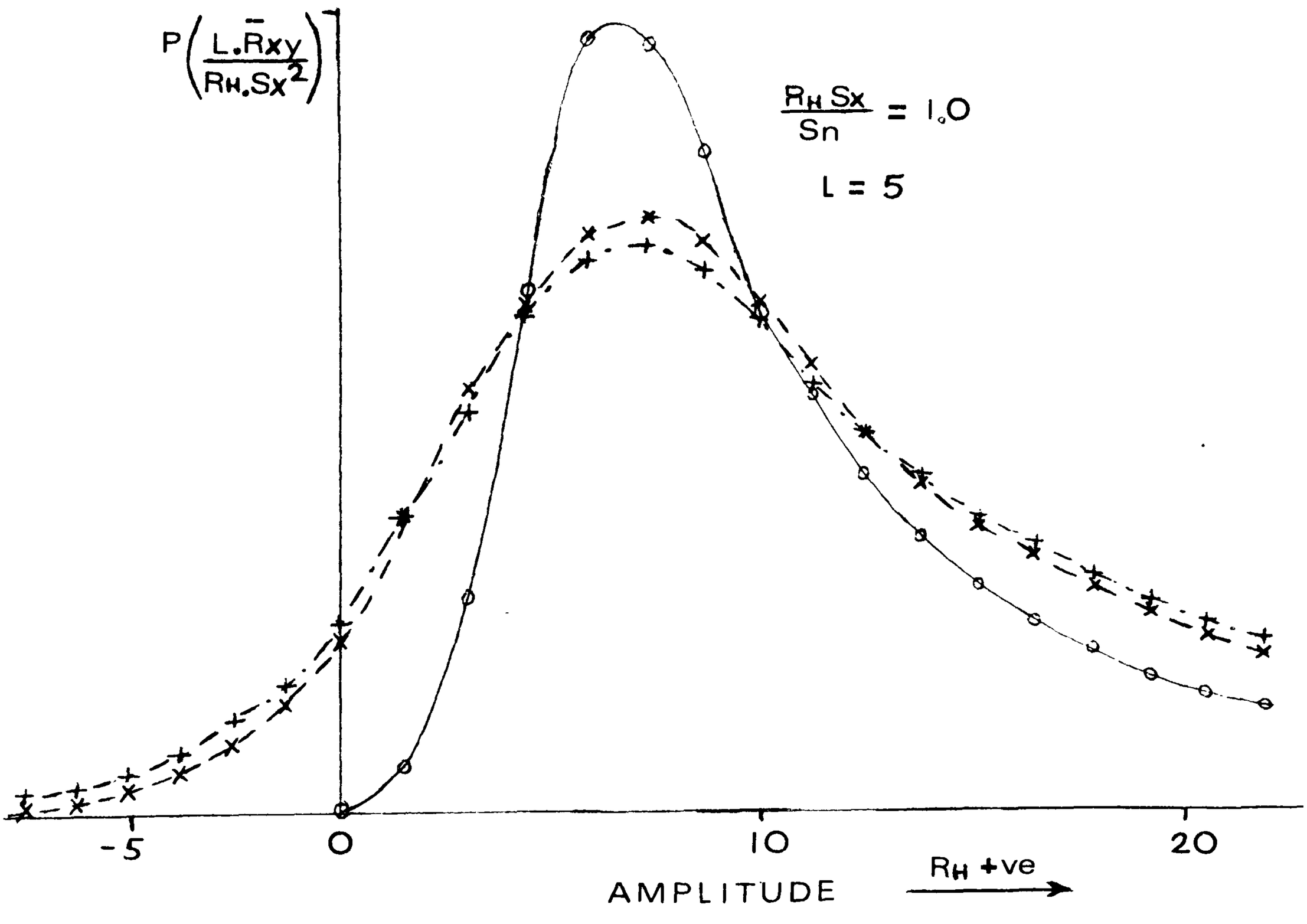

b) <u>The distribution of estimates of the signal-to-noise ratio $\overline{SN}$ as given by equation 2.36</u>

<u>FIGURE 6</u> : Shows the distribution of estimates of SN as predicted by equation 2.36 (———) and as measured from simulation data (- - -)

a) For SN = 0.1

b) For SN = 1.0

c) For SN = 10.0

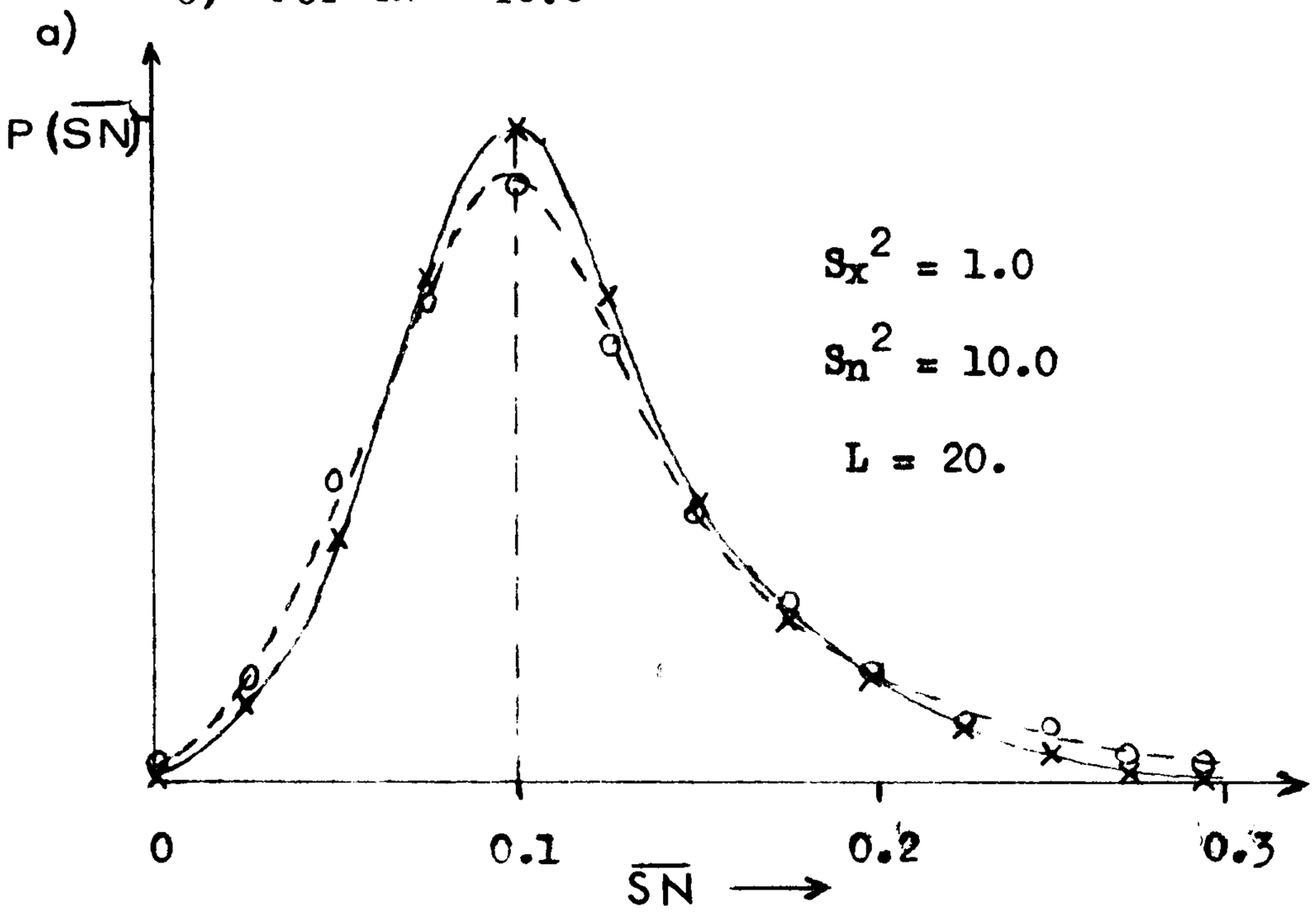

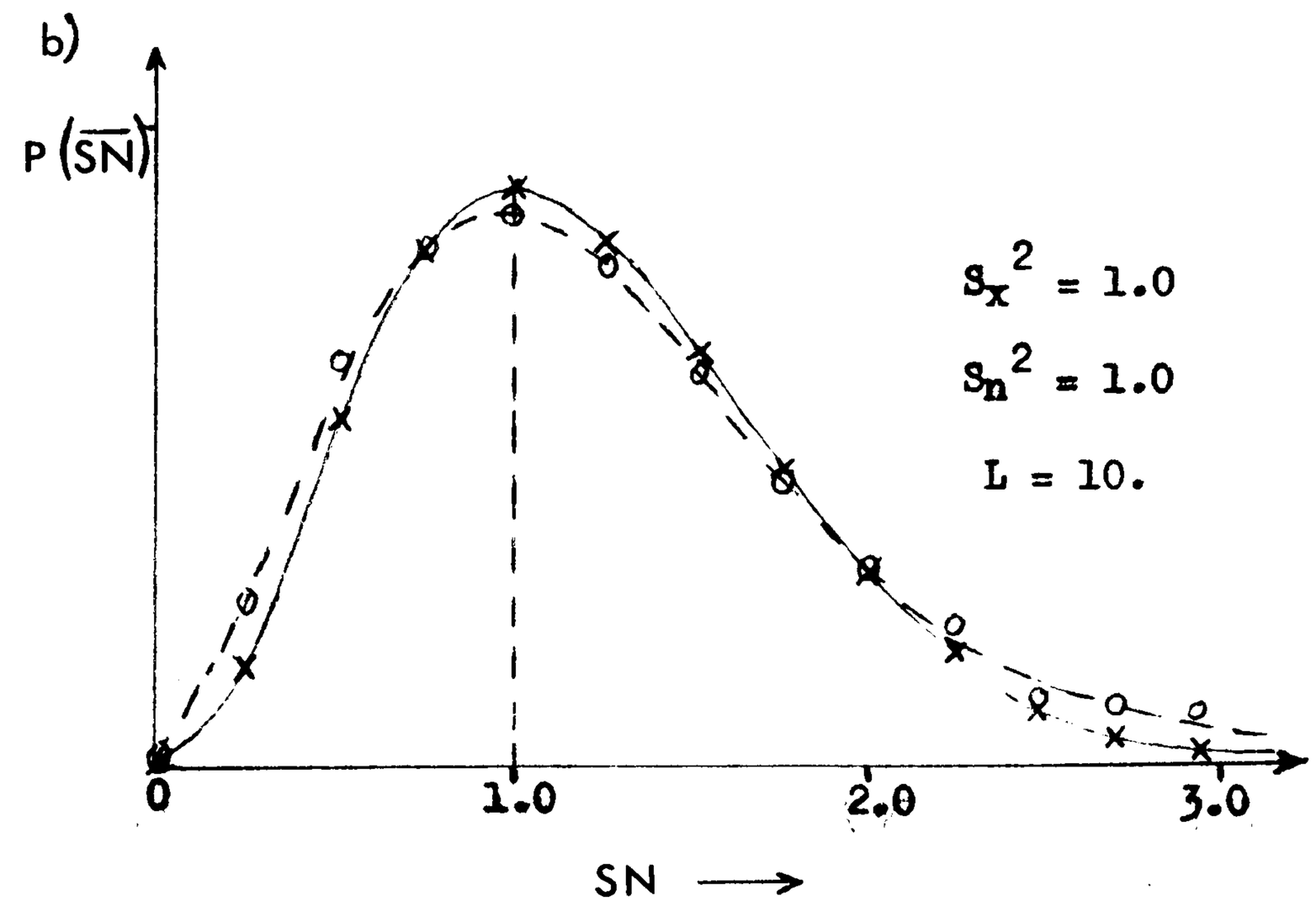

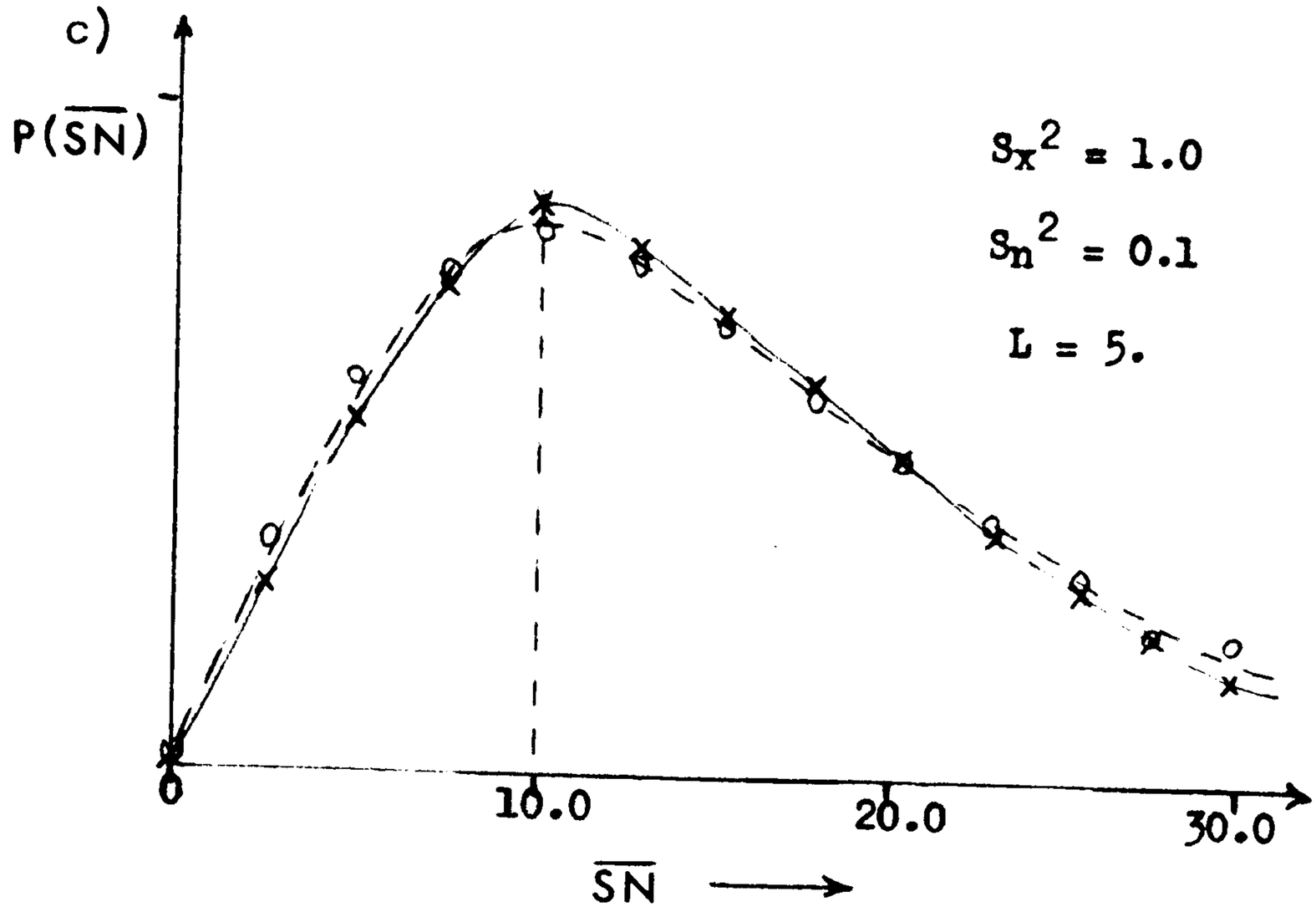

c) <u>The coherency between overlapped data sequences $x_1(t)$, $x_2(t)$</u>

A band-limited white noise Gaussian signal x(t) was sampled at a sufficiently high frequency to avoid aliasing. Groups of two sample records $x_t(i)$, $y_t(i)$, (i=0, 127) were collected where the record $y_t(i)$ was an overlapped record of x(t). The coherency function between $x_t(i)$ and $y_t(i)$ was calculated using 30 independent sets of samples ($x_t(i)$, $y_t(i)$) to calculate $\bar{\phi}xx$, $\bar{\phi}xy$, $\bar{\phi}yy$. The experiment was repeated for different degrees of overlap p in the range $0 \leqslant p \leqslant T$. Figure 7 shows the variation in $\bar{C}xy$ as a function of the overlap P/T

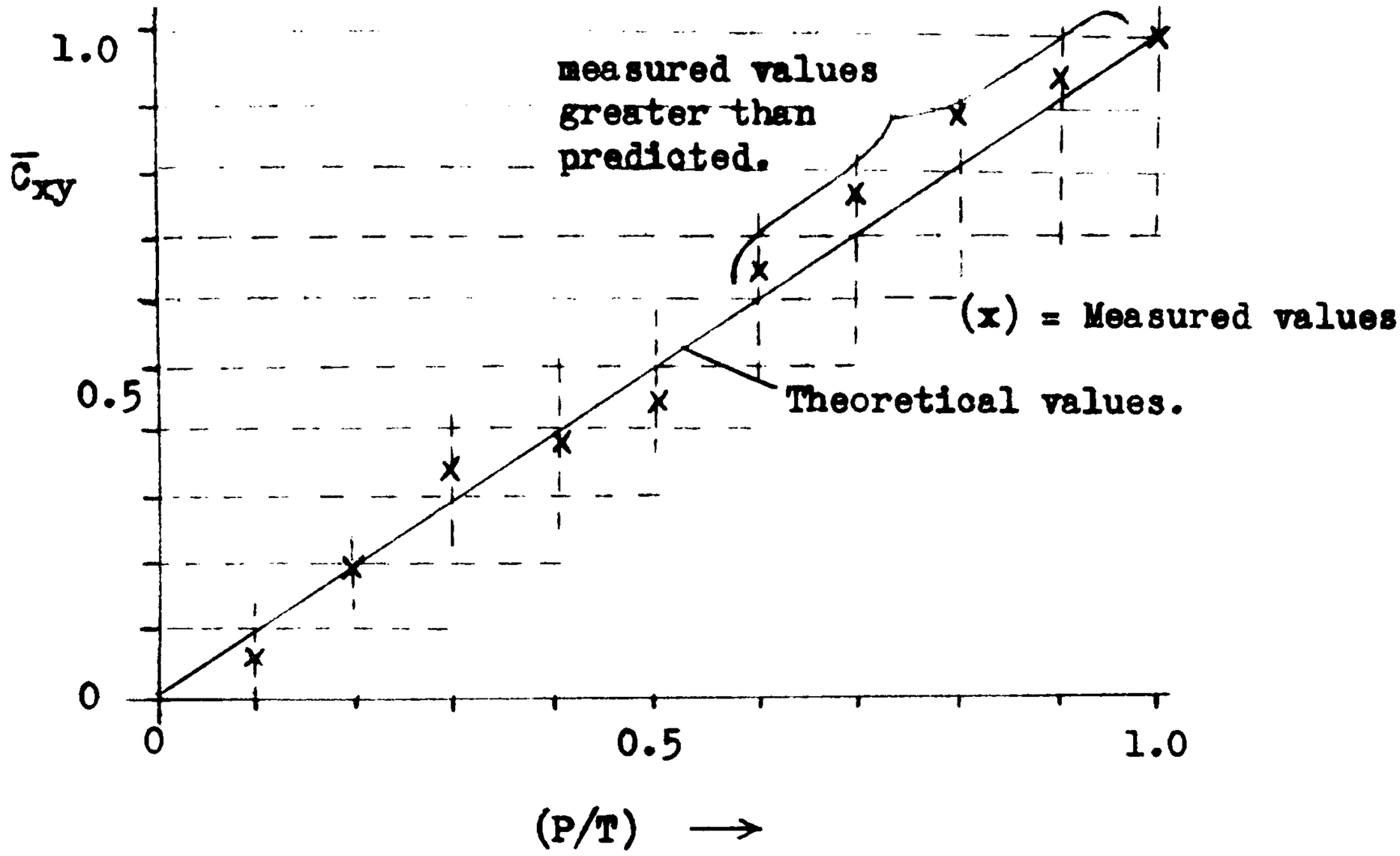

FIGURE 7 Shows the relationship between the coherency and the degree of overlap of two sample records of a signal x(t)

The results would indicate that the predicted result given by equation 2.100 tends to underestimate the true coherency. This might be due to $\phi xx(w)$ having a cut-off less than half the sampling frequency. Under these conditions the auto-correlation function of x(t) is no longer a dirac-delta pulse at $\tau=0$ but has finite width in τ. Thus under these conditions adjacent time sample points become correlated and the coherency between overlapped data sequences increases.

d) System tracking results for a second-order system

A second-order system with light damping was simulated on an analog computer such that the natural frequency w_0 could be varied in time:

$$H(w) = \frac{1}{-\frac{w^2}{w_0^2} + j\,\frac{2\zeta}{w_0}\,w + 1} \qquad \ldots\ldots\ldots\ldots\ldots 2.101$$

with $\zeta \simeq 0.1$ and $100 \leqslant w_0 \leqslant 600$ rads/sec.

The resonant frequency of the system is given by:

$$w_R = w_0 \sqrt{\{1 - 2\zeta^2\}} \simeq w_0 \text{ for small } \zeta$$

The system input was band-limited white noise with a cut-off at 1200 rads/sec. The input x(t) and output y(t) were sampled in blocks of 512 points at a frequency, f_s, of 500 Hz. Thus the frequency resolution was approximately 1 Hz and the block time period, T, was 1 second. The spectral estimates $\bar{\phi}xx$, $\bar{\phi}xy$, $\bar{\phi}yy$, were smoothed in the frequency domain over 10 neighbouring points using a triangular data window.

Figures 8-11 show some system tracking results for various variations of w_0 in time. When the time variations in w_0 are slow over the block interval T (Figure 9) the coherency between input and output is approximately the same as in the stationary case (Figure 8). However, when the period of oscillation of w_0 approaches 2T (twice the block period) the coherency decreases in the frequency band around the resonant frequency (Figure 10). Also, the half-power bandwidth of the system is seriously overestimated. When the variations of w_0 in time are random, (Figure 11) the system is accurately tracked as long as the system is slowly changing with respect to the block period T.

The approximate invariance of coherency for slowly varying systems would indicate that we are justified in applying stationary error analysis results to time-varying systems, letting the variance terms (Sx^2, Sn^2 etc.) be functions of time as well as frequency.

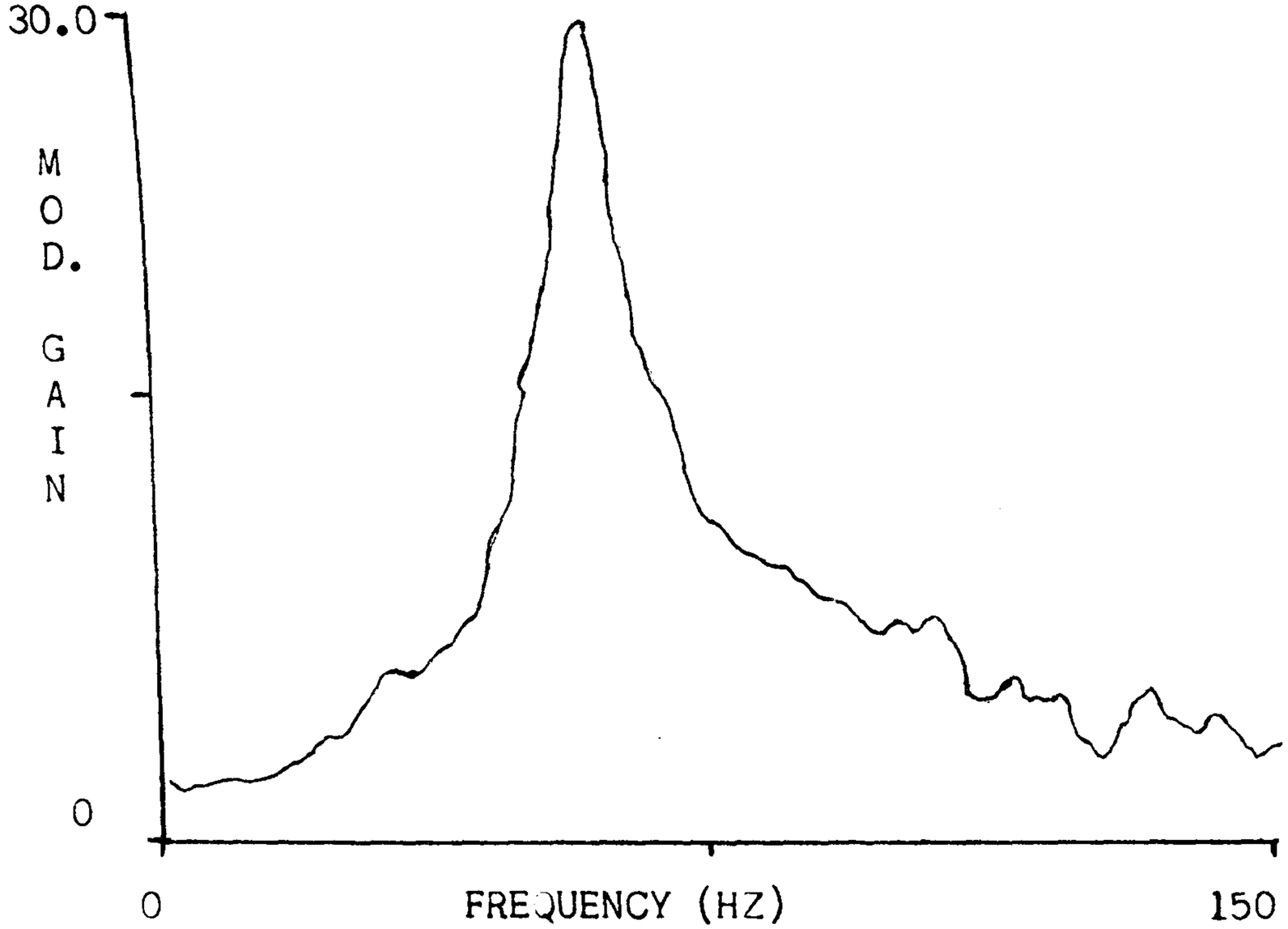

FIGURE 8 : Shows a typical estimate of the frequency response of a second order system obtained when the resonant frequency is not varying with time.

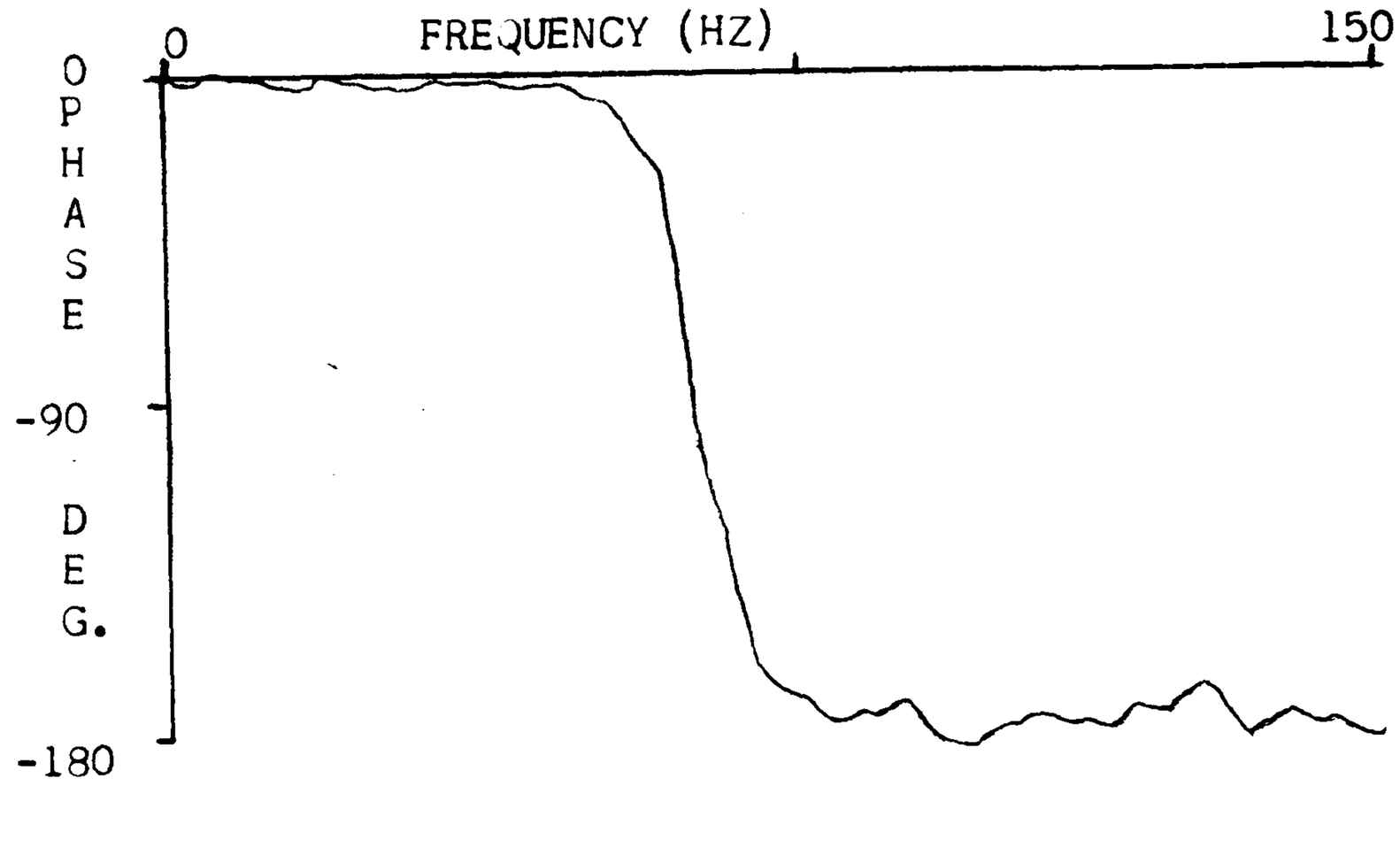

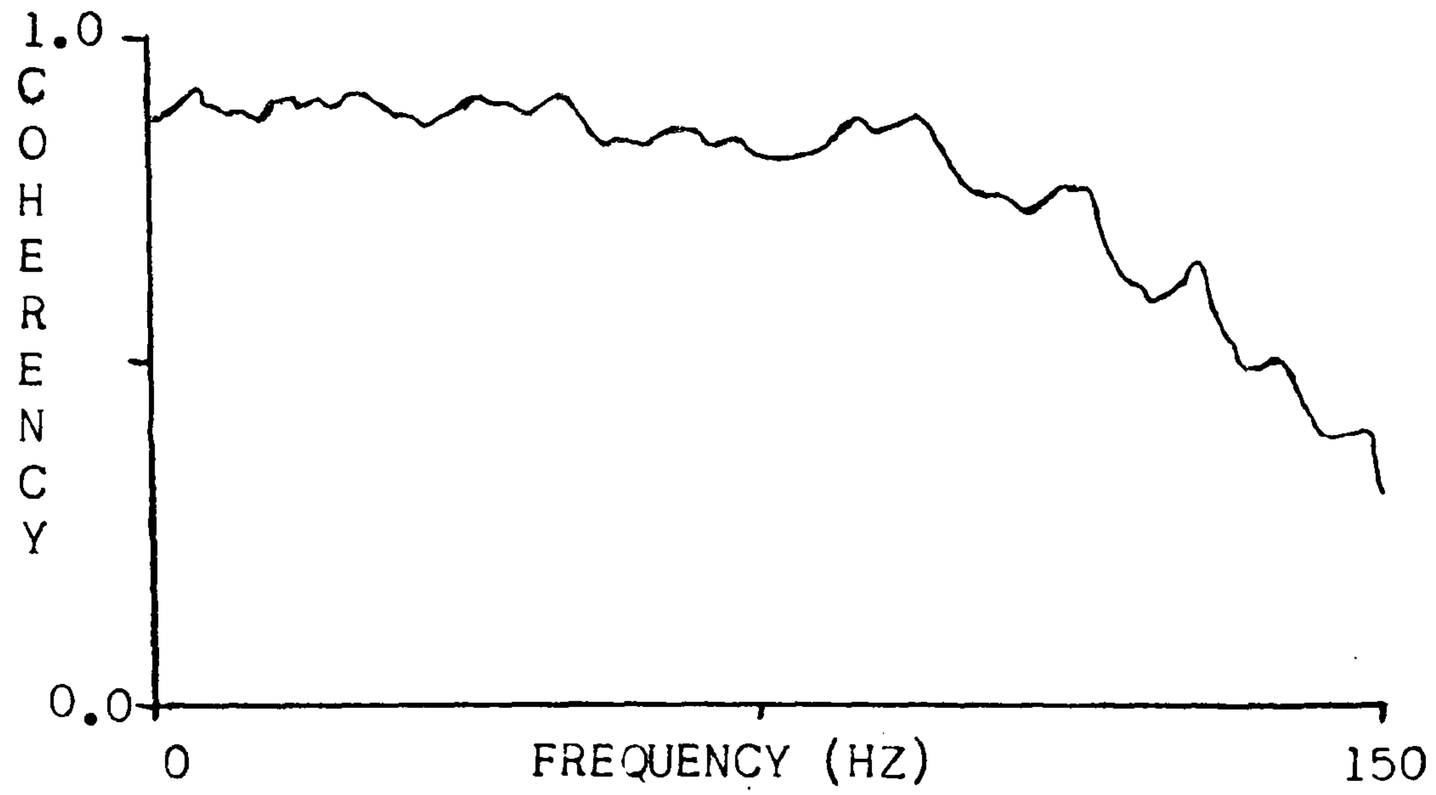

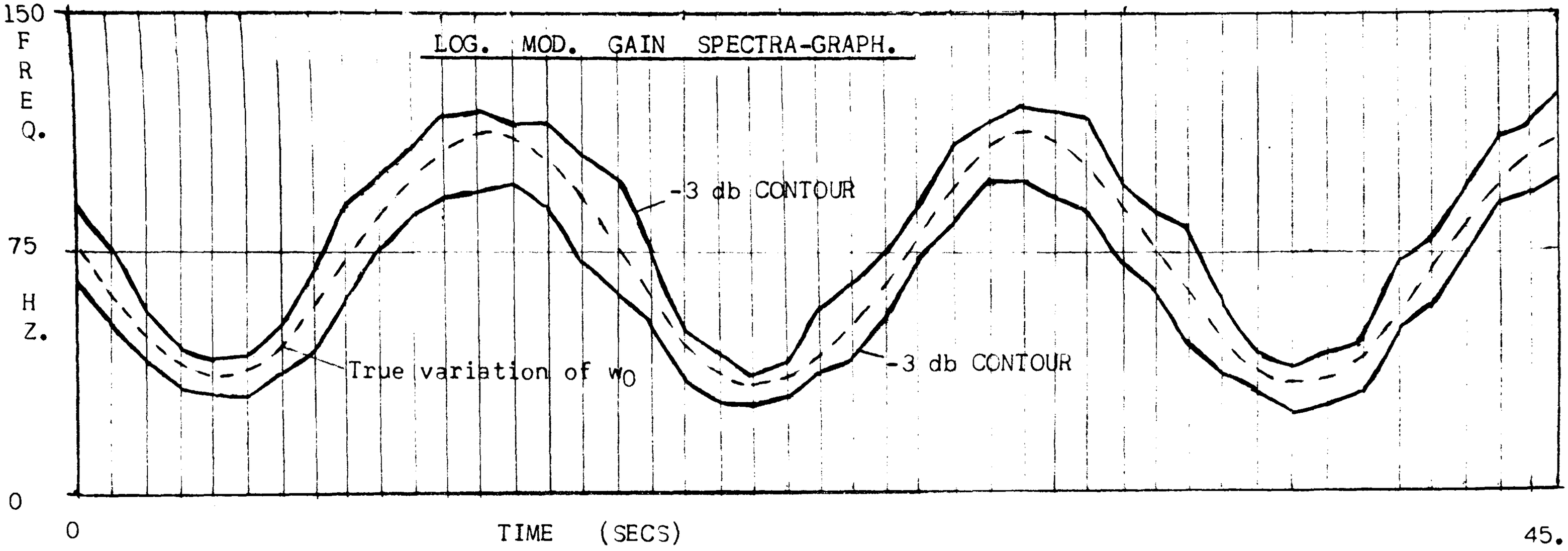

FIGURE 9 : Shows the time spectra-graph of a second order system whose natural frequency is varying sinousoidally with time. A typical coherency is shown on the right. There is little change in the coherency from the stationary case.

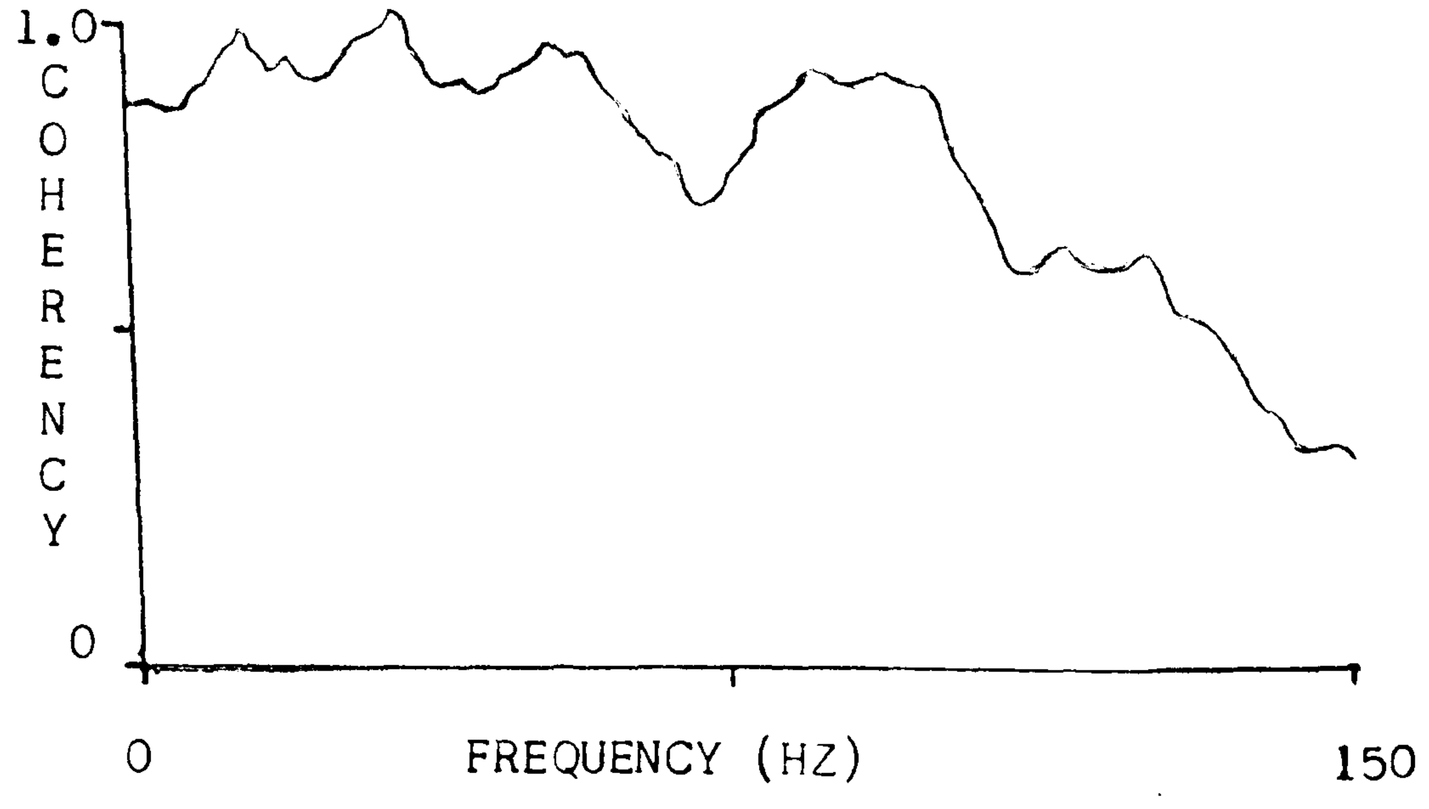

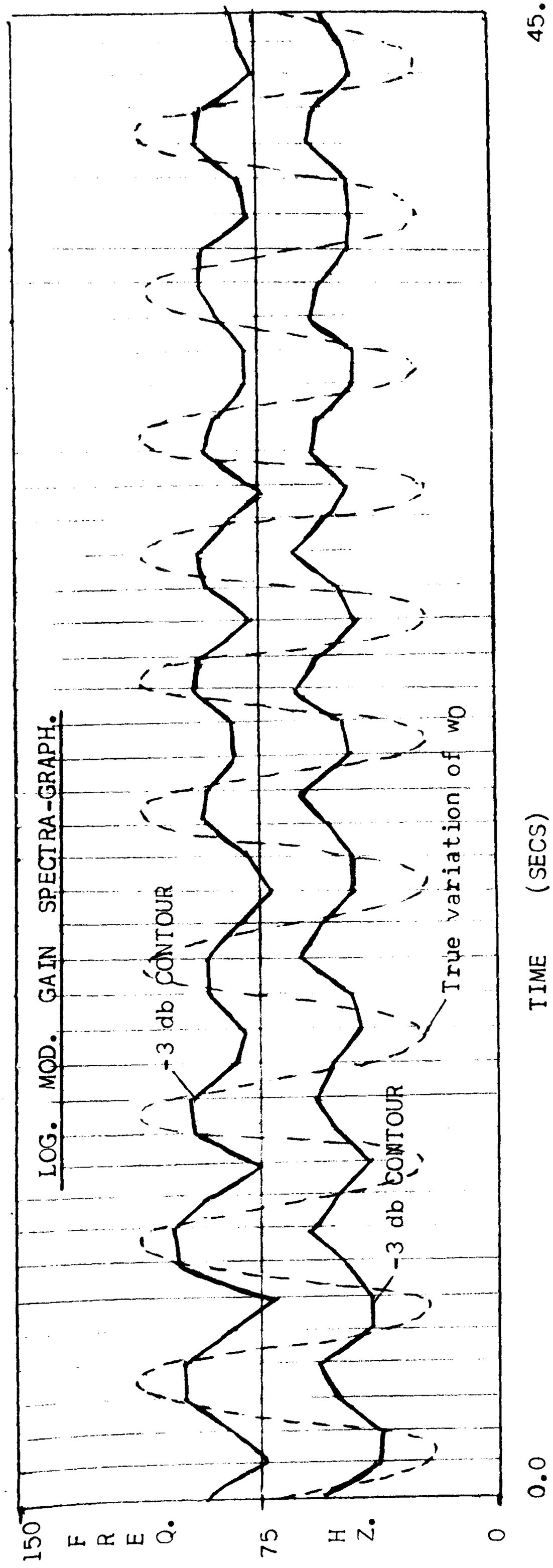

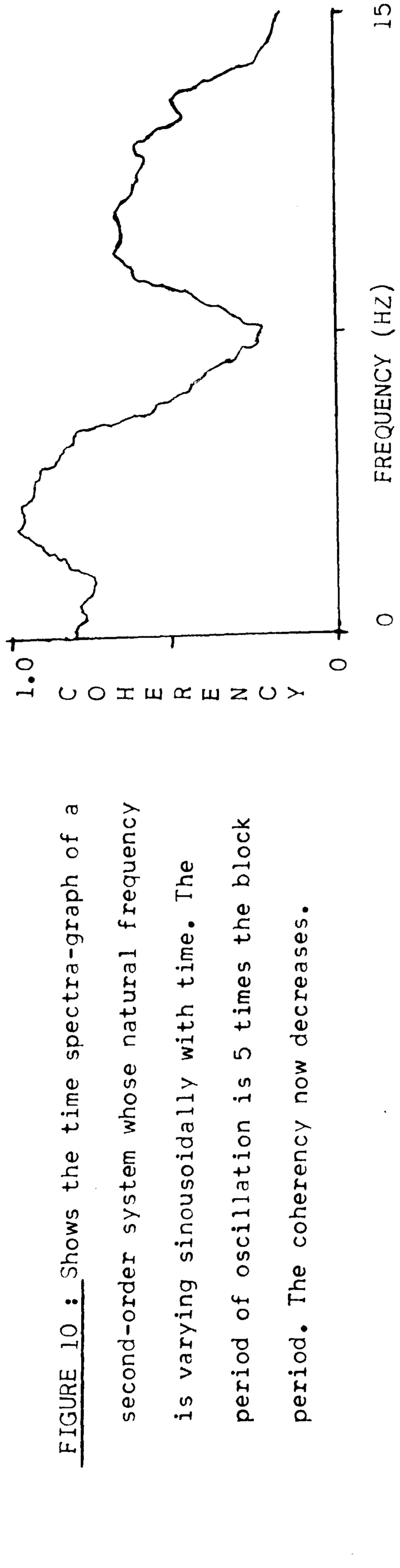

FIGURE 10 : Shows the time spectra-graph of a second-order system whose natural frequency is varying sinusoidally with time. The period of oscillation is 5 times the block period. The coherency now decreases.

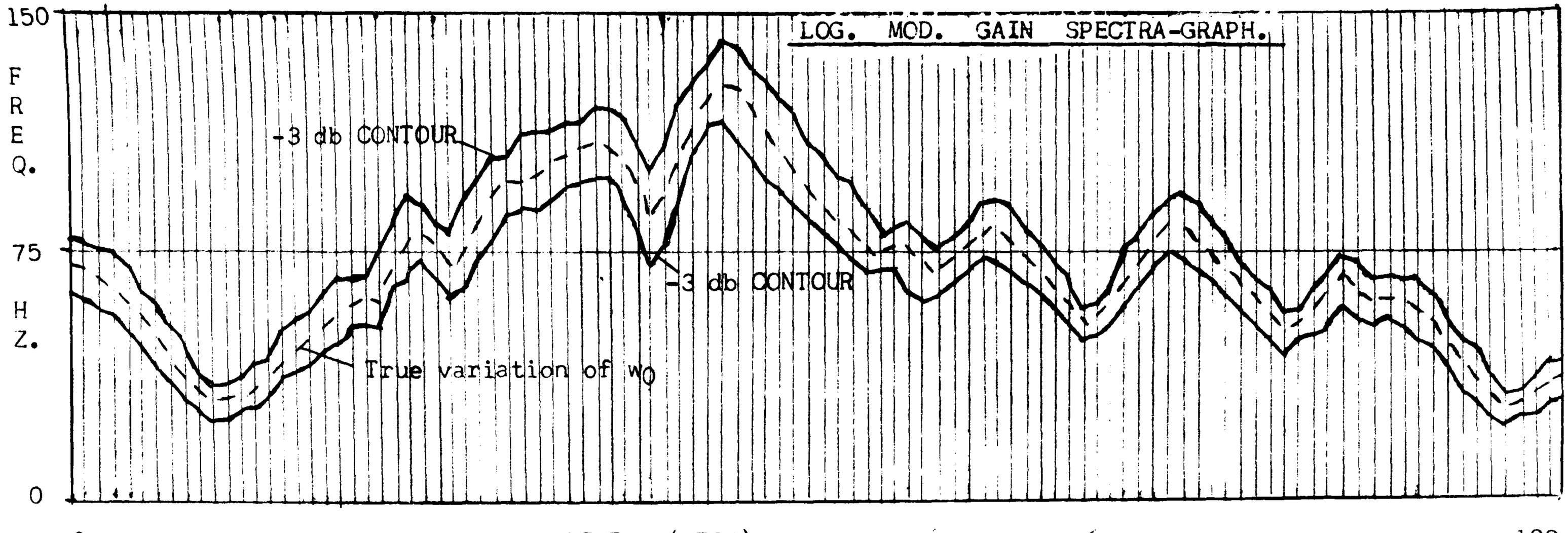

FIGURE 11 : Shows the time spectra-graph of a second order system whose natural frequency is varying randomly with time. The sample coherency (shown right) is approximately the same as in the stationary case.

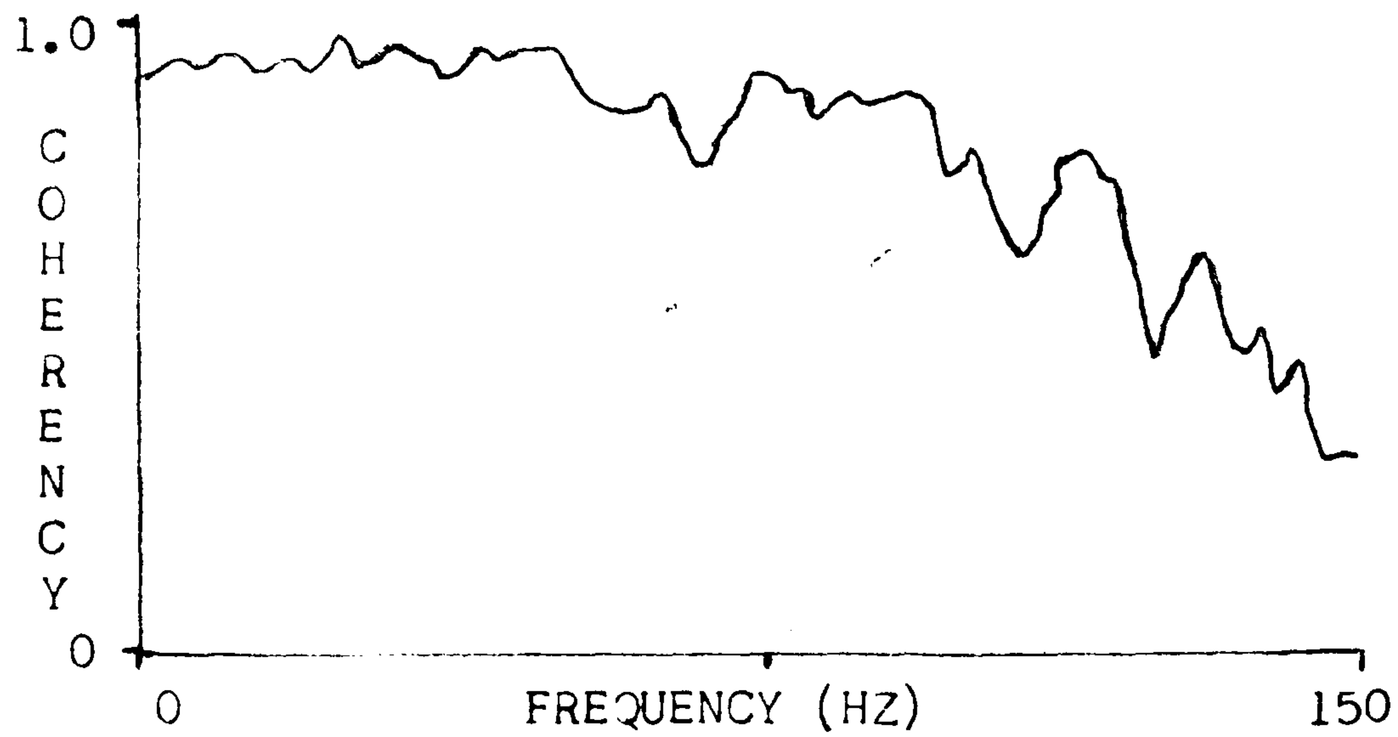

9) APPLICATIONS

Chapters 4 and 5 consider two time-varying situations .

The analysis of speech (Chapter 4) gives an example of the application of spectral analysis to a system whose variations in time may be considered step-like (for instance at the beginning and end of voiced speech sections and at the boundary between two phonemes) or of a slowly varying nature (as sometimes found in long vowel sounds.) It is shown that individual vowels can often be identified using spectral techniques. By testing for stationarity the speech waveform is approximately segmented into stationary sections. The spectral estimates from these sections can be compared with known vowel responses and identified within specified levels of confidence. In another application it is shown how compressed speech may be improved in quality using statistical test results to determine which portions of the speech waveform **should be retained and which can be discarded.**

Chapter 5 investigates some applications of spectral techniques to fatigue rig control and identification of the onset of fatigue cracking. In controlling the loading pattern on a test specimen the response of the rig and of the specimen must be considered. Assuming that the specimen is not loaded beyond its elastic limit, the response is approximately linear. As cracks are formed, the response of the specimen changes. To maintain the required loading pattern, the controller must adapt to these changes and to possible drift in the rig's servo-hydraulic components.

The identification of the onset of cracking necessitates the use of statistical tests which are approximately insensitive to outside random disturbances. The change in the frequency response

of the specimen may be less than 5% over the first 90% of fatigue life. Short-term estimates of the frequency response are subject to random errors, and in testing for stationarity, allowance must be made for variations due to a noisy environment.

REFERENCES

1 GOODMAN, N. R.: 'On the joint estimation of the spectra, cospectrum and quadrature spectrum of a two-dimensional stationary Gaussian process'. Phd. Thesis, Princeton Univ. (1957)

2 TONG, H: 'Some problems in the spectral analysis of bivariate non-stationary stochastic processes'. Phd. Thesis, Univ. of Manchester, (1972)

3 JENKINS, G. M. & WATTS, D. G.: 'Spectral analysis'. Holden Day San Fransisco (1968)

4 AKAIKE, H.: 'On the statistical estimation of the frequency response function of a system having multiple input'. Ann. Inst. Stat. Maths. Vol. 17, pp. 185-210 (1965)

5 AKAIKE, H. & YAMAMMOUCHI, Y.: 'On the statistical estimation of frequency response functions' Ann. Inst. Stat. Maths. Vol. 14, No. 1, pp. 23-56 (1962)

6 BLACKMAN, R. B. & TUKEY, J. W.: 'The measurement of power spectra'. Dover Publications Inc. New York (1958)

7 ADRABBO, N. A. & PRIESTLEY, M. B.: 'On the prediction of non-stationary processes'. Jnl. Royal Stat. Soc. (B) Vol. 29, pp. 570-585 (1967)

8 ADRABBO, N. A. & PRIESTLEY, M. B.: 'Filtering non-stationary signals'. Jnl. Royal Stat. Soc. (B) Vol 31 pp. 150-9 (1969)

9 PRIESTLEY, M. B.: 'Evolutionary spectra and non-stationary processes'. Jnl. Royal Stat. Soc. (B) Vol. 27 pp. 204-37 (1965)

10 PRIESTLEY, M. B. & SUBBA-RAO, T.: 'A test for non-stationarity

of time series'. Jnl. Royal Stat. Soc. (B) Vol. 31, pp. 140-9 (1969)

11 PRIESTLEY, M. B.: 'Design relations for non-stationary processes'. Jnl. Royal Stat. Soc. (B) Vo. 28 pp. 228-40 (1966)

12 SUBBA-RAO, T.: 'The fitting of non-stationary time series models with time-dependent parameters'. Jnl. Royal Stat. Soc. (B) Vol. 32, pp. 312-22 (1970)

13 TUKEY, J: 'One degree of freedom for non-additivity'. Biometrics Vol. 5, pp. 232-42 (1949)

14 CRAMER, H.: 'On some classes of non-stationary processes'. Proc. 4th Berkeley Symposium on Math. Stat. & Prob. Vol. 2, pp. 57-8, Univ. of California Press (1960)

15 JENKINS, G. M.: 'Cross-spectral analysis and the estimation of linear open-loop transfer functions.' Symposium on Time Series Analysis, pp. 267-78 (Ed. M. Rosenblatt) J. Wiley (1963)

16 KOLMOGOROV, A.: Stationary sequences in Hilbert space'. Bull. Maths. Univ. of Moscow, Vol. 2 No. 6 (1941)

17 WHITTLE, P.: 'Prediction and regulation'. English Univ. Press (1963)

18 WIENER, N.: 'Generalised harmonic analysis'. Act. Math. Vol. 55, p. 117

19 BENDAT, J. S. & PIERSOL, A. G.: 'Random data: analysis & measurement procedures'. Wiley Interscience (1972)

20 PAPOULIS, A.: 'Probability, random variables and stochastic processes'. McGraw Hill Book Co. New York (1965)

21 WATSON, G. N.: 'A treatise on the theory of Bessel functions'.

22 GRADSTEYN, I. S. & RHYZIK, I. M.: 'Tables of integrals series and products'. Academic Press Inc. (1965)

23 WELLSTEAD, P. E.: 'Real time spectral analysis'. Phd. Thesis, Univ. of Warwick (1971)

24 PIERSOL, A. G.: 'Spectral analysis of non-stationary spacecraft vibration data'. N.A.S.A. Washington D.C. NASA CR-341 (Dec. 1965)

25 DURRANI, T. S. & NIGHTINGALE, J. M.: 'Probability distributions for discrete Fourier spectra'. Proc. I.E.E. Vol. 120, No. 2 pp. 299-311 (Feb. 1973)

CHAPTER 3

SPECTRAL ANALYSIS OF CLOSED-LOOP SYSTEMS

LIST OF SYMBOLS USED

$x(t)$: Gaussian system input with zero mean and variance σx^2

$y(t)$: system output. Gaussian with zero mean and variance σy^2

$n(t)$: the noise in the forward loop section. Gaussian with zero mean and variance σn^2. Uncorrelated with $x(t)$ or $r(t)$

$r(t)$: the noise introduced in the feedback loop. Gaussian with zero mean and variance σr^2. Uncorrelated with $x(t)$ or $n(t)$

$z(t)$: the feedback signal

$e(t)$: $= x(t)-z(t)$

T : block time period

f_s : sampling frequency

w_0 : frequency resolution $\frac{(2\pi)}{T}$ radians/sec.

N : block size (number of samples)

$\hat{X}(Kw_0)$: discrete Fourier coefficient at frequency Kw_0 $(0 \leqslant K \leqslant N/2)$ obtained from the transformation of a block of N samples of $x(t)$

$\hat{Y}(Kw_0)$: discrete Fourier coefficient of $y(t)$

$\hat{E}(Kw_0)$: discrete Fourier coefficient of $e(t)$

$\hat{Z}(Kw_0)$: discrete Fourier coefficient of $z(t)$

$\hat{N}(Kw_0)$: discrete Fourier coefficient of n(t). (Not directly accessible from sampling x(t), e(t) etc.)

$\hat{R}(Kw_0)$: discrete Fourier coefficient of r(t) (Again, not directly accessible from sampling x(t), e(t))

$\bar{\phi}xx(Kw_0)$: estimate of the power spectrum of x(t) at frequency (Kw_0) taken as the average value of L independent estimates

$\bar{\phi}yy(Kw_0)$: mean estimate of the power spectrum of y(t)

$\bar{\phi}ee(Kw_0)$: mean estimate of the power spectrum of e(t)

$\bar{\phi}rr(Kw_0)$: mean estimate of the power spectrum of r(t) obtained by sampling r(t) alone. (Not usually accessible)

$\bar{\phi}\hat{r}\hat{r}(Kw_0)$: best obtainable estimate of the power spectrum of r(t) through sampling x(t), e(t), y(t), z(t)

$\bar{\phi}nn(Kw_0)$: mean estimate of the power spectrum of n(t), obtained by sampling n(t) directly

$\bar{\phi}\hat{n}\hat{n}(Kw_0)$: best obtainable estimate of the power spectrum of n(t)

$\bar{\phi}zz(Kw_0)$: mean estimate of the power spectrum of z(t)

$\bar{\phi}xy(Kw_0)$: cross-spectrum estimate between x(t) and y(t)

$\bar{\phi}xe(Kw_0)$: cross-spectrum estimate between x(t) and e(t)

$\bar{\phi}xz(Kw_0)$: cross-spectrum estimate between x(t) and z(t)

$\bar{\phi}xr(Kw_0)$: mean estimate of the cross-spectrum between x(t) and r(t). As L becomes large, ϕxr goes to zero as x(t) and r(t) are uncorrelated.

$\bar{\phi}xn(Kw_0)$: mean estimate of the cross-spectrum between x(t) and n(t)

$\bar{G}(Kw_0)$: mean estimate of the forward-loop frequency response at frequency (Kw_0)

$\bar{H}(Kw_0)$: mean estimate of the feedback-loop frequency response

A : true value of A (may be complex)

$\hat{A}$: single estimate of A

$\bar{A}$: estimate of A obtained as the mean of L independent estimates

M_A : magnitude of A $\{= |A|\}$

θ_A : angle the vector $\overrightarrow{O \to A}$ makes with the real axis in the complex plane. Thus $A = M_A \exp(j.\theta_A)$

R_A : real part of A

I_A : imaginary part of A

$p(\bar{A})$: amplitude probability distribution of $\bar{A}$

$p(\bar{A} : \bar{B})$: conditional amplitude probability distribution of $\bar{A}$ given $\bar{B}$

$p(\bar{A}, \bar{B})$: joint distribution of $\bar{A}$ and $\bar{B}$

L : the number of independent estimates used to find $\bar{\phi}xx$, $\bar{\phi}xy$ etc.

$Sx^2(Kw_0)$: half-power of x(t) in the bandwidth $(K-\frac{1}{2})w_0 \leqslant w \leqslant (K+\frac{1}{2})w_0$

$Sr^2(Kw_0)$: half-power of r(t) in the bandwidth $(K-\frac{1}{2})w_0 \leqslant w \leqslant (K+\frac{1}{2})w_0$

$Sn^2(Kw_0)$: half-power of n(t) in the bandwidth $(K-\frac{1}{2})w_0 \leqslant w \leqslant (K+\frac{1}{2})w_0$

σA^2 : variance of variable A

μ_A : mean value of A

$N(\mu, \sigma^2)$: Gaussian distribution with mean μ and variance σ^2

1) INTRODUCTION

In Chapter 2 (Section 3) it was shown that bias errors due to finite frequency resolution could be reduced by choosing a longer block period, T. Goodman and Akaike have investigated the statistical distributions associated with functions of bivariate complex Gaussian sequences and their results can be applied directly to short-term spectral estimates of linear open-loop systems. In many cases it is found that 'random' errors due to finite observation time are a more serious concern than inherent bias errors.

A similar study of closed-loop systems involves distributions associated with tri-variate complex Gaussian sequences and as far as the author is aware, little or no research has been published in this area. Wellstead (1971) suggested a possible approach approximating the distributions associated with closed-loop frequency response estimates by a complex transformation of the open-loop distributions. This was found to give satisfactory results when the noise in the feedback loop was negligible (see Figure 1). This is to be expected, as the system essentially reverts to the bivariate complex situation under these conditions.

To derive the sampling distributions of short-term spectral estimates of closed-loop systems under conditions when r(t) cannot be neglected, it is sufficient to consider the distributions of estimates of G(w), H(w) and best estimates of the noise spectra $\phi nn(w)$ and $\phi rr(w)$. All other distributions, for instance those associated with estimates of $\phi xy(w)$, $\phi xz(w)$, $\phi xe(w)$ and the overall closed-loop gain, can be derived from a suitable transformation of distributions encountered in the open-loop case.

FIGURE 1 Shows the closed-loop system configuration where H(w) and G(w) are linear. It is assumed that any 3 of x(t), e(t), y(t), z(t) can be measured directly

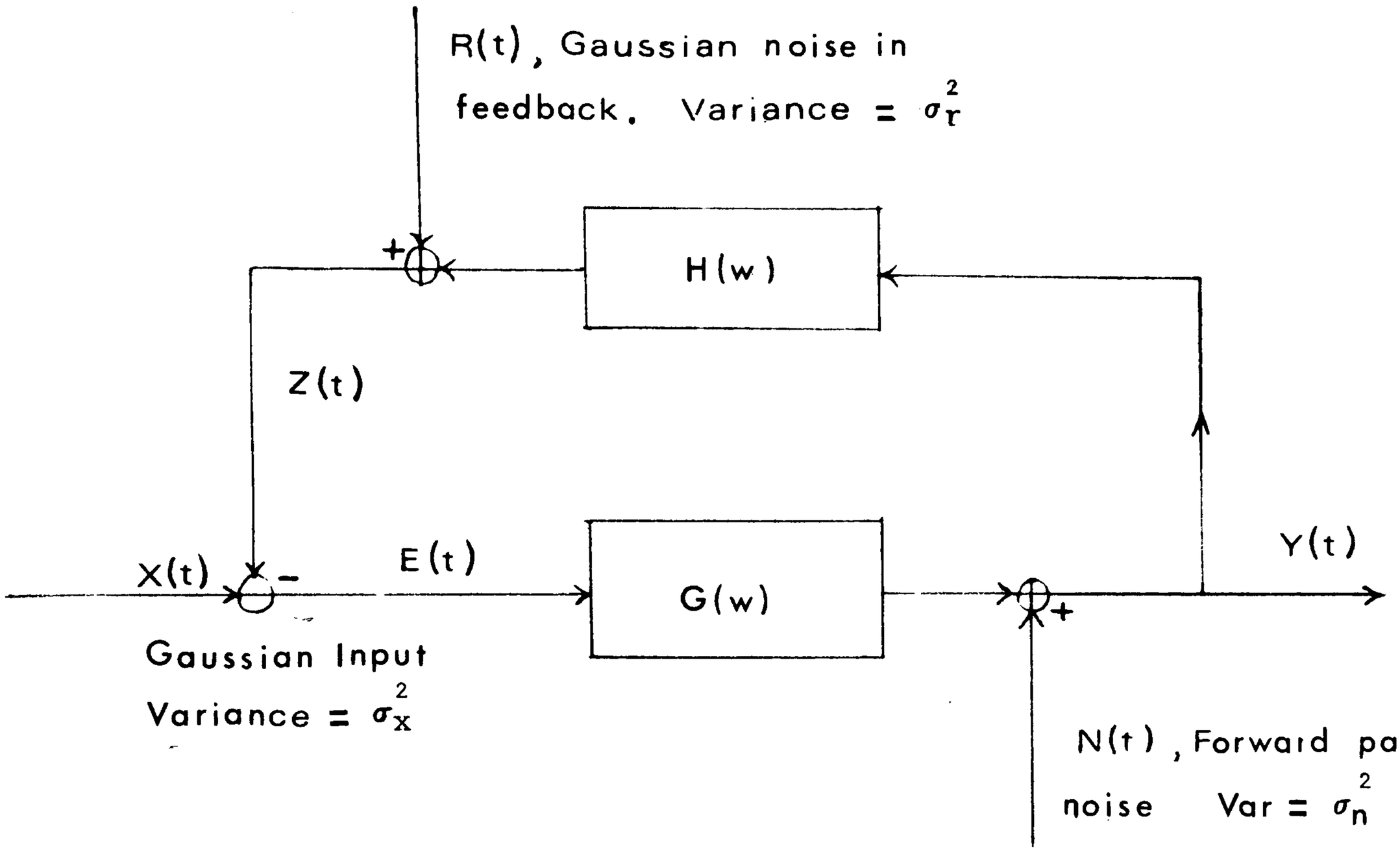

2) RANDOM ERRORS IN CLOSED-LOOP ESTIMATES (extension of open-loop distributions)

It is assumed (Figure 1) that the output, y(t) , and any two of x(t),z(t) and e(t) can be sampled and hence the 4^{th} variable calculated. As in Chapter 2, it is assumed that the block period, T, and the sampling frequency, f_s, have been suitably chosen so that aliasing, and bias errors due to finite frequency resolution, can be neglected. The sampling distributions are derived assuming a rectangular data window is used on the sampled versions of x(t), y(t) etc. If a Hanning or a similar window is used, then adjacent discrete Fourier coefficients $\hat{X}(Kw_0)$, $\hat{X}((K-1)w_0)$, $\hat{X}((K+1)w_0)$ become correlated and the number of degrees of freedom associated with spectral estimates

obtained using frequency smoothing is correspondingly reduced.

If the block period, T, is chosen such that the impulse response functions $g(\tau)$, $h(\tau)$ are effectively zero for some $\tau > \tau max$ where $\tau max << T$ then the following relationships approximately hold:

$$\hat{Y} \simeq \frac{G(\hat{X} + \hat{R}) + \hat{N}}{(1 + HG)} = G\hat{E} + \hat{N} \quad \ldots\ldots\ldots 3.1$$

$$\hat{Z} \simeq \frac{G.H.\hat{X} + H.\hat{N} + \hat{R}}{(1 + HG)} = H.\hat{Y} + \hat{R} \quad \ldots\ldots\ldots 3.2$$

$$\hat{E} \simeq \frac{\hat{X} - \hat{R} - H.\hat{N}}{(1 + HG)} = \hat{X} - \hat{Z} \quad \ldots\ldots\ldots 3.3$$

where $\hat{X}$, $\hat{Y}$, $\hat{E}$ etc. are the complex discrete Fourier coefficients at some general frequency Kw_0 ($w_0 = \frac{2\pi}{T}$), ($0 \leqslant K \leqslant N/2$), obtained by transforming blocks of N samples of x(t), y(t), e(t). The discrete transform algorithm is given in Chapter 2. The dependence on frequency w is henceforth assumed except in cases of ambiguity.

In general we are interested in estimates of:

$$\bar{\phi}xe = \frac{1}{L}\sum_{i=1}^{L} \hat{\phi}^{i}_{xe} = \frac{1}{L}\sum_{i=1}^{L} \hat{X}_i *. \hat{E}_i \quad \ldots\ldots\ldots 3.4$$

$$\bar{\phi}xy = \frac{1}{L}\sum_{i=1}^{L} \hat{\phi}^{i}_{xy} = \frac{1}{L}\sum_{i=1}^{L} \hat{X}_i *. \hat{Y}_i \quad \ldots\ldots\ldots 3.5$$

$$\bar{\phi}xz = \frac{1}{L}\sum_{i=1}^{L} \hat{\phi}^{i}_{xz} = \frac{1}{L}\sum_{i=1}^{L} \hat{X}_i *. \hat{Z}_i \quad \ldots\ldots\ldots 3.6$$

$$\left[\frac{\overline{G}}{(1+HG)}\right] = \bar{\phi}xy \,/\, \bar{\phi}xx \quad \text{(Overall frequency response)} \quad \ldots 3.7$$

$$\bar{G} = \bar{\phi}xy \,/\, \bar{\phi}xe \quad \text{(Forward loop frequency response)} \quad \ldots\ldots 3.8$$

$$\overline{H} = \bar{\phi}xz \,/\, \bar{\phi}xy \quad \text{(Feedback loop frequency response)} \quad \ldots\ldots 3.9$$

$$\bar{\phi}\,\hat{n}\hat{n} = \bar{\phi}yy + |\bar{G}|^2\,\bar{\phi}ee - 2\,RL\,\{\bar{G}.\,\bar{\phi}ye\} \quad \ldots\ldots 3.10$$

$$\bar{\phi}\hat{r}\hat{r} = \bar{\phi}zz + |\bar{H}|^2 . \bar{\phi}yy - 2\,RL.\{\bar{H} . \bar{\phi}zy\} \quad \ldots\ldots\ldots 3.11$$

plus estimates of the auto-spectra of x(t), y(t), e(t) and z(t) defined in a similar manner to $\bar{\phi}xx$ in Chapter 2. The mean values may be found as an average over L successive time blocks or over L adjacent frequency points, as in the open-loop case. The distributions of $\hat{X}_i$, $\hat{N}_i$ and $\hat{R}_i$ are given by:

$$p_X(\hat{X}_i) = \underset{\text{complex}}{N} (0, Sx^2) \quad \ldots\ldots\ldots\ldots\ldots 3.12$$

$$p_N(\hat{N}_i) = \underset{\text{complex}}{N} (0, Sn^2) \quad \ldots\ldots\ldots\ldots\ldots 3.13$$

$$p_R(\hat{R}_i) = \underset{\text{complex}}{N} (0, Sr^2) \quad \ldots\ldots\ldots\ldots\ldots 3.14$$

These distributions are arrived at by the same argument used by Tukey for the open-loop case. Again, the real and imaginary coefficients are approximately independent. In addition $\hat{X}_i$, $\hat{N}_i$ and $\hat{R}_i$ are all mutually independent.

The power in x(t) over the frequency band $Kw_0 \pm w_0/2$ $(0 \leqslant K \leqslant N/2)$ is evenly distributed between the real and imaginary coefficients of $\hat{X}(Kw_0)$. Thus the variance term Sx^2 is equivalent to half the power in this bandwidth. Sx^2 is dependent on the centre frequency Kw_0. A similar relationship holds for Sn^2 and Sr^2. To obtain estimates of the power spectrum <u>density</u> functions equations 3.4 to 3.6 and 3.10, 3.11 must be normalised by the factor $1/w_0$ as in the open-loop case.

If the relationships indicated by equations 3.1 to 3.3 are substituted in equations 3.4 to 3.9, the spectral estimates can be rewritten in terms of the independent inputs, $\hat{X}$, $\hat{N}$, and $\hat{R}$ and the system frequency parameters, G, H.

$$\bar{\phi}xy \simeq \frac{G.\ \bar{\phi}xx + G.\ \bar{\phi}xr + \bar{\phi}xn}{(1 + H.G)} \quad \ldots\ldots\ldots 3.15$$

$$\bar{\phi}xe \simeq \frac{\bar{\phi}xx - \bar{\phi}xr - H.\ \bar{\phi}xn}{(1 + H.G)} \quad \ldots\ldots\ldots 3.16$$

$$\bar{\phi}xz \simeq \frac{G.H.\ \bar{\phi}xx + H.\ \bar{\phi}xn + \bar{\phi}xr}{(1 + H.G)} \quad \ldots\ldots\ldots 3.17$$

$$\left[\overline{\frac{G}{1 + H.G)}}\right] \simeq \frac{G}{1 + H.G} + \frac{G.\ \bar{\phi}xr + \bar{\phi}xn}{(1 + H.G)\ \bar{\phi}xx} \quad \ldots\ldots\ldots 3.18$$

$$\bar{G} \simeq G + \frac{(1 + H.G)\ \bar{\phi}xn}{\bar{\phi}xx - \bar{\phi}xr - H.\ \bar{\phi}xn} \quad \ldots\ldots\ldots 3.19$$

$$\bar{H} \quad H + \frac{(1 + H.G)\ \bar{\phi}xr}{G\ \bar{\phi}xx + \bar{\phi}xn + G\ \bar{\phi}xr} \quad \ldots\ldots\ldots 3.20$$

The noise estimates $\bar{\phi}\hat{n}\hat{n}$ and $\bar{\phi}\hat{r}\hat{r}$ are considered at a later stage in this chapter.

Letting the cross-spectral terms involving X, N and R go to zero in equations 3.15 to 3.20, the expected values of the parameters (found by letting L tend to ∞) are given. We now investigate the sampling distributions associated with equations 3.15 to 3.18

i) Sampling distributions associated with $\bar{\phi}xy$, $\bar{\phi}xe$ and $\bar{\phi}xz$

The distributions of the cross-spectral terms are obtained by an extension of the theory developed for the cross-spectrum, $\bar{\phi}xy$, in the open-loop case. We consider the distribution associated with $\bar{\phi}xz$ and quote similar results for $\bar{\phi}xe$ and $\bar{\phi}xy$.

Equation 3.17 can be rewritten in the form:

$$\bar{\phi}xz \simeq \left[\frac{G.H}{(1 + G.H)}\right] . \left\{\bar{\phi}xx + \frac{\bar{\phi}xn}{G} + \frac{\bar{\phi}xr}{G.H}\right\} \quad \ldots\ldots 3.21$$

In deriving the distribution of the error in the open-loop frequency response it was shown (see equation 2.27) that:

$$p(\bar{M}xn, \bar{\theta}xn : \bar{\phi}xx) = \frac{L.\bar{M}xn \ .exp \ (- \bar{M}xn^2.L \ / \ 2.Sn^2. \ \bar{\Phi}xx)}{2\pi \ . \ Sn^2 \ . \ \bar{\phi}xx} \quad . . \ 3.22$$

where L is the number of independent estimates used to find the mean value $\bar{\phi}xx$ and:

$$\bar{\phi}xn = \bar{M}xn.exp \ (j \ \bar{\theta}xn)$$

The distribution of the term $\phi xn \ / \ G$ in equation 3.21 is given by a complex transformation of equation 3.22. Defining a new variable:

$$A = \bar{\phi}xn \ / \ G$$

the distribution of A is given by:

$$p(M_A,\theta_A : \bar{\phi}xx) = \frac{L. \ |G|^2.M_A.exp \ (- M_A{}^2. \ L. \ |G|^2 \ / \ 2.Sn^2.\bar{\phi}xx)}{2\pi \ . \ Sn^2 \ . \ \bar{\phi}xx} \quad . . . . . \ 3.23$$

Similarly the distribution of a variable B defined as:

$$B = \bar{\phi}xr \ / \ \{ \ G \ . \ H \ \}$$

is given by:

$$p(M_B, \theta_B : \bar{\phi}xx) = \frac{L. \ |G|^2.|H|^2.M_B.exp \ (\ -L.M_B{}^2.|G|^2.|H|^2 \ / \ 2.Sr^2.\bar{\phi}xx)}{2.\pi \ .Sr^2 \ . \ \bar{\phi}_{xx}. . . . . \ 3.24}$$

The distributions given by equations 3.23 and 3.24 are bivariate Gaussian distributions with independent ordinates. Further, as r(t) and n(t) are uncorrelated, the variables A and B are independent if $\bar{\phi}xx$ is fixed. Thus the variable C (= A + B) is also jointly normal with zero mean and variance:

$$VAR \ (C) = \sigma_c{}^2 = \frac{\bar{\phi}xx}{L} \left\{ \frac{Sr^2}{|G|^2.|H|^2} + \frac{Sn^2}{|G|^2} \right\} \quad . . . . . \ 3.25$$

Relating the cross-spectrum $\bar{\phi}xz$ to C using equation 3.21:

$$\bar{\phi}xz = \frac{G.H}{(1 + G.H)} \ . \ \{\bar{\phi}xx + C \} \quad . . . . . \ 3.26$$

The distribution of $\bar{\phi}xz$ is obtained by a complex transformation of the distribution of $(\bar{\phi}xx + C)$. Letting:

$$D = \bar{\phi}xx + C$$

the distribution of D is given by:

$$p(D) = \int_0^\infty p_c\left((D - \bar{\phi}xx) : \bar{\phi}xx\right) . p(\bar{\phi}xx) . d\,\bar{\phi}xx$$

where $p_c(C : \bar{\phi}xx)$ is the bivariate Gaussian distribution with zero mean and variance σ_c^2 (equation 3.25) and $\bar{\phi}xx$ is Chi-square distributed with 2 L degrees of freedom. Integrating with respect to $\bar{\phi}xx$ (reference 2):

$$p(M_D , \theta_D) = \frac{L^{(L+1)} . M_D^{\,L} . \exp\ (L . M_D . \cos\theta_D / \sigma^2)}{2 . \pi . \sigma^2 . Sx^{L+1} . \Gamma(L)} .$$

$$. \frac{K_{L-1}\left\{ \frac{L . M_D . (Sx^2 + \sigma^2)^{\frac{1}{2}}}{\sigma^2 . Sx} \right\}}{(Sx^2 + \sigma 2)^{\frac{L-1}{2}}} \qquad \ldots\ldots\ldots 3.27$$

where $\Gamma(L) = (L-1)!$

$K\nu\ (x) =$ Modified Bessel function of order ν

and $\sigma^2 = \frac{Sx^2}{L} . \left(\frac{Sr^2}{|G|^2 . |H|^2} + \frac{Sn^2}{|G|^2} \right)$

This distribution is similar in form to the distributions associated with cross-spectral estimates in Chapter 2 (see equation 2.23). Indeed, equation 3.27 can be adapted directly to give the joint distribution of the real and imaginary coefficients of $\bar{\phi}xy$ in the open-loop case. To obtain the distribution of $\bar{\phi}xz$ from equation 3.27 we must perform the complex transformation T given by:

$$T = \frac{G . H}{(1 + G . H)}$$

The Jacobian of this transformation is given by:

$$J(M_D , \theta_D) = \begin{vmatrix} \frac{\partial \bar{M}xz}{\partial M_D} & \frac{\partial \bar{M}xz}{\partial \theta D} \\ \frac{\partial \bar{\theta}xz}{\partial M_D} & \frac{\partial \bar{\theta}xz}{\partial \theta_D} \end{vmatrix} = \begin{vmatrix} M_T & 0 \\ 0 & 1 \end{vmatrix} = M_T$$

Thus:

$$p(\bar{M}xz , \bar{\theta}xz) = \frac{p_{M_D,\theta_D}(\bar{M}xz / M_T , \bar{\theta}xz - \theta_T)}{J(M_D , \theta_D)} \quad \ldots\ldots 3.28$$

Figure 2 shows typical equal probability contours of the distribution given by equation 3.28.

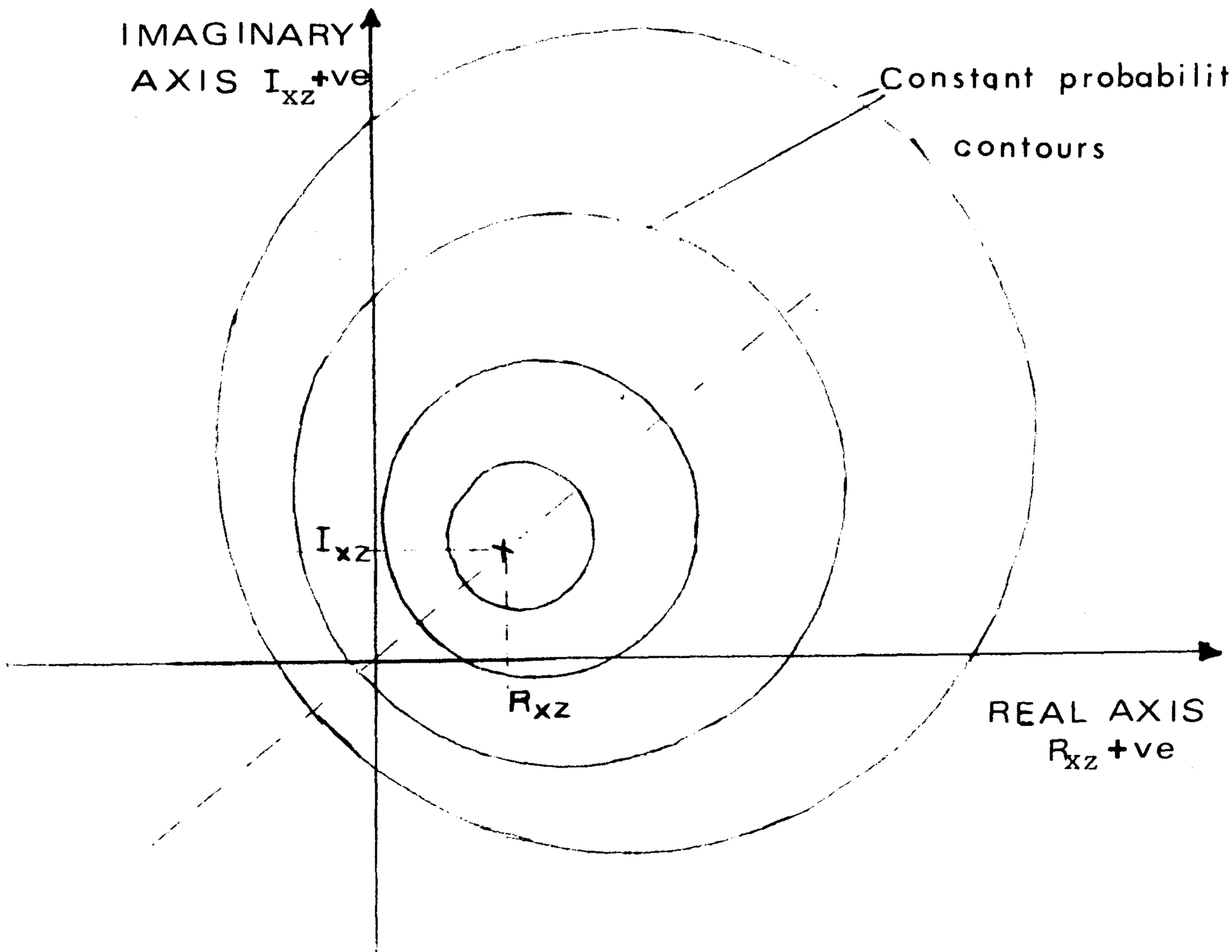

FIGURE 2: Shows the general form taken by equal probability contours of the distribution of $\bar{\phi}xz$

The distributions associated with $\bar{\phi}xe$ and $\bar{\phi}xy$ may be arrived at in a similar manner.

The distribution of $\bar{\phi}xe$ is given by letting:

$$\sigma^2 = \frac{Sx^2}{L} \cdot \{Sr^2 + |H|^2 \cdot Sn^2\}$$

in equation 3.27 and defining the transformation T by:

$$T = 1 / (1 + H.G)$$

The distribution of $\bar{\phi}xy$ is obtained by letting:

$$\sigma^2 = \frac{Sx^2}{L} \cdot \{ Sr^2 + Sn^2/|G|^2\}$$

. . . . defining T as G / (1 + H.G).

ii) <u>Sampling distribution of overall closed-loop gain estimates</u>

The error in the closed-loop gain estimate found from equation 3.18 is approximately given by:

$$\bar{\varepsilon} = \frac{G.\ \bar{\phi}xr + \bar{\phi}xn}{(1 + HG).\bar{\phi}xx} \quad \ldots\ldots\ldots\ldots\ldots\ldots 3.29$$

Using the same arguments as in the previous section, the conditional distribution, given $\bar{\phi}xx$, of a variable:

$$f = \frac{G.\ \bar{\phi}xr + \bar{\phi}xn}{(1 + H.G)}$$

is given by:

$$p(f : \bar{\phi}xx) = \underset{\text{complex}}{N}\left(0, \frac{(|G|^2.Sr^2 + Sn^2).\bar{\phi}_{xx})}{M_T{}^2 . L} \right) \quad \ldots\ldots\ldots 3.30$$

where $M_T{}^2 = |1 + GH|^2$.

This is a similar situation to the open-loop case except that the effective noise variance as seen at the output y(t) is given by:

$$\sigma n^2 = \frac{|G|^2.\ Sr^2 + Sn^2}{M_T{}^2}$$

in the closed loop case. The error in the closed-loop gain is given by $\bar{\varepsilon} = f / \bar{\phi}xx$. The distribution of $\bar{\varepsilon}$ is given by equation 2.28

in Chapter 2 with σn^2 above replacing Sn^2.

3) STATIONARITY TESTING OF CLOSED-LOOP SYSTEMS

Complete stationarity testing of the closed-loop system involves independent testing of five parameters. The sampling of three 'loop' signals gives only three effective degrees of freedom. Thus as in the open-loop case it is not possible to test one parameter alone holding the rest as measured constants.

In the open-loop case, the stationarity test (equation 2.37) requires prior knowledge of the noise variance. This is approximated by a 'best estimate'. The same approach can be employed in the closed-loop case except that two tests are now required for complete stationarity of G and H. If both or either of the tests fail it is not possible to tell (in statistical terms) which of the frequency response functions (G or H) has changed. This **must be resolved by** reference to the particular physical situation.

Let ϕ^1_{xy}, ϕ^1_{xx}, ϕ^1_{xz} and ϕ^2_{xy}, ϕ^2_{xx}, ϕ^2_{xz} be two sets of independent estimates, averaged over L_1, L_2 blocks respectively. Let:

$$T = \frac{\bar{\phi}xy}{\bar{\phi}xx} = \frac{G}{(1 + G.H)} + \bar{\varepsilon} \quad \ldots\ldots\ldots 3.31$$

$$S = \frac{\bar{\phi}xz}{\bar{\phi}xx} = \frac{G.H}{(1 + G.H)} + \bar{\delta} \quad \ldots\ldots\ldots 3.32$$

The conditional distributions of $\bar{\varepsilon}$ and $\bar{\delta}$ given $\bar{\phi}xx$ are Gaussian with zero mean and independent real and imaginary coefficients:

$$p(\bar{\varepsilon} : \bar{\phi}xx) = \underset{\text{complex}}{N}\left(0, \frac{1}{L.\bar{\phi}xx} . \frac{|G|^2 . Sr^2 + Sn^2}{|1 + HG|^2}\right) \ldots 3.33$$

and:

$$p(\bar{\delta} : \bar{\phi}xx) = \underset{\text{complex}}{N}\left(0, \frac{1}{L.\bar{\phi}xx} . \frac{|H|^2 . Sn^2 + Sr^2}{|1 + HG|^2}\right) \ldots 3.34$$

It is worth noting that the variance of the error in the overall frequency response estimate, T, is dependent upon the system parameters G and H. In the open-loop case, the variance is a function of the ratio Sn^2 / Sx^2, and does <u>not</u> depend on the system response.

The variance terms in equations 3.33 and 3.34 are approximated by substituting best estimates as seen at the output Y, and in the feedback loop Z. The derivation of these terms is identical to that followed in Chapter 2 (equations 2.29 to 2,36). It can be shown that:

$$\hat{\sigma}_{\varepsilon}^{\,2} \simeq \frac{(\bar{\phi}yy - |T|^2 . \bar{\phi}xx)}{2 . (L-1) . \bar{\phi}_{xx}} \quad \ldots\ldots\ldots\ldots\ldots\ldots 3.35$$

$$\hat{\sigma}_{\delta}^{\,2} = \frac{(\bar{\phi}zz - |S|^2 . \bar{\phi}xx)}{2 . (L-1) . \bar{\phi}_{xx}} \quad \ldots\ldots\ldots\ldots\ldots\ldots 3.36$$

If the product G.H is constant for the two periods of estimation, then:

$$T_1 - T_2 = \varepsilon_1 - \varepsilon_2 = f \qquad \text{and:}$$

$$p(f : \phi^1_{xx} , \phi^2_{xx}) \simeq \underset{\text{complex}}{N} (0 , \{\hat{\sigma}_{\varepsilon 1}^{\,2} + \hat{\sigma}_{\varepsilon 2}^{\,2}\}) \quad \ldots\ldots 3.37$$

Similarly if the ratio G/H is constant for the two periods of estimation then:

$$S_1 - S_2 = \delta_1 - \delta_2 = g \qquad \text{and:}$$

$$p(g : \phi^1_{xx} , \phi^2_{xx}) \simeq \underset{\text{complex}}{N} (0 , \{\hat{\sigma}_{\delta 1}^{\,2} + \hat{\sigma}_{\delta 2}^{\,2}\}) \quad \ldots\ldots 3.38$$

By squaring f and g and normalising their respective variances we obtain variables that are approximately Chi-square distributed with 2 degrees of freedom and unit variance. As in the open-loop case, the approximation is improved if we consider the stationarity over a wide frequency band. In general, if we wish to test stationarity over M adjacent frequency points, then the variables:

$$\bar{f} = \sum_{i=1}^{M} |f_i|^2 / \sigma_{f_i}^2 \quad \ldots\ldots\ldots\ldots\ldots\ldots \quad 3.39(a)$$

and:

$$\bar{g} = \sum_{i=1}^{M} |g_i|^2 / \sigma_{g_i}^2 \quad \ldots\ldots\ldots\ldots\ldots\ldots \quad 3.39)b)$$

are Chi-square distributed with 2M degrees of freedom. Knowledge of the particular situation may preclude variations in G and H such that the product, GH, or the ratio, G/H, are liable to remain constant. In such circumstances it is only necessary to test one variable. Some applications to human operator tracking tasks are presented in Chapter 6.

4) SAMPLING DISTRIBUTIONS ASSOCIATED WITH FORWARD-LOOP GAIN ESTIMATES (extension to tri-variate complex Gaussian systems)

The distributions developed so far for closed-loop systems are extensions of open-loop results. However the sampling distributions of $\bar{G}$ and $\bar{H}$ cannot be obtained by transformation of open-loop results. The distribution associated with estimates of $\bar{G}$ (equations 3.8, 3.19) is derived in this section. The distribution of estimates of the feedback loop gain, $\bar{H}$, can be found by following an identical procedure (Section 5). From equation 3.19, the error in estimates of G is approximately given by:

$$Eg = \frac{(1 + H.G).\bar{\phi}xn}{\bar{\phi}xx - \bar{\phi}xr - H\bar{\phi}xn} \quad \ldots\ldots\ldots\ldots \quad 3.40$$

If equation 3.40 is rearranged:

$$Eg = \frac{1 + H.G}{Z - H} \quad \ldots\ldots\ldots\ldots \quad 3.41(a)$$

$$\text{where } Z = \frac{\bar{\phi}xx - \bar{\phi}xr}{\bar{\phi}xn} \quad \ldots\ldots\ldots\ldots \quad 3.41(b)$$

We derive the distribution of Z and then consider the complex transformation described by equation 3.41(a).

Derivation of sampling distribution of Z

This involves finding the distribution of $\bar{\phi}xn$ given $\bar{\phi}xx$ and the distribution of U (= $\bar{\phi}xx$ - $\bar{\phi}xr$) given $\bar{\phi}xx$. As n(t) and r(t) are independent it can be seen that U and $\bar{\phi}xn$ are independent if $\bar{\phi}xx$ is kept constant. Knowing the distributions of U and $\bar{\phi}xn$, the distribution of the ratio U / $\bar{\phi}xn$ is derived, maintaining $\bar{\phi}xx$ as a constant. Finally the dependence on $\bar{\phi}xx$ is dropped by integrating for all $\bar{\phi}xx$.

In previous derivations, the terms $\bar{\phi}xx$, $\bar{\phi}xn$ and $\bar{\phi}xr$ have been the mean values obtained from L independent estimates. To avoid complicated scale factors we now consider $\bar{\phi}_{xx}$,$\bar{\phi}xn$ etc. to be the sum of L independent estimates. As Z involves the ratio of two estimates the factor L is lost and the final distribution is the same as that obtained by considering $\bar{\phi}xx$, $\bar{\phi}xn$ and $\bar{\phi}xr$ as mean values.

From equation 3.22:

$$p(\bar{M}xn\ ,\ \bar{\theta}xn\ :\ \bar{\phi}xx) = \frac{\bar{M}xn\ exp\ \left(-\ \bar{M}xn^2\ /\ 2\cdot Sn^2\cdot \bar{\phi}xx\right)}{2\pi\ .\ Sn^2\ .\ \bar{\phi}xx} \quad \ldots\ldots\ 3.42(a)$$

and similarly:

$$p(\bar{M}xr\ ,\ \bar{\theta}xr\ :\ \bar{\phi}xx) = \frac{\bar{M}xr.exp\ \left(-\ \bar{M}xr^2\ /\ 2.Sr^2.\bar{\phi}xx\right)}{2\pi.\ Sr^2\ .\ \bar{\phi}xx} \quad \ldots\ldots\ 3.42(b)$$

However, U = $\bar{\phi}xx$ - $\bar{\phi}xr$. Performing the complex transformation to obtain the distribution of U :

$$p(Mu,\ \theta u\ :\ \bar{\phi}xx) = \frac{p(\bar{M}xr\ ,\ \bar{\theta}xr\ :\ \bar{\phi}xx)}{J(\bar{M}xr\ ,\ \bar{\theta}xr)} \quad \ldots\ldots\ 3.43$$

where $J(\bar{M}xr\ ,\ \bar{\theta}xr) = \begin{vmatrix} \frac{\partial Mu}{\partial \bar{M}xr} & \frac{\partial Mu}{\partial \bar{\theta}xr} \\ \frac{\partial \theta u}{\partial \bar{M}xr} & \frac{\partial \theta u}{\partial \bar{\theta}xr} \end{vmatrix} = \frac{1}{Mu}$

and $\bar{M}xr$ and $\bar{\theta}xr$ are replaced in terms of Mu, θu and $\bar{\phi}xx$. Making the substitution:

$$p(Mu,\ \theta u : \bar{\phi}xx) = \frac{Mu}{2\pi . Sr^2 . \bar{\phi}xx} \cdot \exp\left\{ \frac{-(\bar{\phi}xx - Mu . \cos \theta u)^2 - (Mu . \sin \theta u)^2}{2 . Sr^2 \cdot \bar{\phi}xx} \right\}$$

. . . . 3.44

As $\bar{\phi}xn$ and U are independent if $\bar{\phi}xx$ is fixed, the joint distribution of $\bar{\phi}xn$ and U is given by:

$$p(Mu,\ \theta u,\ \bar{M}xn,\ \bar{\theta}xn : \bar{\phi}xx) = p(Mu,\ \theta u : \bar{\phi}xx) . p(\bar{M}xn,\ \bar{\theta}xn : \bar{\phi}xx) \quad . . 3.45$$

We now find the distribution of Mz, θz given $\bar{\phi}xx$. It can be seen that:

$$Mz = Mu / \bar{M}xn\ ,\ \theta z = \theta u - \bar{\theta}xn$$

The distribution of Mu, Mxn, θz, given $\bar{\phi}xx$ is found by substituting for θu in terms of θz and $\bar{\theta}xn$, and integrating over the complete range of $\bar{\theta}xn$, ($0 \leqslant \bar{\theta}xn \leqslant 2\pi$) :

$$p(\bar{M}xn,\ Mu,\ \theta z : \bar{\phi}xx) = \int_0^{2\pi} p(\bar{M}xn,\ Mu,\ \bar{\theta}xn,\ \{\theta z + \bar{\theta}xn\} : \bar{\phi}xx) \cdot \left| \frac{\partial \theta z}{\partial \bar{\theta}xn} \right| \cdot d\bar{\theta}xn$$

where $\theta u = \theta z + \bar{\theta}_{xn}$. Making the appropriate substitutions from equations 3.42(a) and 3.44 it is found that:

$$p(\bar{M}xn,\ Mu,\ \theta z : \bar{\phi}xx) = K \cdot \int_0^{2\pi} \exp\ \left(\frac{Mu \cos\ (\bar{\theta}xn + \theta z)}{Sr^2} \right) d\bar{\theta}xn$$

where the coefficient K includes all terms not involving $\bar{\theta}xn$.

$$K = \frac{\bar{M}xn . Mu}{4\pi^2 . Sn^2 . Sr^2 . \bar{\phi}xx^2} \exp\left\{ -\left[\frac{\bar{\phi}xx}{2 . Sr^2} + \frac{Mu^2}{2\ Sr^2 . \bar{\phi}xx} + \frac{\bar{M}xn^2}{2\ Sn^2\ \bar{\phi}xx} \right] \right\}$$

Integrating using standard integrals (reference 3) :

$$p(\bar{M}xn, Mu, \theta z : \bar{\phi}xx) = 2.\pi . K . I_0 (Mu / Sr^2) \quad \ldots . 3.46$$

where $I_0(x)$ = Modified Bessel function of order zero.

The above procedure is repeated to find $p(Mz, \theta z : \bar{\phi}xx)$

$$p(Mz, \theta z : \bar{\phi}xx) = \int_0^\infty \bar{M}xn . p(\bar{M}xn, Mz.\bar{M}xn, \theta z : \bar{\phi}xx) . d\bar{M}xn$$

where Mu is replaced in terms of Mz and $\bar{M}xn$. This integral is of the form:

$$p(Mz, \theta z : \bar{\phi}xx) = K_1 \int_0^\infty \bar{M}xn^3 . \exp(-\alpha.\bar{M}xn^2) . I_0(\beta . \bar{M}xn) . d\bar{M}xn \quad \ldots\ldots\ldots\ldots . 3.47$$

where from equation 3.46 we find:

$$K_1 = \frac{Mz . \exp(-\bar{\phi}xx / 2.Sr^2)}{2.\pi . Sn^2 . Sr^2 . \bar{\phi}xx^2}$$

$$\alpha = \frac{1}{2.\bar{\phi}xx} . \left[\frac{1}{Sn^2} + \frac{Mz^2}{Sr^2} \right]$$

and $\beta = \dfrac{Mz}{Sr^2}$

Integrating with respect to $\bar{M}xn$ (using standard integral formulae, reference 4) :

$$p(Mz, \theta z : \bar{\phi}xx) = \frac{K_1}{2\alpha^2} . \exp(\beta^2 / 4.\alpha) . L_1(-\beta^2 / 4.\alpha) \quad \ldots 3.48$$

where $L_N(x)$ = Laguerre polynomial of order N and $L_1(x) = (1-x)$

Dropping the dependence on $\bar{\phi}xx$ the distribution of Mz, θz alone is given by:

$$p(Mz, \theta z) = \int_0^{\infty} p(Mz, \theta z : \bar{\phi}xx) \cdot p(\bar{\phi}xx) \; d\,\bar{\phi}xx \quad \ldots\ldots 3.49$$

Substituting for K_1, α and β in equation 3.48 and letting $p(\bar{\phi}xx)$ equal the Chi-square distribution with 2L degrees of freedom and variance Sx^2 we find:

$$p(Mz,\theta z) = \int_0^{\infty} K_2 . \bar{\phi}xx^{L-1} . \exp\ (- \lambda\, \bar{\phi}xx) \cdot (1 + \delta . \bar{\phi}xx) \cdot d\,\bar{\phi}xx \ldots 3.50$$

where λ can be shown to be greater than zero for all values of Sx^2, Sr^2, Sn^2. Integrating by parts:

$$p(Mz, \theta z) = K_2 . \frac{\Gamma(L)}{\lambda^{L}} + \delta . \frac{\Gamma(L+1)}{\lambda^{L+1}} \quad \ldots\ldots 3.51$$

where $\Gamma(L)$ = Gamma Integral = $(L-1)!$ and the coefficients are found to be:

$$K_2 = \frac{Mz \;.\; Sr^2}{2^L \;.\; Sn^2 \;.\; \pi \;.\; Sx^{2L} .\; \Gamma(L) \;.\; \left\{ \frac{Sr^2}{Sn^2} + Mz^2 \right\}}$$

$$\delta = \frac{Mz^2}{2.Sr^2 \;.\; (Sr^2 / Sn^2) + Mz^2}$$

$$\text{and } \lambda = \frac{1}{2.Sr^2} \left[1 - \frac{Mz^2}{(Sr^2 / Sn^2) + Mz^2} \right] + \frac{1}{2.Sx^2}$$

Substituting for K_2, λ and δ in equation 3.51 and rearranging:

$$p(Mz, \theta z) = \frac{Mz \;.Sr^2 \;.Sn^2}{\pi . \{Sr^2 + Sn^2 . Mz^2\}^2} \cdot \left\{ 1 + \frac{Sx^2}{Sr^2 + Sn^2 . Mz^2} \right\}^{L} \cdot \left[1 + \frac{L \;.Mz^2}{Sr^2 \cdot \left\{ \frac{Sr^2}{Sn^2} + Mz^2 \right\} \cdot \left\{ \frac{1}{Sx^2} + \frac{1}{Sr^2 + Sn^2 . Mz^2} \right\}} \right] \quad \ldots 3.52$$

The distribution of z as given by equation 3.52 is of a complicated form. However, the following properties of $p(Mz, \theta z)$ can be found:

1) If $Mz = 0$ or $Mz = \infty$ then $p(Mz, \theta z)$ is zero (as expected).

2) Equal probability contours in z describe circles about the origin i.e. $p(Mz, \theta z)$ is essentially only a function of the absolute distance from the origin (Mz).

3) Taking a cross-section of $p(Mz, \theta z)$ along the real axis it is found that $p(Mz, \theta z)$ takes the form of a double hump. (See Figure 3 below).

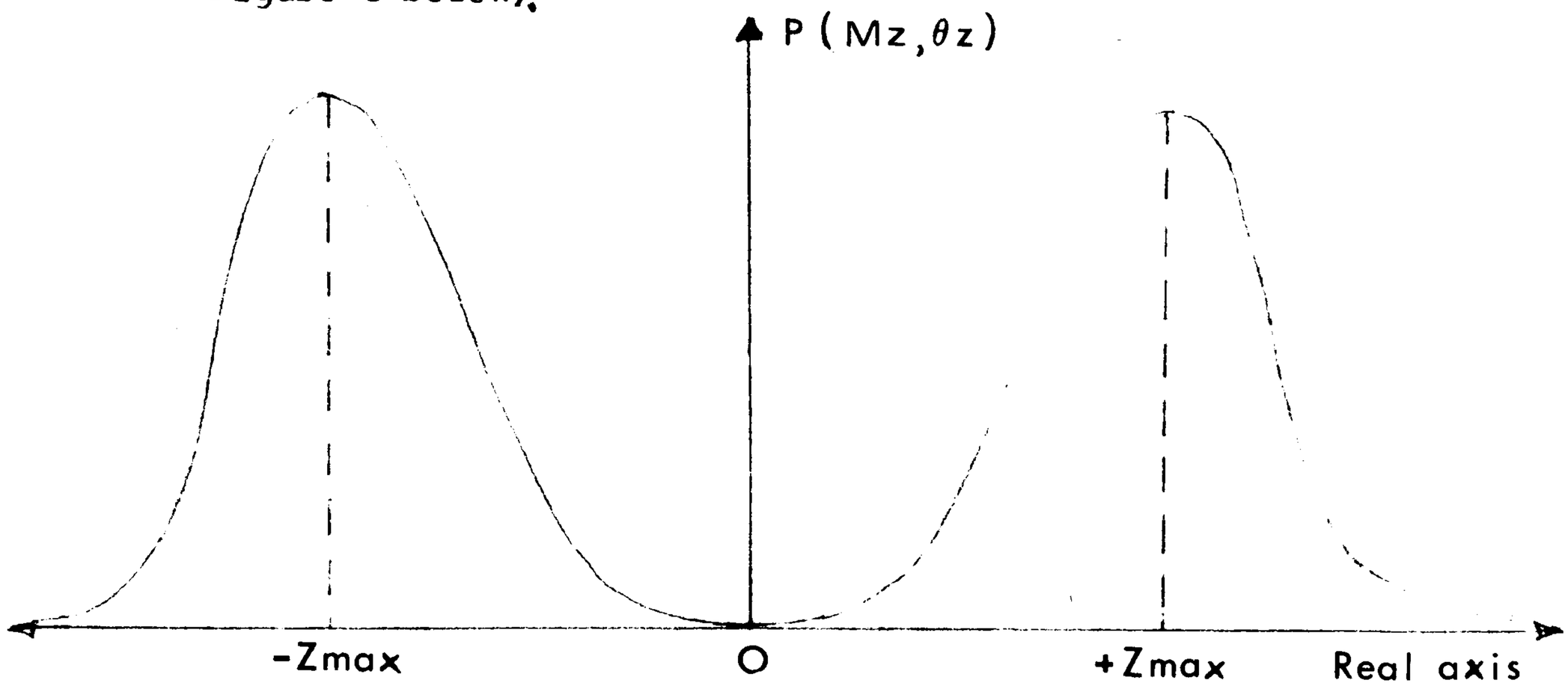

FIGURE 3: Shows a typical cross-section of $p(Mz, \theta z)$ taken along the real-axis of z.

The value of Zmax is a function of Sx^2, Sn^2, Sr^2 and L. Varying each parameter in turn, keeping the remaining terms constant, it is found that:

i) If Sx^2 is increased then Zmax increases

ii) If Sn^2 is increased then Zmax decreases

iii) If Sr^2 is increased then Zmax decreases

However Zmax is more sensitive to changes in Sn^2.

iv) If L is increased then Zmax increases. As $L \rightarrow \infty$ $p(Mz, \theta z)$ $\rightarrow$ dirac delta function at $Mz = \infty$

4) If the noise in the feedback loop is zero (i.e. $Sr^2 = 0$) then equation 3.52 resembles the distribution of the open-loop frequency response error. Remembering for the open-loop case that:

$$\bar{E}g = \frac{\bar{\phi}_{xn}}{\bar{\phi}_{xx}} = \frac{1}{z} \qquad (\text{if } \bar{\phi}xr = 0)$$

It can be shown that:

$$p(\bar{E}g) = p(1/z)\Big|_{Sr^2=0,H=0.}$$

Thus the open-loop frequency response distribution is a particular case of the closed-loop distribution with the feedback noise (Sr^2) and the feedback gain (H) set to zero.

To obtain the distribution of the forward-loop gain estimate we must make the complex transformation given by equation 3.41(a). By applying this transformation to a distribution of the form shown in Figure 3 insight is gained on the nature of errors in the forward-loop frequency response estimate. The transformation is given by:

$$Eg = \frac{T}{z - H} \qquad \text{where } T = 1 + H.G$$

The distribution of Eg is found from the distributions of z by:

$$p(M_E, \theta_E) = \frac{p(Mz, \theta z)}{J(Mz, \theta z)} \qquad \ldots\ldots\ldots\ldots\ldots\ldots 3.53$$

where: $$J(Mz, \theta z) = \begin{vmatrix} \frac{\partial M_E}{\partial Mz} & \frac{\partial M_E}{\partial \theta z} \\ \frac{\partial \theta E}{\partial Mz} & \frac{\partial \theta E}{\partial \theta z} \end{vmatrix}$$

and Mz, θz are rephrased in terms of M_E, θ_E.

This transformation is most easily derived in two stages. First we consider the transformation:

$$w = z - H$$ Under this transformation:

$$Mw = \left(Mz^2 + M_H^2 - 2\,Mz.M_H.\cos\,(\theta_z - \theta_H) \right)^{\frac{1}{2}}$$

$$\theta w = \tan^{-1} \left\{ \frac{Mz.\sin\,\theta z - M_H.\sin\,\theta_H}{Mz.\cos\,\theta z - M_H.\cos\,\theta_H} \right\}$$

The Jacobian of this transformation is given by:

$$J(Mz, \theta z) = \begin{vmatrix} \frac{\partial Mw}{\partial Mz} & \frac{\partial Mw}{\partial \theta z} \\ \frac{\partial \theta w}{\partial Mz} & \frac{\partial \theta w}{\partial \theta z} \end{vmatrix}$$

Evaluating the partial differentials:

$$\frac{\partial Mw}{\partial Mz} = \frac{\{Mz - M_H.\cos\,(\theta z - \theta_H\}}{\{Mz^2 + M_H^2 - 2\,Mz.M_H.\cos\,(\theta z - \theta_H)\}^{\frac{1}{2}}}$$

$$\frac{\partial Mw}{\partial \theta_z} = \frac{Mz.M_H.\sin\,(\theta z - \theta_H)}{\{Mz^2 + M_H^2 - 2.Mz.M_H.\cos\,(\theta z - \theta_H)\}^{\frac{1}{2}}}$$

$$\frac{\partial \theta w}{\partial Mz} = \frac{-M_H.\sin\,(\theta z - \theta_H)}{\{Mz^2 + M_H^2 - 2.Mz.M_H.\cos\,(\theta z - \theta_H)\}}$$

$$\frac{\partial \theta w}{\partial \theta z} = \frac{\{Mz^2 - Mz.M_H.\cos\,(\theta_z - \theta_H)\}}{\{Mz^2 + M_H^2 - 2.Mz.M_H.\cos\,(\theta z - \theta_H)\}}$$

Evaluating the determinant:

$$J(Mz,\ \theta z) = \frac{(Mz^3 - 2.Mz^2.M_H.\cos\ (\theta z - \theta_H) + Mz.M_H^2)}{\{Mz^2 + M_H^2 - 2.Mz.M_H.\cos\ (\theta z - \theta_H)\}} \quad \ldots\ldots 3.54(a)$$

and lastly Mz and θz are rephrased in terms of Mw, θw using the relationships.

$$Mz = \{Mw^2 - M_H^2 + 2.Mw.M_H.\cos\ (\theta w - \theta_H)\}^{\frac{1}{2}} \quad \ldots\ldots\ldots 3.54(b)$$

$$\theta z = \tan^{-1}\left(\frac{Mw.\sin\ \theta w + M_H.\sin\ \theta_H}{Mw.\cos\ \theta w + M_H.\cos\ \theta_H}\right) \quad \ldots\ldots\ldots 3.54(c)$$

Equations 3.54 (a,b,c) can be used directly to obtain the distribution of Mw, θw by substituting appropriately using $p(Mw,\ \theta w) = \frac{p(Mz,\theta z)}{J(Mz,\theta z)}$

Lastly the error term Eg is given by:

$$M_E.\exp\ (j\theta_E) = \frac{M_T.\exp\ (j\theta_T)}{Mw.\exp\ (j\theta w)}$$

$$\text{and} \quad p(M_E,\ \theta_E) = \frac{p(Mw,\ \theta w)}{J(Mw,\ \theta w)} \quad \ldots\ldots\ldots\ldots\ldots 3.55$$

where $Mw = \frac{M_T}{M_E}$, $\theta_w = \theta_T - \theta_E$ and:

$$J(Mw,\ \theta w) = \begin{vmatrix} \frac{\partial M_E}{\partial Mw} & \frac{\partial M_E}{\partial \theta_w} \\ \frac{\partial \theta_E}{\partial Mw} & \frac{\partial \theta_E}{\partial \theta_w} \end{vmatrix} = \frac{M_T}{Mw^2} = \frac{M_E^2}{M_T}$$

$$\text{So } p(M_E,\ \theta_E) = \frac{M_T}{M_E^2} \cdot p_{Mw,\ \theta w}\left(\frac{M_T}{M_E},\ (\theta_T - \theta_E)\right) \ldots 3.56$$

Direct substitution to yield an explicit form for the distribtuion of Eg is cumbersome and not very enlightening. It is simpler to consider the transformation of circles centred about the origin in the z-plane to the E-plane. There are three conditions to consider (see Figure 4)

FIGURE 4 : Shows circles in the Z-plane mapped into the Eg -plane. The origin denotes zero error in estimates of G. The circles are labelled with the ratio Mz/Mh.

$0 = -(1+HG) / H = 1 / (1,-j1)$

If $Mz = \infty$ then $Eg = 0$.

If $Mz = 0$ then $Eg = -(1+HG) / H$

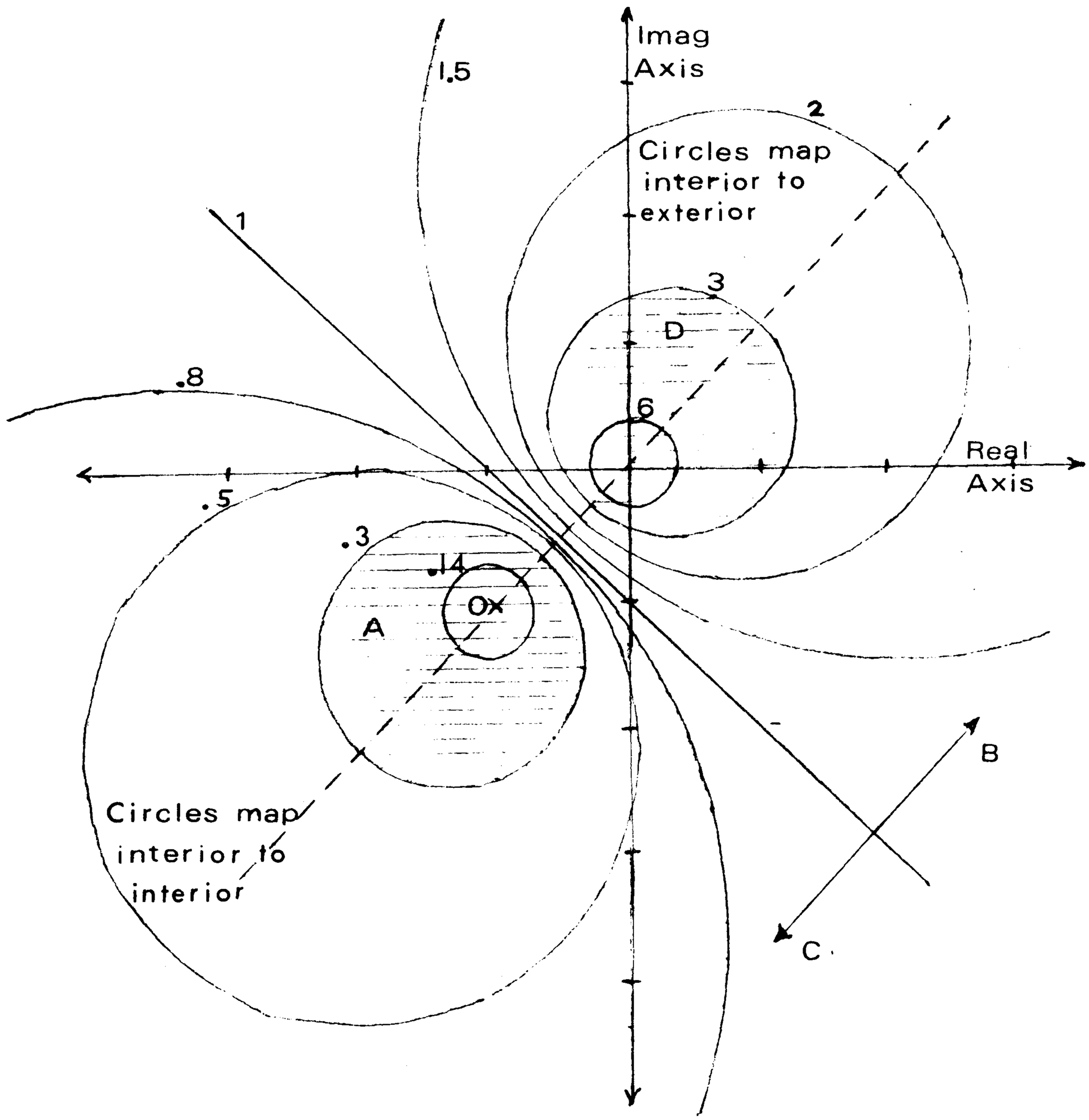

1) Circles in the z-plane of radius $Mz<M_H$

These map to circles in the E-plane with the interior of circles in the z-plane mapping to the interior of circles in the E-plane. As $Mz \to 0$ these circles are centred about $-(1 + H.G) / H$.

2) Circles in the z-plane of radius $Mz=M_H$

This circle maps to a straight line in the E-plane bisecting the line joining $-(1 + H.G) / H$ and the origin at right angles.

3) Circles in the z-plane of radius $Mz>M_H$

These map to circles in the E-plane with the interior of circles in the z-plane mapping to the exterior of circles in the E-plane. As $Mz \to \infty$ the circles in the E-plane become centred about the origin.

Figure 4 shows an example of this transformation for the case where;

$$H / (1 + H.G.) = (1 - j\,1)$$

The circles are marked by the ratio Mz / M_H . The circles enclosing the origin map interior to exterior, those enclosing the point $-(1 + H.G) / H$ map interior to interior.

When the distribution of z is of the form indicated by Figure 3 with a maximum occurring at Zmax there are three cases to consider:

1) $Zmax << M_H$ (under very noisy conditions or in the presence of a large gain in the feedback loop). Under these conditions it is highly likely to obtain estimates centred around the region marked 'A' in Figure 4. This means the estimates are highly biased, with an approximate mean of:

$$\mu_G = G - \frac{1 + H.G}{H} = -\frac{1}{H}$$

remembering that obtaining an estimate at the origin of E corresponds to estimating the forward-loop gain (G) exactly.

2) $Zmax \simeq M_H$ (noise in the system is reduced from case 1 but still considerable.) This represents an intermediate stage, under which it is just as likely to obtain estimates to the right of the straight line (area 'B') as to the left (area 'C'). It is also possible under these conditions to find that the distribution of E exhibits a 'hole' centred about the point $-(1 + HG) / H$ i.e. it is highly unlikely to find estimates in the immediate vicinity of the point H. This phenomenon is indeed shown to exist in simulation results presented in Section 6.

3) $Zmax >> M_H$ (this is the desired case when noise in the system is minimal or L is sufficiently large). Under these conditions it is highly likely to obtain estimates centred around the origin in the region marked 'D' in Figure 4. The approximate mean of estimates $\bar{G}$ is given by:

$$\mu_G \simeq G \quad .$$

By considering the transformation given by equation 3.41(a) in conjunction with the distribution of z given by equation 3.52, it is possible to construct approximate confidence intervals for estimates of G if Zmax (Figure 3) is much greater than the absolute magnitude of the feedback gain. If from equation 3.52 we are α percent confident that values of z lie outside a circle radius M_α, then we are α percent confident that estimates of G lie within the transformed circle, radius M_α, in the E-plane. This technique is used in Chapter 6 to assess models of the human operator response in tracking tasks.

5) DISTRIBUTION OF FEEDBACK FREQUENCY RESPONSE ESTIMATES

The sampling distribution associated with estimates of H is essentially identical to that of the forward-path estimate. Only the alterations required are noted in this section. From equation 3.20 the error in estimates of H is given by:

$$\bar{E}_H = \frac{(1 + H.G)\ \bar{\phi}xr}{G\ \bar{\phi}xx + \bar{\phi}xn - G\ \bar{\phi}xr} \quad \ldots\ldots\ldots\ldots 3.57$$

Rearranging to a form shown by equation 3.41:

$$\bar{E}_H = \frac{1 + G.H}{G} \cdot \left\{ \frac{1}{z - 1} \right\}$$

where now: $z = \frac{(\bar{\phi}xx + \bar{\phi}xn\ /\ G)}{\bar{\phi}xr} = \frac{U}{\bar{\phi}xr}$ . . .(U defined for eq^{un}.3.43)

As is expected the roles of $\bar{\phi}xn$ and $\bar{\phi}xr$ are reversed from those in the previous section.

By inspection the distribution of z is given by equation 3.52 replacing:

1) Sn^2 by Sr^2 and

2) Sr^2 by $Sn^2 / |G|^2$

If G is large then the effect of noise in the forward path on the accuracy of estimates of H is neglibible and the distribution of 1 / z is approximated by equation 2.28 (the distribution of errors in the open-loop frequency response estimate.)

6) SIMULATION RESULTS

The distribution of errors in the forward-loop frequency response was found from simulation tests for an extensive range of system parameters. As in the open-loop simulation tests the Fourier

coefficients X, R and N are assumed Gaussian with zero mean and variance Sx^2, Sr^2, Sn^2 respectively. Thus, to find the distribution of errors in the closed-loop system it is sufficient to form each of the above by taking two independent samples of a Gaussian white noise process as the real and imaginary coefficients and then multiply by the desired scale factor to obtain the correct variance. The loop-signals, $\hat{Y}$, $\hat{E}$ and $\hat{Z}$ can be formed from a combination of $\hat{X}$, $\hat{R}$, $\hat{N}$ and the specified system frequency response gains G, H. The degrees of freedom, L, can be varied by taking average estimates of $\bar{\phi}xx$, $\bar{\phi}xy$ over L independent realisations of $\hat{X}$, $\hat{N}$ and $\hat{R}$.

The amplitude probability distributions of $\bar{G}$ were calculated from ten thousand individual estimates. The complex-plane was divided into a 25 x 25 matrix of squares centred on the true value of G; the square resolution being chosen to suit each particular case. The number of occurrences of estimates of G within each square was recorded and constant probability contours were constructed. These were compared with expected results from equation 3.56 found by numerically integrating the probability distribution over each square and normalising to the total count of ten thousand estimates.

In total twenty-two tests were tried and good correlation was found in each case. Of these twenty-two, the three variations described in Section 5 are displayed. Figures 5, 6 and 7 show results obtained:

i) Under very noisy conditions ($Zmax << |H|$)

ii) Under less noisy conditions ($Zmax \simeq |H|$)

iii) With a high signal-to-noise ratio ($Zmax >> |H|$)

Lastly, Figures 8 and 9 show that the distributions as predicted are a good approximation for two different systems under similar input and noise conditions.

These results would indicate that the distribution of errors in forward-loop and feedback-loop frequency response estimates in the presence of noise both in the forward and feedback path is described by equation 3.56. This analysis has assumed that bias errors due to finite frequency resolution may be neglected.

FIGURE 5 : Shows constant probability contours in the Eg-plane as measured from simulation tests (——), and as predicted by transformation and integration of equation 3.52. (- - -). Contours are plotted from experiments involving 10000 independent estimates of the forward-loop frequency response, G.

As the noise variance S_n^2 increases relative to S_x^2 the variance of estimates of G decreases. However the values are centred around $-(1+HG)/H$. This corresponds to estimating $G = -1/H$, or an infinite closed-loop gain.

SYSTEM PARAMETERS. : $P = -(1+HG)/H$, $H = (10, j0)$, $G = (1, j0)$

$S_x^2 = 0.28$, $S_n^2 = 0.4$, $S_r^2 = 0.14$, $L = 3$.

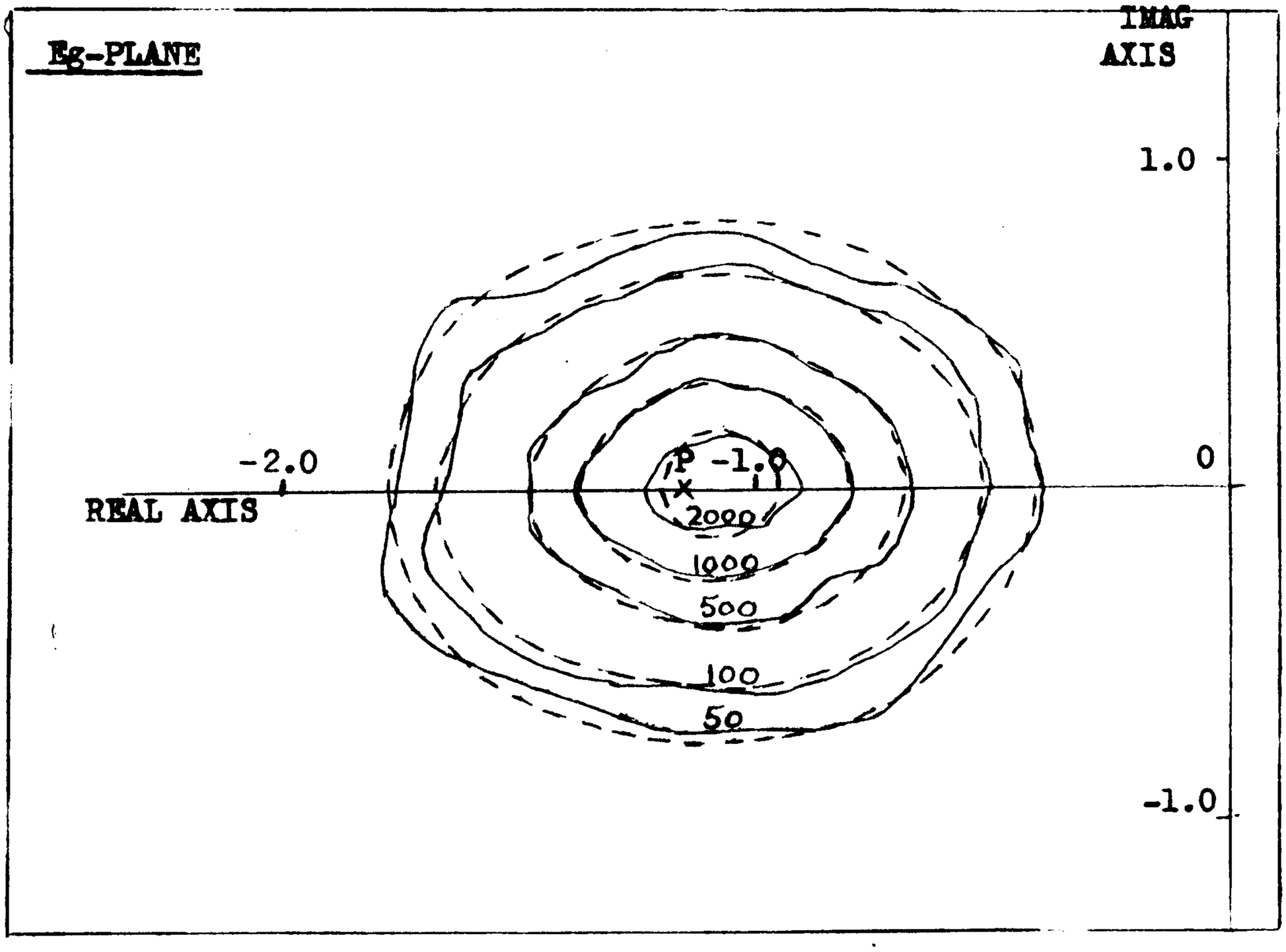

FIGURE 6 : Shows constant probability contours in Eg-plane,

a) As found from simulation tests (——)

b) As predicted (- - -).

As the noise variance decreases relative to S_x^2, the variance of estimates increases. The mean of the distribution moves away from the -(1+HG)/H point towards the origin. Under certain conditions the probability of obtaining estimates in the neighbourhood of -(1+HG)/H is small and the constant probability contours bend round this point.

SYSTEM PARAMETERS. : P = -(1+HG)/H, H = (10, j0), G = (1, j0),

$S_x^2 = 0.28$, $Sn^2 = 0.05$, $S_r^2 = 0.14$, L=3.

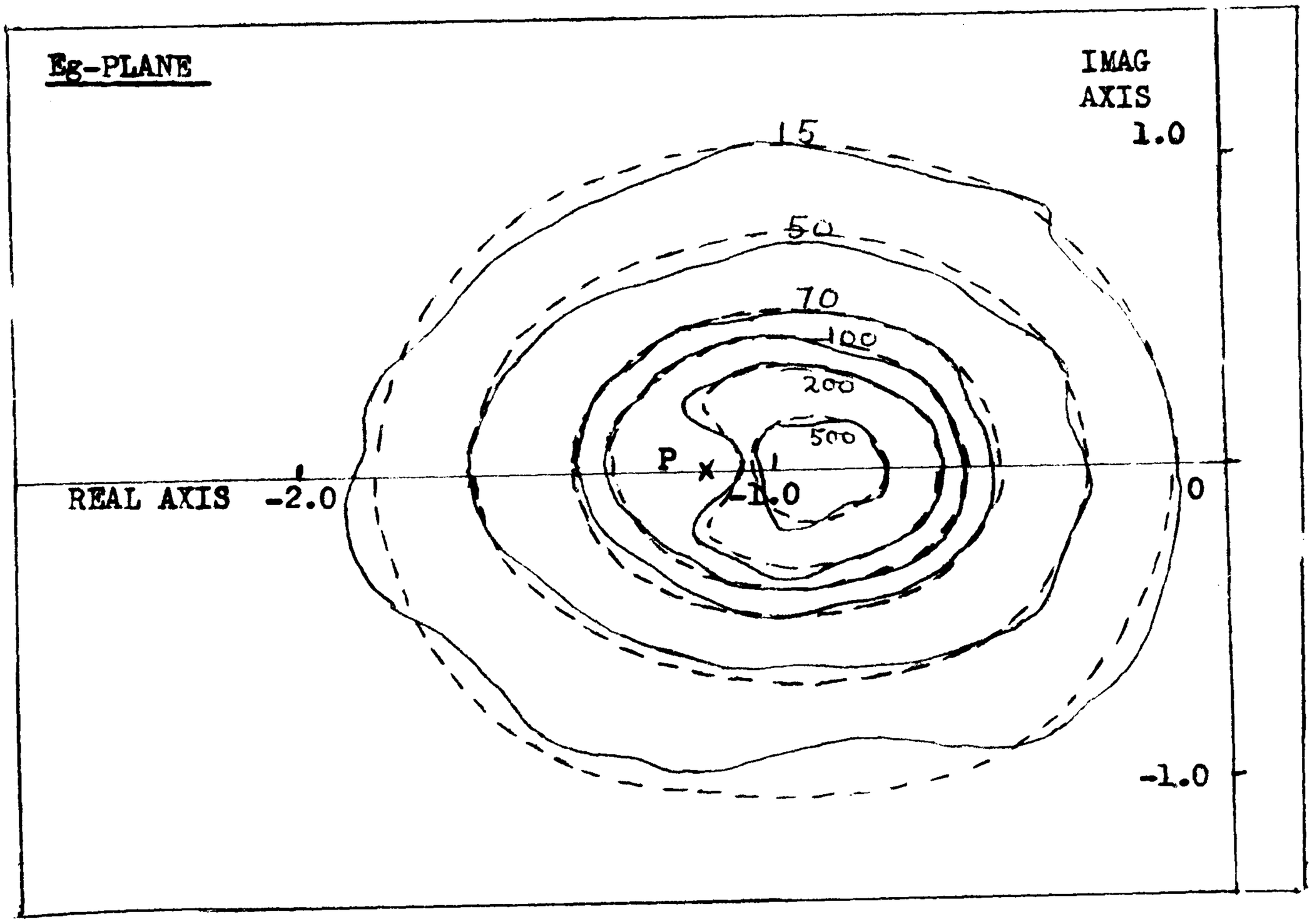

FIGURE 7 Shows constant probability contours in the Eg-plane when the signal to noise ratio is large. Under these conditions estimates are centred about the origin.

The variance of estimates of G now decreases as the noise variance S_n^2 decreases.

SYSTEM PARAMETERS : $H = (10, j0)$, $G = (1, j0)$, $L = 3$

$S_x^2 = 0.28$, $S_n^2 = 0.005$, $S_r^2 = 0.14$

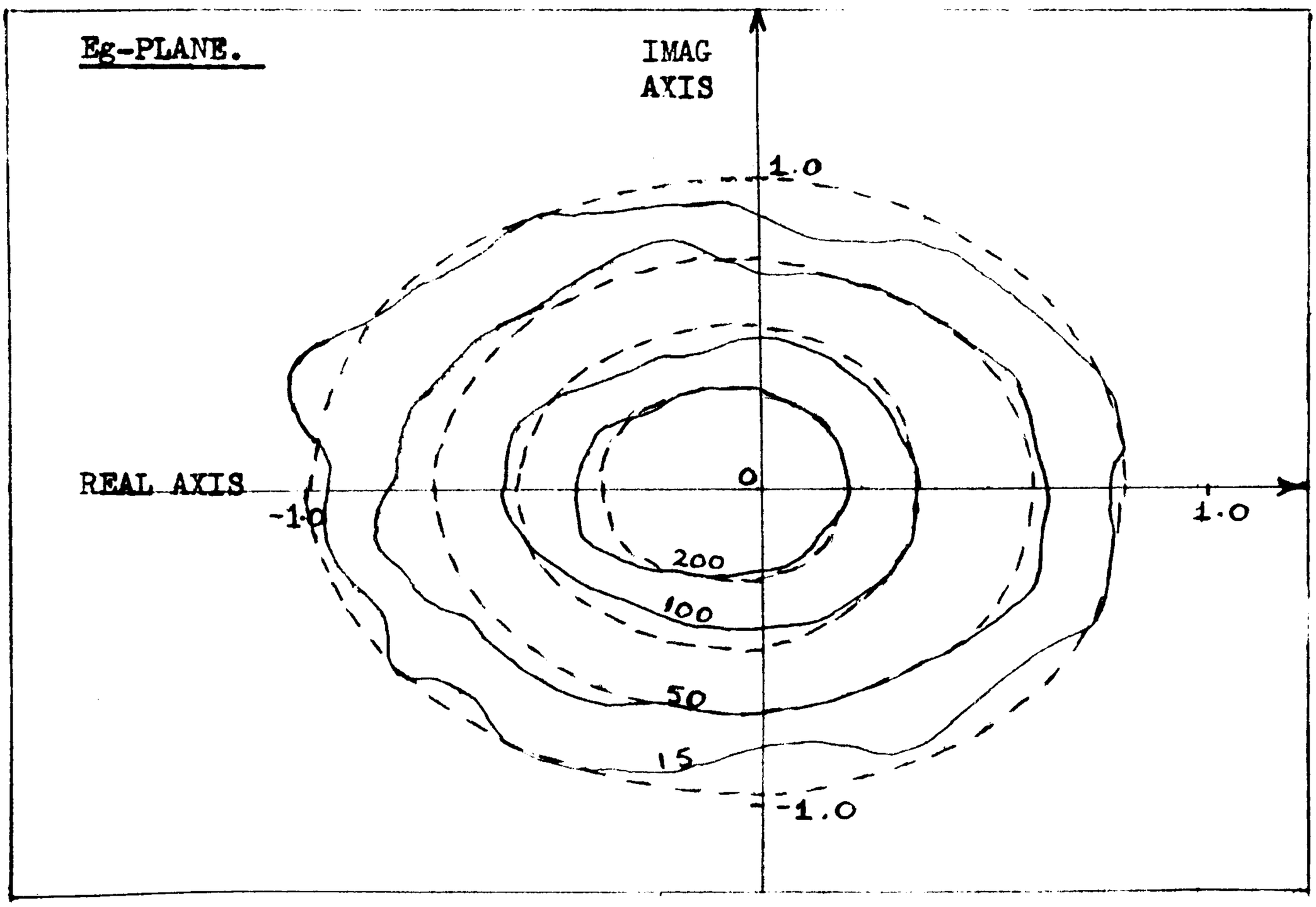

FIGURE 8 : Shows close agreement between measured probability levels (———) and predicted probability levels (- - - -) for estimates of the open-loop frequency response,G. The high probability contours are centred about the point -(1+HG)/H indicating a low signal to noise ratio.

SYSTEM PARAMETERS : $P = -(1+HG)/H$, $H = (7.14, +j7.14)$

$G = (1, j0)$, $L = 5$, $S_x^2 = 0.28$, $S_n^2 = 1.12$, $S_r^2 = 0.14$

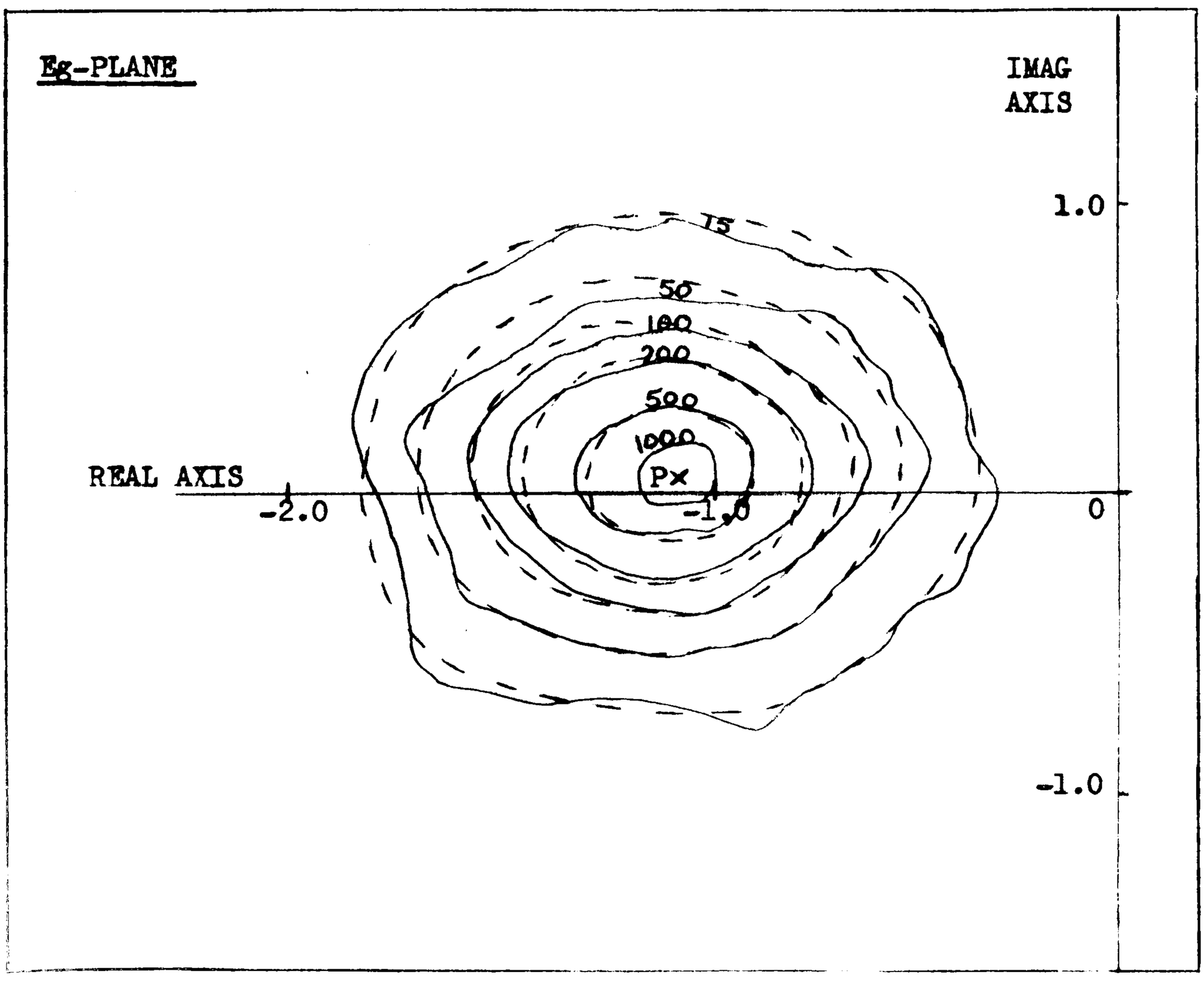

FIGURE 9 : Shows constant probability contours in the Eg-plane under the same noise conditions as in FIGURE 8 , but for a different system. Again their is close agreement between measured and predicted results.

In figures 5-9 the complex plane was divided into a 25 x 25 matrix of squares and the number of occurrences in each square recorded.The total number of estimates taken was 10000. The predicted occurrence in each square was found by integrating the distribution of G over an interval in the Z-plane (eqn . 3.52) corresponding to the mapped square in the Eg-plane. The total probability was normalised to the total number of estimates.

SYSTEM PARAMETERS : $P = -(1+HG)/H$, $H = (10, j0)$, $L = 5$

$G = (0.707, -j0.707)$, $S_x^2 = 0.28$, $S_n^2 = 1.12$, $S_r^2 = 0.14$

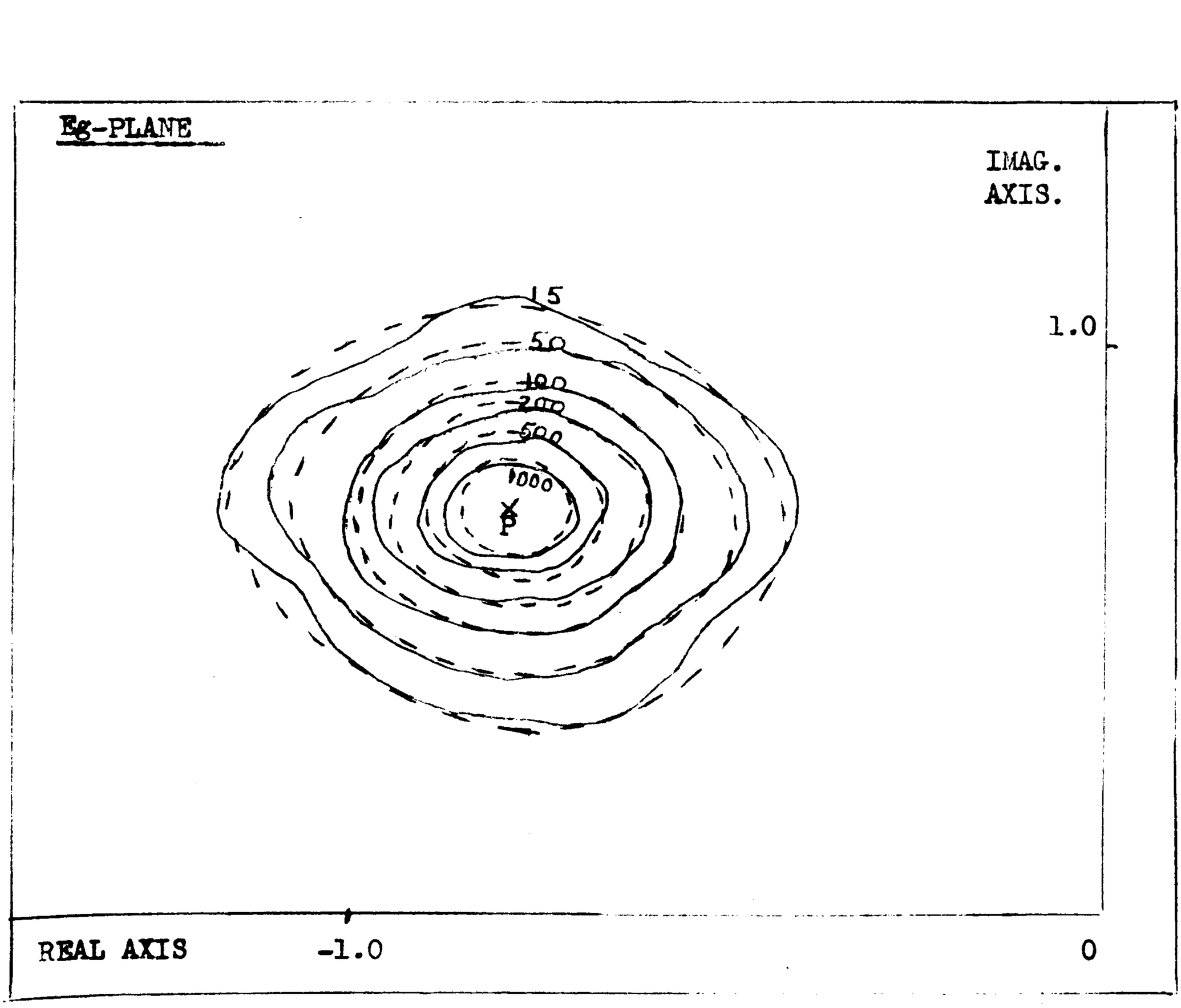

7) NOISE ESTIMATES IN CLOSED -LOOP SYSTEMS

In the open-loop system it was shown that estimates of the noise spectrum were Chi-square distributed with 2L - 2 degrees of freedom. In closed-loop systems, estimates of the forward path noise, $\bar{\phi}\hat{n}\hat{n}$, and the feedback noise, $\bar{\phi}\hat{r}\hat{r}$ are shown to be approximately Chi-square distributed with 2L - 2 degrees of freedom when the signal-to-noise ratio is large, but the approximation becomes worse as the signal-to-noise ratio decreases.

From equations 3.10 and 3.11 it can be shown that:

$$\bar{\phi}\hat{n}\hat{n} \simeq \bar{\phi}nn - |\bar{E}g|^2 . \bar{\phi}ee \quad \ldots\ldots\ldots\ldots\ldots\ldots \quad 3.58$$

and $$\bar{\phi}\hat{r}\hat{r} \simeq \bar{\phi}rr - |\bar{E}h|^2 . \bar{\phi}yy \quad \ldots\ldots\ldots\ldots\ldots \quad 3.59$$

where $\bar{E}g$ and $\bar{E}h$ are the errors in estimates of G and H respectively. As the number of estimates L taken to find the average values $\bar{\phi}ee$, $\bar{\phi}yy$ etc. tends to infinity, $\bar{E}g$ and $\bar{E}h$ go to zero and the estimates of the noise spectra tend to their true values. When the ratios Sx^2 / Sn^2 and Sx^2 / Sr^2 are large then the terms $|\bar{E}g|^2 . \bar{\phi}ee$ and $|\bar{E}h|^2 . \bar{\phi}yy$ are almost independent of the noise signals n(t) and r(t) and can be shown to be Chi-square distributed with 2 degrees of freedom. Thus as $\bar{\phi}nn$ and $\bar{\phi}rr$ are Chi-square distributed with 2L degrees of freedom, the best estimates of these are approximately Chi-square distributed with 2L - 2 degrees of freedom. Figure 10 would indicate that this is indeed the case.

As the signal-to-noise ratios decrease, the terms $|\bar{E}h|^2 . \bar{\phi}yy$ and $|\bar{E}g|^2 . \bar{\phi}ee$ become highly correlated with the noise terms. Under these conditions the noise spectra estimates tend to underestimate the true values. If the noise term, n(t), dominates the error signal e(t), then:

$$\bar{\phi}ee \simeq \left|\frac{H}{1 + H.G}\right|^2 . \bar{\phi}nn \quad \ldots\ldots\ldots\ldots\ldots\ldots\ldots\ldots 3.60$$

and the error in estimates of G was shown in Section 5 to be $\simeq$

$- (1 + H.G) / H.$

Thus the term $|\bar{E}g|^2 . \bar{\phi}ee$ in equation 3.58 is of the same order of magnitude as $\bar{\phi}nn$ and the best estimate of the noise spectrum severely underestimates the true value. A similar argument applies to estimates of the auto-spectrum of the noise in the feedback loop. The distribution of noise spectra estimates under these conditions is shown in Figure 11.

For most cases of system identification, it is necessary to choose L so that the variance of system estimates is reduced to acceptable levels. Under these conditions, estimates of the noise spectra are approximately Chi-square distributed with 2L - 2 degrees of freedom.

FIGURE 10 : Shows the amplitude distribution of estimates of the Noise auto-spectrum a) As obtained by measuring the noise signal.

b) From best estimates of the noise signal.

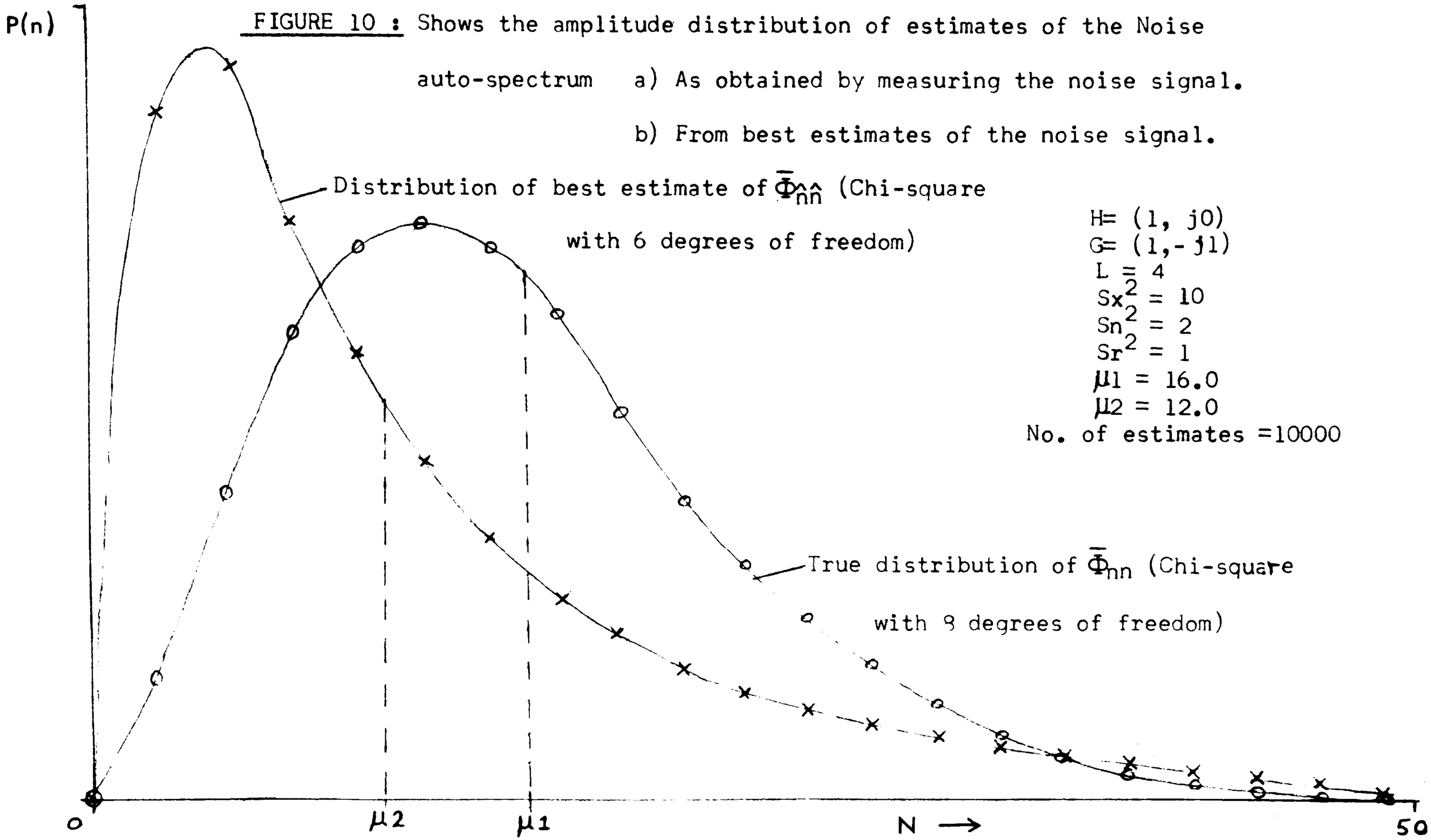

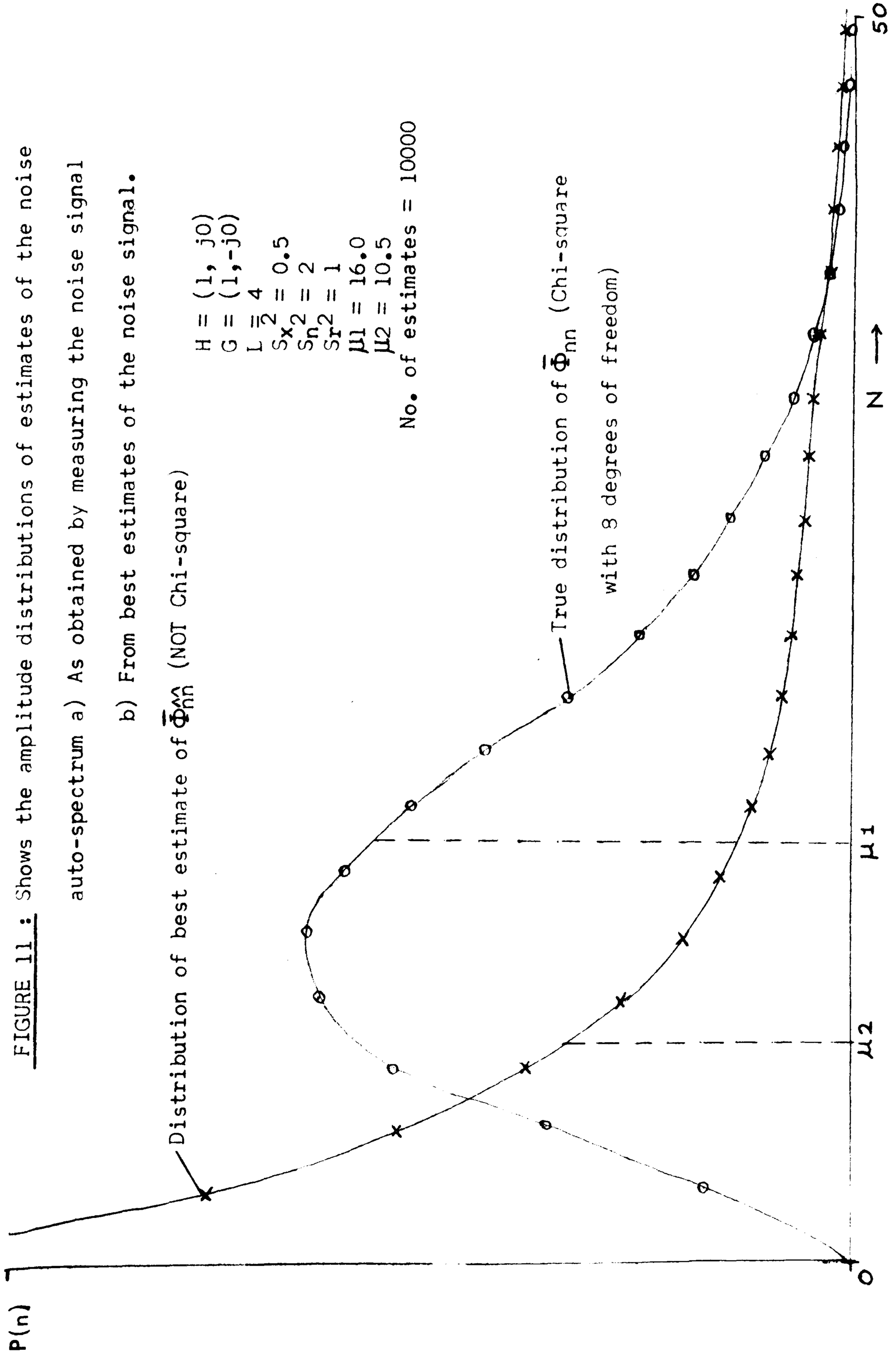

FIGURE 11 : Shows the amplitude distributions of estimates of the noise

8) CONCLUSIONS

The results of this chapter extend the 'random' error analysis of short-term spectral estimates to include closed-loop systems with noise both in the forward and feedback paths.

Initial results for the distribution of cross-spectral estimates and estimates of the overall frequency response involve a fairly straightforward extension of results found in Chapter 2. The distribution of estimates of the forward path gain and feedback gain, however, require an approach involving distributions of tri-variate complex Gaussian sequences. The resulting distributions show clearly that, unlike the open-loop case, estimates of G and H can be severely biased under noisy conditions, if L, the degrees of freedom, is chosen too small. This fact is not apparent from an initial consideration of equations 3.19 and 3.20.

The distribution has been derived for a linear Gaussian system where the noise inputs are uncorrelated with each other and with the input. Using similar arguments to those in Chapter 2, it is expected that the distributions are a good approximation even when $x(t)$, $n(t)$ and $r(t)$ are non-Gaussian.

In Chapter 6 the response of a human operator performing a tracking task in closed-loop mode is examined. It is shown, using the stationarity tests given by equations 3.39 (a,b) and the theoretical distribution of estimates as given by equation 3.56, that his mode of response depends on the frequency content of the input signal.

REFERENCES

1 WELLSTEAD, P. E.: 'Real time spectral analysis'. Phd. thesis, Univ. of Warwick (1971)

2 GRADSTEYN, I. S. & RHYSIK, I. M.: 'Tables of integrals series & products'. No. 9, p. 340. Academic Press (1965)

3 As above : No. 3937, p. 488.

4 As above : No. 10, p. 718.

5 TONG, H: 'Some problems in the spectral analysis of bivariate non-stationary Gaussian processes'. Phd. thesis, Univ. of Manchester, Chapter 5 (1972)

6 BENDAT, J. S. & PIERSOL, A.G.: 'Measurement and analysis of random data'. Wiley Interscience (1972)

7 PAPOULIS, A.: 'Probability random variables and stochastic processes'. McGraw Hill (1965)

8 CRAMER, H.: 'Mathematical methods of statistics'. Princeton Univ. Press (1946)

CHAPTER 4.

SPECTRAL ANALYSIS OF SPEECH

LIST OF SYMBOLS USED

$x(t)$: output signal from the throat microphone after amplification and filtering

$y(t)$: output signal from the crystal microphone held in front of the mouth after amplification and filtering

$n(t)$: a combination of external noise picked up by the crystal microphone and all sounds not generated by the vocal chords or from the larynx

$\hat{X}(w)$: short-term Fourier transform of $x(t)$

$\hat{Y}(t)$: short-term Fourier transform of $y(t)$

$\bar{\phi}_{xx}(w)$: smoothed short-term estimate of the power spectrum of $x(t)$

$\bar{\phi}_{yy}(w)$: smoothed short-term estimate of the power spectrum of $y(t)$

$\bar{\phi}_{\hat{n}\hat{n}}(w)$: best obtainable smoothed estimate of the power spectrum of $n(t)$ $(= \bar{\phi}_{yy} - |\bar{H}|^2 . \bar{\phi}_{xx})$

$\bar{H}(w)$: estimate of the frequency response between $x(t)$, $y(t)$. Is equivalent to the best obtainable estimate of the vocal tract frequency response as the two filter/amplifier networks modifying the outputs from the throat and crystal microphones have identical dynamic characteristics

$\bar{C}_{xy}(w)$: a short-term estimate of the coherency between

x(t) and y(t)

f_s : sampling frequency

T : time taken to fill a block of N samples

N : block size (number of time samples)

w : angular frequency (radians/sec)

Ω : frequency normalised in terms of the voice pitch fundamental frequency

$P_{a,b}(\lambda)$: the Fisher distribution with a,b degrees of freedom and argument λ such that $0 \leqslant \lambda \leqslant \infty$

1) INTRODUCTION

Estimation of the vocal tract transfer function, and spectral analysis of the speech waveform using Fourier techniques (references 1-20) have been subjects for research for many years. In general, the phonetic content of speech is difficult to recover for three reasons:

a) Individual phonemics are often badly enunciated or missed completely

b) Different accents change the phonetic characteristics

c) Many phonemic sounds are themselves slowly transient and not stationary phenomena, thence it is difficult to identify the phonemic boundaries.

This chapter makes use of results obtained in Chapter 2, and shows how these results can be used in the time-varying case to identify both slow changes where two phonemic sounds merge and sharp step-like changes.

The speech measurement system is shown in Figure 1. A throat microphone is placed on a level with the 'voice box.' This ensures that the pick-up is obtained from the vocal chords while feedback from the jaw and small bone structure of the throat is minimised. As the throat microphone is placed higher on the throat the waveform is more contaminated by this bone feedback. The mouth crystal microphone is held 12 inches from the mouth and suitably masked to avoid distortion due to breathing. The mouth-to-microphone distance and the inclination angle are maintained constant to avoid phase changes in the measured frequency response. Figure 2 shows the schematic block diagram for speech analysis.

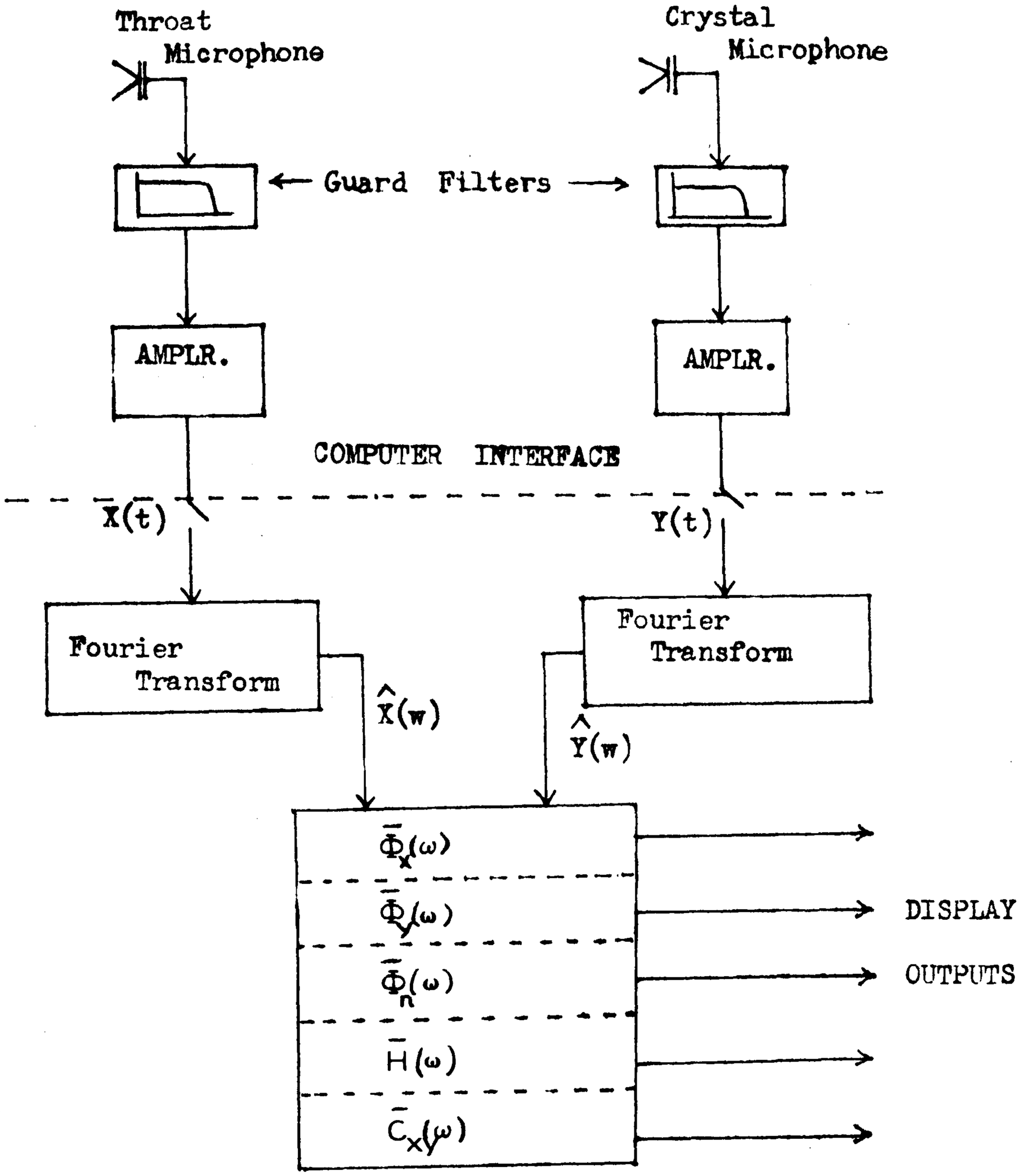

FIGURE 1 : Shows the speech analysis hardware components plus the basic software operations.

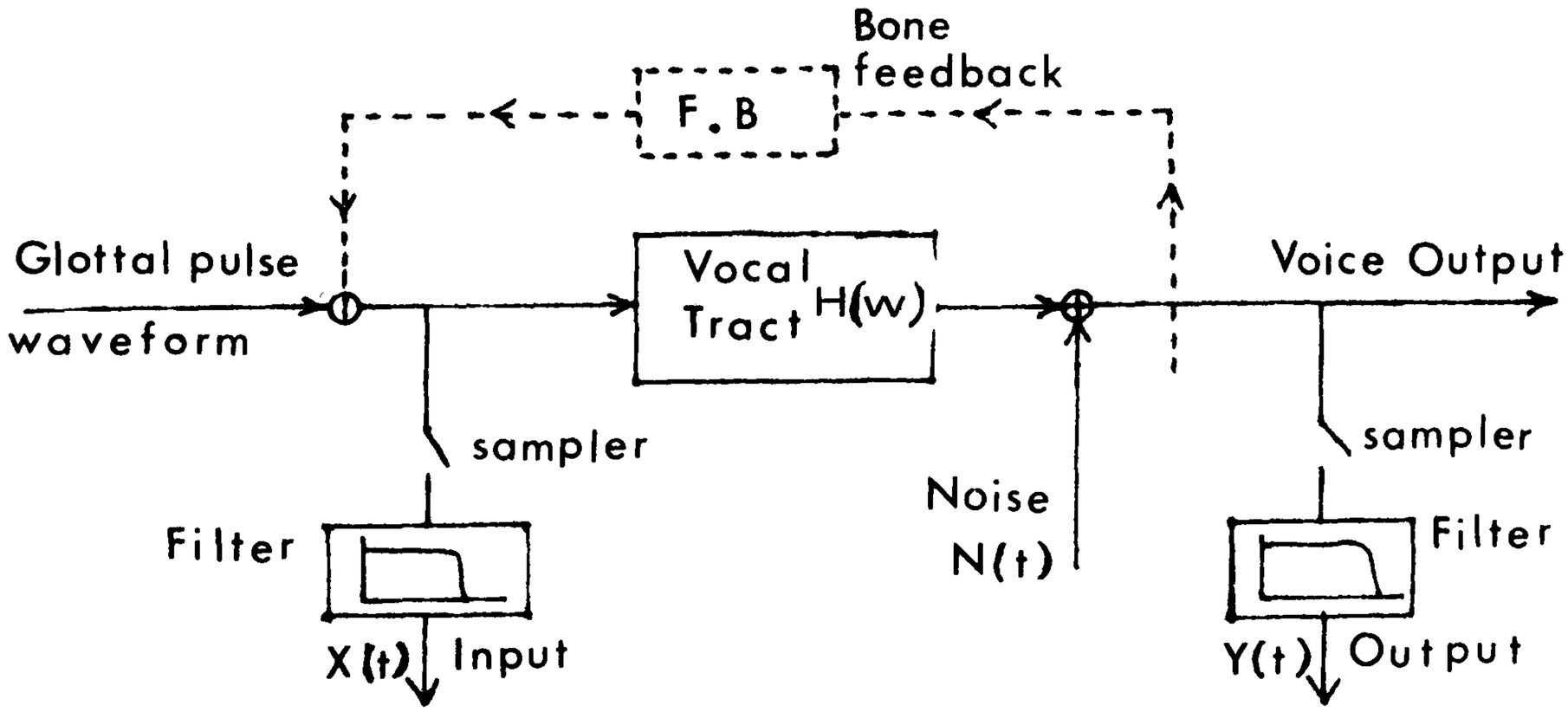

FIGURE 2 Shows the block schematic of the speech analysis system

The frequency response estimate is not a direct measure of the vocal tract, as the input does not access the glottal pulse waveform direct. Any feedback loops in the system are essentially time-invariant in nature. The sounds generated at the mouth do not all originate from the throat, only voiced sounds. Hence in certain cases, the specification of a frequency response is impossible from the measured input/output signals. Thus any phonemic identification system must rely on more than the measured frequency response alone. In the most general case, a phoneme may be defined by any sub-group of 4 functions: input/output auto-spectra, noise spectrum and frequency response.

Changes in voice amplitude and voice pitch (used mainly to convey emotional responses in speech) introduce changes in the speech waveform which can be independent of phonemic changes. Thus any system of analysis must normalise to the signal variance and to the voice pitch.

Section 2 details the normalisation methods used and the choice of parameters for the frequency response analysis. Section 3 outlines the statistical tests used to identify phonemic constants, while Sections 4 and 5 give results obtained in identifying certain phonemes. Lastly Section 6 outlines an application of phonemic identification to the compiling of compressed speech. The results obtained are recorded on a cassette (supplied with this thesis) and a statistical survey of 'merit' based on this tape is presented.

2) SPEECH ANALYSIS AND VOICE PITCH DETECTION

a) Choice of short-term Fourier analysis parameters

1) Voiced speech

Sampling frequency : 10 kHz

Block size (N) : 256 points

Block period (T) = 25 msecs

Frequency resolution = 40 Hz

Smoothed over 4 frequency points.

Typically voiced speech sections are seldom shorter than 100 msecs and individual phonemes are often held this long. Exceptions might be the short 'i' as in sit or the short 'u' as in cut.

ii) Unvoiced speech

Frequency resolution is less essential for unvoiced speech, but the duration of short transients such as K, T, P, may be $\leqslant$10 msecs. Thus Fourier parameters were chosen as follows:

Sampling frequency (Fs) : 20 kHz

Block size (N) : 256 points

Block duration $\simeq$ 10 msecs

Frequency resolution $\simeq$ 80 Hz

Smoothed over 10 frequency points.

The speech signal was sampled at 20 kHz. During unvoiced speech, the data blocks were loaded with every time sample obtained; during voiced speech every other time data point was taken. The choice of voiced/unvoiced was made from an analysis of the variance of the throat microphone signal over 20 sample points. The threshold trip level was somewhat arbitrary and was set to suit the individual. Under normal speech conditions (i.e. no shouting or whispering) this form of voice detection was found adequate. Thus each phoneme has a voiced/unvoiced characteristic as an initial identifier.

The identification procedures for voiced speech require the spectral estimates to be normalised both in terms of signal variance and voice pitch. Normalising to the signal variance is straightforward; normalising to the voice

pitch is more complicated.

Previous spectral techniques for obtaining the voice pitch have utilized the cepstrum (reference 21). This is defined as 'the modulus of the Fourier transform of the logarithm of the normalised speech output auto-spectrum.' Typical results obtained from this analysis are shown in Figure 3, the horizontal scale being in a quasi-time domain, the voice pitch being $1/\tau$ Hz. Figure 3 shows the cepstrum results for the spoken vowel 'ā' (as in Kāte) This form of analysis is costly in computer time and somewhat clumsy.

FIGURE 3 : Shows a typical series of cepstrum results as obtained during voiced speech.

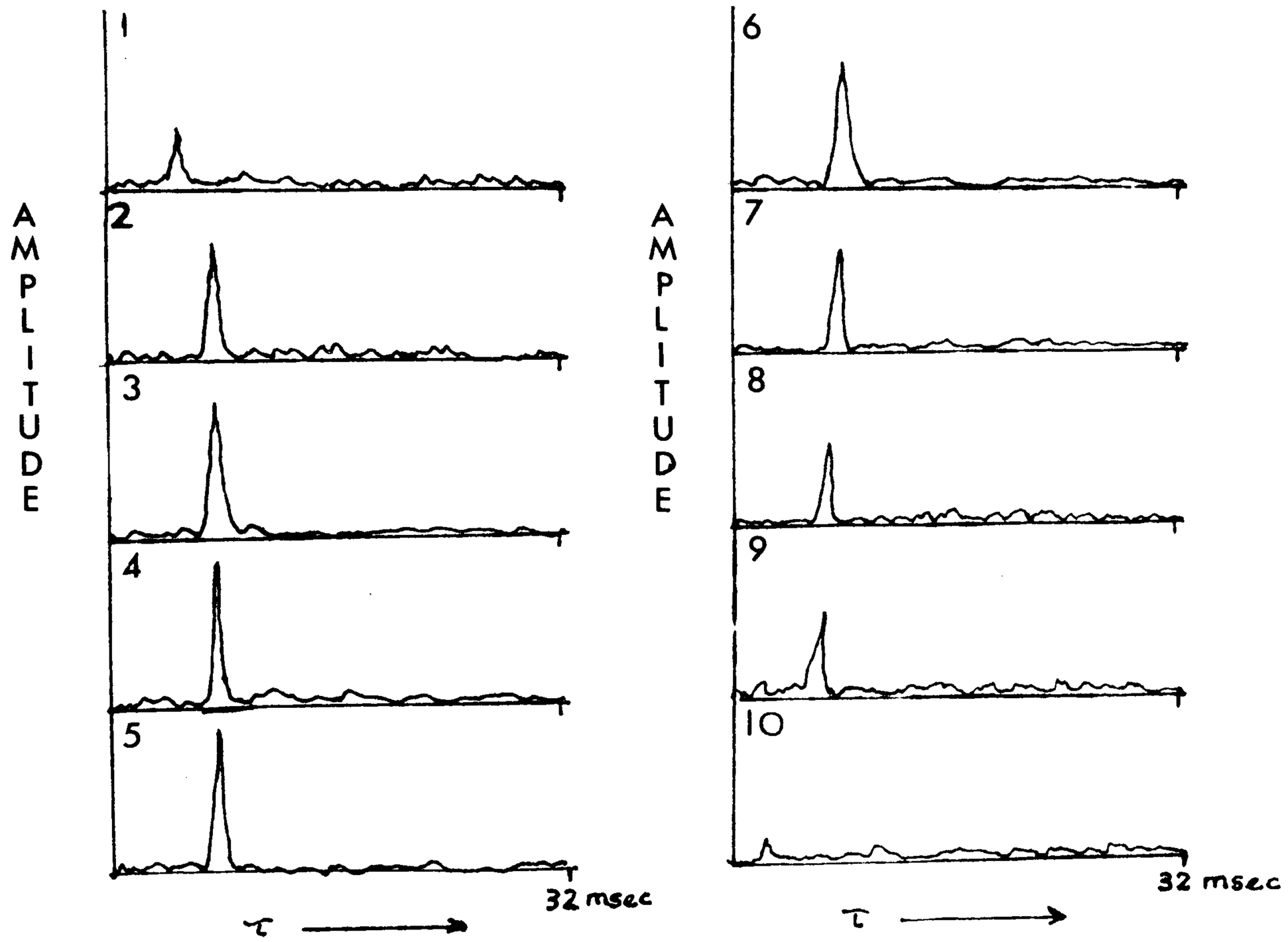

The alternative as used here is more simple and reliable. Figure 4 shows a typical output spectrum as obtained from the throat microphone.

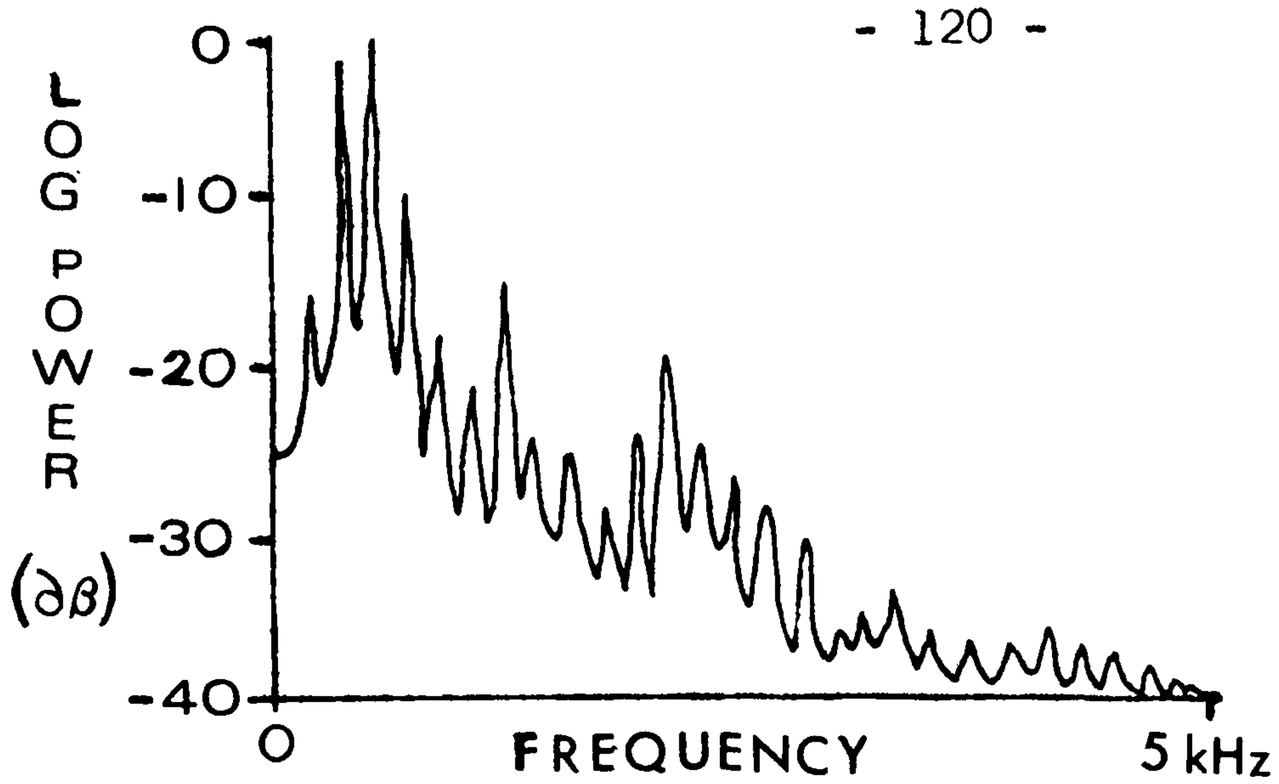

FIGURE 4 : Shows a typical auto-spectral estimate obtained from the throat microphone during voiced speech.

It is found that the first five maxima are always easily discernable in spoken speech, regardless of the vowel sound uttered. The computer program records the frequency of the fifth maximum and divides accordingly to find the voice pitch. This involves the computer in typically less than 30 compare-and-branch steps compared to at least N log N (N = 128) complex multiplications, using an F.F.T. algorithm, to find the cepstrum. The result is also less dependent on the high frequency content of the input spectrum. All vowel phonemes are tabulated and identified as a function of the voice pitch frequency rather than just frequency. This makes the phonemic patterns as far as is possible independent of context and intonation. Whether the patterns are also speaker-dependent was not thoroughly tested. For one female, one male tested the results were inconclusive. It is extremely unlikely that the results are independent of accent.

3) STATISTICAL TESTING OF SPEECH

Considering the schematic block diagram of Figure 2 the feedback loop is considered of secondary importance. Thus the system is treated

as open-loop. The statistical test employed is dependent on the voiced/unvoiced decision.

i) Voiced speech

Four parameters are tested, the input auto-spectrum, the output auto-spectrum, the best estimate of the noise auto-spectrum and the frequency response. The auto-spectra of successive blocks are normalised to their measured total power and smoothed over 4 frequency points in the Ω domain (see end of next paragraph).

Successive block estimates are compared with previous blocks for stationarity. The process is 2-level. The first level compares adjacent blocks while the second level compares blocks one block removed. The first level is sensitive to sudden step changes while the second level gives an indication of slower transients within phonemic sounds. (e.g. the vowel $\grave{a}$ ends as an $\bar{e}\bar{e}$ in many contexts). This two-tier system was envisaged as a possible means of building a degree of sophistication into the analysis system for possible later developments in the pattern recognition side. The concept of frequency was dropped in favour of normalisation to the voice pitch. Thus frequency ω in Hz is replaced by Ω in terms of the voice pitch. Smoothing is conducted in the Ω domain.

An F-test with 8,8 degrees of freedom was used to test the stationarity of the auto-spectral estimates.

$\left\{ F = \phi_1(\Omega) \,/\, \phi_2(\Omega) \right.$ where $\phi_1(\Omega)$ and $\phi_2(\Omega)$ are the estimates to be tested at frequency Ω such that $F \geqslant 1.0 \left.\right\}$

$$P_F = \int_F^{\infty} P_{8,8}(\lambda)\, d\lambda \qquad \ldots\ldots\ldots 4.1$$

where P_F = Probability of $\lambda \geqslant F$ given ϕ_1 and ϕ_2 are samples from a stationary process. Therefore the probability that a change has occurred is given by $(1-P_F)$. However, if $F = 1$ (the expected value in this case for stationary

systems) we wish the probability of change to equal zero. Thus equation 4.2 is used to give a mean stationarity confidence level:

$$CONF = \frac{200}{\Omega max} \int_0^{\Omega max} \int_1^{F(\Omega)} P_{8,8}(\lambda) \, d\lambda \, d\Omega \quad .... 4.2$$

where the constant term $200/\Omega max$ ensures CONF varies from 0-100%. In the discrete case the integral in Ω is a normalised summation over the frequency band 0 - Ωmax.

This test is used on the 3 auto-spectral estimates with the number of degrees of freedom in the test on the noise spectrum estimate reduced to 6,6.

The stationarity test on the frequency response estimate is given by equation 2.42 in Chapter 2. Again a mean level over Ω is obtained. Thus 8 confidence figures (4 for adjacent blocks, 4 for estimates one block removed) are obtained per test. In many cases only a subset of these are used.

ii) Unvoiced speech

The test procedure is similar to that for voiced speech with the following differences:

a) The frequency range of interest extends up to 10 kHz. There is no normalisation to Ω .

b) The frequency response function and input spectra contain less information. In many cases consonants are formed at the front of the mouth. (e.g. s,t,p,m,n, d, etc.) The input spectrum is useful in detecting the gutteral consonants (e.g. k,g).

4) CATEGORISATION OF THE VOWEL PHONEMES

This section presents diagrams of spectra and frequency response functions for the common vowels. The vowel responses as shown are taken

as the mean values obtained for those vowels as they appeared in a variety of contexts. Table 1 lists the distinguishing features of each of the vowels.

- - - - - - - - -

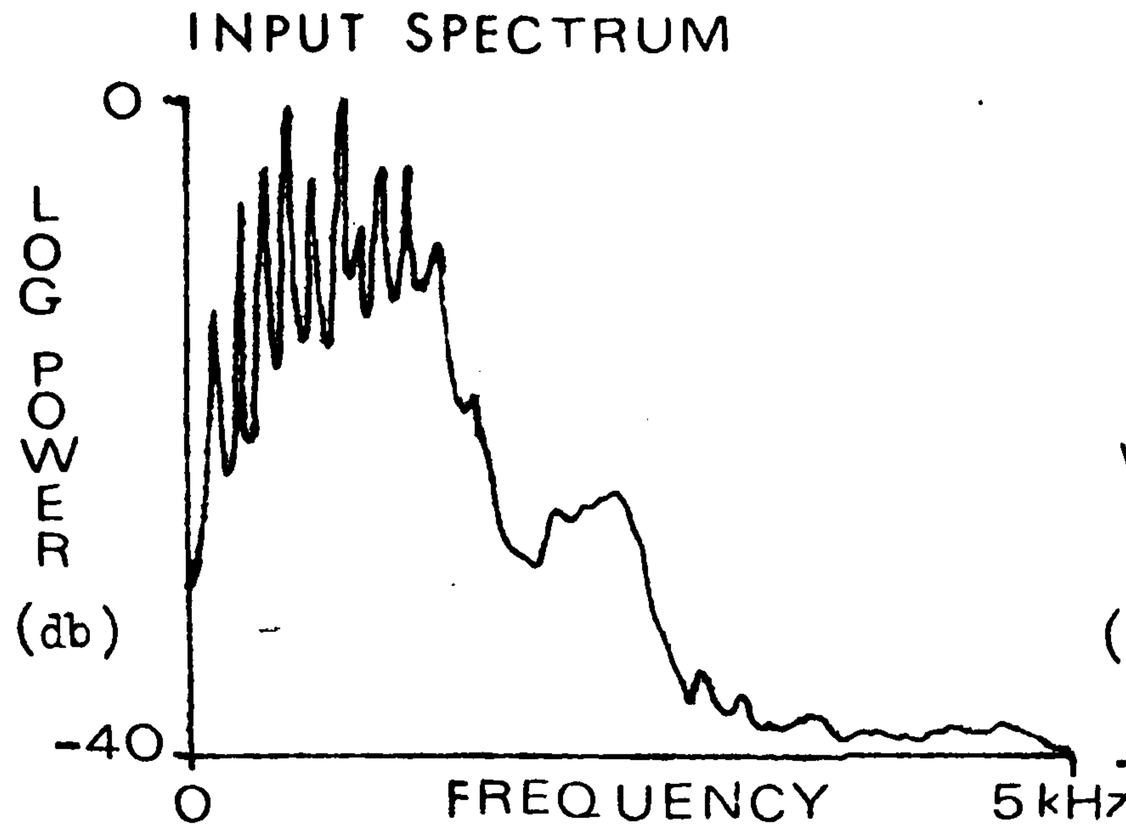

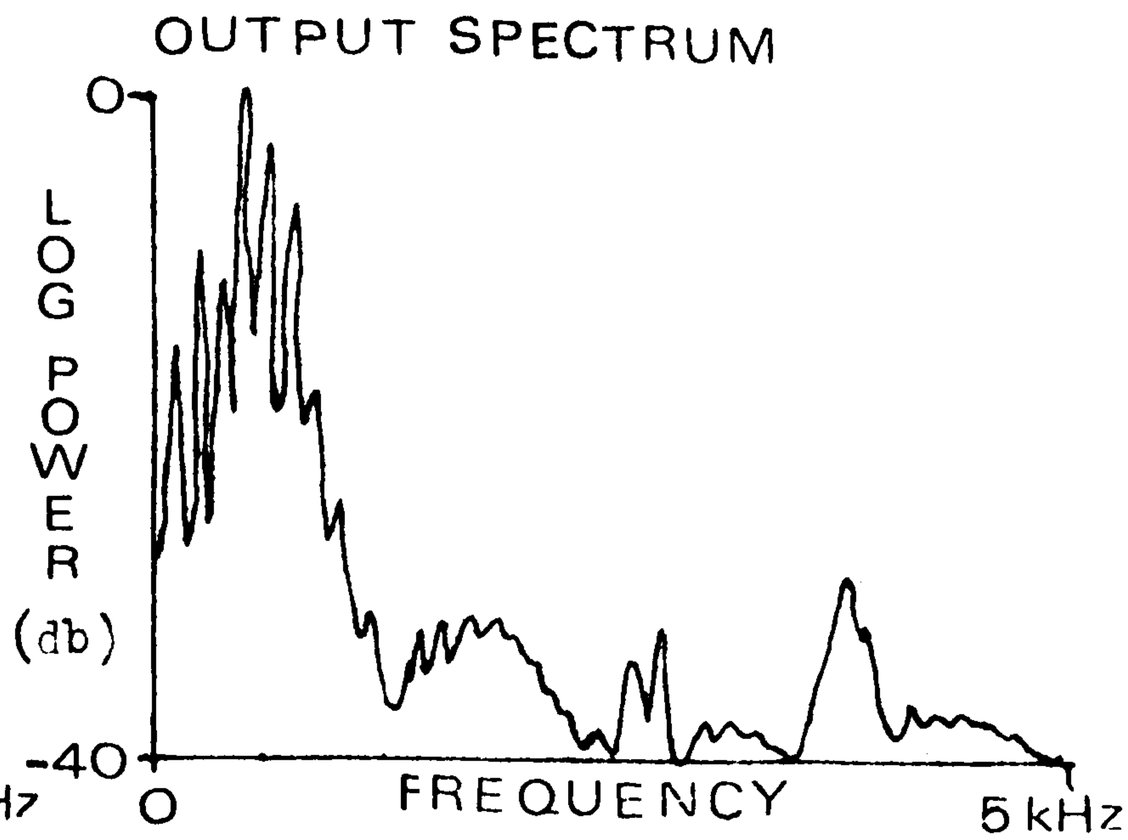

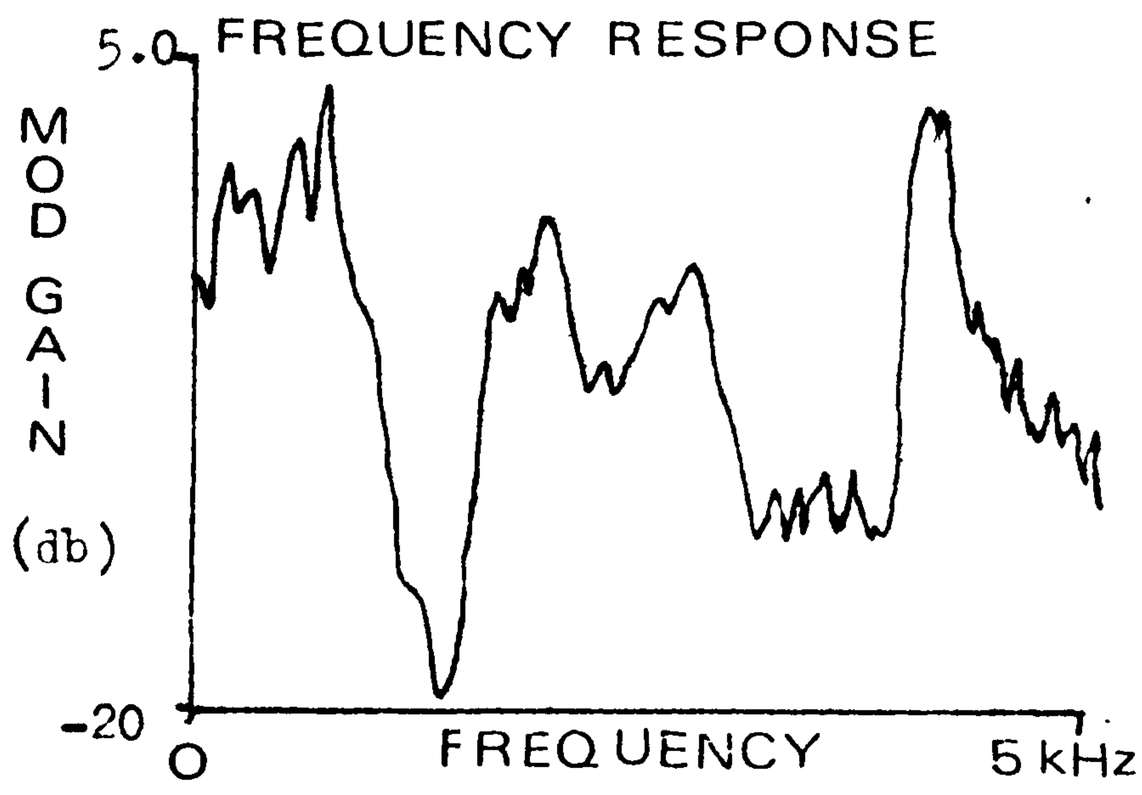

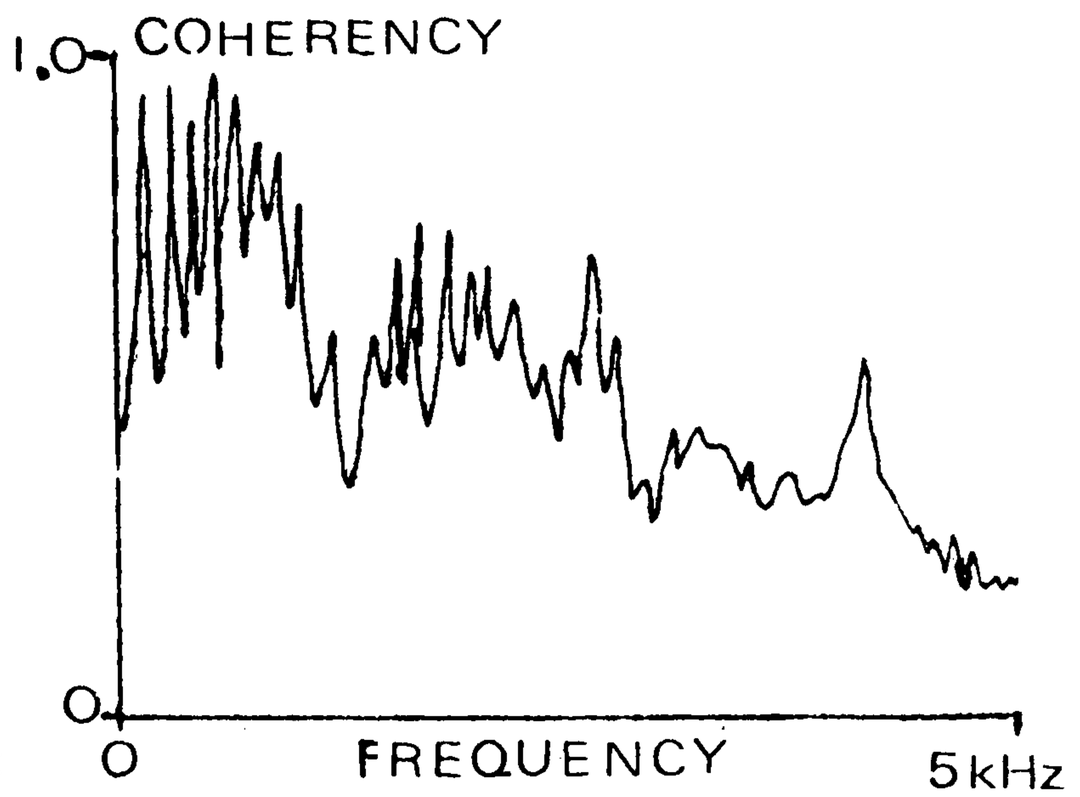

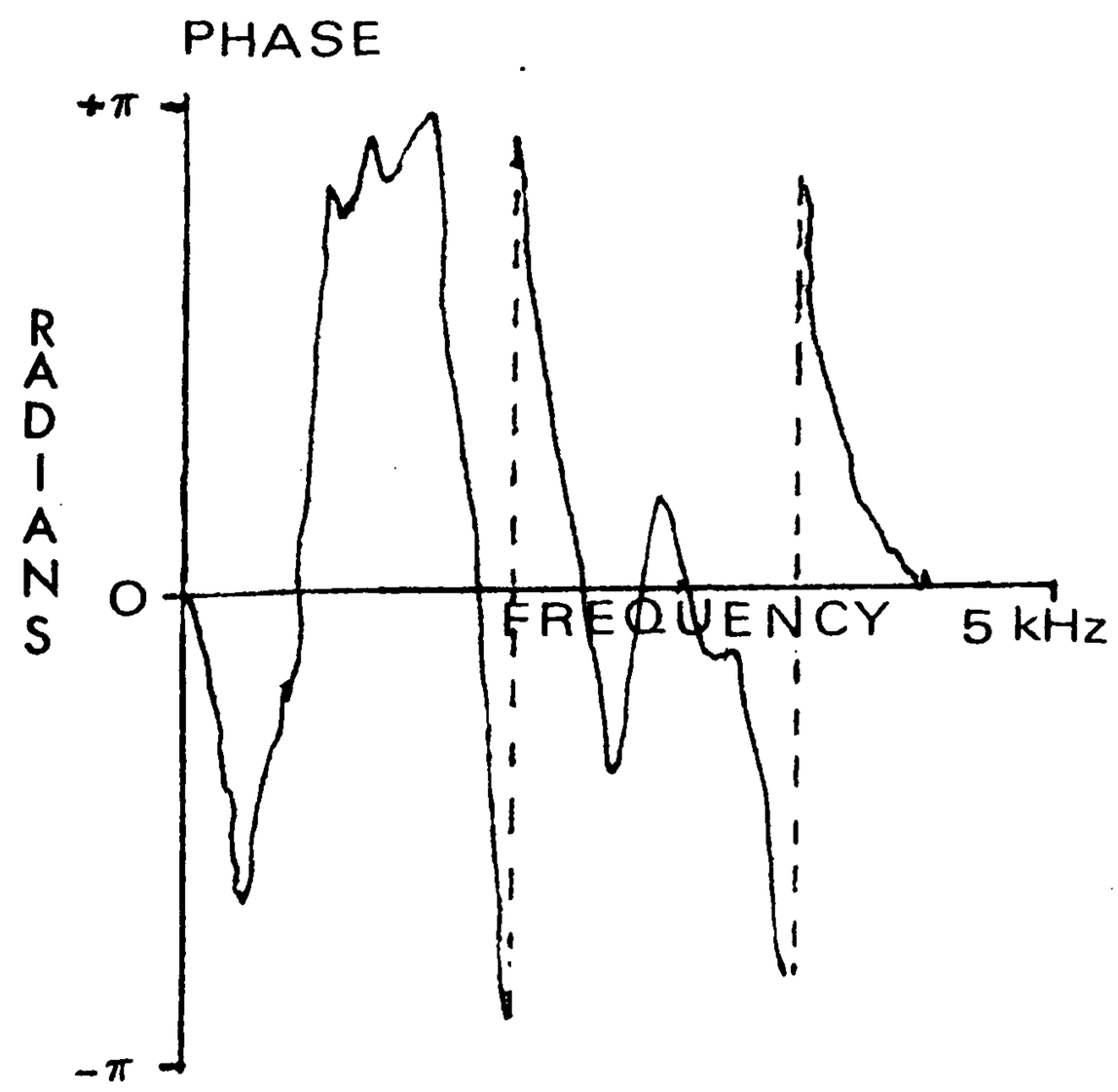

VOWEL NAME : ŏ

AS IN :- H ŏ T

FIGURE 5

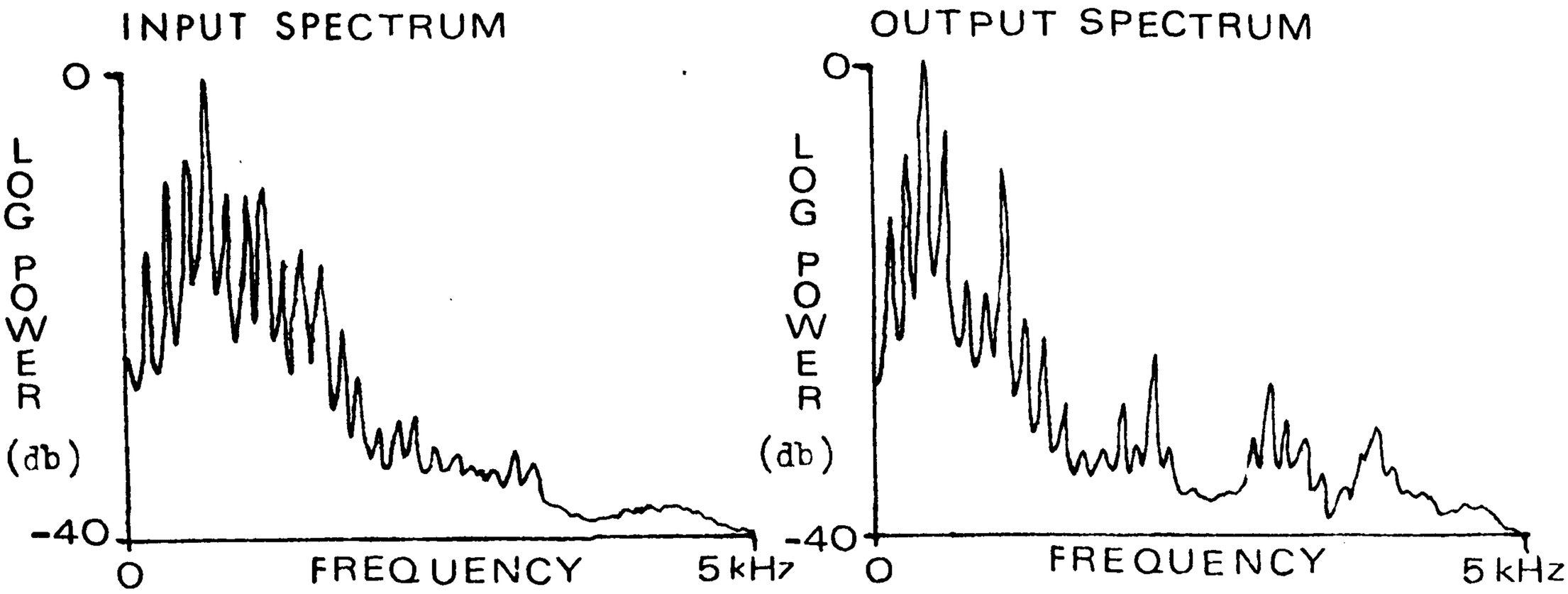

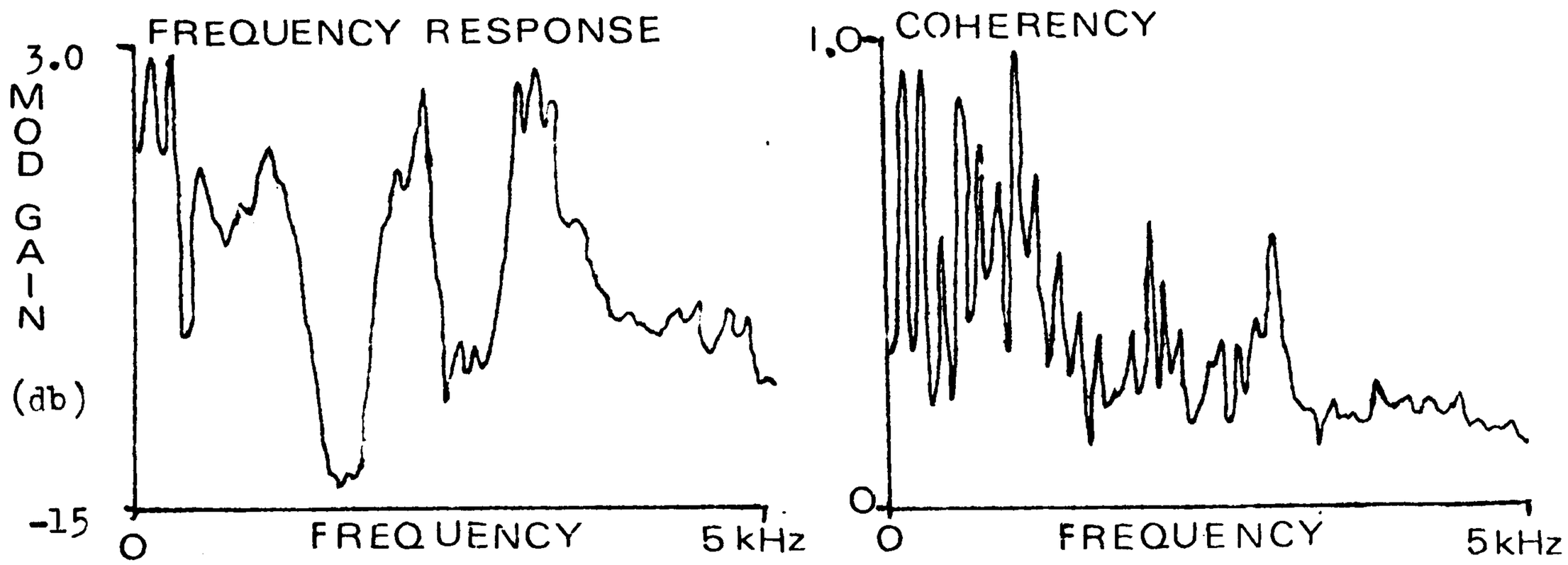

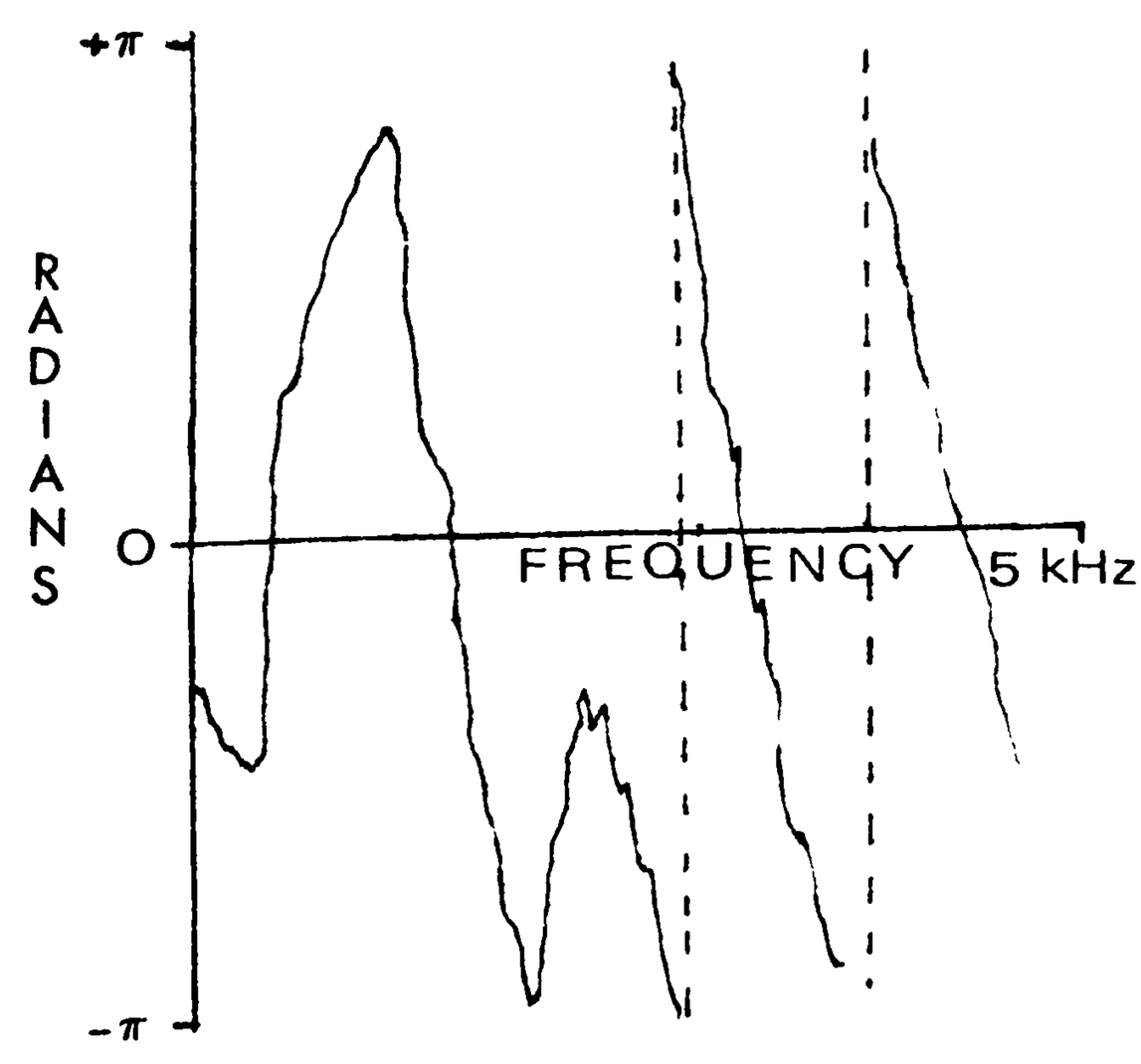

VOWEL NAME : $\bar{O}$

AS IN :- D $\bar{O}$ T E

FIGURE 6

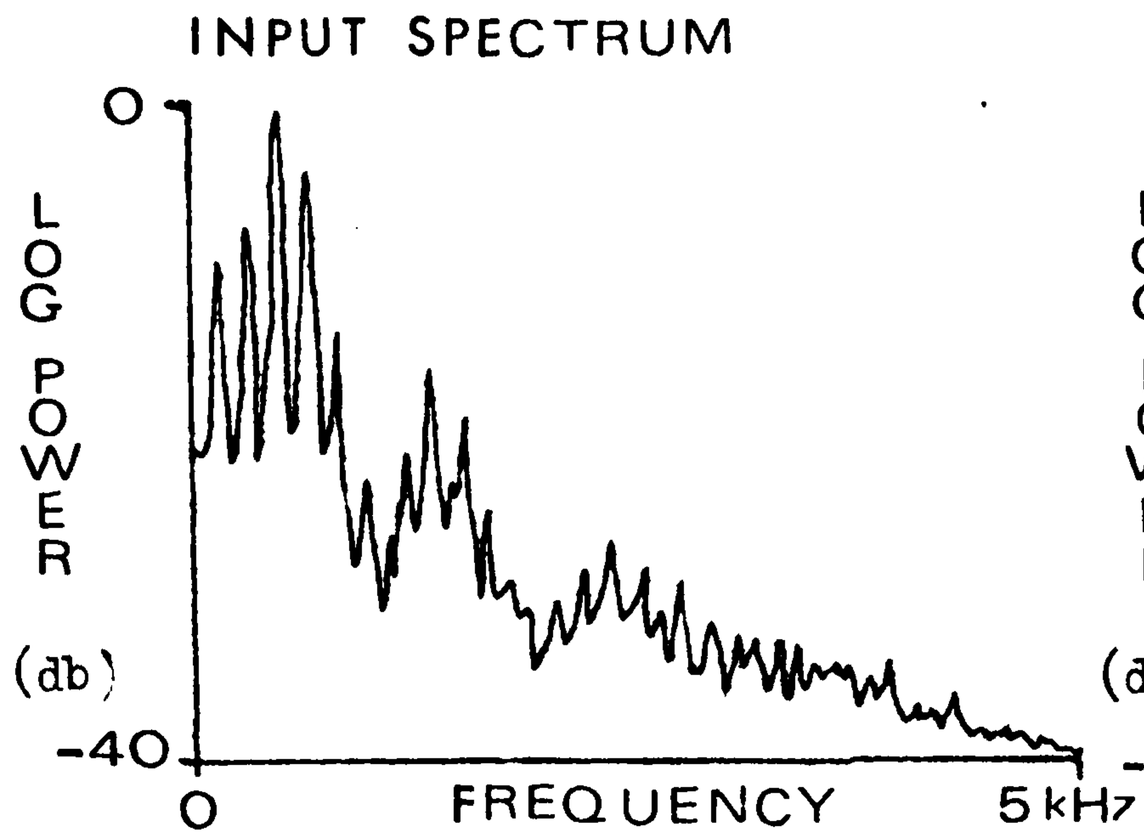

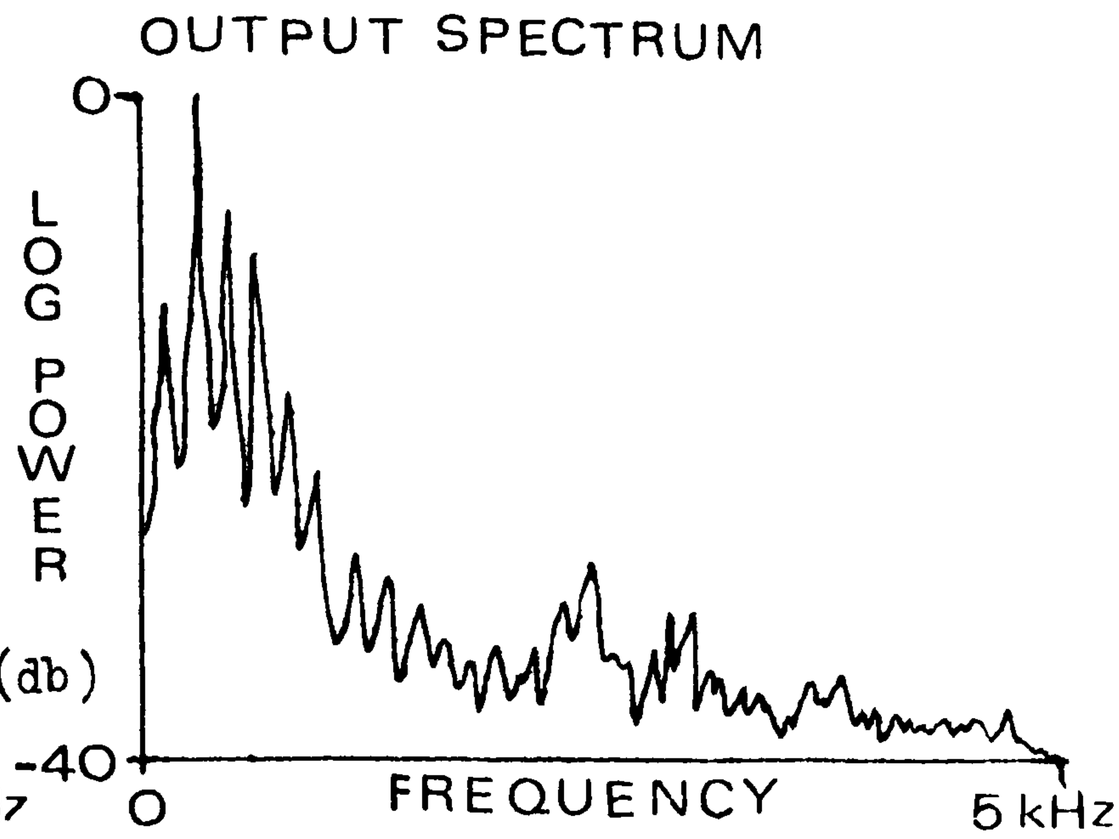

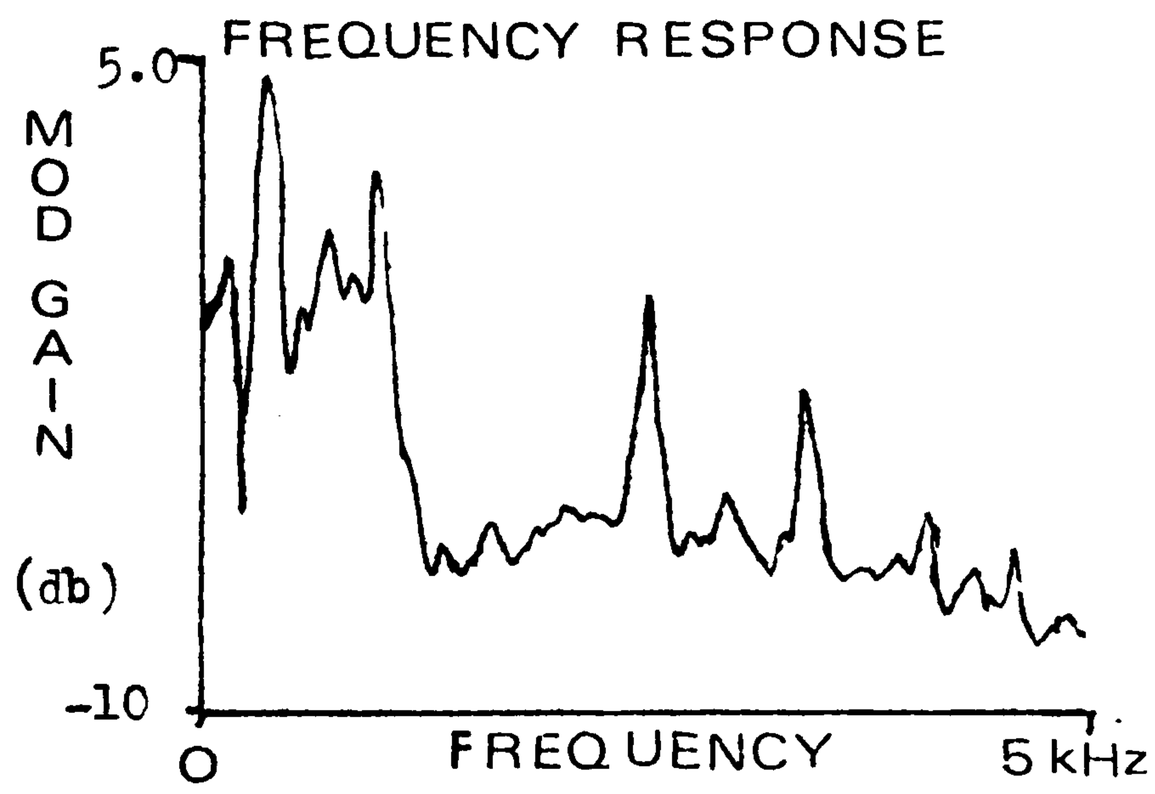

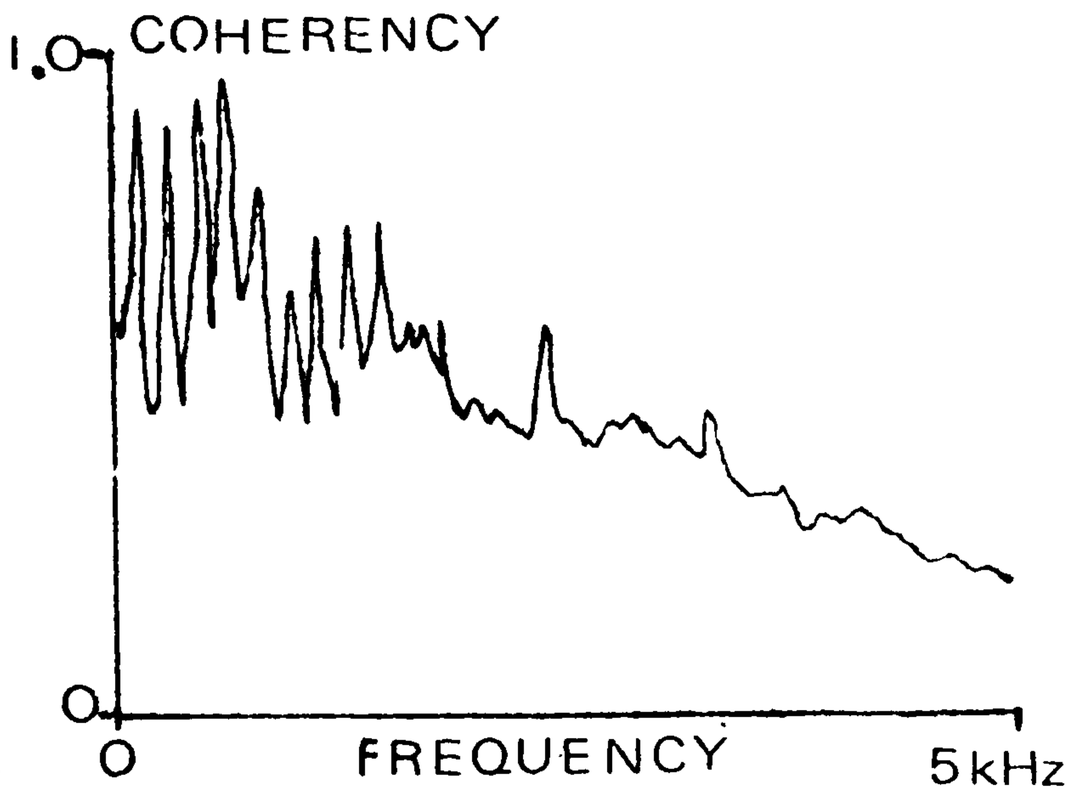

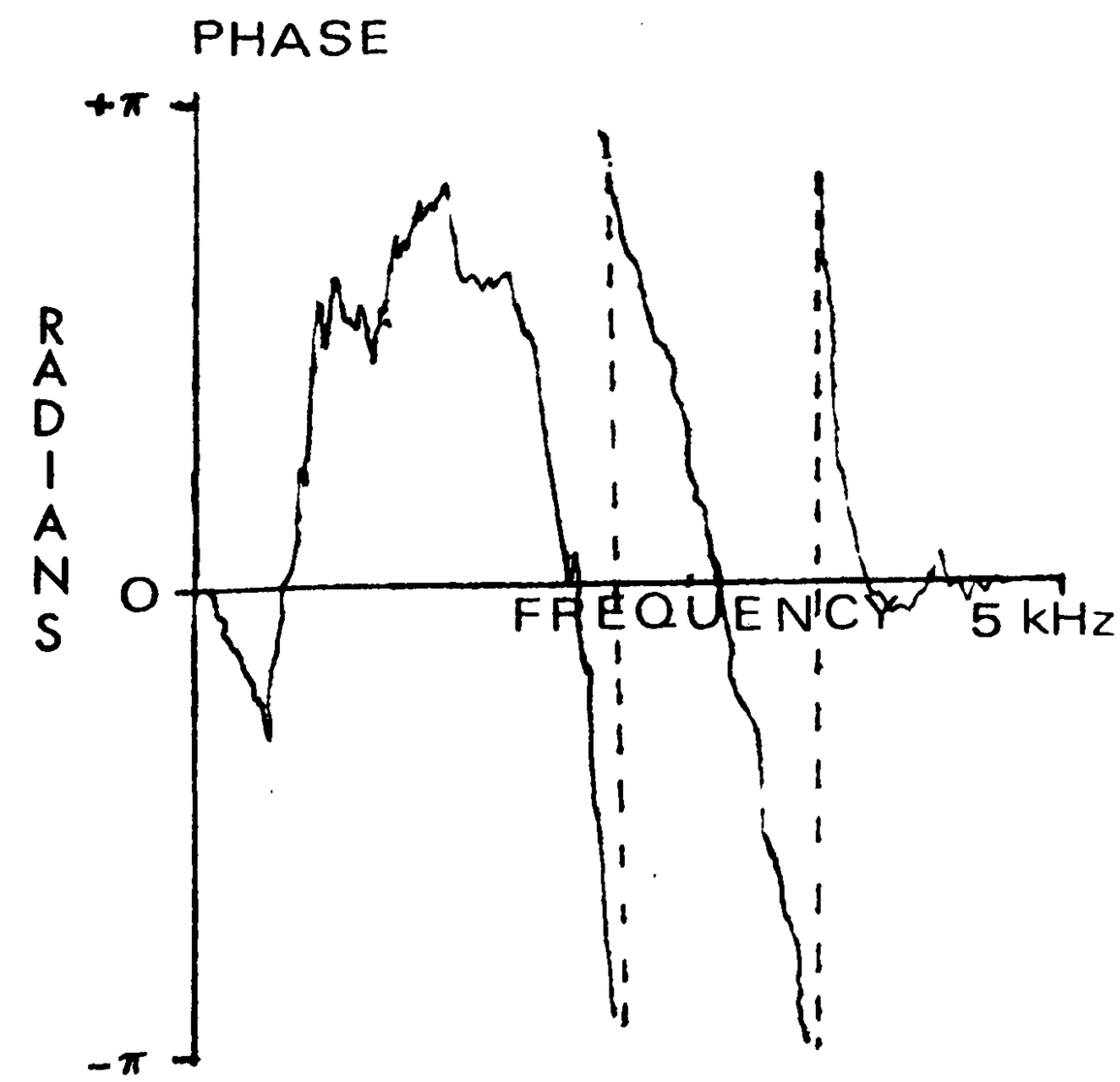

VOWEL NAME : o͡o

AS IN :- S o͡o T

FIGURE 7

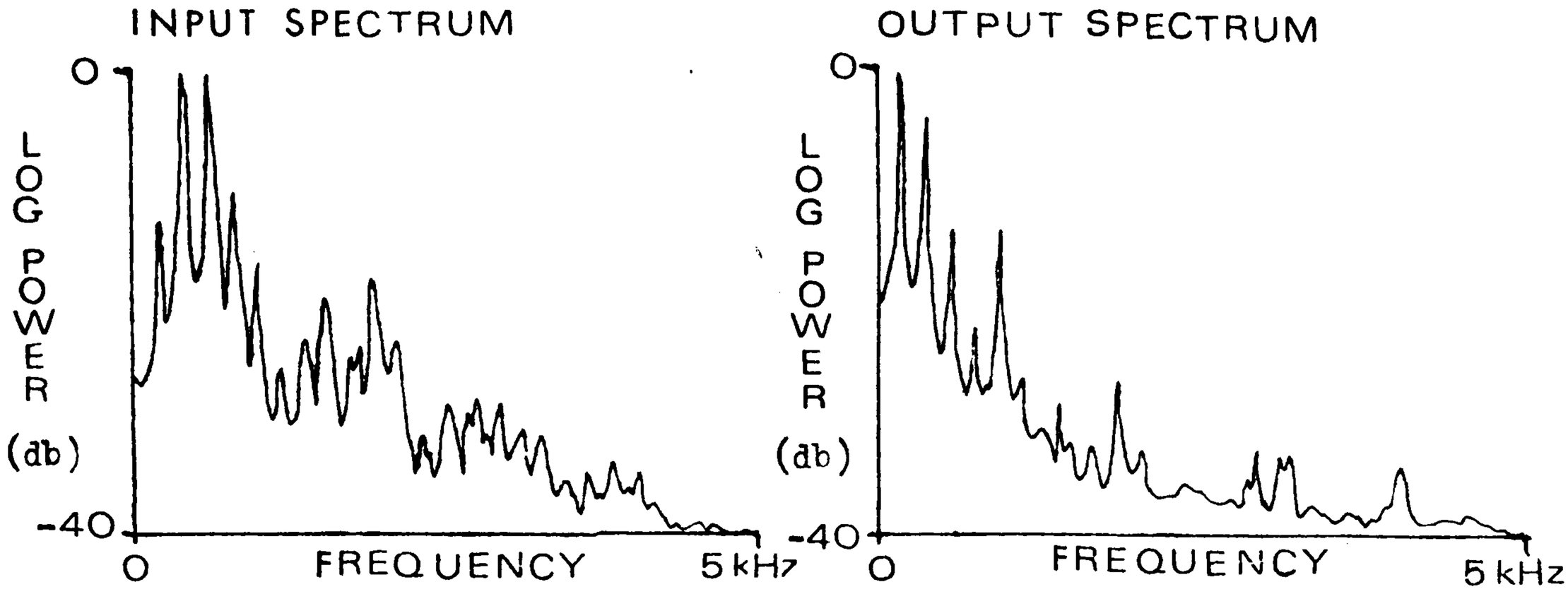

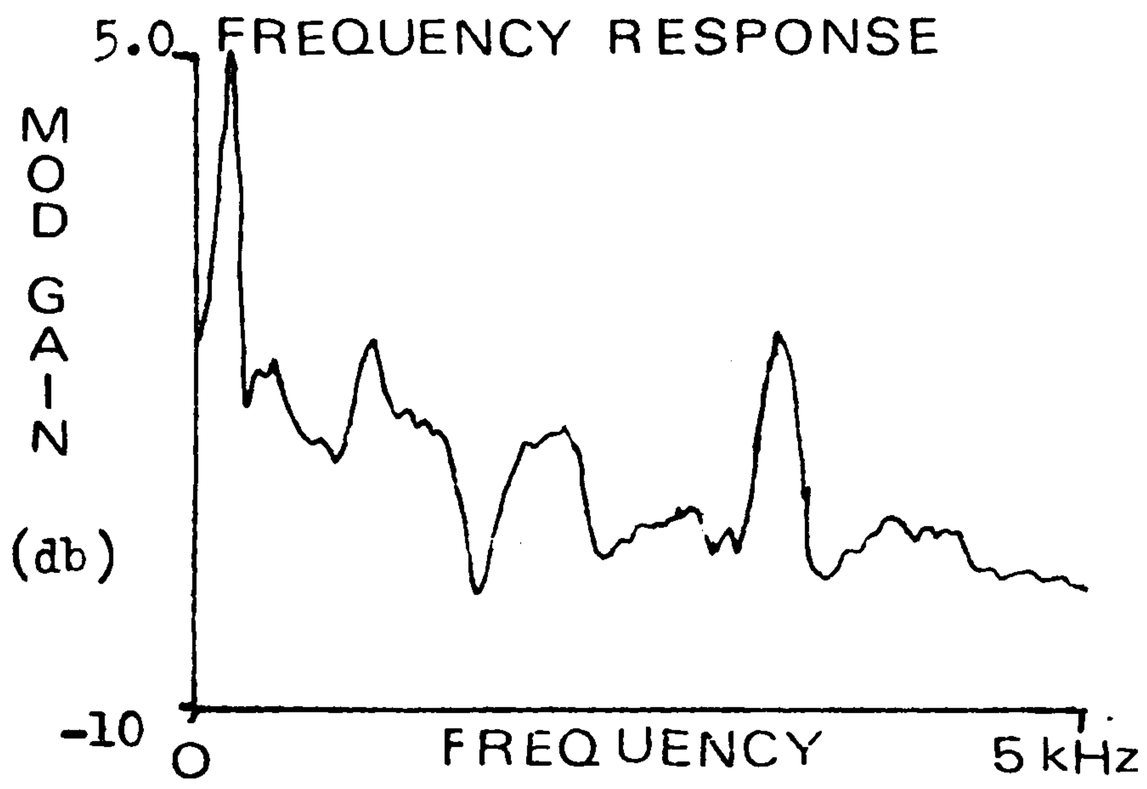

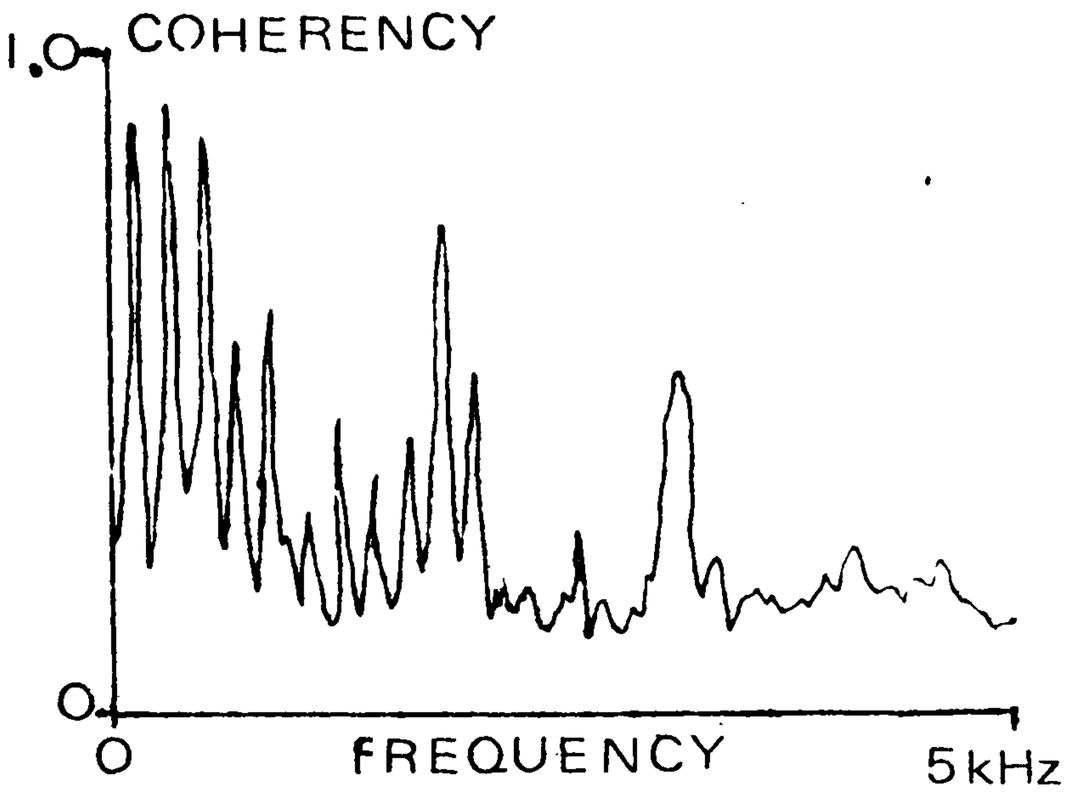

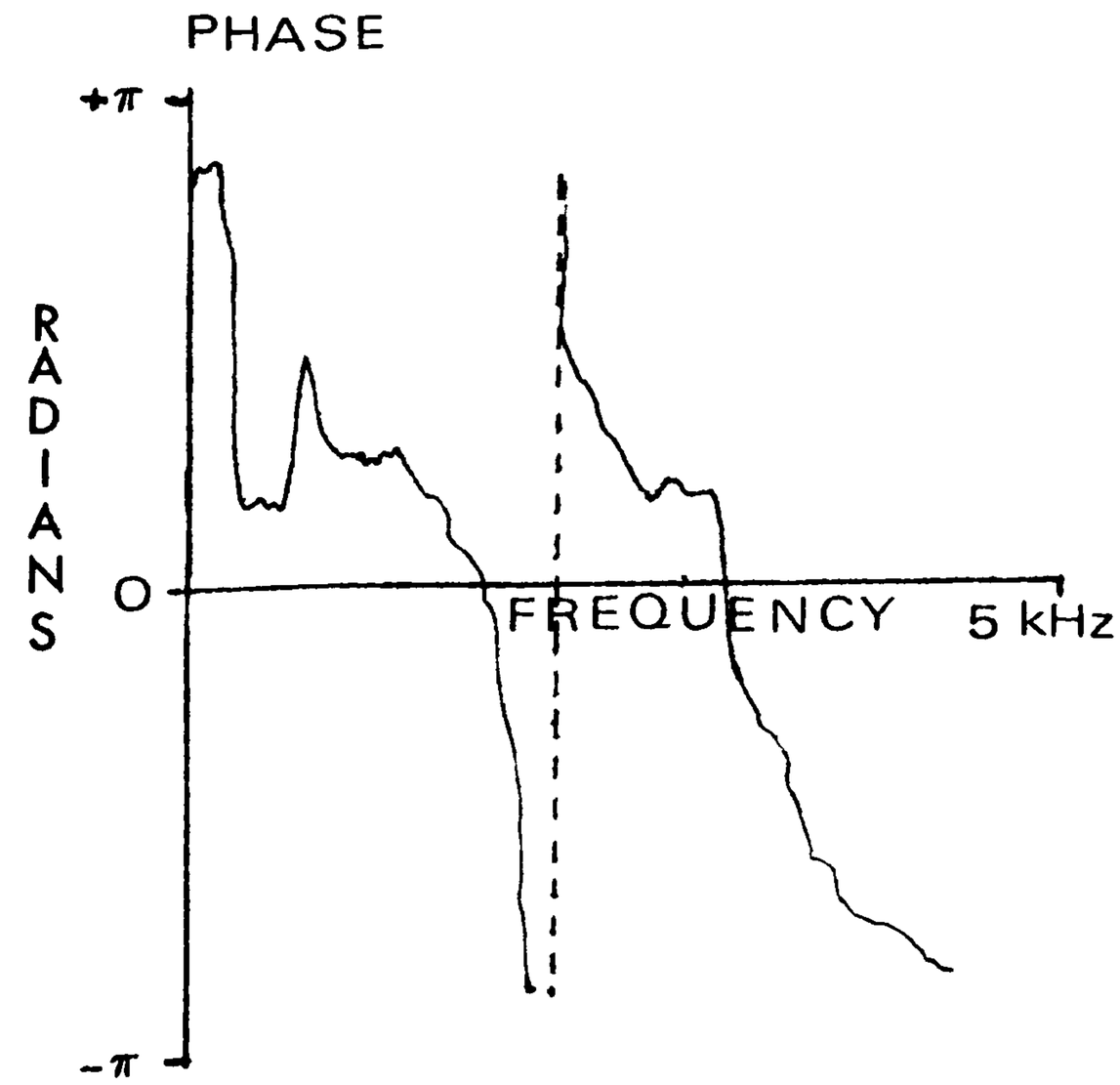

VOWEL NAME : $\overline{O}$

AS IN :- L $\overline{O}$ O T

FIGURE 8

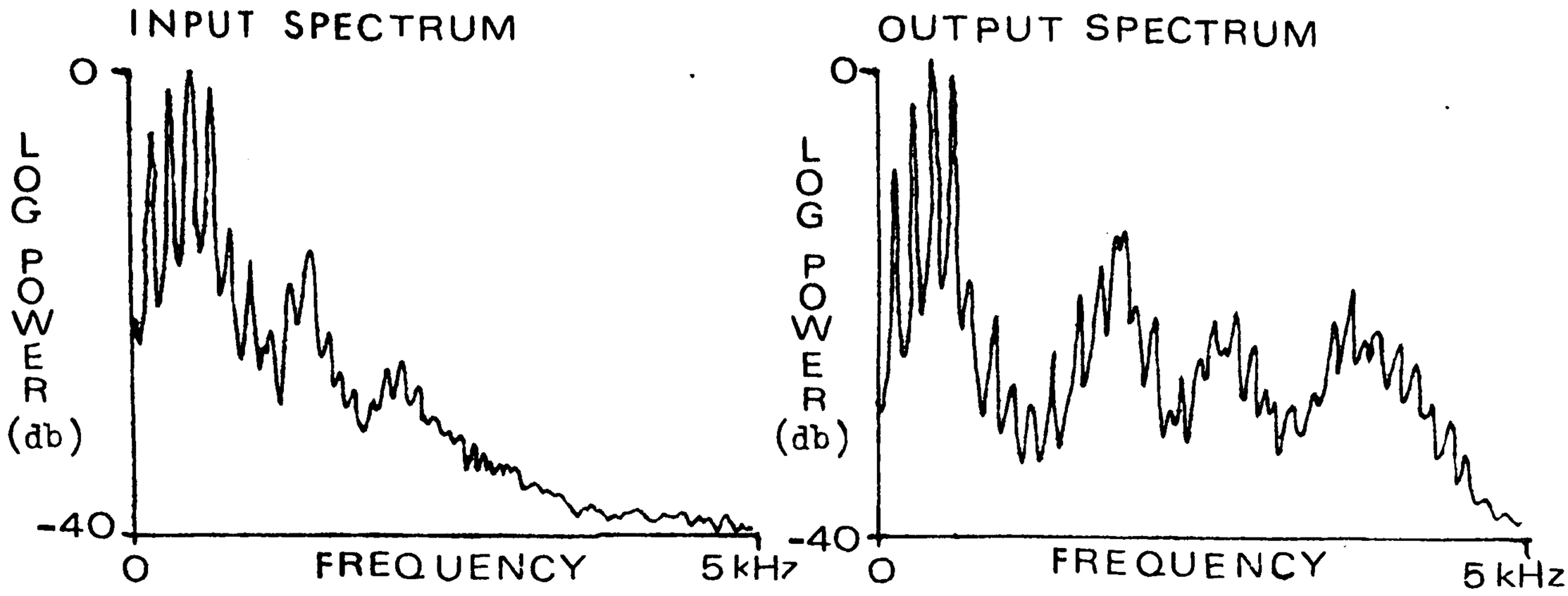

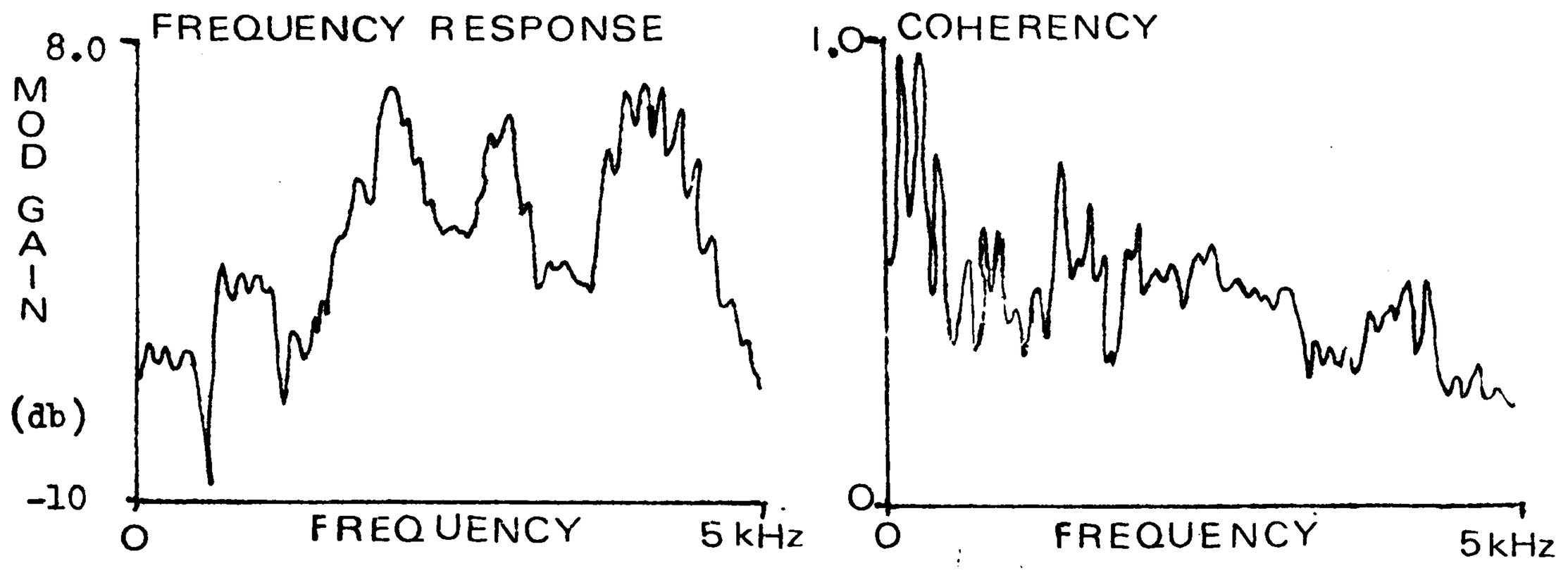

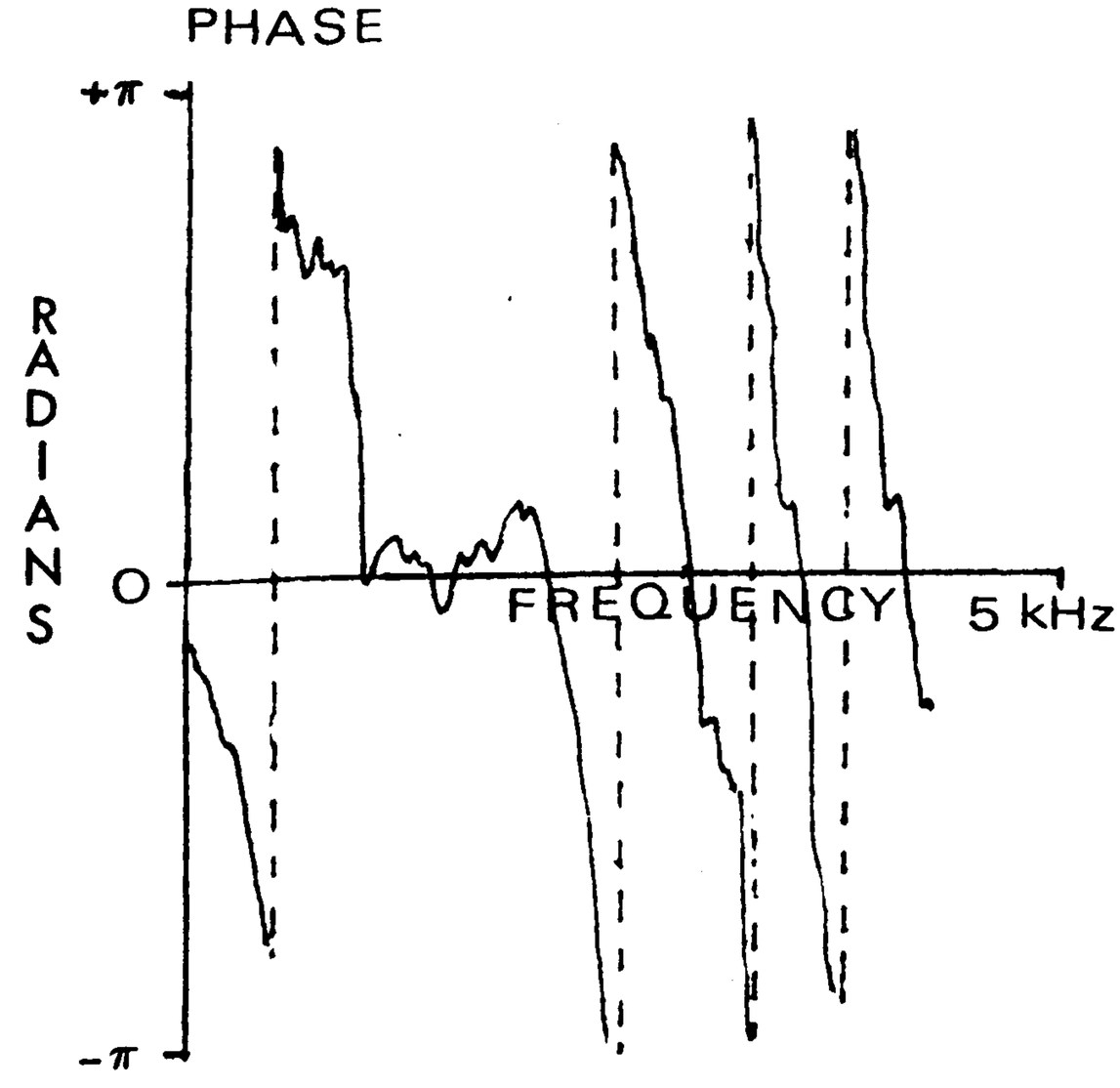

VOWEL NAME : $\bar{A}$

AS IN :- K $\bar{A}$ T E

FIGURE 9

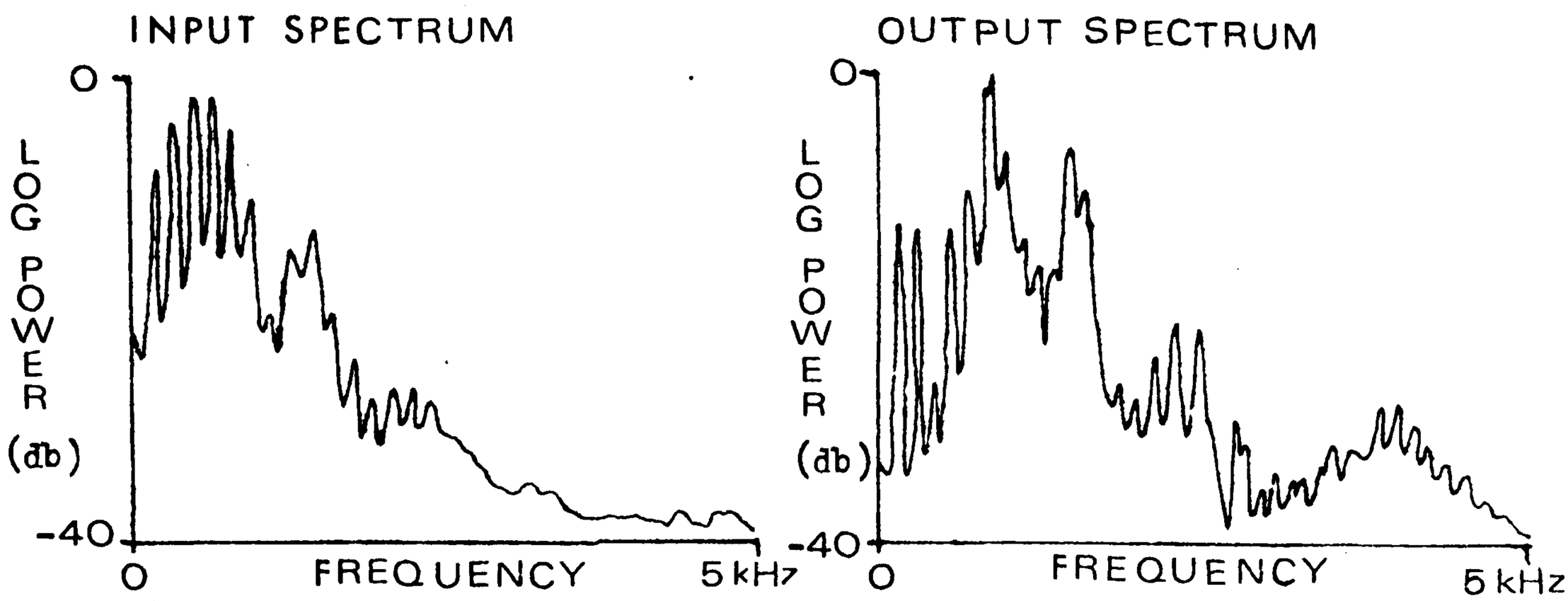

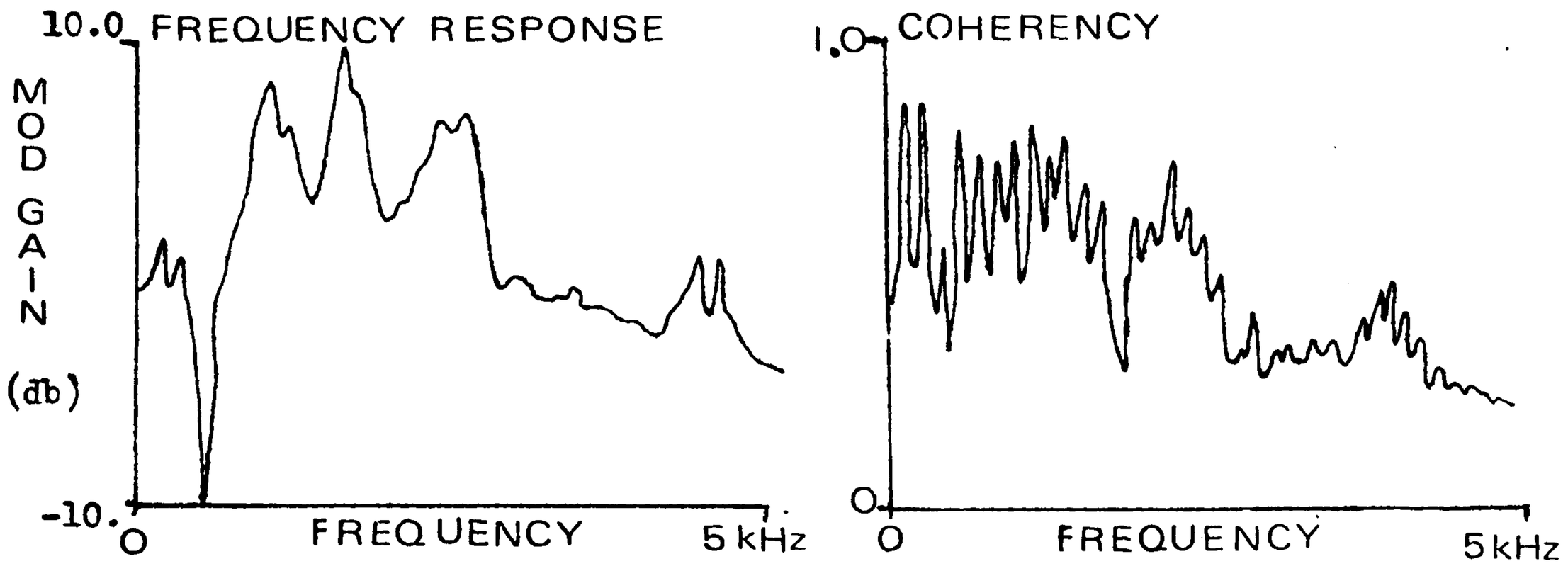

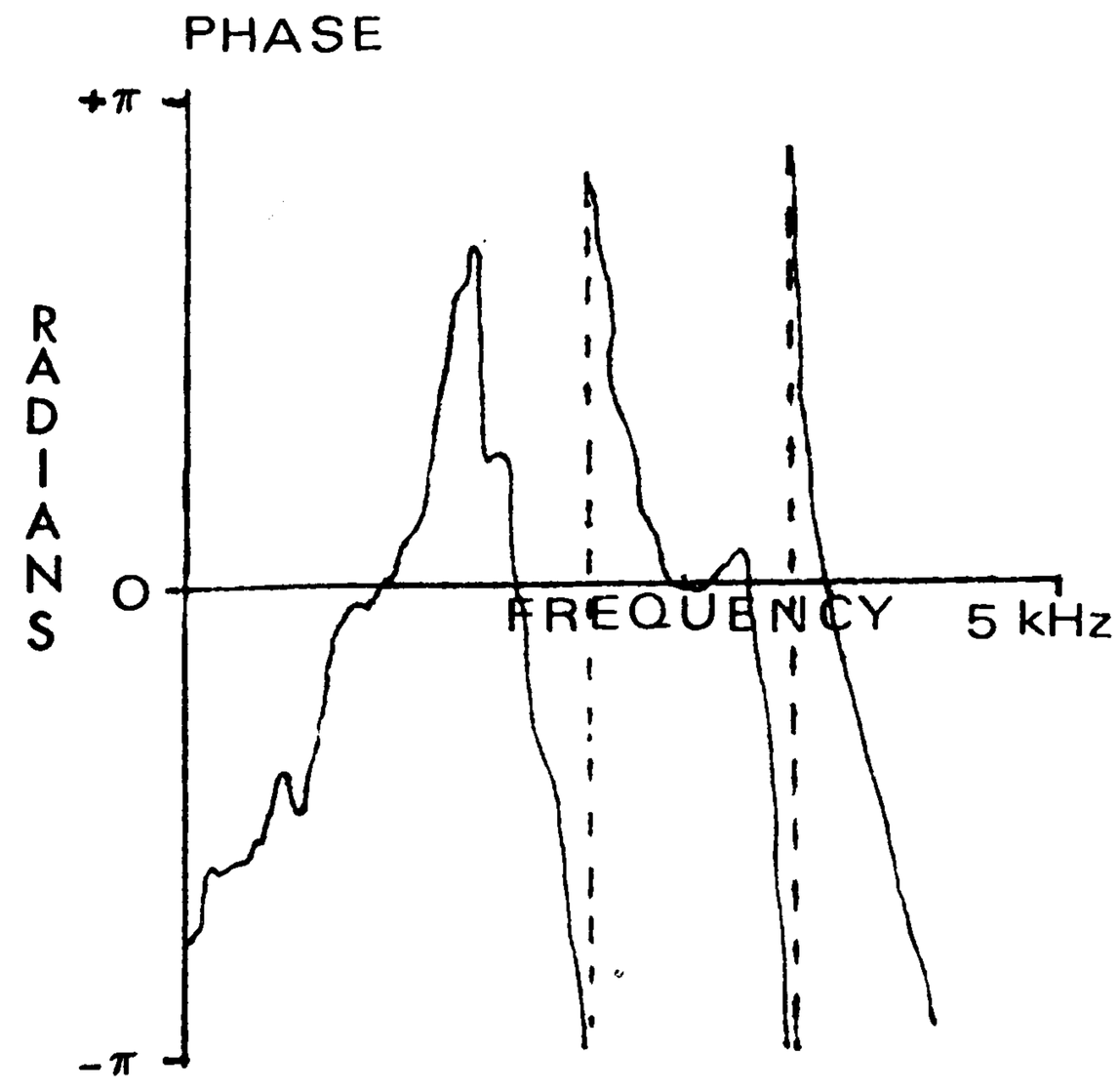

VOWEL NAME : Ă

AS IN :- C Ă T

FIGURE 10

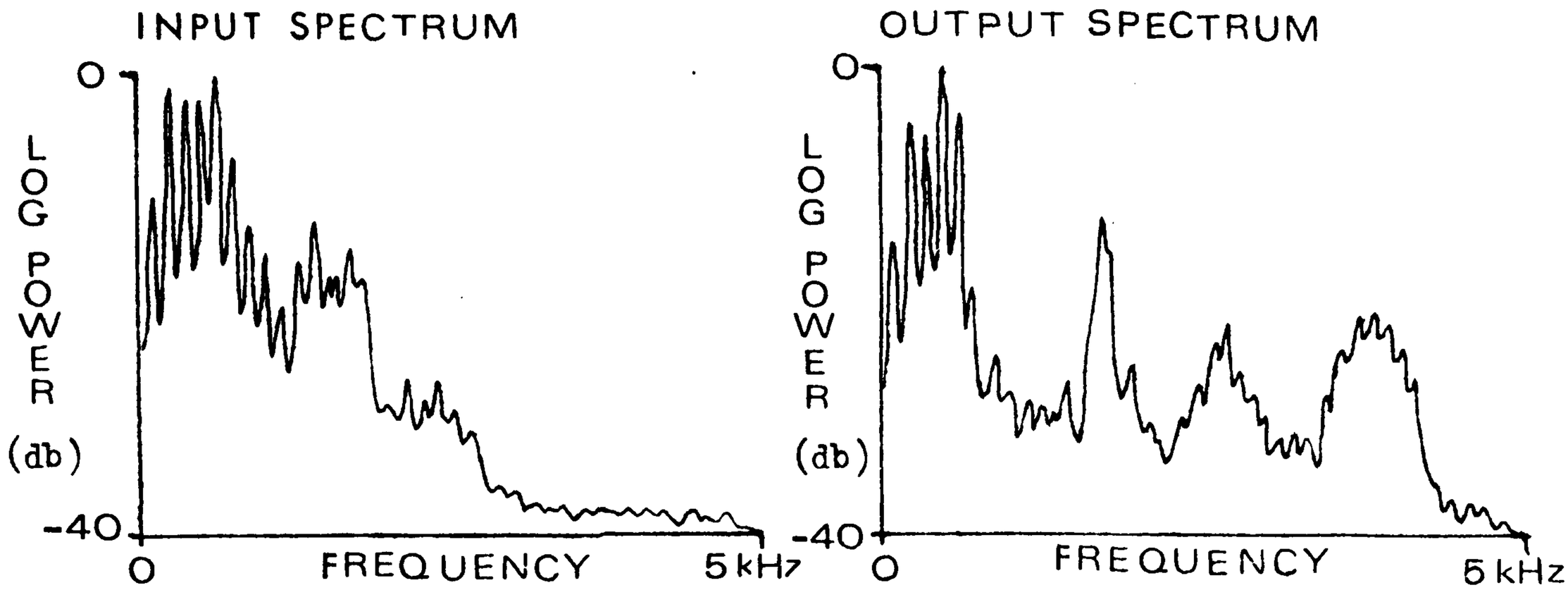

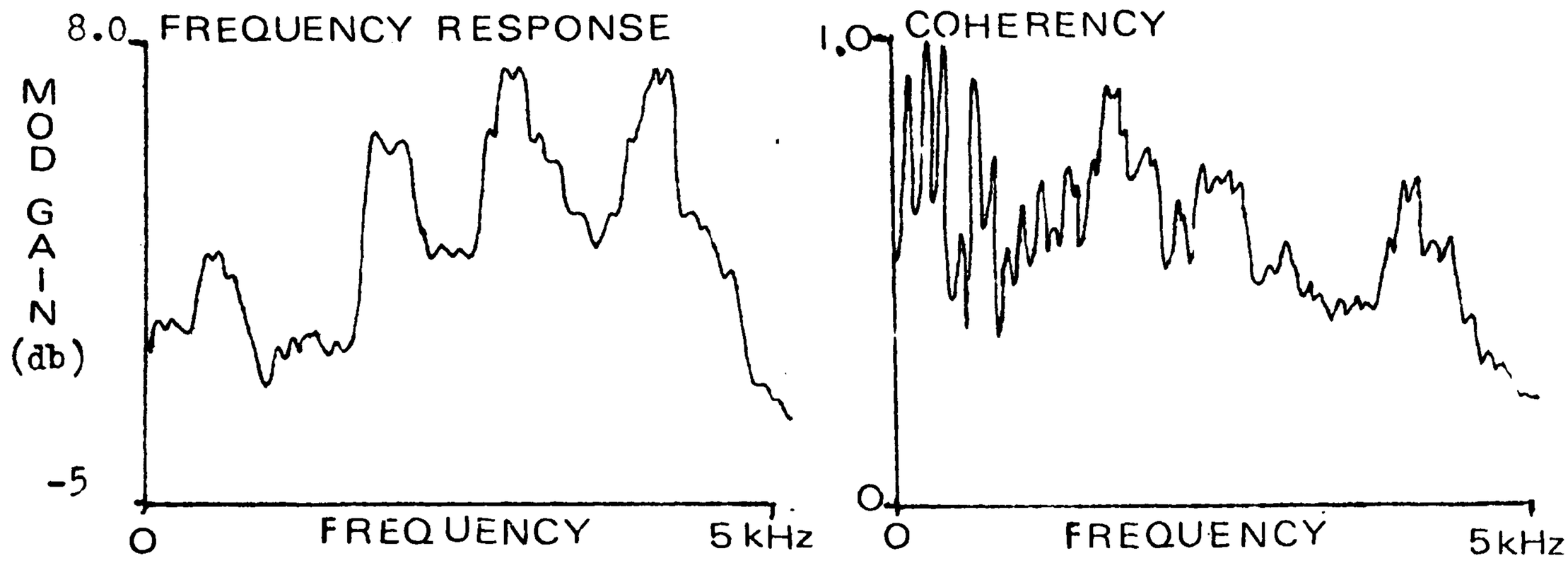

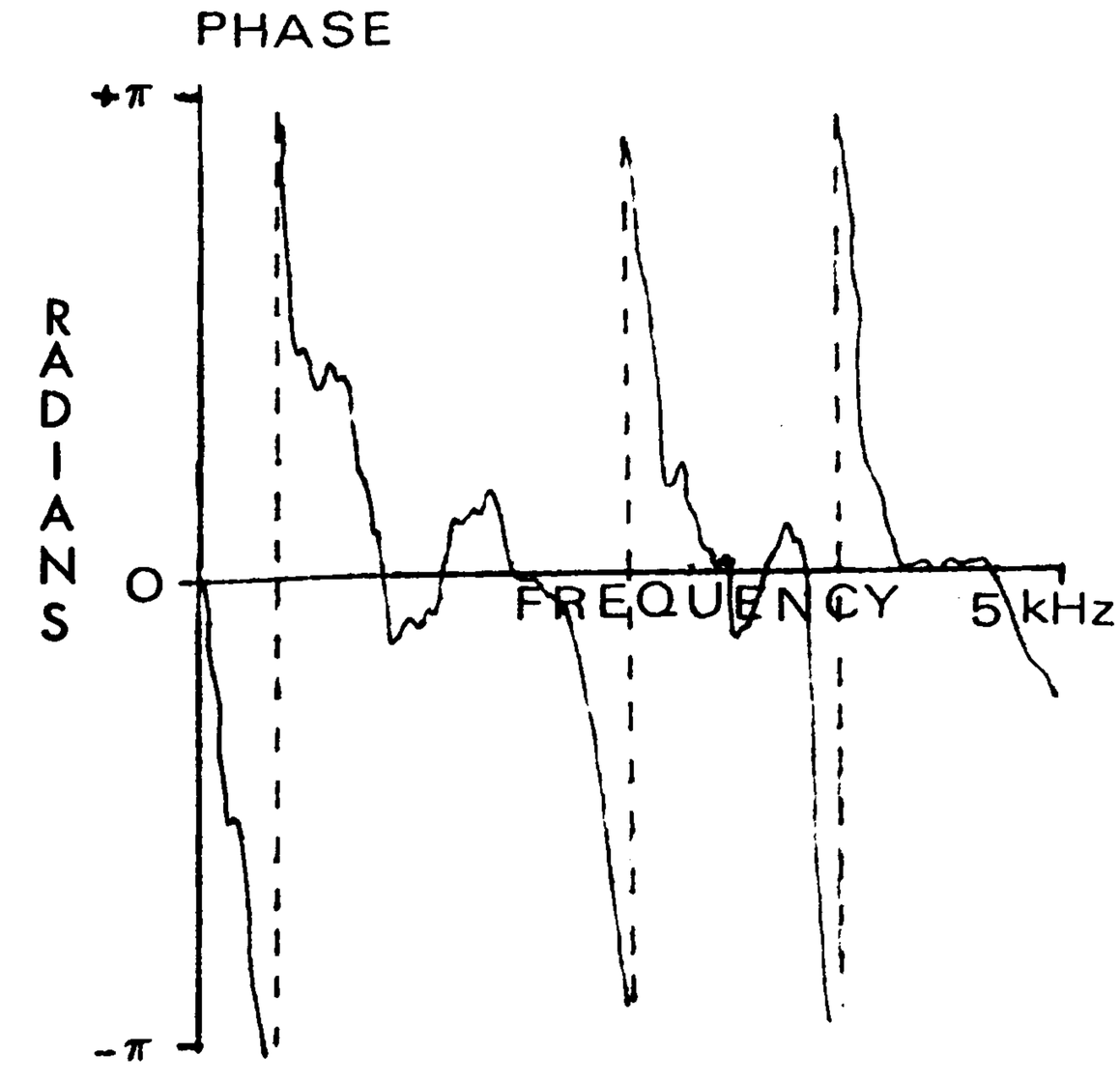

VOWEL NAME : $\breve{E}$

AS IN :- S $\breve{E}$ T

FIGURE 11

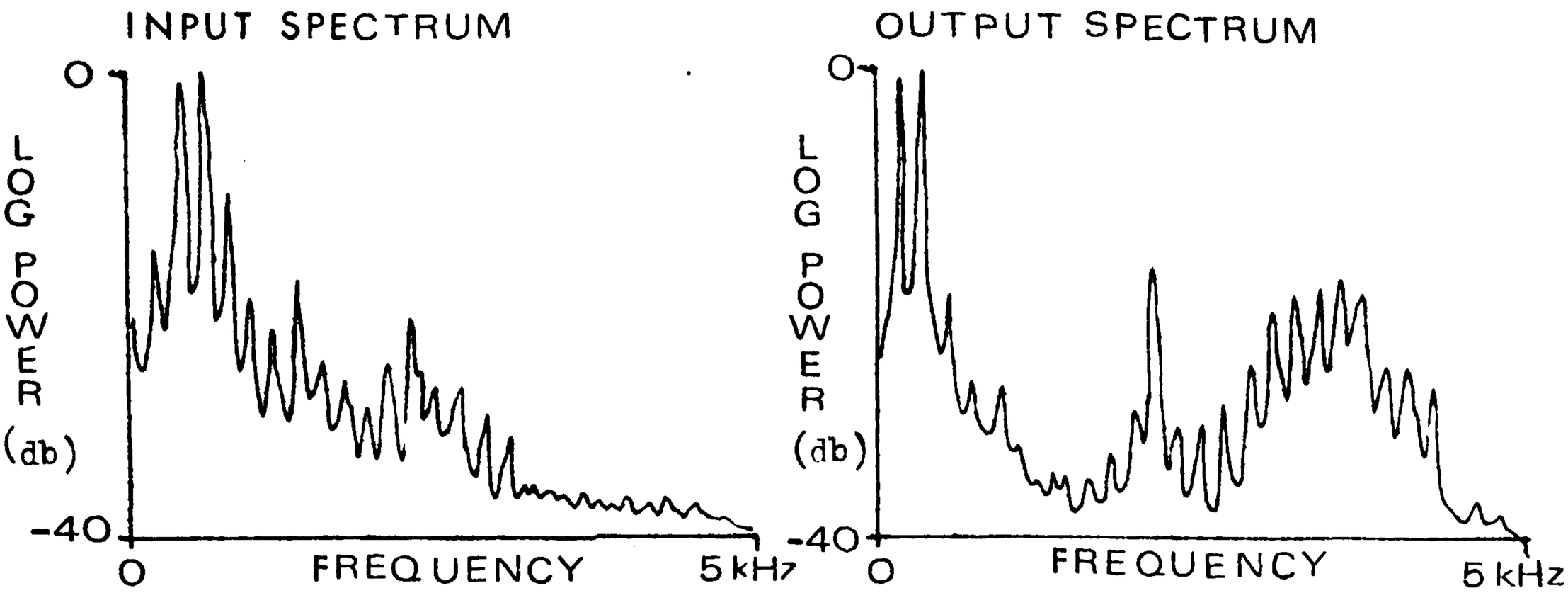

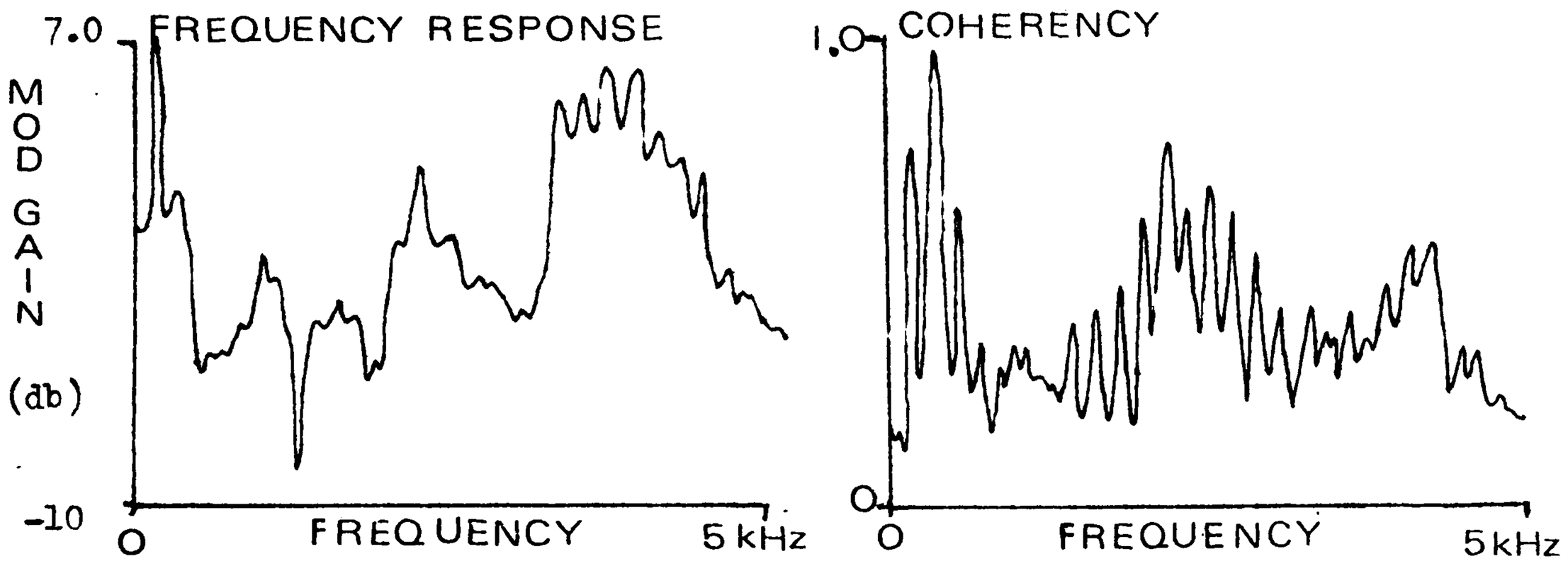

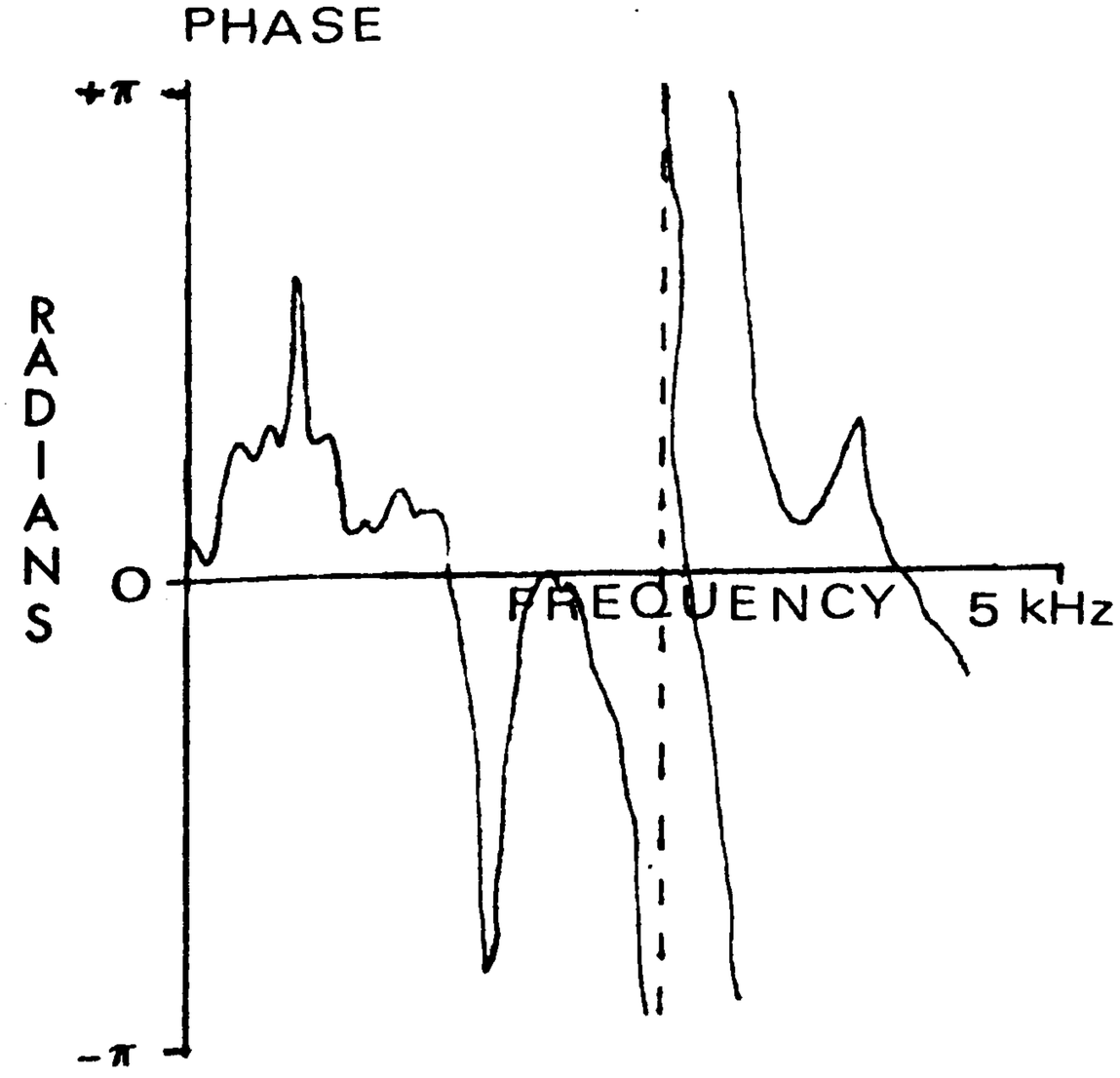

VOWEL NAME : $\overline{\text{EE}}$

AS IN :- F $\overline{\text{EE}}$ T

FIGURE 12

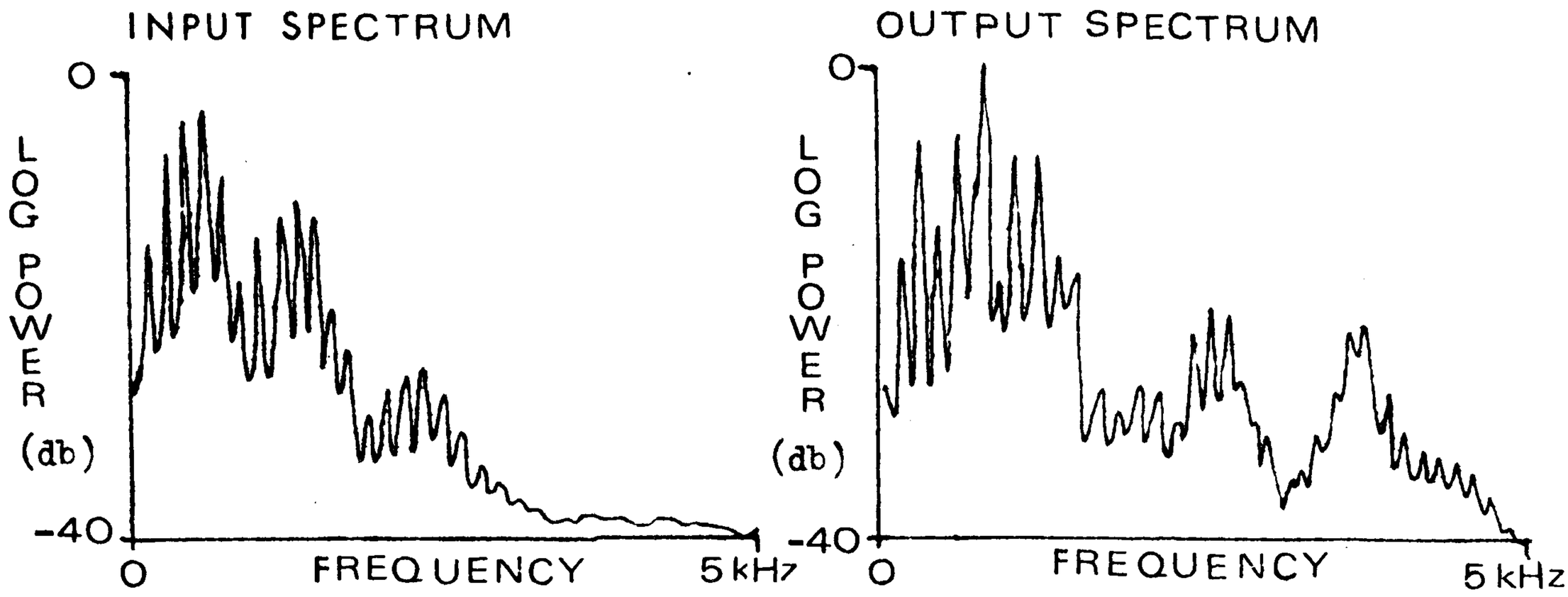

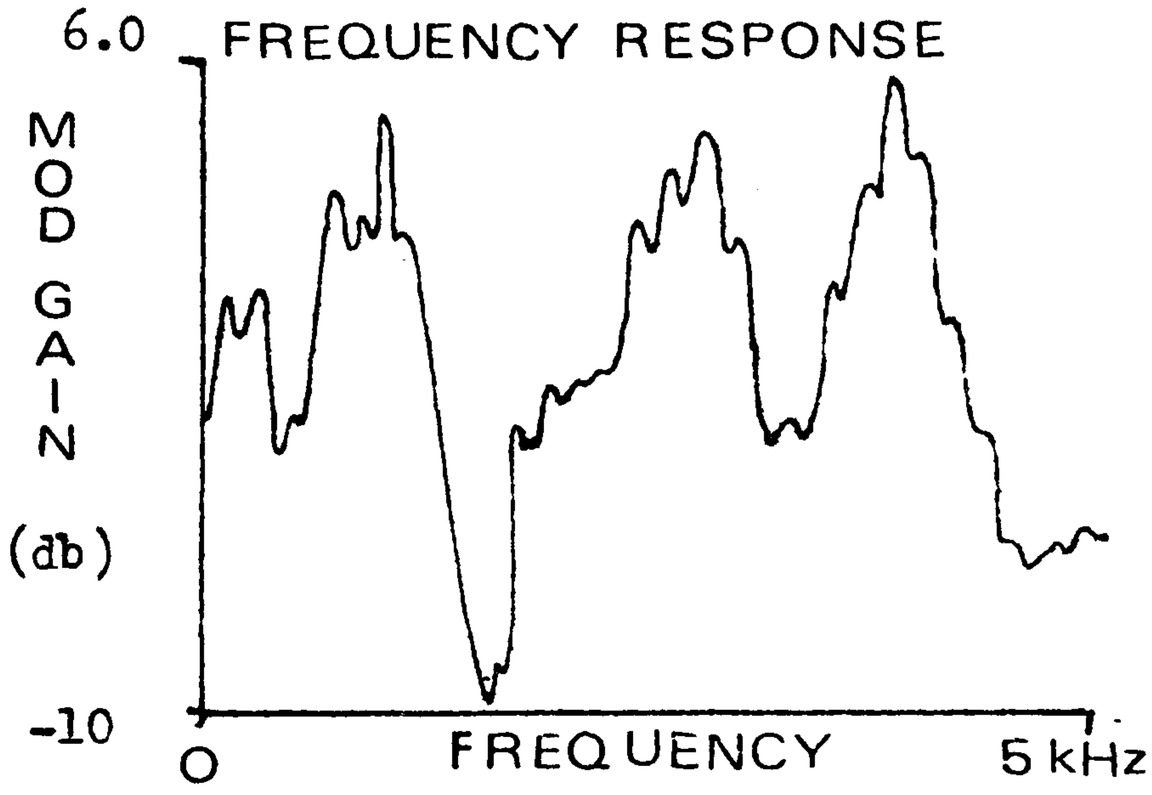

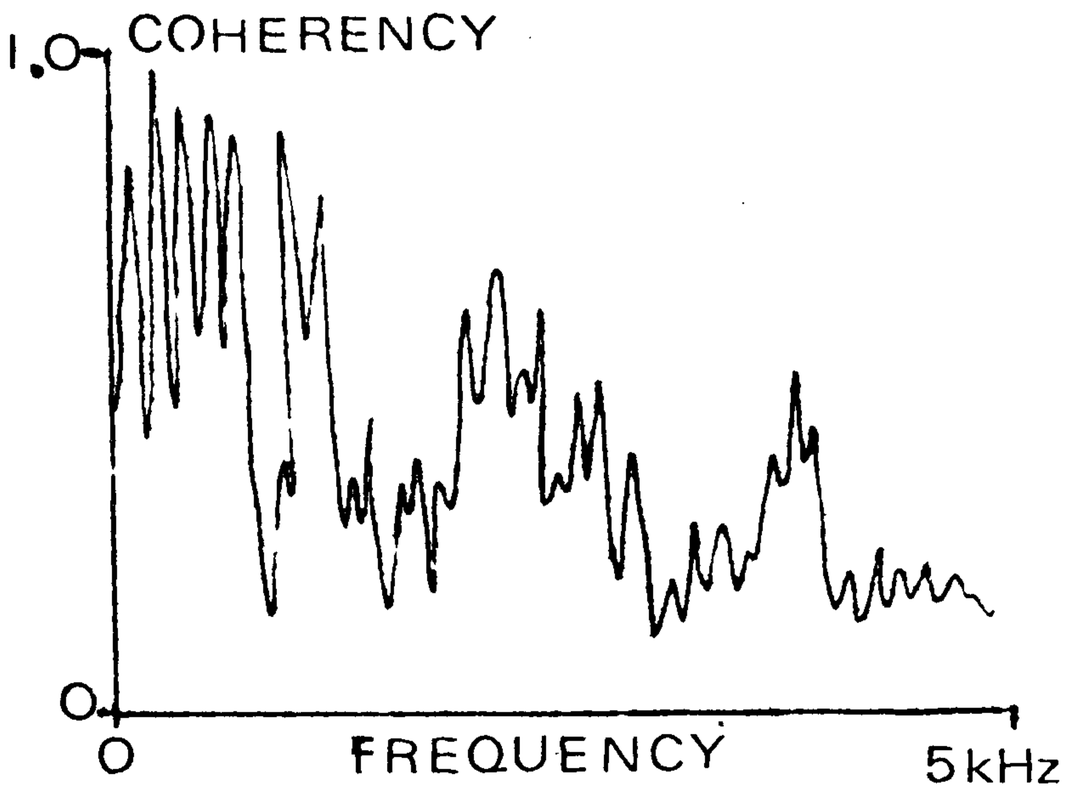

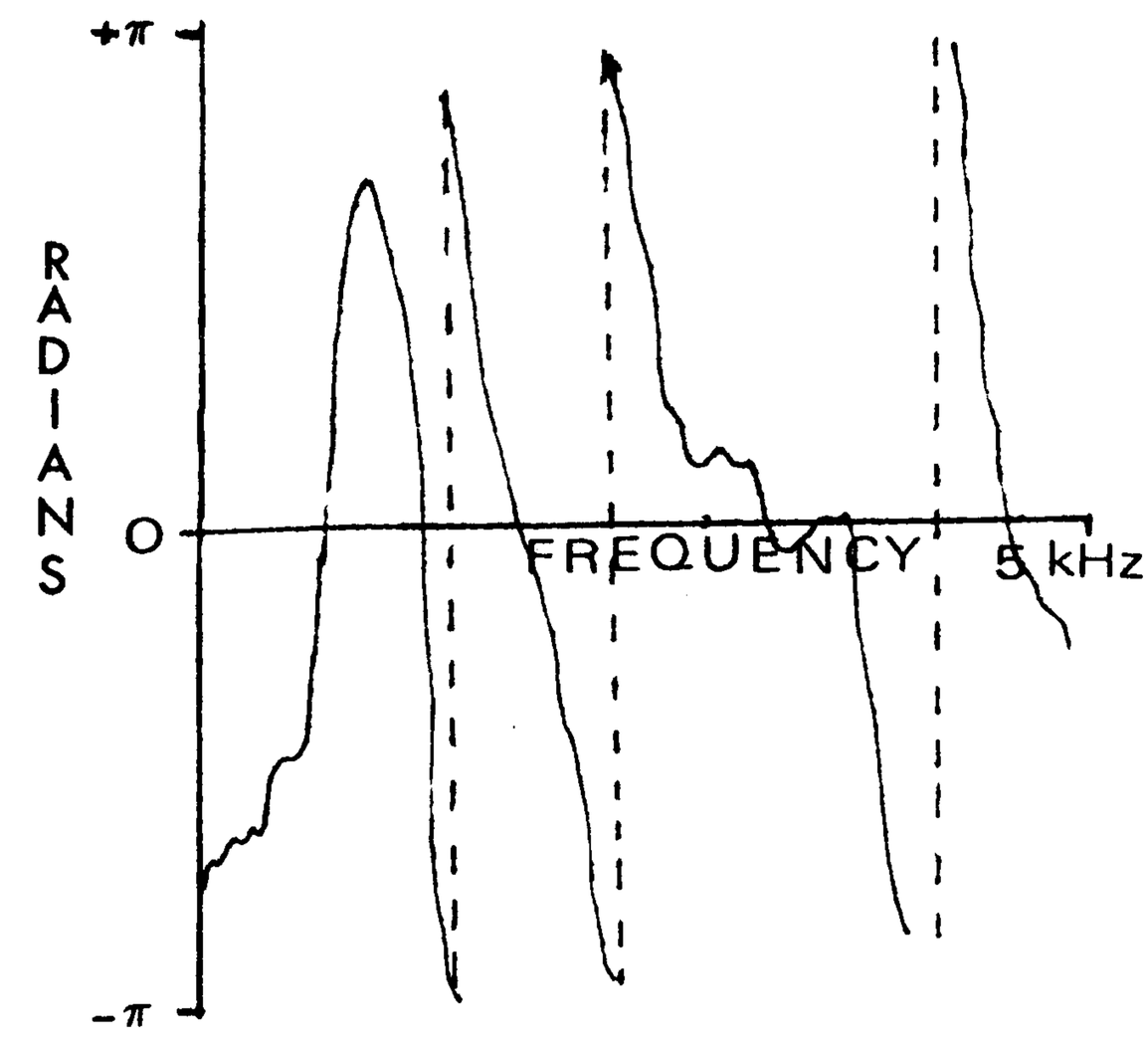

VOWEL NAME : $\bar{I}$

AS IN :- B $\bar{I}$ K E

FIGURE 13

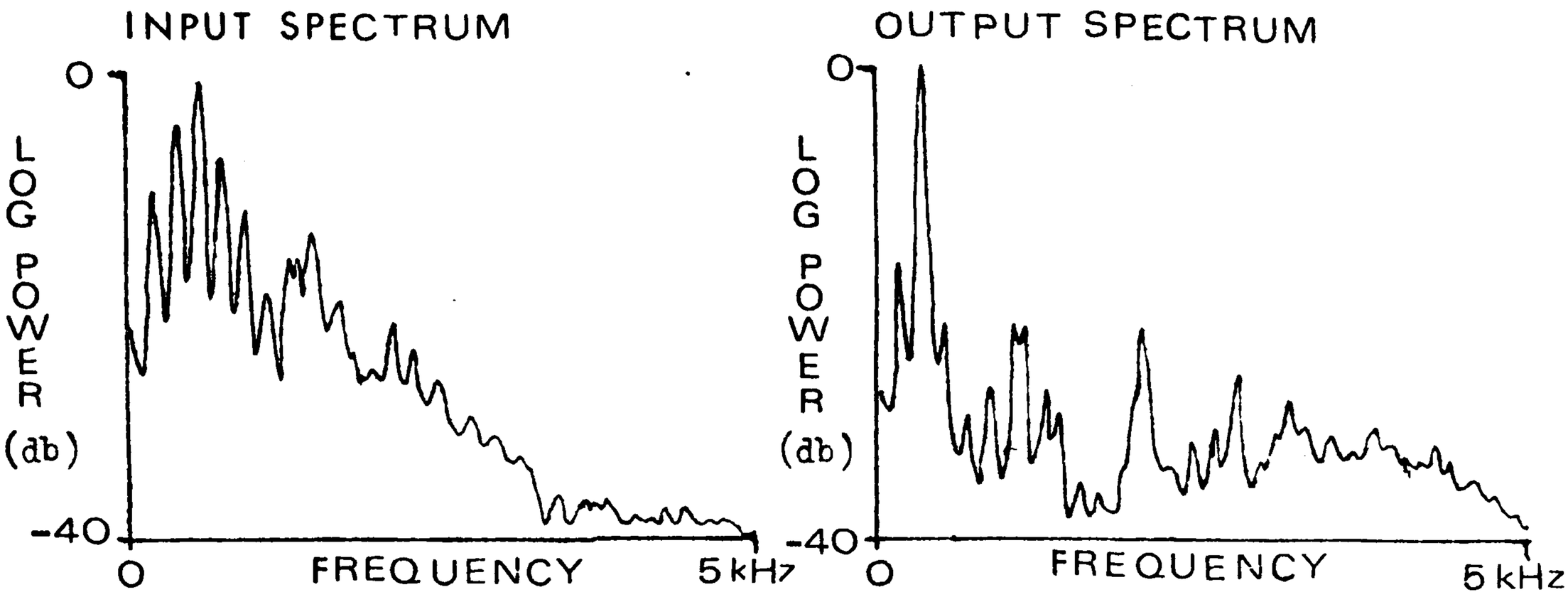

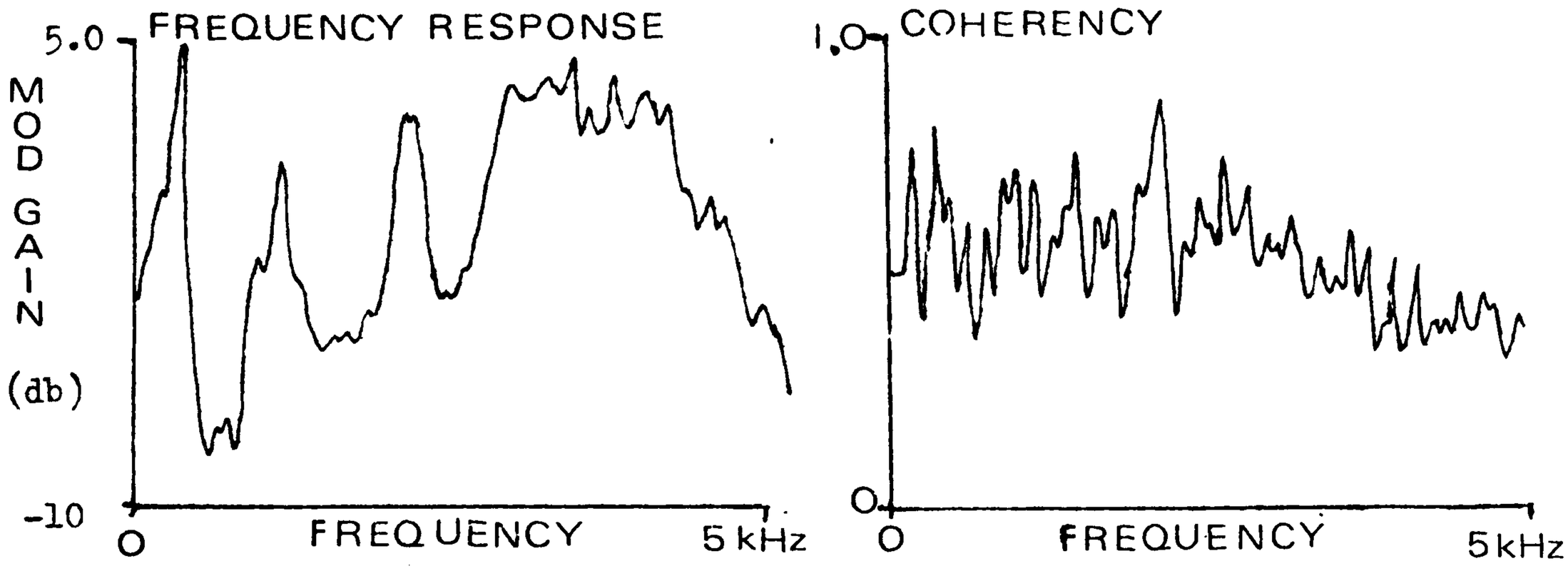

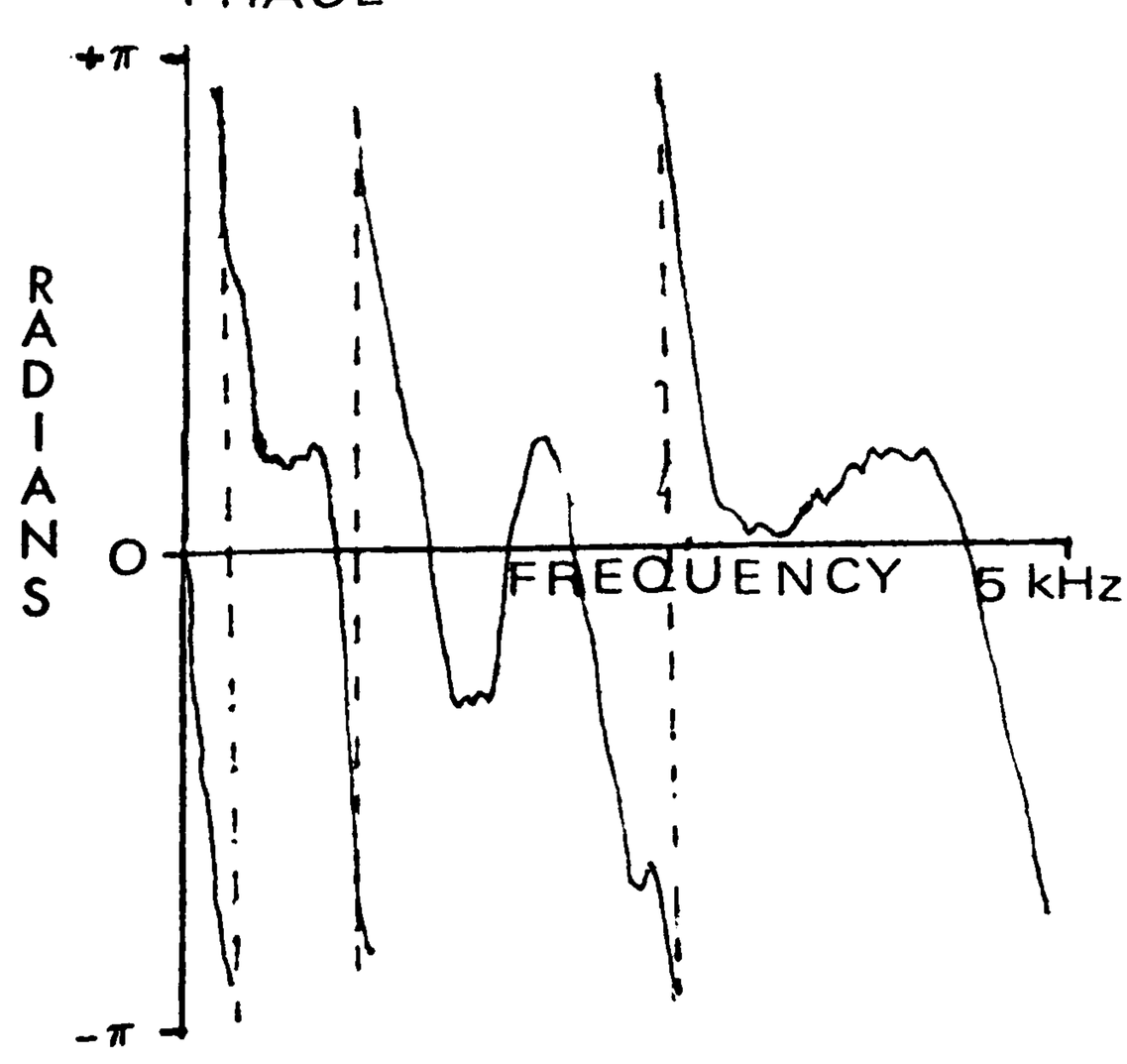

VOWEL NAME : $\breve{I}$

AS IN :- S$\breve{I}$T

FIGURE 14

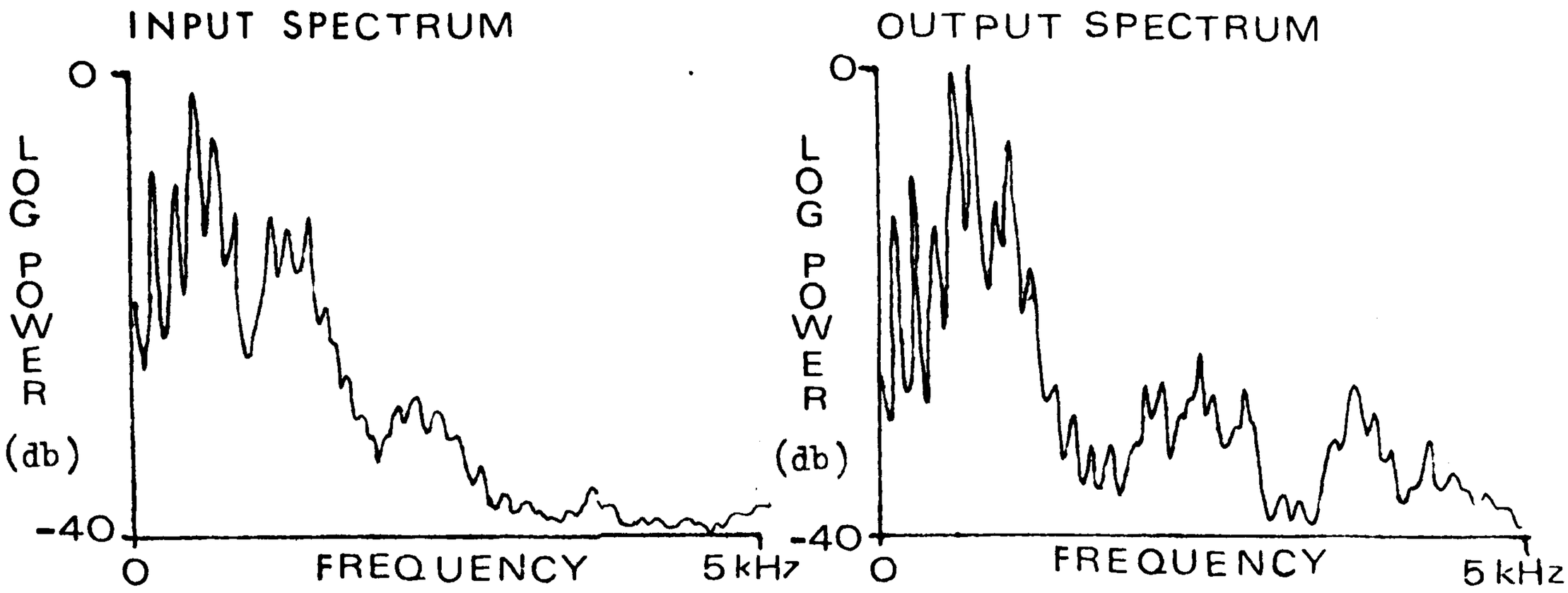

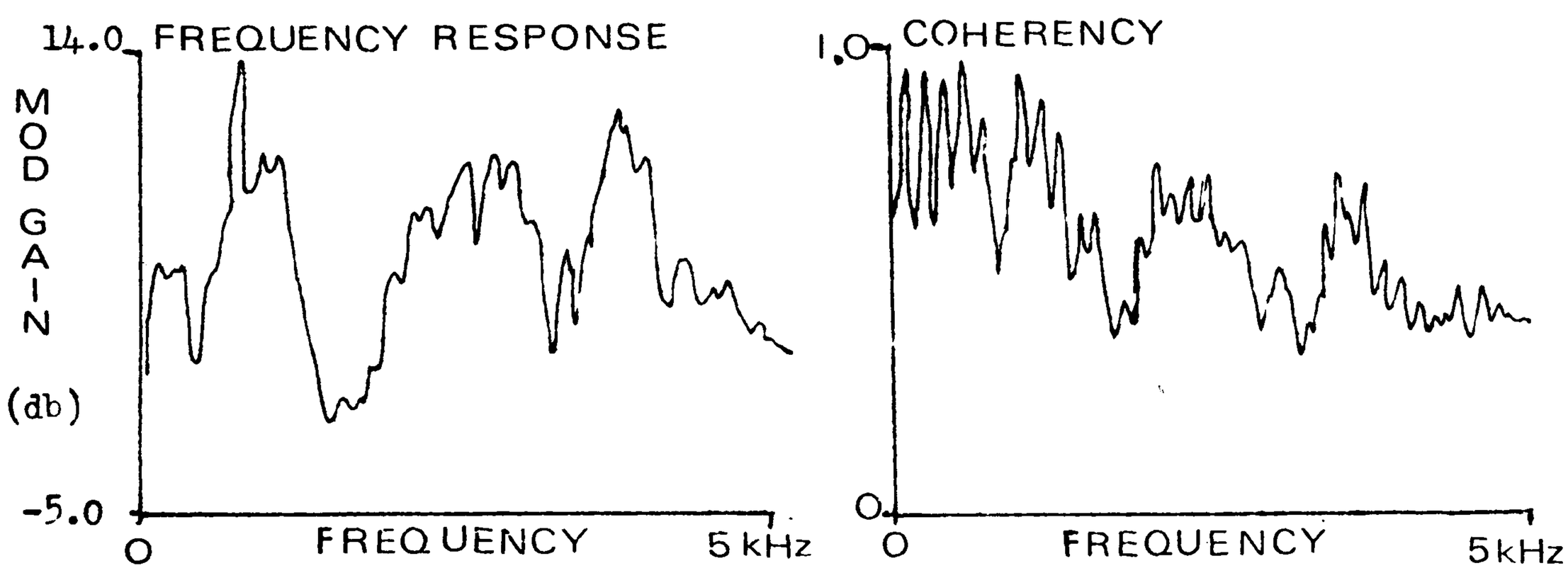

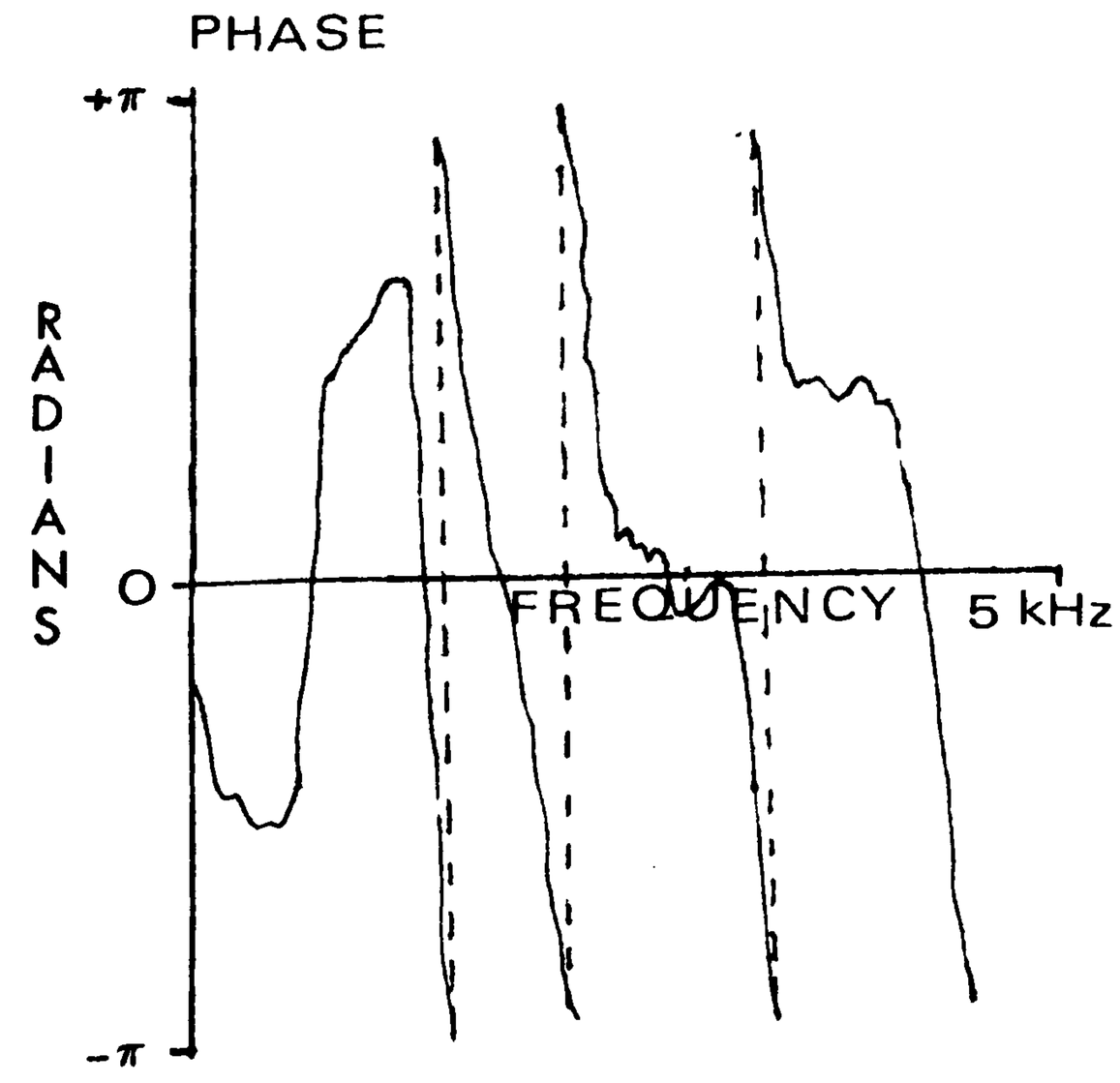

VOWEL NAME : $\breve{U}$

AS IN :- C $\breve{U}$ T

FIGURE 15

TABLE 1: BRIEF CLASSIFICATION OF VOWEL PHONEMES

VOWEL	SPECTRUM	COMMENT
$\breve{O}$	INPUT	1st & 2nd formants present
	OUTPUT	1st formant only, 2nd suppressed
	FREQ. RES.	Zero suppressing top band of 1st formant
$\bar{O}$	INPUT	1st formant dominant (broad)
	OUTPUT	1st formant & minor 2nd & 3rd formants
	FREQ. RES.	Zero suppressing top band of 1st formant followed by 2 peak for 2nd & 3rd formants
$\breve{OO}$	INPUT	Narrow 1st formant followed by 2nd formant
	OUTPUT	1st formant only
	FREQ. RES.	Zero suppressing top band of 1st formant
$\bar{OO}$	INPUT	4 formants present. 4th is sometimes lost
	OUTPUT	1st formant. Voice pitch is dominant
	FREQ. RES.	High gain at voice pitch
$\bar{A}$	INPUT	1st three formants present
	OUTPUT	Formants 1 through 4 present
	FREQ. RES.	Unity initial gain followed by 3 peaks coinciding with 2nd, 3rd and 4th formants
$\breve{A}$	INPUT	1st three formants present
	OUTPUT	Low end of 1st formant suppressed. Top half appears as a narrow peak. Followed by 2nd formant

VOWEL	SPECTRUM	COMMENT
$\breve{A}$	FREQ. RES.	Zero at 3 x voice pitch followed by 3 close peaks with middle peak dominant
$\breve{E}$	INPUT	1st three formants present
	OUTPUT	4 formants present
	FREQ. RES.	Low gain at top end of 1st formant followed by three evenly spread peaks
$\bar{E}E$	INPUT	1st and 3rd formants present as peaks
	OUTPUT	1st formant shows at 1 x voice pitch and 2 x voice pitch. Broad 'hump' on 4th formant (3 & 4 merged)
	FREQ. RES.	High gain at voice pitch. Peak for 4th formant
$\bar{I}$	INPUT	1st three formants present
	OUTPUT	Broad 1st formant followed by 3rd & 4th. 2nd formant merged with 1st
	FREQ. RES.	Peak for 1st formant. 2 peaks for 3rd & 4th formants. Zero for 2nd formant
$\breve{I}$	INPUT	1st & 2nd formants present
	OUTPUT	Narrow 1st formant at 2 x voice pitch. Zero for 2nd formant. Slight rise over 3rd & 4th formants.
	FREQ. RES.	Peak at 2 x voice pitch. Followed by 2 zeros interspaced by a minor peak. Broad peak over 4th formant.

VOWEL	SPECTRUM	COMMENT
$\breve{U}$	INPUT	1st three formants present.
	OUTPUT	1st three formants present.
	FREQ. RES.	Peak at top end of 1st formant followed by zero and 2 peaks on 2nd & 3rd formants.

The term formant has been used loosely in Table 1. Briefly the formants describe the possible resonances generated by the vocal tract. However Table 1 in conjunction with the Figures 5 - 15 show that the individual short and long vowel sounds can be identified separately. Possible exceptions are $\breve{U}$ and $\bar{I}$, $\bar{A}$ and $\breve{E}$. These two pairs are difficult to distinguish using the present system. The response, as shown, for each vowel was the mean of 20 separate utterances of the vowel in different contexts. Section 5 shows a brief example of identification of vowels in connected speech. However, no extensive tests were performed and the development of a detailed phonemic recognition scheme is beyond the scope of this chapter.

5) EXAMPLE OF IDENTIFICATION OF VOWEL PHONEMES WITHIN A COMPLEX CONNECTED UTTERANCE

Two examples are shown. In deriving the vowel responses in the previous section many more examples (20 per vowel) were tried but for space considerations cannot be presented here.

a) The connected utterance $\bar{a}$, $\bar{e}\bar{e}$, $\bar{i}$, $\bar{o}$, $\bar{o}\bar{o}$

This is a connected utterance of the long vowels. Figure 16 (a,b,c) shows the input, output spectra-graphs and frequency response spectra-graph respectively. Each block was compared with the vowel responses

shown in Section 4, using the stationarity tests from Section 3. The stationarity confidence levels for the input spectrum, output spectrum and frequency response, as found for adjacent blocks, were averaged to give a mean stationarity confidence interval. If this mean value was less than 20% (i.e. confidence of stationarity $\geqslant$ 80%) then the vowel was regarded as positively identified. The + sign at the top of the diagrams shows a positive identification while a - sign indicates a failure. For the examples shown all the vowel sounds were correctly identified. In some of the examples used to specify the vowel responses the $\breve{i}$ and $\breve{u}$, $\breve{e}$ and $\bar{a}$ were occasionally doubly defined under this process.

Figure 17 shows the variation of the 8 stationarity parameters over the same sequence of vowels. Slow changes in the $\bar{a}$ and $\bar{oo}$ are detected. These are not marked as phonetic changes but as transients within one phoneme. By comparing adjacent blocks these slow changes are missed.

b) <u>The word SPITOON</u>

A similar process was followed for the word SPITOON to identify the $\breve{i}$ and $\bar{oo}$. Figure 18 shows the time spectra-graphs while Figure 19 shows the variations in the 8 stationarity parameters. The silent 'N' was not clearly detected. The 'S' and 'T' are easily identified from the spectra-graphs. These phonemes are defined entirely by the output spectrum alone.

FIGURE 16 : Shows Time Spectra-graphs obtained from analysis of the phonemes
$\overline{A}$-$\overline{EE}$-$\overline{I}$-$\overline{O}$-$\overline{OO}$

a) Frequency Response
b) Input Spectrum
c) Output Spectrum

16 a) IDENTIFICATION RESULTS

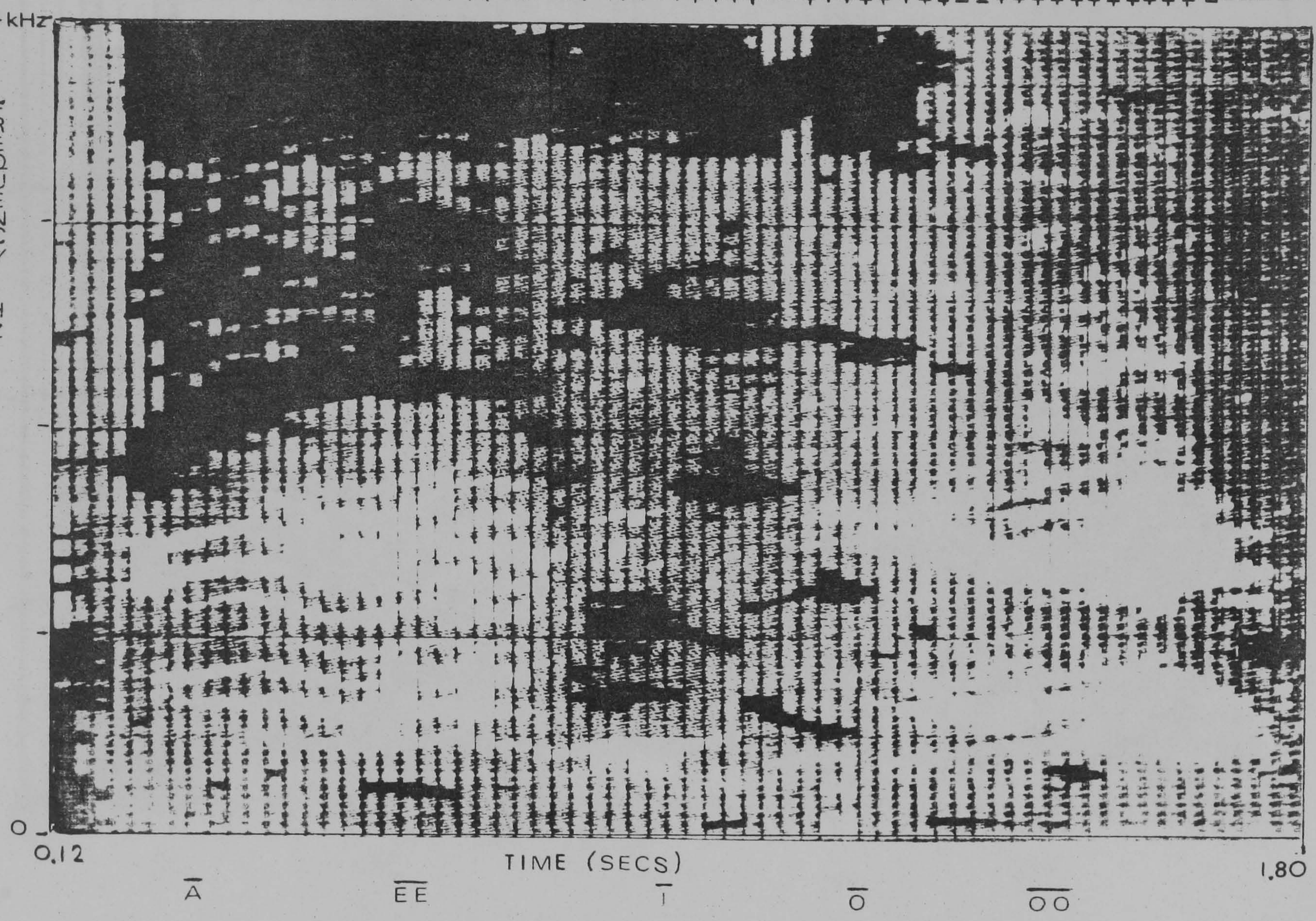

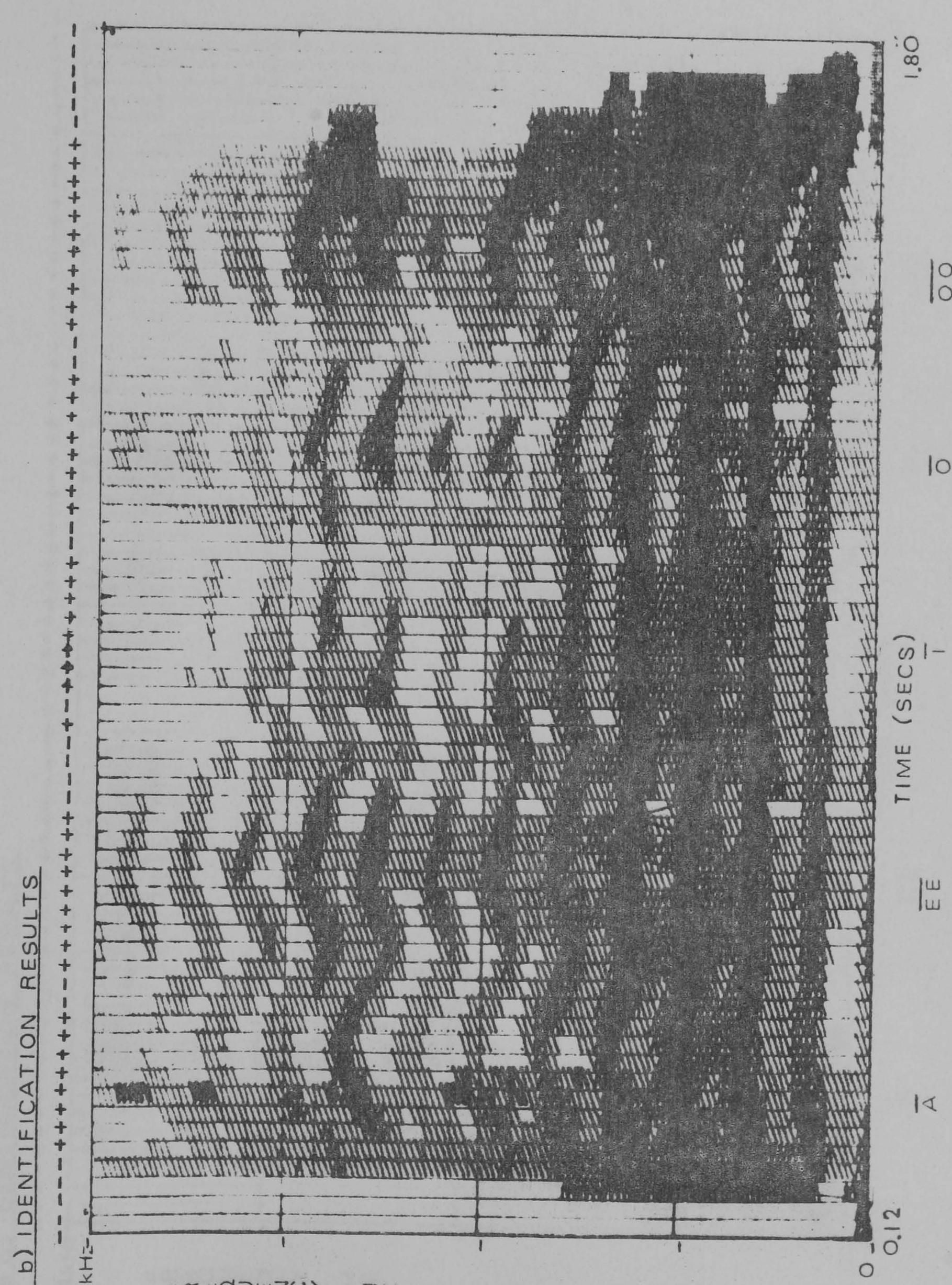
16 b) IDENTIFICATION RESULTS
2 kHz
FREQUENCY IN
0
0.12
TIME (SECS)
1.80

16 c) IDENTIFICATION RESULTS

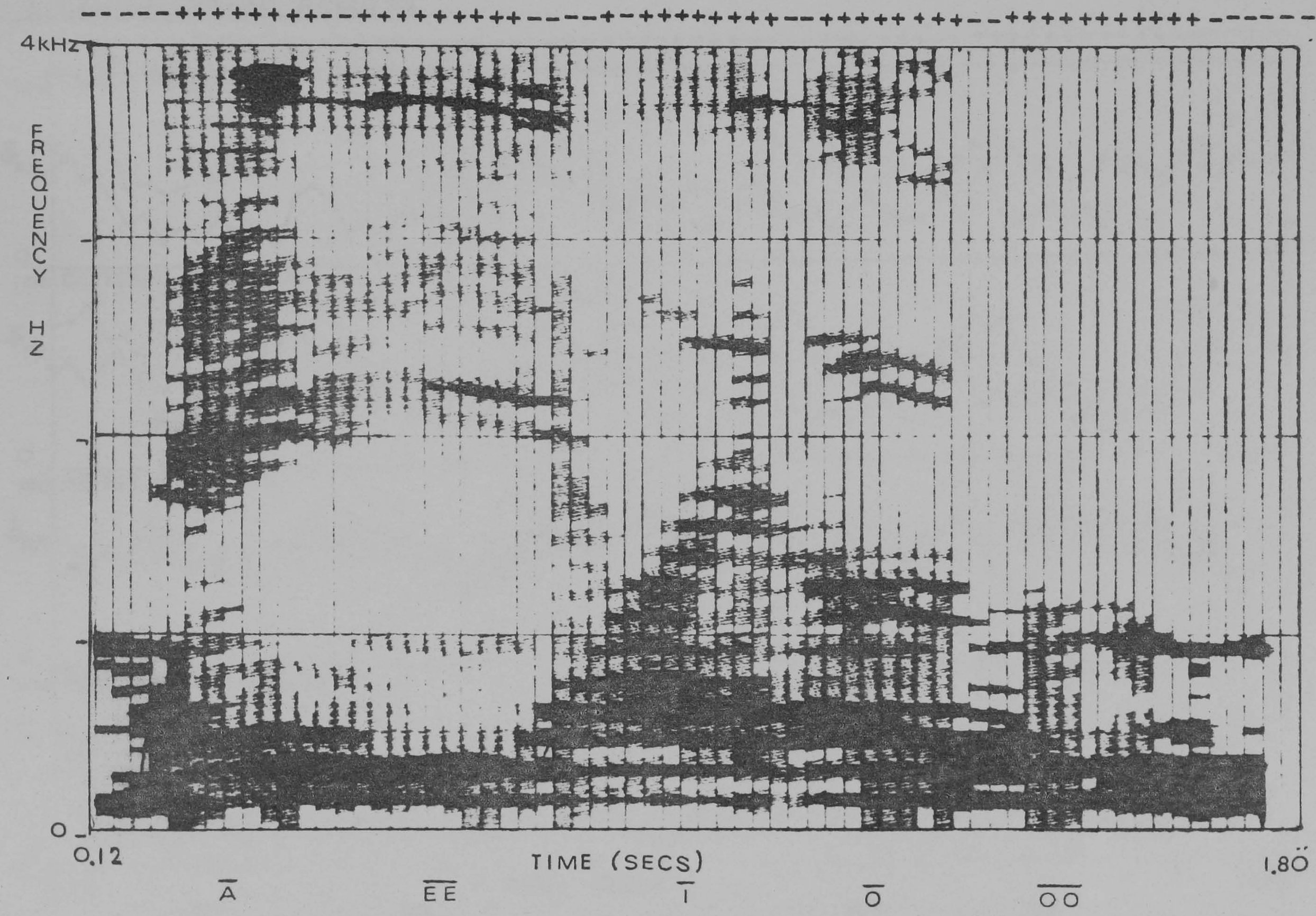

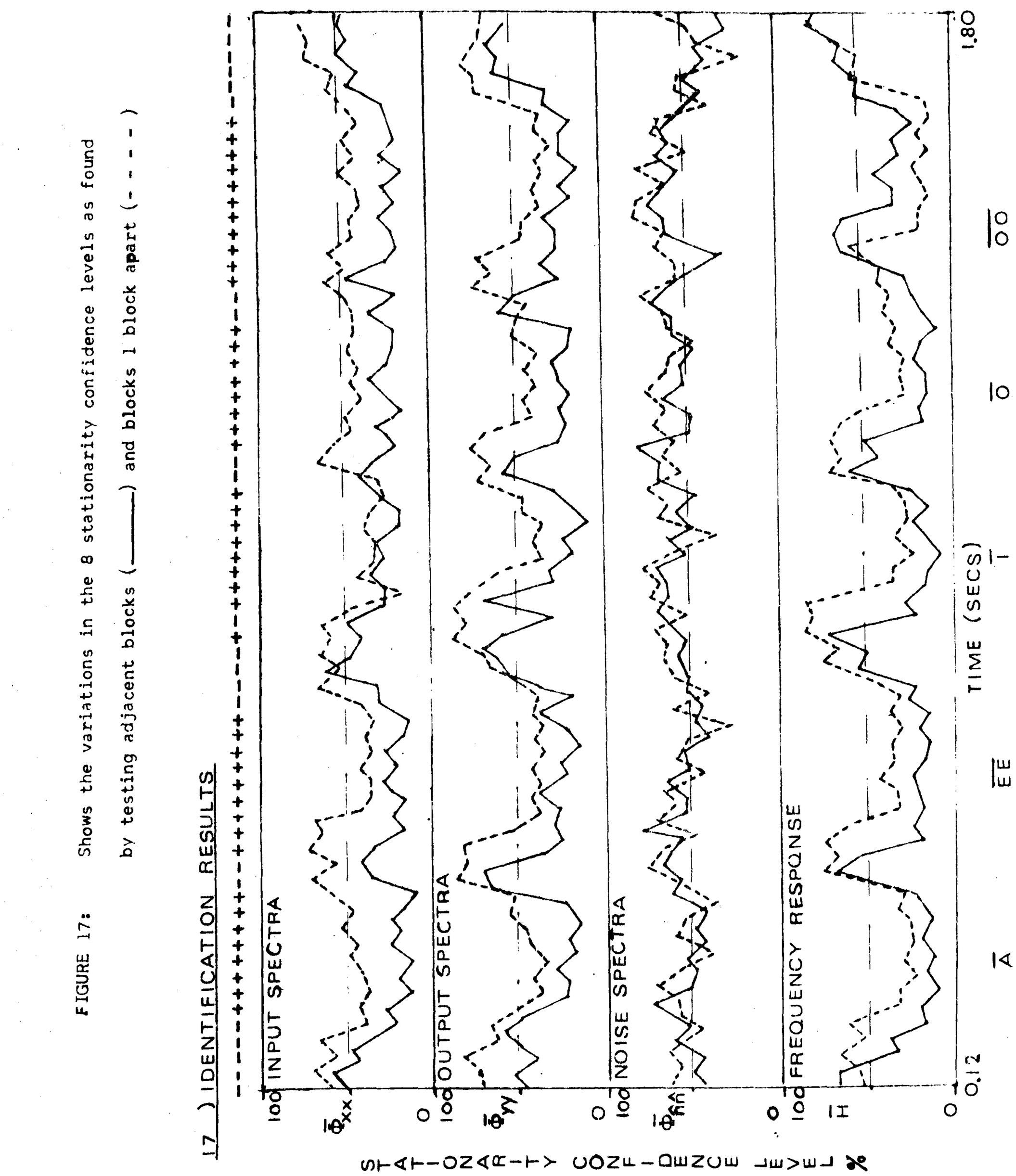

FIGURE 17: SHOWS THE VARIATIONS IN THE 8 STATIONARITY CONFIDENCE LEVELS AS FOUND BY TESTING ADJACENT BLOCKS (——) AND BLOCKS 1 BLOCK APART (- - - -)

FIGURE 13 : Shows the Time Spectra-graphs obtained from analysis of the word spitoon

a) FREQUENCY RESPONSE
b) INPUT AUTO-SPECTRUM
c) OUTPUT AUTO-SPECTRUM.

18 a) IDENTIFICATION RESULTS

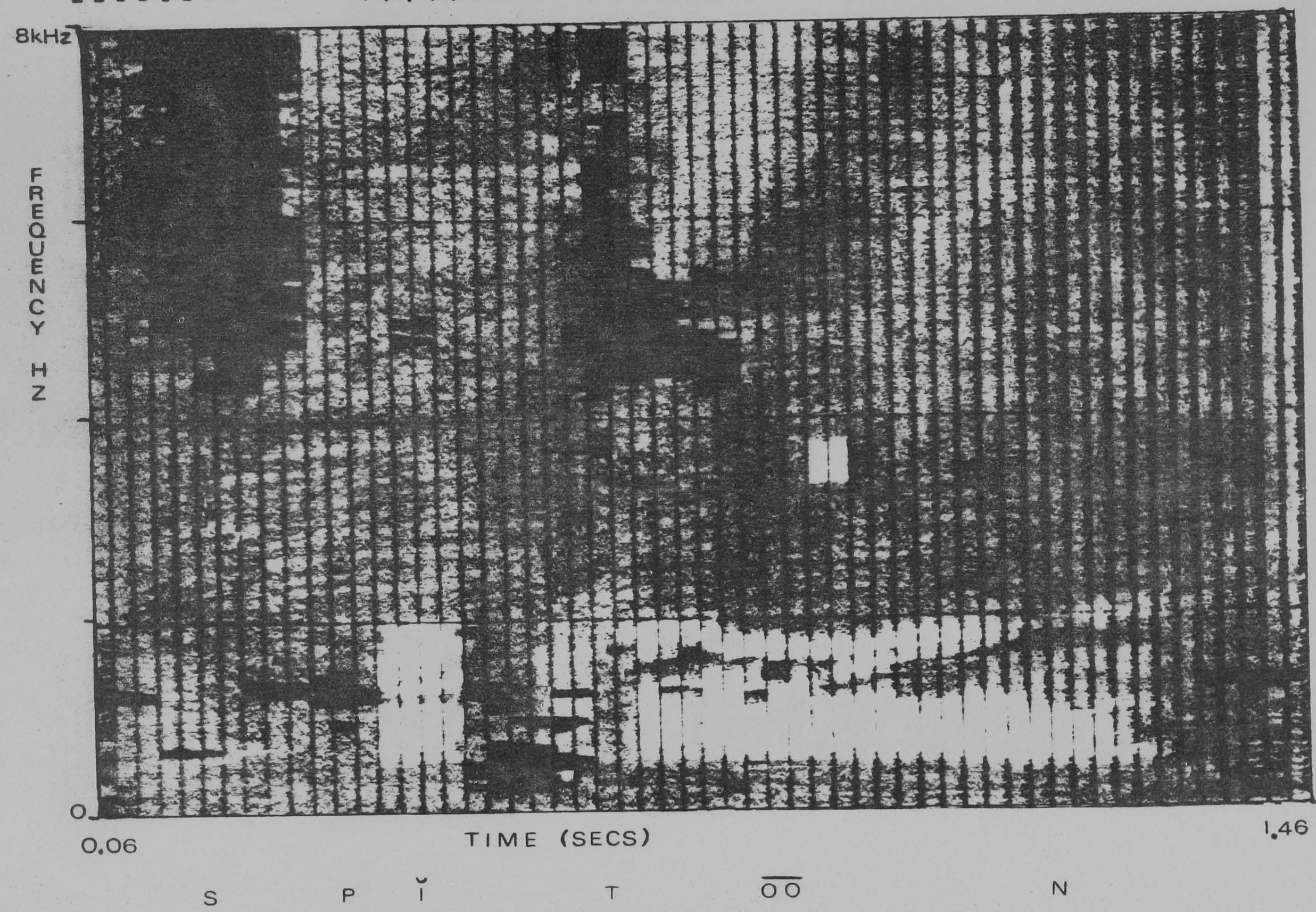

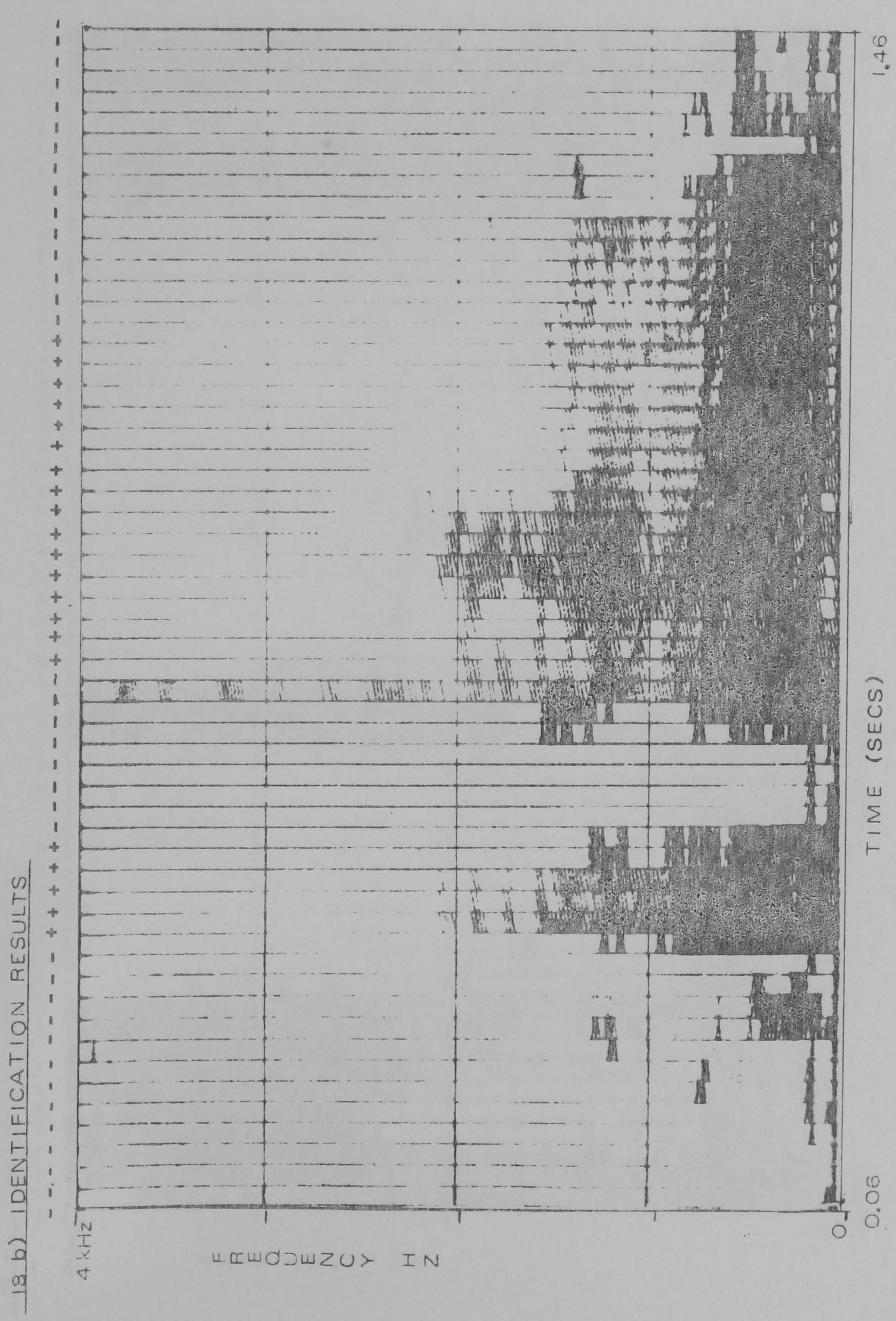
18 b) IDENTIFICATION RESULTS
4 kHz
FREQUENCY IN
0
0.06
TIME (SECS)
94.1
N

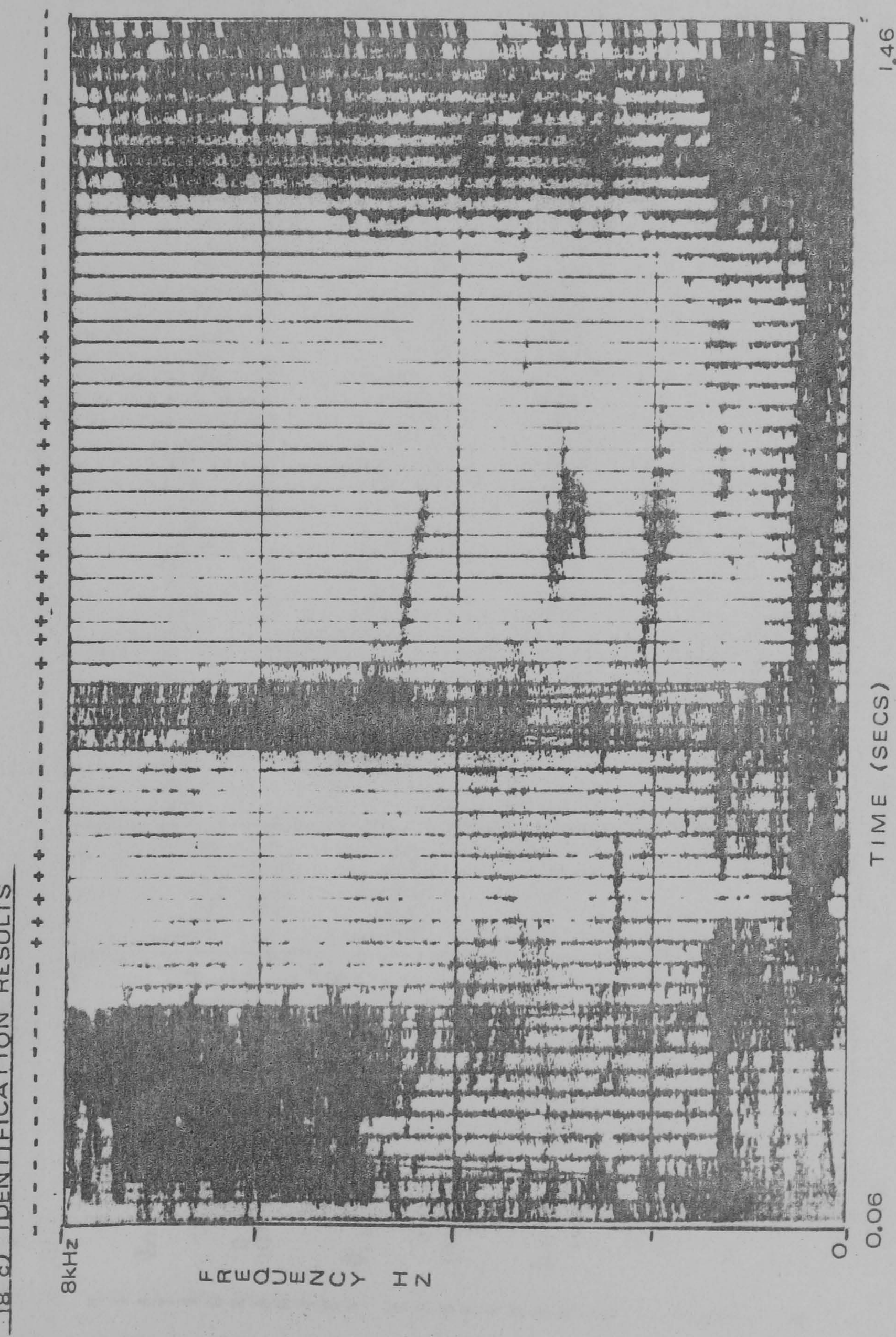
18 c) IDENTIFICATION RESULTS
8kHz
FREQUENCY IN
0
0.06
TIME (SECS)
1.46

FIGURE 19 : Shows the variations in the 8 stationarity confidence levels by testing adjacent blocks (——) and blocks 1 block time apart(- - -) IDENTIFICATION RESULTS

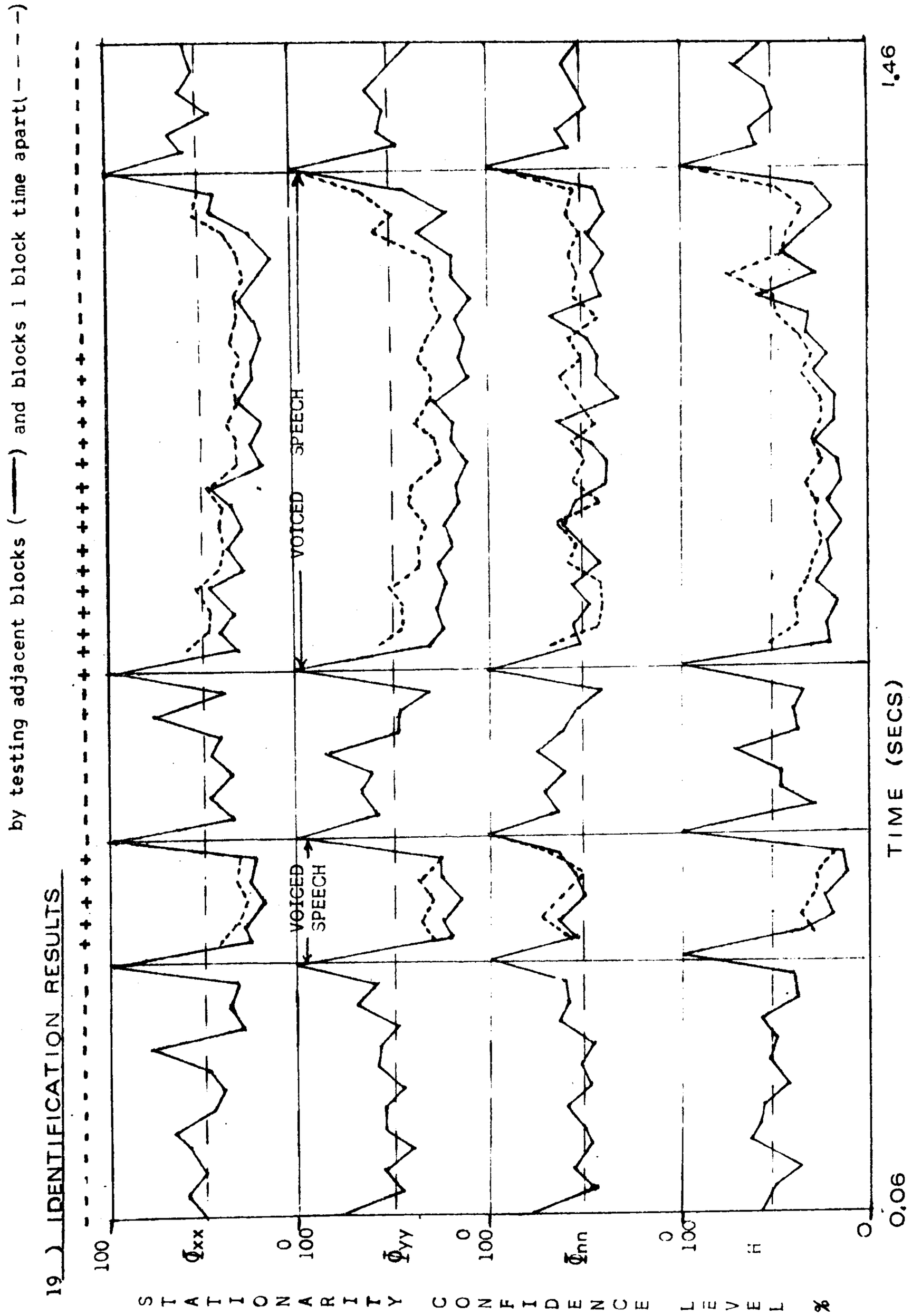

6) APPLICATION TO COMPRESSED SPEECH

The process of speeding up speech to compress information content is used extensively in talking books for the blind and in numerous instances where fast information retrieval is needed. Traditionally the speech time waveform is segmented periodically and chunks are cut out without regard to their information content. Using this method, speech rates up to 400 words per minute can be understood. The method employed here used the stationarity tests for open-loop systems (see Chapter 2) to identify sections of approximate time invariance and segment accordingly. The stationary segments were spliced together. As the degree of compression increased the beginning and end sections of these stationary segments were dropped.

The method of testing for stationarity was different from that used in phoneme identification. The statistical tests were the same, but only adjacent frequency blocks were tested. The best estimate of the noise spectrum was not tested for stationarity. The spoken sections of speech were not normalised to the voice pitch and were analysed over a frequency range of 0 - 5 KHz. Unvoiced speech was analysed over a frequency range 0 - 10 KHz and the complete speech waveform sampled at 20 KHz. The largest of the 3 stationarity parameters measured was taken as the stationarity confidence level for that block. A change was noted if this level was $>$ 80% (i.e. 80% confident that a change has occured). The following sentence was compressed both periodically and using the stationarity testing for word rates varying from 120-400 w.p.m.: "This is a speeded-up section of speech to test the principle of phonemic sectioning as opposed to random sectioning."

Forty people were asked to identify the sentence by listening

first to the 400 w.p.m. recording and then at successively slower speeds until they could repeat the sentence. The number of words picked out was recorded for each playback speed. They were then asked to decide whether the sentence was more comprehensible at 400 w.p.m. using phonemic or periodic sectioning. This last question is to a degree subjective, in that a person can be biased by his previous performance and by whether he was tested on the periodically compressed or phonemically compressed records. Table 2 shows the total number of words identified at each playback speed for the two types of speech compression. The tests would indicate a significant improvement in the information retrieval capabilities using phonemic compression (about 40 w.p.m.). The recording is of poor quality due to the automatic recording level monitor on the cassette recorder used. This means that machine noise dominates the initial section of each recording. However, all tests are affected equally.

TABLE 2. SHOWS THE RESULTS OF COMPARISON TESTS ON PHONEMICALLY & PERIODICALLY COMPRESSED SPEECH

SPEECH RATE IN W.P.M.	TOTAL NO. OF WORDS RECOGNIZED	
	PHONEMICALLY COMPRESSED	PERIODICALLY COMPRESSED
400	122	63
360	273	146
320	621	486
280	778	736
240	800	800
200	800	800
PREFERENCE VOTE	72	8

7) CONCLUSIONS

The use of a throat microphone to access the input signal to the speech system increases the information that can be obtained about phonemic content in the speech waveform. This is especially true for voiced speech. The vowel sounds can be classified and successfully identified for short connected speech segments. The recognition system makes no serious attempt to optimise the identification routine in terms identifying key characteristics for each phoneme. Clearly for voiced vowel sounds each vowel sound could be characterised by only a few salient features; a number less than ten would be suggested from an initial scan of the results presented. This might further improve identification results but was considered beyond the immediate scope of this chapter.

The results confirm that statistical tests developed for stationary open-loop systems can be applied to the time-varying case for a class of systems whose parameters are subject to 'step' changes. In this case the 'step' is considered the interface of two phonetic utterances.

However, time spectra-graphs of speech are extremely difficult to interpret even for trained operators. If the phonetic changes are indeed step-like, this is hard to understand. Consideration of the choice of analysis parameters such as sampling frequency and frequency resolution give some insight into this problem.

If we restrict ourselves to considering voiced speech then the physical limitations imposed suggest the following requirements:

a) The waveform generated from the 'voice box' is pulse-like with a fundamental frequency of around 100 Hz. Harmonics higher than 5 KHz are effectively filtered out by the vocal tract. It is reasonable to assume that each phoneme will be maintained for at least 2 cycles

of the voice generator (20 msecs) and that any changes in the vocal tract shape will not be registered for approximately a further 10 msecs. Sampling the voice signal at 10 KHz we require a block time period in the order of 30 msecs or a block size of 300 points.

b) The pulse-like nature of the output from the 'voice box' means that the speech spectrum will not be broad band but contain narrow peaks. To avoid undue bias in the results due to lack of frequency resolution adjacent peaks must remain separated. The peaks are spaced approximately 100 Hz apart, hence a frequency resolution of at least 50 Hz is required.

The requirements of (a) and (b) are just met by choosing the block size N to be 256 points. However no margin is left for smoothing the results in time (intoducing bad tracking qualities) or in frequency (introducing bias errors). Clearly we must sacrifice one restriction to reduce random errors to an acceptable degree. In this chapter we have sacrificed frequency resolution by smoothing over adjacent frequency points. In general the speech spectra-graphs presented by different researchers have circumnavigated this dilemma in different ways and hence their results differ markedly. Even on allowing for frequency smoothing, random error will be sufficient to blur any step changes that may be present. This suggests that approaching the speech recognition problem by considering the statistics of the spectral estimates is essential.

Allowing for accurate measurement of the spectral parameters a more serious source of error lies in the original assumption that each vowel sound is itself a stationary phenomenon. Examples such as $\bar{a}$, $\bar{i}$ tend to end as an $\overline{ee}$ and hence the recognition patterns used for these vowels will overlap with those used for $\overline{ee}$. Voice pitch and context will also change the emphasis placed on a particular vowel

sound. This chapter normalises all vowel spectra to the voice pitch, but this does not allow for trends in voice pitch over the measurement interval. Similarly changes in overall loudness during the measurement interval will cause a further bias. Consider the following simplified example.

Let $X(t,w)$ be approximated over an interval $t \in T$ by:

$$X(t,w) = G(t).X(w) = (1 + \alpha t)\, X(w)$$

Taking the short-term Fourier transform of $x(t)$ on the interval T:

$$X_T(u) = \frac{1}{T}\int_{-T/2}^{T/2}\int_{-\infty}^{\infty} (1 + \alpha t).X(w)\, e^{+jwt}\, dw\, e^{-jut}\, dt$$

Performing the integration:

$$X_T(u) = \int_{-\infty}^{\infty} X(w)\, \frac{\sin\frac{(u-w)T}{2}}{\frac{(u-w)T}{2}} \cdot dw + j\alpha \int_{-\infty}^{\infty} X(w) \left\{ \frac{2\sin\frac{(u-w)T}{2}}{T(u-w)^2} - \frac{\cos\frac{(u-w)T}{2}}{\frac{(u-w)}{2}} \right\} dw \quad \ldots\ldots\ldots 4.3$$

The first term in equation 4.3 is that expected if the system were stationary. The second term is due to the time-dependent overall gain of the system $G(t)$. This example is equivalent to changing the loudness of a phoneme in a simple manner during a short interval T of say 30 msecs. This represents only three to four cycles of the voice pitch fundamental and it is reasonable to assume $\alpha T << 1$. Thus normalising each successive block to the sampled signal variance should account for errors due to change in loudness.

Changes in the voice pitch over individual time data blocks lead to more serious bias errors. Consider:

$$X(t,w) \simeq X_0(w) + t.\frac{dX_0(w)}{dt} + \frac{t^2}{2}\,\frac{d^2X_0(w)}{dt^2} \quad \ldots\ldots 4.4$$

- - - - in the short interval $t \in T$.

Taking the short-term Fourier transform of $x(t)$ on the interval T:

$$X_T(u) \simeq \frac{1}{T}\int_{T/2}^{T/2}\int_{-\infty}^{\infty}\left\{X_0(w) + t.\frac{dX_0(w)}{dt} + \frac{t^2}{2}.\frac{d^2X_0(w)}{dt^2}\right\}\exp(+jwt)\,dw$$

$$\exp(-jut)\,dt \quad \ldots\ldots\ldots\ldots\ldots\ldots 4.5$$

Integrating with respect to t:

$$X_T(u) \simeq \int_{-\infty}^{\infty}\frac{X_0(w)\,\sin\frac{(u-w)T}{2}}{\frac{(u-w)T}{2}}\,dw \quad +$$

$$+ j\int_{-\infty}^{\infty}\frac{dX_0(w)}{dt}\left\{\frac{2\sin\frac{(u-w)\,T}{2}}{T\,(u-w)^2} - \frac{\cos\frac{(u-w)\,T}{2}}{(u-w)}\right\}dw \quad +$$

$$+\int_{-\infty}^{\infty}\frac{d^2X_0(w)}{dt^2}\left\{\frac{T\sin\frac{(u-w)T}{2}}{4(u-w)} + \frac{\cos\frac{(u-w)T}{2}}{(u-w)^2} - \frac{2\sin\frac{(u-w)T}{2}}{T(u-w)^3}\right\}dw$$

$$\ldots\ldots\ldots 4.6$$

The last two terms in equation 4.6 represent expected bias errors due to the time dependence of $X(w)$. The speech input waveform contains sharp peaks at harmonics of the voice pitch. A slow change in voice pitch can lead to a relatively rapid change in $\phi_{xx}(w)$ as illustrated in Figure 21.

For a small change in the voice pitch frequency from say w_1 to w_2 over a short interval T the power spectrum changes by amounts δ_1 at w_1 and δ_2 at w_2 which are large. For sharply peaked spectra with bandwidths less than $2|w_1 - w_2|$ this change may be in the order of the original peak amplitude, A. Clearly under these circumstances terms involving $\frac{dX_0(w)}{dt}$ and $\frac{d^2X_0(w)}{dt^2}$ in equation 4.6 cannot be ignored.

FIGURE 21: Illustrates how a small change in the voice pitch can lead to a large change in the voice spectrum at given frequencies

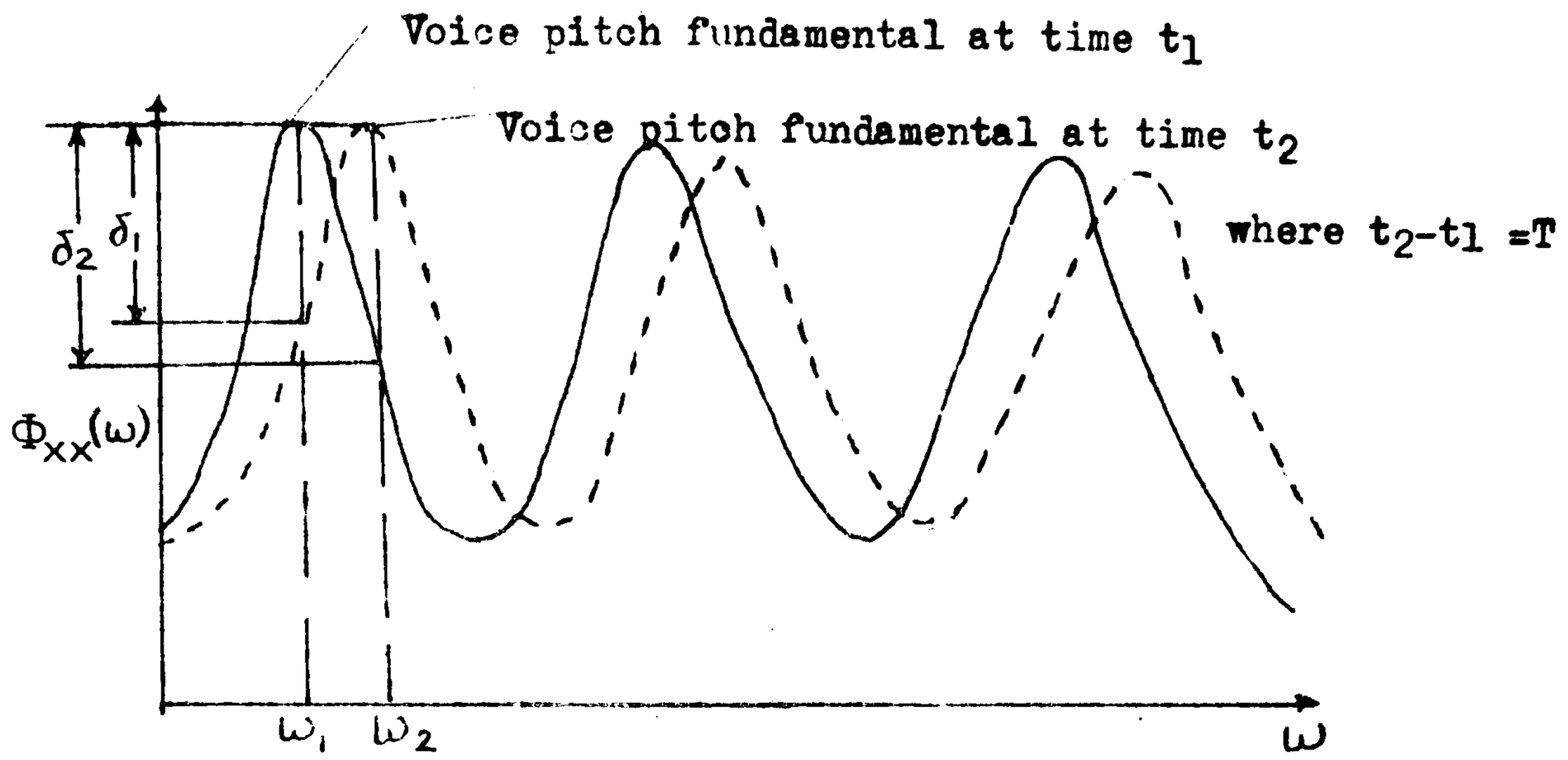

Typically in speech we find: $T \simeq 30$ msecs, $w_1 \simeq 100$ Hz, $w_2 \simeq 110$ Hz (= maximum change in interval T) and, as already discussed, the bandwidth of the peaks is less than 50 Hz. The maximum change expected in $\phi_{xx}(w)$ would be in the order of A/4 in the interval T. Assuming $\frac{d^2X_0(w)}{dt^2}$ to be small, this would give:

$$\left|\frac{dX_0(w)}{dt}\right|_{\max \forall w} \simeq A/4T \qquad \text{where } A = \sqrt{\phi_{xx}(w)} \text{ at } t_1 \qquad \ldots\ldots\ldots\ldots 4.7$$

We have briefly discussed possible sources of error due to changes in the voice pitch and voice amplitude. A similar procedure can be followed for considering bias errors due to changes in the vocal tract response over individual block intervals. These changes are relatively slow over individual phonetic sounds and can often be neglected entirely as they usually mark the interface between two phonemes.

The feedback loop suggested in Figure 1 can be neglected if the

throat microphone is correctly positioned. The input spectra obtained for all the spoken vowels bear close resemblance to each other. This indicates that these spectra represent filtered versions of the 'voice box' output rather than filtered versions of the signal as picked up by the crystal microphone. However it must be emphasised that a major problem in speech analysis is gaining access to the input signal to the vocal tract.

Allowing for a perfect analysis technique it is still doubtful whether a flexible speech recognition system can be developed which is able to cope with long connected passages. The system here can identify sections of voiced speech and may be a useful tool for correcting or analysing speech defects (see references 15 and 20). Other applications to compressed speech would indicate some improvement in terms of intelligibility at the cost of simplicity and computing time. In terms of producing talking books for the blind the improvement in quality is perhaps hard to justify in terms of the extra cost involved. As a means of efficient communication over long distances the extra cost could well be justified.

REFERENCES

1 OPPENHEIM, A. V.: 'Speech spectro-grams using the Fast Fourier Transform'. I.E.E.E. Spectrum 7, No. 8, pp. 57-66 (1970)

2 MIYAMOTO, E.: 'Intelligible artificial voice'. Japan Electrical Eng. No. 34, pp. 36-39 (1969)

3 FATTER, J. W.: 'Continuous speech recognition & synthesis'. National Aerospace Elec. Conf. pp.435-440, (1970)

4 BENINGHOF, W. J.: 'Investigation of an efficient representation of speech spectra for segmentation and classification of speech sounds'. I.E.E.E. Au-18, pp. 33-40, (March, 1970)

5 FANT, C. G. M.: 'Accoustic theory of speech production'. Mouton, The Hague (1960)

6 JACOBSON, FANT & HALLE: ' Preliminaries to speech analysis'. M.I.T. Press (1963)

7 LIEBERMAN, A. M.: 'Perception of the speech code'. Psychological Review, Vol 74, No. 6 (Nov. 1967)

8 OPPENHEIM, A. V.: 'Homomorphic analysis of speech'. I.E.E.E. Trans Au-16, p. 221 (1968)

9 CARR, P. B. TRILL, D.: 'Long-term larynx excitation spectra'. J. Accoust. Soc. Am. pp. 2033-40 36, (1964)

10 HOLMES, J. N.: 'An intestigation of the volume velocity wave-form at the larynx during speech by means of an inverse filter'. Proc. of the speech communication seminar, Stockholm, Sweden (1962)

11 LOBANOV, B. M.: 'More about the structure of the speech signal and the principles of its analysis '. I.E.E.E. Au-18 pp. 316-17 (March 1970)

12 HOLMES, J. N.: 'Speech synthesis'. Mills & Boon (1972)

13 HERSCHER, M. B. & COX, R. B.: 'A practical speech recognition system'. Systems pp. 32-5 (March/April 1974)

14 ATAL, B. S.: 'Determination of the vocal tract shape directly from the speech wave'. Jnl. Accoust. Soc. Am. p. 65, 47 (1970)

15 CRICHTON, R. G.& FALLSIDE, F.: 'Linear prediction model of speech product -ion with applications to deaf speech training.' I.E.E. Proc. Vol 121 No. 8 pp. 865-72 (Aug. 1974)

16 FLANAGAN, J. L.: 'Speech analysis, synthesis and perception'. Springer Verlag, 2nd ed. (1972)

17 MAKHOUL, J. I. & WOLF, J. J.: 'Linear prediction and the spectral analysis of speech'. Bolt Beranek & Newman Report p. 2304 (1972)

18 ITAKURA, F.: 'Extraction of feature parameters of speech by statistical methods'. 8th symposium on speech information pro-cessing . R.I.E.C. Tohoku Univ. Japan (1971)

19 ITAKURA, F. & SAITO, S.: 'Digital filtering techniques for speech analysis'. British Accoust. Soc. I.O.P. 7th International Congress on Accoustics 27C1 (1971)

20 'Special section on speech analysing aids for the deaf'. I.E.E.E Trans. Au-20, pp. 2-41 (1972)

21 NOLL, A. M.: 'Short-term spectrum and cepstrum techniques for vocal pitch detection'. Jnl. Accoustic Soc. Am. 36, pp. 296-302 (1964)

22 BOGNER, R. E.& FLANAGAN, J. L.: 'Frequency multiplication of speech signals'. I.E.E.E. Trans. Au-17 p.202

23 INDIRESAN, P. V.: 'Interrupted speech and the possibility of increas-ing communication efficiency'. Jnl. Acoust. Soc. Am. 35 (March 1963)

24 FAIRBANKS, G., EVERITT, W. L., JAEGER, R. S.: 'Method for time or frequency expansion of speech'. I.R.E. Trans. Au-2 pp. 7-11 (Jan. 1954)

25 VILLIG, F.: 'An apparatus for speech compression and expansion and replaying visible speech records'. Jnl. Acoust. Soc. Am. 22, pp. 754-761

26 GILL, J. S., MORRIS, R. J., EDWARDS, M.G.: 'A helium speech compressor operating in the time-domain'. Paper for I.E.E. Conference 'Electronic Engineering in Ocean Technology' (1970)

27 BEETLE, D. H., CHAPMAN, W. D.: 'Flexible analogue time compression of short utterances'. I.E.E.E. Trans Au-16 (1968)

28 FRASER, J. M., BULLOCK, D. B., LONG, N. G.: 'Overall characteristics of a T.A.S.I. system'. B.S.T.J. 41 (1962)

29 BOGNER, R. E.: 'Frequency division in speech bandwidth reduction'. I.E.E.E. Trans. COM-13 4 (Dec. 1965)

30 SCHROEDER, M. R.: 'Vocoders: Analysis and synthesis of speech'. Jnl. Accoust. Soc. Am. Vol 22 p. 162 onwards (1950)

31 SEVERWRIGHT, J. S., LOCKHART, G. B.: 'Digital speech transmission using interruption techniques'. Conference on Digital Processing of Signals in Communications, held at the University of Loughborough (1972).

CHAPTER 5.

APPLICATIONS TO FATIGUE ANALYSIS

LIST OF SYMBOLS USED

For signal generation section

x(t)	: input signal to shift register
y(t)	: summed output of shift register suitably weighted
h(i), i=1,N	: weighting function in order of decreasing magnitude
h_k	: weighting function assigned to the k^{th} stage of the shift register
p(a)	: desired amplitude probability function with amplitude (a)
M(v)	: characteristic function of p(a)
p'(a)	: model amplitude distribution function
M'(v)	: characteristic function of p'(a)
Fc	: clock frequency of shift register
λ	: clock period of shift register = 1/Fc
ϕ_x (f)	: one-sided power spectrum density function of x(t)
ϕ_y (f)	: one-sided power spectrum density function of y(t)
$H_D(f)$	: desired power transfer function = $\phi_D(f)/ \phi_x(f)$
$\phi_D(f)$	: one-sided desired power spectrum
H(f)	: model transfer function = $\phi_y(f)/ \phi_x(f)$
σ^2	: signal variance of $\phi_D(f)$
E(h)	: error function describing the accuracy of the model H(f) to the desired $H_D(f)$

For Fatique Rig Control section

x(t)	: original input loading signal before compensation
x'(t)	: compensated input loading signal as delivered to rig

$y(t)$: achieved loading signal

$\hat{H}_E(jw)$: short-term estimate of frequency response between x and y at frequency w

$H_D(jw)$: desired frequency response between x and y

$\hat{E}(jw)$: difference between desired and estimated frequency response between x and y

$\phi_{xx}(w)$: input auto spectrum of x(t)

$\phi_{xy}(jw)$: cross-spectrum between x and y

$\phi_{yy}(jw)$: achieved auto-spectrum of y(t)

N : number of sample points in Fourier block

T : update period of controller

K : correction factor for compensator update

C(jw) : compensator frequency response

Fs : sampling frequency

1) INTRODUCTION

This chapter investigates three aspects of fatigue testing. Broadly these are: a) The generation of a loading signal whose characteristics can be specified by the user.

b) The control of the loading rig to ensure that demanded loads are actually achieved.

c) Statistical analysis of the test specimen's response to identify the onset of fatigue cracking.

In the first section it is shown how the weighted output of a pseudo-random noise generator (P.R.B.S.) can approximate desired amplitude probability and power spectrum characteristics simultaneously. Several examples are given. The second section deals with control of fatigue loading rigs by a method of frequency compensation of the input loading signal so that the achieved load has the desired characteristics (in this case a time-delayed version of the original input) Section three makes use of stationarity tests developed in Chapter 2 for open-loop systems to identify changes in the measured frequency response of the test specimen. Some examples are given from test runs conducted on notched aluminium and steel rods subjected to random cantilever bending.

2(i) GENERATION OF SIGNALS WITH SPECIFIED STATISTICS

Much fatigue testing has assumed the loading time history to be Gaussian. Generation of Gaussian signals with a specified power spectrum is in general simple, as the response of any time invariant linear filter to a normally-distributed signal has a normal distribution. For other distributions it is difficult to satisfy constraints simultaneously on both the amplitude distribution and the frequency content. The basic difficulty arises since altering the amplitude distribution by passing the signal through a non-linear device will modify the power spectrum, and passing the signal through

a linear network in general modifies the amplitude distribution. (1,2)

The technique introduced in this chapter utilises a shift register supplied with a binary (+1, -1) input signal which approximates to band-limited white noise. The shift register itself may be used to generate a binary pseudo-random input signal by appropriate feedback. Outputs from a selected number of stages of the shift register are added together in a linear element, the contribution from each stage having an appropriate weight. These weights can be determined so that, subject to certain limitations, the final signal has statistical properties approximating the required functions. This permits a very simple implementation.

The method finally selected generates the magnitudes of the weights so that the output signal has, as closely as possible, the specified amplitude probability function. The allocation of these weights in position along the shift register and the sign associated with each weight is then determined to approximate the required power spectrum. These two stages of the design are independent and discussed in turn. Figure 1 shows the block diagram of the proposed generator with the input sequence to the shift register generated by appropriate feedback.

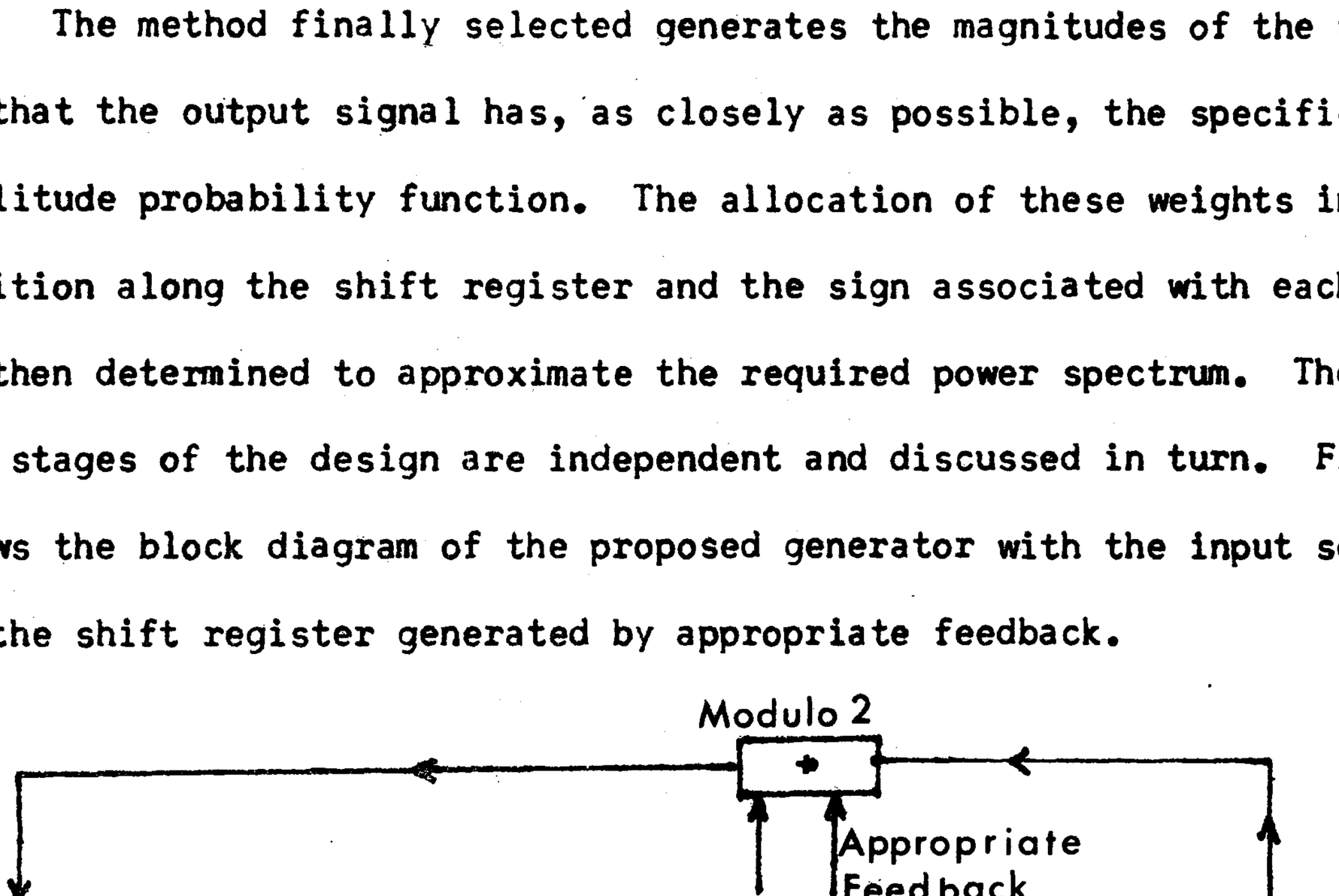

FIGURE 1: BASIC GENERATOR

2(ii) GENERATION OF SPECIFIED AMPLITUDE DISTRIBUTION

When x(t) and its delayed versions are statistically independent, the amplitude distribution of y(t) is the multiple convolution of the amplitude distributions of N square waves of magnitude $\pm$hi (i=1,N). This is approximated to the desired distribution by choosing the weights hi such that the model characteristic function of y(t) given by:

$$M'(v) = \prod_{i=1}^{N} (\cos (hi \cdot v)) \quad \ldots\ldots\ldots 5.1$$

approximates the given characteristic function.

$$M(v) = \int_{-A}^{+A} p(a) \cos(v.a) \, da \quad \ldots\ldots\ldots 5.2$$

where p(a) is the given amplitude probability distribution.

The position and sign of the weights along the shift register do not affect the amplitude probability distribution, only the resulting power spectrum of y(t). The notation adopted here is that weights along the shift register are denoted hi for i = 1, N, whilst the sequence of weights in order of decreasing magnitude are written h(i), again for i = 1, N.

The weights h(j) are chosen in decreasing magnitude by selecting successive weights to give correspondence between the zeros of the given characteristic function and the zeros of the approximation for increasing v. Since the characteristic function of a zero-mean random square wave of amplitude $\pm$h is a cosine function of v, with periodic zero crossings at h.v = $\pi/2$, $3\pi/2$, $5\pi/2$ etc. any given characteristic function with periodic zero crossings can be approximated arbitrarily closely by a cosine product series (3) otherwise significant errors can arise regardless of the number of terms in the approximation.

As each zero not already modelled of the characteristic function is located, the order of the zero is also found. The function is modelled in the neighbourhood of the zero by $A(\cos(h(j).v))^k$ where k is an integer

giving the number of weights with value h(j), and A is a constant.

To assess the accuracy of the final approximation, the derived characteristic function M'(v) is smoothed by a Hanning window of the form $\frac{1}{2}\{1 + \cos \pi v/Vmax\}$, where Vmax is the position of the last modelled zero, and the smoothed function transformed to give p'(a), the model amplitude distribution.

A cost function:

$$C = \int_{-A}^{+A} | p(a) - p'(a) | \quad da \quad \ldots\ldots\ldots 5.3$$

is then computed to assess the accuracy of the model.

Experimentally values of C in the range 0.03 to 0.29 have been encountered, values greater than 0.05 corresponding to characteristic functions not possessing periodic zero crossings.

The range of application of this method to different amplitude probability distributions has not been fully investigated. In the form presented here only even functions can be modelled. However, by a process of discarding negative values or inverting them and then biasing the output with a D.C. value, the restriction to even-valued functions is removed. This process will not however retain the desired spectral characteristics. Successful modelling of the triangular, rectangular, normal and semi-circular amplitude functions has been achieved, although the accuracy of the last did not match that of the first three. This poorer result was due to non-periodic cross-over points in the characteristic function of the semi-circular amplitude distribution. The amplitude function of a sine-wave was also modelled, but with less success than the four mentioned above. This can be appreciated on observing the amplitude distribution of a sine-wave (see results section) which exhibits a sharp cut-off at $\pm A$, the amplitude of the sine-wave. This sharp cut-off is impossible to achieve by convoluting a series of square-wave amplitude distributions. Amplitude

distributions with smooth characteristics about some central amplitude are most suitable for modelling by this method.

2(iii) MODELLING OF POWER SPECTRA BY WEIGHTING AND ADDING THE N-OUTPUTS OF A PSEUDO-RANDOM BINARY NOISE GENERATOR

From the preceding section the magnitudes of the chosen number of weights can be determined. It remains to order these weights with appropriate signs to successive stages of the shift register, so that the final output y(t) has a power spectrum as close as possible to the specified function. In the notation employed h(i) has been determined for all i, but the values have not been allocated positions along the register nor given appropriate signs to specify hi.

The total power of y(t) is already determined by its amplitude distribution so only the shape of the desired power spectrum need be specified. From a knowledge of $\phi_D(f)$ and the spectrum of the signal applied to the shift register $\phi_x(f)$, the desired power gain of the weighting network, $H_D(f)$ is given by:

$$H_D(f) = \phi_D(f) / \phi_x(f) \quad \ldots\ldots\ldots 5.4$$

The power gain H(f) of a weighting network hi, i = 1,N, depends solely on the weights hi. A quadratic error function, E(h) is chosen to describe the 'goodness' of the model H(f).

$$E(h) = \int_0^{Fc/2} | H_D(f) - H(f) |^2 \, df + K(\Sigma_{i=1}^{N} hi^2 - \sigma^2)^2 \quad \ldots\ldots\ldots 5.5$$

The last part of this error function models the error in the total power present in the signal y(t). The variable K is chosen to secure convergence in the Powell hillclimb routine when used. It ensures that any minima found in E(h) are centred around the hyper-sphere of $\Sigma hi^2 = \sigma^2$.

The best obtainable power spectrum using N weights is given by the global minimum of the function E(h) in N-dimensional space, and a hill-climb technique or a modified axis search as appropriate is used to find this minimum.

It is possible to attain any one of three objectives using the techniques described below. Firstly the best power spectrum model using an N-term weighting function can be found without respect to the amplitude distribution of y(t); secondly the best power spectrum model with a specified amplitude distribution can be found; lastly a compromise solution embodying the weighted sum of both the previous criteria is available.

The desired power spectrum is only modelled at frequencies less than half the clock frequency of the shift register, Fc. By attenuating the desired spectrum at frequencies above Fc/4, the unwanted frequency components above Fc/2 can be significantly reduced. The higher frequency components are present because of the nature of $\phi_x(f)$ which is of the form:

$$\phi_x(f) = \lambda \sin^2(\pi f \lambda)/(\lambda \pi f)^2 \quad \ldots\ldots\ldots 5.6$$

with maxima at 3Fc/2, 5Fc/2 etc. If the power transfer function has a zero at Fc/2, then it will also have zeros at 3Fc/2, 5Fc/2 etc. as will be shown.

From Figure 1:

$$y(t) = \sum_{i=1}^{N} hi.x(t - (i-1)\lambda) \quad \ldots\ldots\ldots 5.7$$

Taking the Fourier transform of y(t) and multiplying by the complex conjugate of the result we get $\phi_y(f)$, the power spectrum of y(t), expressed in terms of $\phi_x(f)$.

$$\phi_y(f) = \sum_{i=1}^{N}\sum_{k=1}^{N} hi.hk.\exp(-j2.\pi.(i-k)\lambda).\phi_x(f) \quad \ldots\ldots 5.8$$

From this, the power transfer function relating $\phi_y(f)$ to $\phi_x(f)$

can be defined.

$$H(f) = \sum_{i=1}^{N}\sum_{k=1}^{N} hi.hk.\ \exp(-j2\pi f(i-k)\lambda) \quad \ldots\ldots\ldots 5.9$$

H(f) is periodic with period Fc.

By defining the desired power spectrum $\phi_D(f)$ of y(t), the desired transfer function $H_D(f)$ is also uniquely defined.

$$H_D(f) = \phi_D(f).(\pi f \lambda)^2 / \lambda \sin^2(\pi \lambda f) \quad \ldots\ldots\ldots 5.10$$

Therefore if $\phi_D(f)$ has a zero at Fc/2, so will $H_D(f)$, and zeros will be introduced at 3Fc/2, 5Fc/2 etc. because of the periodicity of H(f).

Many choices of error function describing the 'goodness' of fit of H(f) are suitable. The one chosen (equation 5.5) is of the integral error squared form with an added term matching the total powers. Expanding equation 5.5:

$$E(h) = \int_0^{Fc/2} H_D(f)^2\ df + \int_0^{Fc/2} H(f)^2\ df - 2\int_0^{Fc/2} H_D(f).H(f)\ df$$

$$+ K(\sigma^2 - \sum_{i=1}^{N} hi^2)^2 \quad \ldots\ldots\ldots\ldots 5.11$$

To perform this integration $H_D(f)$ is modelled over the desired frequency range $(0 \rightarrow Fc/2)$ by a Fourier series with a sufficient number of terms to ensure reasonable accuracy in the model.

$$H_D(f) = \sum_{i=0}^{P} Ai\ \cos(2\pi if/Fc) \quad \ldots\ldots\ldots 5.12$$

where: $Ai = \frac{4}{Fc}\int_0^{Fc/2} H_D(f)\ \cos(2\pi if/Fc)\ df$

and: $A_0 = \frac{2}{Fc}\int_0^{Fc/2} H_D(f)\ df$

P is chosen to give sufficient accuracy to the model.

The integration of equation 5.11 is lengthy but straightforward, and only the result is quoted here.

$$E(h) = \sum_{i=1}^{P} A_i^2 \, Fc/4 + A_0^2 \, Fc/2 + \sum_{i=1}^{N} hi^2 \sum_{j=1}^{N} hj^2 \, Fc/2$$

$$+ \sum_{i=1}^{N-1} Ti^2 \, Fc - 2 \sum_{i=1}^{N} hj^2 . A_0 . Fc/2 + \sum_{k=1}^{N-1} A_k \, T_k \, Fc/2$$

$$+ K(\Sigma_{i=1}^{N} hi^2 - \sigma^2)^2 \qquad \ldots\ldots\ldots\ldots\ldots\ldots\ldots\ldots \quad 5.13$$

where: $T_k = \sum_{j=1}^{N-k} hj . h_{j+k}$

Equation 5.13 can be differentiated with respect to each hi to give the gradient of the error function over the function space. This gradient and its derivative $\partial^2 E(h) / \partial hi^2$ may be used in a Powell hill-climbing routine.

In determining the section of the N-space to be searched to find the global minimum, certain restrictions can be introduced to speed up the process. Considering the weighting function as depicted in Figure 1 and the resultant transfer function as given by equation 5.9, then reversing the weighting function or inverting it has no effect on H(f). Furthermore, none of the h(i)'s will have magnitude greater than σ , the R.M.S. value of y(t). So in N-dimensional space the following restrictions can be placed on the magnitudes of the h(i).

$$-\sigma \leqslant hi \leqslant \sigma \qquad\qquad i=1,N$$

$$h_1 > |h_N|$$

The method adopted to find the global minimum in E(h) depends on the nature of E(h) and the value of N. When E(h) is smooth with few secondary minima and N is relatively small the Powell hill-climb routine is suitable, otherwise the user must rely on a reasonably sophisticated axis search routine.

The Powell hill-climb process chosen finds the best model for an N-length weighting network. Several different starting-points are tried

and a variable step length algorithm steps in a chosen direction to the minimum point in this direction. The minimum is the new starting point for repeating the process in a non-parallel direction. This is repeated N + 1 times, the $(N + 1)^{th}$ direction being defined by the two points given by the initial starting point and the current minimum. The minimum in the $(N + 1)^{th}$ direction is taken as the new starting point, and the process is repeated with the j^{th} direction of the old iteration becoming the $(j - 1)^{th}$ direction for the new iteration. When this process yields no new minimum, a local search is conducted to ensure the point found is indeed a minimum and not a point on a ridge, and the resultant hi values are taken as the optimum N-length weighting function modelling the desired transfer function. This gives the optimum weighting sequence when no regard is given to the constraints imposed due to meeting a specification on the amplitude distribution of y(t). One method of constraining the amplitude distribution is to use the weights h(i) found in 2(ii) and allocate these weights in correct sequence along the shift register such that the sum of the squared differences between the optimum weighting sequence and the ordered weights is a minimum. This condition reduces to fitting h(1) to the largest ordinate, h(2) to the next largest etc. with suitable signs attached (see Appendix A).

The restrictions on using this hill-climb procedure are two-fold. Firstly the hill-climb is only practical when N is fairly small (12 was found to be a reasonable maximum) and secondly the nature of the surface of E(h) will determine the efficiency of the method. Lastly there is no guarantee that by fitting the global minimum by the desired weighting function found from Section 2(ii), the best model is obtained.

Therefore for large weighting functions ($N \geqslant 12$), an axis search was

used to find the best minimum. Computationally the axis search is much simpler, with no convergence problems, and a stepping vector that is preset.

The user specifies a starting point on the error function surface and the maximum and minimum step length to be taken. The program starts searching at maximum step-length in h_1 until $h_1 > \sigma$. At each point the weighting function as found in 2(ii) is fitted (as discussed above) and the error in the resultant modelled transfer function evaluated. The program then takes the point giving the minimum error found as the starting point for a search in h_2. This continues up to h_N and then back to h_1. If a complete search in all dimensions is made and no new minimum is found, then the step-length is decreased and the process continues. On reaching the preset minimum step-length the user can either reset the minimum step and continue, or print out the best fit found so far and start again from a different starting point.

The success of the axis search is less dependent on the nature of the function E(h) but is inefficient in the number of iterations needed to find the minimum sufficiently accurately. However, the final result does give the best fitted order of the weights h_i, as found in Section 2(ii) without relying so heavily on assuming the best order is automatically found by fitting the weights to the global minimum in a least squares distance sense.

2(iv) RESULTS

This section gives some results achieved and the mode of operation of the computer programs.

Figure 2 shows the results obtained in modelling four amplitude probability functions. The cost function C is given by equation 5.3. Figures 2a, 2b (rectangular and triangular amplitude distributions respectively) are accurately modelled as their characteristic

functions exhibit periodic zero crossing. Figure 2c is a reasonable approximation to a semi-circular distribution but the model is not as good as 2a or 2b. The characteristic function of 2c has non-periodic zero crossings. Figure 2d shows the model of the amplitude distribution of a sine wave. This model does not obtain the sharp cut-off required.

FIGURE 2: AMPLITUDE DISTRIBUTION MODELS

(————) = desired distribution (- - - - -) = modelled distribution

a) Rectangular Distribution

σ^2 = 8.3125 volts^2 C = 0.05

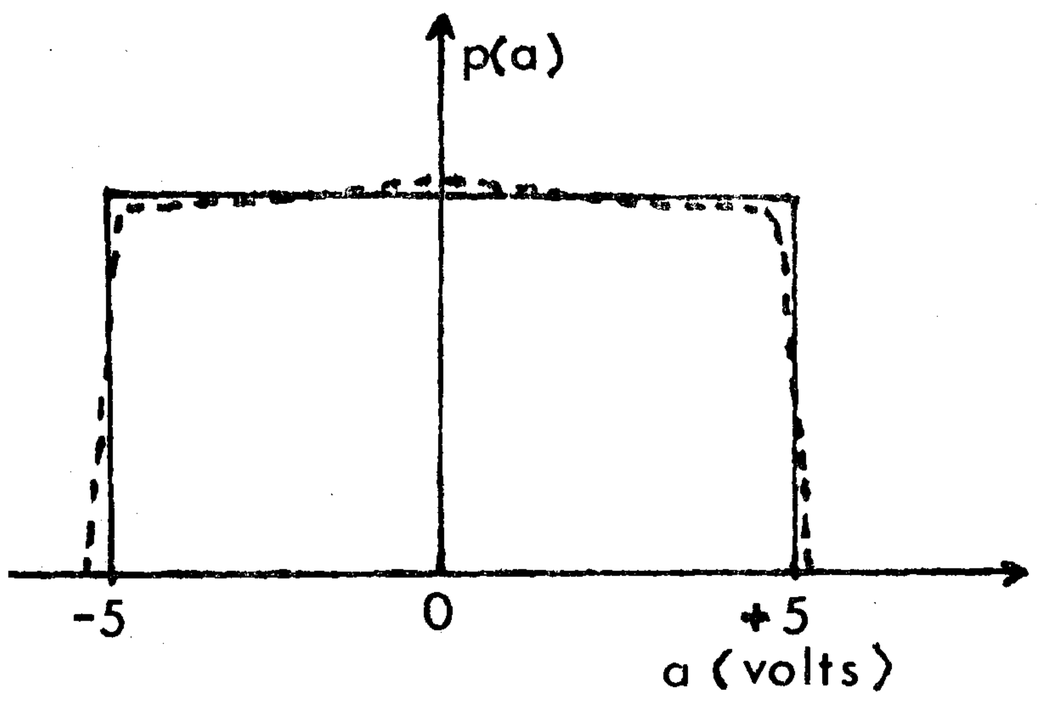

b) Triangular Distribution

σ^2 = 4.1875 volts^2 C = 0.03

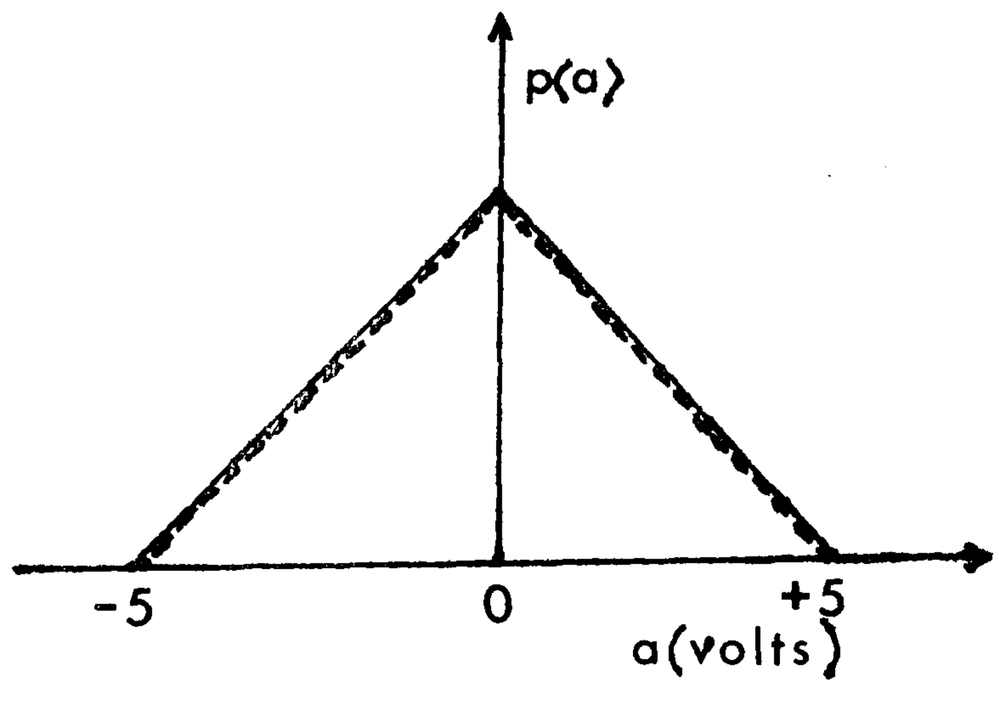

c) Semi-circular Distribution

σ^2 = 0.1587 volts^2 ^{2} = 0.12

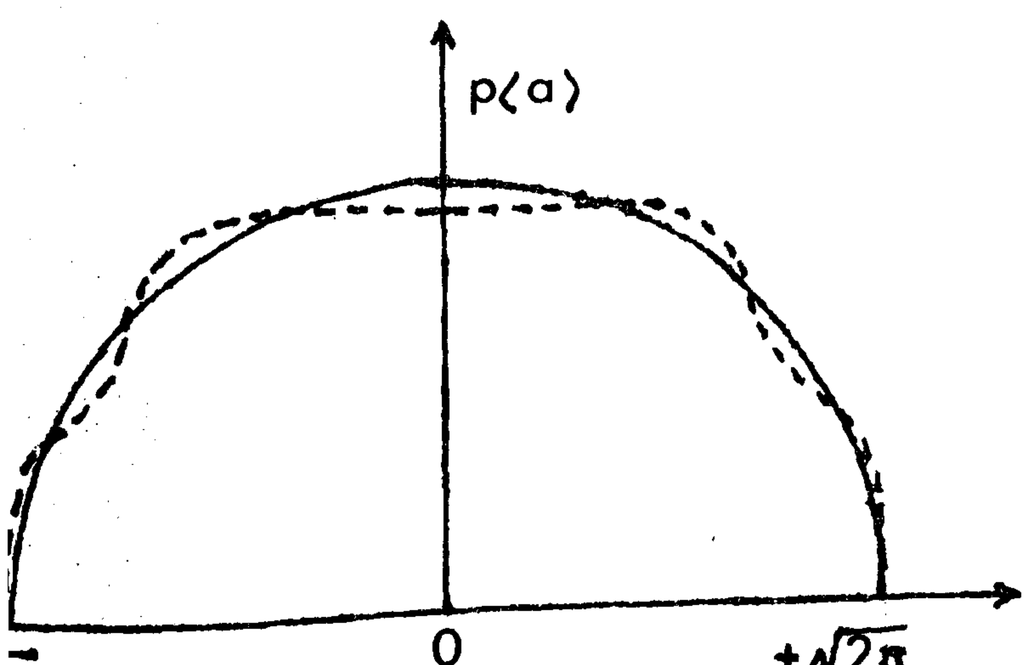

d) Sine-wave Amplitude Distribution

σ^2 = 12.50 volts^2 C = 0.29

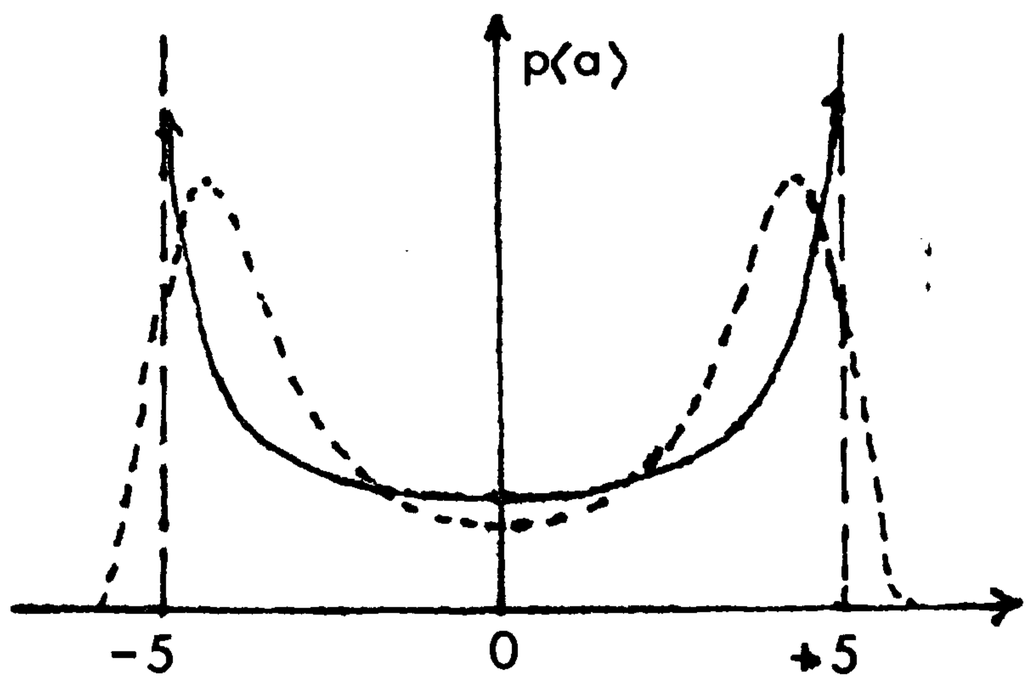

Table 1 shows the calculated weighting function for each type of amplitude distribution.

TABLE 1 (Weighting values are given in volts)

a) RECT-ANGULAR	NO. OF PTS	b) TRI-ANGULAR	NO. OF PTS	c) CIR-CULAR	NO. OF PTS	d) SINE-WAVE	NO. OF PTS
2.50	1	1.25	2	0.326749	1	3.258587	1
1.25	1	0.625	2	0.178405	1	0.523237	1
0.625	1	0.3125	2	0.093895	1	0.230969	1
0.3125	1	0.15625	2	0.075940	1	0.125676	1
0.15625	1	0.078125	2	0.043034	1	0.0625	1
0.078125	1	0.03906	2	0.027911	1	0.052815	1
0.03906	1	0.01953	2	0.024470	1	0.036243	1
0.01953	1	0.00976	2	0.020650	1	0.029073	1
0.00976	1	0.00488	2	0.017861	1	0.018941	1
0.00488	1	0.00244	2	0.012710	1	0.016234	1
0.00244	1			0.011545	1	0.010549	1
0.00122	1			0.009625	1	0.008143	1
				0.008141	15	0.004753	1
						0.003041	1
						0.002031	5

The computer program was able to identify weighting function values accurately to six decimal places. However, for on-line use the shift-register generating procedure has an accuracy of approximately $\pm$ 1mv in 10 volts due to round-off in digital to analogue conversion, so weights less than 1mv were not computed. There is no theoretical restriction on the number of weights used: a maximum of fifty is

allowed in the present program.

The first three distributions (rectangular, triangular and semi-circular) were each modelled to three types of power spectra. Figure 3 shows the models obtained.

FIGURE 3: POWER SPECTRUM MODELS

KEY

——— : Desired power spectrum

- - - - - - : Model obtained with triangular distribution

..... : Model obtained with rectangular distribution

—·—·— : Model obtained with semi-circular distribution

a) Rectangular Power Spectrum Model

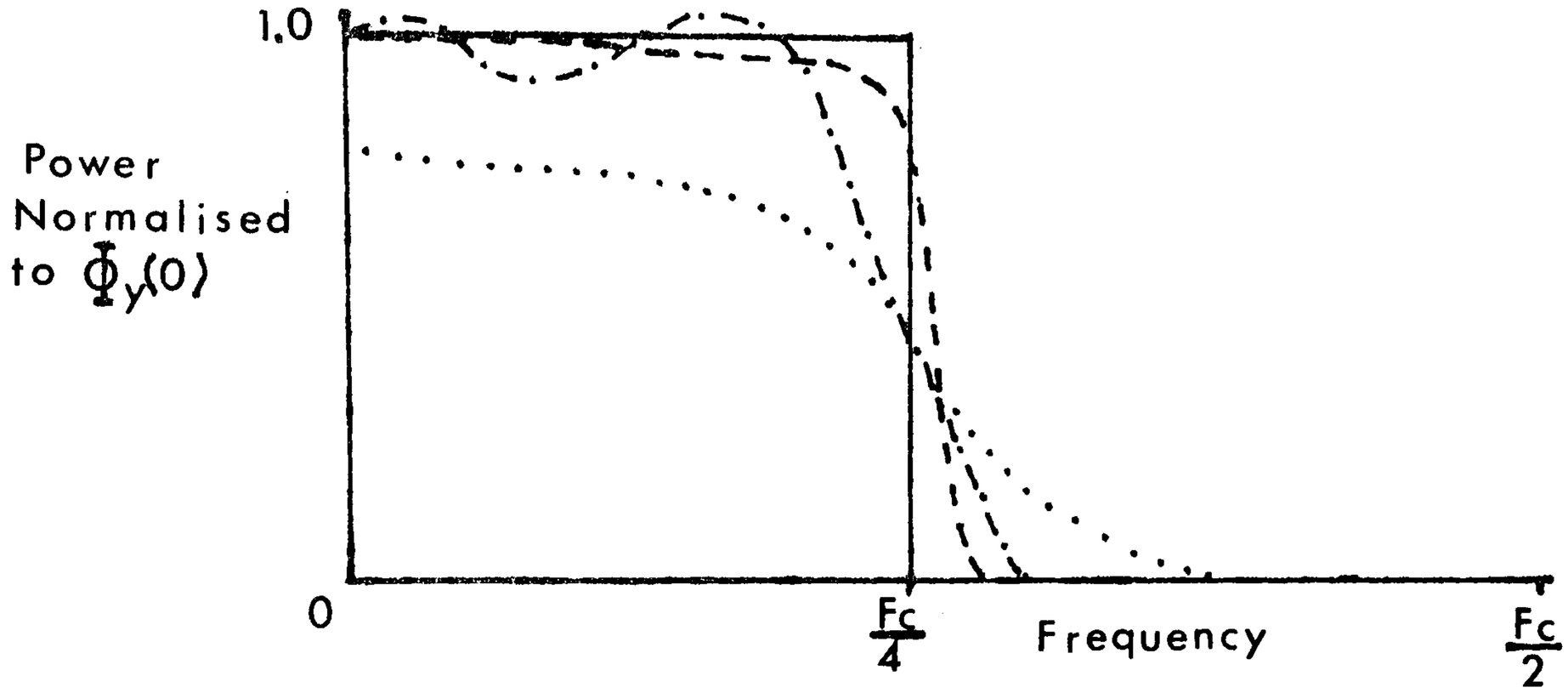

b) Power Spectrum with 6dB/Octave Cut-off

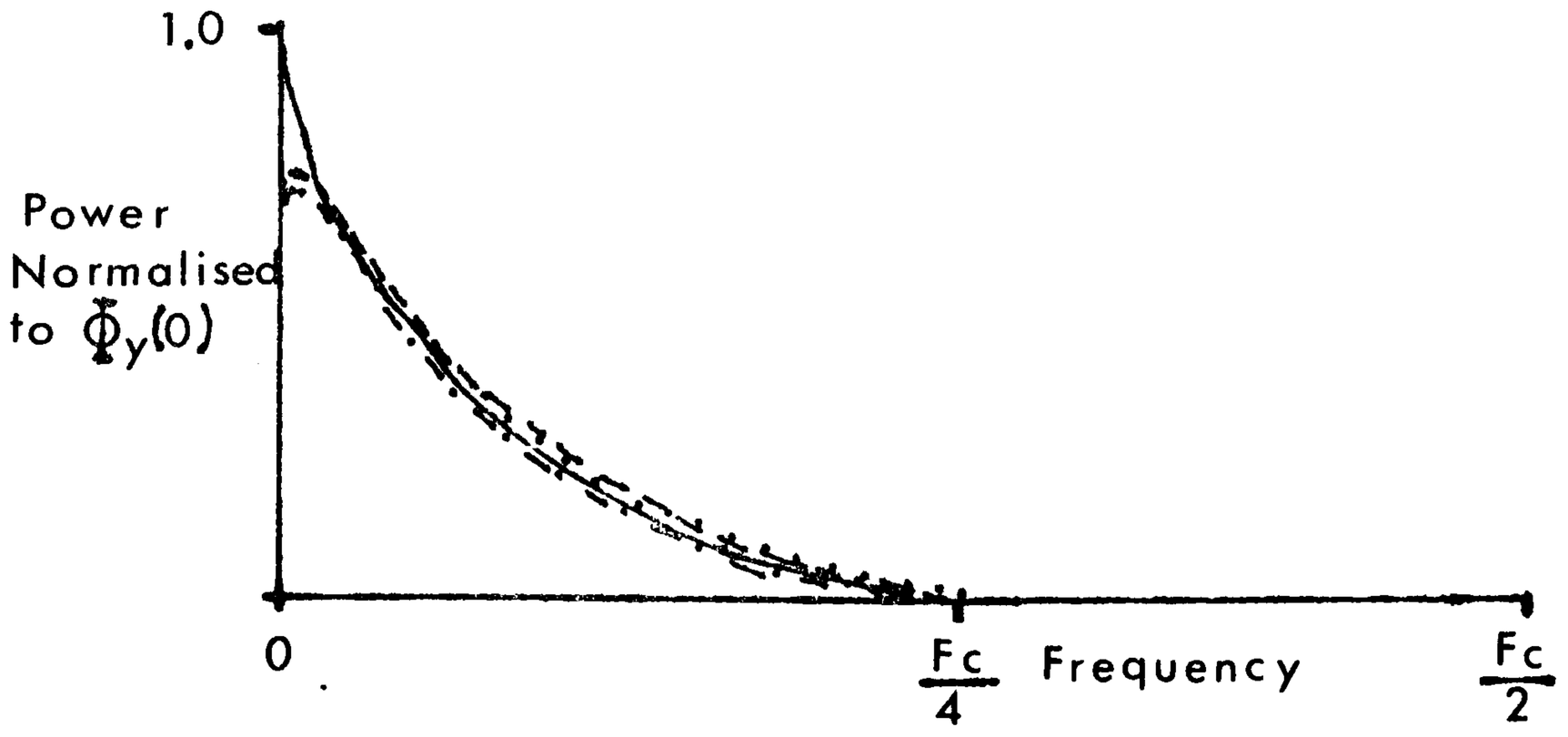

c) Band Pass Spectrum

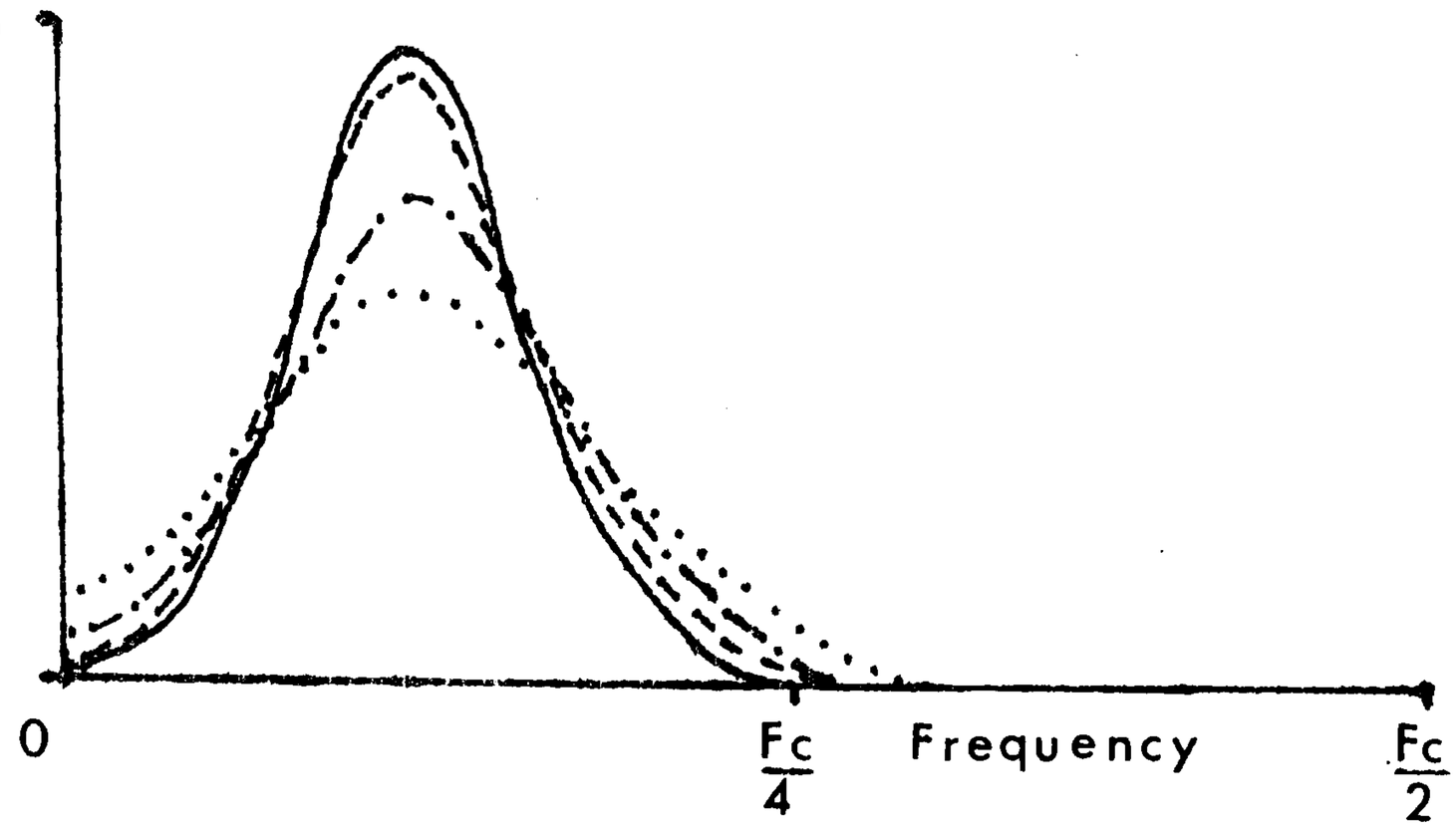

The ability to order a given series of weights along the shift register to approximately achieve the desired output power spectrum depends on the form taken by the impulse response of a filter, fed with band-limited white noise, whose output has the desired power characteristics. The shift register is acting as a digital filter. Good matching of the weights obtained in Section 2(i) to this impulse response will ensure a reasonable model of the output power spectrum.

One method of ordering the weights along the shift register is to recover the impulse response of a minimum phase linear network from the amplitude and slope characteristics of the desired output power spectrum, assuming the input to be white noise. The weights are then matched, (biggest to biggest as previously discussed) to this impulse response.

This method was not used here for two reasons:

a) The recovered impulse response is only one of a family of possible filters and may not give the best possible model.

b) The recovery process is computationally awkward and inaccurate when the desired spectrum is only specified up to some

maximum frequency Fc/2.

Details of the operating modes of computer programs developed for signal generation are listed in Appendix B at the end of this chapter.

3(i) FATIGUE RIG CONTROL

Although an input signal with the desired amplitude probability and power spectrum distributions may be generated and used to drive an electro-mechanical or servo-hydraulic loading system, the dynamics of the loading rig may severely alter the achieved loading pattern. This is particularly important at higher frequencies which can be attenuated due to the low-pass characteristics of the rig.

One method of achieving desired peaks in the signal is to drive the machine cycle by cycle using a constant velocity input and wait for the machine to catch up. A simple 'bang-bang' time domain controller for use on linear systems is proposed in Appendix C. However, in general, this form of control is undesirable from two aspects:

a) The power spectrum is modified.

b) The relative phases between frequency components are changed.

An alternative is to incorporate the rig as the forward-loop component in a closed-loop system, with a suitably designed controller in the feedback-loop. The performance of this type of system has the disadvantage of being input-dependent and subject to stability considerations.

A third, more appealing, method is to compensate for the effects of the rig dynamics by modifying the characteristics of the input signal. Two possible approaches make use of frequency response analysis or the adoption of a model reference system.

The second approach requires a mathematical approximation to the

rig transfer function to be made initially. The parameters of this mathematical model are then estimated and updated continuously using sampled data of the force delivered and force achieved time signals. The input driving function is then modified by the inverse of the modelled rig transfer function such that the signal demanded to signal achieved has a unity gain and zero phase frequency response. The disadvantages of this system are:

a) The initial mathematical model used is dependent on individual rig characteristics

b) The output signal may be a time-delayed version of the input, with no cost to the user. This is difficult to build into the model reference system as the choice of a suitable time delay is arbitrary.

The system adopted operates using a similar principle to that of model reference, except that the compensation required on the input demanded signal is calculated directly from the measured frequency response between input demanded and input achieved.

The demanded driver signal x(t) may be generated internally by the computer or externally using a random signal generator. Ideally, y(t) the output driving signal, should be a time-delayed version of x(t); the time constant of the time delay being chosen such that the phase compensation introduced by the compensator is minimised. This ensures y(t) has the demanded amplitude probability and power spectrum distributions.

The signals x(t) and y(t) are sampled at a frequency fs such that the power in x(t) above frequencies of fs/2 is negligible. The samples are taken in blocks of $N(= 2^M)$ points and Fourier transformed (using

FIGURE 4: SHOWS COMPUTER/RIG INTERFACE

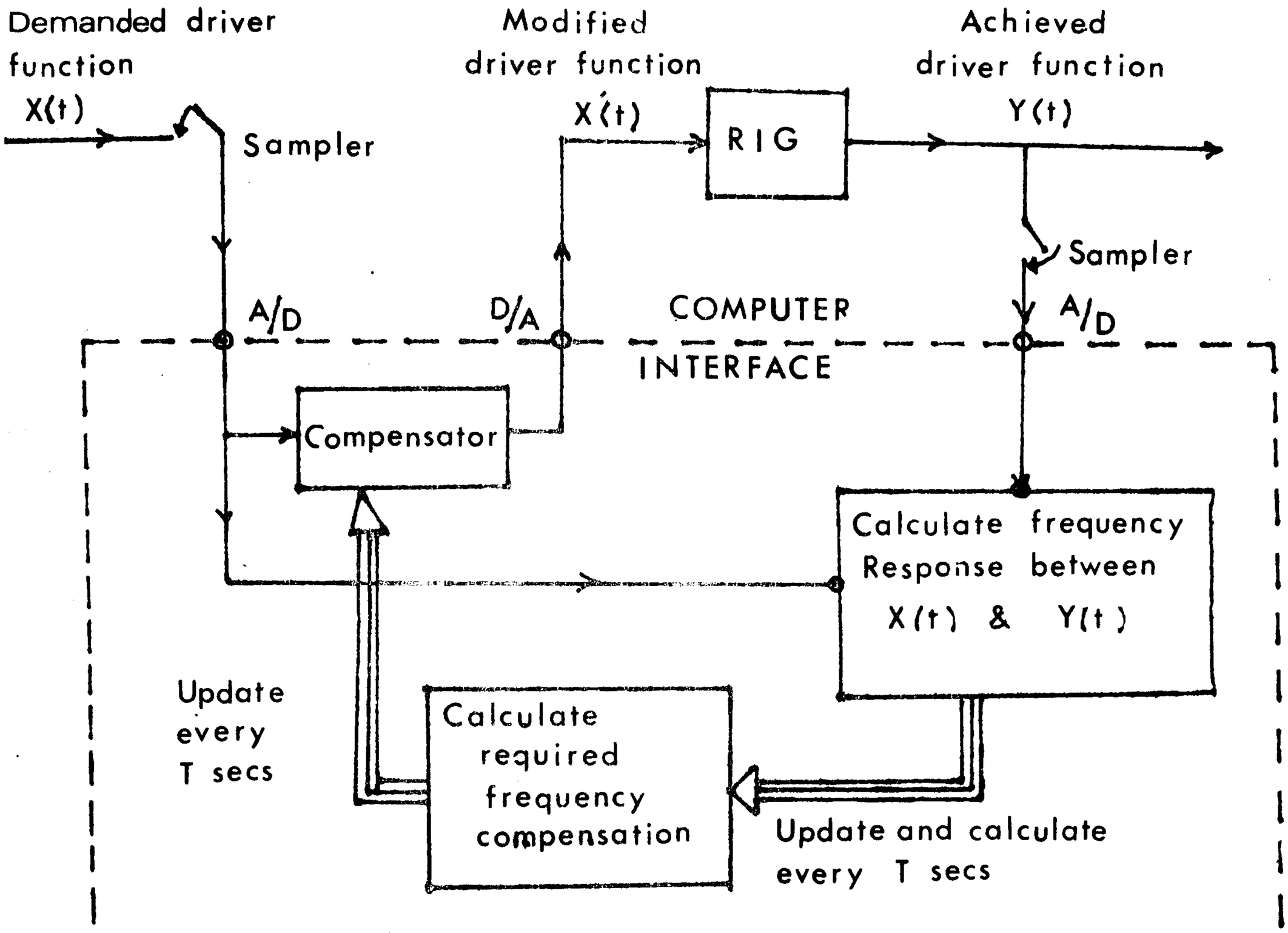

FIGURE 5: SHOWS A TYPICAL RIG FREQUENCY RESPONSE COMPARING IT WITH THE DESIRED IDEAL FREQUENCY RESPONSE

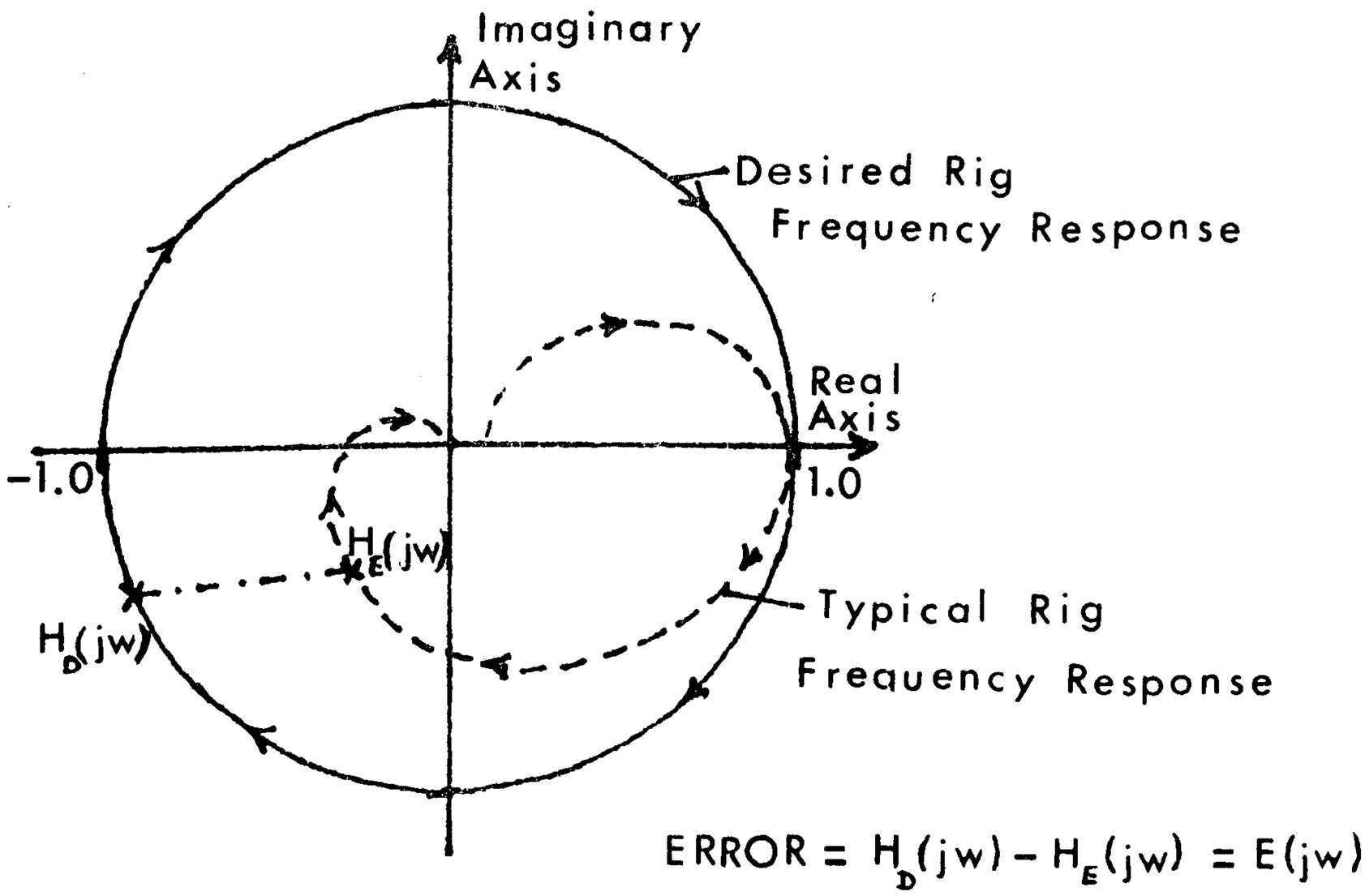

a digital F.F.T. algorithm) to produce N/2 + 1 complex Fourier coefficients at discrete frequency intervals Wo (wo = fs/N)

$$\hat{X}(KWo) = \frac{1}{N}\sum_{I=0}^{N-1} Xt(I)\ \mathcal{E}^{-jWoIK} \quad \ldots\ldots\ldots 5.14(a)$$

$$\hat{Y}(KWo) = \frac{1}{N}\sum_{I=0}^{N-1} Yt(I)\ \mathcal{E}^{-jWoIK} \quad \ldots\ldots\ldots 5.14(b)$$

The auto-spectrum $\hat{\phi}_{xx}(KWo)$ and cross-spectrum $\hat{\phi}_{xy}(KWo)$ are then calculated by:

$$\hat{\phi}_{xx}(KWo) = \hat{X}^*(KWo) \cdot \hat{X}(KWo) \quad \ldots\ldots\ldots 5.15(a)$$

$$\hat{\phi}_{xy}(KWo) = \hat{X}^*(KWo) \cdot \hat{Y}(KWo) \quad \ldots\ldots\ldots 5.15(b)$$

where * denotes the complex conjugate.

The estimated frequency response between x(t) and y(t) is then averaged over L such individual time blocks. The number of blocks, L, is chosen to give the desired update period T on the compensator:

$$T = L \cdot N/fs \text{ secs} \quad \ldots\ldots\ldots 5.16$$

$$\hat{H}_E(KWo) = \bar{\phi}_{xy}(KWo) \,/\, \bar{\phi}_{xx}(KWo) \quad \ldots\ldots\ldots 5.17$$

for $0 \leqslant K \leqslant N2$ where :—

$$\bar{\phi}_{xy}(KWo) = \frac{1}{L}\sum_{I=1}^{L} \hat{\phi}_{xy}^{I}(KWo) \quad \ldots\ldots\ldots 5.18(a)$$

$$\bar{\phi}_{xx}(KWo) = \frac{1}{L}\sum_{I=1}^{L} \hat{\phi}_{xx}^{I}(KWo) \quad \ldots\ldots\ldots 5.18(b)$$

The number of estimates, L, used to calculate $\hat{H}_E^T(jw)$ is taken above as the time average of L independent estimates. As L increases the variance in $\bar{H}_E^T(jw)$ decreases at the expense of T, the update period, becoming large. This can be avoided by smoothing over adjacent frequency points instead of, or as well as, over time. Frequency smoothing can however introduce bias into estimates of $\bar{H}_E(jw)$ as well as decreasing the frequency resolution. For the fatigue rigs used in experiments presented

in this chapter, the frequency resolution was sufficient to allow significant frequency smoothing without introducing detrimental bias errors.

The compensator frequency characteristics are now calculated so that the error E(jw) is decreased:

$$Cnew(jw) = Cold(jw) + K \frac{E(jw)}{H_E(jw)} \cdot Cold(jw) \quad \ldots \quad 5.19$$

where Cnew(jw) = New compensator frequency response

Cold(jw) = Current compensator frequency response

E(jw) = Current error = $H_D(jw) - H_E(jw)$

and K is some constant such that $0 \ll K \ll 1$.

The choice of K determines the ability of the compensator to correct itself in response to possible changes in the rig dynamics. When K = 1.0 the compensator acts in a 'bang-bang' mode, such that the complete error is compensated in one step. When K=0 the compensator is non-responsive to the rig dynamics. The compensator is usually set to unity at the beginning of a run. The user has four parameters to adjust:

a) <u>The choice of the sampling frequency</u> is determined by the frequency content in the driving signal x(t). f_s must be greater than or equal to twice the maximum significant frequency component in x(t).

b) <u>The update period T</u> is chosen such that there is sufficient time to calculate an accurate estimate of the frequency response $H_E^T(jw)$. The accuracy of $H_E^T(jw)$ depends on the input signal to output noise ratio (i.e. noise introduced by the rig and measuring devices). As this ratio decreases, the accuracy decreases and T must increase to achieve a consistent estimate. For most rigs, noise is not a severe problem, but in situ testing may present noise problems. A method of choosing T automatically to ensure $H_E^T(jw)$ lies within certain bounds of the true value with a given confidence level is a subject for further consideration.

The results of Chapter 2 give the theoretical basis for such a process.

c) The block size N. Together with the update period T this determines the number of independent estimates used in forming $H_E{}^T(jw)$. As N is increased, the frequency resolution is also increased. N must be chosen to give sufficient frequency resolution over the frequency range of interest.

d) The constant K in equation 5.19. The choice of K affects the choice of the previous two parameters. It is found that if K is set equal to 1 and frequency smoothing is in operation the system can go unstable under noisy conditions. This is due to errors at frequency f_1 being propagated to adjacent frequencies by the frequency smoothing. The initial impetus is supplied by sampling errors in $H_E{}^T(jw_1)$. (These are due to short-term measurement under noisy conditions.) These errors are introduced into a neighbouring frequency f_2 where perhaps there is no error initially. At the next update period the error at frequency f_2 is transferred further along the line, the system corrects for a non-existent error, further compounding the error at f_1. This effect of frequency instability can be limited by smoothing only over frequency bands, with adjacent bands remaining independent. This has the effect of limiting the possible range of propagation of the instability and it was found for the rigs used that this was sufficient to ensure stability under most conditions (even with T very short).

With K equal to 1.0 the compensator acts in the form of a statistical sample and hold action with a 'bang-bang' error correction. As K decreases, the compensator response to changes in the rig driver dynamics is impaired. However, the control process can never go unstable through the choice of K (except in the form of frequency error propagation just mentioned.)

The variance in an (integral error)^2 cost function over frequency given by:

$$COST(T) = \int_0^{fs/2} \left\{ H_D{}^T(jw) - H_E{}^T(jw) \right\}^2 \, dw$$

is however increased by increasing K.

The limitations of this technique of compensatory driving are threefold:

a) Where the input power in the original signal x(t) is small compared to the noise introduced in the system, the frequency response estimate is subject to large variance. Thus in regions of low input-power, it may be advisable to have a 'do-nothing' compensator so that noise is not introduced by possible large errors in the estimated frequency response. This has little effect on the resulting time signal y(t) as x(t) contained minimal frequency components over these ranges anyway.

b) In trying to achieve overall unity gain there is a possibility of x'(t) (see Figure 4) exciting non-linearities in the rig driving system. These non-linearities usually take the form of amplifier saturation or distortion and hysteresis. In these cases there is little that can improve the situation as it is simply a case of overdriving the machine.

c) The low-pass characteristics of loading machines ensure that at high frequencies, whatever the demanded input, the output is negligible. By trying to counteract very low gains the user runs into the problems laid out in(b). Thus the overall frequency response can only be modified up to some frequency Fmax. The power spectrum $\phi_{xx}(f)$ must have dropped to negligible levels by this frequency for the compensatory system just

described to operate.

The process was implemented on a Rank Xerox Sigma 5 computer. It can, however, if written in suitable assembler code, be suited to a small 8K word mini-computer with an appropriate interface.

3(ii) RESULTS

Two loading rigs were used to test the viability of the control scheme: a Derritron electro-magnetic vibrator and a larger servo-hydraulic rig.

a) RUN RESULTS USING A 3-PEAKED INPUT SPECTRUM WITH A GAUSSIAN AMPLITUDE PROBABILITY FUNCTION

Steel and aluminium rods were subjected to cantilever bending (the set-up is shown in detail in the last part of this chapter), using an electro-magnetic vibrator as the loading rig. Figure 6 shows the rig frequency response before and after compensation. The compensated frequency response is shown to be a pure time-delay in the frequency range 0-70 Hz.

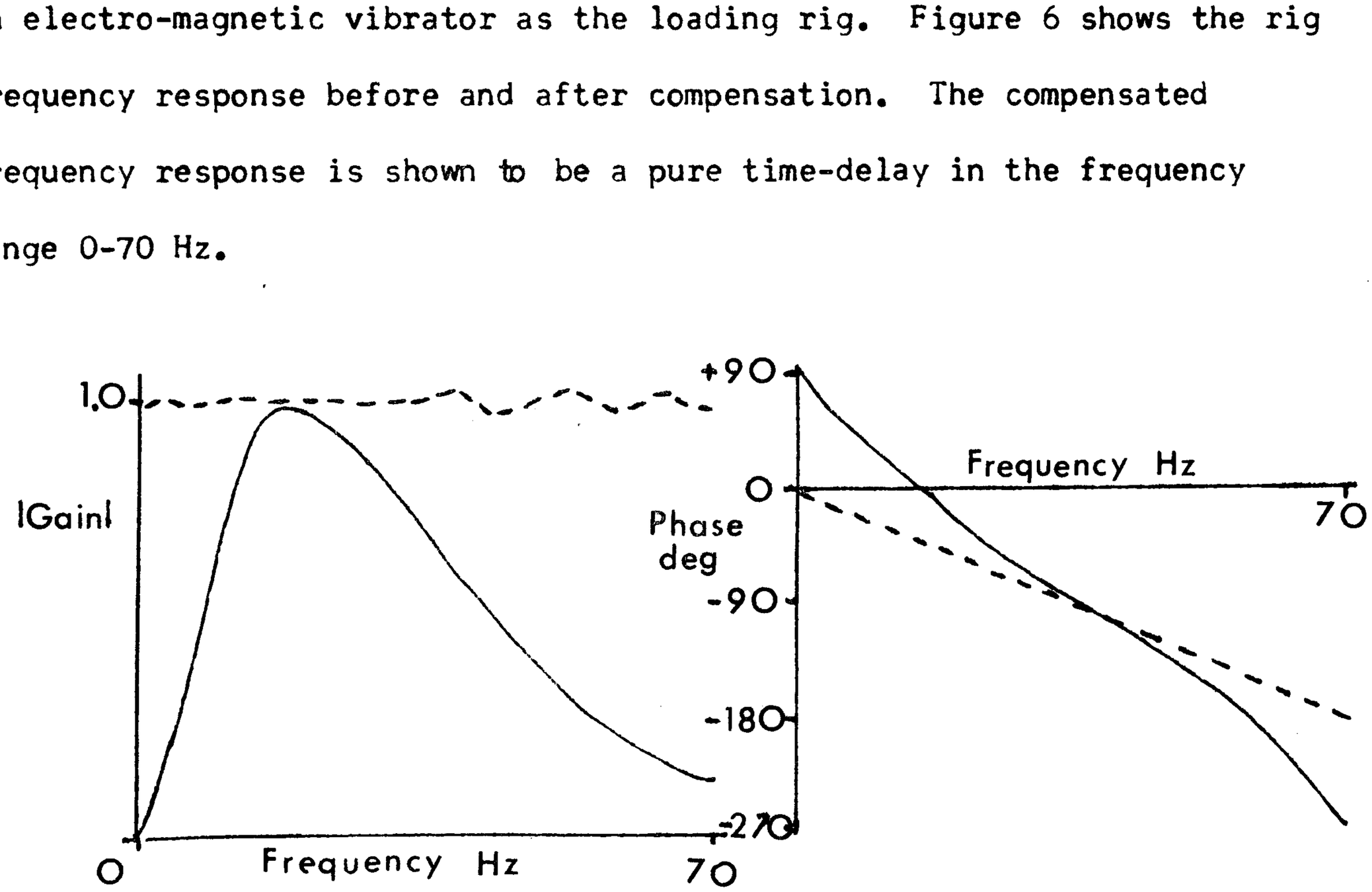

FIGURE 6: SHOWS a) Measured Rig Frequency Response without compensation (—)
b) Measured Rig Frequency Response with compensation (-- -)

Figures 7 and 8 show the effect of compensation on the achieved power spectrum and amplitude probability distribution.

FIGURE 7: SHOWS a) The demanded auto-spectrum (———)

b) The non-compensated auto-spectrum (– – – –)

c) The compensated auto-spectrum (– · – · –)

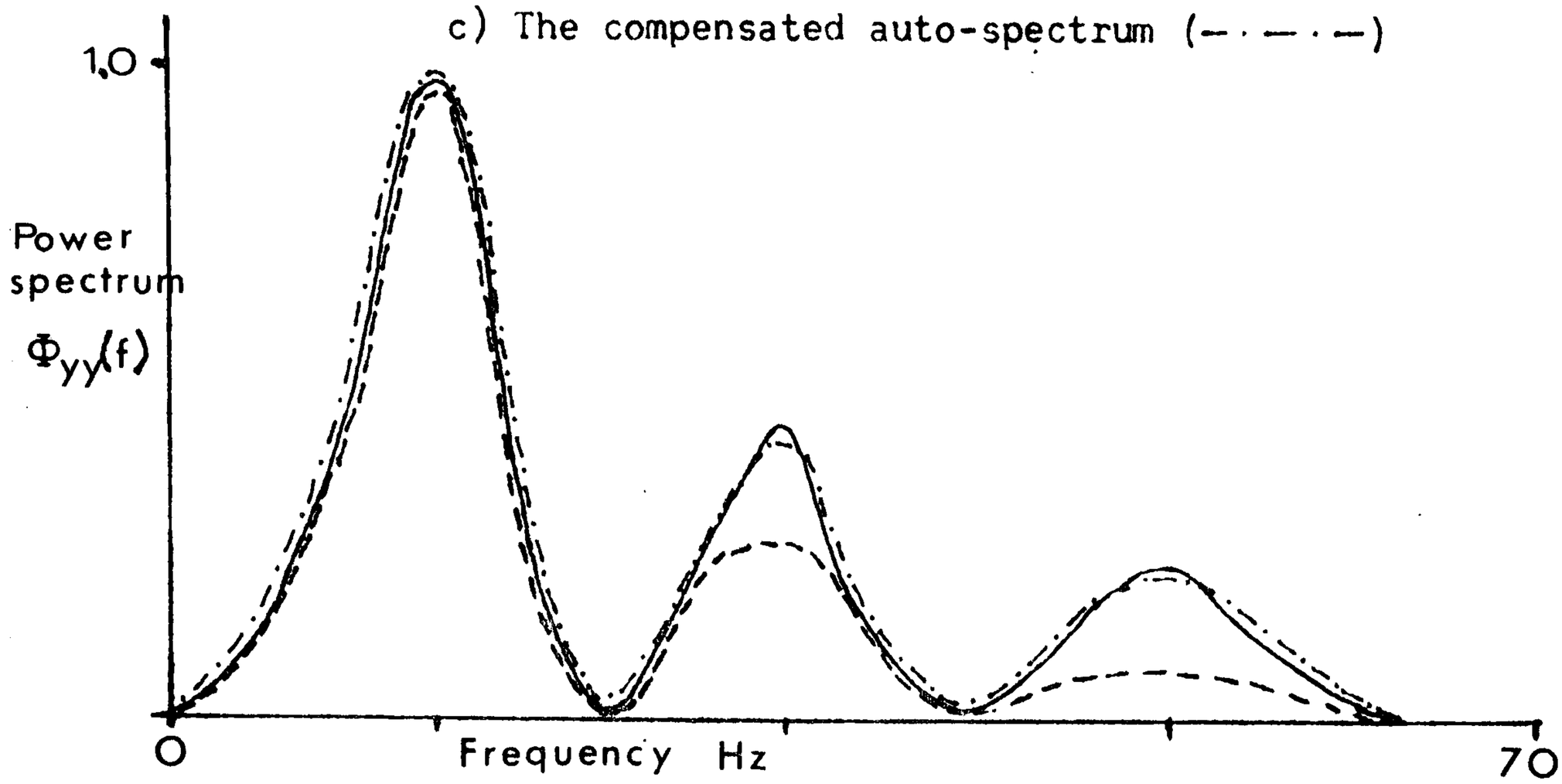

FIGURE 8: SHOWS THE AMPLITUDE PROBABILITY DISTRIBUTION OF

a) The desired input (———)

b) The achieved output without compensation (– – – – –)

c) The achieved output with compensation (– · – · –)

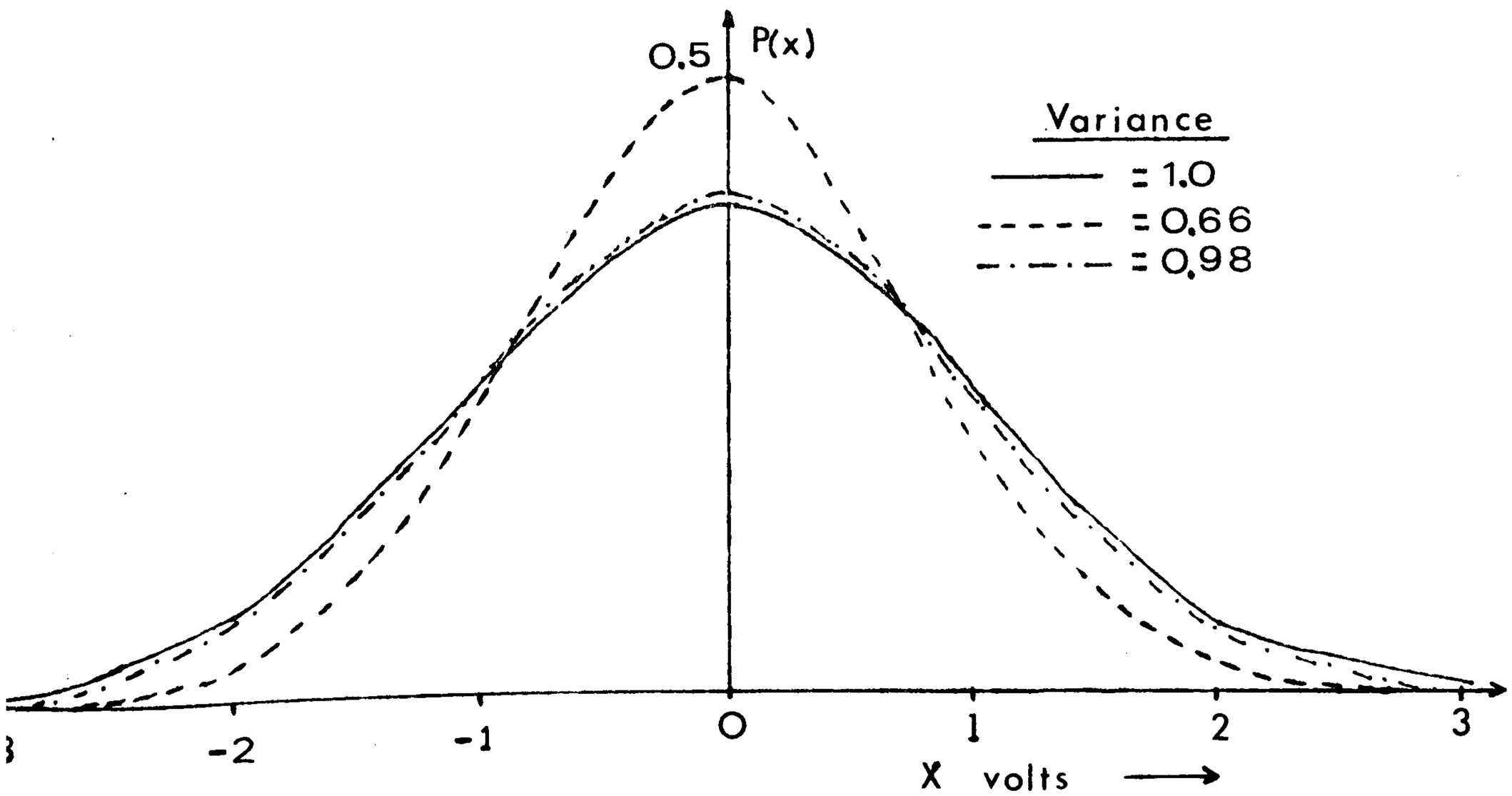

Figures 6, 7, and 8 show that for a 3-peaked input spectrum the power spectrum and amplitude probability functions are almost exactly restored using compensation. The change in the amplitude probability distribution is not in its shape but only in its variance. For the case next discussed, the change is more marked.

b) RUN RESULTS USING A 2-PEAKED INPUT-SPECTRUM WITH RECTANGULAR AMPLITUDE PROBABILITY DISTRIBUTION

Similar tests as shown in the previous section were repeated for a different input signal. Figures 9 and 10 show that the power spectrum is again recovered but, more importantly perhaps, the rectangularity of the amplitude distribution is to a large degree restored.

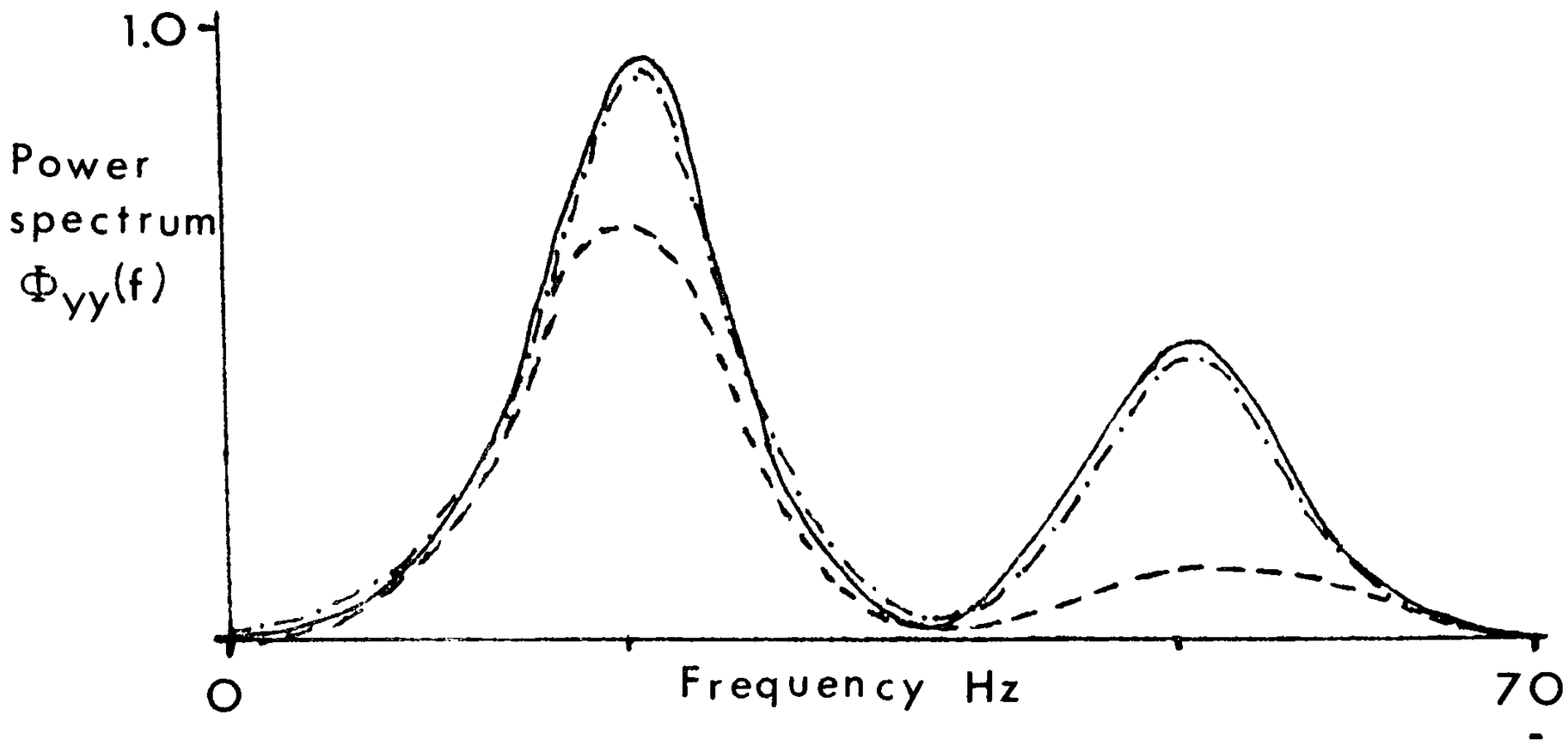

FIGURE 9: SHOWS a) The demanded auto-spectrum (———)

b) The non-compensated achieved auto-spectrum (- - - - -)

c) The compensated achieved auto-spectrum (—·—·—)

FIGURE 10: SHOWS a) The original amplitude distribution as desired (——)

b) The achieved amplitude distribution without compensation (– – – – – –)

c) The achieved amplitude distribution with compensation (. — . — . —)

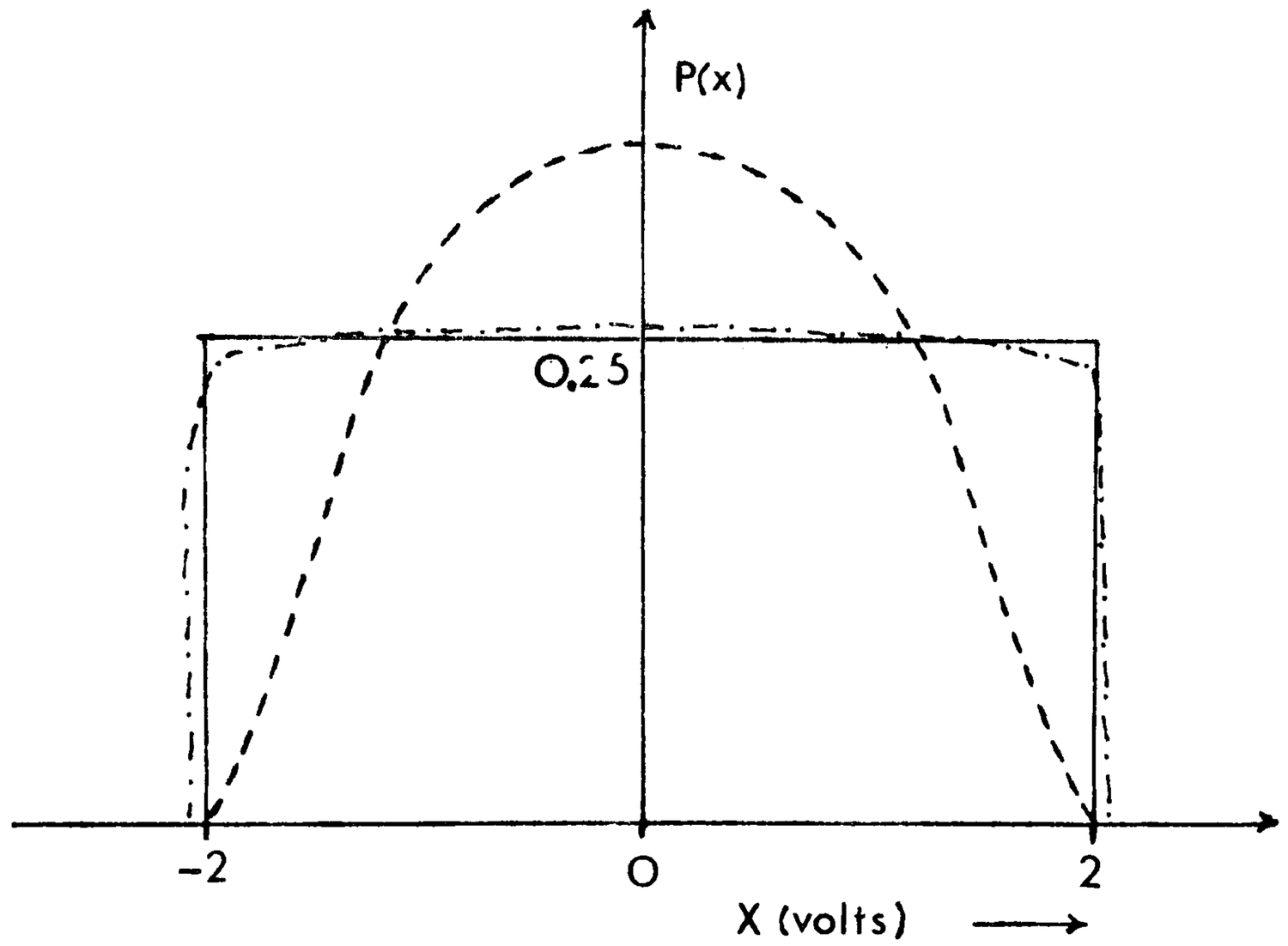

Although the compensated amplitude distribution is approximately rectangular, there is still some residual rounding, as the frequency response of the loading rig was only modified up to 70 Hz.

Six tests (3 without compensation, 3 with) were performed with each form of spectral input. The results presented were consistently achieved for each mode of system input. The parameter values chosen for the compensation were as follows:

K = 1.0 (in equation 3.6)

fs = 140 Hz = sampling frequency

N = 512 (block size)

T ≏ 18 seconds (update period)

Estimates were smoothed over 5 points in the frequency domain.

c) RECOVERY OF PEAK TROUGH DISTRIBUTION ON A SERVO-HYDRAULIC RIG

Defining the properties of a loading signal in terms of its auto-spectrum and amplitude probability is inadequate for the fatigue engineer. An alternative is to characterise a signal by its peak-trough probability matrix. This is defined as the probability of obtaining a peak-trough pair of amplitudes A_1, A_2 over the complete range $-\infty \leqslant A_1, A_2 \leqslant +\infty$. The joint peak-trough probability matrix is thus an upper triangular matrix (it is meaningless to have a signal peak value less than its paired trough). A constant velocity signal with specified peak-trough characteristics was generated (11) on a G.E.C. 90/2 computer. This signal was fed through the compensation system onto a servo-hydraulic rig applying a cantilever bending moment to a bearing structure. The peak-trough matrices of the original signal (Figure 11), the uncompensated achieved signal (Figure 12) and the compensated achieved signal (Figure 13) were measured over a half-hour period using the Sigma 5 computer. Figure 13 shows that the original peak-trough matrix is almost completely recovered by using compensation, whereas without compensation, the large amplitude peak-trough pairs are not achieved. The rig frequency response is very similar to that depicted in Figure 6, and is not repeated. Appendix C outlines the type of signal generated by the G.E.C. 90/2 computer for attaining a peak-trough matrix and gives a simple time-domain method of controlling the servo-rig as an alternative to the compensation method described here.

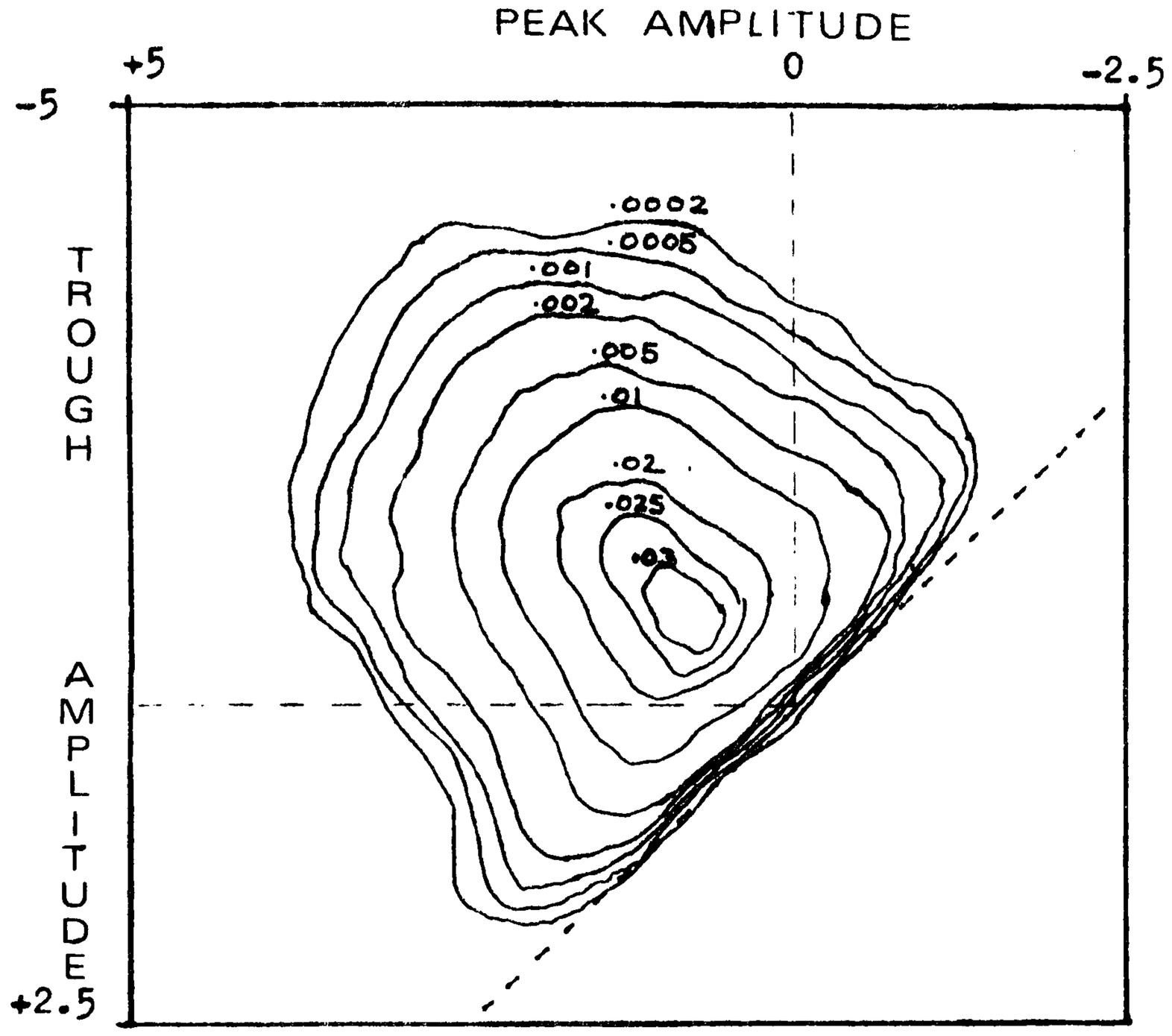

FIGURE 11 : Shows the Peak/Trough distribution of the original signal input.

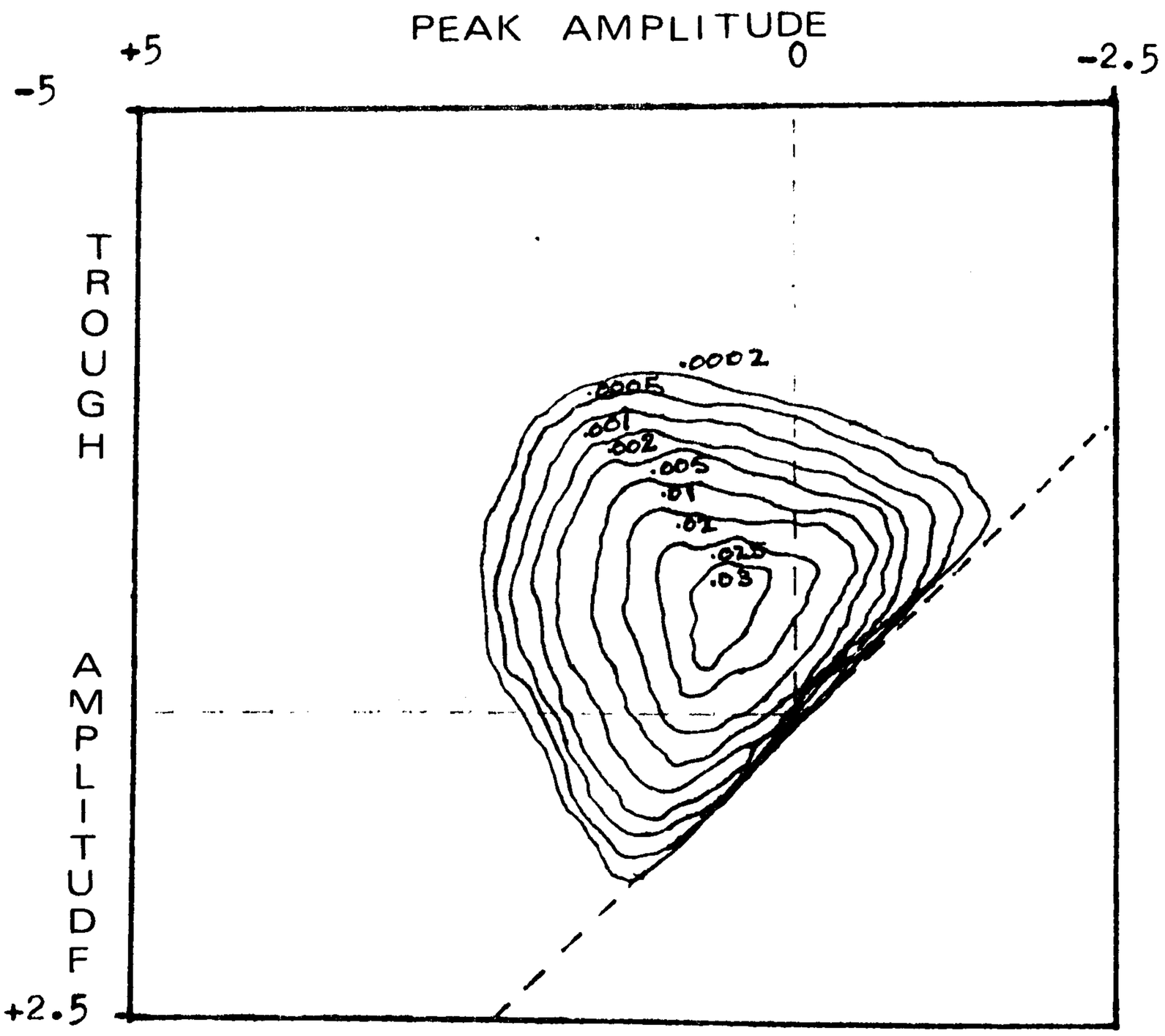

FIGURE 12 : Shows the achieved Peak/Trough distribution without compensation.

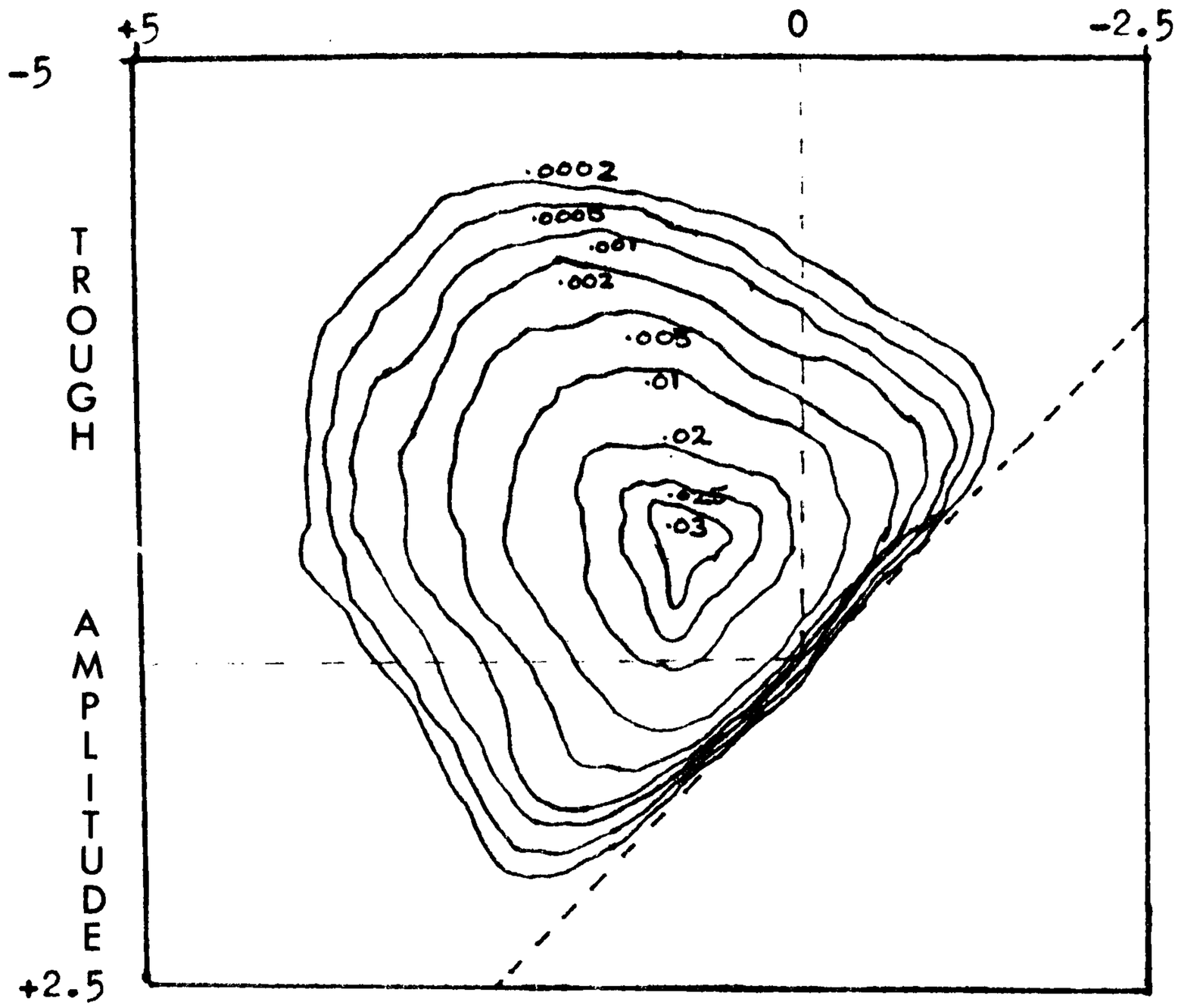

FIGURE 13: Shows the Peak/Trough distribution of the compensated loading signal.

The need for rig control depends on how accurately the engineer wishes to simulate loading time histories under laboratory conditions. When using a hydraulic servo-rig it is possible to dynamically tune the rig response to the particular task involved. However this has three drawbacks:

i) It is a lengthy procedure

ii) It does not take account of changes in the specimen's response during a test.

iii) On changing the specimen the rig must be retuned.

4(i) DETECTION OF FATIGUE CRACKING IN ALUMINIUM AND STEEL RODS

Forty fatigue tests, twenty on aluminium rods and twenty on steel, were performed, each specimen being tested to destruction. Figure 14

gives the specification for the rig and aluminium rod used. The mild steel rod was of the same dimensions.

Three input loading spectra were used, the two already shown in Figures 7 and 9 plus a third wide-band signal with a break point at 40 Hz and a cut-off of 6dB/octave.

Six tests were performed with each loading spectrum on the aluminium and steel rods in turn. The results presented show a typical response for each of the 6 groups of tests. Lastly a series of four tests was conducted, two on steel rods and two on aluminium, with each of the rods pre-work-hardened.

The input force to resulting displacement frequency response function was continually estimated over 18-second intervals throughout the specimen's fatigue life (typically 45-60 minutes for aluminium and 150-180 minutes for steel). A representative sample of the frequency response over the frequency range 0-70 Hz was taken at around 20% of fatigue life (when no fatigue cracks are present and work-hardening has ceased). This response was compared with estimates obtained over various stages in the specimen's life. Two cost functions were calculated:

a) The mean stationarity confidence interval satisfied over the frequency range 0-70 Hz. (as described in Chapter 2, equation 2.42)

b) The integral error squared function given by:

$$\text{COST} = \int_0^{70\ \text{Hz}} \left\{ H_1(jw) - H_2(jw) \right\}^2 \, dw \quad \ldots\ldots 5.20$$

where H_1 is the representative sample and H_2 is the estimate being tested.

Figures 15 - 21 show the change in the confidence level, together with the cost function as a function of % sample life.

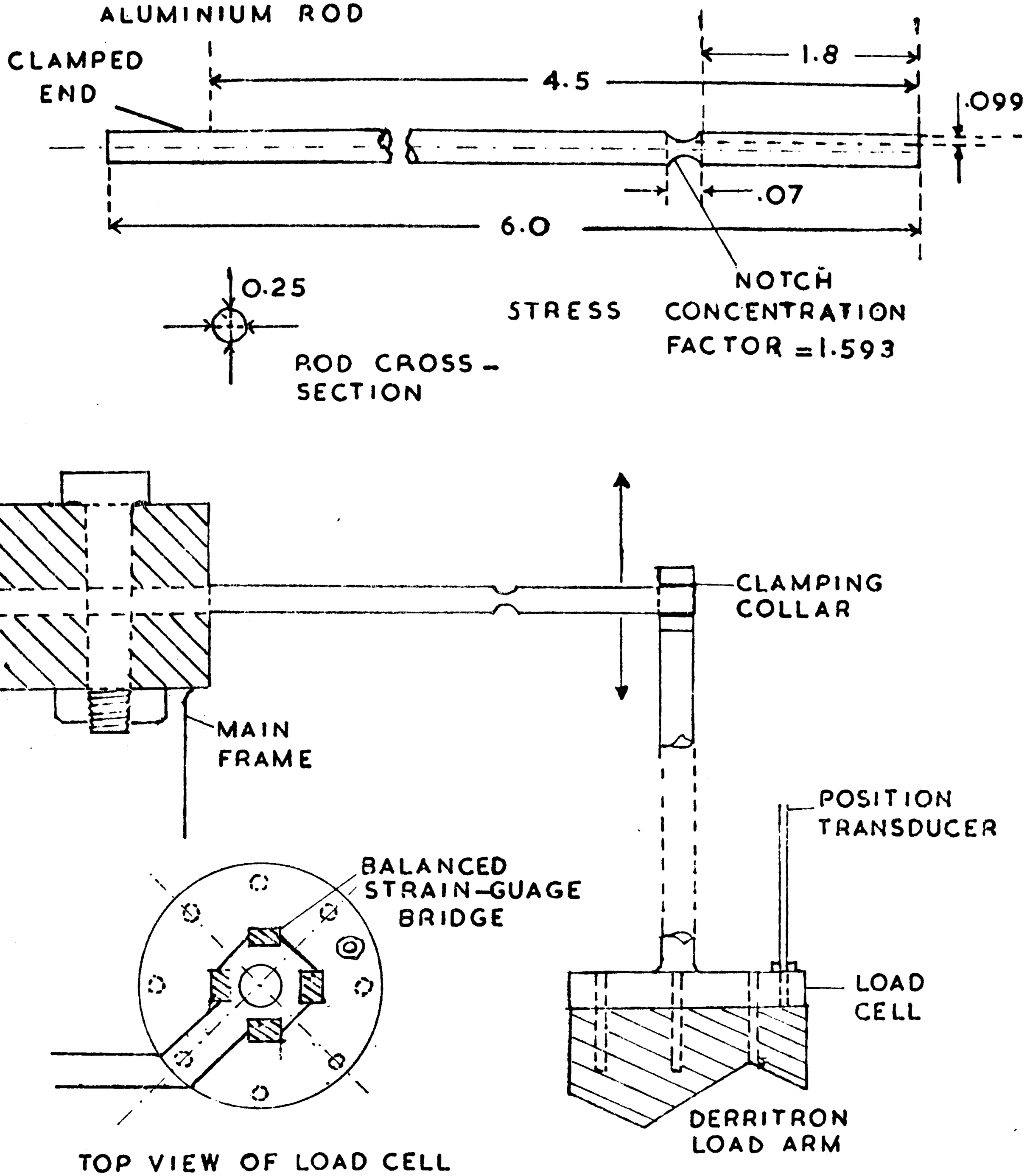

FIGURE14 : SHOWING LOADING CONFIGURATION ON ALUMINIUM ROD SUBJECTED TO CANTILEVER BENDING.

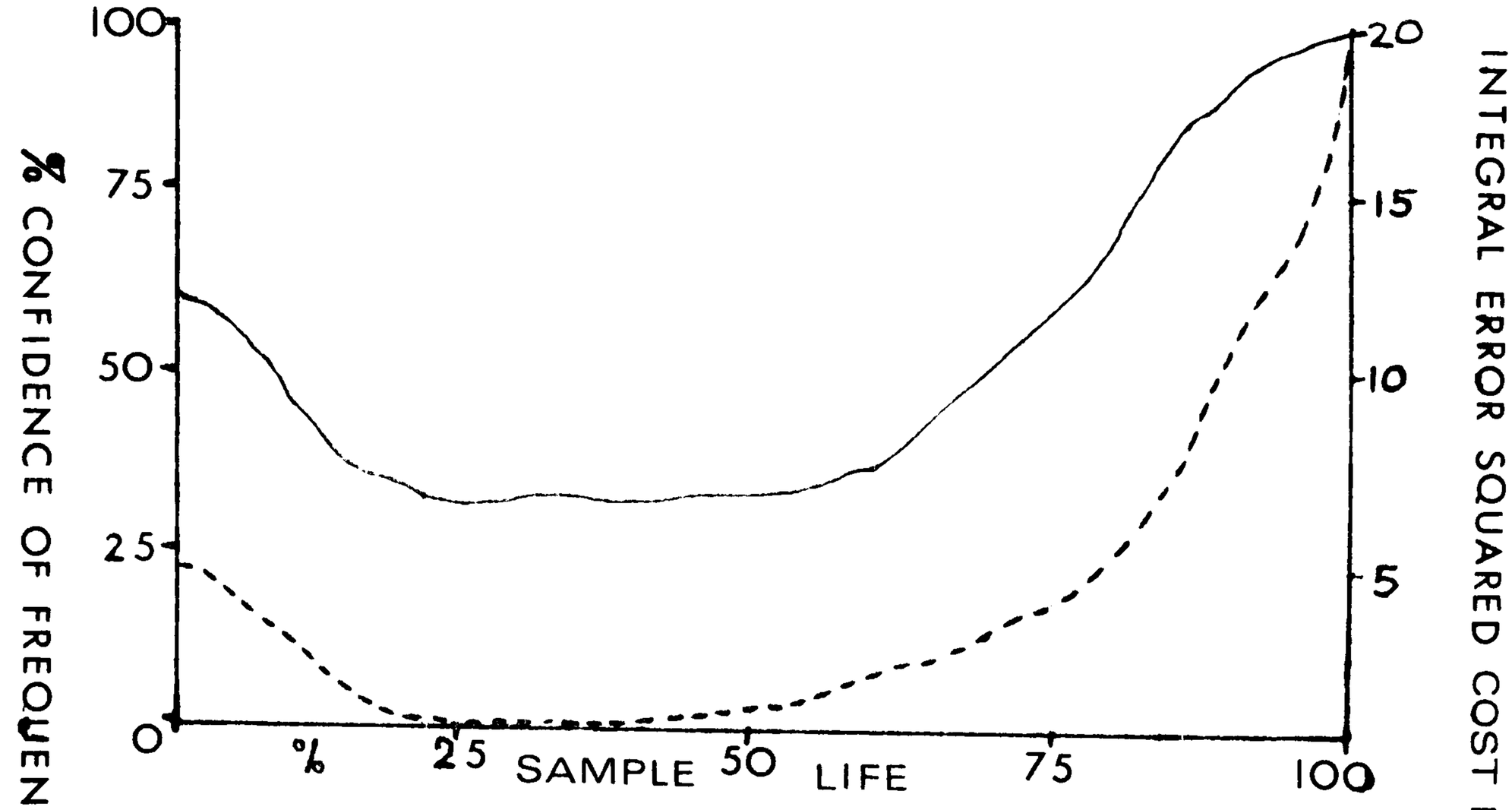

FIGURE 15 : Shows the change in response of an aluminium rod against % fatigue life for the 3-peaked loading spectrum.

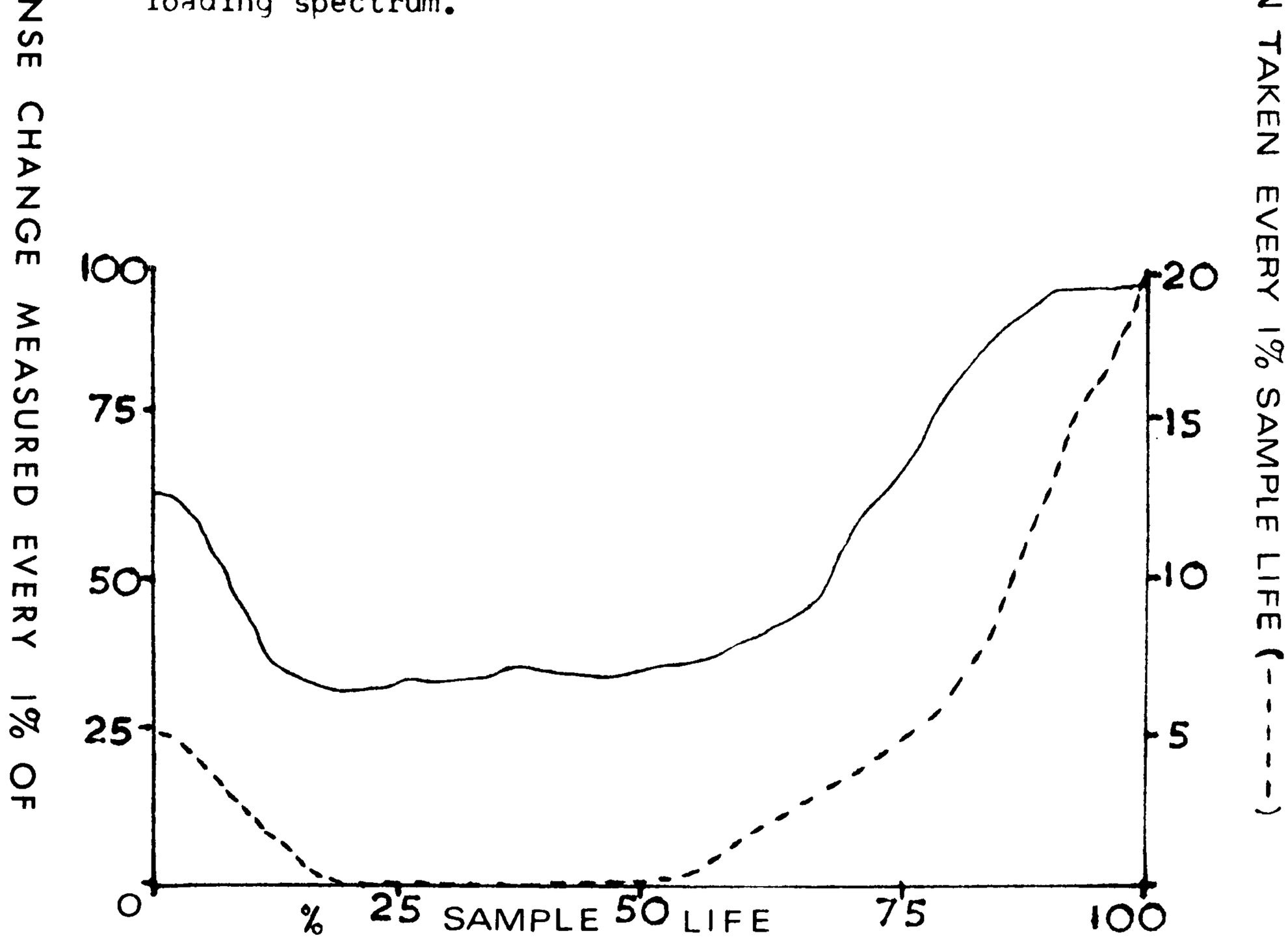

FIGURE 16 : Shows the change in response of an aluminium rod against %fatigue life for the 2-peaked loading spectrum.

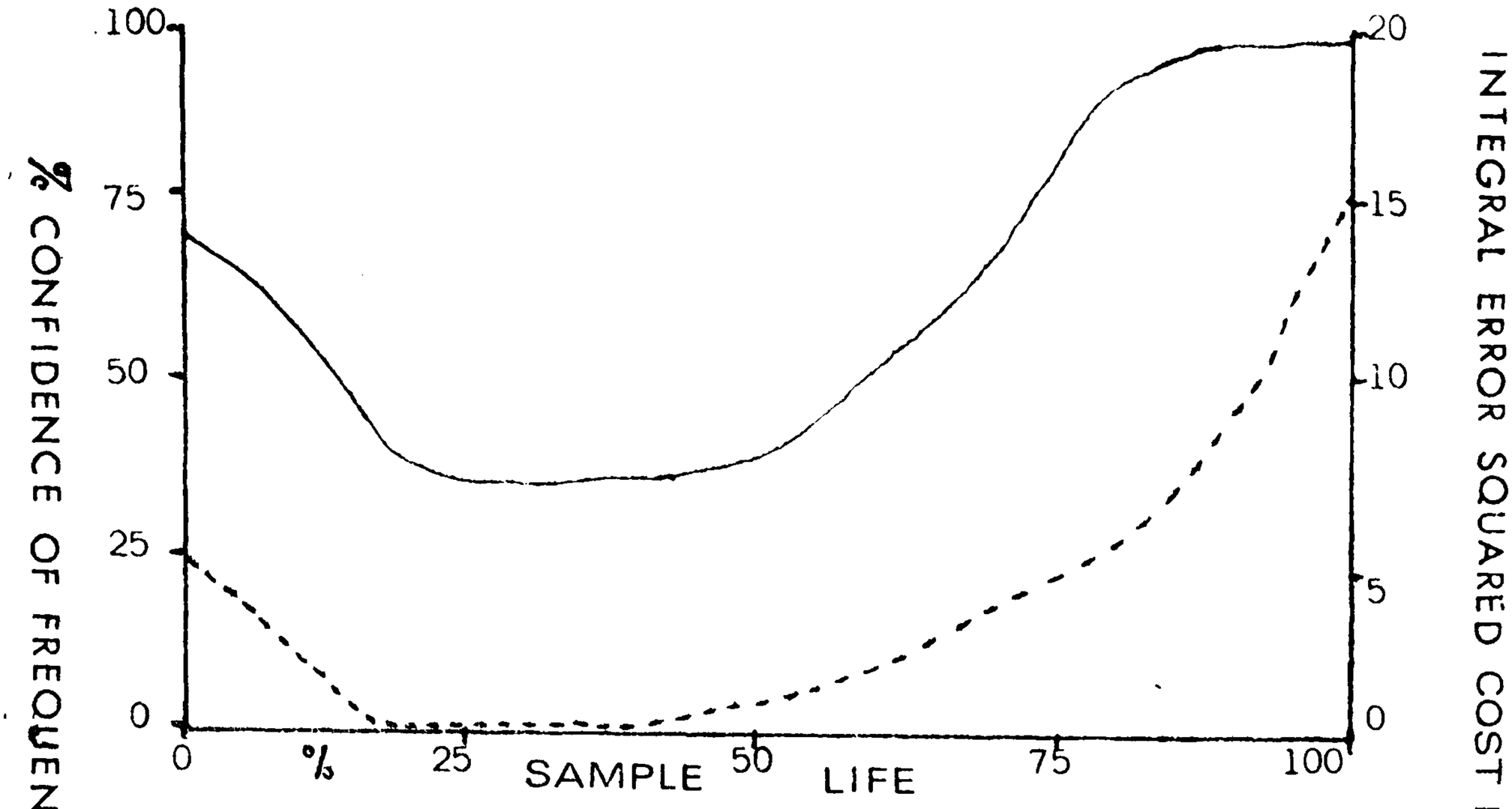

FIGURE 17 : Shows the change in response of an aluminium rod against % fatigue life for the broad band loading spectrum.

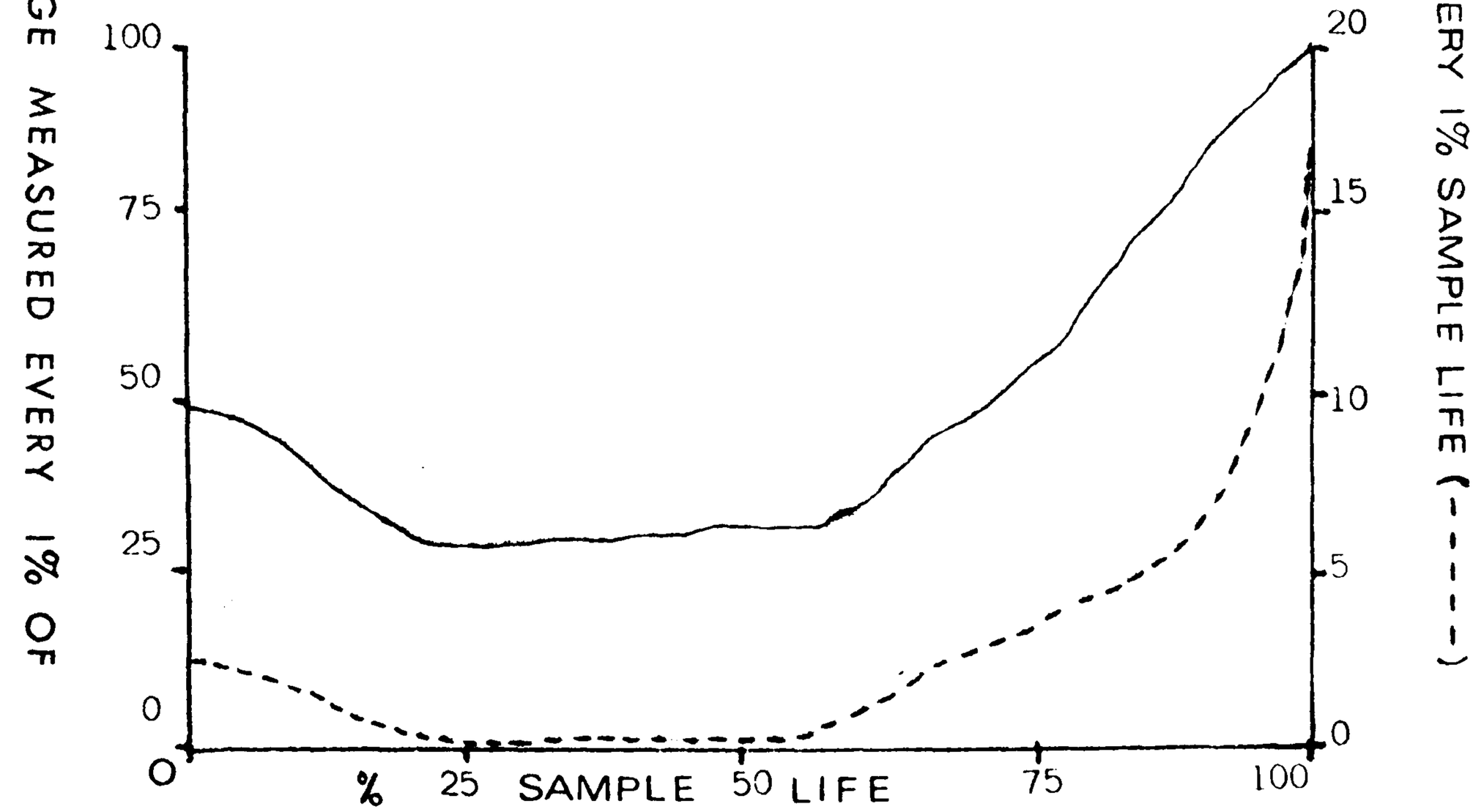

FIGURE 18 : Shows the change in response of a steel rod against % fatigue life for the 3-peaked loading spectrum.

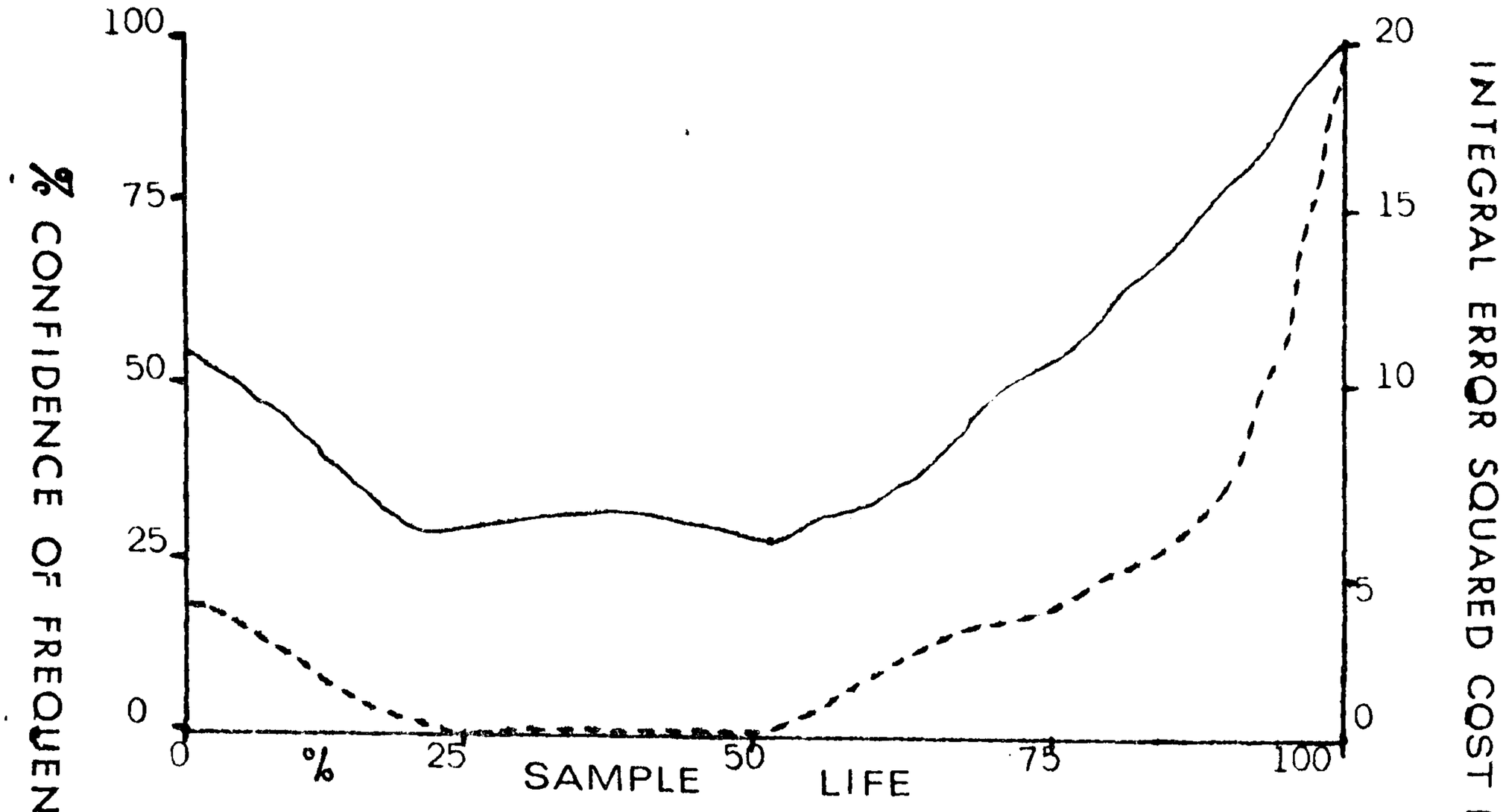

FIGURE 19 : Shows the change in response of a steel rod against % fatigue life for the 2-peaked loading spectrum

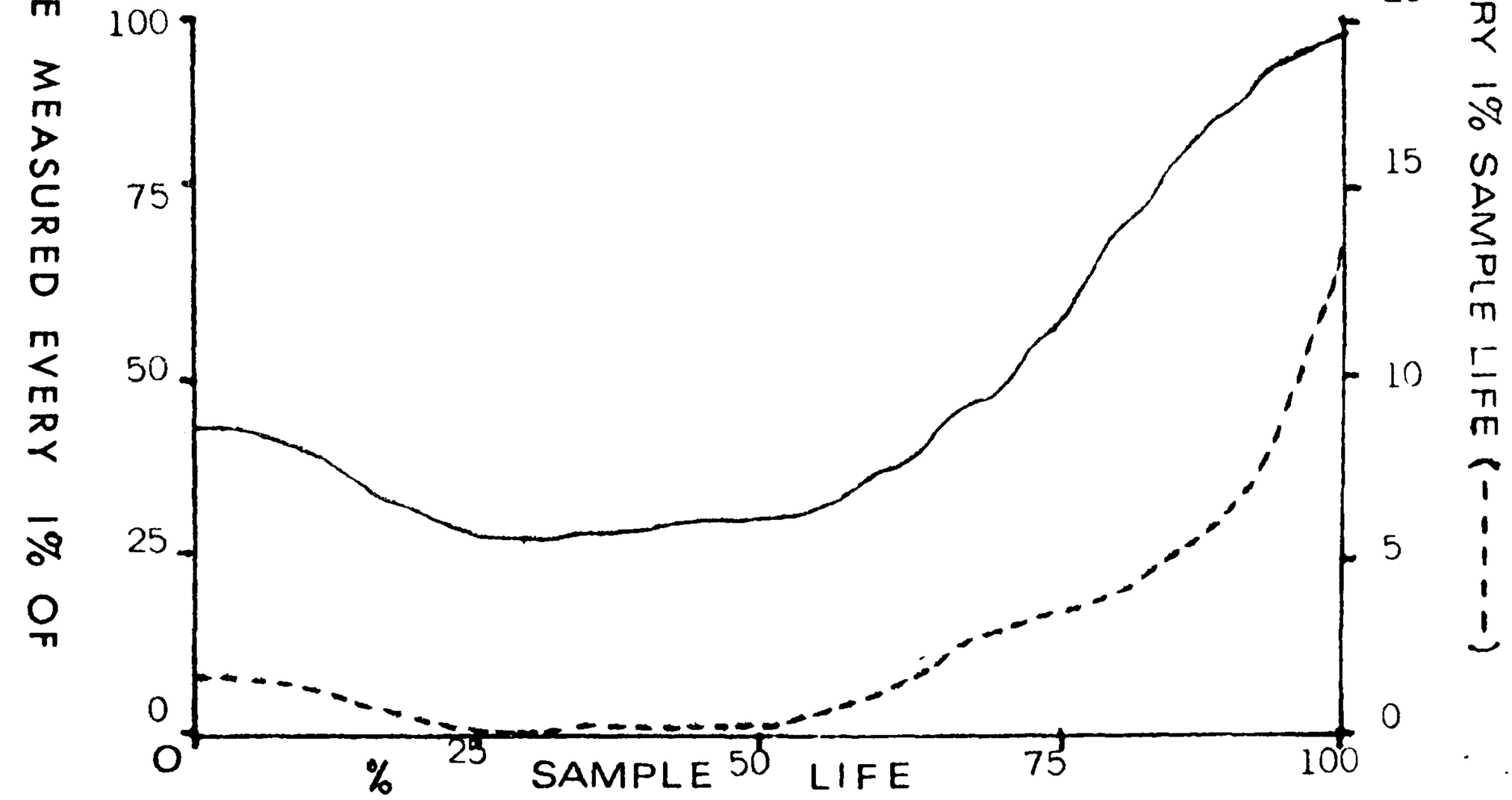

FIGURE 20 : Shows the change in response for a steel rod against % fatigue life for the 2- peaked loading spectrum.

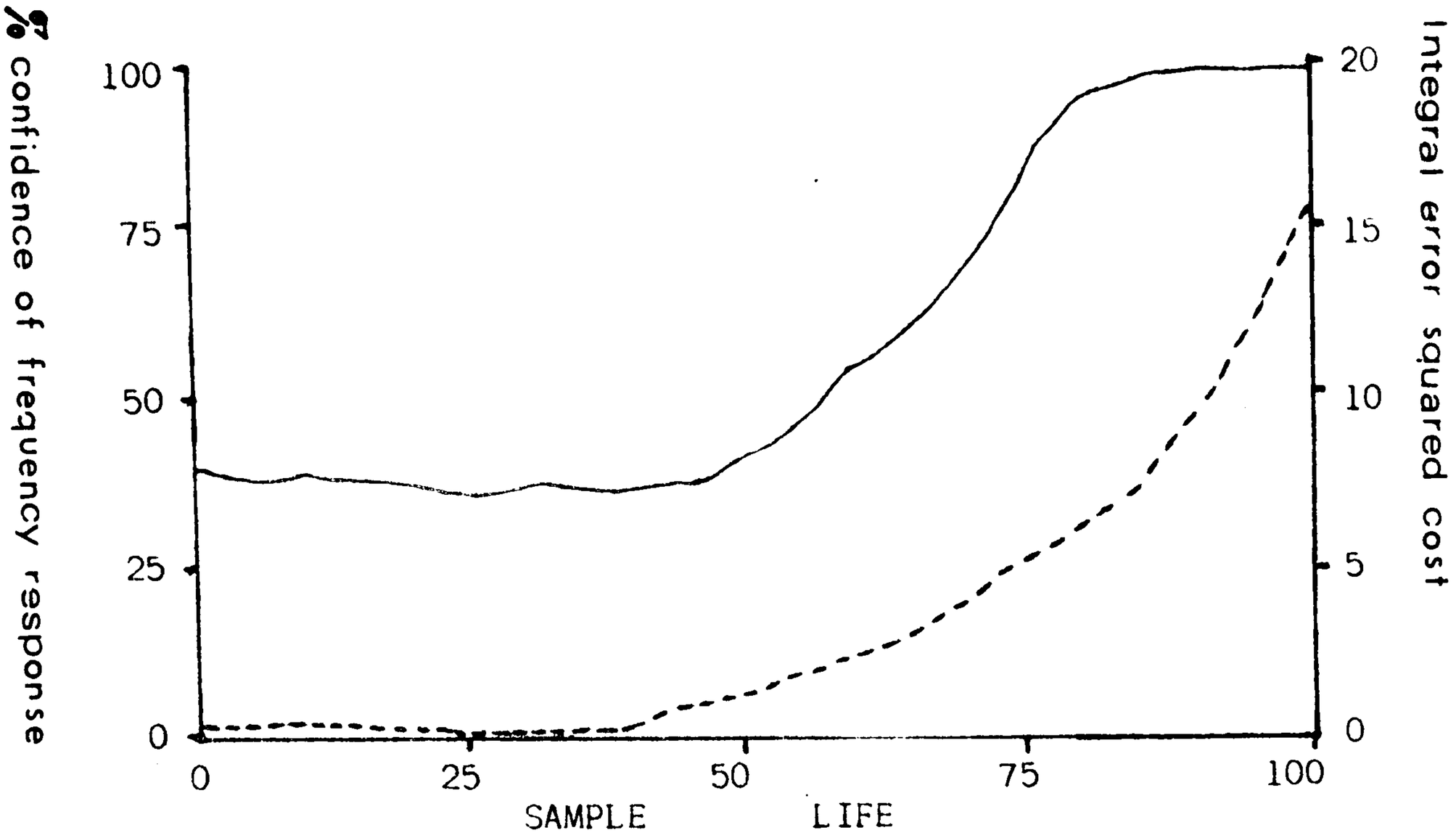

FIGURE 21 : Shows the change in response for an aluminium rod under broad-band loading when the rod has been pre-work-hardened.

The specimen's fatigue life divides into 3 regions: an initial region where work-hardening is in progress, an intermediate region where no fatigue cracks have yet started, and a final period where fatigue cracking is present and the sample is approaching failure. It is the identification of the final period which is of interest.

The stress concentration at the notch surface causes dislocations in the metal lattice structure to move in such a way as to relieve the stress. This movement of dislocations will only occur when the local stress is sufficient to overcome the pinning of dislocations at grain boundaries. The dislocations congregate at the notch surface, eventually forming a fatigue crack. The stress concentration at the tip of the fatigue crack

is higher than in surrounding areas, and hence once a fatigue crack has started, it is more likely that the crack will grow than that secondary cracking will appear. As the fatigue crack increases in depth, the mean stress level across the remaining non-affected cross-section of the notch will increase. Thus the deflection of the cantilever for a given loading will increase, changing the frequency response. Figure 22 shows that in general for the case described the change in the frequency response is more marked at higher frequencies. The prediction of fatigue cracking using this simplistic approach meets practical difficulties.

FIGURE 22: SHOWS THE MODULUS FREQUENCY RESPONSE FOR AN ALUMINIUM SPECIMEN SUBJECTED TO BROAD BAND LOADING

a) As measured between 25-30% sample life

b) As measured between 80-85% sample life

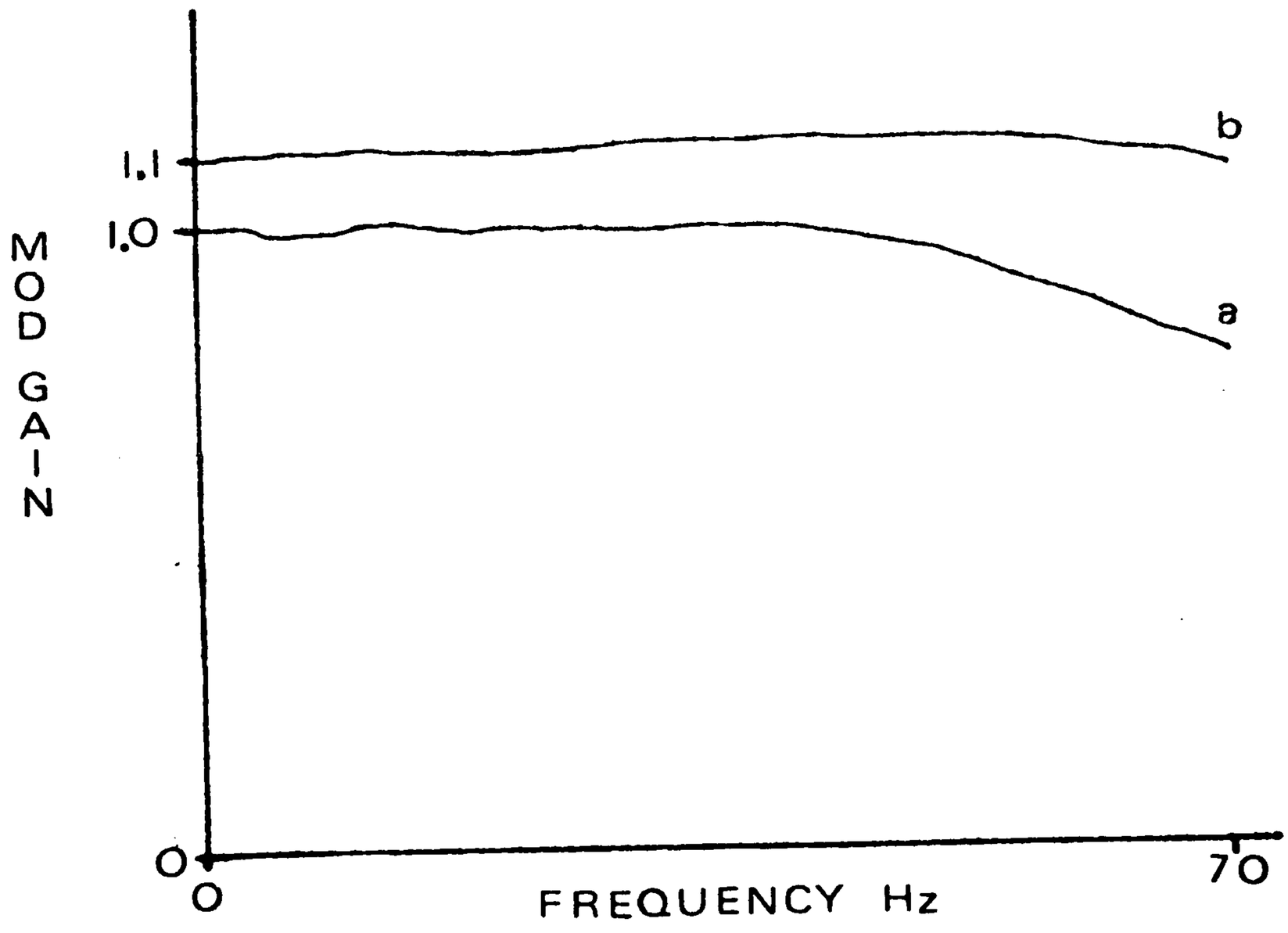

The rate of propagation of the fatigue crack and hence the rate of change in the frequency response, is a function both of the stress concentration at the tip of the crack and of the depth of the crack. As the crack depth increases, the stress concentration at the tip of the crack increases, and this in turn causes an increase in the rate of propagation of the crack. Complete failure occurs when this cycle becomes self-perpetuating within the time taken to sufficiently decrease the external loading.

The acceleration of cracking means that initial changes (from about 50-90% sample life) are small compared with those encountered over the last 10% of life. Thus initial changes found using equation 4.1 are lost due to short-term random sampling errors. However, when combined with the stationarity confidence test the onset of cracking can be identified early on and quite consistently. An indication that changes are due to fatigue cracking and not due to drift in the loading and measuring circuit is demonstrated by the high degree of correlation between results presented here and those presented by Fisher (14) on similar specimens, using eddy current analysis to detect cracking.

Given three loading signals, each with similar R.M.S. values, the following effects can be noted:

a) The narrow band-spectra maintain high stress levels in the specimens for a greater proportion of fatigue life. Hence the rate of propagation of the crack is faster (in terms of % sample life) than that observed using broad band spectra.

b) The higher stress levels induced by the narrow band spectra might be expected to cause the onset of cracking earlier in the fatigue

life. This is not the case. The presence of high frequency loading cycles in the broad band spectrum causes initial cracking to occur at about 45% fatigue life for the tests run on the aluminium samples, while cracking occurs at about 55% fatigue life for narrow band input loading. This effect was less marked for the steel samples.

c) The stationarity test confidence level results are more sensitive to changes in the frequency response than the COST measure taken from equation 4.1. This is especially true when the coherency is near unity.

The results presented in this chapter show the application of Fourier techniques to fatigue rig control and the application of some statistical tests for identifying the onset of cracking under random loading conditions. The section showing a method of generating signals with specified statistics is an essential preliminary to an integrated computer-controlled fatigue testing system, and provided standard test signals for the tests conducted.

5) APPENDIX A

Consider the weighting function $g_1 \ldots . g_N$ found as the optimum model to the desired auto-spectrum. From modelling the amplitude distribution the weights $h_1 \ldots . h_N$ are obtained. Let $g_1 \ldots . g_N$ and $h_1 \ldots . h_N$ be ordered according to their absolute magnitudes i.e. $h_1 \geqslant h_2 \geqslant h_3$ and $g_1 \geqslant g_2 \geqslant g_3$ etc.

Lemma

The best fit to $g_1 \ldots . g_N$ in the least squares sense is obtained by fitting the largest remaining weight in h to the largest remaining weight in g with the appropriate sign attached.

Proof

Consider the case of N = 2.

To prove $(h_1 - g_1)^2 + (h_2 - g_2)^2 \leqslant (h_2 - g_1)^2 + (h_1 - g_2)^2$

Expanding and cancelling terms in common:

$$-h_1g_1 - h_2g_2 \leqslant -h_2g_1 - h_1g_2$$

or $$h_1g_1 + h_2g_2 \geqslant h_2g_1 + h_1g_2$$

or $$(h_1 - h_2) \cdot (g_1 - g_2) \geqslant 0$$

But: $\text{sign}(h_1) = \text{sign}(g_1)$, and $h_1 \geqslant h_2$, $g_1 \geqslant g_2$ Q. E. D.

Extending to the case of N = 3, we have to prove:

$$(h_1 - g_1)^2 + (h_2 - g_2)^2 + (h_3 - g_3)^2 \leqslant (h_2 - g_1)^2 + (h_1 - g_2)^2 + (h_3 - g_3)^2 \quad \ldots (a)$$

$$\leqslant (h_3 - g_1)^2 + (h_2 - g_2)^2 + (h_1 - g_3)^2 \quad \ldots (b)$$

$$\leqslant (h_1 - g_1)^2 + (h_3 - g_2)^2 + (h_2 - g_3)^2 \quad \ldots (c)$$

$$\leqslant (h_3 - g_1)^2 + (h_1 - g_2)^2 + (h_2 - g_3)^2 \quad \ldots (d)$$

$$\leqslant (h_2 - g_1)^2 + (h_3 - g_2)^2 + (h_1 - g_3)^2 \quad \ldots (e)$$

Using the proof for N = 2: expression (a) is minimised by exchanging h_1 and h_2. Expression (b) is minimised by exchanging h_3 and h_1. Expression (c) is minimised by exchanging h_2 and h_3. Expression (d) is first decreased by exchanging h_3 and h_1 and then minimised by exchanging h_3 and h_2. A similar process can be followed on expression (e). Thus a proof for N = 2 is sufficient for proving the case of N = 3. By a process of inductive reasoning, the proof can be extended for all N.

APPENDIX B

PROGRAM DESCRIPTION OF USER RUN-TIME ACTIONS FOR AMPLITUDE PROBABILITY MODELLING

The program includes 9 possible actions; the sequence of operations is chosen by the user.

1) Calculation of characteristic function, M(v), of required amplitude probability function. User specifies the initial value V_0, the final value V_f, and the number of points to be calculated in this interval.

2) Graphical display of current M(v) and the latest model M'(v) on a V.D.U. screen.

3) Search for zero of M(v) in a region specified by the user. The region is specified by use of cross-wires on a graphical display.

4) Calculation of the order of the zero found by 3.

5) Print-out of weighting function.

6) Call to the cross-wires of the V.D.U. which can be used:

   a) To specify point from which to look for a zero of M(v).

   b) To specify new limits for calculating M(v) i.e. enlarging a section of a current plot.

7) Normalisation of M(v) i.e. M(v)/M'(v). This tells the user the accuracy of the model over the range considered.

8) The inverse Fourier transform of a smoothed version of M'(v) together with a graphical display of the modelled amplitude probability function.

9) The integral |error| between the desired amplitude function and the model amplitude function.

APPENDIX C

This appendix develops a simple 'bang-bang' controller for achieving a specified peak-trough probability matrix. The input signal to the rig is of constant velocity form +v, -v where $v = dx/dt$ (x = signal level) The controller is presented as an operating algorithm.

a) SET-UP PROCEDURE

The test rig is driven with a triangular input waveform, $x(t)$, of the specified slope $\pm v$. The amplitude of this waveform is chosen such that $y(t)$, the achieved output, just achieves the desired slope $\pm v$.

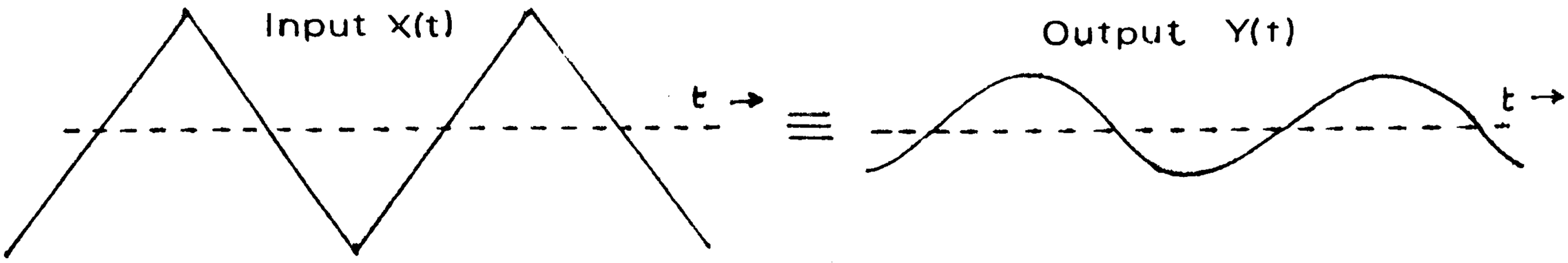

Slope ±V — Slope ±V just attained

The turn-around amplitude of the output A_0 is now recorded and stored (A_0).

CONTROL ALGORITHM

1) Get next peak-trough pair (Pn, Tn)

2) Is $(Pn - Tn\text{-}1) \leqslant A_0$

   Yes: Set Clevel = $Tn\text{-}1 + \frac{Pn - Tn\text{-}1}{2}$

   No: Set Clevel = $Pn - A_0$

3) Sample output $y(t)$

4) Is $y(t) \leqslant$ Clevel

   Yes: Generate $x(t)$ with slope +v

   No: Generate $x(t)$ with slope -v

5) If slope of $x(t)$ = +v go to 3

6) Is $(Pn - Tn) \leqslant A_0$

Yes: Set Clevel = $Pn - \frac{Pn - Tn}{2}$

No: Set Clevel = $Tn + A_0$

7) Sample output y(t)

8) Is $y(t) \leqslant$ Clevel

Yes: Generate x(t) with slope -v

No: Generate x(t) with slope +v

9) If slope of x(t) = -v go to 7

10) Go to 1

Where Pn, Tn are the current values of the peak-trough pair to be attained; Pn-1, Tn-1 the past pair just attained. The generation of peak-trough values is described in the last section of reference 12. This algorithm only applies to systems that are approximately linear in their dynamic response. The algorithm is repetitious in its method of achieving peaks and then troughs. This would normally be included in one series of tests with signal inversion for changing from a peak search to a trough search.

APPENDIX D.

The following gives a brief description of the program logic for controlling the fatigue rig to ensure the desired loading pattern is achieved.

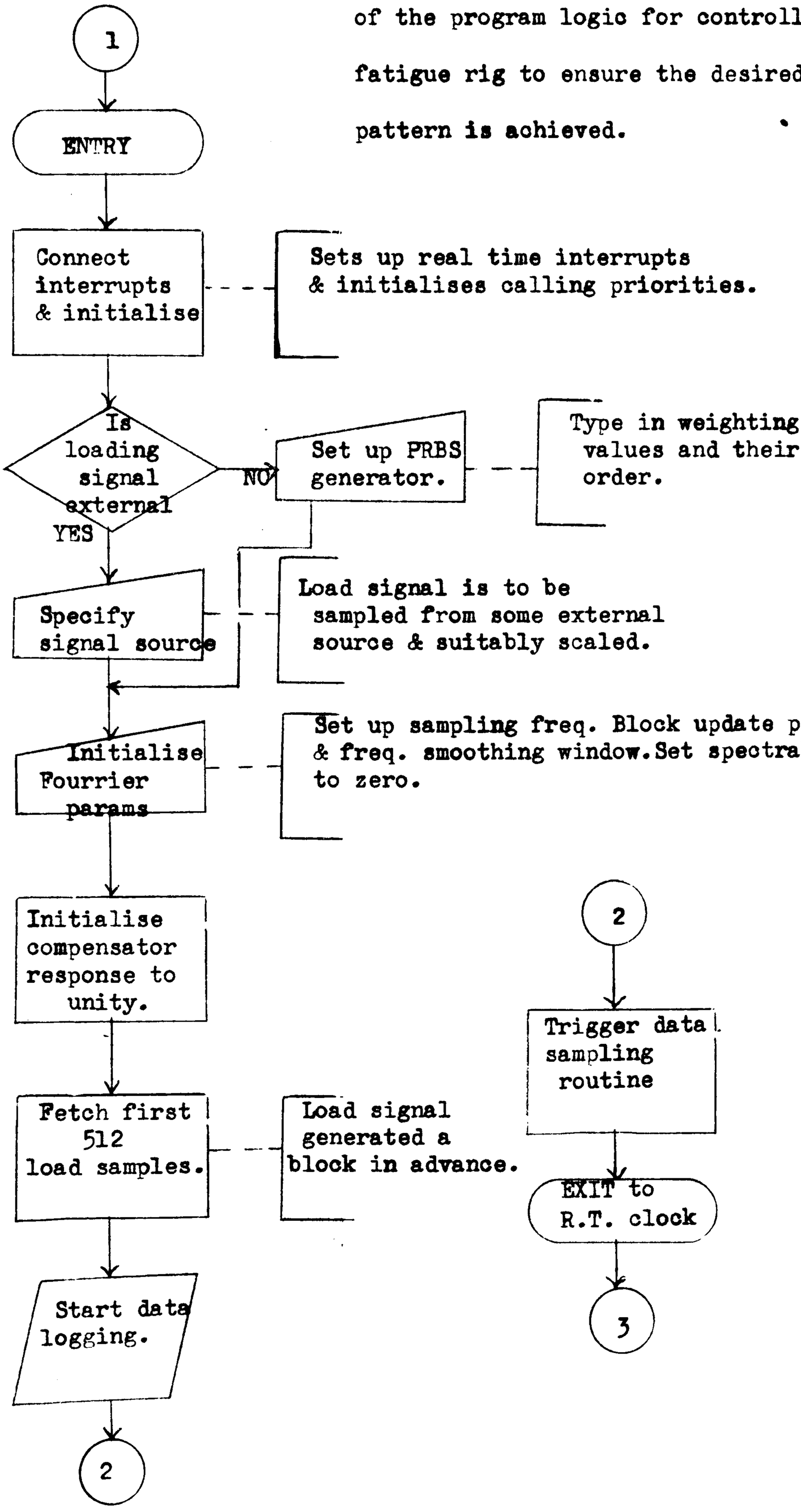

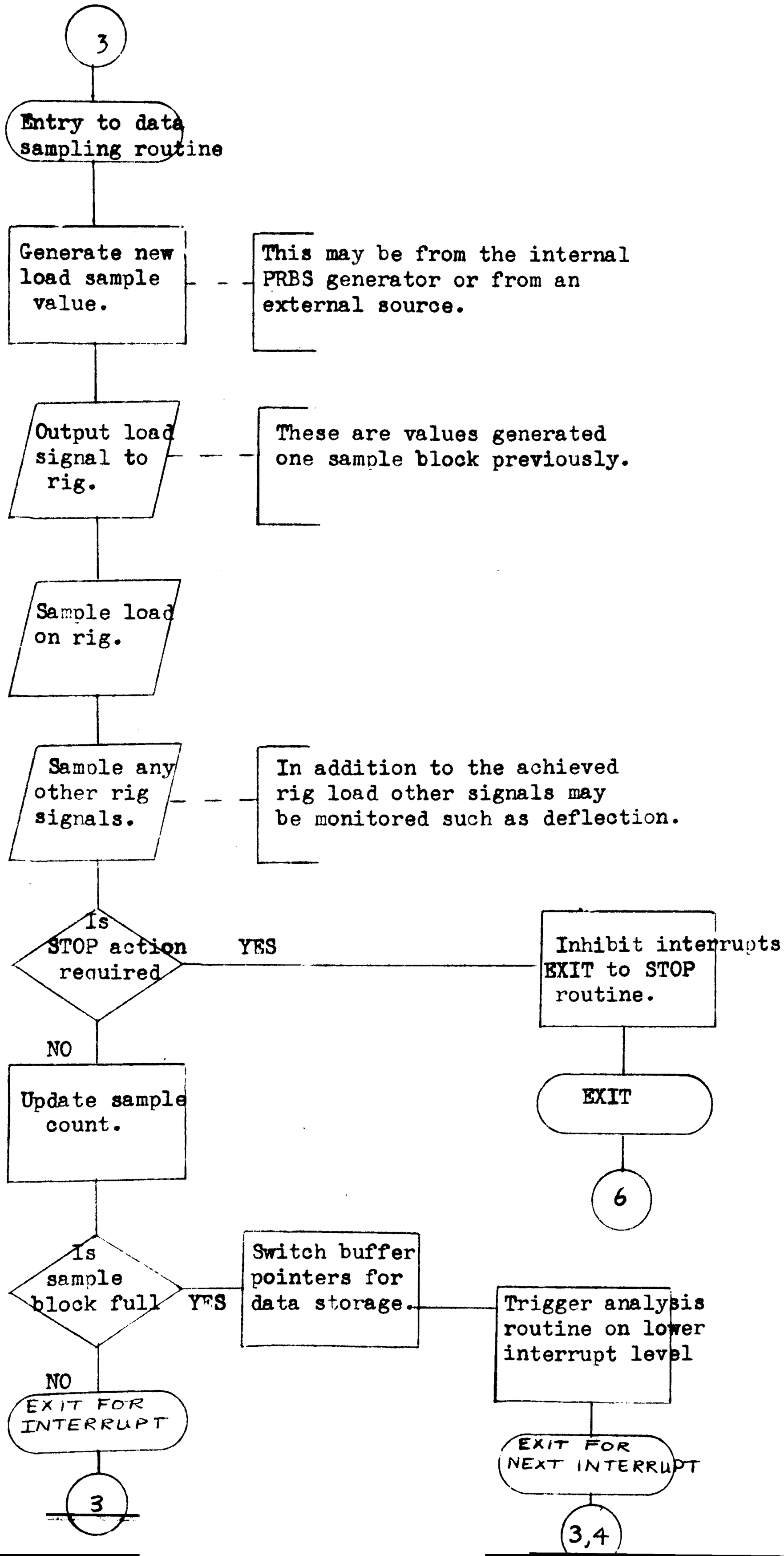
3
Entry to data sampling routine
Generate new load sample value.
This may be from the internal PRBS generator or from an external source.
Output load signal to rig.
These are values generated one sample block previously.
Sample load on rig.
Samole any other rig signals.
In addition to the achieved rig load other signals may be monitored such as deflection.
Is STOP action required
YES
Inhibit interrupts EXIT to STOP routine.
EXIT
6
NO
Update sample count.
Is sample block full
YES
Switch buffer pointers for data storage.
Trigger analysis routine on lower interrupt level
NO
EXIT FOR INTERRUPT
EXIT FOR NEXT INTERRUPT
3
3,4

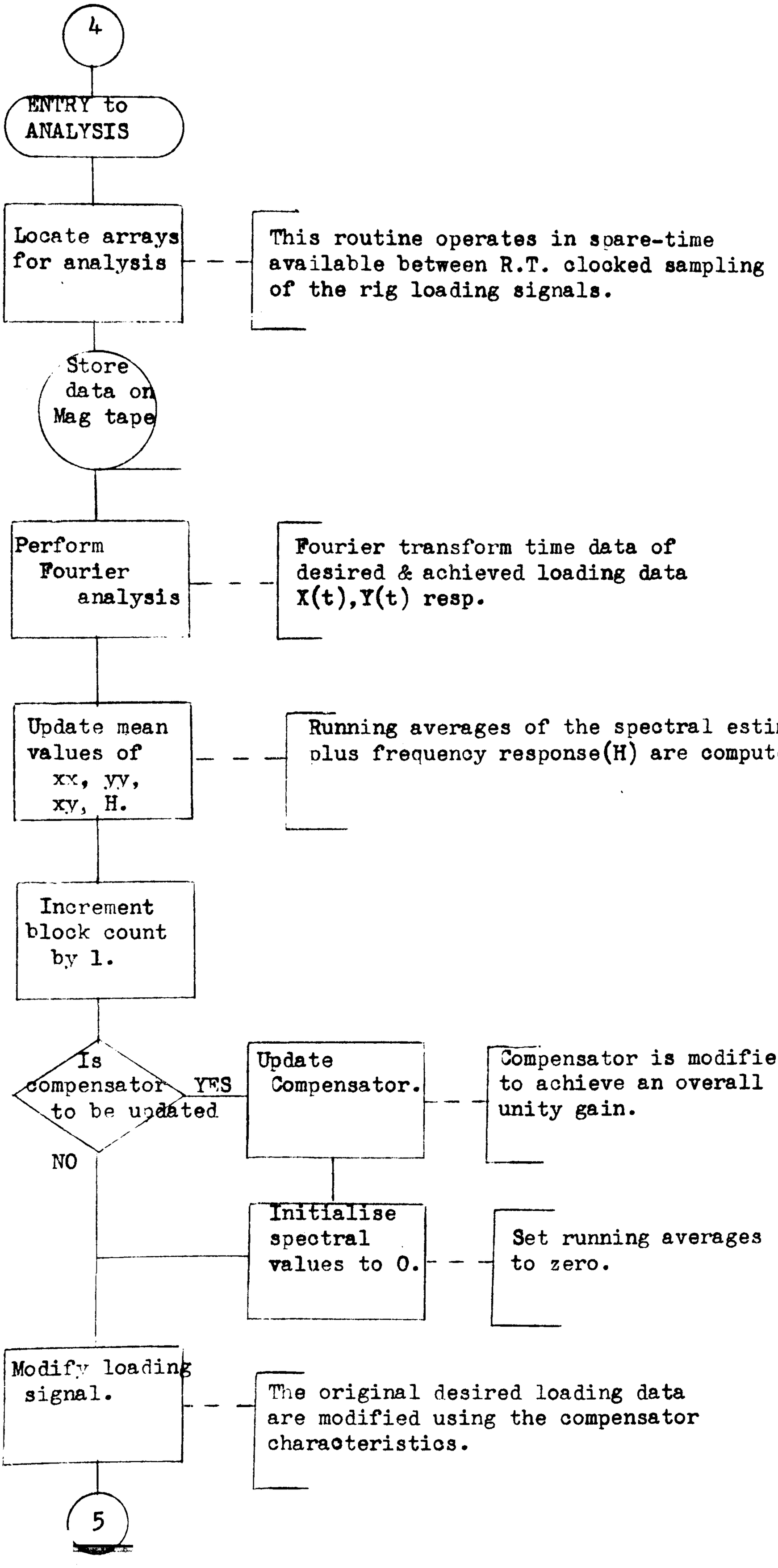
4
ENTRY to ANALYSIS
Locate arrays for analysis
This routine operates in spare-time available between R.T. clocked sampling of the rig loading signals.
Store data on Mag tape
Perform Fourier analysis
Fourier transform time data of desired & achieved loading data X(t),Y(t) resp.
Update mean values of xx, yy, xy, H.
Running averages of the spectral estimates plus frequency response(H) are computed .
Increment block count by 1.
Is compensator to be updated
YES
Update Compensator.
Compensator is modified to achieve an overall unity gain.
NO
Initialise spectral values to 0.
Set running averages to zero.
Modify loading signal.
The original desired loading data are modified using the compensator characteristics.
5

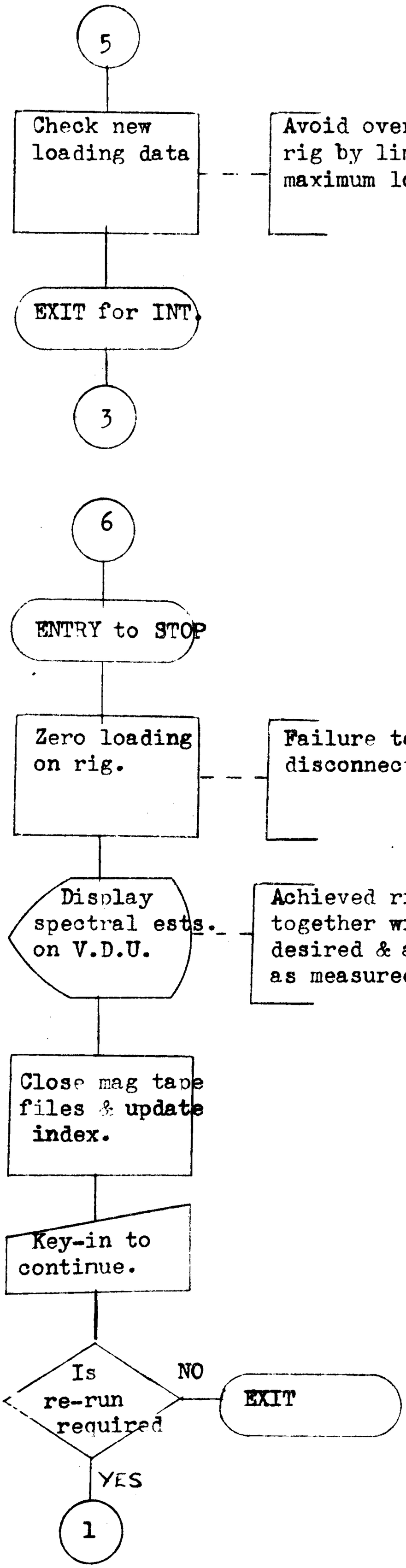
5
Check new loading data
Avoid overloading the rig by limiting the maximum load.
EXIT for INT.
3
6
ENTRY to STOP
Zero loading on rig.
Failure to comply will disconnect power to rig.
Display spectral ests. on V.D.U.
Achieved rig response is plotted together with power spectra of desired & achieved loading signals as measured on the most recent update.
Close mag tape files & update index.
Key-in to continue.
Is re-run required
NO
EXIT
YES
1

REFERENCES

1 WEST, J. C., DOUCE, J. L. LEARY, B.G.: 'Frequency spectrum distortion of random signals in non-linear feedback systems'. Proc. I.E.E., 108, C 13, p. 259 (1961)

2 GUJAR, J. G. & KAVANAGH, R. J.: 'Generation of random signals with specified probability density functions and power density spectra'. I.E.E.E. Transactions on Automatic Control, (Dec. 1968) pp. 716-20

3 LUCACS, E.: 'Characteristic functions'. Charles Griffin & Co.Ltd (1960)

4 GOLOMB, S.W.: 'Shift Register sequences'. Holden Day (1967)

5 DOUCE, J. L.: 'An introduction to the Mathematics of servo-mechanisms'. English Univ. Press Ltd. (1963)

6 BLACKMAN, R. B. & TUKEY, J. W.: 'The measurement of power spectra'. Dover Publications (1958)

7 HAMMING, R. W.: 'Numerical methods for scienctists and engineers'. McGraw Hill (1962)

8 BEKEY, G. E.: 'System identification: an introduction and a survey'. Simulation Vol. 15 No. 4, Oct.(1970)

9 BARRETT, J. F. & COALES, J. F.: 'An introduction to the analysis of non-linear control systems with random inputs'. Proc. I.E.E. 103 p. 190 (1955)

10 SWANSON, S. R.: 'Random load fatigue testing: a state of the art survey'. Materials Research and Standards, Vol. 8 No. 1,(April 1968)

11 BENDAT, J. S. & PIERSOL, A. G.: 'Random data analysis and measurement procedures'. Wiley Interscience(1972)

12 SHERRATT, F. & DAVALL, P. W.: 'Advances in computer-controlled random load fatigue testing'. Univ. of Warwick Report(1974)

13 SHERRATT, F. & FISHER, B.: "Statistical measurements on servo-hydraulic fatigue machines'. Univ. of Warwick Report (March 1971)

14 FISHER, B.: 'Random load fatigue damage accumulation in mild steel'. Phd. Thesis, Univ. of Warwick (1971)

15 HUANG, T. C. & LANZ, R. W.: 'Investigation of fatigue failure of materials under broad-band random vibrations'. A.I.A.A. J10(8) pp. 977-8

16 LUCKE, J. W.& BROWN, G. W.: 'Fatigue data processing with a small digital computer'. I.S.A. Trans. 11 pp. 128-134(1972)

17 REDKIN, V. B.: 'Stability of a multi-variable system for controlling a fatigue testing process with random loading'. Automatika 18 pp. 28-34 (1973) - I.A.A 13 (12) : A73-27949

18 SCHUETZ, W.: 'Technical evaluation report on the AGARD symposium on random load fatigue'. AGARD: - AR 54 STAR N73-28884

19 KICIMAN, M. O.: 'Prediction of failure for a multiple load-path system under random loading'. Middle East Technical Univ. Jnl. of Pure and Applied Sciences 5 83-93 (1972) I.A.A. 13(4):A73-15075

20 ITAGAKI, I. & SHINOZUKA, M.: 'Application of Monte-Carlo technique to fatigue-failure analysis under random loading'. Probabilistic aspects of fatigue proceedings of the Symposium 1971, A.S.T.M.(1972) I.A.A. 13(3):A73-13236

21 DOUCE, J.L. & DAVALL, P.W. : 'Generation of signals with specified statistics'. I.E.E. Proc. ,Oct. 1973, pp. 1278-82. (Chapter 5, Section 2).

CHAPTER 6

APPLICATIONS TO HUMAN OPERATOR TRACKING TASKS - A COMPARISON OF AUDIO AND VISUAL DISPLAYS

LIST OF SYMBOLS USED

$x(t)$: band-limited Gaussian white noise with zero mean and variance σx^2. As the cut-off frequency is varied the variance is maintained constant

$e(t)$: the error signal presented to the operator via the visual or audio display. The operator is required to minimise this error

$z(t)$: (= $y(t)$) the operator's response to the error signal

$e(t)$: $e(t) = x(t) - z(t)$

The corresponding Fourier transforms of $x(t)$, $y(t)$, $e(t)$ and $z(t)$ are as defined in Chapter 3.

$G(jw)$: the forward-loop frequency response, incorporating the display, operator and joystick dynamics

$H(jw)$: the overall closed-loop frequency response relating the input $x(t)$ to the output $y(t)$. (= $G / (1 + G)$).

ϕnn : the power spectrum of that part of the output signal $y(t)$ which is not linearly related to the input $x(t)$

w_0 : frequency resolution (= $2\pi / T$)

N : block size for Fourier analysis

T : block period

f_s : sampling frequency

1) INTRODUCTION

Chapters 4 and 5 show two applications of the statistical results of Chapter 2 in identifying time variations in open-loop linear systems. The results of Chapter 3 may be used to identify changes in the human operator describing function when performing tracking tasks, and to obtain confidence levels for models of the operator's response. The task configuration is essentially a closed-loop situation where the operator is presented with an error signal marking the difference between his output and the input signal to be tracked.

In this chapter the effect of the choice of error signal display on the operator's response is investigated. A comparison between various audio error displays and a visual display is made both in terms of the response to stationary input signals (i.e. fixed frequency content) and in terms of monitoring the change in the operator's response to a step change in the frequency bandwidth of the input signal. A five parameter linear model of the operator's response is proposed, and the model is justified using some of the statistical tests developed in Chapter 3.

Many models of the human operator response have been proposed. Briefly, these models fall into three categories: linear models (reference 1), sampled data models (reference 2) and non-linear models (reference 3). For a wide range of applications it has been shown that the linear cross-over model on lines proposed by Krendel and McRuer (1953) gives a good approximation to measured human operator describing functions. Exceptions are when the input signal to be tracked is of very low frequency content (< 0.2 Hz) under which

conditions the operator exhibits a threshold type non-linearity, and when the input signal contains high frequency components (> 1.5 Hz) where the operator degenerates to a 'bang-bang' mode of control.

Comparison of various forms of multi-dimensional visual and tactile displays has been attempted (references 5 to 7) and generally results have indicated that the human operator responds equally well to visual and tactile presentation of information. Similar studies of one type of audio display (reference 8) also indicate no appreciable loss of performance. Initial studies in this chapter contained in Appendix A would, however, indicate considerable down-grading of the human operator's response to audio stimuli in one-dimensional tracking tasks.

In designing an audio display to either complement or replace a visual display, it is necessary to ensure that the operator's performance is optimised, in terms of the display, for a wide range of operating conditions. In this chapter a method of comparing and modelling an operator's response for various audio and visual displays is proposed (Appendix A) and the operator's change in response for a step change in the dynamics of the input signal is investigated.

Section 2, together with the paper presented in Appendix A, outlines the experimental set-up and the types of audio and visual displays used. The operator describing function is modelled using a modified 5-parameter cross-over model, and a plausible physical interpretation of the results in terms of the model parameters is presented.

The assumption that the model used is a good representation of

the operator's response using audio displays and that his response is essentially stationary for fixed input dynamics is investigated in Section 3. It is assumed that the model describing function represents the true response of the operator and that deviations from this model during the test were due to short-term measurement inaccuracies due to noise in the system. This noise may be due to non-linearity in the response, uncontrolled movements of the force joystick and discretisation errors in the analogue-to-digital sampling. Using the statistical results of Chapter 3 for closed-loop systems, the goodness of fit of the model to measured results is found.

It is well known (references 9 to 12) that the human operator's mode of response depends on the dynamics of the plant to be controlled and on the frequency content of the signal to be tracked. The transient behaviour of the response to step changes in the plant dynamics has been investigated (reference 13) for visual displays. In Section 4 the transient behaviour of an operator's response to step changes in the dynamics of the input signal is investigated for the audio and visual displays used. The response stationarity and the applicability of the model during these periods of transient response are verified using the statistical results of Chapter 3.

Lastly, Section 5 outlines some problems involved in extending the analysis procedure to two-dimensional and multi-dimensional displays.

2) COMPARISON OF HUMAN OPERATOR'S PERFORMANCE USING VISUAL AND AUDIO DISPLAYS

The results of this section are fully discussed in Appendix A.

To avoid duplication, only the basic test procedure is outlined here, together with some further explanation of the phase response of the human operator at very low frequencies. Figure 1 shows the schematic block diagram for the closed-loop configuration.

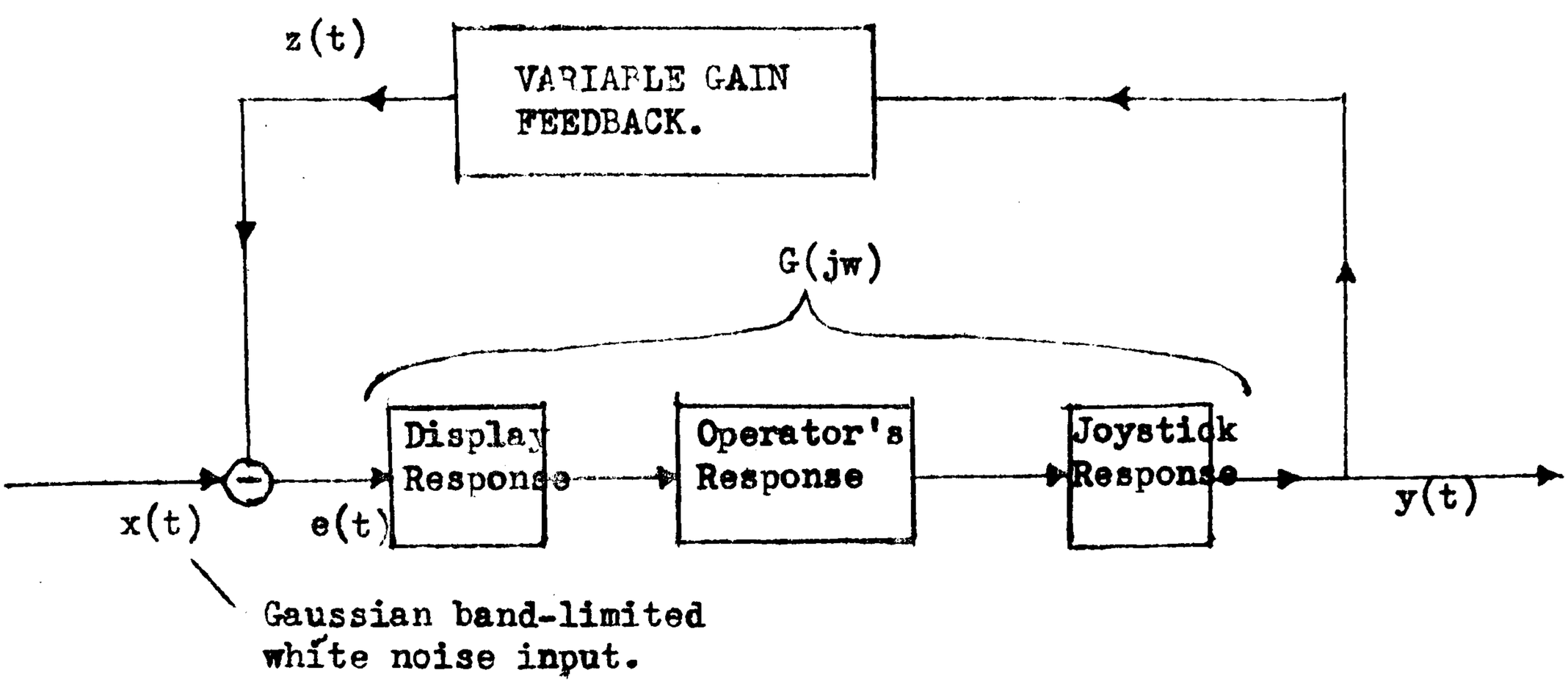

FIGURE 1 : SHOWS THE TEST CONFIGURATION FOR AN OPERATOR PERFORMING A SINGLE AXIS TRACKING TASK

a) SUMMARY OF METHOD

The signals $x(t)$, $e(t)$, $y(t)$ and $z(t)$ were sampled every 0.2 seconds. Short-term Fourier estimates were obtained using a block size of 128 samples. Five input cut-off frequencies were used, 0.3, 0.5, 0.7, 1.0 and 1.5 Hz. Each test, at a fixed cut-off frequency, lasted 10 minutes; thus, approximately 25 blocks of 128 samples were collected for each input cut-off. The average response of the operator was calculated from the mean values of $\bar{\phi}xx$, $\bar{\phi}xe$ and $\bar{\phi}xy$ obtained over the 25 blocks. The frequency response estimates were calculated (dependence on frequency is assumed) by:

$\bar{G}$ = $\bar{\phi}xy$ / $\bar{\phi}xe$ = forward-loop gain

$\bar{H}$ = $\bar{\phi}xy$ / $\bar{\phi}xx$ = overall closed-loop gain

over the frequency range $0 \leqslant f \leqslant 2.5$ Hz. The frequency resolution w_0 = 2.5 / 64 Hz. or approximately 0.04 Hz. The response functions were modelled over a frequency range $0 \leqslant f \leqslant$ input cut-off; beyond this range the signal-to-noise ratio drops off and estimates become inaccurate. The block time period $T \simeq 25$ seconds. A best estimate of the noise spectrum for each input cut-off is given by:

$$\bar{\phi}nn = \bar{\phi}yy + |\bar{G}|^2 \bar{\Phi}ee - 2\,RL\,(\bar{G}\,\bar{\Phi}ye) \quad \ldots\ldots\ldots 6.1$$

It is assumed (see Chapter 3, Section 7) that $\bar{\phi}nn$ is approximately Chi-square distributed with 2L - 2 degrees of freedom, where L = 25. This assumption is justified by L being relatively large and the coherency between x(t) and y(t) being fairly high (>0.5 for all cases) within the frequency range $0 \leqslant f \leqslant$ input cut-off.

For a description of the model used and the method of fitting the model parameters to measured results, refer to Appendix A.

b) <u>EXPLANATION OF LOW-FREQUENCY PHASE RESPONSE FOR THE MEASURED HUMAN OPERATOR DESCRIBING FUNCTION</u>

In many cases it is found that the measured forward-loop response exhibits a phase 'droop' at low frequencies. It might be expected that the phase estimate would tend to zero phase shift. Consideration of the physical situation leads to a simple explanation of this phenomenon.

It is found that due to inherent reaction time delays the best the operator can hope to achieve is a time-delayed version of the input signal (This is true when the input signal is random. If the

operator is asked to track a deterministic signal such as a sine-wave then he is able to employ predictor methods to anticipate future response)

FIGURE 2 : SHOWS A TYPICAL CLOSED-LOOP FREQUENCY RESPONSE WHERE WE CONSIDER THE CASE LETTING $w_0 \rightarrow 0$

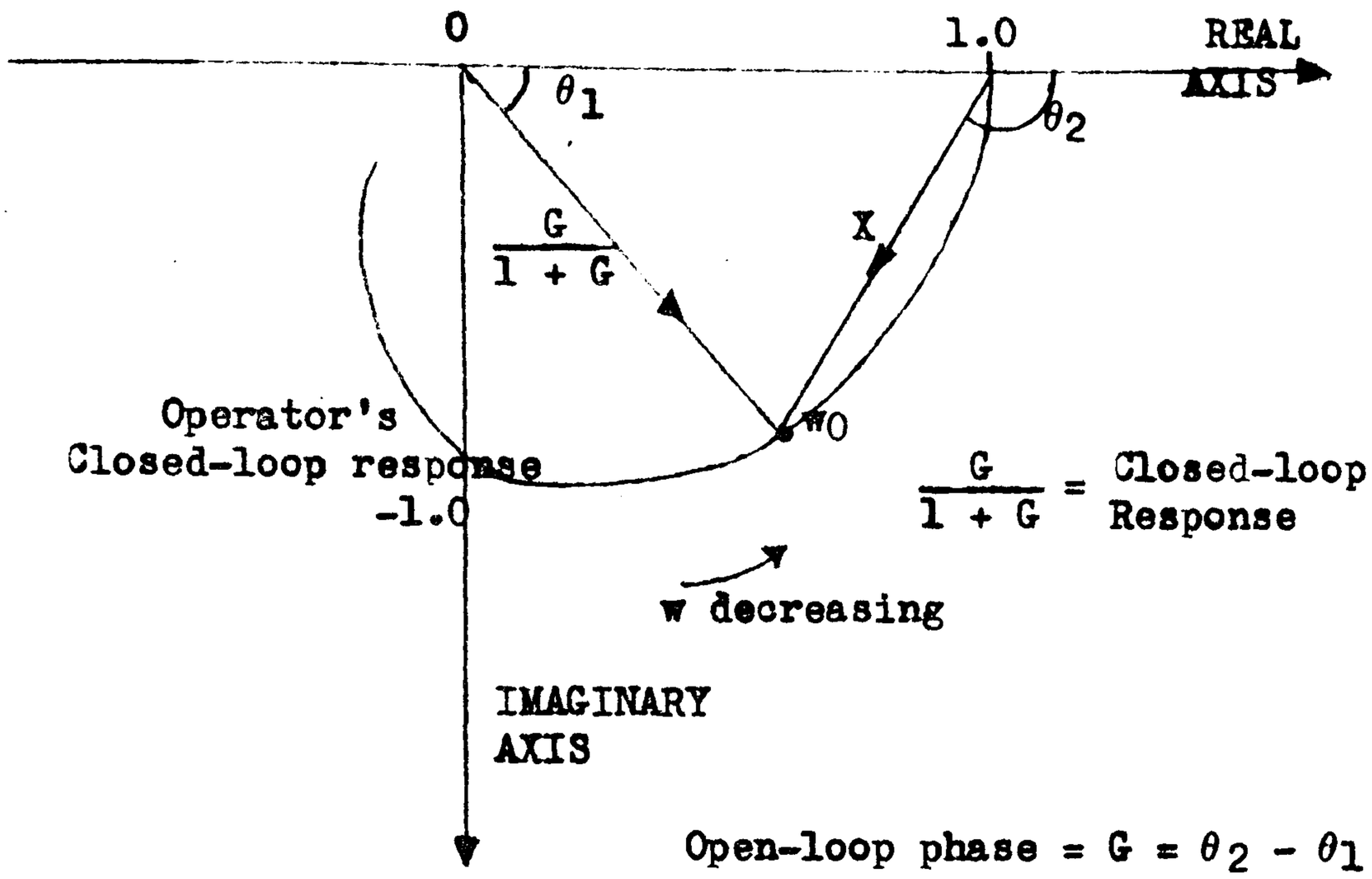

On considering Figure 2 three situations can occur:

i) If the operator over-reacts and his closed-loop gain is greater than unity at low frequencies then the forward-loop phase shift, given by $(\theta_2 - \theta_1)$, will tend to zero. This is often the case in tests with an input cut-off in the mid-frequency range (0.5 Hz to 0.7 Hz) where the operator will try to track the higher frequency variations with a corresponding tendency to over-react to lower frequency changes.

ii) If the operator has an overall unity gain at low frequencies then the forward-loop phase shift will tend to $-\pi/2$. This is often

approximately the case when the input signal is slowly-varying and the operator has time to adjust his gain. Figure 9 in Appendix A is an example of such a case.

iii) If the overall gain is less than unity at low frequencies then the forward-loop phase shift will tend to $-\pi$. This occurrence is perhaps more likely to occur when the operator is controlling a complex plant and he is less certain of the action to be taken to reduce the error. The model as used can only predict a phase shift of $-\pi/2$ at low frequencies unless the lag term with time constant T_S (Appendix A) is allowed to take the form of an integrator. It is considered in Appendix A that T_S represents a lag introduced by the operator to maintain stability when the input signal contains high frequency components. When controlling a plant with complex dynamics (typically of the form $1/P(jw)$, where $P(\cdot)$ is a polynomial in (jw)) the overall response can go unstable at much lower frequencies due to the phase shift introduced by the plant. Under these conditions, one method of regaining stability is to let T_S take on much larger values, hence bending the closed-loop response inside the -1 point.

3) JUSTIFICATION OF ASSUMPTION OF STATIONARITY

The results presented in Appendix A assume the operator's response to be stationary for a fixed input cut-off frequency. Figures 9 and 10 in Appendix A indicate that the model would appear to be a good representation of the measured response for low-frequency input cut-offs. The assumption is less certain at high-frequency cut-offs.

It is assumed that the modelled frequency response, $G_M(jw)$, is the true operator's response and that deviations from this value

are due to short-term estimation errors in a noisy environment. The noise variance at a given frequency Kw_0 ($0 \leqslant K \leqslant 64$) is given by half the power in n(t) in the frequency band $Kw_0 \pm w_0 / 2$. Thus:

$$Sn^2(Kw_0) \simeq \bar{\phi}nn(Kw_0) / 2 \quad \ldots\ldots\ldots\ldots\ldots\ldots 6.2$$

where $\bar{\phi}nn(Kw_0)$ is given by equation 6.1. For each block of data the operator's response $\hat{G}_i$ ($1 \leqslant i \leqslant 25$) is estimated. The estimates are smoothed over 5 adjacent frequency points to reduce random errors.

The distribution of a variable:

$$\hat{z}_i = \frac{(1 + \hat{G}i)}{(\hat{G}i - G_M)} \quad \ldots\ldots\ldots\ldots 6.3$$

where $(1 \leqslant i \leqslant 25)$, is given by equation 3.52, where the noise variance Sn^2 is found from equation 6.2 and the noise in the feedback loop is assumed negligible. The confidence interval satisfied by z_i is found by integrating equation 3.52 over the range $0 \leqslant z \leqslant \hat{z}_i$.

The mean confidence level satisfied by the i^{th} estimate is found by taking the average over the frequency range $0 \leqslant f \leqslant$ fCUT-OFF. The lower this confidence level the greater the confidence placed on the model.

$$CONF_i = \frac{1}{Kmax} \sum_{K=0}^{Kmax} \int_0^{\hat{z}_i(Kw_0)} p(z).\,dz \quad \ldots 6.4$$

where p(z) is given by equation 3.52.

Each operator response was tested in this manner. The results for a single operator using the mark-space audio display are shown in Figure 3. Similar results for the same operator using the beat frequency audio display are presented in Figure 4. These two displays are chosen as being representative of the 'worst' and 'best' audio displays respectively. Figure 5 shows typical results obtained for

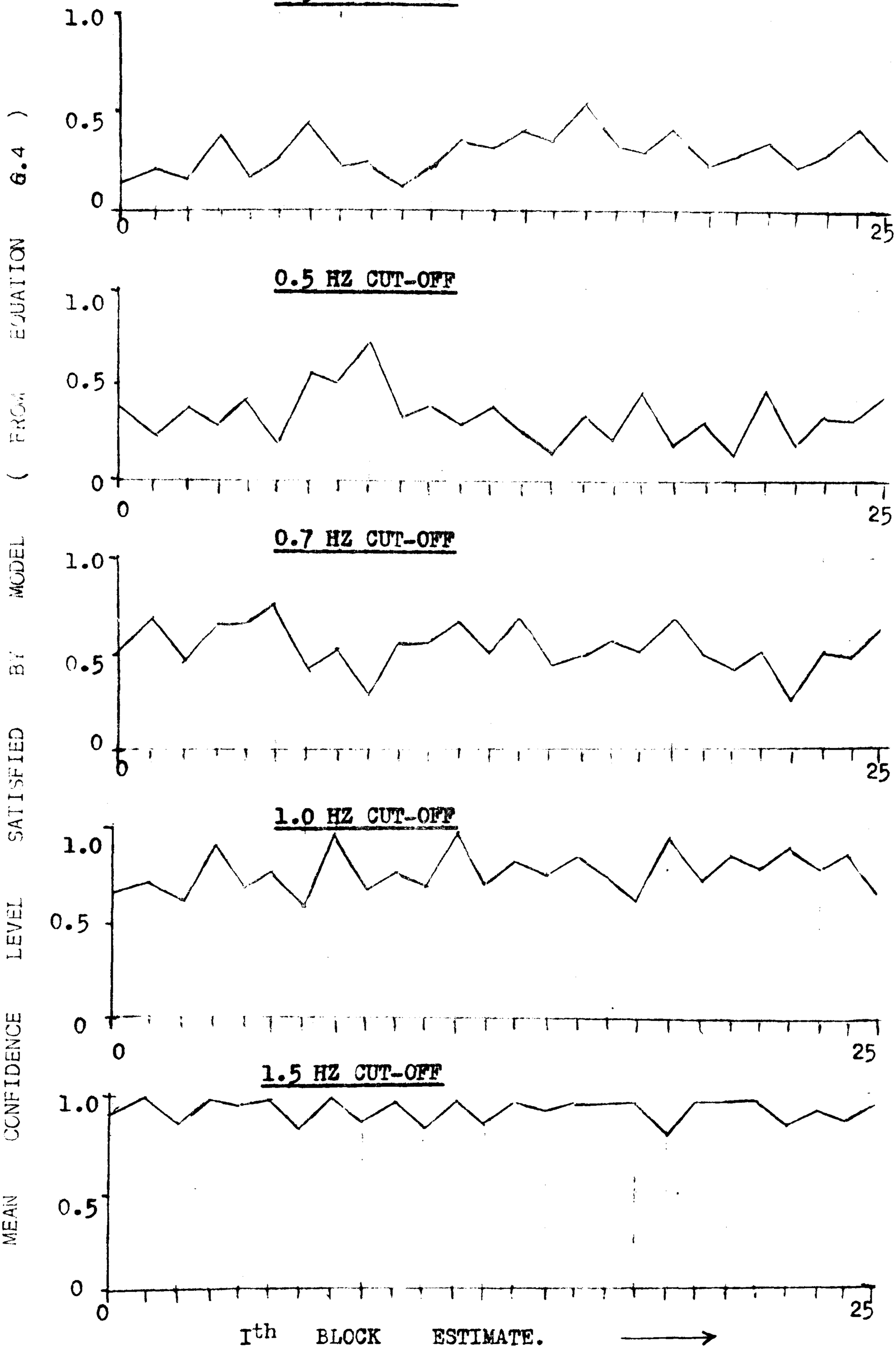

FIGURE 3 : Shows variations in the confidence placed on the model found by comparing the model with measured response data using the Mark-space ratio audio display.

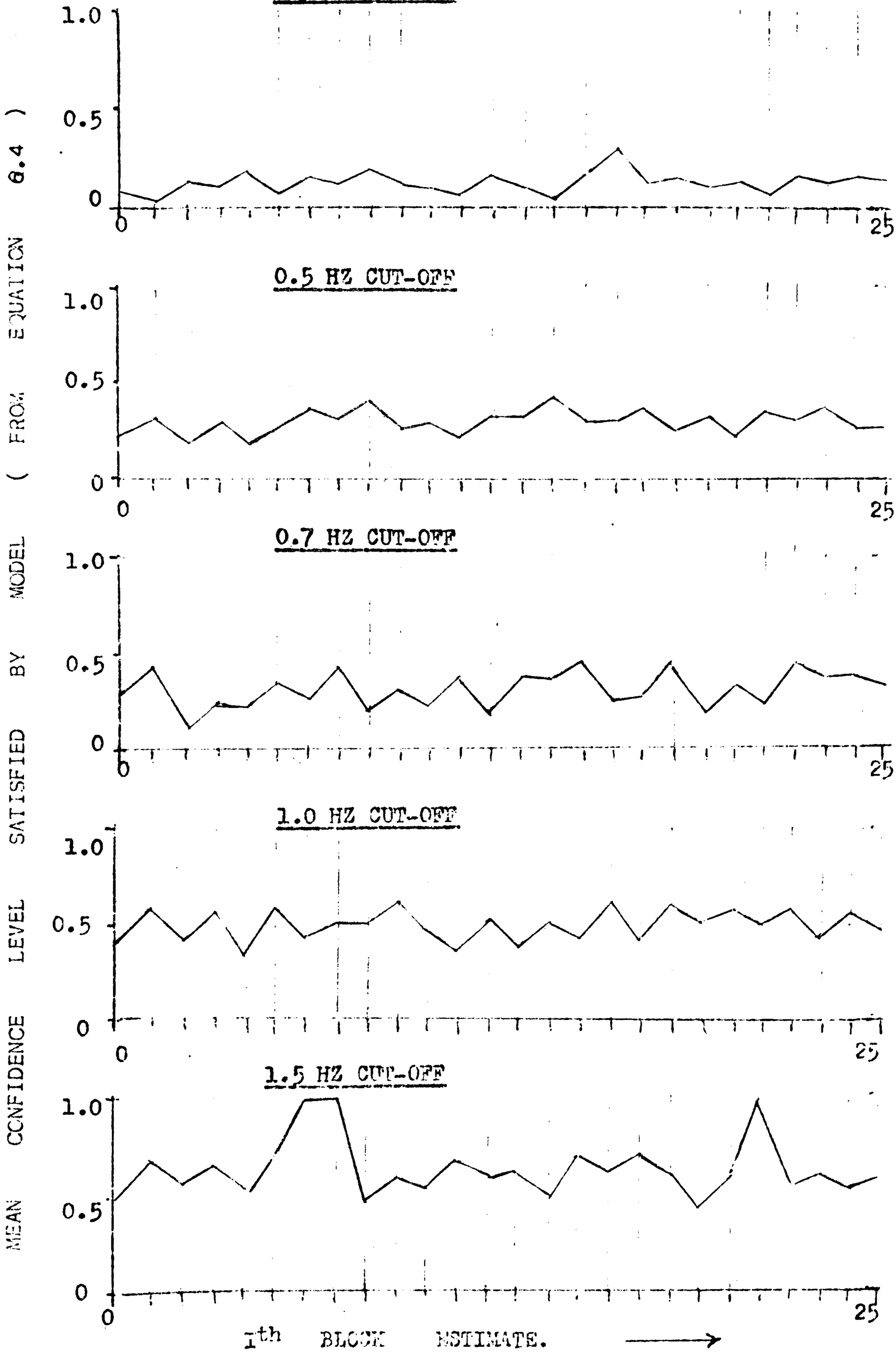

FIGURE 4 : Shows variations in the confidence placed on the model found by comparing the model with measured response data using the Beat-frequency audio display.

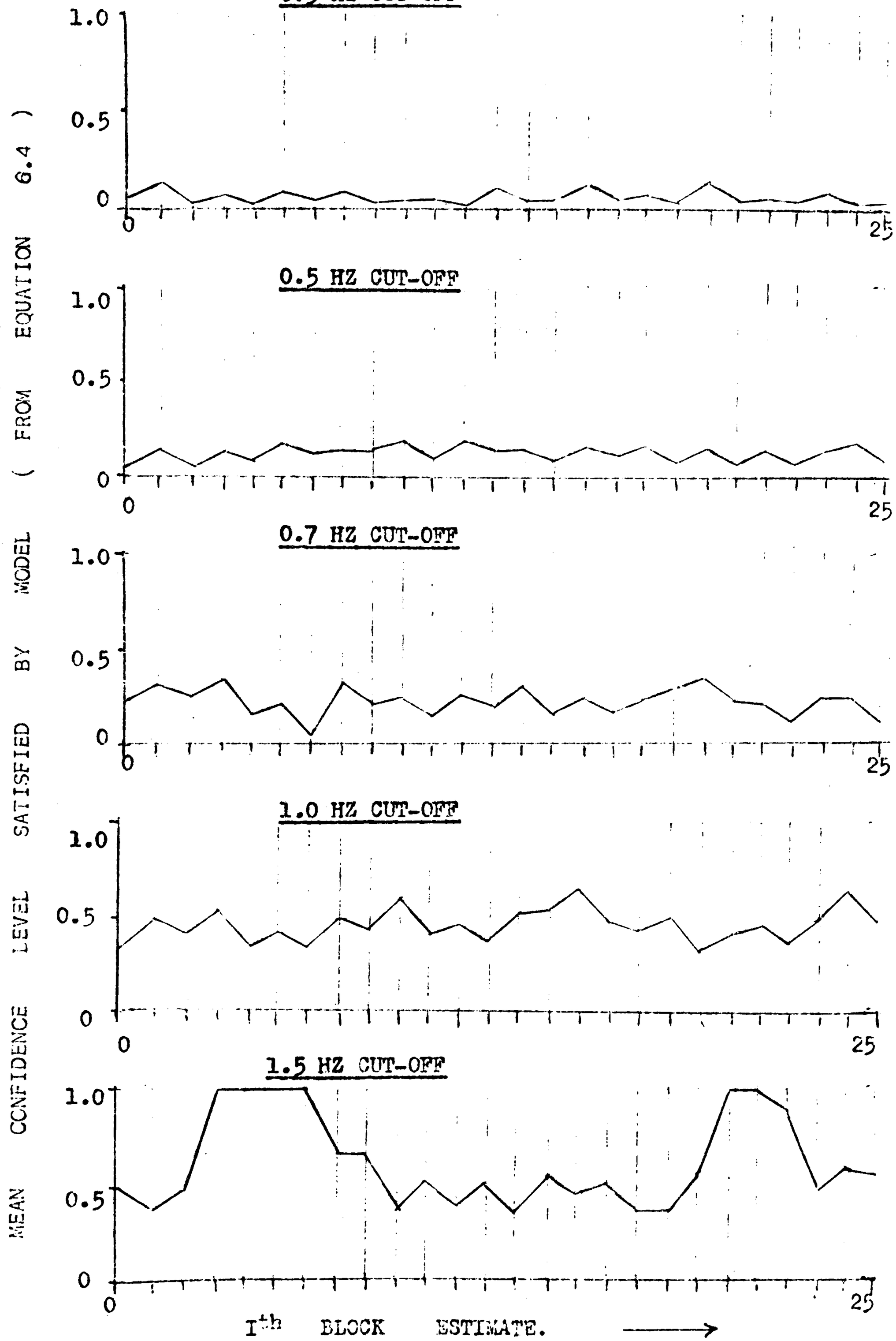

FIGURE 5 : Shows variations in the confidence placed on the model found by comparing the model with measured response data using the ~~visual display~~

the visual display.

From Figure 3, it is doubtful whether the response using the mark-space audio display can be modelled above frequencies of 0.7 Hz. This is confirmed by the coherency results for high frequency tests using this display shown in Figure 4 of Appendix A.

For the beat frequency and visual diplays the response may be considered stationary for fixed input cut-off frequencies below 1.5 Hz.

The visual display response at 1.5 Hz is apparently stationary except for two short intervals where the confidence level increases significantly. On comparing the overall closed-loop responses calculated from the stationary and non-stationary segments (Figure 6) it would appear that the two levels correspond to two different modes of response. A similar effect can be seen in Figure 4 using the beat frequency display with the input cut-off frequency at 1.5 Hz. On comparing the overall closed-loop responses obtained from the stationary and non-stationary segments of this record, however, it was found that the high confidence levels indicated that the operator had ceased to respond almost completely. This drop-out phenomenon was fairly common using the 1.5 Hz cut-off signal for all the audio displays.

FIGURE 6 : SHOWS THE TWO MODES OF RESPONSE USING THE VISUAL DISPLAY TO AN INPUT SIGNAL WITH A FREQUENCY CUT-OFF AT 1.5 Hz.

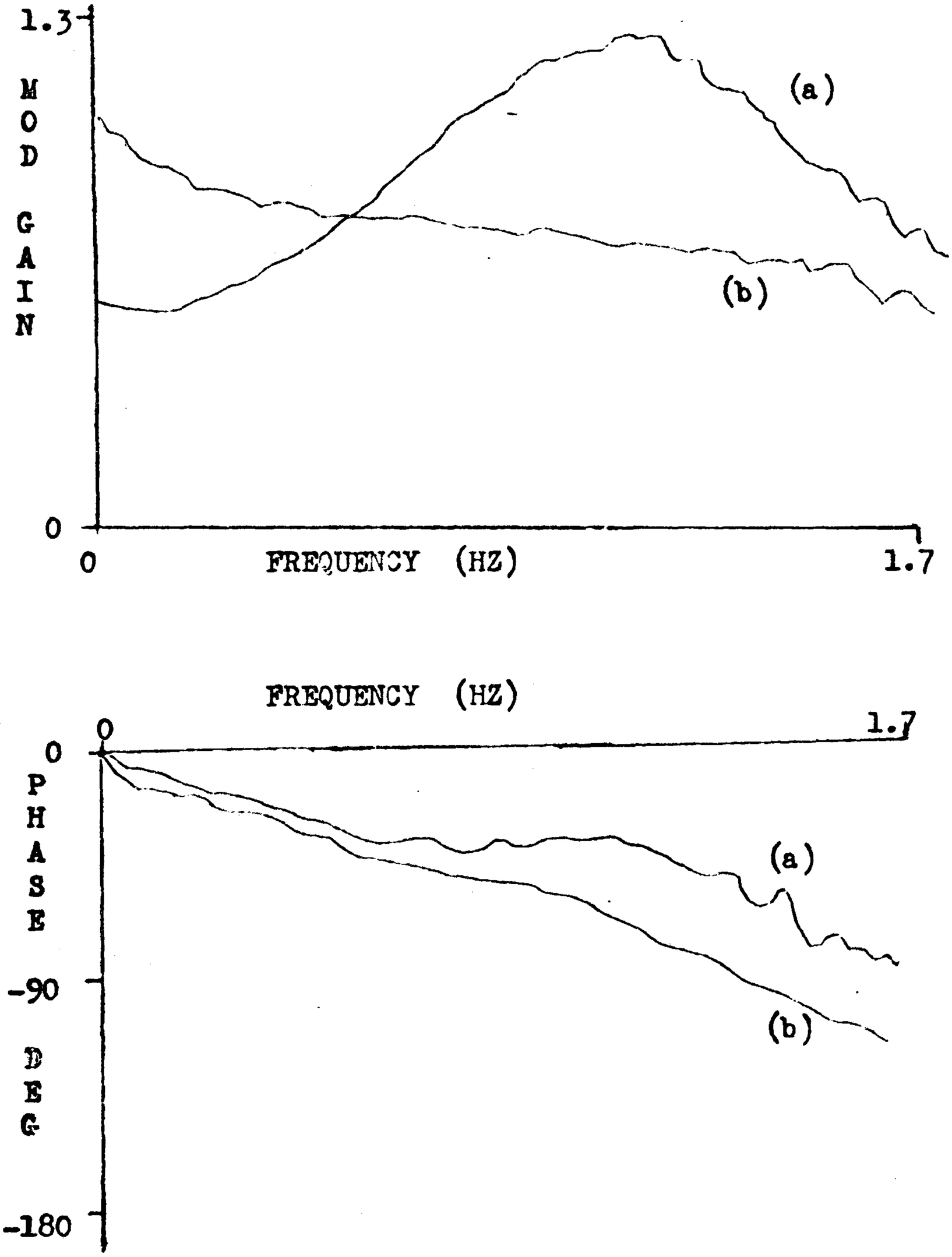

Response (a) is maintained for short periods before the operator lapses to the mode of response shown by (b).

For the 0.3, 0.5, 0.7 and 1.0 Hz input cut-off frequencies, the model was found to be satisfactory for all displays with the exception of the mark-space display at 1.0 Hz.

Further, the assumption of stationarity for fixed input signal dynamics was satisfied at the 0.8 level of significance for all tests with input cut-offs below 1.5 Hz.

4) INVESTIGATION OF TRANSIENTS IN THE OPERATOR'S FREQUENCY RESPONSE FUNCTION WITH STEP CHANGES IN THE FREQUENCY CHARACTERISTICS OF THE INPUT SIGNAL

a) TEST PROCEDURE AND ANALYSIS

The operator was asked to track a band-limited Gaussian signal whose cut-off frequency underwent two step changes, 0.5 Hz → 1.0 Hz → 0.5 Hz. Each frequency cut-off was maintained for approximately three minutes: this period being considered sufficient for the operator to attain a steady state response. Fourier estimates of the input, $x(t)$, output, $y(t)$ and the error, $e(t)$ were obtained using a block size of 64 samples. The signal sampling frequency was set as before at 5 Hz. Thus the functions ϕxx, ϕxy and ϕxe were estimated every 12 seconds. To reduce random errors the estimates were smoothed over 5 frequency points. Ideally, the estimate update period should be less than 12 seconds; however, further reduction decreases the block size and hence decreases the frequency resolution to an unacceptable level. To offset this disadvantage, successive block estimates were overlapped by a factor of 0.5 (Figure 7).

FIGURE 7 : SHOWS METHOD OF OVERLAPPING BLOCKS OF TIME SAMPLES TO IMPROVE TRACKING QUALITIES IN ESTIMATES OF THE OPERATOR'S RESPONSE

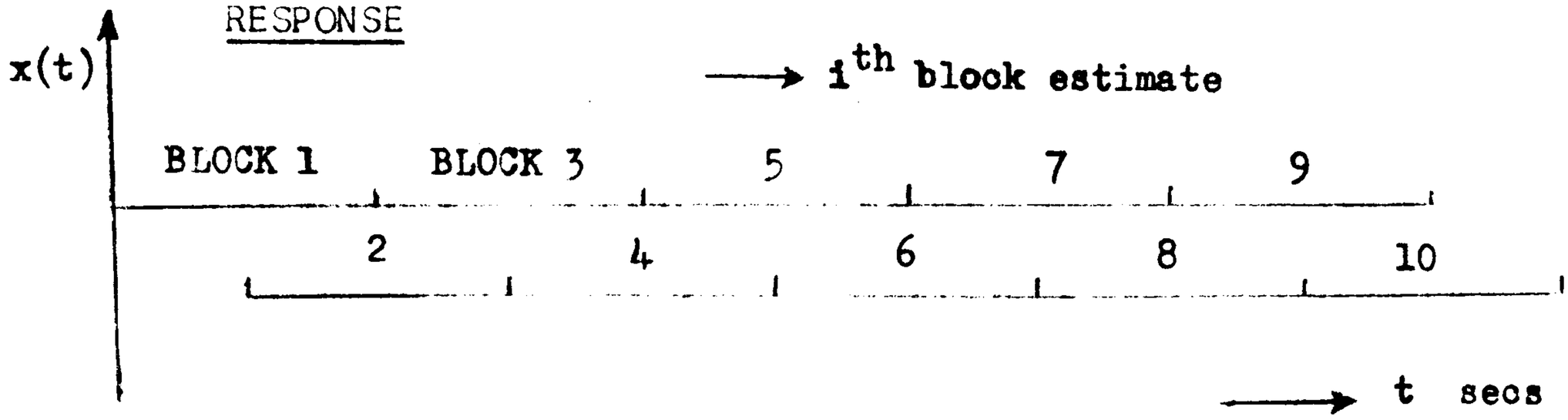

Successive estimates of the overall gain, ($\bar{H}_i(k.w_0)$ = $\bar{\phi}^i_{xy}(Kw_0)$ / $\bar{\phi}^i_{xx}(Kw_0)$, $(0 \leqslant K \leqslant 32)$ and for i = 1,3,5 . .) were tested for stationarity, using the methods described in Chapter 3, Section 3(iii). For the particular situation described here it is sufficient to use a single test, as the feedback-loop dynamics are constrained to be stationary. An overall stationarity confidence level in the frequency range, $0 \leqslant f \leqslant$ fCUT-OFF, was calculated for each adjacent block estimate $\bar{H}_i$ using equation 3.37, where the variance term is calculated from equation 3.35.

The operator's measured describing function was modelled, using methods outlined in Appendix A, at each block interval (i = 1,2,3 ...) and variations in the model parameters were recorded. The confidence placed in each model estimate was found using similar methods as described in the previous section. For this case, the noise variance is calculated for each block rather than over the entire record.

b) RESULTS

All the operators were tested using both the visual and audio displays. It was found that the model could be accepted at the 0.3

level of significance for all the tests except those using the mark-space audio display. Fitting operator response models using this display and the 1.0 Hz input cut-off signal led to fluctuations in the model parameters which could more likely be assigned to severe non-linearity in the response.

The results for a single operator are presented in Figures 8-17. The variations in each model parameter are discussed in turn and discrepancies found with other operators are noted.

VARIATIONS IN THE GAIN PARAMETER, K

As the input cut-off frequency increased from 0.5 Hz to 1.0 Hz the gain parameter decreased. For the visual display, a new stable level was found within two block periods of the change in input. For the audio displays a new stable level took longer to achieve. In the case of the mark-space ratio display no detectable change occurred.

For a step down in the input cut-off frequency the gain increased again. A new stable value was found quickly using the visual display. It was found that the beat frequency audio display results closely matched the visual in this respect.

VARIATIONS IN TIME DELAY, τ

For an increase in the input cut-off frequency the time delay parameter decreased when the visual and beat frequency audio displays were used. In the case of the visual display, the parameter decreased abruptly and then returned to a higher level: this effect was not detected using the beat frequency display. For the matching frequency and matching amplitude displays, it was occasionally noticed that the time delay increased. No significant change could be detected using the mark-space ratio display.

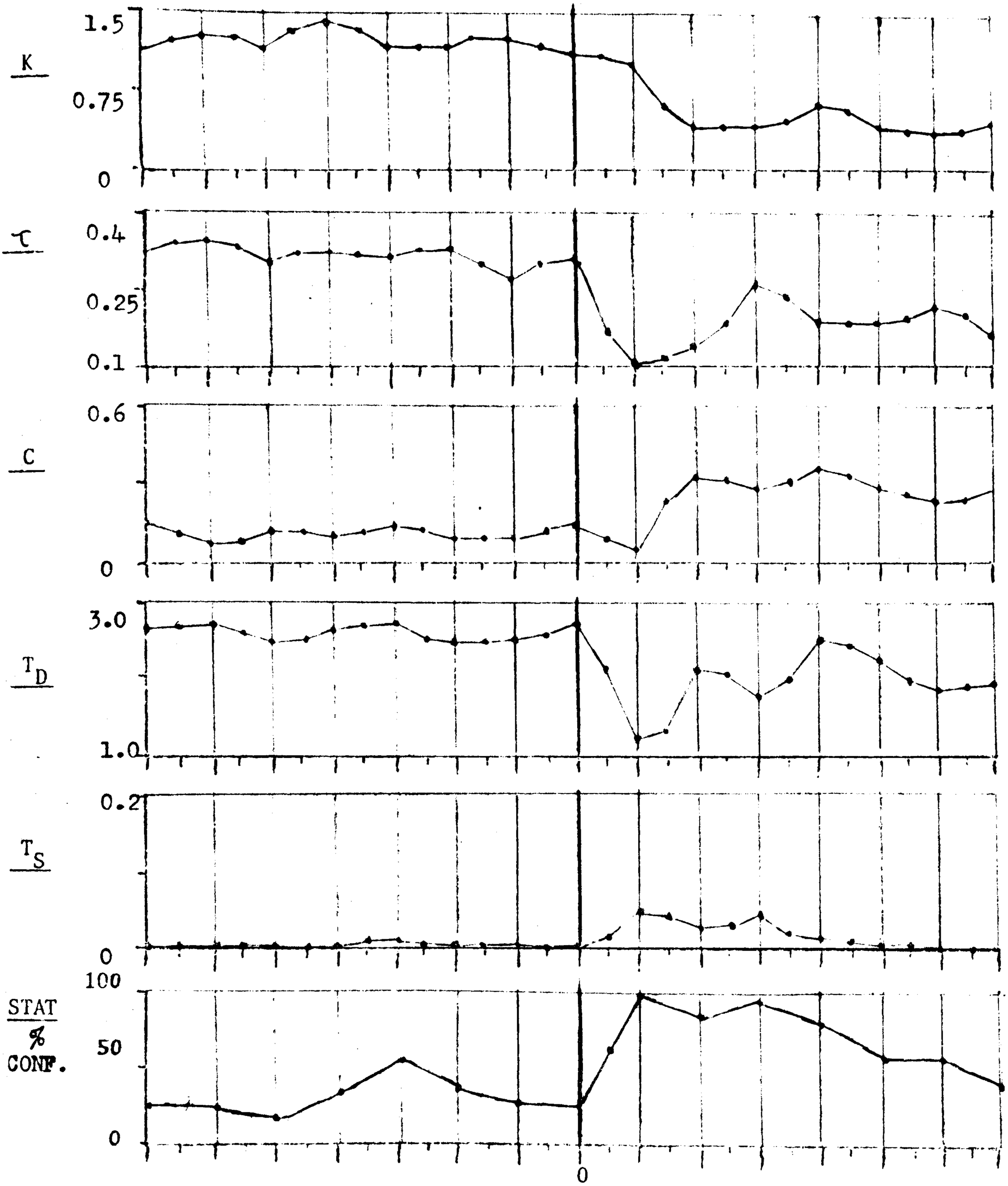

FIGURE 8 : Shows variations in the model parameters for a step change in the input signal cut-off frequency going from 0.5→1.0 Hz using the visual display.

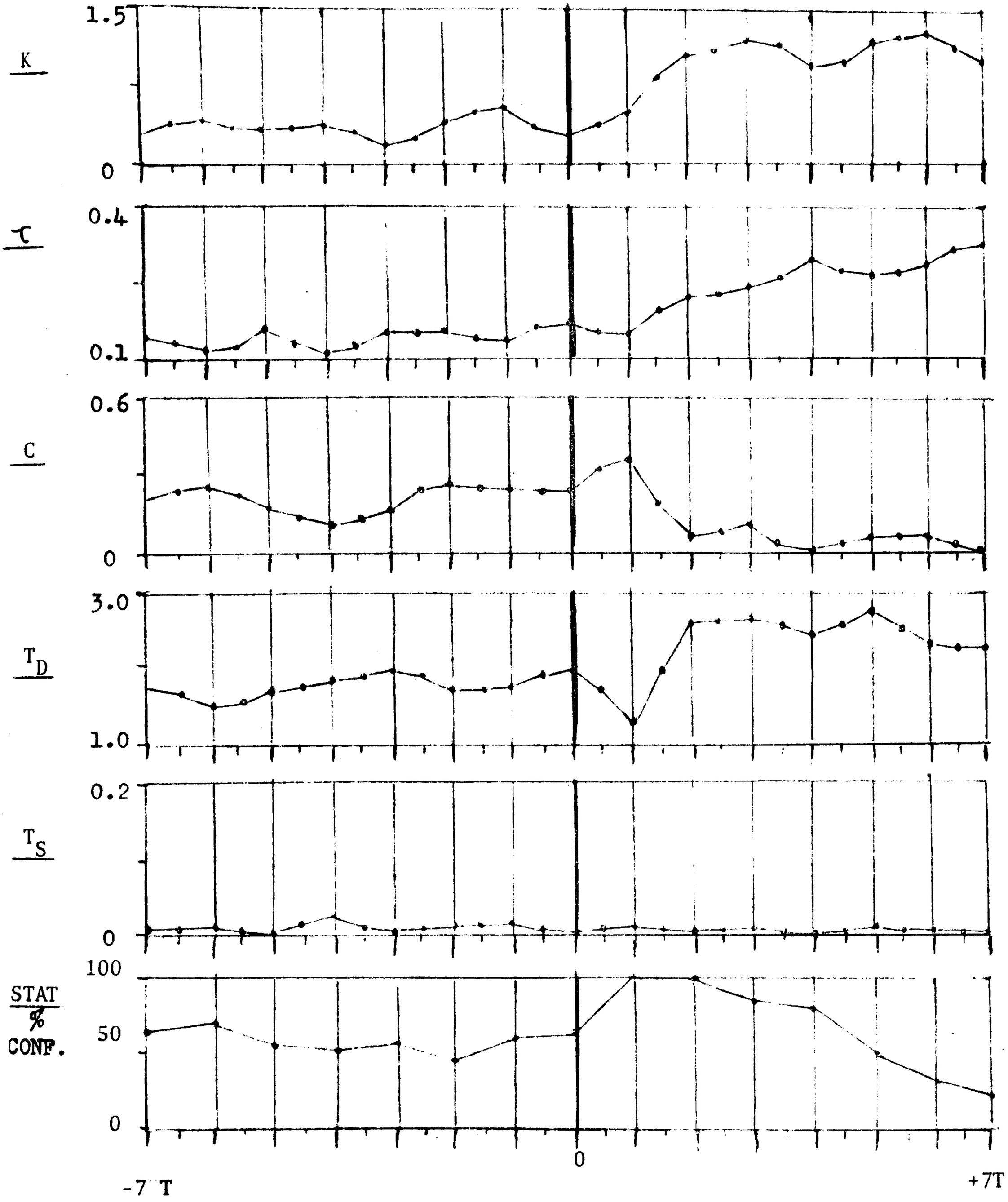

FIGURE 9 : Shows variations in the model parameters for a step change in the input signal cut-off frequency going from 1.0→0.5 Hz using the visual display.

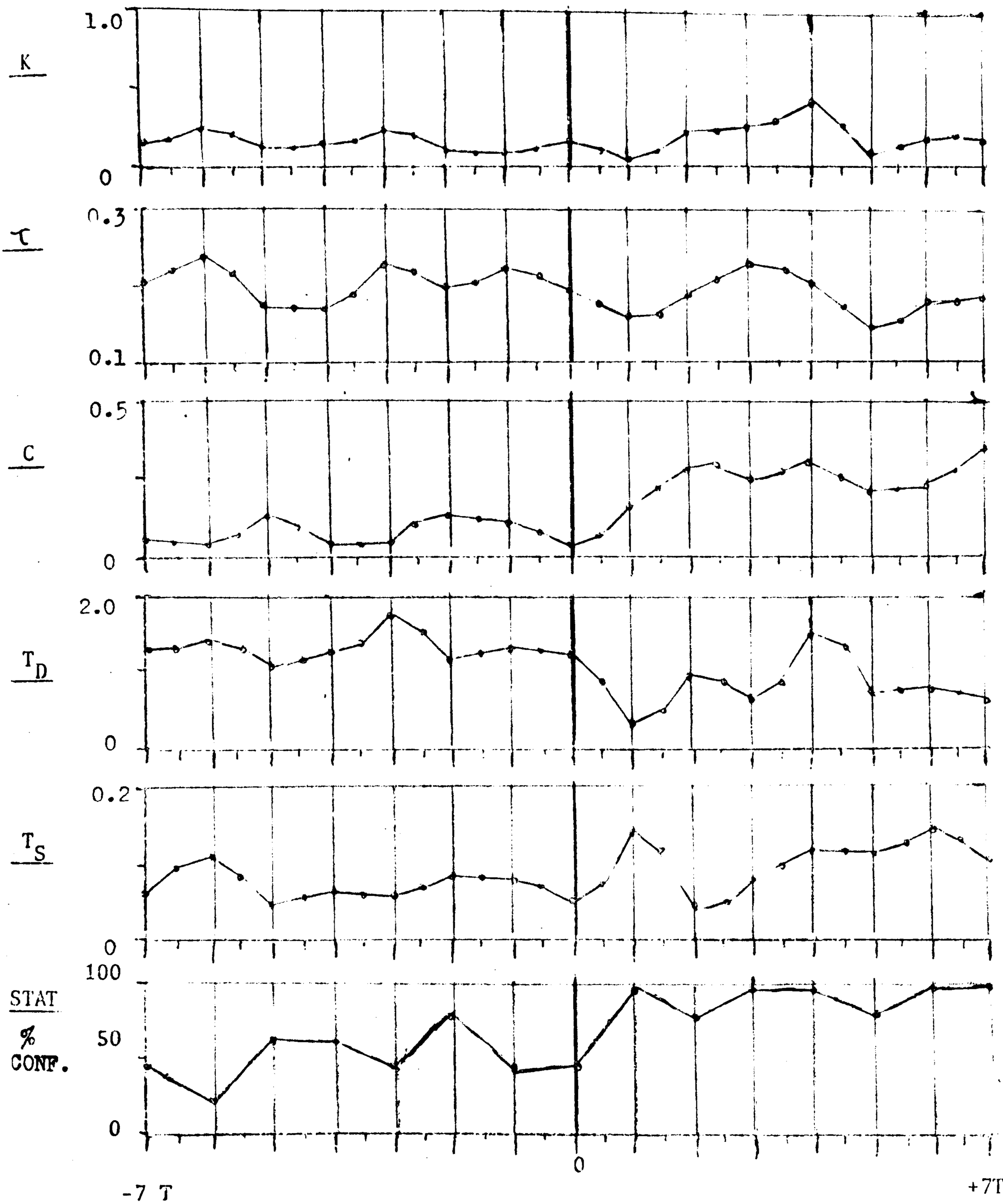

FIGURE 10: Shows variations in the model parameters for a step change in the input signal cut-off frequency going from 0.5→1.0 Hz using the Mark-space ratio audio display.

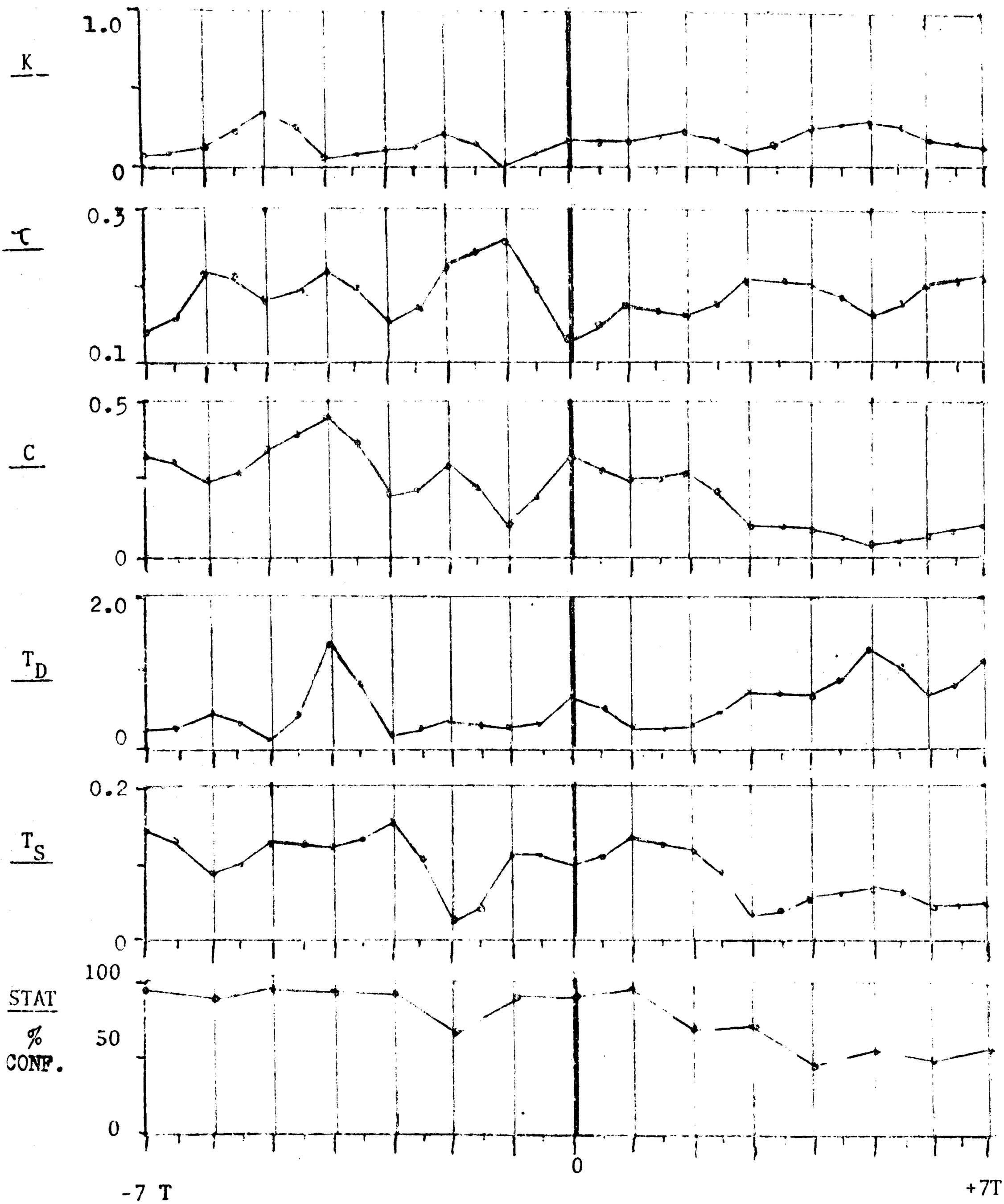

FIGURE 11: Shows variations in the model parameters for a step change in the input signal cut-off frequency going from 1.0→0.5 Hz using the Mark-space ratio audio display.

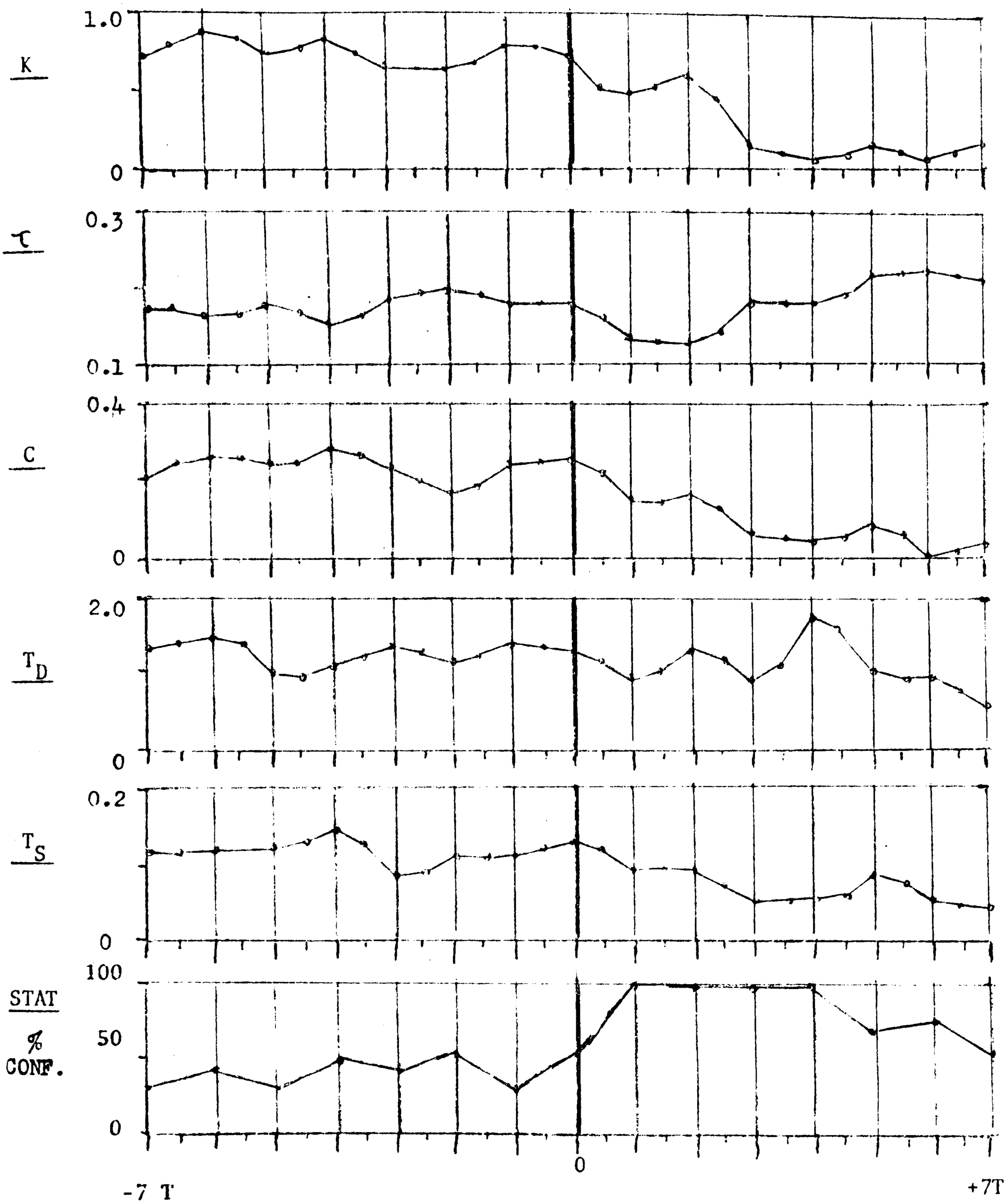

FIGURE 12 : Shows variations in the model parameters for a step change in the input signal cut-off frequency going from 0.5→1.0 Hz using the Matching frequency audio display.

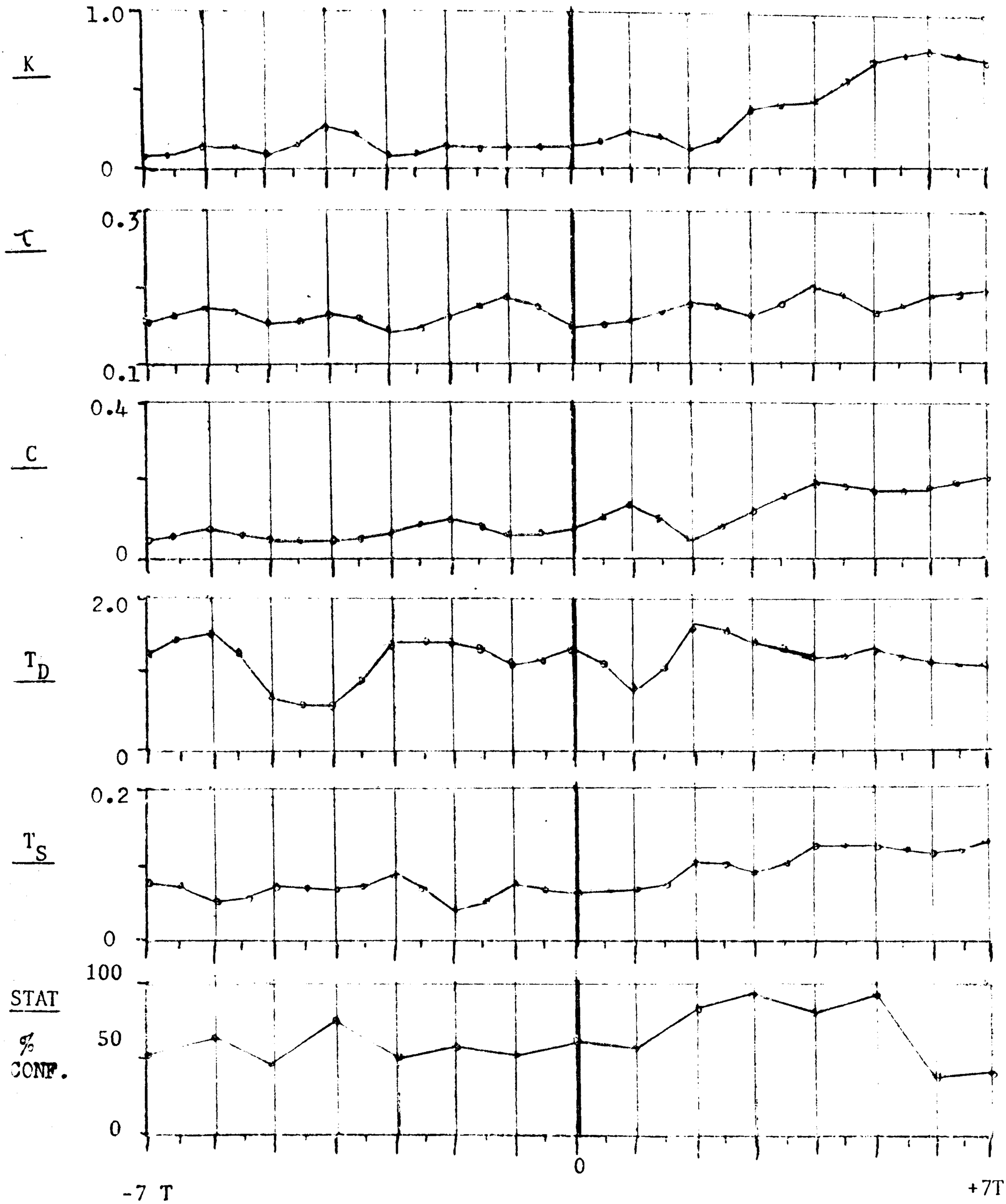

FIGURE 13 : Shows variations in the model parameters for a step change in the input signal cut-off frequency going from 1.0→0.5 Hz using the Matching frequency audio display.

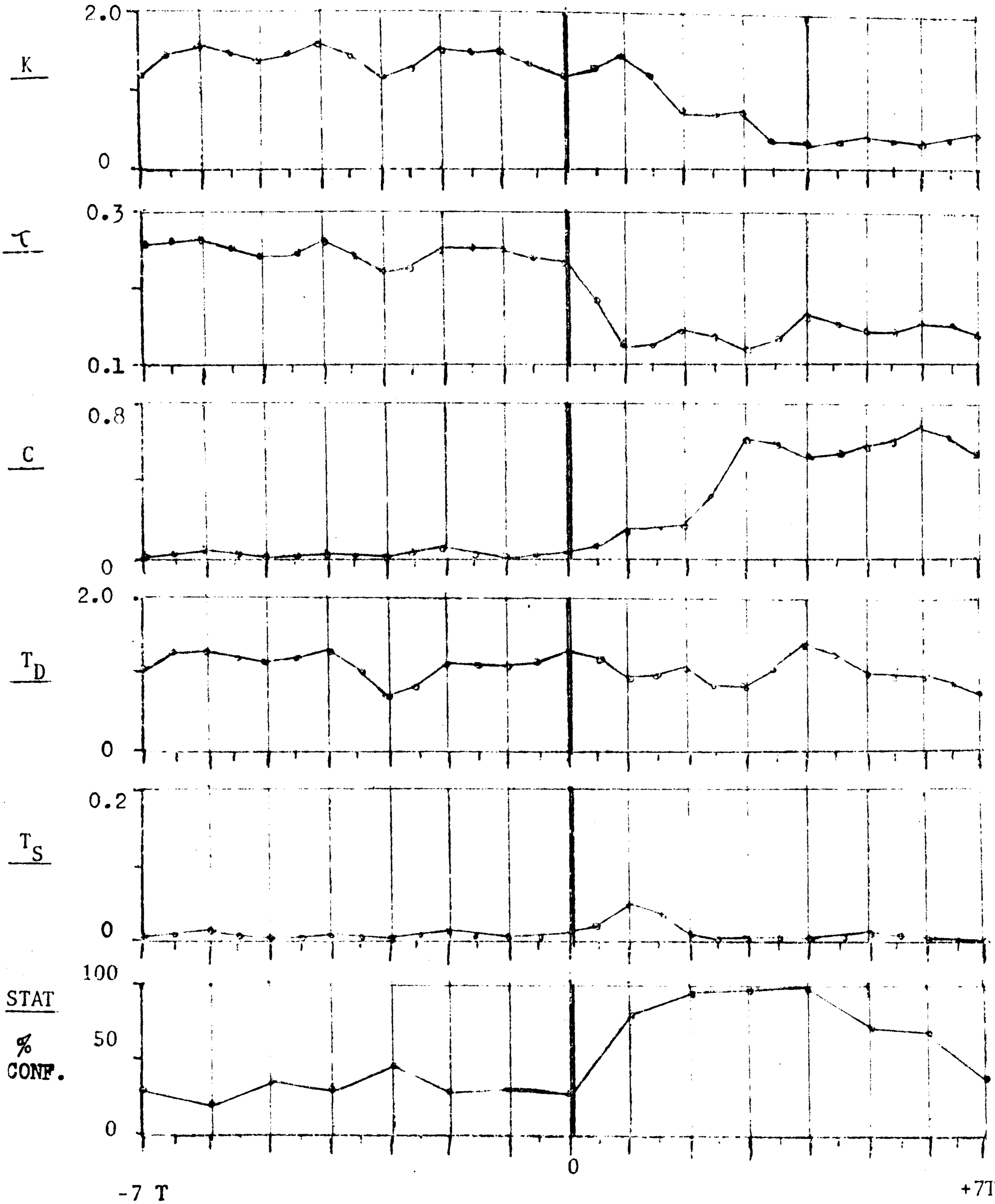

FIGURE 14 : Shows variations in the model parameters for a step change in the input signal cut-off frequency going from 0.5→1.0 Hz using the Beat frequency audio display.

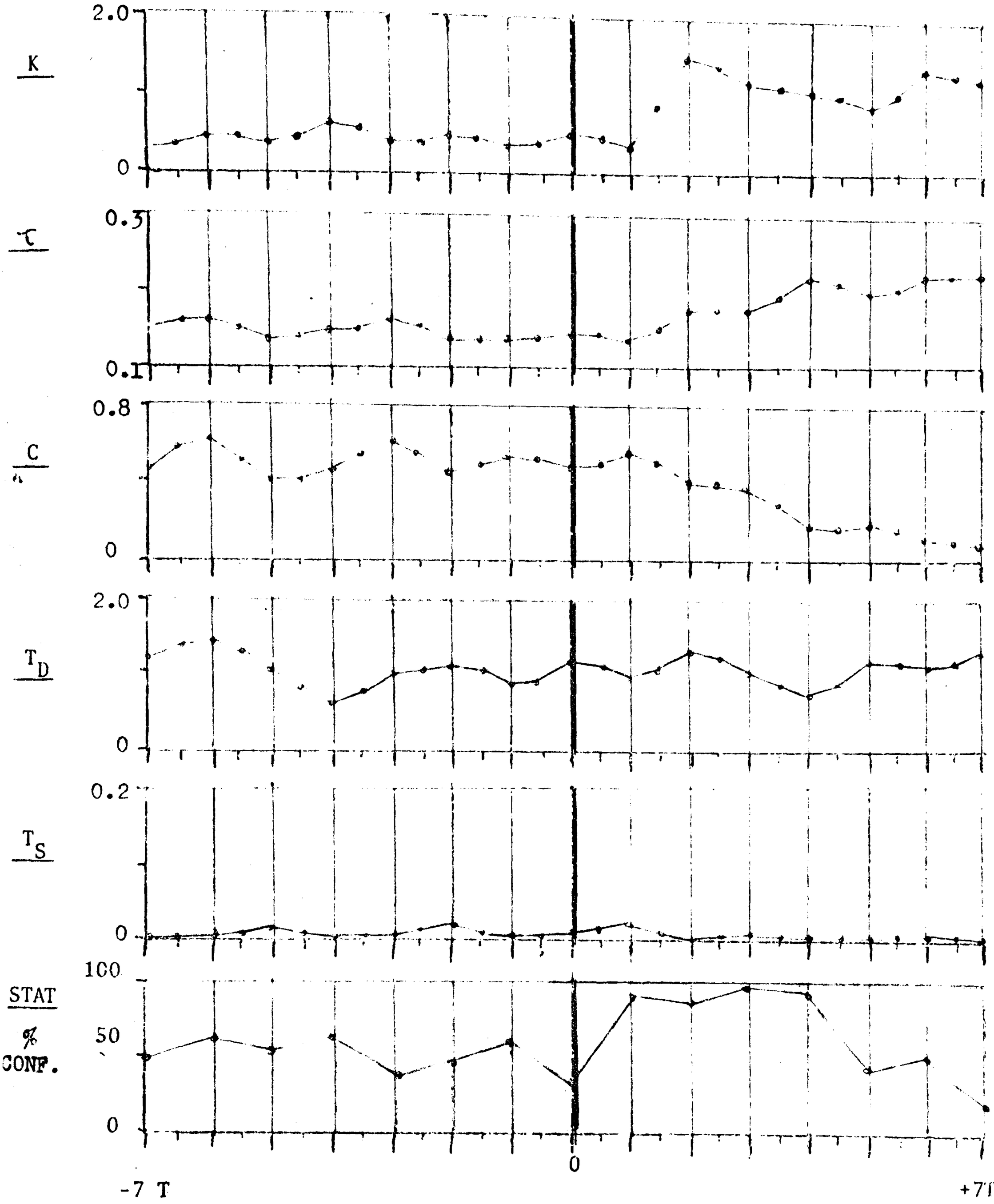

FIGURE 15 : Shows variations in the model parameters or a step change in the input signal cut-off frequency going from 1.0→0.5 Hz using the Beat frequency audio display.

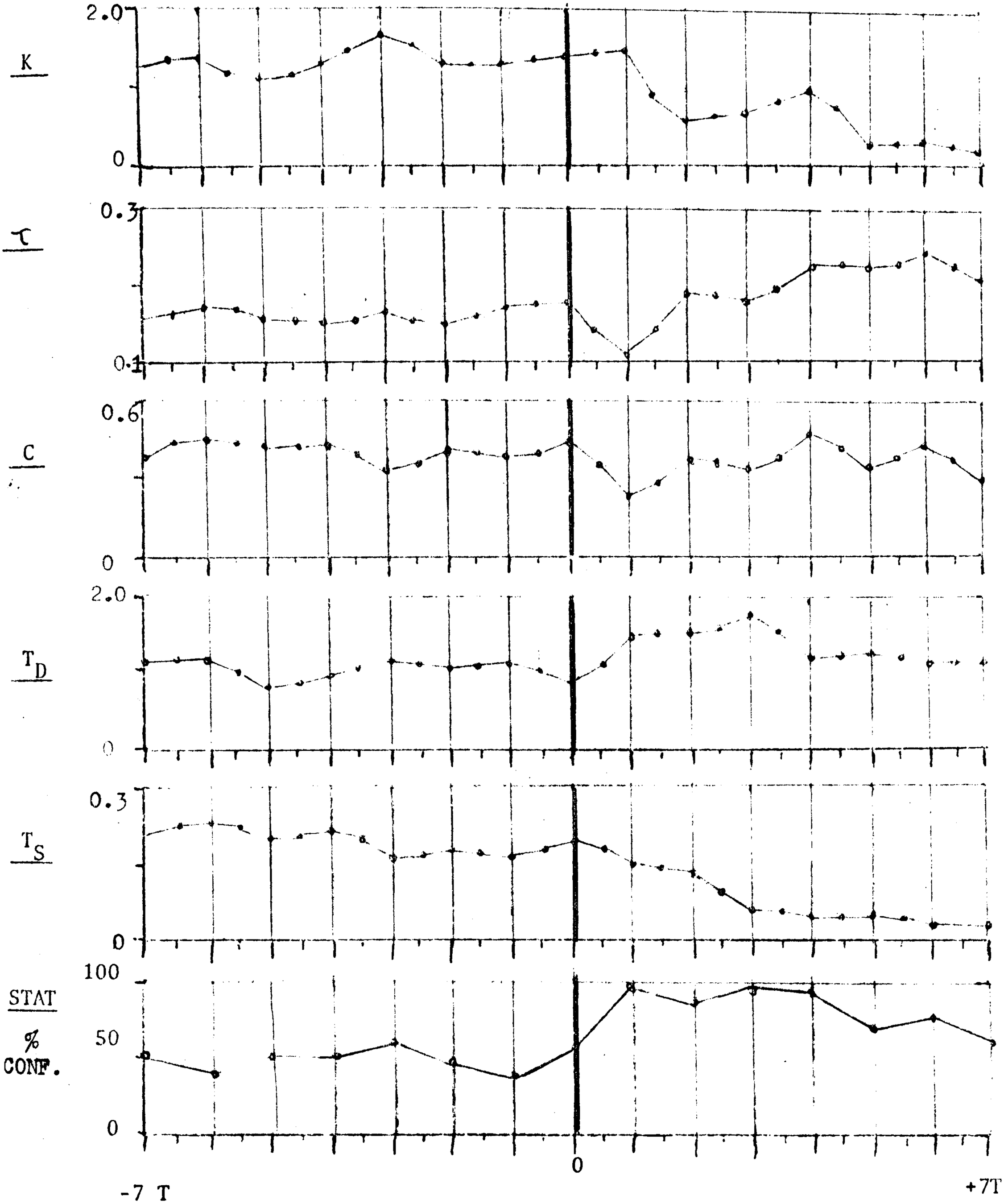

FIGURE 16 : Shows variations in the model parameters for a step change in the input signal cut-off frequency going from 0.5→1.0 Hz using the Matching Amplitude audio display.

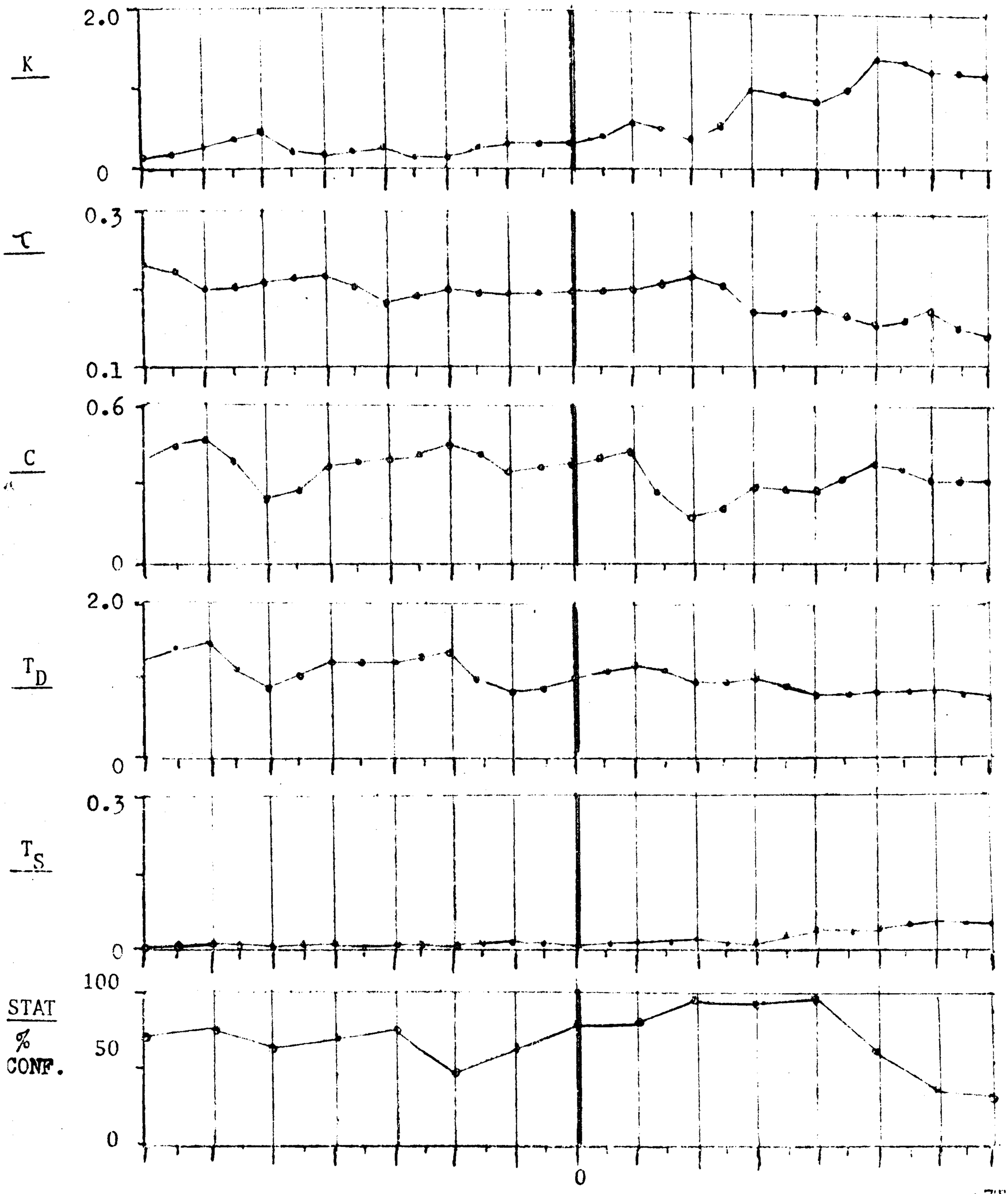

FIGURE 17 : Shows variations in the model parameters for a step change in the input signal cut-off frequency going from 1.0→0.5 Hz using the Matching Amplitude audio display

For the visual and beat frequency displays, the decrease would indicate an awareness on the part of the operator that a more complex signal required greater attention. It is suggested that the increase in time-delay using the other audio displays indicated an inability to interpret the error signal. This effect has been noted by Elkind and Sprague (see reference 13).

As the input signal cut-off frequency decreased again the time delay slowly increased for the visual and beat frequency displays. The change is less rapid than the step down.

VARIATIONS IN THE INTEGRATOR TIME CONSTANT, C

No overall trends in this parameter could be detected. The type of change depended on the display used. For the visual mark-space ratio and beat frequency displays the value of C increased as the input cut-off frequency increased, although variations in the mark-space ratio test results make any conclusions using this display doubtful. For the matching frequency and matching amplitude displays, the reverse was found. As the input cut-off frequency increased, the value of C decreased.

VARIATIONS IN THE DERIVATIVE TIME CONSTANT, T_D

An increase in T_D indicates that the operator is using derivative control on the error signal. Little or no change could be detected in T_D using the audio displays. Using the visual display T_D decreased as the input cut-off frequency increased. As in the case of variations in the time delay parameter, the initial decrease was often partly recovered.

VARIATIONS IN THE LAG TIME CONSTANT, T_S

No appreciable change in T_S could be found using the visual and beat frequency displays. For the frequency matching and amplitude matching displays, T_S decreased as the input cut-off frequency increased. This is consistent with the increase shown in the time-delay parameter, τ, for these displays.

VARIATIONS IN THE STATIONARITY CONFIDENCE LEVEL

The operator's response was in all cases found to be approximately stationary before a change in the input signal had occurred. A marked increase in the stationarity confidence level was noted immediately following a change in the input. This increase in general returned to a lower level after 7 block periods and in many cases sooner.

The variations in model parameter values just described were consistently detected for four of the five operators tested. For the fifth operator, no conclusions could be drawn from the results using the matching frequency and beat frequency displays. This is partly explained by the audio-gram shown in Appendix A, which shows a hearing loss in the mid-frequency band: however, it is unlikely that this discrepancy can be completely explained by this hearing loss.

5) SOME EXTENSIONS TO TWO-DIMENSIONAL AND MULTI-DIMENSIONAL DISPLAYS

In extending the analysis procedure to include two-dimensional displays, it is necessary to calculate four forward-loop frequency response functions. Figure 18 shows the block schematic for the analysis of a two-dimensional display.

FIGURE 18 : SHOWS THE SCHEMATIC BLOCK DIAGRAM FOR THE ANALYSIS OF A TWO-DIMENSIONAL DISPLAY

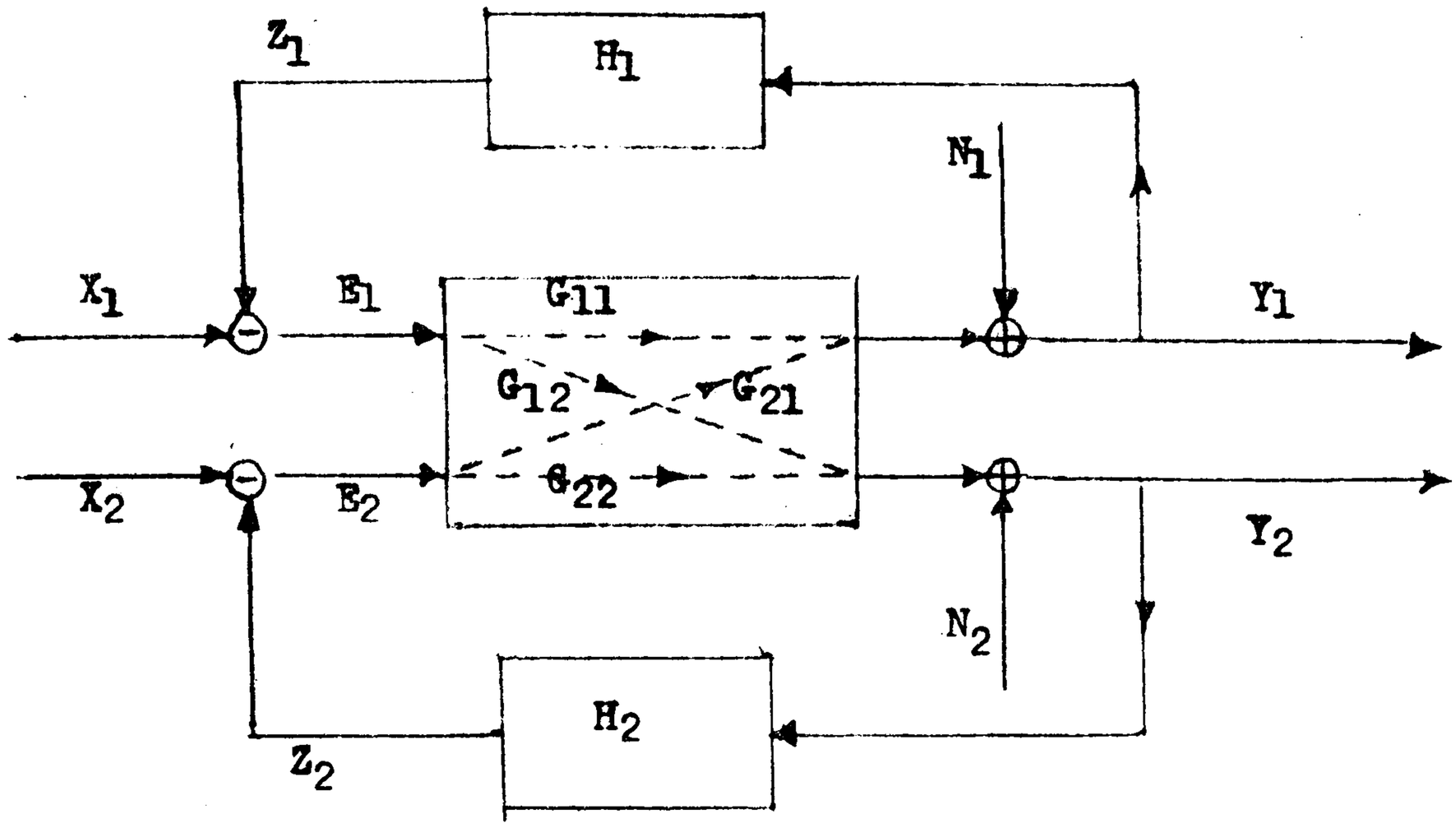

Unbiased estimates of the four forward-loop gain functions are given by:

$$\bar{G}_{11} = \bar{\phi}_{x_1 y_1} / \bar{\phi}_{x_1 e_1}$$

$$\bar{G}_{22} = \bar{\phi}_{x_2 y_2} / \bar{\phi}_{x_2 e_2}$$

$$\bar{G}_{12} = \frac{\bar{\phi}_{x_2 y_1}}{\bar{\phi}_{x_1 e_1}} \cdot \frac{\bar{\phi}_{x_1 x_1}}{\bar{\phi}_{x_2 x_2}}$$

$$\bar{G}_{21} = \frac{\bar{\phi}_{x_1 y_2}}{\bar{\phi}_{x_2 e_2}} \cdot \frac{\bar{\phi}_{x_2 x_2}}{\bar{\phi}_{x_1 x_1}}$$

Stapleford et al (see reference 7) have shown that the cross-coupling terms $\bar{G}_{12}$, $\bar{G}_{21}$ are negligible for visual displays when there is no cross-coupling in the response dynamics. Thus four optimising parameters can be put forward to compare responses of audio and visual two-dimensional displays.

As in the one-dimensional case, G_{11} and G_{22} are optimal when the output tracks the input exactly, i.e. $G_{11} = G_{22} = 1.0$ for all frequencies. Thus cost functions as proposed in Appendix A can be used to compare the responses obtained from different displays. Ideally, there should be no cross-coupling. Under these conditions, the outputs $y(t)$ and $y_2(t)$ become independent. A cost function marking departure from this ideal is given by:

$$G_{FACT} = \int_0^{Fc} |\bar{G}_{12}| \cdot df$$

The phase response is of secondary importance. A similar cost factor can be defined for G_{21}.

In the design of multi-dimensional audio displays, care must be taken to make the audio feedbacks in each dimension distinct from each other. For instance, the combination of frequency pitch to indicate errors in the Y-axis and amplitude to indicate errors in the X-axis would make detection of Y-error easier at large X-errors (large amplitudes). Further, a base reference of zero error is easily defined in the X-axis by modulating the amplitude in left or right ears, but not so easily defined in the Y-axis, where a reference tone is required. The resulting audio signal even in two dimensions is extremely complex.

A further complication in examining the response to two-dimensional displays is the possible introduction of non-linearities.

This applies even to the visual display where an operator is more likely to correct large errors in one axis and ignore errors in the other axis if they are relatively small.

Lastly, most displays in two dimensions have concentrated on a rectangular set of coordinates. It is highly conceivable that the choice of another reference frame (e.g. polar coordinates) might be more suitable for the design of audio displays. Indeed, it is simpler to design easily distinguishable audio feedback signals in a polar set of axes.

6) CONCLUSIONS

Section 2 and Appendix A outline a simple method of comparing one-dimensional displays. It was found that the cost functions give a reasonably objective appraisal of the performance of the displays tested, without recourse to a detailed analysis of the measured frequency response functions.

The plausibility of the model suggested by confidence level testing in Section 3, together with its physical interpretation, justify its use in explaining changes in the mode of response with change in the input signal dynamics.

The drop-out phenomenon exhibited in some of the audio tests for high frequency cut-off input signals would indicate an inability to interpret the audio display. Other changes in the response sometimes found in tests using the 1.5 Hz input signal cut-off indicate that the operator varied between two modes of response: a highly damped mode in which high frequency components in the error function are simply ignored (indicated in Figure 6(b)) and a resonant mode

(indicated by Figure 6(a)). The amounts of time spent in each mode would indicate that the former is easier to maintain.

By calculating the average values (i.e. for all five operators tested) of the model parameters for each type of test, it is possible to plot the change in the parameters as a function of the cut-off frequency of the input signal. Figure 19 shows a comparison of the model parameters for the visual display and what was considered to be the best audio display (Appendix A). The parameter variations shown can be considered as characteristic of the respective displays, although, as has been mentioned, each operator may vary quite considerably from this characteristic response. In comparing the characteristic responses (Figure 19) it can be seen that the use of signal derivative control, Ts, is more marked for the visual display and that stability is maintained for the audio display by the introduction of a lag time-constant T_D. This would indicate that less error signal information is retrieved by the operator using an audio display than using the visual display.

It is seen (Section 4) that not only is the operator's response down-graded using the audio displays but also that his reaction to changes in the frequency content of the input signal is in all cases less immediate than for the visual display and in some cases not detectable. The use of overlapped blocks of time samples to track variations in the response parameters gives a clearer picture of the parameter variations. The reduction in block size decreases the sampling interval and enhances tracking qualities at the expense of frequency resolution. It can be argued that the human operator can

GAIN FACTOR , K

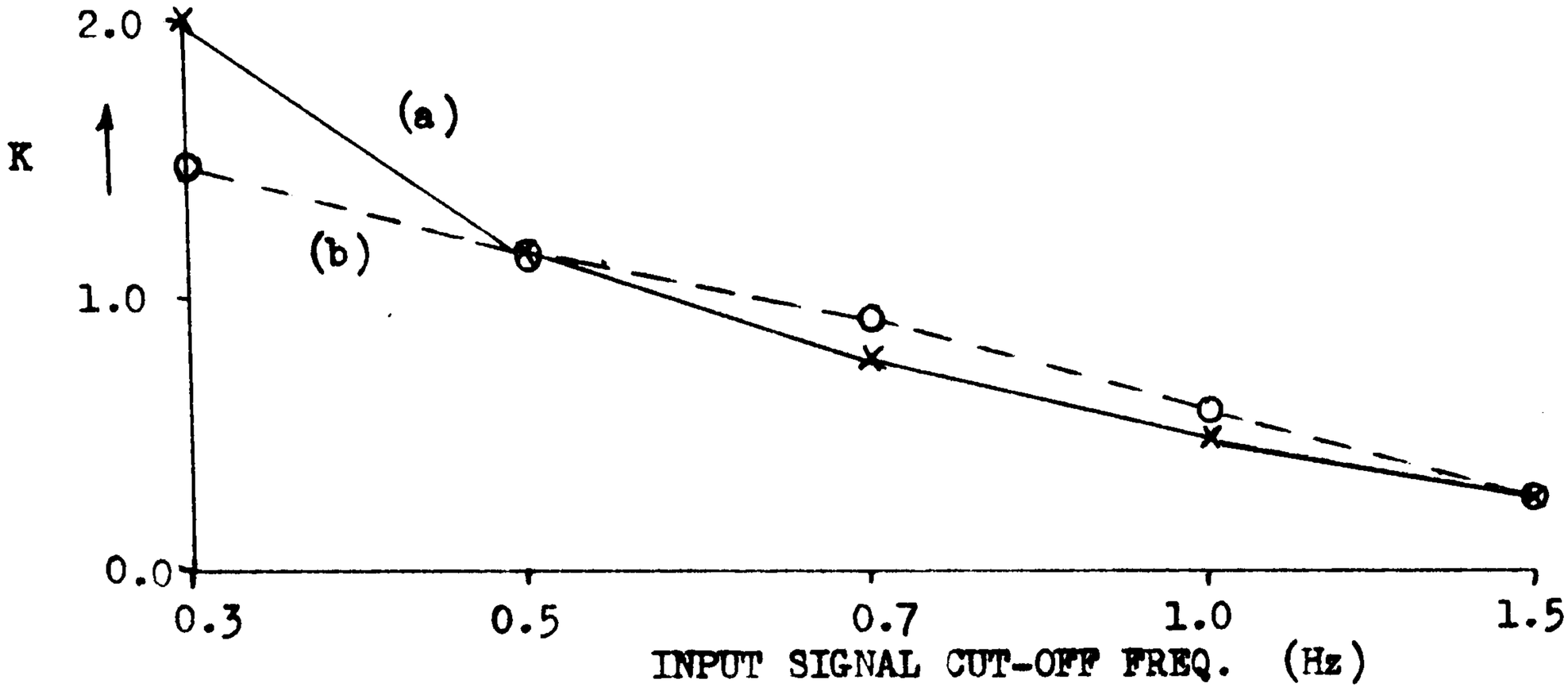

TIME DELAY , τ

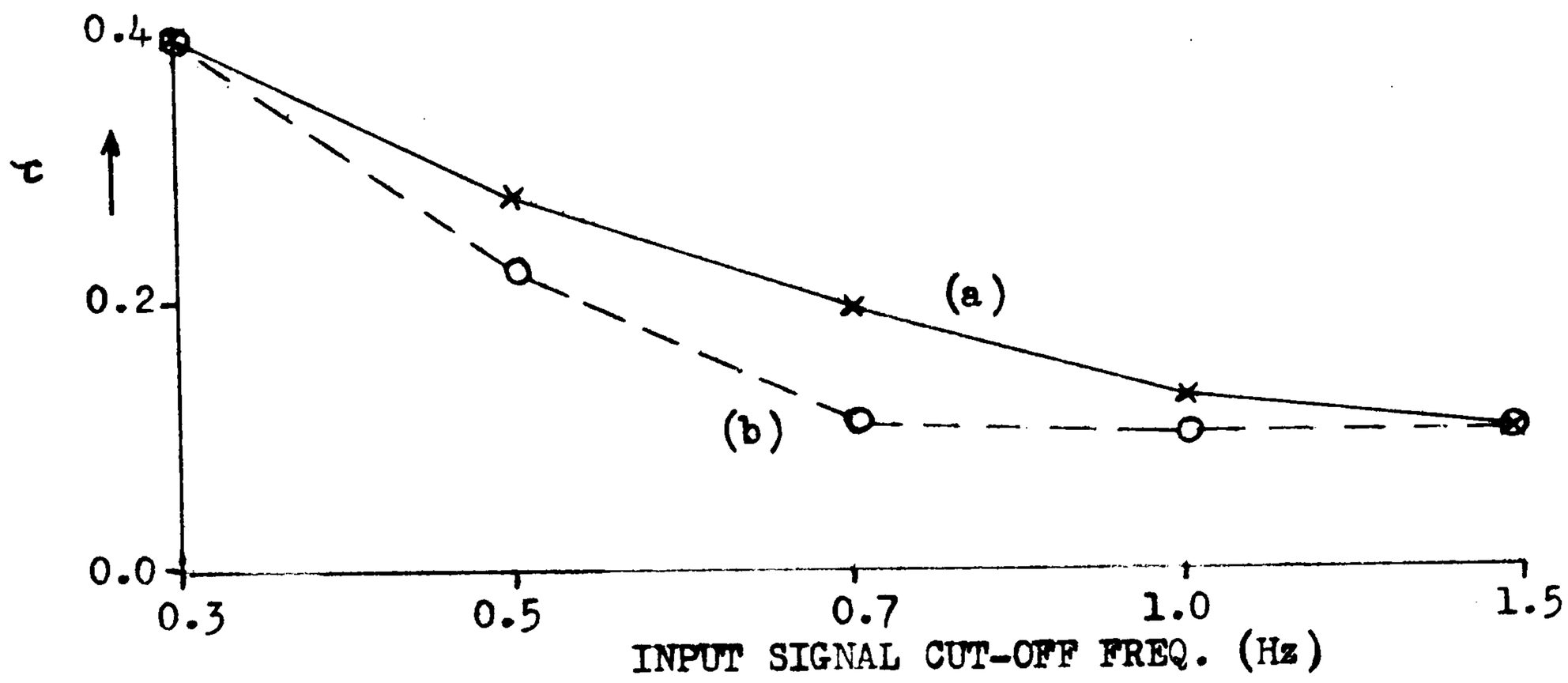

INTEGRATOR CONSTANT , C

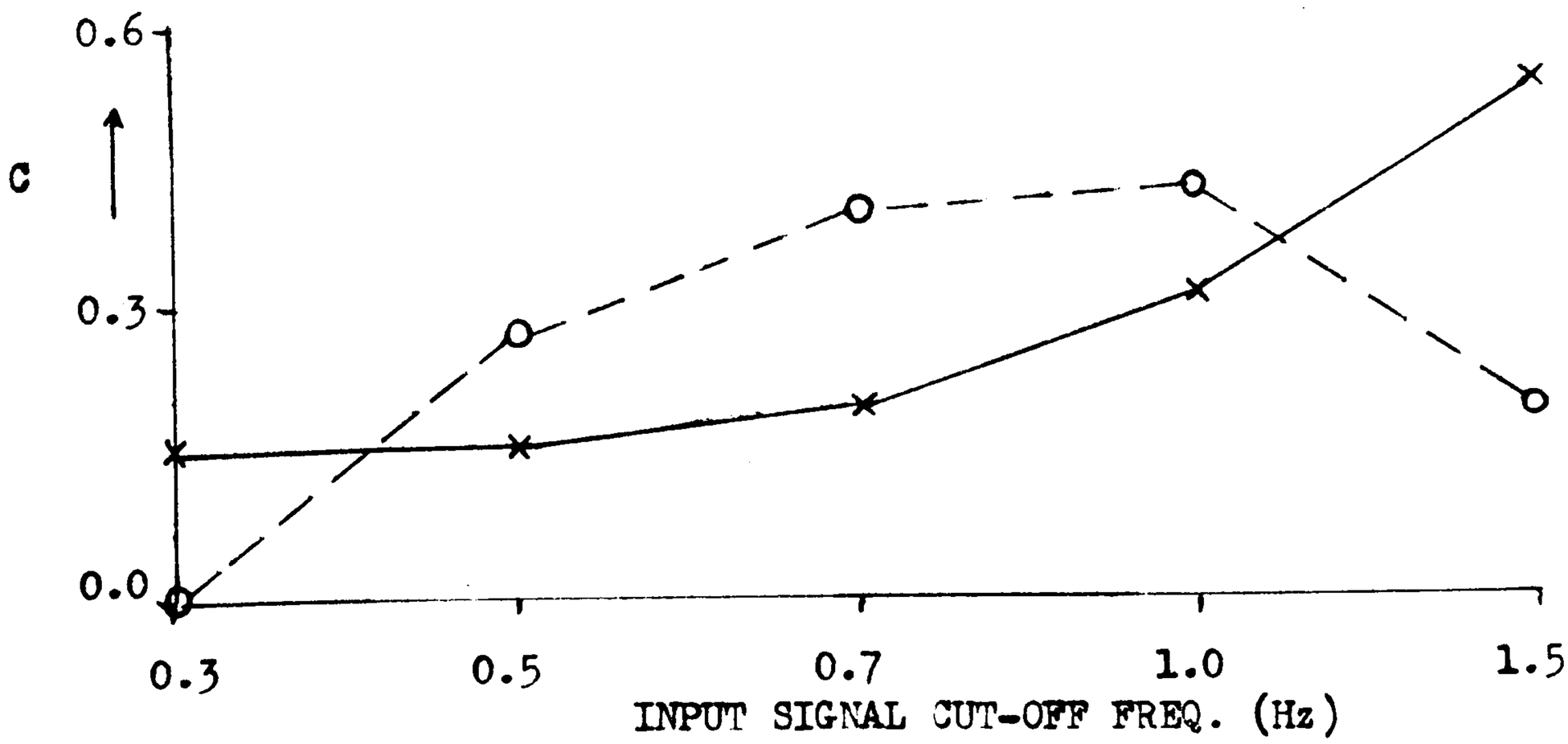

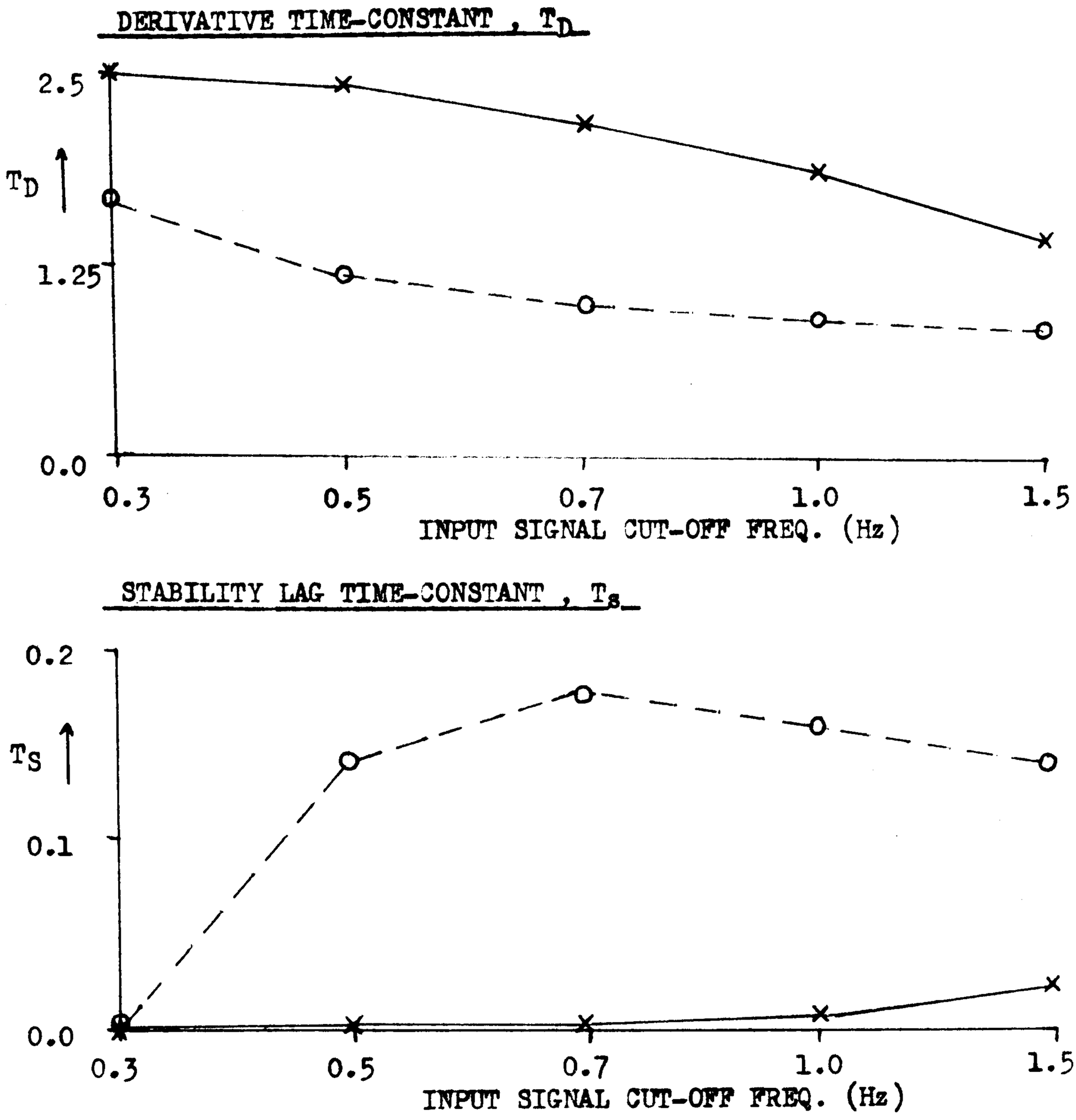

FIGURE 19 Plots the average variations in the model parameters against the input signal cut-off frequency for :-

a) the visual display (——) and

b) the best audio display as found in appendix A.

(ie. The Beat frequency audio display) (– – –)

The parameter values represent the average as obtained for the five operators tested.

nevertheless vary his dynamic response much faster than the time it takes to collect a block of data. The changes in the model parameters are then at best filtered versions of the true changes. However, it is significant that the response continues to alter for some considerable time after a step change in the input has occurred. This might be explained by the operator's adopting a trial and error mode of response adaptation, with the period between changes being fairly long.

Finally some problems in extending the analysis procedure to include comparison of two-dimensional audio and visual displays indicate a large area for future research. Assumptions of linearity need to be confirmed and displays based on different sets of coordinates must be compared. This requires an extension of the statistical theory to include two input/two output closed-loop systems.

7) APPENDIX A

(A paper published in Research Bulletin. 'A method for the comparative evaluation of visual and auditory displays'. P. W. Davall & J. M. Gill. (October 1974))

SUMMARY

In reading and mobility aids for the blind it is desirable to design the display to optimise the man-machine interface. This paper describes a possible method for comparing various displays.

Five subjects used compensatory tracking with random input signals (five different cut-off frequencies) with five one-dimensional displays where the error is represented by:

(i) Visual : deflection

(ii) Auditory : mark-space ratio

(iii) Auditory : matching frequency

(iv) Auditory : beat frequency

(v) Auditory : amplitude matching

The significance of the coherency between the input signal and the subjects' output is discussed. The measured closed-loop frequency response is compared to that obtained from a modified form of cross-over model. Finally two performance parameters are proposed for assessing the various displays.

1) INTRODUCTION

Research on the design of auditory displays has usually been motivated by the desire to provide non-visual displays for those who cannot use vision or to supplement a visual display particularly in aeronautical applications.

Pollack and Ficks (1954) studied multi-dimensional auditory displays in which each variable had only two states. They found that, in general, multiple stimulus encoding is a satisfactory procedure for increasing the information transmission rate associated with such displays. Mudd (1965) studied the relative effectiveness of frequency, intensity, duration and interaural difference dimensions of a pure-tone binary display. Frequency proved to be the most effective dimension for the purposes of cuing; intensity was the least effective.

Roffler and Butler (1968a) found that listeners could locate auditory stimuli accurately in the vertical plane when the stimulus was complex and included frequencies above 7 kHz. Roffler and Butler (1968b) then found that subjects tended to place the audio stimuli on a vertical scale in accordance with their respective pitch. Higher-pitched sound were perceived as originating above lower-pitched sounds.

Vinje and Pitkin (1971) studied human operator dynamics for aural compensatory tracking using pitch of the tone to represent the magnitude of the tracking error. Error polarity was indicated, in the two-ear display, by switching the tone between ears as a function of error sign. For the one-ear display, error polarity was indicated by using modulated and unmodulated tones. The describing function and remnant data indicated that humans can control as well with aural cues as with visual cues for input signals with cut-off frequencies of 0.27 to 0.56 Hz.

A variety of two-dimensional auditory displays have been built; for instance, Black (1968) developed a display where the horizontal coordinate was represented by time delay and amplitude of the signal

and the vertical coordinate by frequency (100-400 Hz). Fish and Beschle (1973) also used frequency (200-7000 Hz) for representing the vertical position of the scan but interaural intensity differences (up to 40 dB) for the horizontal.

Phillips and Seligman (1974) developed a multi-dimensional auditory display in which frequency, amplitude and timbre are all utilized. Robinson (Gill, 1974) also developed a two-dimensional display, as a non-visual equivalent to the cathode ray oscilloscope, where the frequency of the signal depends on the vertical coordinate and time delay for the horizontal. However, there has been little systematic comparison of the various types of auditory displays even though Kramer (1962) mentioned the need for this over a decade ago.

This paper describes a method for comparing various displays and applies the technique to one visual and four auditory one-dimensional displays. The technique can be extended to multi-dimensional displays.

2) EXPERIMENTAL METHOD AND ANALYSIS

The human operator was presented with an error signal, e(t), which was the difference between the input, x(t), and the output, y(t) (Figure 1). The output was measured from two strain gauges (making two arms of a bridge section) strapped across a stiff joystick. The choice of a force, as opposed to a position, joystick considerably reduces the response time delay introduced by the muscle motor action of the arm. The input, x(t), was band-limited Gaussian white noise. Five bandwidths of 0.3, 0.5, 0.7, 1.0 and 1.5 Hz were used for each form of error signal presentation. The operator's task was

Figure 1: Shows closed loop configuration for human operator tracking tests.

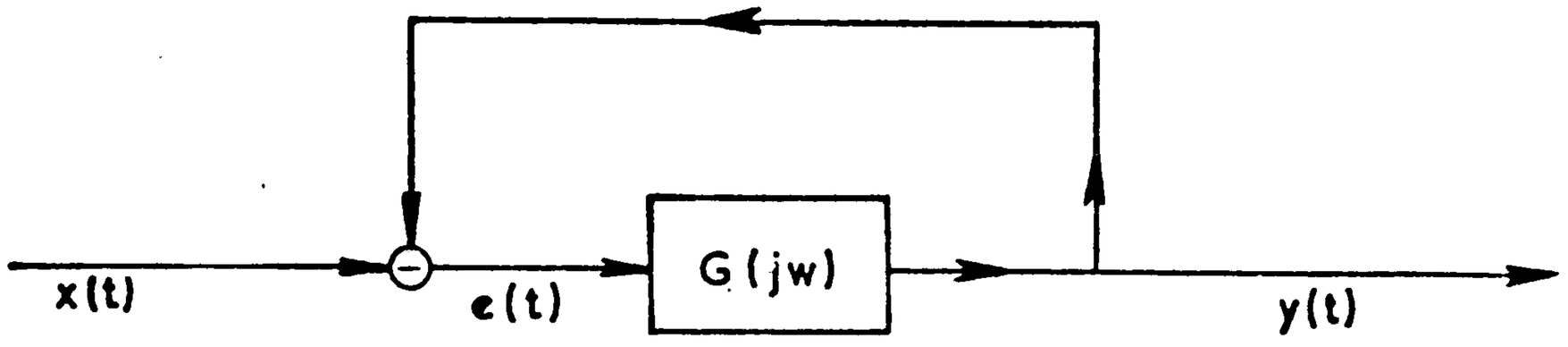

Figure 2: Shows the zero error state for mark space audio feedback error signal presentation.

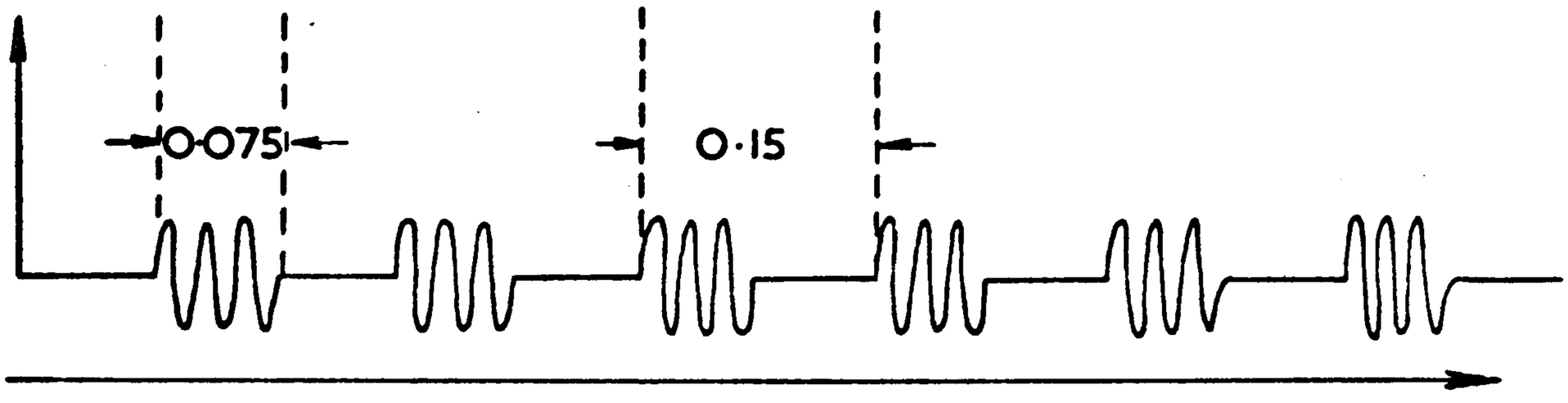

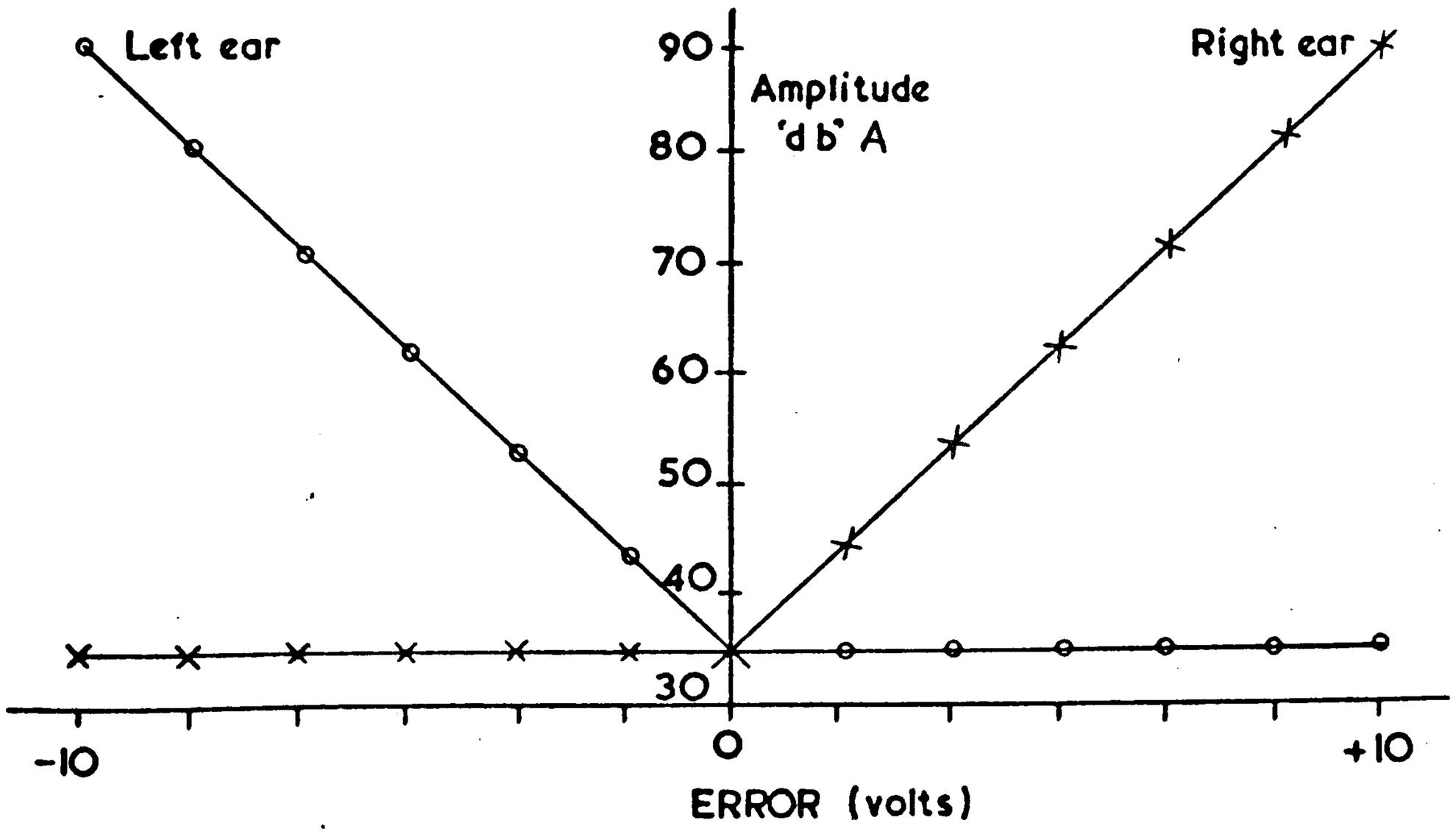

Figure 3: Shows the Amplitude v Error function for left and right ears for the amplitude matching audio test.

to minimise the error.

2.1) ERROR SIGNAL PRESENTATION

(i) Visual feedback

A horizontal line on a cathode ray tube display moved vertically about a centre zero, the deflection being a function of the error signal. By pushing on the joystick the line was moved up the screen while pulling brings the line down. Full scale deflection was ±10 cm. in response to an error signal of ±10 volts (0.5 kg per volt).

(ii) Mark-space audio feedback

The error signal was presented as short bursts of a single tone. Pulling the joystick reduced the duration of the pulses and increased the silent periods, while pushing reversed the effect. The fundamental clocking period for repeating the pulses was 0.15 seconds (Figure 2). The zero error state was defined as unity mark-space ratio between noise and silence.

(iii) Matching frequency feedback

A 1 kHz square-wave was fed to the left ear as a reference tone while a variable frequency square-wave of equal amplitude was fed to the right ear. The frequency of the variable signal was controlled by the joystick and could vary from zero to 3 kHz for full scale error deflection of -10 volts to +10 volts. Zero error was recorded when the two inputs were of matching frequency.

(iv) Beat frequency feedback

The signal inputs were the same as those described in (iii), except that both inputs were presented to both ears simultaneously. The effect is different from (iii) in that signals of three frequencies

can be heard. As well as the two fundamental frequencies, a beat frequency is present. This beat frequency decreases as the two fundamentals come closer together. The advantage of this form of frequency matching is that it does not require the operator to be tone sensitive.

(v) Amplitude matching feedback

A 1 kHz square-wave was presented to both ears. The amplitude presented to each ear, as a function of the error signal, is shown in Figure 3. The loudness of the tone presented in each ear was approximately a linear function of the error (the ear being a logarithmic device to a first approximation). Zero error was recorded when the amplitudes were matched.

2.2) ANALYSIS

$x(t)$	:	signal input
$y(t)$	:	system output
$e(t)$	:	error signal, $x(t) - y(t)$
$\hat{X}i(jw)$	:	i^{th} short-term Fourier estimator of $X(jw)$ at frequency w
$\bar{H}(jw)$	:	frequency response estimate relating $X(jw)$ to $Y(jw)$ at frequency w
$\bar{G}(jw)$	:	open-loop frequency response estimate relating $E(jw)$ to $Y(jw)$ at frequency w
$\bar{\phi}xx(w)$	:	estimate of the auto-spectrum of $x(t)$ at frequency w
$\bar{\phi}xy(jw)$	:	estimate of the cross-spectrum between x and y at frequency w
$\overline{C^2xy(w)}$	:	squared coherency estimate between X and Y at frequency w

The signals x(t), y(t) and e(t) were sampled five times per second. Approximately ten-minute records were taken for each type of input signal (0.3, 0.5, 0.7, 1.0 and 1.5 Hz cut-off frequencies).

The sample records were divided into blocks of N (128 in this case) points for Fourier analysis using a radix '2' fast Fourier algorithm (Blackman and Tukey (1958); Wellstead (1971)) producing N/2 spectral coefficients over the frequency range $0 \rightarrow 2.5$ Hz. Approximately 25 short-term estimates of E(jw), X(jw) and Y(jw) were obtained for each input cut-off frequency.

$$\hat{X}_i(jw) = \frac{1}{N} \sum_{K=0}^{N-1} x_t^i(k).\exp(-jwk) \quad \ldots\ldots\ldots 2.1$$

where k denotes the k^{th} time sample in the i^{th} block and for $w = \{2.\pi.0.039.L\}$,$0 \leqslant L \leqslant N/2$ where 0.039 is the frequency resolution in Hz. Similar expressions are used to calculate Yi(jw) and Ei(jw).

The overall closed-loop frequency response as estimated between x(t) and y(t) was calculated as follows:

$$\bar{H}(jw) = \bar{\phi}xy(jw) \,/\, \bar{\phi}xx(jw) \quad \ldots\ldots\ldots\ldots\ldots 2.2$$

and the human operator frequency response (open-loop) relating e(t) and y(t) is given by:

$$\bar{G}(jw) = \bar{\phi}xy(jw) \,/\, \bar{\phi}xe(jw) \quad \ldots\ldots\ldots\ldots\ldots 2.3$$

where:

$$\bar{\phi}xx(jw) = \sum_{i=1}^{25} \hat{X}i(jw) * \hat{X}i(jw) \quad \ldots\ldots\ldots 2.4$$

$$\bar{\phi}xy(jw) = \sum_{i=1}^{25} \hat{X}i(jw) * \hat{Y}i(jw) \quad \ldots\ldots\ldots 2.5$$

$$\bar{\phi}xe(jw) = \sum_{i=1}^{25} \hat{X}i(jw) * \hat{E}i(jw) \quad \ldots\ldots\ldots 2.6$$

where * denotes the complex conjugate

MODELLING THE HUMAN OPERATOR RESPONSE

For each test mean estimates of $\bar{H}(jw)$ and $\bar{G}(jw)$ were obtained. These represented the average performance over each ten minute test. A linear model of the human operator, similar to the more complex cross-over models (Young (1969); Krendel, McRuer & Graham (1966)) was used:

$$G_H(jw) = \frac{K.\exp(-jw\tau).(1 + jwT_D)}{(c + jw).(1 + jwT_S).(1 + jwT_L)} \quad \ldots\ldots\ldots\ldots 2.7$$

where:

K : an arbitrary gain factor which can be varied over a large range by the operator

τ : human operator's response time delay

T_D : a velocity lead response reacting to the rate of change in the error signal. The degree of velocity control exhibited is found to be dependent on the frequency content of the input

c : a measure of the integral action of the operator. c is small when the operator is able to track slowly-varying trends in the mean level of the error signal.

T_S : a low-pass element modelling the operator's ability to disregard high frequency content in the error signal which may be due to his own reaction time delay acting in a closed-loop mode.

T_L : a fixed low-pass element measuring the inability of the muscles to respond to frequency changes (T_L = 0.04, cut-off about 4 Hz)

The parameters of interest are τ, (the reaction time delay), T_D (the operator's ability to react not only to the magnitude of the error but also to the manner in which it is changing) and c (a measure of the operator's ability to follow the mean level of the signal accurately). A Powell hill-climb routine (Fletcher and Powell, 1963) was implemented to model the responses obtained for $\bar{G}(jw)$ and $\bar{H}(jw)$ in each test in terms of the model described in equation 2.7. The fixed low-pass element T_L was chosen to achieve a cut-off at about 4 Hz while T_S, the stability factor, was only allowed to operate on high frequency cut-off tests. This is consistent with experience in that no stability problems were encountered in low frequency tests. Thus the Powell hill-climb routine was used to optimise the parameters K, τ, T_D and c. The gain factor K acts in choosing the magnitude of the human operator's open-loop characteristic response. The limits imposed on K are physical limitations and not of direct interest to his mode of response. The restrictions on the values assumed by τ, T_D and c were taken from previous results, and from trial and error. The following limits were chosen:

$$0.1 \leqslant K \leqslant 20$$

$$0.1 \leqslant \tau \leqslant 0.6$$

$$0.0 \leqslant c \leqslant 1.0$$

$$0.0 \leqslant T_D \leqslant 4.0$$

and where applicable:

$$0.0 \leqslant T_S \leqslant 0.3$$

RESPONSE EVALUATION

The concept of a measure of 'goodness' for a particular form of error signal presentation is subjective to a degree. However, for

specific tasks, such as continuous tracking and control tasks as presented here, two parameters may be considered to give a measure of the performance of one form of display against another.

The ideal operator response is achieved when y(t) follows x(t) exactly. Under these conditions the magnitude of the closed-loop frequency response is unity over all frequencies of interest. Deviations from this unity gain represent a loss. Thus a factor given by:

$$G_{FACT} = \frac{1}{Fmax} \int_{0}^{Fmax} \left| \bar{H}(jw) - 1.0 \right| . dw \quad .... 2.8$$

gives a number by shich the gain response is characterised. Fmax is chosen as some maximum frequency of interest for which the display is to be used. Each operator's response can thus be characterised by a factor G_{FACT}. The greater G_{FACT}, the greater the overall deviation from the ideal response.

The amplitude of the overall response does not completely characterise the response. Phase shifts in the response can also be detrimental to the performance of a particular form of error signal presentation. The ideal phase characteristics are again zero phase shift over all frequencies of interest. Thus a phase 'goodness' parameter is proposed:

$$P_{FACT} = \frac{1}{Fmax} \int_{0}^{Fmax} \left| \theta_H(jw) \right| . dw \quad ..... 2.9$$

where $\theta_H(jw)$ is the phase shift, in radians, of the closed-loop response $\bar{H}(jw)$. Fmax is chosen as before.

Thus each operator's response to a particular form of error signal presentation is characterised by two 'goodness' parameters.

The display which minimises these two parameters can be judged to give the best response. However, for individual applications the weight placed on the amplitude factor as opposed to the phase factor is a matter of choice.

3) RESULTS AND DISCUSSION

In assessing the operator's performance, the coherency between the input and the operator's output presents a measure of the extent to which his output (at a given frequency) resulted as a direct response (albeit perhaps a wrong one) to the input. It is defined by:

$$C^2_{xy}(jw) = \frac{|\phi^2_{xy}(jw)|}{\phi xx(w) \cdot \phi yy(w)} \quad \ldots\ldots\ldots\ldots\ldots\ldots 3.1$$

at frequency w where $0 \leqslant C^2_{xy} \leqslant 1$.

When the coherency equals one, the output can be defined exactly as a linear function of the input. When the coherency is zero, the output is uncorrelated with the input (indicating a lack of response or possible nonlinearities).

Figures 4 and 5 show the mean coherency squared results measured for two operators. The mean coherency was taken over the frequency range zero to cut-off for each test, and the results for each type of error signal presentation and for each input cut-off frequency are displayed. Figure 4 was typical of results obtained for four of the five operators tested. The visual test showed a high level of coherency over the complete range of inputs used. The spread being typically $0.6 \leqslant C^2_{xy} \leqslant 0.95$.

The results for the mark-space test (A1) show a low level of coherency on all tests. As the input cut-off frequency increases, the

operator is less able to track correctly and the coherency falls. Indeed, it is doubtful whether the very high frequency tests (1.0 and 1.5 Hz cut-off) can be tracked at all using the mark-space ratio feedback.

The matching frequency test (A2) shows an all-round improvement on the mark-space test, while beat frequency feedback (A3) is probably the best display used over the frequency ranges of interest. It must be noted that although amplitude matching (A4) performed well for low frequency inputs (slightly better even than A3), the operators found greater difficulty in matching amplitudes quickly than in matching frequencies.

Figure 5 shows the exception to the rule. For this operator the amplitude matching tests results were consistently better than either frequency test. This is possibly explained by the hearing defect shown in the operator's audiogram (Figure 6). However, the case is made that an audio display must be tailored to suit the individual.

CLOSED-LOOP FREQUENCY RESPONSE

Figure 7 shows the closed-loop frequency response results as measured at each input cut-off frequency for each type of error signal presentation. The results are shown for a single operator.

At low input cut-off frequencies the closed-loop gain response is approximately flat and approaching unity, while the phase response shows the phase shift slowly increasing with frequency. The ideal response is defined as unity gain over all frequencies with zero phase shift. As the input cut-off frequency increases, the gain response decreases sharply with unity gain only occurring at very low frequencies.

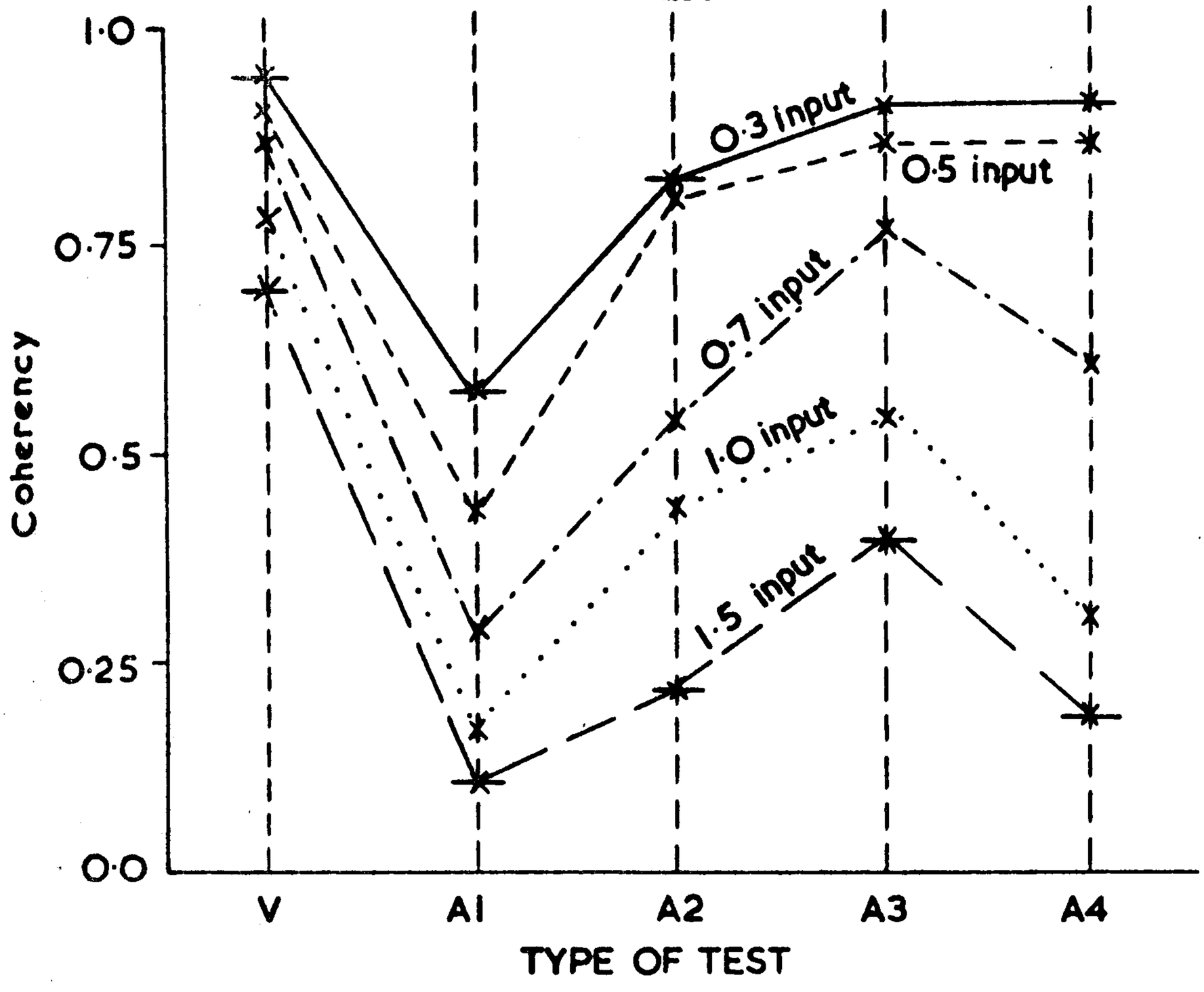

Figure 4: Shows the Mean Coherency level obtained for a single operator for each form of display and at each input cut-off frequency
(The mean level is taken over the frequency range O-cut off)

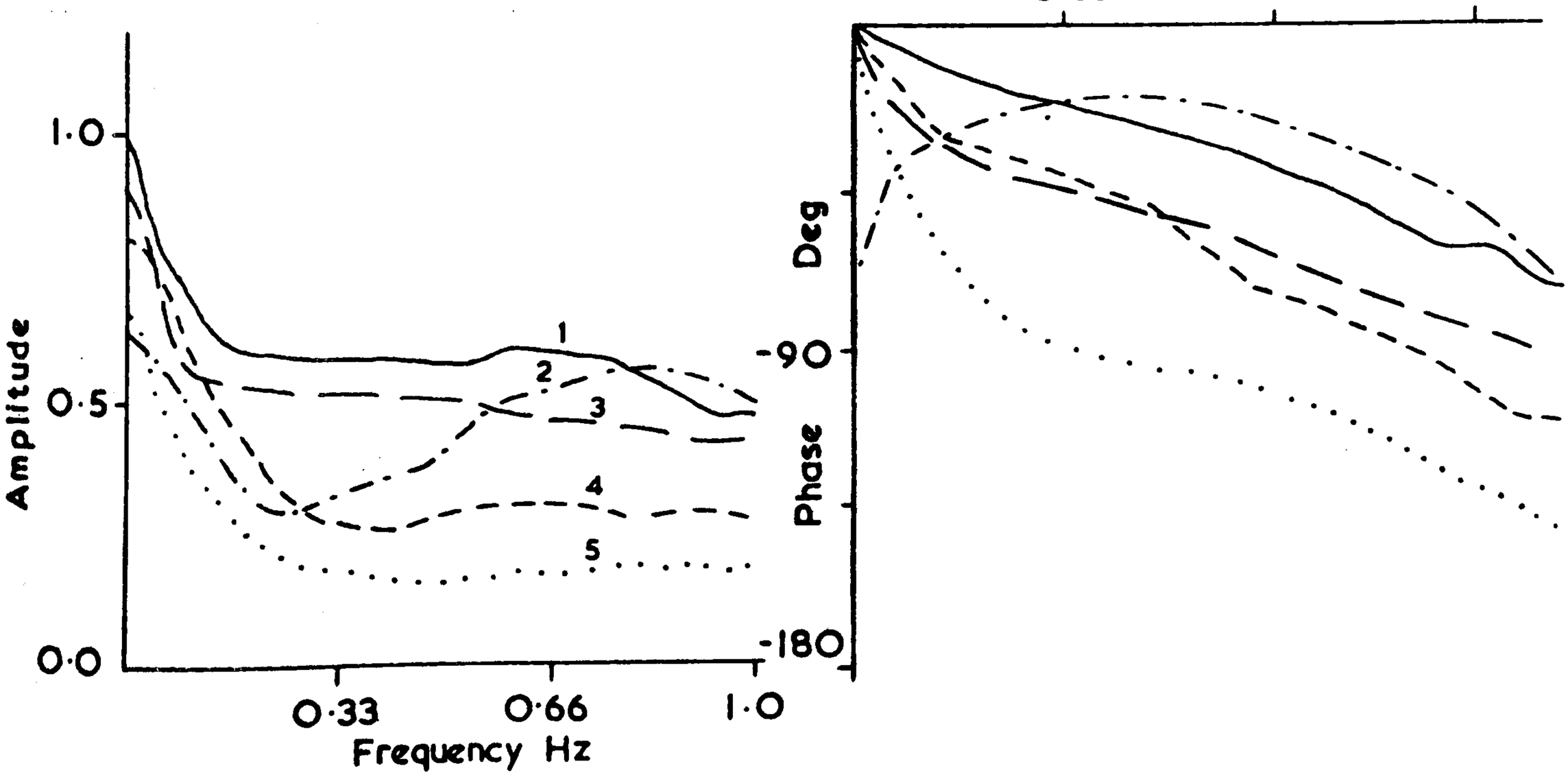

Figure 8: Shows the results obtained (for all 5 operators) for the Doppler matching audio feedback with an input cut-off frequency of 0·7 Hz.

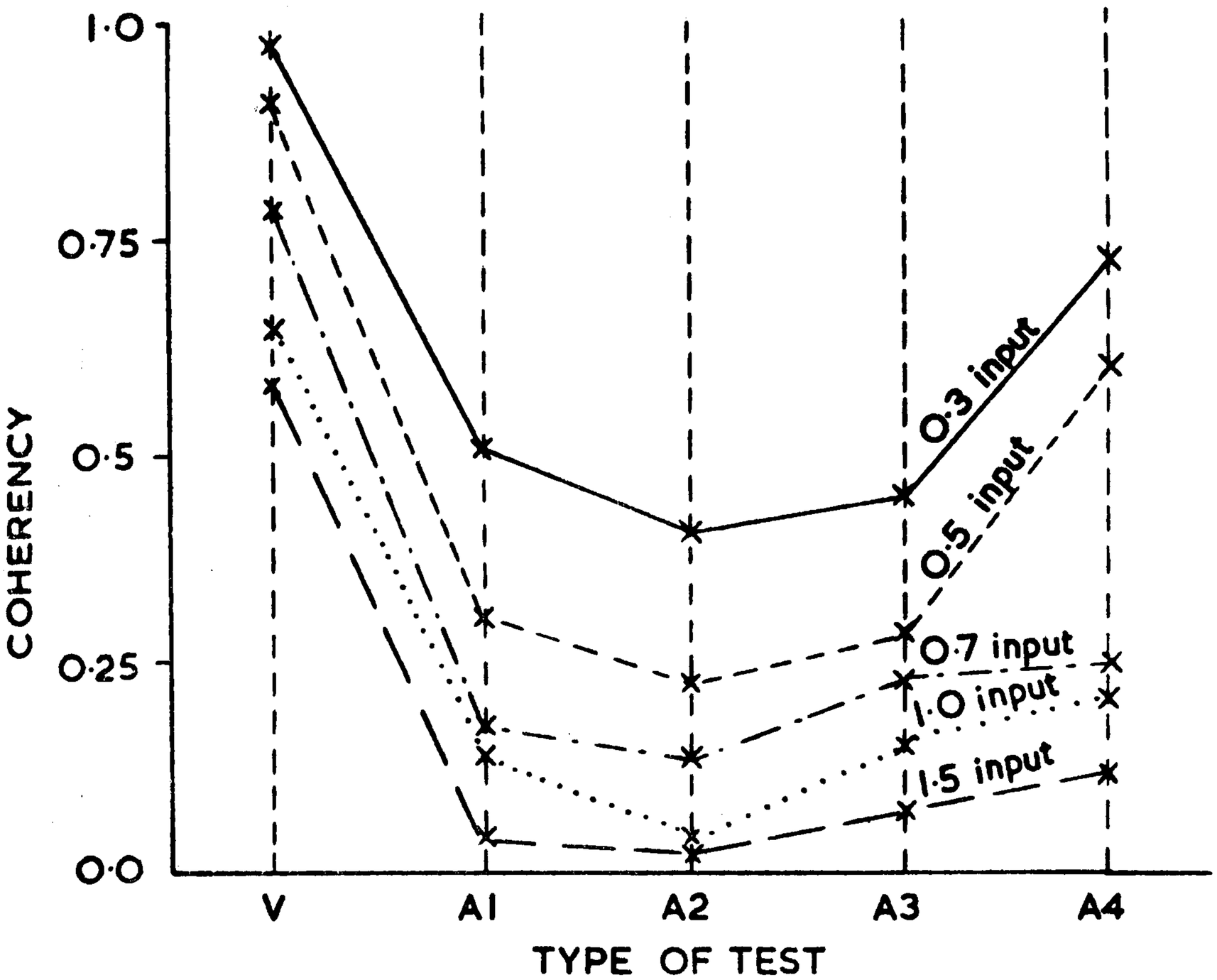

FIGURE 5. Shows the Mean Coherency level obtained for a single operator for each form of display and at each input cut-off frequency.

(The mean level is taken over the frequency range O-cut off)

Operator No. 2.

V - Visual
A1 - Mark Space matching
A2 - Matching Frequency
A3 - Doppler matching Frequency
A4 - Amplitude matching

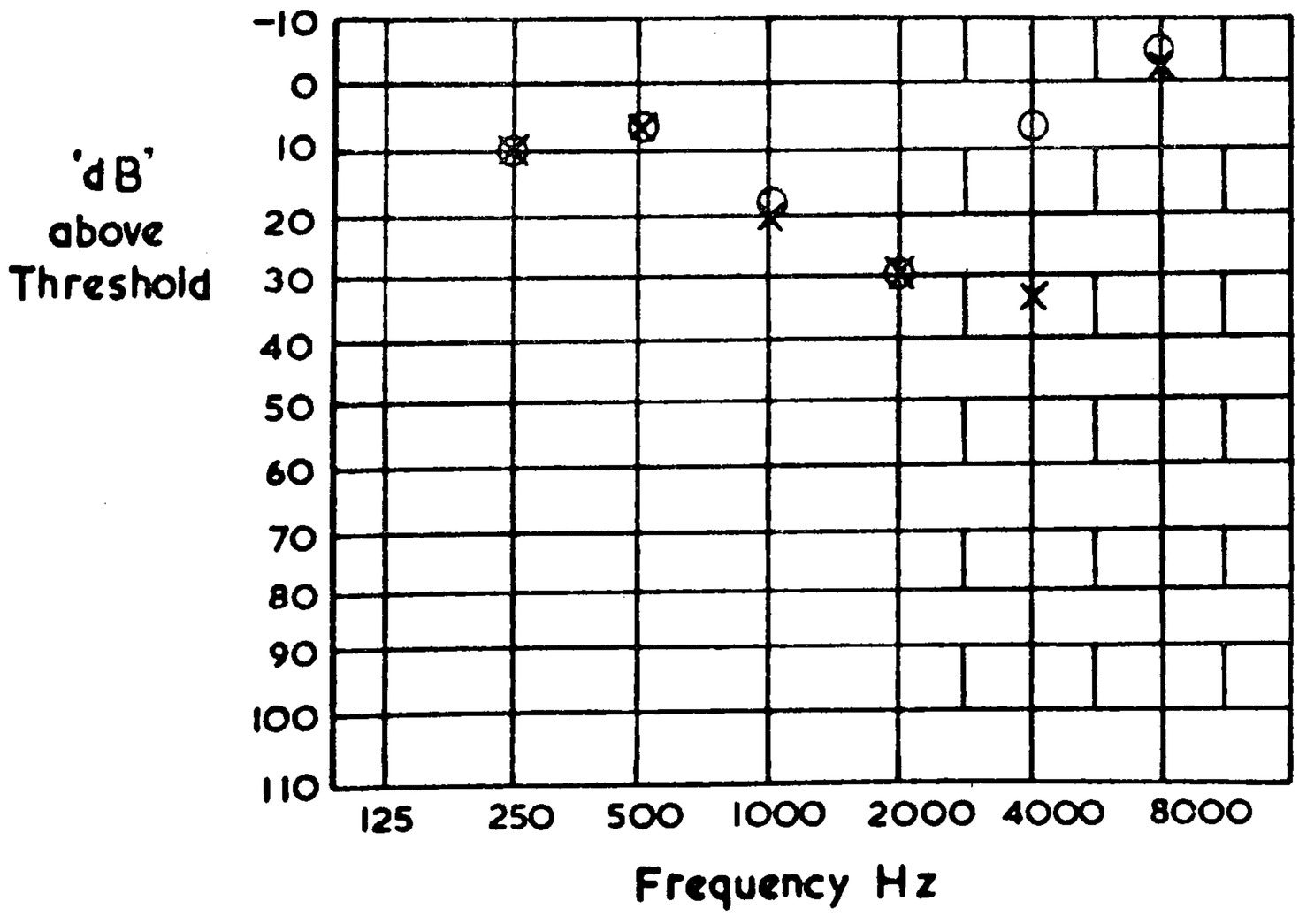

FIGURE 6. Shows the results of an audiometer tests on operator No. 2.

{ Left ear---X
Right ear---O }

a) 0·3 CUT-OFF

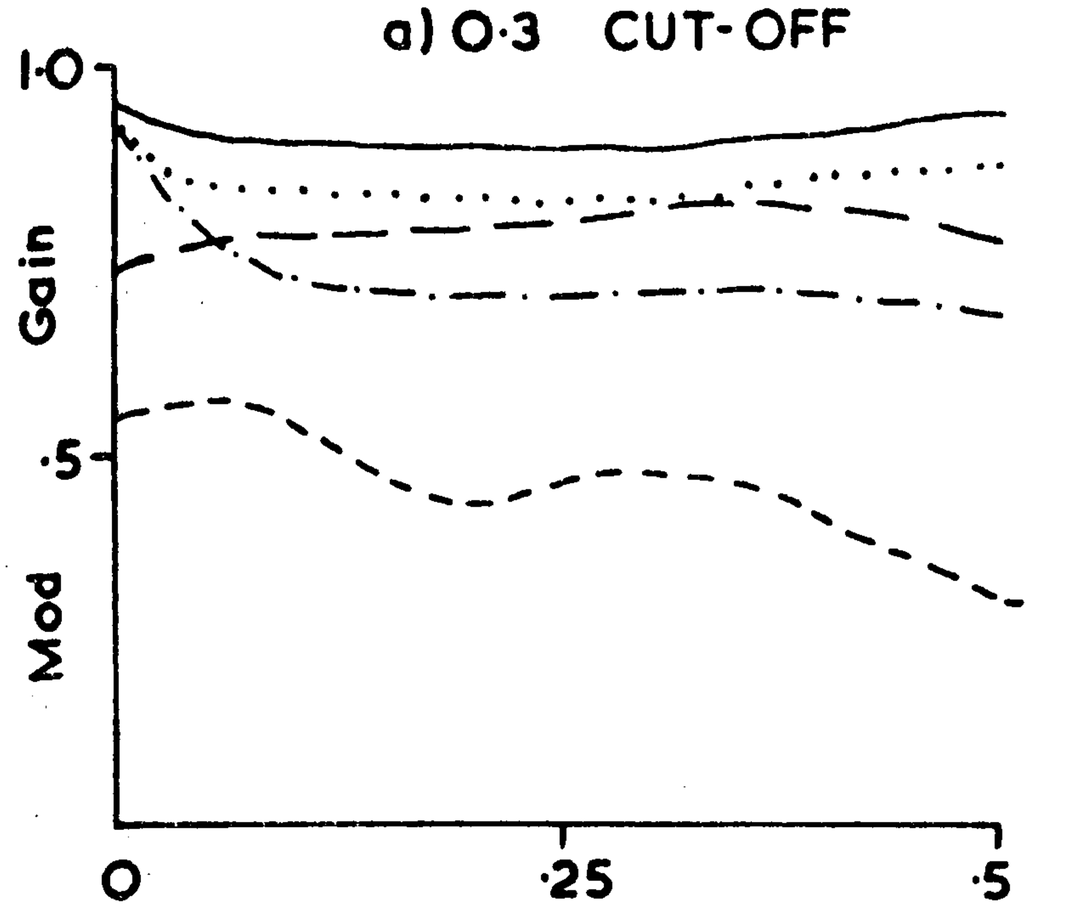

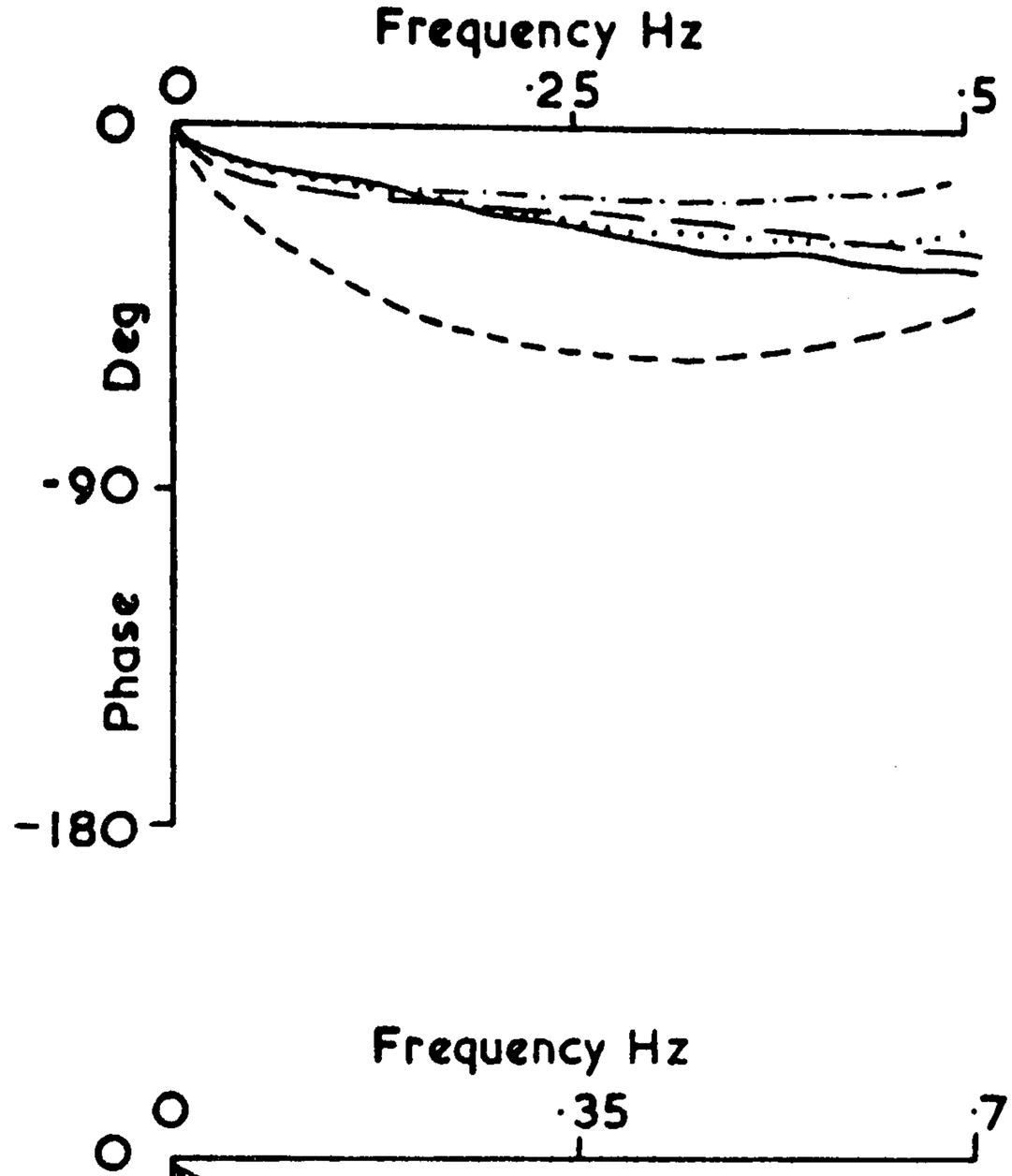

b) 0·5 CUT-OFF

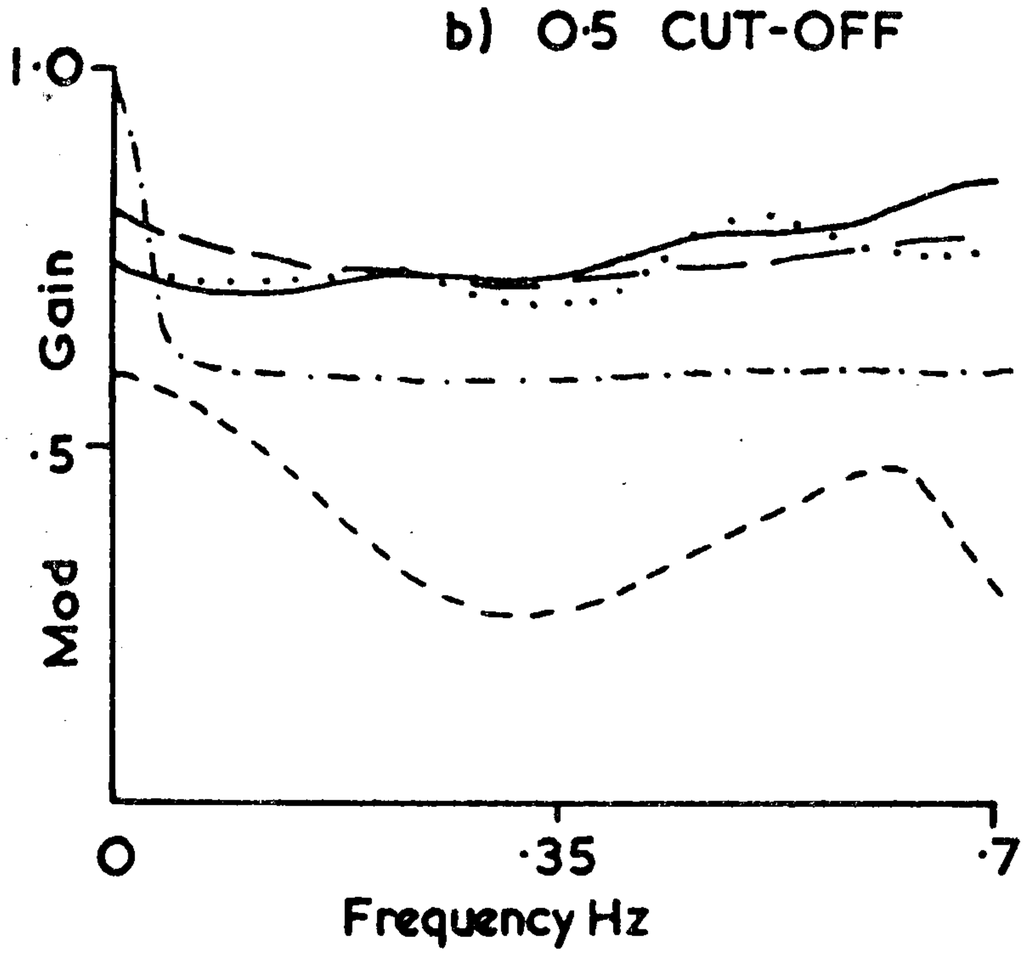

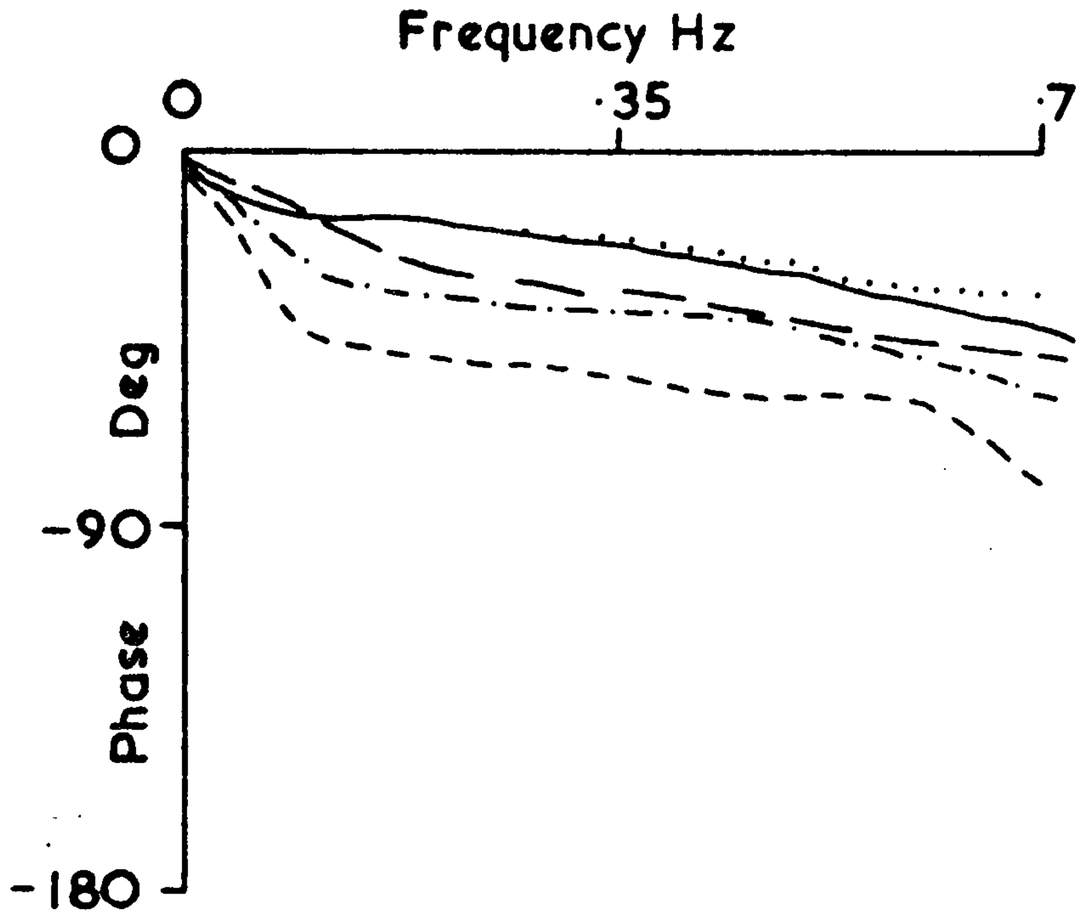

c) 0·7 CUT-OFF

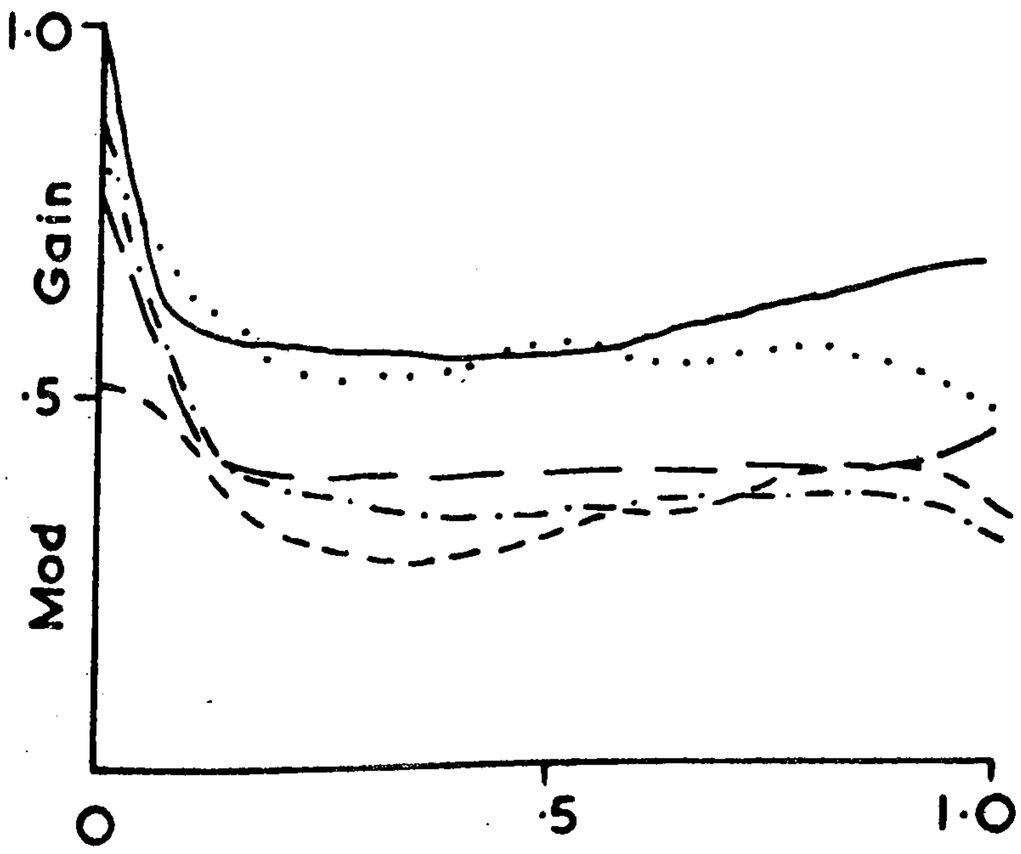

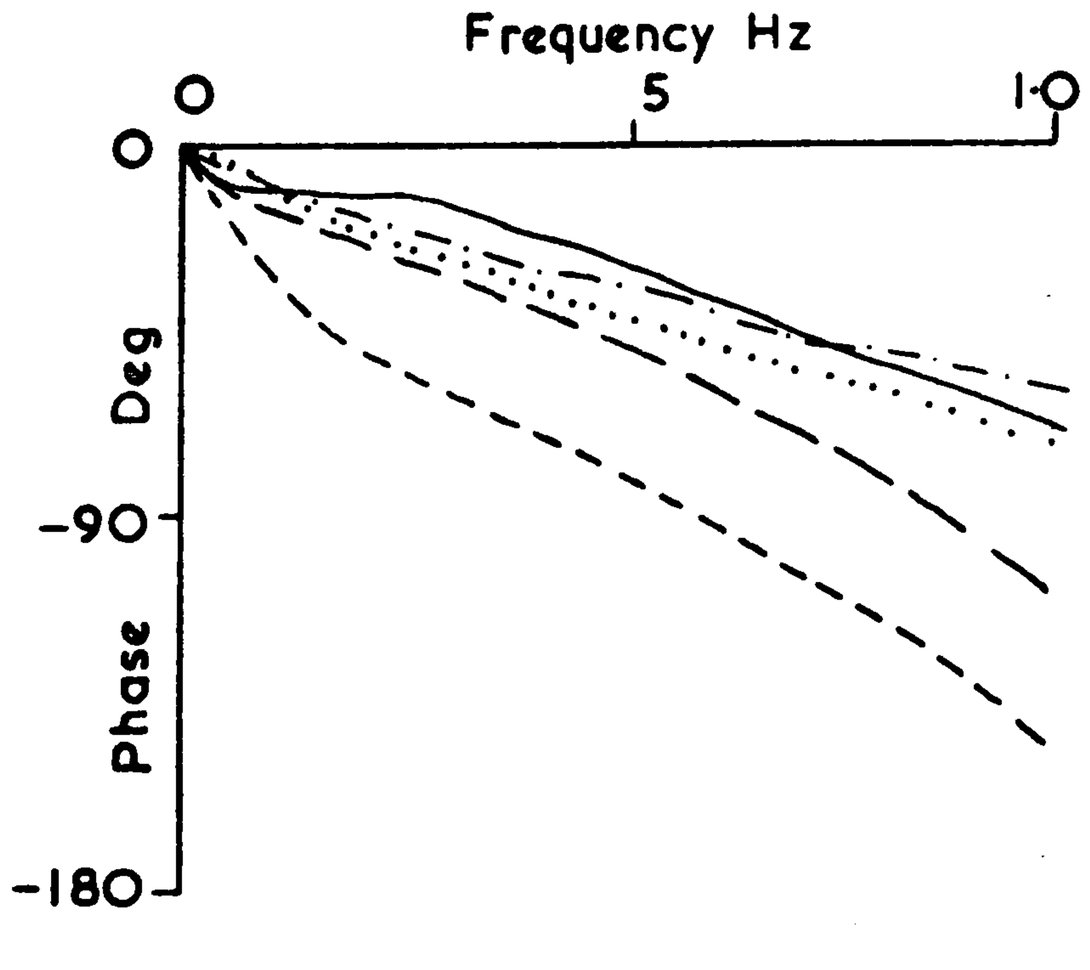

d) 1·0 CUT-OFF

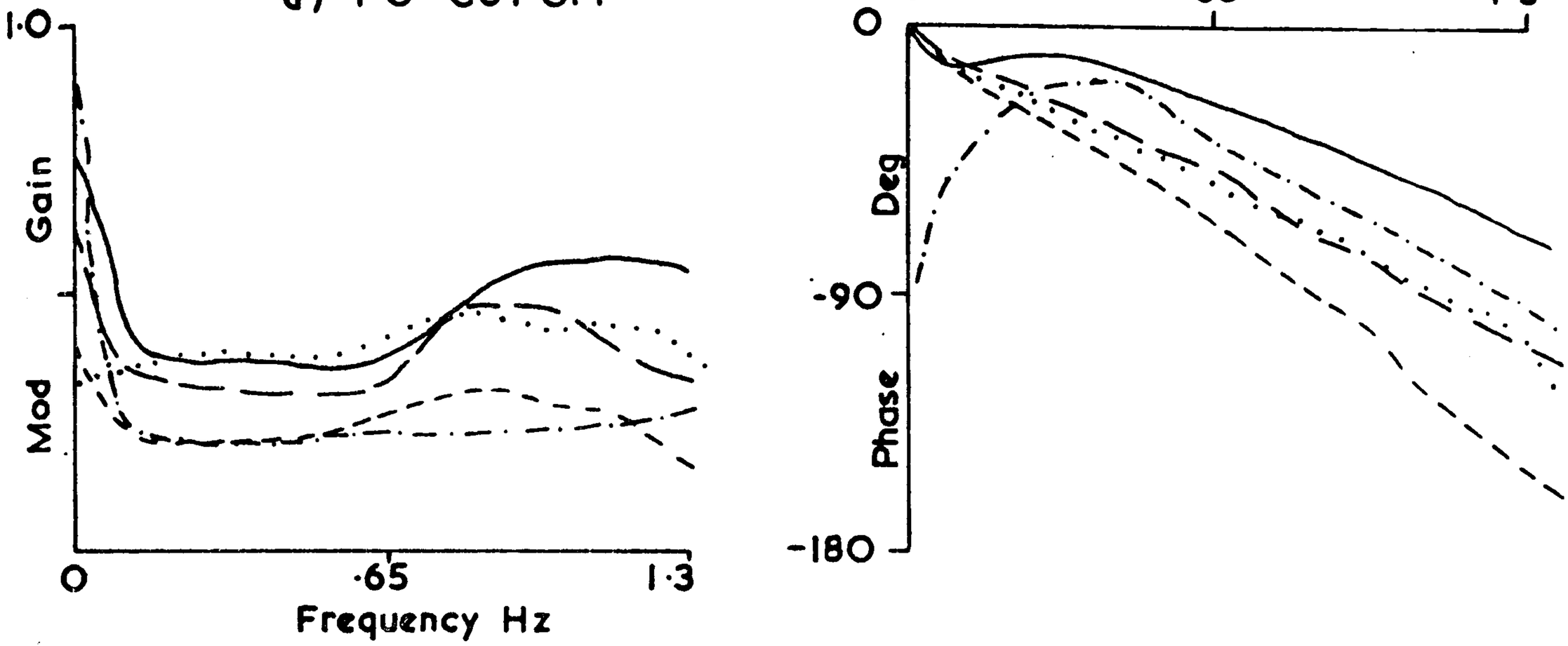

e) 1·5 CUT-OFF

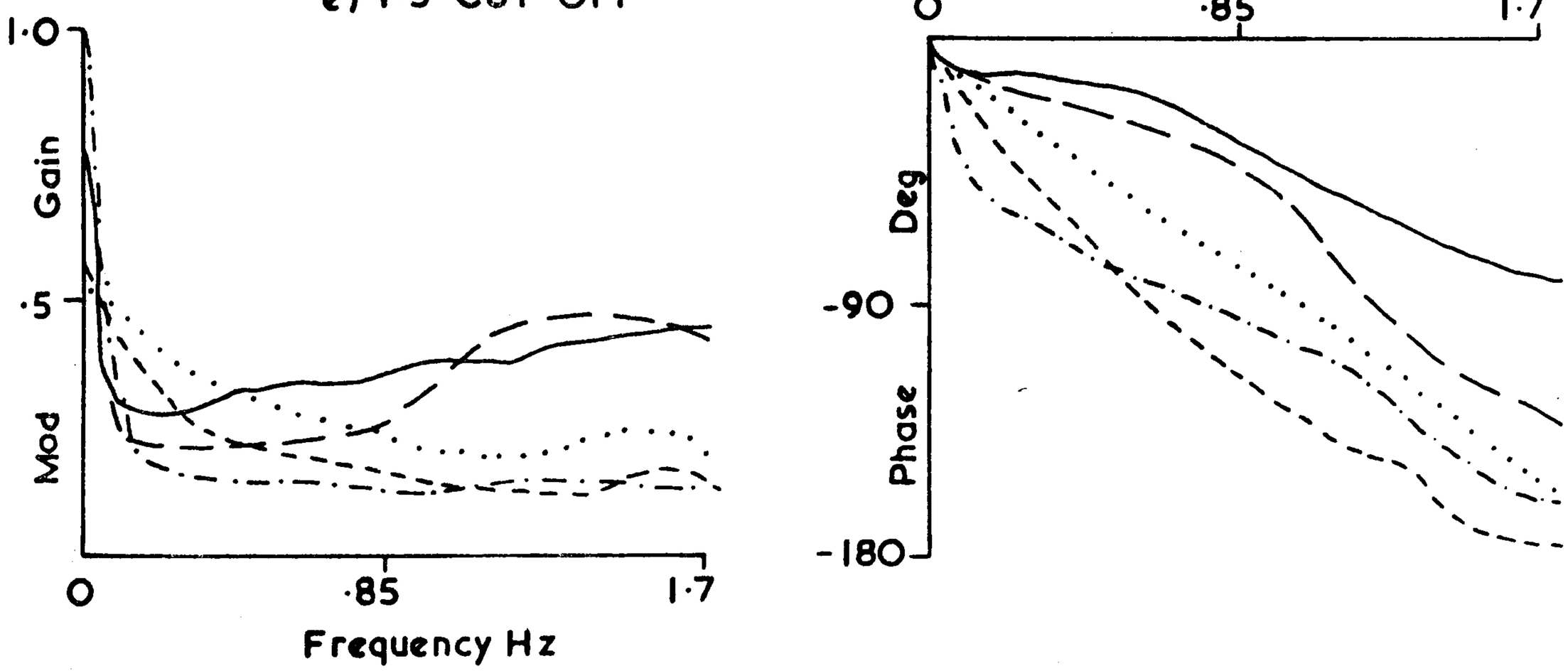

Figure 7: Shows the measured Closed Loop Frequency Response at each input cut off frequency for each of the visual and audio error signal presentations. The results are shown for a single operator.

Visual (V) ——————
Mark Space (A1) - - - - - - - -
Matching Frequency (A2) —·—·—·—·—··
Doppler Matching (A3) ·····
Amplitude Matching (4) —— —— ——

The rate of increase in phase shift is greater than expected by extrapolation of the low frequency results. Thus, in general, the operator changes his mode of operation as the input cut-off frequency increases. In some cases the inherent time delay in the operator's response leads to a resonant peak in the closed-loop response.

In measuring the operator's response, it must be recognised that his response will change as his concentration and skill vary. For this reason untrained operators were used to try to nullify any skill discrepancies in the results. Possibly a fairer test on which to base conclusions on the acceptability of any particular form of auditory display would be conducted with trained operators. However, the authors believe that initial reactions are as true a guide as any. There is no quantative way to allow for concentration lapses.

Figure 8 shows the range of results obtained for one particular test (beat audio error signal presentation with 0.7 Hz input cut-off frequency) for all five operators. The result for operator number 2 shows a resonant peak in the gain response at about 0.8 Hz while the phase shift at low frequencies tends to $-\pi/2$ (unlike the other operators). This type of response occurs when the operator is over-reacting to changes in the input signal and subsequently over-correcting. Again the variations in the responses measured would tend to advocate the case for tailoring the audio display to the individual.

HUMAN OPERATOR MODELLING

The model used (equation 2.7) has the advantage that the parameters can be given a physical interpretation. The Powell hill-climbing technique used to minimise a cost function between measured

and modelled response values found the global minimum in the cost function over the parameter N - vector space and within the boundary values chosen. The choice of boundary values for the parameters was based on previous values used and on experience, taking into account the physical limitations imposed by the human operator. The error function minimised was of the integral error squared form given by:

$$\text{COST} = \frac{\int_0^{Fmax} (H_{MEAS}(jw) - H_{MOD}(jw))^2 \, dw}{\int_0^{Fmax} (H_{MEAS}(jw))^2 \, dw} + \frac{\int_0^{Fmax} (G_{MEAS}(jw) - G_{MOD}(jw))^2 \, dw}{\int_0^{Fmax} (G_{MEAS}(jw))^2 \, dw} \quad \ldots\ldots 3.2$$

where $H_{MEAS}(jw)$: measured closed-loop response

$H_{MOD}(jw)$: model closed-loop response

$G_{MEAS}(jw)$: measured open-loop response

$G_{MOD}(jw)$: model open-loop response

and $H_{MOD}(jw) = \frac{G_{MOD}(jw)}{1 + G_{MOD}(jw)}$

This cost function and hill-climb process thus optimises the model parameters in terms of both open-loop and closed-loop measurements simultaneously. Figures 9 and 10 show typical results obtained from this modelling process for a visual test.

Table 1 lists the parameter values obtained from modelling the tests conducted on a single operator. A complete table for all five operators is not included for reasons of space. However, several points can be inferred from the result presented which are borne

out in the results obtained for the other operators.

The human operator gain (K) is a function of the sensitivity of the joystick and of the particular test environment chosen. However, as the input cut-off frequency increases, the gain decreases. This is borne out by Table 1 for all the various forms of error signal presentation. It is also noticeable that the mark-space presentation (A1) displays the lowest overall gain figures, which is compatable with predictions made from the coherency results. The beat frequency presentation (A4) comes closest to the figures presented for the visual presentation; this again might be expected from the coherency results.

The lead factor (T_D) is a measure of the velocity control exerted by the operator; the larger the value of T_D, the greater the velocity control exerted (i.e. the more sensitive the response to rate of change in the error function).

The operator appears to maintain an approximately constant level of velocity control until, at high frequencies, he no longer responds to velocity but degenerates into a form of 'bang-bang' control. Under this last mode of operation it is purely the sign of the error that decides the controlling action. For some audio tests, notably the mark-space test, this degeneration into a form of 'bang-bang' control occurs at input cut-off frequencies as low as 1 Hz and possibly even lower.

The operator's time delay (τ) decreases as the input cut-off frequency increases (Figure 11); this result is well known. However, a slight increase in time delay was found at the high frequencies for the audio tests. This might be explained by the fact that, at high

frequencies, signal interpretation becomes more complicated for the audio tests. This suggestion is only tentative, and further tests are required.

The lag constant (T_S) is perhaps the most difficult to explain in physical terms. Due to the operator's time delay response, the closed-loop response has a tendency to exhibit resonances at frequencies where the phase shift in the output leads to positive feedback. Thus the operator can find himself correcting high frequency components in the error signal which are not in fact present in the original input. All the operators tended to counteract this by ignoring, to a greater or lesser extent, high frequency changes in the error signal. The model, as given by equation 2.7, allows for this in the form of a low-pass element with a time constant T_S. The greater T_S, the lower the break frequency for the low-pass element. All the tests display low values of T_S for the 0.3 Hz cut-off with T_S increasing for the 0.5 and 0.7 Hz cut-off frequencies. Beyond 0.7 Hz it depends on the test as to the degree of damping used. There appears to be a mode of operation for some of the audio tests in which the closed-loop resonance effect goes unnoticed and hence uncontrolled. This may be a function of the information being lost in the audio feedback at high frequencies. This is certainly true of the amplitude matching and beat frequency presentations.

Lastly, the integrator factor (c) attempts to measure the ability of the operator to track low frequency trends in the mean level of the signal. Surprisingly, the mark-space tests show up quite well in this respect, at low frequencies being similar to the visual response. However, the variations in this constant are more a function of the

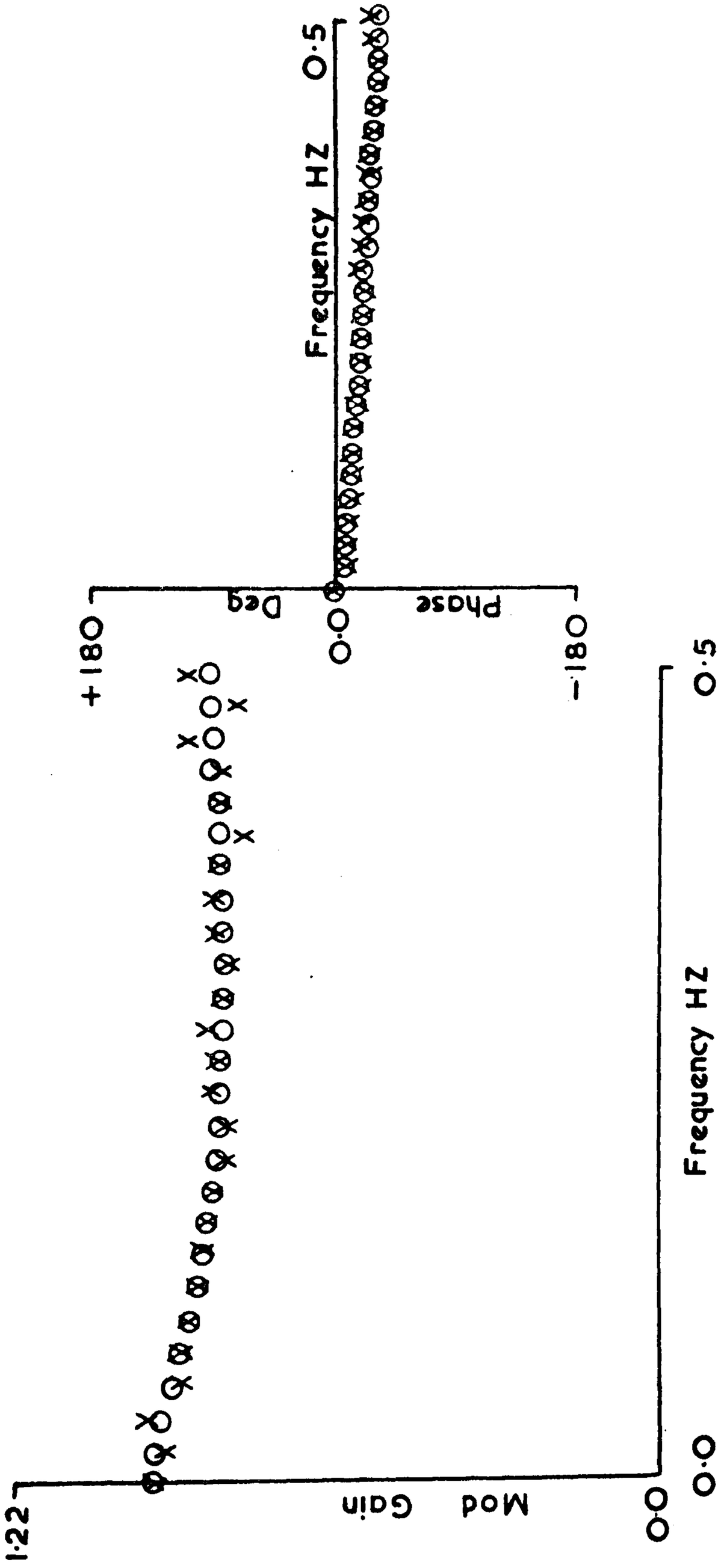

Figure 9b: Shows the Measured and Modelled Frequency Response:-
CLOSED LOOP
for human operator subjected to tracking a band limited white noise input with 0·3 HZ cut-off.
The error was presented visually.

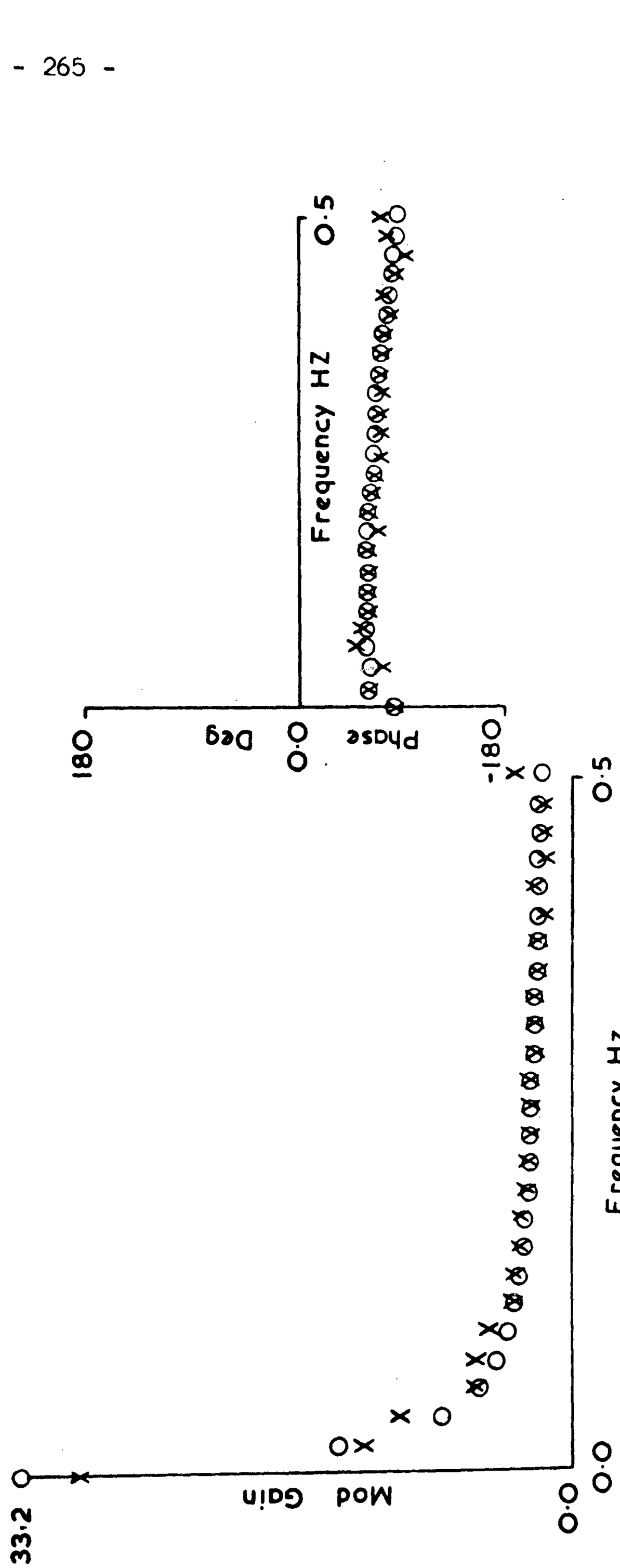

Figure 9a: Shows the Measured and Modelled Frequency Response :-
OPEN LOOP
for a human operator subjected to tracking a band limited
white noise input with 0.3 HZ cut-off.
The error was presented visually.

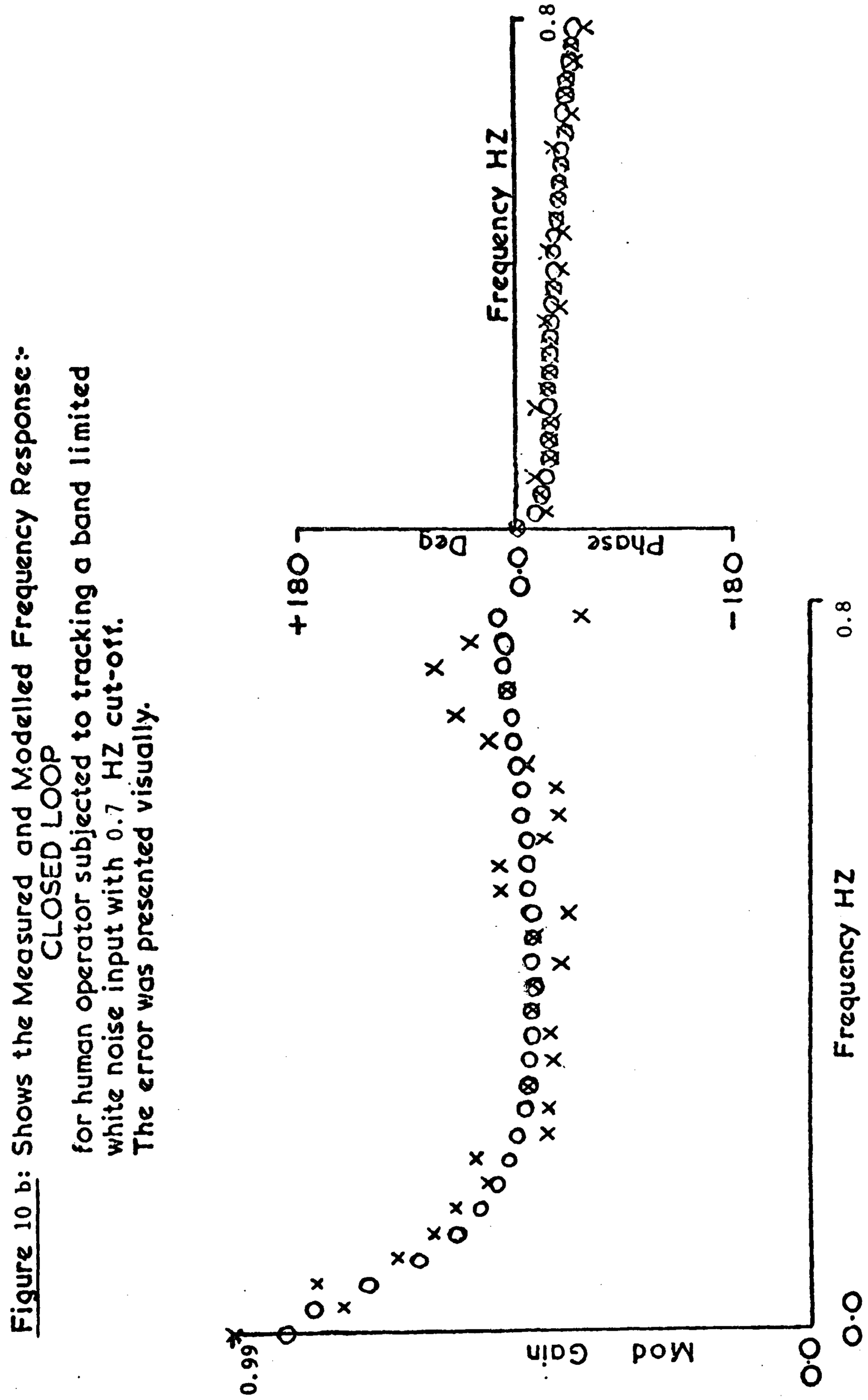

Figure 10 b: Shows the Measured and Modelled Frequency Response:-
CLOSED LOOP
for human operator subjected to tracking a band limited
white noise input with 0.7 HZ cut-off.
The error was presented visually.

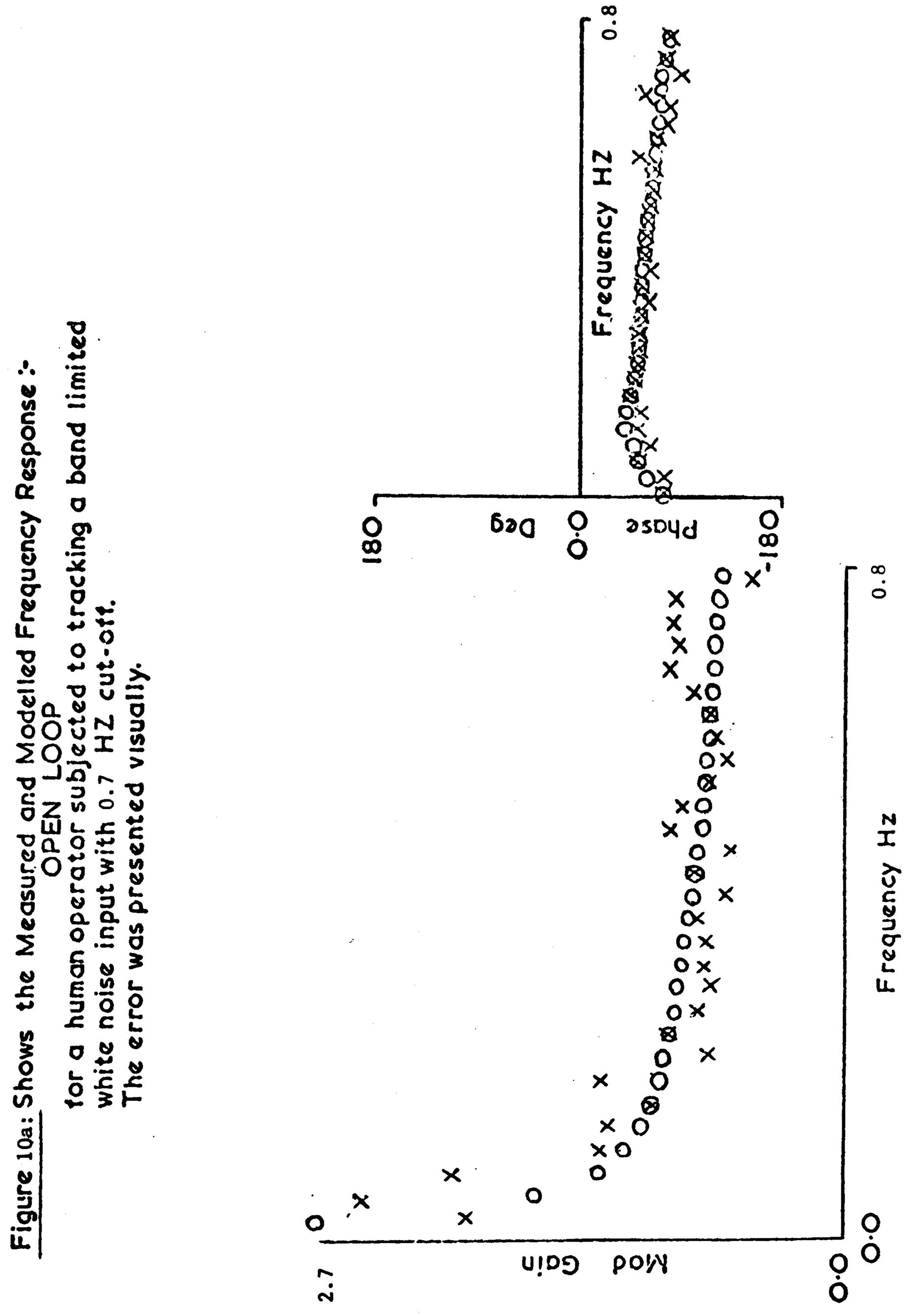
Modelled Frequency Response :-
LOOP
bjected to tracking a band limited
7 HZ cut-off.
visually.
Measured and
OPEN LO
for a human operator subj
white noise input with 0.7
The error was presented v
Figure 10a: Shows the
180
Deg
0.0
Phase
-180
Frequency HZ
0.8
2.7
Mod Gain
0.0
0.8
Frequency Hz
0.0

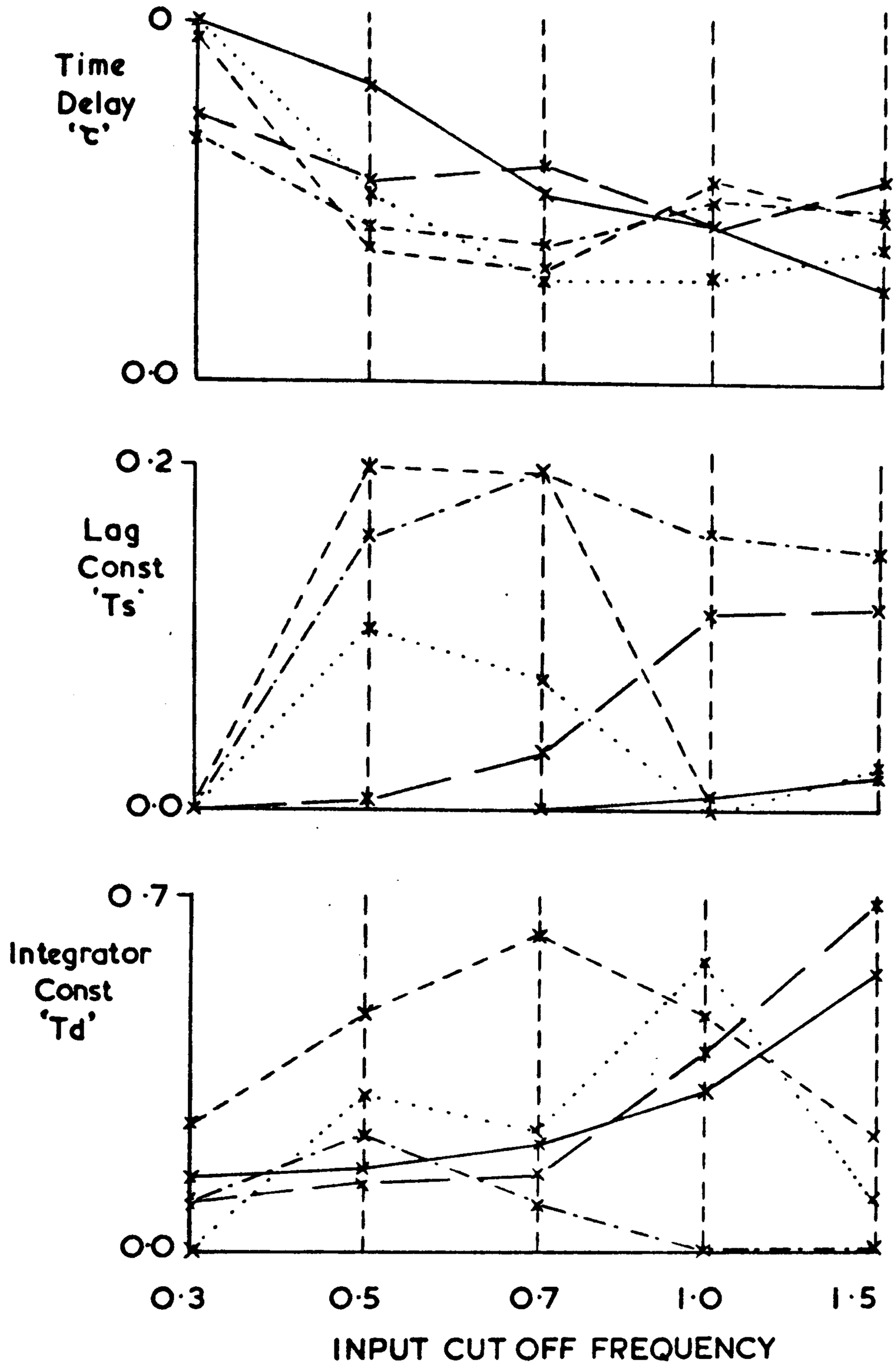

Figure 11: Shows the variation of 3 Model parameters with change in the input cut off Frequency for each form of Error signal presentation and for a single operator.

Visual ——————————

Mark Space —— —— ——

Matching Frequency —·—·—·—·—·—

Doppler . . . . . .

Amplitude Matching – – – – – – – – –

operator's long-term concentration and hence little can be said.

It must be emphasised that the discussion of changes in the model parameters is only applicable to these particular tests. Any firmer conclusions require a large number of subjects tested many times. However, the trends listed were consistently reproduced in tests conducted for a second time on a single operator and lend weight to the applicability of the model. The model cost function values listed in Table 1 give further reason for believing the model to be creditable.

DISPLAY PERFORMANCE ESTIMATES

Although a detailed study of the measured operator responses for various types of error presentation is instructive, it is too cumbersome a method for classifying particular forms of display. There are two ways of classifying an operator's response for a given input in terms of modulus gain response and phase response. Equation 2.8 defines a factor G_{FACT} which gives a measure of the mean square deviation from unity gain over the frequency range of interest, while equation 2.9 describes a similar factor P_{FACT} assessing the deviation of the phase response from a desired zero phase shift. These factors are listed in Table 1 for each test. The weight placed on G_{FACT} as opposed to P_{FACT} depends on the type of task to be performed.

The ideal values are:

$$G_{FACT} = 0.0$$

$$P_{FACT} = 0.0$$

It can be seen that the visual display comes top on both counts (see Table 1). The beat frequency test just has the edge on the amplitude matching test, followed by the frequency matching test.

TABLE 1 Shows Operator Model Parameter Values Plus Error Performance Figures for Single Operator

TEST

Type of display	Input Cut-off frequency Hz	K	τ	C	T_D	T_S	COST	G_{FACT}	P_{FACT}
Visual	0.3	2.1	0.40	0.15	2.59	0.0	0.021	.08	10.6
Visual	0.5	0.94	0.33	0.17	2.26	0.0	0.02	.20	18.0
Visual	0.7	0.78	0.21	0.22	1.96	0.0	0.02	.30	24.0
Visual	1.0	0.43	0.18	0.33	1.77	0.0	0.013	.46	33.7
Visual	1.5	0.40	0.10	0.57	1.45	0.02	0.025	.57	42.0
Mark space	0.3	0.41	0.3	0.10	1.30	.004	0.02	.54	38.0
Mark space	0.5	0.27	0.24	0.16	1.41	.08	0.017	.69	45.4
Mark space	0.7	0.27	0.23	0.16	.87	.06	0.04	.72	72.2
Mark space	1.0	0.26	0.23	0.4	.72	0.10	0.023	.77	92.2
Mark space	1.5	0.33	0.18	0.70	0.35	0.09	0.07	.86	108.7
Matching Freq	0.3	1.02	0.27	0.11	1.17	.001	0.013	.32	23.1
Matching Freq	0.5	0.79	0.17	0.25	1.24	.11	0.015	.40	25.5
Matching Freq	0.7	0.36	0.16	0.20	1.31	.07	0.009	.61	46.5
Matching Freq	1.0	0.19	0.20	0.0	1.33	0.0	0.024	.75	63.6
Matching Freq	1.5	0.21	0.19	0.08	0.67	.004	0.035	.83	87.8
Beat	0.3	1.52	0.40	0.0	1.46	.003	0.024	.14	18.1
Beat	0.5	1.42	0.21	0.32	1.01	0.16	0.016	.22	28.7
Beat	0.7	0.97	0.12	0.25	1.02	0.20	0.02	.37	48.4
Beat	1.0	0.53	0.12	0.60	1.09	0.16	0.017	.58	59.8
Beat	1.5	0.28	0.15	0.13	1.05	0.154	0.02	.75	100.6
Amplitude	0.3	1.22	0.39	0.26	1.16	.002	0.022	.25	23
Amplitude	0.5	1.25	0.15	0.49	0.99	0.2	0.009	.33	29
Amplitude	0.7	0.59	0.13	0.64	1.15	0.189	0.02	.55	48.5
Amplitude	1.0	0.28	0.23	0.48	1.2	0.0	0.06	.67	60
Amplitude	1.5	0.10	0.18	0.25	1.9	0.05	0.04	.81	80.2

The mark-space test comes out bottom. This ordering agrees substantially with the other results presented, and confirms that G_{FACT} and P_{FACT} would appear to give a reliable performance index.

4) CONCLUSIONS

The experiments show that the human operator's performance depends on the frequency content of the input. It would appear that for visual tracking tasks the operator can adapt his response to suit the input. However, it was found that his adaptability and hence his performance was impaired by audio presentation of the signal. Contrary to comments made by Vinje and Pitkin (1971), the human operator's response to the audio cues presented in these experiments was consistently inferior to visual. However, the audio presentations used here are different from those used by the above authors.

The linear model used to describe the operator's response fitted the measured response well for low frequency input tests. However, when the input signal contained high frequency components, the operator's response might be better described by the incorporation of a non-linear 'bang-bang' element in the model. For this reason the physical interpretation of the model parameters is still open to argument. The description presented here is, however, subjectively consistent with the experience of the subjects tested.

The presentation of a gain and phase cost function to measure the 'goodness' of the operator's response has the advantage of retaining information about phase response in its crudest form while retaining overall information on the modulus of the response. A simple presentation of error variance to input variance gives no

useful information about the nature of the response.

Finally, this paper serves as an introduction to a more thorough analysis of two- and three-dimensional audio displays as an alternative or in conjunction with visual displays. Extension to two-dimensional displays introduces cross-coupling effects, which, although not too serious for visual tracking tasks, could prove detrimental to performance for certain combinations of audio displays.

REFERENCES: APPENDIX A

BLACK, W. L.: 'An acoustic pattern presentation'. Research Bulletin, No. 16, pp. 93-132 (May, 1968)

BLACKMAN, R. B. & TUKEY, J. W.: 'The measurement of power spectra'. Dover Publication (1958)

FISH, R. M. & BESCHLE, R. G.: 'An auditory display capable of presenting two-dimensional shapes to the blind'. Research Bulletin, No. 26, pp. 5-18, (June, 1973)

FLETCHER, R. & POWELL, M. J. D.: 'A rapidly convergent descent method for minimisation'. British Computer Jnl. Vol. 6, pp. 163-8 (1963)

GILL, J. M.: 'Auditory and tactual displays for sensory aids for the visually impaired'. Research Bulletin, No. 29, to be published

KRAMER, H. J.: 'Stimulus variables in auditory projective testing'. Research Bulletin, No. 1 pp. 33-40 (Jan. 1962)

KRENDEL, E. S. MCRUER, D. T. & GRAHAM, D.: 'The analysis and synthesis of manual closed-loop control systems'. I.E.E.E.Int. Convention Rec. pp. 193-5 (1966)

MUDD, S. A.: 'Experimental evaluation of binary pure-tone auditory displays'. Jnl. of Applied Psychology, Vol. 49, No. 2, pp. 112-121 (1965)

PHILLIPS, J. A. & SELIGMAN, P. M.: 'Two instruments for the blind engineer'. Research Bulletin, No. 27, pp. 187-216 (April, 1974)

POLLACK, I. & FICKS, L.: 'Information of elementary multi-dimensional auditory displays'. Jnl. Acoustical Soc. Am. Vol. 26, No.2, pp. 155-8 (March, 1954)

ROFFLER, S. K. & BUTLER, R. A.: 'Factors that influence the localization of sound in the vertical plane'. Jnl. Acoustical Soc. Am., Vol. 43, No. 6, pp. 1255-9 (1968)

ROFFLER, S. K. & BUTLER, R. A.: 'Localization of tonal stimuli in the vertical plane'. Jnl. Acoustical Soc. Am., Vol. 43, No. 6, pp. 1260-6 (1968)

VINJE, E. W. & PITKIN, E. T.: 'Human operator dynamics for aural compensatory tracking'. 7th Annual Conference on Manual Control, NASA SP-281, pp. 339-48 (June, 1971)

WELLSTEAD, P.E.: 'Aspects of real time spectral analysis'. Phd. Thesis, Univ. of Warwick (1971)

YOUNG, L. P.: 'On adaptive manual control'. I.E.E.E. MMS-10, pp. 292-331, (Dec, 1969)

REFERENCES : CHAPTER 6

1 KRENDEL, E. S. & MCRUER, D. T.: 'Dynamic response of human operators'. W.A.D.C. Tech. Report 57-509 (1958)

2 BEKEY, G. A.: 'The human operator as a sampled data system'. I.E.E.E. HFE-3 pp. 43-9 (1962)

3 'Final Report, human dynamics study'. Goodyear Aircraft Co. Akion Ohio Report GER-4750 (1962)

4 ELLKIND, J. I. & DARLEY, D. L.: 'The normality of signals and describing function measurements of simple manual control systems'. I.E.E.E. HFE-4 pp. 52-60 (1963)

5 SEELEY, H. F. & BLISS, J. C.: 'Compensatory tracking with visual and tictile displays'. I.E.E.E. HFE-7 pp. 84-90 (1966)

6 HILL, J. W.: 'Describing function analysis of tracking performance using two tactile displays'. I.E.E.E. MMS-11 pp. 92-100 (1970)

7 STAPLEFORD, R. L., MCRUER, D. T. & MAGDALENO, R. E.: 'Pilot describing function measurements in a multi-loop task'. I.E.E.E. HFE-8 pp. 113-128 (1967)

8 VINJE, E. W., PITKIN, E. T.: 'Human operator dynamics for aural compensatory tracking'. 7th Annual Conference on Manual Control NASA SP-281 pp. 339-48 (June, 1971)

9 SHERIDAN, T. B.: 'Human operators' time-varying transfer characteristics in the study of perception and fatigue'. Proc. Symposium on Recent Developments in Automatic Control pp. 161-165 (1966)

10 SHERIDAN, T. B.: 'Time-variable dynamics of human operator systems'. Air force Cambridge Research Centre, Bedford, Mass., report No. AFCRC TN-60-196 (1960)

11 'Some conclusions from a special issue on revision of opinions by men and machine systems'. I.E.E.E. HFE-7 pp. 125-30 (1966)

12 WIERENGA, R. D.: 'An evaluation of a pilot model based on Kalman filtering and optimal control'. I.E.E.E. MMS-10 pp. 108-23 (1969)

13 ELKIND, J. I. & SPRAGUE, L. T.: 'Transmission of information in simple manual control systems'. I.E.E.E. HFE-2 pp. 58-62 (1961)

14 BEKEY, G. A. & MEISSINGER, H. F.: 'Mathematical models of human operators in simple two-axis manual control systems'. I.E.E.E. HFE-6 pp. 42-53 (1965)

15 BEKEY, G. A. & NEAL, C. B.: 'Identification of sampling intervals in sampled data models of the human operator'. I.E.E.E. MMS-9 pp. 138-42 (1968)

16 BLISS, J. C.: 'A provisional bibliography on tactile displays'. I.E.E.E. MMS-11 p. 101 (1970)

17 SKOLNICK, A.: 'Stability and performance of manual control systems'. I.E.E.E. HFE-7 pp. 115-124 (1966)

18 COSTELLO, R. G. & HIGGINS, T. J.: 'An inclusive classified bibliography pertaining to modelling the human operator as an element in an automatic control system'. I.E.E.E. HFE-7 pp. 174-81 (1966)

19 DUEY, J.W. & CHERNIKOFF, R.: 'The use of quickening in one co-ordinate of a two-dimensional tracking system'. I.E.E.E. HFE-1 pp. 21-25 (1960)

20 ROIG, R. W.: 'A comparison between human operator and optimum linear controller R.M.S. error performance'. I.E.E.E. HFE-3 pp. 18-22 (1962)

21 SEELEY, H. F. & BLISS, J. C.: 'Compensatory tracking with visual and tactile displays'. I.E.E.E. HFE-7 pp. 84-90 (1966)

CHAPTER 7

CONCLUSIONS AND SOME SUGGESTIONS FOR FUTURE RESEARCH

The statistical aspects of short-term spectral estimation as developed in Chapters 2 and 3 are shown to have wide application in the analysis of open-loop and closed-loop time-varying systems.

The use of confidence interval and stationarity tests in determining the accuracy of projected mathematical models, and in monitoring the time-varying aspects of the system response, has led to some new developments in the fields of speech analysis, fatigue testing and display comparison in human operator tracking tasks.

In Chapter 2 the effect of noise in open-loop spectral estimation is examined in detail. The distribution of cross-spectral estimates is shown to differ markedly from the classical Chi-square approximation under noisy conditions. In particular, the finite probability of obtaining negative estimates is clearly demonstrated using the derived distribution.

From the distribution of frequency response estimates, a stationarity test which is essentially sensitive to variations in the system and not to variations in the input is suggested. This test is widely used in Chapters 4 and 5.

By considering the open-loop frequency response distribution, it is shown that the variance is a function of the signal-to-noise ratio of the system and not the system response. On this basis, the statistics of an estimate of the signal-to-noise ratio are derived. It is shown that the traditional coherency estimate does not give direct information on

the likely variance in the frequency response estimate.

A heuristic extension of stationary spectral analysis to include slowly-varying linear systems indicates that the statistical distributions derived for stationary systems can be modified to include slowly-varying oscillatory processes, if the bandwidth of oscillation is considerably less than the fundamental frequency resolution $2\pi/T$ (where T = block estimation period). Under these conditions, the variance terms for the distributions may be approximately replaced by their time-varying equivalents.

Lastly, a preliminary investigation of the joint distributions of overlapped estimates is undertaken. The distribution associated with auto-spectral estimates is derived. Future work should extend this to a complete investigation of overlapped cross-spectrum and frequency response estimates.

The analysis of speech (Chapter 4) and fatigue (Chapter 5) are chosen as two examples of time-varying situations where the nature of the time variation is markedly different.

In Chapter 3 the statistics of closed-loop spectral estimates are examined. Of major importance is the extension to tri-variate Gaussian systems. Little research has previously been conducted on the distributions associated with tri-variate complex systems.

The distribution of closed-loop cross-spectral estimates and estimates of the overall closed-loop frequency response are derived from complex transformations of the open-loop case. The derivation of the closed-loop overall frequency response distribution leads to a two-part stationarity test for closed-loop systems. This test can only

determine the joint stationarity of the forward and feedback path responses. In many cases this may be sufficient, but the development of stationarity tests which are sensitive to variations in individual closed-loop parameters would be preferable. A fundamental limitation to the development of such a series of stationarity tests is that the variance of estimates of the forward- and feedback-loop response is a function of the system being measured. This was not the case in the open-loop system.

In the open-loop case it is possible to use signal-to-noise ratio estimates to calculate the variance of frequency response estimates. In the closed-loop situation it is useful to estimate the forward and feedback path noise spectra. It is shown that the distributions associated with such estimates are approximately Chi-square with 2L - 2 degrees of freedom when the signal-to-noise ratios are large, but that this approximation is seriously misleading under noisy conditions. A preliminary investigation suggests that as the signal-to-noise ratio decreases, the number of degrees of freedom associated with the distribution also decreases. This conclusion is based on simulation results and needs theoretical confirmation.

The distributions are applicable to stationary systems : to fully justify their use in time-varying situations it must be shown that the relationships between input/output and feedback short-term Fourier estimates are similar to those encountered in stationary systems, with added bias and variance terms that may be effectively suppressed by a suitable choice of the estimation period T. Tong (1972) provided some plausible arguments justifying this assumption for the case of slowly-varying oscillatory systems. However, an extension of the arguments

used in Chapter 2 is required.

Chapter 6 makes use of the results of Chapter 3 both to validate the proposed linear model of the operator's response and to test for response stationarity.

In Chapter 4 the use of a throat microphone to define a system input enables a reasonably simple phonemic recognition system to be implemented. The vowel phonemes can be consistently identified and preliminary results for some consonants indicate that the system can be extended. Improvements in compressed speech intelligibility using so-called 'phonemic compression' (essentially just compressing the stationary speech segments and deleting the non-stationary sections) would indicate that not only vowels but also consonant phonemics are retained.

It is to be noted that random errors due to short-term estimation make the reading of a speech spectragraph extremely difficult and in many cases impossible, even when the information is in fact present. Thus interpretation using statistical methods is essential. The stationarity test developed in Chapter 2 is shown to be sufficiently robust to detect changes in the vocal tract frequency response even in a very noisy environment.

In the long-term development of a connected speech recognition system, a more serious problem is the absence of complete phonemic information in the speech wave. On first listening to the compressed speech tape, the listener has great difficulty in picking out more than three or four words at 400 w.p.m. If the listener is familiar with the sentence before listening to the tape, he experiences little or no trouble in understanding it. This indicates the strong influence of

predictor-corrector methods used by the brain in deciphering spoken speech. If one is pre-conditioned to expect a limited range of utterances, then the brain reacts to cues rather than rely on exact interpretation. The requirement of intelligent interpretation is almost impossible for a computer. Thus, in the view of the author, for the purposes of man-machine communication, it is more profitable to rely on a restricted set of code instructions.

Alternative applications of stationarity testing to transmission bit rate reductions in communications are more promising.

A contrasting time-varying situation is presented in the identification of fatigue cracking in aluminium and steel rods (Chapter 5). Here we are looking for slow trends in the response. If the input driver signal is sinousoidal, it is well known that there are small changes in the amplitude and phase of the response as cracking sets in. This effect cannot be detected visually under random load conditions. In Chapter 5 it is shown that changes do occur and can be detected using statistical testing techniques on the measured frequency response. These changes may be due to:

a) Deforming the specimen beyond the plastic limit

b) Fatigue cracking

c) Drift in the testing equipment

d) A slow change in the input load spectrum.

By designing an input load compensation system to ensure the achieved load matches the original desired load both in terms of spectral and amplitude distribution characteristics, the effects of (a) and (d) above can be practically eliminated. Possible load saturation of the

fatigue rig driver due to changes in the specimen's response as cracking occurs can also be avoided. By monitoring the response of amplifiers and transducers in the circuit, errors due to drift can be allowed for. In many cases drift occurs in the D.C. and very low frequency range, and ignoring changes in these frequency components eliminates this as a major source of error . That the changes detected are not a function of the load signal characteristics is indicated by the consistent changes monitored under varied load conditions. In designing a load compensation system, the choice of analysis parameters to guarantee consistent results is based on the statistical considerations of Chapter 2.

Although much research on the dynamics of the human operator response in tracking task situations has been carried out , there has been little or no serious attempt to utilise the results in fields other than the aerospace industry. A major field of application is in the design of audio, tactile and visual aids for the handicapped. Currently such aids as sonic torches for the visually handicapped, audio C.R.T. displays, and many household gadgets have been manufactured without serious regard to the maximum effectiveness of these aids.

In Chapter 6 an attempt is made to outline a method of display comparison, both in terms of overall response characteristics and in terms of variations in the model parameters. A major facet of any display is the ability of the operator to respond to changes in the dynamics of the input signal to be tracked. In tracking transients in the model parameters for step changes in the input dynamics, care must be taken to ensure that the model is representative of the measured response, and that the transients are a function of the changes in the response mode of the

operator and not due to short-term sampling errors. The sampling distributions for closed-loop systems as developed in Chapter 3 provide confidence intervals for the model and enable the response stationarity to be monitored.

The physical justification of the linear model chosen is based on a combination of physical restrictions and the subjective appraisal of the operators used. From the model the phenomenon of increased phase lag at very low frequencies can be explained.

Contrary to previous results it is shown that audio displays are inferior to visual displays both in terms of overall response characteristics and in the ability of the operator to adapt his response to changes in the input dynamics. Non-linearities in the operator's response when tracking signals with high frequency components make it unreasonable to qualify his response in terms of the linear model parameters under these conditions. In the mid-frequency ranges his response is known to be approximately linear.

The experiments involved one-dimensional displays. Extension to two- and three-dimensional displays requires careful consideration of the statistics of multi-input, multi-output closed-loop systems. In its full complexity, this problem involves finding the distribution of frequency response estimates when the inputs are correlated and for multi-path feedback. For the purposes of display analysis it is sufficient to consider the case where the inputs are uncorrelated and the feedback is single path. This is a major topic for future research.

LISTING OF MAJOR COMPUTER PROGRAMS

1) SPECTRA 2

This program is written to be compatible with an integrated data analysis system implemented on a Rank Xerox Sigma 5 computer. Time data is taken from files held on magnetic tape. The program can calculate input/output and cross-spectra together with frequency response estimates for up to 2 input/output closed-loop systems (i.e. 8 time variables). Auto-spectral, cross-spectral and open-loop frequency response estimates can be tested for stationarity using tests described in Chapter 2.

2) FATIGUE RIG CONTROL

Implementation of real time control of fatigue loading rig by input compensation.

3) HUMAN OPERATOR TRACKING TASK

This program samples the output from the force generator and generates the appropriate error signal for display on a C.R.T. scope or using audio display. The program is written for two-dimensional displays, but may be used for one-dimensional tests.

4) MODELLING OF HUMAN OPERATOR RESPONSE

This program uses a Powell hill-climb routine to minimise the cost function between measured and modelled response. The measured response is read from paper tape. The model and the cost function are described in Chapter 6.

5) FAST FOURIER ALGORITHM

Performs discrete Fourier transform on an N-complex array ($N = 2^M$, M 9). The transform can perform either way. The output is ordered. Recorded transform times using Rank Xerox Sigma 5 computer are as follows:

i) 512 point transform 0.3 secs

ii) 256 point transform 0.12 secs

iii) 128 point transform 0.05 secs.

The program is written to be Fortran IV, Macro-Symbol compatible.

All programs are written in Extended Fortran IV where possible. Where speed of execution is essential, a Macro-Symbol code is used. Standard system sub-routines referenced in the program listings are given below.

1) BUFFERIN : inputs record from magnetic tape, disc or paper tape as specified

2) BUFFEROUT : outputs record of data to specified device

3) CHECK : checks for completion of data output to V.D.U. storage scope

4) CHOOSE : input routine from V.D.U. terminal : specifies jump action to be taken within program

5) CLOSEFIL : closes data file on magnetic tape

6) COCINIT : initialises V.D.U. terminal for data transfer

7) CWRITE : program for writing TEXT to V.D.U.

8) DISAB : disables real time interrupt. Interrupt level is specified by user.

9) ENAB : enables real time interrupt

10) ENDFILE : puts end-of-file marker on specified device

11) ERASE : erases V.D.U. screen

12) FETCH : fetch required file (specified by name) from designated source (e.g. magnetic tape, disc)

13) HOME : homes cursor on V.D.U. to top of page

14) LABEL1 : enables user to input text to label graphs on V.D.U. screen. Position specified by displayed cross-wires on screen.

15) MINPUT : inputs filed time sample data from magnetic tape

16) MOUTPUT : outputs data sample point to magnetic tape

17) OPENFIL : open data file on magnetic tape

18) RADCS : analogue to digital sampling routine

19) RDAC : digital to analogue sampling routine

20) RD,RDNC : reads character input from V.D.U. terminal. New-line command can be suppressed.

21) RELEASE : releases OV file to restart program or continue on subsequent jobs

22) REWIND : rewinds specified I/C device

23) SKIPFILE : skips specified number of files on I/O device

24) TIMER : triggers specified real time interrupt at pre-determined rate

25) TPLOT : plots line on V.D.U. storage scope from current position to specified coordinates

26) TRIGR : triggers specified real time interrupt

27) WAIT : drops out of interrupt level. On next trigger to that level control is returned to the next statement after the WAIT call.

28) WT,WTNL : writes character string to V.D.U. terminal. New-line command may be suppressed.

SPECTRA 2

AUTHOR : P. W. DAVALL

LANGUAGE : FORTRAN IV/MACRO-SYMBOL

```
      SUBROUTINE MP
C
C
C
C
C
C
C     PRØGRAM USES INTERRUPT 2Z69 PLUS 2 C8C INTERRUPTS.
C     USING !FØRTRANH G0,S 0PTION.
C     TAPES ØN UNIT T1 MUST BE INITIALISED BY THE USER BEFØRE
C     RUNNING DATA ANALYSIS PACKAGE,ASPECIAL SET ØF TAPE HEADER CARDS
C     IS USED FØR THIS PURPØSE.
C        SCØPE ØF PRØGRAM
C     USED WITHIN D.A. PACKAGE THIS PRØGRAM CAN CALCULATE JLL
C     USEFUL PARAMETERS ØF LINEAR SYSTEMS WITH LESS THAN 8 VARIABLES.
C     ØF TYPICAL INTEREST MAY BE FØR INSTANCE :
C        1)AUTØ-SPECTRA
C        2)CRØSS-SPECTRA BETWEEN 2 CHANNELS.
C        3)PARAMETERS ØF SINGLE INPUT/ØUTPUT LINEAR SYSTEMS
C        4)CØHERENCY ESTIMATES BETWEEN TWØ CHANNELS.
C        5)SINGLE INPUT/ØUTPUT CLØSED LØØP LINEAR SYSTEMS.
C        6)TWØ INPUT/ØUTPUT LINEAR SYSTEMS.
C        7)TWØ INPUT/ØUTPUT CLØSED LØØP LINEAR SYSTEMS.
C
C     FØR FUTURE REF THE FØURIER ALGØRITHM REQLIRES A BLANK
C     CØMMØN ØF RE(1024),IM(1024),N,M,ISIGN,FCØS(129),FCTR IN THAT ØRDER
C     RE = REAL DATA ARRAY
C     IM = IMAGINARY DATA ARRAY
C     N=2**M
C     N=BLØCK SIZE.
C     FCØS = FØURIER WEIGHTING INDEX.
C     ISIGN = TRANSFØRM DIRECTIØN
C     FCTR = NØRMALISING FACTØR FØR FØRWARD TRANSFØRM.
C
C
C
C
C
```

```
C
C          INITIALISE COC AND GET INDEX ON TO TIME DATA FILES
C
C
      COMMON /SET2/INDEXO(90)
      CALL COCINIT(2,1S)
      CALL GETINDX(100,INDEXO)
 1    CALL HOME
      CALL ERASE
      REWIND 101
C
C
C          CHOOSE ACTION
C          A) CREATE FOURIER FILE OF TIME DATA ON TO.
C          B) ACCESS FOURIER FILE ALREADY CREATED ON T1.
C
C
      CALL CHOOSE(55,'(F)OURIER ANALYSIS,(P)LOT,(S)TATIONARITY TEST,(E)X
     &IT !!',1,'F,P,S,E;',J)
      GO TO (2,3,4,5) J
5     CALL RELEASE
2     CALL FFTFILE
      GO TO 1
3     CALL FFTPLOT
      GO TO 1
4     CALL STATOL
      GO TO 1
      RETURN
      END
```

```
C
C
C
      SUBROUTINE FFTFILE
C
C        CREATE FOURIER FILE OF TIME DATA FILE ON TO.(FOURINR FILE ON T1)
C
C
      DIMENSION RCHAN(90)
      COMMON RE(1024),IM(1024),N,M,ISIGN,FCOS(129),FCTR,AR(8,512)/HEADER
     &/ICHAN(90)/SET1/INDEX1(90)/SET2/INDEXO(90)
      REAL IM
      EQUIVALENCE (RCHAN,ICHAN)
C
C
C        WRITE INDEX OF TIME FILES ON TO TO V.D.U.
C
C
      CALL HOME
      CALL ERASE
      CALL WTNL(27,'  FILE         NO OF SAMPLES')
      NFILES=INDEXO(1)
      DO 10 I=1,NFILES
      N=1+I*2
      CALL WT(8,INDEXO(N))
      N=61+I
 10   CALL WTNL(6,'       ',INDEXO(N))
C
C        FETCH REQUIRED FILE ON TO.
C
      CALL FILEFET(NSAMP)
      REWIND 101
      CALL BUFFERIN(101,1,INDEX1,90,IST)
C
C        CHECK TAPE ON T1 INITIALISED IN CORRECT FORMAT FOR FOURIER FILES.
C
      CALL T1CHECK(IFLAG)
```

```
      IF (IFLAG .EQ. 1) RETURN
C
C
C        CHECK FOURIER FILE NAME IS NOT ALREADY ON T1,
C        IF IT IS ON,CHANGE FILE NAME
C
      NFILES=INDEX1(3)
      IF (NFILES .EQ. 0) GO TO 6
 8    DO 7 I=1,NFILES
      N=5+I*2
      IF (ICHAN(1) .NE. INDEX1(N) .OR. ICHAN(2) .NE. INDEX1(N+1)) GO TO
     &7
      CALL WT(23,'(DUPLICATE FILE NAME : ')
      CALL WTNL(8,ICHAN(1))
      IBC=-8
      CALL RDNL(31,'MODIFY NAME FOR FOURIER FILE : ',IBC,ICHAN(1))
      GO TO 8
 7    CONTINUE
 6    CONTINUE
C
C
C        SET UP BLOCK SIZE FOR FOURIER ANALYSIS.
C        SET UP TIME DOMAIN DATA WINDOW.
C        SET UP SAMPLING PARAMETERS OF FOURIER FILE
C
      FSAMP=1.0/RCHAN(69)
      NFPOS=INDEX1(3)+1
      CALL WT(22,'(SAMPLING FREQUENCY = ',FSAMP)
      CALL WT(4,' (1/')
      CALL WT(8,ICHAN(67))
      CALL WTNL(1,')')
 20   CONTINUE
      CALL RDNL(44,'BLOCK SIZE FOR FOURIER ANALYSIS N=2**M  M = ',M)
      IF (M .GT. 9 .OR. M .LT. 2) GO TO 20
      CALL RDNL(30,'SAMPLES TAKEN EVERY I PTS  I= ',ISKSAMP)
      N=2**M
      N2=N/2
```

```
      ISIGN=-1
      FRES=FSAMP/(N*ISKSAMP)
      IF (ISKSAMP .LT. 1) ISKSAMP=1
      NBLCK=NSAMP/(N*ISKSAMP)
      IF (NBLCK .LT. 1) NBLCK=1
      ICHAN(7)=N
      RCHAN(8)=FRES
      ICHAN(9)=NBLCK
      ICHAN(10)=NFPOS
      N4=N/4+1
      DO 4 I=1,N4
    4 FCOS(I)=COS((I-1)*6.2831854/N)
      INDEX1(3)=NFPOS
      CALL SKIPFILE(101,NFPOS)
      CALL BUFFEROUT(101,1,RCHAN,90,IST)
      I=-1
      CALL RDNL(41,'DO YOU WANT A HANNING TIME DATA WINDOW : ',I,IHAN)
      NMOD=0
      FCTR=N
      IF (IHAN .NE. &ZE8404040) GO TO 11
      CALL RDNL(27,'NO OF PTS TO BE MODIFIED = ',NMOD)
      IF (NMOD .LT. 1) NMOD=0
      IF (NMOD .GT. N2) NMOD=N2
      IF (NMOD .EQ. 0) GO TO 11
      FCTR=N-2.0*NMOD
      DO 12 I=1,NMOD
   12 FCTR=FCTR+(1.0+COS(-3.1415926+(I-1)*3.1415926/NMOD))
   11 CONTINUE
      NVAR=ICHAN(3)
      DO 1 I=1,NBLCK
      DO 2 J=1,N
      DO 2 K=1,ISKSAMP
      CALL MINPUT(ITEST,AR(1,J))
    2 CONTINUE
C
C
C         INPUT TIME DATA IN BLOCKS OF N PTS .CARRY OUT FOURIER TRANSFORM
```

```
C          AND OUTPUT TO FOURIER FILE ON T1.
C
       DO 1 J=1,NVAR
       DO 3 K=1,N
       RE(K)=AP(J,K)*RCHAN(15+(J-1)*6)
       IF (K .LE. NMOD) RE(K)=RE(K)*0.5*(1.0+COS(-3.1415926+(K-1)*3.14159
      &26/NMOD))
       IF (K .GE. (N-NMOD+1)) RE(K)=RE(K)*0.5*(1.0+COS(-3.1415926+(N-K)*3
      &.1415926/NMOD))
       RE(N+K)=0.0
       IM(K)=0.0
  3    IM(N+K)=0.0
       CALL FFA
       DO 5 K=1,N2
  5    RE(K+N2)=IM(K)
       CALL BUFFEROUT(101,1,RE,N,IST)
  1    CONTINUE
C
C
C          CLOSE FOURIER FILE ,UPDATE INDEX ON T1.
C
       ENDFILE 101
       ENDFILE 101
       N2=5+2*NFPOS
       INDEX1(N2)=ICHAN(1)
       INDEX1(N2+1)=ICHAN(2)
       N2=60+NFPOS
       INDEX1(N2)=NBLCK
       IF (ITEST .NE. 1) CALL WTNL(17,'END OF DATA FOUND')
       REWIND 101
       CALL BUFFEROUT(101,1,INDEX1,90,IST)
       REWIND 101
C
C          RETURN TO MP.
       RETURN
       END
```

```
C
C
C
      SUBROUTINE FFTPLOT
C
C        CALCULATES AND PLOTS REQUIRED SPECTRAL ESTIMATES FROM FOURIER
C        FILES ON T1.
C
      COMMON RE(1024),IM(1024),N,M,ISIG,FCOS(129),FCTR,AR(8,512)/HEADER
     &/ICHAN(90)/SET1/INDEX1(90)
      COMPLEX FVALUE(9),F1,F2,F3,F4
      REAL IM
      DIMENSION RCHAN(90),IV(8),DUMP(512),FT1(512),FT2(512),FT3(512),
     &FT4(512),FS1(512),FS2(512),FS3(512),FS4(512)
      DIMENSION PAPE(20),IPAPE(20)
      EQUIVALENCE (PAPE,IPAPE)
      EQUIVALENCE (RCHAN,ICHAN),(FT1,RE(1)),(FT2,RE(513)),(FT3,IM(1)),(F
     &T4,IM(513)),(FS1,AR(1)),(FS2,AR(513)),(FS3,AR(1025)),(FS4,AR(1537)
     &)
C
C
C        FETCH TAPE INDEX ON T1.
C
    1 REWIND 101
      CALL BUFFERIN(101,1,INDEX1,90,IST)
C
C
C        CHECK FOR CORRECT TAPE FORMAT.
      CALL T1CHECK(IFLAG)
      IF (IFLAG .EQ. 1) RETURN
      NFILES=INDEX1(3)
      CALL HOME
      CALL ERASE
C
C
C        OUTPUT NAMES OF FOURIER FILES ON V.D.U.
      CALL WTNL(28,'    FILE          NO OF BLOCKS')
```

```
      CALL RD(I,IV(2))
      I=1
      CALL RD(2,'*P',I,IV(3))
      I=1
      CALL RD(I,IV(4))
      I=1
      CALL RD(4,')/(P',I,IV(5))
      I=1
      CALL RD(I,IV(6))
      I=1
      CALL RD(2,'*P',I,IV(7))
      I=1
      CALL RD(I,IV(8))
      CALL WTNL(1,')')
      NCHAN=ICHAN(3)
C
C
C        CHECK FOR CORRECT FUNCTION FORMAT,TRY AGAIN IF WRONG.
C
 21   ITDIM=0
      IBDIM=0
      DO 3 I=1,8
      IF (IV(I) .GT. NCHAN .OR. IV(I) .LT. 0) GO TO 22
      IF (I .LE. 4 .AND. IV(I) .NE. 0) ITDIM=ITDIM+1
      IF (I .GT. 4 .AND. IV(I) .NE. 0) IBDIM=IBDIM+1
 3    IF (IV(I) .EQ. 0) IV(I)=9
      IDIM=((ITDIM-IBDIM)+ISIGN(1,(ITDIM-IBDIM)))/2
      FVALUE(9)=CMPLX(1.0,0.0)
C
C
C        READ IN START AND FINISH POINT FOR PLOT ROUTINES IN TERMS
C        OF FOURIER BLOCKS ON T1.
C
      IST=IBL1
      CALL RDNL(23,'START BLOCK FOR PLOT = ',IBL1)
      IF (IBL1 .EQ. 0 .OR . IBL1 .GT. 1000000) IBL1=IST
      IST=IBL2
```

```
      DO 2 I=1,NFILES
      N=5+I*2
      CALL WTSP(4)
      CALL WT(8,INDEX1(N))
      CALL WTSP(6)
 2    CALL WTNL(INDEX1(60+I))
C
C
C        FETCH REQUIRED FOURIER FILE ON T1.
C
      CALL FFET1(NBLCK)
C
C
C        DEFAULT VALUES FOR PLOT ROUTINE
C        FPLOT=0
C        IBL1=1
C        IBL2=NBLCK
C        SMOOTH=1
C        ILOG=FALSE
C        DC SUPPRESSION=FALSE
C        CARRIAGE RETURN CHARACTER LEAVES IBL1,IBL2,FPLOT,SMOOTH WITH
C        PREVIOUS VALUES
C
      IBL2=NBLCK
      IBL1=1
      FPLOT=0.0
      SMOOTH=1.0
C
C
C        CHOOSE REQUIRED FOURIER FUNCTION IN FORM --
C        (P12*P34)/(P56*P78)
C        IF ANY OF 1-8 ARE ZERO THE CONST 1.0 IS ASSUMED.
C
 22   CALL WTNL(14,'(((**FUNCTION**!')
      I=1
      CALL RD(13,'FUNCTION = (P',I,IV(1))
      I=1
```

```
      CALL RDNL(22,'LAST BLOCK FOR PLOT = ',IBL2)
      IF (IBL2 .EQ. 0 .OR. IBL2 .GT. 1000000) IBL2=IST
      IF (IBL2 .GT. NBLCK) IBL2=NBLCK
      IF (IBL1 .GT. IBL2)IBL1=IBL2
C
C
C        SET UP FREQ RESOLUTION,MAX POSS. FREQ FOR PLOT,MAX NO OF PTS FOR PLOT
C
      N=ICHAN(7)
      FRES=RCHAN(8)
      N2=N/2
      FMAX=FRES*(N2-1)
C
C
C        SKIP TO START POS IN FOURIER FILE ON T1.
C
      ISET=IBL1-1
      IF (ISET .EQ. 0) GO TO 4
      DO 5 I=1,ISET
      DO 5 J=1,NCHAN
 5    CALL BUFFERIN(101,1,RE,N,IST)
 4    CONTINUE
C
C
C        INITIALISE REGISTERS CONTAINING SPECTRAL ESTIMATES TO ZERO
C
      DO 10 I=1,1024
      IM(I)=0.0
 10   RE(I)=0.0
      ISET=IBL2-IBL1+1
C
C
C        CALCULATE SPECTRAL AVERAGE OVER ISET BLOCKS
C
      DO 6 I=1,ISET
C
C
```

```
C          INPUT FOURIER DATA FOR ALL CHANNELS
C
      DO 7 J=1,NCHAN
      CALL BUFFERIN(101,1,DUMP,N,IST)
      DO 7 K=1,N
      AR(J,K)=DUMP(K)
 7    CONTINUE
C
C
C          CALCULATE 4 REQUIRED CROSS-SPECTRA AND ADD TO SPECTRAL REGISTERS
C
      DO 9 J=1,N2
      JN2=J+N2
      DO 8 K=1,NCHAN
 8    FVALUE(K)=CMPLX(AR(K,J),AR(K,JN2))
      F1=CONJG(FVALUE(IV(1)))*FVALUE(IV(2))
      F2=CONJG(FVALUE(IV(3)))*FVALUE(IV(4))
      F3=CONJG(FVALUE(IV(5)))*FVALUE(IV(6))
      F4=CONJG(FVALUE(IV(7)))*FVALUE(IV(8))
      FT1(J)=REAL(F1)+FT1(J)
      FT1(JN2)=FT1(JN2)+AIMAG(F1)
      FT2(J)=FT2(J)+REAL(F2)
      FT2(JN2)=FT2(JN2)+AIMAG(F2)
      FT3(J)=FT3(J)+REAL(F3)
      FT3(JN2)=FT3(JN2)+AIMAG(F3)
      FT4(J)=FT4(J)+REAL(F4)
 9    FT4(JN2)=FT4(JN2)+AIMAG(F4)
 6    CONTINUE
C
C
C          CALCULATE MEAN
C
      DO 11 I=1,1024
      RE(I)=RE(I)/ISET
 11   IM(I)=IM(I)/ISET
C
C
```

```
C          SET UP PLOTTING PARAMETERS
C
 20    CALL HOME
       CALL ERASE
       CALL WTNL(16,'PLOTTING ROUTINE')
       CALL WT(11,'MAX FREQ = ',FMAX)
       CALL WT(4,' (1/')
       CALL WT(8,ICHAN(67))
       CALL WTNL(1,')')
       CALL WTNL(15,'NO OF POINTS = ',N2)
       RST=FPLOT
       CALL RDNL(20,'MAX FREQ FOR PLOT = ',FPLOT)
       IF (FPLOT .EQ. 0.0 .OR. FPLOT .GT. 1.0E20) FPLOT=RST
       IF (FPLOT .GT. FMAX) FPLOT=FMAX
       NPLOT=(N2-1)*FPLOT/FMAX+1
       RST=SMOOTH
       CALL RDNL(26,'NO OF PTS FOR SMOOTHING = ',SMOOTH)
       IF (SMOOTH .EQ. 0.0 .OR. SMOOTH .GT. 1.0E20) SMOOTH=RST
       I=-1
       CALL RDNL(17,'DC SUPPRESSION ? ',I,IDC)
       I=-1
       CALL RDNL(11,'LOG PLOT ? ',I,ILOG)
       I=-1
       CALL RDNL(17,'PAPER TAPE DUMP ? ',I,IP)
       IF (IP .NE. 8ZE8404040) GO TO 42
       IPAPE(1)=ICHAN(1)
       IPAPE(2)=ICHAN(2)
       DO 32 J=1,8
       K=0
       IF (IV(J) .NE. 9) K=IV(J)
 32    IPAPE(2+J)=K
       IPAPE(11)=NPLOT
       IPAPE(12)=ISET
       IPAPE(13)=ILOG
       PAPE(14)=FPLOT
       PAPE(15)=SMOOTH
       CALL BUFFEROUT(105,1,PAPE,15,IST)
```

```
 42    CONTINUE
       CALL HOME
       CALL ERASE
       DO 12 I=1,8
 12    IF (IV(I) .EQ. 9) IV(I)=0
C
C
C         OUTPUT FUNCTION CALCULATED AS TITLE FOR GRAPH.
C
       CALL WTSP(25)
       CALL WT(15,'FUNCTION = (PHH',IV(1))
       CALL WT(2,'HH',IV(2))
       CALL WT(4,'*PHH',IV(3))
       CALL WT(2,'HH',IV(4))
       CALL WT(6,')/(PHH',IV(5))
       CALL WT(2,'HH',IV(6))
       CALL WT(4,'*PHH',IV(7))
       CALL WT(2,'HH',IV(8))
       CALL WTNL(1,')')
       CALL WTSP(20)
       CALL WTNL(40,'========================================')
       CALL WT(16,'((START BLOCK = ',IBL1)
       CALL WTNL(19,'       LAST BLOCK = ',IBL2)
       CALL WT(16,'FREQ IN UNITS OF')
       CALL WT(3,' 1/')
       CALL WTNL(8,ICHAN(67))
C
C
C         SMOOTH SPECTRAL ESTIMATES.
C
       CALL AVERAG(FT1,FS1,N,SMOOTH)
       CALL AVERAG(FT2,FS2,N,SMOOTH)
       CALL AVERAG(FT3,FS3,N,SMOOTH)
       CALL AVERAG(FT4,FS4,N,SMOOTH)
       VAR=0.0
       PMAX=0.0
C
```

```
C
C          CALCULATE REQUIRED AMPLITUDE AND PHASE.
C          AMPLITUDE = DUMP(1-N2) , PHASE = DUMP(N2+1-N)
C
      DO 14 I=1,NPLOT
      F1=CMPLX(FS1(I),FS1(I+N2))
      F2=CMPLX(FS2(I),FS2(I+N2))
      F3=CMPLX(FS3(I),FS3(I+N2))
      F4=CMPLX(FS4(I),FS4(I+N2))
      F1=(F1*F2)/(F3*F4)
      IF (I .NE. 1) F1=F1*(2.0**IDIM)
      DUMP(I)=CABS(F1)
      IF (I .EQ. 1 .AND. IDC .EQ. 8ZE8404040) DUMP(1)=0.0
      DUMP(I+N2)=0.0
      IF (DUMP(I) .GT. 0.0) DUMP(I+N2)=ATAN2(AIMAG(F1),REAL(F1))
      VAR=VAR+DUMP(I)
 14   IF (DUMP(I) .GT. PMAX) PMAX=DUMP(I)
      IF (IDC .EQ. 8ZE8404040) DUMP(1)=DUMP(2)
      PMIN=0.0
      DO 15 I=1,NPLOT
      IF (ILOG .NE. 8ZE8404040) GO TO 33
      IF (DUMP(I) .GT. 0.0)DUMP(I)=10.0*ALOG10(DUMP(I)/VAR)
      IF (IDIM .EQ. 0) DUMP(I)=DUMP(I)*2.0
      IF (DUMP(I) .EQ. 0.0) DUMP(I)=-100.0
 33   IF (IP .NE. 8ZE8404040) GO TO 15
      PAPE(1)=DUMP(I)
      PAPE(2)=DUMP(I+N2)
      CALL BUFFEROUT(105,1,PAPE,2,IST)
 15   IF (DUMP(I) .LT. PMIN) PMIN=DUMP(I)
C.
C
C          CALL GRAPH PLOTTING ROUTINE
C
      CALL PLOTTER(FMAX,PMAX,PMIN,ILOG,DUMP,N,FPLOT,VAR,SMOOTH)
C
C
C          CHOOSE NEXT ACTION
```

```
C
 17    CALL CHOOSE(79,'REPEAT PLOT (RP)(NEW DATA (ND)(NEW FUNCTION (NF)(C
      &HANGE FILE (CF)(EXIT (EX)  !!',2,'RP,ND,NF,CF,EX;',IAC)
       CALL WT(1,'(')
       IF (IAC .EQ. 0) GO TO 17
       CALL SKIPFILE(101,0)
       CALL BUFFERIN(101,1,ICHAN,90,IST)
       GO TO (20,21,22,1,24),IAC
 24    REWIND 101
       RETURN
       END
```

```
C
C
C
      SUBROUTINE FFA
C
C
C        FAST FOURIER ALGORITHM.
C        FORWARD TRANSFORM       ISIGN=-1
C        TAKES N (2**M) DATA PTS FROM RE(1-N) (REAL DATA PTS) ,IM(1-N)
C        (IMAGINARY DATA PTS) AND PUTS N COMPLEX COEFFS IN ASCENDING FREQ ORDER
C        BACK INTO REAL AND IMAGINARY DATA ARRAYS.
C        THE LAST N/2 PTS ARE THE ALIASED PAIRS OF THE PREVIOUS N/2 PTS.
C        FOR THE INVERSE TRANSFORM ISIGN=+1,AND DATA IS LOADED AS FOR
C        FORWARD TRANSFORM WITH ALIASED PAIRS IN LAST N/2 PLACES.
C        TIME FOR 512 PTS TRANSFORM = 0.25 SECS ON SIGMA 5
C
C
      DIMENSION FCOS(129)
      COMMON RE(1024),IM(1024),N,M,ISIGN,FCOS,FCTR,AR(8,512)
      REAL IM
      DOUBLE PRECISION ONEONE
      DATA ONEONE/9Z100000001/
      N2=N/2
      N4=N2/2
      NP=N4+1
      NB=N
      NC=0
      ND=NB
      J2=1
      N2J=NB
      NX=N2+1
      DO 3 J=1,M
      NI=J2
      N2J=N2J/2
      J2=J2+J2
      IN2J=-N2J
      DO 2 I=1,NI
```

```
      IN2J=IN2J+N2J
S         LW,5        IN2J
S         AI,5        1
S         LW,9        IN2J
S         CW,9        N4
S         BL          4S
S         SW,9        NX
S         LCW,5       9
S4        LW,9        FC0S-1,5
S         STW,9       W1
      IF (IN2J .GT. N4) W1=-W1
S         LW,7        N4
S         AI,7        2
S         SW,7        5
S         LW,9        FC0S-1,7
S         MW,9        ISIGN
S         STW,9       W2
S         LW,6        IN2J
S         AW,6        NB
S         LW,4        IN2J
S         SLS,4       1
S         AW,4        NC
S         LW,7        4
S         AW,7        N2J
S         LW,5        6
S         AW,5        N2
S         LW,1        N2J
S1        AD,4        0NE0NE
S         AD,6        0NE0NE
S         LW,8        W1
S         FMS,8       RE-1,7
S         LW,10       W2
S         FMS,10      IM-1,7
S         FSS,8       10
S         LW,9        W1
S         FMS,9       IM-1,7
S         LW,10       W2
```

```
S           FMS,10      RE-1,7
S           FAS,9       10
S           LW,10       RE-1,4
S           LW,12       10
S           FAS,10      8
S           STW,10      RE-1,6
S           LW,11       IM-1,4
S           LW,13       11
S           FAS,11      9
S           STW,11      IM-1,6
S           FSS,12      8
S           STW,12      RE-1,5
S           FSS,13      9
S           STW,13      IM-1,5
S           BDR,1       1S
  2         CONTINUE
          NB=NC
          NC=ND
  3       ND=NB
C
C
C           TRANSFER DATA TO OUTPUT REGISTER AND NORMALISE IF REQUIRED.
C
          IAR=0
          IF (NB .EQ. 0) IAR=N
          IF (ISIGN .GT. 0) FCTR=1.0
          DO 5 I=1,N
          J=I+IAR
          RE(I)=RE(J)/FCTR
  5       IM(I)=IM(J)/FCTR
          RETURN
          END
```

```
C
C
C
      SUBROUTINE FFET1(NBLCK)
C
C        FETCHES FOURIER FILE ON T1 WITH HEADER IN D.A.FORMAT.
C        OUTPUTS DETAILS OF FILE TO V.D.U. RETURNS WITH NO. OF FOURIER
C        BLOCKS IN NBLCK.
C
      COMMON /HEADER/ICHAN(90)/SET1/INDEX1(90)
      DIMENSION RCHAN(90),NAME(2)
      EQUIVALENCE (RCHAN,ICHAN)
    3 IBC=-8
      CALL RDNL(28,'WHICH FILE DO YOU REQUIRE : ',IBC,NAME)
      NFILES=INDEX1(3)
      DO 1 I=1,NFILES
      J=5+I*2
    1 IF (NAME(1) .EQ. INDEX1(J) .AND. NAME(2) .EQ. INDEX1(J+1)) GO TO 2
      GO TO 3
    2 CONTINUE
      I=(J-5)/2
      CALL SKIPFILE(101,I)
      CALL BUFFERIN(101,1,RCHAN,90,IST)
      CALL HOME
      CALL ERASE
      IBC=-8
      CALL WT(12,'FILE NAME : ')
      CALL WTNL(IBC,ICHAN(1))
      CALL WT(10,'IND VAR : ')
      CALL WT(IBC,ICHAN(65))
      CALL WT(11,'   UNITS : ')
      CALL WTNL(IBC,ICHAN(67))
      CALL WT(17,'INCREMENT STEP = ',RCHAN(69))
      CALL WTNL(14,'START VALUE = ',RCHAN(70))
      CALL WTNL(21,'FOURIER BLOCK SIZE = ',ICHAN(7))
      CALL WT(18,'FREQ RESOLUTION = ',RCHAN(8))
      CALL WT(15,'NO OF BLOCKS = ',ICHAN(9))
```

```
      CALL WT(21,'((DEPENDENT VARIABLES')
      CALL WT(39,'((   NO   NAME          UNITS         SCALE')
      NVAR=ICHAN(3)
      IBC=8
      CALL WTNL
      DO 4 I=1,NVAR
      N=11+(I-1)*6
      CALL WT(2,'  ',I)
      CALL WTSP(4)
      CALL WT(IBC,ICHAN(N))
      CALL WTSP(4)
      CALL WT(IBC,ICHAN(N+2))
    4 CALL WTNL(4,'    ',RCHAN(N+4))
      IBC=40
      CALL WT(12,'((COMMENT : ')
      CALL WTNL(IBC,ICHAN(71))
      CALL WT(IBC,ICHAN(81))
      CALL WT(2,'(((')
      NBLCK=ICHAN(9)
      RETURN
      END
```

```
C
C
C
      SUBROUTINE AVERAG(RAWD,SMDAT,NPTS,SMOOTH)
C
C        SMOOTHS SPECTRAL ESTIMATES USING TRIANGULAR WINDOW.
C        RAWD=UNSMOOTHED DATA
C        SMDAT=SMOOTHED DATA
C        NPTS=SIZE OF FOURIER BLOCK.
C        SMOOTH=REAL VALUED NO OF PTS FOR SMOOTHING
C
      DIMENSION RAWD(512),SMDAT(512)
      DO 1 I=1,NPTS
    1 SMDAT(I)=RAWD(I)
      IF (SMOOTH .LE. 2) RETURN
      N2=NPTS/2
      EXT=SMOOTH/2.0
      IEXT=EXT+0.1
      DO 2 I=2,N2
      SMDAT(I)=0.0
      SMDAT(I+N2)=0.0
      IST=I-IEXT
      IFIN=I+IEXT
      FACT=0.0
      DO 3 J=IST,IFIN
      IF (J .LT. 2 .OR. J .GT. N2) GO TO 3
      ACT=1.0-IABS(I-J)/EXT
      FACT=FACT+ACT
      SMDAT(I)=SMDAT(I)+ACT*RAWD(J)
      SMDAT(I+N2)=SMDAT(I+N2)+ACT*RAWD(J+N2)
    3 CONTINUE
      SMDAT(I)=SMDAT(I)/FACT
    2 SMDAT(I+N2)=SMDAT(I+N2)/FACT
      RETURN
      END
```

```
C
C
C
      SUBROUTINE PLOTTER(FMAX,PMAX,PMIN,ILOG,DUMP,N,FPLOT,VAR,SMOOTH)
C
C         PLOT GRAPH OF REQUIRED SPECTRAL FUNCTION ON V.D.U.
C         FMAX=MAX POSS FREQ FOR PLOT
C         PMAX=MAX FN VALUE
C         PMIN=MIN FN VALUE
C         ILOG=INDICATOR FOR LOG PLOT
C         DUMP=ARRAY FOR PLOTTING
C         N=BLOCK SIZE
C         FPLOT= MAX FREQ OF PLOT
C         VAR=SIGMA AMPLITUDE
C         SMOOTH=NO OF PTS FOR SMOOTHING
C
      DIMENSION DUMP(512)
      NSMOOTH=SMOOTH+0.1
C
C
C           CALCULATE NO OF PTS TO PLOT
C
      N2=N/2
      NPLOT=(N2-1)*(FPLOT/FMAX)+1
C
C
C           DRAW AXES AND LABEL PHASE PLOT
C
      CALL TPLOT(0,640,500)
      CALL TPLOT(-1,650,500)
      CALL TPLOT(-1,650,412)
      CALL TPLOT(-1,640,412)
      CALL TPLOT(0,650,412)
      CALL TPLOT(-1,650,238)
      CALL TPLOT(-1,640,238)
      CALL TPLOT(0,650,238)
      CALL TPLOT(-1,650,150)
```

```
      CALL TPLOT(-1,640,150)
      CALL TPLOT(0,1000,315)
      CALL TPLOT(-1,1000,325)
      CALL TPLOT(-1,825,325)
      CALL TPLOT(0,825,315)
      CALL TPLOT(-1,825,325)
      CALL TPLOT(-1,650,325)
      CALL TPLOT(0,700,525)
      CALL WT(18,'PHASE (DEG) V FREQ')
      CALL TPLOT(0,600,495)
      CALL WT(4,'+180')
      CALL TPLOT(0,600,407)
      CALL WT(4,' +90')
      CALL TPLOT(0,600,320)
      CALL WT(4,'   0')
      CALL TPLOT(0,600,233)
      CALL WT(4,' -90')
      CALL TPLOT(0,600,145)
      CALL WT(4,'-180')
      F=FPLOT/2.0
      CALL TPLOT(0,760,310)
      CALL WT(F)
      CALL TPLOT(0,910,310)
      CALL WT(FPLOT)
      CALL TPLOT(0,650,325)
      XINC=350.0/(NPLOT-1)
C
C
C         PLOT PHASE
C
      DO 2 I=1,NPLOT
      X=650.0+(I-1)*XINC
      Y=325.0+175.0*DUMP(N2+I)/3.1415926
 2    CALL TPLOT(-1,X,Y)
C
C
C         CHOOSE REQUIRED TYPE OF AMPLITUDE PLOT
```

```
C
      IF (ILOG .NE. 8ZE8404040) GO TO 3
C
C
C        DRAW AXES AND LABEL LOG AMPLITUDE PLOT
C
      CALL TPLOT(0,600,560)
      CALL TPLOT(-1,600,550)
      CALL TPLOT(-1,350,550)
      CALL TPLOT(0,350,560)
      CALL TPLOT(-1,350,550)
      CALL TPLOT(-1,100,550)
      CALL TPLOT(0,290,570)
      CALL WT(F)
      CALL TPLOT(0,530,570)
      CALL WT(FPLOT)
      CALL TPLOT(0,20,550)
      CALL WT(3,'  0')
      CALL TPLOT(0,100,550)
      INT=ABS(PMIN)/5.0+1
      PMIN=INT*5.0
      YINC=-450.0/INT
      DO 4 I=1,INT
      Y=550.0+YINC*I
      CALL TPLOT(-1,100.0,Y)
      CALL TPLOT(-1,90.0,Y)
      CALL TPLOT(0,20.0,Y)
      NP=-I*5
      CALL WT(NP)
    4 CALL TPLOT(0,100.0,Y)
      CALL TPLOT(0,150,70)
      CALL WT(21,'AMPLITUDE (DB) V FREQ')
      XINC=500.0/(NPLOT-1)
      CALL TPLOT(0,100,550)
C
C
C        PLOT LOG AMPLITUDE
```

```
C
      DO 5 I=1,NPLOT
      X=100.0+(I-1)*XINC
      Y=550.0-ABS(DUMP(I)/PMIN)*450.0
 5    CALL TPLOT(-1,X,Y)
      GO TO 6
C
C
C        DRAW AXES AND LABEL LIN AMPLITUDE PLOT
C
 3    CALL TPLOT(0,600,90)
      CALL TPLOT(-1,600,100)
      CALL TPLOT(-1,350,100)
      CALL TPLOT(-1,350,90)
      CALL TPLOT(0,350,100)
      CALL TPLOT(-1,100,100)
      CALL TPLOT(-1,100,325)
      CALL TPLOT(-1,90,325)
      P=PMAX/2.0
      CALL TPLOT(0,1,325)
      CALL WT(P)
      CALL TPLOT(0,100,325)
      CALL TPLOT(-1,100,550)
      CALL TPLOT(-1,90,550)
      CALL TPLOT(0,1,550)
      CALL WT(PMAX)
      CALL TPLOT(0,150,575)
      CALL WT(16,'AMPLITUDE V FREQ')
      CALL TPLOT(0,290,70)
      CALL WT(F)
      CALL TPLOT(0,530,70)
      CALL WT(FPLOT)
      CALL TPLOT(0,100,100)
      XINC=500.0/(NPLOT-1)
C
C
C        PLOT LIN AMPLITUDE VALUES
```

```
C
      DO 7 I=1,NPLOT
      X=100.0+(I-1)*XINC
      Y=100.0+(DUMP(I)/PMAX)*450.0
 7    CALL TPLOT(-1,X,Y)
C
C
C        OUTPUT PLOT PARAMETERS FOR GRAPH
C
 6    CALL TPLOT(0,650,100)
      CALL WT(18,'SIGMA AMPLITUDE = ',VAR)
      CALL TPLOT(0,650,80)
      CALL WT(16,'MAX AMPLITUDE = ',PMAX)
      CALL TPLOT(0,650,60)
      FRES=FMAX/(N2-1)
      CALL WT(11,'FREQ RES = ',FRES)
      CALL TPLOT(0,650,40)
      CALL WT(12,'SMOOTHING = ',NSMOOTH)
      CALL WT(4,' PTS')
C
C
C        USER CAN NOW LABEL GRAPH TO OWN SPECIFICATION.
C
      CALL TPLOT(0,650,20)
      I=1
      CALL RD(2,'!!!',I,J)
      IF (I .EQ. 0) GO TO 11
 10   ICHAR=8Z40404040
      CALL JOY(ICHAR,IX,IY)
      IF (ICHAR .EQ. 8Z0D404040) GO TO 11
      IF (IX .GT. 640) GO TO 12
      IF (IX .GT. 600 .OR. IX .LT. 100) GO TO 10
      IF (IY .GT. 550 .OR. IY .LT. 100) GO TO 10
      FREQ=FPLOT*(IX-100.0)/500.0
      AMP=PMAX*(IY-100.0)/450.0
      IF (ILOG .EQ. 8ZE8404040) AMP=-PMIN*(IABS(550-IY))/450.0
      GO TO 13
```

```
12    IF (IX .GT. 1000 .OR. IX .LT. 650) GO TO 10
      IF (IY .LT. 150 .OR. IY .GT. 500) GO TO 10
      FREQ=FPLOT*(IX-650.0)/350.0
      AMP=180.0*(IY-325.0)/175.0
13    CALL TPLOT(0,IX,IY)
      IF (IX .GT. 910) IX=910
      IF (IX .GT. 490 .AND. IX .LE. 600) IX=490
      CALL TPLOT(-1,IX,IY+5)
      CALL WT(2,'F=',FREQ)
      CALL TPLOT(0,IX,IY+20)
      CALL WT(2,'Y=',AMP)
      GO TO 10
11    CONTINUE
      CALL LABEL1
      CALL HOME
      CALL ERASE
      RETURN
      END
```

```
C
C
C
      SUBROUTINE WTSP(NSP)
C
C        WRITE SPACES ON V.D.U.
C
      N=NSP
      IF (N .EQ. 0) RETURN
      IF (N .LT. 0) N=N+1
      DO 1 I=1,N
      IF (N .LE. 0) CALL WT(2,'H ')
      IF (N .GT. 0) CALL WT(2,'  ')
    1 CONTINUE
      RETURN
      END
```

```
C
C
C
      SUBROUTINE T1CHECK(IFLAG)
C
C        CHECK FORMAT HEADER FOR T1 TAPE
C
      COMMON /SET1/INDEX1(90)
      IFLAG=0
      IF (INDEX1(1) .EQ. 8ZE2D7C5C3 .AND. INDEX1(2) .EQ. 8ZE3D9C1F2)RETU
     &RN
      I=-1
      CALL RDNL(21,'WRONG TAPE ON UNIT T1',I,J)
      IFLAG=1
      RETURN
      END
```

```
      CALL WTNL
      CALL WT(19,'DEPENDANT VARIABLES')
      CALL WTNL
      CALL WT(28,'CHANNEL      NAME        UNITS')
      CALL WTNL
      M=N00FCH
      IF (M.GT.9) M=9
      DO 10 I=1,M
      N0=8Z404040F0+I
      CALL WT(4,N0)
      CALL WTSP(7)
      CALL WT(8,CHAN(1,I))
      CALL WTSP(4)
      CALL WT(8,CHAN(3,I))
      CALL WTNL
10    CONTINUE
      CALL WT(12,'((COMMENT : ')
      CALL WTNL(40,IAR(71))
      CALL WT(40,IAR(81))
      END
```

```
C
C
C
      SUBROUTINE FILE FET(N)
C
C        FETCH REQUIRED FILE ON TO,OUTPUT HEADER TO V.D.U.
C
      DIMENSION IAR(90)
      DIMENSION SPARE(4)
      DIMENSION NAME(2),CHAN(6,11)
      DIMENSION INAM(2)
      INTEGER FORMAT,RECSIZE,CHAN
      DIMENSION INDNAM(2),INDUNIT(2)
      COMMON /HEADER/NAME,NOOFCH,FORMAT,RECSIZE,INCREMENT,SPARE,CHAN
      EQUIVALENCE (IAR,NAME)
      EQUIVALENCE (SC1,CHAN(5,1)),(SC2,CHAN(5,2)),(SC3,CHAN(5,3)),
     1(SC4,CHAN(5,4)),(SC5,CHAN(5,5)),(SC6,CHAN(5,6)),(SC7,CHAN(5,7)),
     1(SC8,CHAN(5,8)),(SC9,CHAN(5,9))
      EQUIVALENCE (INDNAM,CHAN(1,10)),(INDUNIT,CHAN(3,10)),
     1(SCIND,CHAN(5,10)),(INDTYP,CHAN(6,10))
1     CONTINUE
      ITEXCNT=-8
      CALL RDNL(28,'WHICH FILE DO YOU REQUIRE  ',ITEXCNT,INAM)
      CALL FETCH(INAM,N,IAR)
      IF (N.EQ.-1) GO TO 1
      CALL HOME
      CALL ERASE
      ITEXCNT=-8
      CALL WT(12,'FILE NAME : ')
      CALL WTNL(ITEXCNT,IAR(1))
      CALL WT(20,'INDEPENDANT VARIABLE')
      CALL WTNL
      CALL WT(10,'   0       ')
      CALL WT(8,CHAN(1,10))
      CALL WT(4,' IN ')
      CALL WT(8,CHAN(3,10))
      CALL WTNL
```

```
C
C
C
      SUBROUTINE GETINDX(IU,INDEX)
C
C        GET TAPE INDEX ON UNIT IU AND PUT INDEX IN ARRAY INDEX.
C
      DIMENSION INDEX(90)
      INTEGER UIEC/'UIEC'/
      REWIND IU
1     CALL SKIPFILE(IU,1)
      CALL BUFFERIN(IU,1,INDEX,90,IST)
      IF(IST.EQ.2) GOTO 1
      CALL BUFFERIN(IU,1,INDEX,90,IST)
      I=1
      IF (INDEX(2) .NE. UIEC) CALL RDNL(23,'NOT D.A. TAPE ABORT PROG',I,
     &J)
      REWIND IU
      END
```

```
C
C
C
      SUBROUTINE STATOL
C
C
C
C     THIS SUBROUTINE TESTS THE STATIONARITY OF AN OPEN-LOOP SYSTEM
C     WHOSE INPUT CHANNEL IS IN, & OUTPUT CHANNEL IS IOUT. CONFIDENCE
C     INTERVALS ARE RETURNED FOR AUTO-SPECTRAL ESTIMATES OF PXX,PYY,PNN
C     AND H,THE FREQUENCY RESPONSE. THE PROGRAM TAKES THE FIRST ESTIMATE
C     OVER BLOCKS IST1 TO IF1 & THE SECOND ESTIMATE OVER BLOCKS IST2
C     TO IF2, WHERE IST2 IS GREATER THAN IF1.
C
C
C
      COMMON RE(1024),IM(1024),N,M,FCOS(129),FCTR,RA(512,8)/HEADER/ICHAN
     &(90)/SET1/INDEX1(90)
       DIMENSION PXX1(256),PXX2(256),PYY1(256),PYY2(256),PXY1(256),PXY2(2
     &56),SMX(256),SMY(256),SMXY(256),DUMP(512),PX(2),PY(2),XY(2)
       DIMENSION ICOUNT(256)
       COMPLEX PXY1,PXY2,SMXY,XJW,YJW,XY
       EQUIVALENCE (PXX1,RE),(PXX2,RE(257)),(PYY1,RE(513)),(PYY2,RE(769))
     &,(PXY1,IM),(PXY2,IM(513)),(DUMP,RA(3585)),(SMX,RA),(SMY,RA(257)),(
     &SMXY,RA(513)),(ICOUNT,RA(1025))
C
C      GET INDEX ON TAPE UNIT 1.
C
       REWIND 101
       CALL BUFFERIN(101,1,INDEX1,90,IST)
       CALL T1CHECK(IFLAG)
       IF (IFLAG .EQ. 1) RETURN
       NFILES=INDEX1(3)
       CALL HOME
       CALL ERASE
C
C      GET REQUIRED FOURIER FILE
```

```
C
C       SET UP INITIAL SPECTRAL VALUES TO ZERO
C
 11     DO 4 I=1,256
        PXX2(I)=0.0
        PYY2(I)=0.0
  4     PXY2(I)=CMPLX(0.0,0.0)
C
C       ADD UP NAV FOURIER BLOCKS TO FORM PXX,PYY,PXY.
C
        DO 3 I=1,NAV
        DO 5 J=1,NCHAN
        CALL BUFFERIN(101,1,DUMP,N,IST)
        DO 5 K=1,N
  5     RA(K,J)=DUMP(K)
        DO 6 J=1,N2
        PXX2(J)=PXX2(J)+RA(J,IN)**2+RA(J+N2,IN)**2
        PYY2(J)=PYY2(J)+RA(J,IOUT)**2+RA(J+N2,IOUT)**2
        XJW=CMPLX(RA(J,IN),RA(J+N2,IN))
        YJW=CMPLX(RA(J,IOUT),RA(J+N2,IOUT))
  6     PXY2(J)=PXY2(J)+CONJG(XJW)*YJW
  3     CONTINUE
C
C       NORMALISE ESTIMATES OVER TIME.
C
        DO 7 I=1,N2
        ICOUNT(I)=0
        SMX(I)=0.0
        SMY(I)=0.0
        SMXY(I)=CMPLX(0.0,0.0)
        PXX2(I)=PXX2(I)/NAV
        PYY2(I)=PYY2(I)/NAV
  7     PXY2(I)=PXY2(I)/NAV
C
C       SMOOTH ESTIMATES OVER FREQUENCY.
C
        IF (NSMOOTH .LT. 3) GO TO 15
```

```
C       CHOOSE CHANNELS FOR SYSTEM INPUT & OUTPUT.
C
        CALL FFET1(NBLCK)
 22     CALL RDNL(26,'SYSTEM INPUT CHANNEL NO = ',IN)
        CALL RDNL(27,'SYSTEM OUTPUT CHANNEL NO = ',IOUT)
        N=ICHAN(7)
        N2=N/2
        NCHAN=ICHAN(3)
        CALL WTNL(13,'BLOCK SIZE = ',N)
        CALL WTNL(21,'NO OF SPECTRAL PTS = ',N2)
        CALL RDNL(26,'NO OF PTS FOR SMOOTHING = ',NSMOOTH)
C
C       CHOOSE SECTIONS OF DATA FOR 2 ESTIMATES.
C       DECIDE FREQUENCY RANGE OF INTEREST.
C
        CALL WTNL(24,'ESTIMATE 1 SPECIFICATION')
        CALL RDNL(14,'START BLOCK = ',IST1)
        CALL RDNL(12,'END BLOCK = ',IF1)
        CALL WTNL(24,'ESTIMATE 2 SPECIFICATION')
        CALL RDNL(14,'START BLOCK = ',IST2)
        CALL RDNL(12,'END BLOCK = ',IF2)
        CALL RD(22,'FROM SPECTRAL PT NO = ',IPT1)
        CALL RDNL(4,' TO ',IPT2)
        J=-1
        CALL RDNL(33,'IS NOISE CONSIDERED STATIONARY ? ',J,ISTAT)
        NSET=1
        NAV=IF1-IST1+1
        ISET=IST1-1
 12     CONTINUE
C
C       CALCULATE 2 ESTIMATE VALUES.
C       SKIP TO BEGINNING SECTION OF FOURIER DATA.
C
        IF (ISET .EQ. 0) GO TO 11
        DO 2 I=1,ISET
        DO 2 J=1,NCHAN
 2      CALL BUFFERIN(101,1,DUMP,N,IST)
```

```
      SMX(1)=PXY2(1)
      SMY(1)=PYY2(1)
      SMXY(1)=PXY2(1)
      ICOUNT(1)=1
      DO 8 I=IPT1,IPT2
      IST=I-NSMOOTH/2
      IFIN=I+NSMOOTH/2
      DO 8 J=IST,IFIN
      IF (J .LT. 2 .OR. J .GT. N2) GO TO 8
      ICOUNT(I)=ICOUNT(I)+1
      SMX(I)=SMX(I)+PXX2(J)
      SMY(I)=SMY(I)+PYY2(J)
      SMXY(I)=SMXY(I)+PXY2(J)
8     CONTINUE
      DO 9 J=IPT1,IPT2
      PXX2(J)=SMX(J)/ICOUNT(J)
      PYY2(J)=SMY(J)/ICOUNT(J)
9     PXY2(J)=SMXY(J)/ICOUNT(J)
15    IF (NSET .EQ. 2) GO TO 10
C
C     GO BACK & CALCULATE SECOND ESTIMATE.
C     TRANSFER CURRENT ESTIMATE TO FIRST REGISTER.
C
      NAV=IF2-IST2+1
      ISET=IST2-IF1-1
      DO 13 I=IPT1,IPT2
      PXX1(I)=PXX2(I)
      PYY1(I)=PYY2(I)
13    PXY1(I)=PXY2(I)
      NSET=2
      GO TO 12
C
C     ZERO INITIAL CONFIDENCE INTERVALS.
C     PERFORM STATIONARITY TEST AS AVERAGE SUM OVER FREQ RANGE OF
C     INTEREST.
C
10    CONXX=0.0
```

```
      CONYY=0.0
      CONNN=0.0
      CONH=0.0
C
C     SWAP BUFFERS IF NECESSARY
C
      L1=IF1-IST1
      L2=IF2-IST2
      IF (L1 .LE. L2) GO TO 40
      I=IF1
      J=IST1
      IST1=IST2
      IF1=IF2
      IST2=J
      IF2=I
      DO 41 I=IPT1,IPT2
      DUMP(I)=PXX1(I)
      DUMP(N2+I)=PYY1(I)
      XJW=PXY1(I)
      PXX1(I)=PXX2(I)
      PYY1(I)=PYY2(I)
      PXY1(I)=PXY2(I)
      PXX2(I)=DUMP(I)
      PYY2(I)=DUMP(N2+I)
      PXY2(I)=XJW
 41   CONTINUE
 40   CONTINUE
      NLIM=NSMOOTH/2+1
      ICALC=0
      DO 14 I=IPT1,IPT2
      PX(1)=PXX1(I)
      PX(2)=PXX2(I)
      PY(1)=PYY1(I)
      PY(2)=PYY2(I)
      XY(1)=PXY1(I)
      XY(2)=PXY2(I)
C
```

```
C       SET UP DEGREES OF FREEDOM OF ESTIMATES.
C
        L1=(IF1-IST1+1)*NSMOOTH
        L2=(IF2-IST2+1)*NSMOOTH
        IF (I .LE. NLIM) L1=(IF1-IST1+1)*(NLIM-1+I)
        IF (I .LE. NLIM) L2=(IF2-IST2+1)*(NLIM-1+I)
        IF ((N2-I) .LT. NLIM) L1=(IF1-IST1+1)*(NSMOOTH/2+1+N2-I)
        IF ((N2-I) .LT. NLIM) L2=(IF2-IST2+1)*(NLIM+N2-I)
        IF (I .LE. (NLIM+1) .OR. (N2-I) .LT. (NLIM-1)) ICALC=0
        IF (I .EQ. 1) L1=(IF1-IST1+1)
        IF (I .EQ. 1) L2=IF2-IST2+1
C
C       DO STATIONARITY TEST ON ITH FREQ POINT.
C
        CALL STATION(PX,PY,XY,L1,L2,CH,CXX,CYY,CNN,ISTAT,ICALC)
C
C       ADD UP TO FIND MEAN CONFIDENCE LEVEL.
C
        CONXX=CONXX+CXX
        CONYY=CONYY+CYY
        CONNN=CONNN+CNN
  14    CONH=CONH+CH
        NPTS=IPT2-IPT1+1
        CONXX=CONXX/NPTS
        CONYY=CONYY/NPTS
        CONNN=CONNN/NPTS
        CONH=CONH/NPTS
C
C       DISPLAY CONFIDENCE INTERVAL.
C
        CALL WT(6,'CXX = ',CONXX)
        CALL WT(7,' CYY = ',CONYY)
        CALL WT(7,' CNN = ',CONNN)
        CALL WTNL(6,' CH = ',CONH)
        CALL SKIPFILE(101,0)
        CALL BUFFERIN(101,1,ICHAN,90,IST)
C
```

```
C       CHOOSE NEXT ACTION.
C
        CALL CHOOSE(18,'(RE)PEAT,(EX)IT,!!',2,'REPEAT,EXIT;',J)
        GO TO (20,21) J
  20    CALL HOME
        CALL ERASE
C
C       GO BACK & CHOOSE NEW SECTION OF DATA,
C
        GO TO 22
  21    REWIND 101
        RETURN
        END
```

```
C
C
C
      SUBROUTINE STATION(PXX,PYY,PXY,L1,L2,CH,CXX,CYY,CNN,ISTAT,ICALC)
      DIMENSION PXX(2),PYY(2),PXY(2),PNN(2),H(2)
      COMPLEX PXY,H
C
C     CALCULATE NOISE AUTO-SPECTRAL ESTIMATES
C
      PNN(1)=PYY(1)-(CABS(PXY(1))**2)/PXX(1)
      PNN(2)=PYY(2)-(CABS(PXY(2))**2)/PXX(2)
C
C     DO F-TEST ON PXX,PYY,PNN PUTTING CONFIDENCE RESULT IN CXX,CYY
C     CNN RESP.
C
C
      V1=PXX(1)
      V2=PXX(2)
      ICNT=1
1     CONTINUE
      FINT=(V1*L1)/(V2*L2)
      IF (L2 .GT. 2) GO TO 10
      VAR=13.0
      GO TO 11
10    VAR=(L1+L2)*L1
      VAR=VAR/(((L2-1.0)**2)*(L2-2.0))
      VAR=SQRT(VAR)
11    EX=L1
      EX=EX/L2
      FLIM=EX+3.0*VAR
      IF (FINT .LT. FLIM) GO TO 12
      PF=100.0
      GO TO 2
12    NSTEPS=91
      IF ((L1+L2) .GT. 1000) NSTEPS=183
      STEP=FINT/(NSTEPS-1.0)
      F=0.0
```

```
      P=FPROB(F,L1,L2,COEFF,LC,ICALC)*STEP/3.0
      ICALC=1
      MULT=2
      DO 18 K=2,NSTEPS
      MULT=MULT*2
      IF (MULT .GT. 4) MULT=2
      IF (K .EQ. NSTEPS) MULT=1
      F=(K-1)*STEP
 18   P=P+FPROB(F,L1,L2,COEFF,LC,ICALC)*MULT*STEP/3.0
C
C     SET CONFIDENCE INTERVAL PF.
C
      IF (P .GE. 0.5) PF=P-0.5
      IF (P .LT. 0.5) PF=0.5-P
      PF=PF*200.0
      IF (PF .GT. 100.0) PF=100.0
 2    GO TO (5,4,3) ICNT
 5    ICNT=2
C
C     SET UP PYY CONFIDENCE TEST
C     STORE PXX CONFIDENCE RESULT.
C
      V1=PYY(1)
      V2=PYY(2)
      CXX=PF
      GO TO 1
 4    ICNT=3
C
C     SET UP PNN CONFIDENCE TEST.
C     STORE PYY CONFIDENCE RESULT.
      L1=L1-1
      L2=L2-1
      CYY=PF
      PF=100.0
      IF (L1 .EQ. 0 .OR. L2 .EQ. 0) GO TO 3
      V1=PNN(1)
      V2=PNN(2)
```

```
      GØ TØ 1
 3    CNN=PF
C
C     STØRE PNN CØNFIDENCE RESULT.
C
      L1=L1+1
      L2=L2+1
      CH=100.0
      IF (L1 .EQ. 1 .ØR. L2 .EQ. 1) RETURN
C
C     CALCULATE EXPECTED NØISE VARIANCE FØR ESTIMATES.
C     DØ STATIØNARITY TEST ØN H GIVEN PXX1,PXX2
C
      IF (ISTAT .NE. 8ZE8404040) GØ TØ 20
      PNN(1)=(PNN(1)*L1+PNN(2)*L2)/(L1+L2)
      PNN(1)=PNN(1)*(L1+L2)/(L1+L2-1)
      PNN(2)=PNN(1)
      GØ TØ 21
20    PNN(1)=PNN(1)*L1/(L1-1)
      PNN(2)=PNN(2)*L2/(L2-1)
21    H(1)=PXY(1)/PXX(1)
      H(2)=PXY(2)/PXX(2)
      X2=CABS(H(1)-H(2))**2
      VAR=PNN(1)/(PXX(1)*L1)+PNN(2)/(PXX(2)*L2)
      CH=1.0-EXP((-X2)/(2.0*VAR))
7     CH=CH*100.0
      RETURN
      END
```

```
      FUNCTION FPROB(F,L1,L2,COEFF,LC,ICALC)
      IF (F .GT. 0.0) GO TO 1
      FPROB=0.0
      IF (L1 .EQ. 1) FPROB=FLOAT(L2)
1     F1=F+1.0
      LIM1=L1-1
      LIMTOT=L1+L2-1
      IF (ICALC .EQ. 1) GO TO 3
      LC=0
      COEFF=1.0
      R=1.0
      DO 2 I=L2,LIMTOT
      COEFF=COEFF*I
      IF (I .LT. LIMTOT) COEFF=COEFF/R
      IF (COEFF .LT. 1.0E60) GO TO 2
      J=ALOG10(COEFF)
      COEFF=COEFF/(10.0**J)
      LC=LC+J
2     R=R+1.0
      COEFF=ALOG10(COEFF)
3     CONTINUE
      IF (F .EQ. 0.0) RETURN
      R=ALOG10(F)*LIM1
      R1=ALOG10(F1)*(LIMTOT+1)
      R=R-R1
      FPROB=10.0**(R+COEFF+LC)
      RETURN
      END
```

FATIGUE RIG CONTROL

AUTHOR : P. W. DAVALL

LANGUAGE : FORTRAN IV/MACRO-SYMBOL

```
      SUBROUTINE MP
C
C
C
C     THIS PROGRAM CONTROLS A FATIGUE TEST RIG COMPENSATING FOR THE RIG
C     DYNAMICS IN ORDER TO LOAD THE SPECIMEN WITH THE REQUIRED LOADING
C     PATTERN. THE LOADING SIGNAL IS SPECIFIED BY THE USER AT RUN TIME.
C     ACHIEVED LOADING & POSN. DATA MAY BE LOGGED ON MAG TAPE FOR LATER
C     ANALYSIS. AN INTERNAL PRBS GENERATOR IS USED FOR SIGNAL OUTPUT.
C     THE GENERATOR SIGNAL IS OUTPUT ON CHANNEL 1 WHILE THE ACHIEVED
C     LOAD,POSN AND START STOP LINES ARE ANALOGUE INPUTS 1,2,3 RESP.
C     THE PROGRAMMED TEST IS STOPPED BY INPUTTING +6.0V ON LINE 3.
C
C
C
C
      COMMON /FRTG/FRIG1
      COMMON RE(1024),IM(1024),N,M,ISIGN,FCOS(129),FCTR
      COMMON /SET1/X(1024),Y(1024),XJW(256),X0JW(256),YJW(256),PXY(256),
     &PXX(256)
      COMMON /SET2/TF(256),CONT(256)
         COMMON /SET3/ IREG,PRBS(24),NPRBS
      COMMON /SET4/KPT,NMOD,KS,IOPEN,GAMP,NSMOOTH,ICLOCK,NEST
      COMMON /SET5/COST,PHASE,SIGMAX,NCNT,CORRECT,CSTMIN,ITRAP,NLIM
     &,COST1
      COMMON /SET6/IWAIT
      COMMON /SET8/XTT(1024)
      COMMON /SET9/IEXT,INHIBIT
      COMPLEX XJW,X0JW,YJW,PXY
      COMPLEX TF,CONT
      REAL IM
      CALL COCINIT(2,1S)
1     CALL HOME
      CALL ERASE
      VOUT=0.0
      CALL RDAC(1,VOUT)
      CALL WTNL(36,'ANALOGUE OUTPUT 1 = DRIVING FUNCTION')
```

```
      CALL WTNL(36,'ANALOGUE INPUT 1 = ACHIEVED FUNCTION')
      CALL WTNL(33,'ANALOGUE INPUT 2 = POSITION INPUT')
      CALL WTNL(21,'INPUT 3 = STOP ACTION')
      CALL WTNL(40,'ANALOGUE INPUT 4 = EXTERNAL INPUT SIGNAL')
         IREG=8ZAAAAAAAA
C
C     SET UP RUN TIME CHARACTERISTICS.
C     GAMP=EXTERNAL AMPLIFIER GAIN IN ACHIEVED LOAD SIGNAL.
C     NLIM <256
C     NMOD = NO OF BLOCKS BEFORE CONTROLLER UPDATES,SAMPLE & HOLD TYPE
C     COMPENSATION USED.
C     0<CORRECT<1.0
C
      CALL RDNL(21,'NO OF P.R.B.S. WTS = ',NPRBS)
      IF (NPRBS .EQ. 0) GO TO 30
      CALL WTNL(30,'(((      INPUT WEIGHTING VALUES')
      CALL WTNL(23,'          NO      WEIGHT')
      DO 2 I=1,NPRBS
      CALL WT(10,'            ',I)
 2     CALL RDNL(5,'      ',PRBS(NPRBS+1-I))
 30   CONTINUE
      CALL RDNL(29,'TEST SAMPLING TIME (MSECS) = ',ICLOCK)
      CALL RDNL(24,'AMPLIFIER GAIN FACTOR = ',GAMP)
      CALL RDNL(30,'MAX AMP DRIVER SIGNAL LEVEL = ',SIGMAX)
      CALL RDNL(28,'MAX PT FOR TF MEASUREMENT = ',NLIM)
      CALL RDNL(32,'SMOOTHING FACTOR (ODD NUMBER) = ',NSMOOTH)
      J=-1
      CALL RDNL(33,'IS SIGNAL GENERATED EXTERNALLY : ',J,IEXT)
      IF (IEXT .EQ. 8ZE8404040) CALL RDNL(32,'EXTERNAL INPUT SCALING FAC
     &TOR = ',FRIG1)
      CALL RDNL(47,'STATIONARITY TESTING INTERVAL (NO OF BLOCKS) = ',NMO
     &D)
      CALL RDNL(37,'% CORRECTION FACTOR FOR CONTROLLER = ',CORRECT)
C
C     OUTPUT RUN SPECIFICATIONS TO LINE-PRINTER.
C
      WRITE(108,6)
```

```
 6     FORMAT(1H1,40X,18HRUN SPECIFICATIONS)
       WRITE(108,7)
 7     FORMAT(40X,18H******************)
       WRITE(108,8)
 8     FORMAT(5X,25HP.R.B.S. WEIGHTING VALUES)
       DO 9 I=1,NPRBS
 9     WRITE(108,10) I,PRBS(NPRBS+1-I)
 10    FORMAT(5X,I3,5X,F7.5)
       WRITE(108,11) NSMOOTH,NMOD,CORRECT
 11    FORMAT(5X,26HNO OF PTS FOR SMOOTHING = ,I3,5X,22HBLOCK UPDATE PERI
      &OD = ,I3,5X,20HCORRECTION FACTOR = ,F6.2)
       WRITE(108,17) ICLOCK,NLIM,GAMP
 17    FORMAT (1HO,5X,14HSAMPLE TIME = ,I3,7H MSECS.,5X,28HMAX PT FOR TF
      &MEASUREMENT = ,I3,5X,17HAMPLIFIER GAIN = ,F7.3)
C
C      INITIALISE REGISTERS
C
       IWAIT=0
       PHASE=0.0
       COST=0.0
       COST1=0.0
       CORRECT=CORRECT/100.0
       ITRAP=0
       CSTMIN=1.0E6
       NCNT=0
       KPT=0
       KS=1024
       N=512
       M=9
       ISIGN=-1
       FCTR=N
       ICLOCK=ICLOCK*2
       NEST=NLIM/NSMOOTH
       NLIM=NEST*NSMOOTH+1
       DO 4 I=1,129
  4    FCOS(I)=COS(6.2831853*(I-1)/N)
C
```

```
C     GENERATE INITIAL TIME DATA FROM PRBS & STORE INITIAL FOURIER COEFFS.
C
      INHIBIT=0
      IF (IEXT .NE. 8ZE8404040) GO TO 20
      INHIBIT=1
      CALL DISAB(2Z67)
      CALL TIMER(ICLOCK,2Z67)
      CALL ENAB(2Z67)
 23   CONTINUE
      IF (INHIBIT .LT. 1025) GO TO 23
      INHIBIT=0
      DO 21 I=1,512
 21   RE(I)=XTT(I)
      GO TO 22
 20   CALL RANDMM
 22   DO 12 J=1,512
      Y(512+J)=RF(J)
      X(J)=RE(J)
      XTT(J)=X(J)
 12   IM(J)=0.0
      X(1024)=X(1)
      XTT(1024)=XTT(1)
      CALL FFA
C
C     SET INITIAL CONTROLLER VALUES TO UNITY GAIN.
C
      DO 13 I=1,256
      CONT(I)=CMPLX(1.0,0.0)
      PXX(I)=0.0
      PXY(I)=CMPLX(0.0,0.0)
      TF(I)=CMPLX(1.0,0.0)
      XOJW(I)=CMPLX(RE(I),IM(I))
      XJW(I)=XOJW(I)
 13   XOJW(I)=CONJG(XOJW(I))
C
C     OPEN FILE FOR DATA LOGGING ON MAG TAPE.
C
```

```
      J=-1
      CALL RDNL(27,'DØ YØU WANT TØ ØPEN FILE : ',J,IØPEN)
      IF (IØPEN .EQ. 8ZE8404040) CALL FILEHEAD
C
C     LØG ERRØR CØST FN. ØN LINE-PRINTER.
C
      WRITE(108,16)
 16   FØRMAT(1H1,10X,19HERRØR CØST FUNCTIØN)
      J=-1
      CALL RDNL(30,'TEST READY INDICATE TØ PRØCEED',J,I)
C
C     RUN TEST
C
      CALL WT(16,'TEST IN RUN MØDE')
      CALL DISAB(2Z67)
      CALL TIMER(ICLØCK,2Z67)
      CALL ENAB(2Z67)
      CALL WAIT
C
C     PLØT RESULTS ØF FREQUENCY RESPØNSE FN. AS PERTAINING AT END ØF
C     TEST
C
      CALL ENDTEST
      GØ TØ 1
      RETURN
      END
```

```
C
C
C
      SUBROUTINE FILEHEAD
C
C
C     OPEN FILE HEADER FOR DATA ANALYSIS TAPE.
C
C
      COMMON /HEADER/IH(90)
      COMMON /SET4/KPT,NMOD,KS,IOPEN,GAMP,NSMOOTH,ICLOCK,NEST
      DIMENSION RH(90)
      EQUIVALENCE (RH,IH)
      CALL HOME
      CALL ERASE
      IBC=-8
      CALL RDNL(12,'FILE NAME : ',IBC,IH(1))
      IH(3)=3
      IH(6)=1
      IH(11)=8ZC6C4C5D4
      IH(12)=8ZC1D4C440
      IH(13)=8ZF5D6D3E3
      IH(14)=8ZE2404040
      RH(15)=1.0
      IH(17)=8ZC6C1D7D7
      IH(18)=8ZD3C9C5C4
      IH(19)=IH(13)
      IH(20)=IH(14)
      RH(21)=1.0
      IH(23)=8ZD7D6E240
      IH(24)=8Z40404040
      IH(25)=IH(13)
      IH(26)=IH(14)
      RH(27)=1.0
      IH(65)=8ZE3C9D4C5
      IH(66)=8Z40404040
      IH(67)=8ZD4E2C5C3
```

```
      IH(68)=8ZF2404040
      RH(69)=ICLOCK/2.0
      RH(70)=0.0
C
C     PUT IN REQUIRED COMMENTS FOR CURRENT RUN.
C
      IBC=-80
      CALL RDNL(10,'COMMENT : ',IBC,IH(71))
      WRITE(108,2) IH(1),IH(2)
    2 FORMAT(1H0,10X,A4,A4)
      WRITE(108,3)
    3 FORMAT(10X,10H**********)
      WRITE(108,1) (IH(I),I=71,90)
    1 FORMAT(1H0,20(A4))
      CALL WTNL(12,'OPENING FILE')
      CALL OPENFIL(IH)
      RETURN
      END
```

```
C
C
C
      SUBROUTINE RIGSAMP
C
C
C     SUBROUTINE OUTPUTS A DRIVING SIGNAL TO THE RIG & SAMPLES
C     THE RESULTING ACHIEVED LOAD & POSN. THIS MAY THEN BE RECORDED
C     ON MAGNETIC TAPE.
C
C
      COMMON /FRIG/FRIG1
      COMMON /SET1/X(1024),Y(1024),XJW(256),XOJW(256),YJW(256),PXY(256),
     &PXX(256)
      COMMON /SET4/KPT,NMOD,KS,IOPEN,GAMP,NSMOOTH,ICLOCK,NEST
      COMMON /SET6/IWAIT
      COMMON /SAMPARR/S,SA(4)
      COMMON /SET8/XTT(1024)
      COMMON /SET9/IEXT,INHIBIT
      COMPLEX XJW,XOJW,YJW,PXY
      DIMENSION SV(5)
      EQUIVALENCE (SV,S)
      DATA TEND /6.0/
      DATA V0/0.0/
C
C     INITIAL SET UP PROCEDURE WHEN SYSTEM IS DRIVEN BY EXTERNAL
      DATA ICHAN,NCHAN,GAIN/1,4,10.0/
C     SIGNAL
C
      IF (INHIBIT .EQ. 0) GO TO 6
      CALL RADCS(1,XTT(INHIBIT),GAIN,4)
      INHIBIT=INHIBIT+1
      IF (INHIBIT .GE. 1025) CALL DISAB(2Z67)
      RETURN
    6 CONTINUE
C
C     OUTPUT REQUIRED LOADING SIGNAL.
```

```
C
      CALL RDAC(1,X(KS))
C
C     STORE DEMANDED LEADING SIGNAL.
C
      S=XTT(KS)
C
C     SAMPLE RIG OUTPUT SIGNALS.
C
      CALL RADCS(NCHAN,SA,GAIN,ICHAN)
      IF (SV(4) .LT. TEND) GO TO 1
      VOUT=0.0
      CALL RDAC(1,VOUT)
      CALL DISAB(2Z67)
      IF (IOPEN .EQ. 8ZE8404040) CALL CLOSEFIL
C
C     STOP TEST TRIGGER END ACTION.
C
      CALL TRIGR(2Z69)
      RETURN
 1    SV(2)=SV(2)/GAMP
      IF (IEXT .EQ. 8ZE8404040) XTT(KS)=SV(5)*FRIG1
      SV(3)=X(KS)
C
C     STORE ON MAG. TAPE
C
      IF (IOPEN .EQ. 8ZE8404040) CALL MOUTPUT(SV)
      Y(KS)=SV(2)
C
C     TEST FOR SIGNAL GENERATOR & UPDATING REQUIRED.
C
      IF (KS .EQ. 1024 .OR. KS .EQ. 512) GO TO 4
      GO TO 3
 4    IF (IWAIT .EQ. 0) GO TO 5
      CALL WAIT
      GO TO 4
C
```

```
C       TRIGGER FOURIER ANALYSIS OF OLD DATA & UPDATE PROCEDURE.
C
 5      CALL TRIGR(2Z68)
 3      IF (KS .EQ. 1024) KS=0
C
C       INCREMENT DATA LOADER/OUTPUT ARRAY POINTER.
C
 2      KS=KS+1
        RETURN
        END
```

```
C
C
C
      SUBROUTINE UPDATE
C
C
C     THIS SUBROUTINE CALCULATES THE RIG FREQ. RESPONSE OVER NMOD BLOCKS
C     &THEN CORRECTS THE COMPENSATOR 'CONT' TO ACHIEVE AN OVERALL TIME DELAY
C     FREQ. RESPONSE BETWEEN INPUT DEMANDED AND OUTPUT ACHIEVED LOADING.
C
C
C
      COMMON RE(1024),IM(1024),N,M,ISIGN,FCOS(129),FCTR
      COMMON /SET1/X(1024),Y(1024),XJW(256),XOJW(256),YJW(256),PXY(256),
     &PXX(256)
      COMMON /SET2/TF(256),CONT(256)
      COMMON /SET4/KPT,NMOD,KS,IOPEN,GAMP,NSMOOTH,ICLOCK,NEST
      COMMON /SET5/COST,PHASE,SIGMAX,NCNT,CORRECT,CSTMIN,ITRAP,NLIM
     &,COST1
      COMMON /SET6/IWAIT
      COMMON /SET8/XTT(1024)
      COMMON /SET9/IEXT,INHIBIT
      REAL IM
      COMPLEX TF,CONT
      COMPLEX XJW,XOJW,YJW,PXY
      COMPLEX TRY,TFM
      DIMENSION YF(512),XF(512)
      EQUIVALENCE (YJW,YF),(XOJW,XF)
      IWAIT=1
C
C     SET UP REQUIRED POINTER FROM WHICH ANALYSIS IS TO TAKE PLACE.
C
      KPT=KPT+512
      IF (KPT .EQ. 1024) KPT=0
      ISIGN=-1
      FCTR=N
      DO 1 I=1,512
```

```
      RE(I)=Y(KPT+I)
 1    IM(I)=0.0
C
C     FOURIER TRANSFORM PREVIOUS 512 SAMPLES OF Y(T), OUTPUT ERROR COST
C     FN. TO LINE PRINTER.
C
      CALL FFA
      NCNT=NCNT+1
      IF (NCNT .EQ. 1) WRITE(108,40) COST1
 40   FORMAT (15X,F10.2)
      IF (NCNT .EQ. 1) GO TO 8
C
C     CALCULATE INPUT AUTO-SPECTRUM & INPUT/OUTPUT CROSS-SPECTRUM.
C
      DO 2 I=2,NLIM
      TRY=CMPLX(RE(I),IM(I))
      YJW(I)=TRY*XOJW(I)
 2    XOJW(I)=CABS(XOJW(I))**2
C
C     SMOOTH OVER FREQUENCY AS REQUIRED.
C
      IF (NSMOOTH .LT. 3) GO TO 8
      DO 101 I=1,NEST
      RE(I)=0.0
      RE(512+I)=0.0
      IM(I)=0.0
      IAR=(I-1)*NSMOOTH+1
      DO 100 J=1,NSMOOTH
      RE(I)=RE(I)+REAL(YJW(IAR+J))
      RE(512+I)=RE(512+I)+AIMAG(YJW(IAR+J))
 100  IM(I)=IM(I)+REAL(XOJW(IAR+J))
      RE(I)=RE(I)/NSMOOTH
      RE(512+I)=RE(512+I)/NSMOOTH
      IM(I)=IM(I)/NSMOOTH
 101  CONTINUE
      NSTOP=NEST-1
      DO 102 I=1,NSTOP
```

```
      ISTART=(I-1)*NSM00TH+NSM00TH/2+1
      DRY=(RE(I+1)-RE(I))/NSM00TH
      DIY=(RE(513+I)-RE(512+I))/NSM00TH
      DRX=(IM(I+1)-IM(I))/NSM00TH
103   D0 102 J=1,NSM00TH
      IAR=(ISTART+J)*2
      YF(IAR-1)=RE(I)+(J-1)*DRY
      YF(IAR)=RE(512+I)+(J-1)*DIY
102   XF(IAR-1)=IM(I)+(J-1)*DRX
      N2=NSM00TH/2+1
      ISTART=(NEST-1)*NSM00TH+NSM00TH/2+1
      D0 105 J=1,N2
      IAR=(ISTART+J)*2
      YF(IAR-1)=RE(NEST)
      YF(IAR)=RE(512+NEST)
      TRY=CMPLX(C0S((J-1)*PHASE),SIN((J-1)*PHASE))
      YJW(ISTART+J)=YJW(ISTART+J)*TRY
      YJW(J)=CABS(YJW(N2+1))
      YJW(J)=YJW(J)*TRY
      X0JW(J)=X0JW(N2+1)
 105  XF(IAR-1)=IM(NEST)
 8    CONTINUE
C
C     AVERAGE SPECTRAL ESTIMATES OVER TIME
C
      D0 3 I=2,NLIN
      IM(I)=0.0
      IF (NCNT .EQ. 1) G0 T0 3
      PXX(I)=PXX(I)+CABS(X0JW(I))
      PXY(I)=PXY(I)+YJW(I)
      TF(I)=PXY(I)/PXX(I)
 3    X0JW(I)=C0NJG(XJW(I))
      TF(1)=CMPLX(1.0,0.0)
      IM(1)=0.0
      IF (NCNT .EQ. 1) G0 T0 9
C
C     ESTIMATE INTEGRAL ERR0R SQUARED C0ST FN BETWEEN ACHIEVED
```

```
C       LOADING FREQ. RESPONSE & DESIRED TIME DELAY FREQ. RESPONSE
C
        DO 4 I=2,NLIM
        TFM=CMPLX(COS((I-1)*PHASE),SIN((I-1)*PHASE))
  4     COST=COST+CABS(TFM-TF(I))
  9     LIM=NLIM+1
        DO 5 I=LIM,256
  5     IM(I)=0.0
        IF (NCNT .LT. NMOD) GO TO 6
        COST1=COST/(NMOD-1.0)
        NCNT=0
C
C       CALCULATE BEST AVAILABLE TIME DELAY APPROXIMATION
C       ZERO SPECTRAL ESTIMATES
C
        PHASE=0.0
        DO 7 I=1,256
        IF (I .GT. NLIM) GO TO 50
        PH1=ATAN2(AIMAG(TF(I)),REAL(TF(I)))
        IF (I .GT. 100 .AND. PH1 .GT. 0.0) PH1=PH1-6.2831854
        PHASE=PHASE+PH1
 50     CONTINUE
        PXX(I)=0.0
        PXY(I)=0.0
  7     CONTINUE
        PHASE=PHASE/((NLIM-1.0)*NLIM/2.0)
        IF (PHASE .GT. 0.0) PHASE=0.0
        IF (PHASE .LT. -0.0123) PHASE=-0.0123
        DO 32 I=LIM,256
 32     TF(I)=CMPLX(COS((I-1)*PHASE),SIN((I-1)*PHASE))
        IF (COST1 .LT. CSTMIN) CSTMIN=COST1
C
C       UPDATE CONTROLLER CHARACTERISTICS.
C       MODIFY CONTROLLER TO ACHIEVE DESIRED TIME DELAY OVER NEXT
C       ESTIMATION PERIOD
C
        DO 13 I=1,256
```

```
      TFM=CMPLX(COS((I-1)*PHASE),SIN((I-1)*PHASE))
      TFM=TF(I)+(TFM-TF(I))*CORRECT
 13   CONT(I)=TFM*CONT(I)/TF(I)
 14   COST=0.0
 6    CONTINUE
C
C     GENERATE REQUIRED LOADING SIGNAL FOR NEXT BLOCK OF 512 SAMPLES.
C
      IF (IEXT .NE. 8ZE8404040) GO TO 60
      DO 61 I=1,512
 61   RE(I)=XTT(KPT+I)
      GO TO 62
 60   CALL RANDOM
      DO 64 I=1,512
 64   XTT(KPT+I)=RE(I)
 62   CALL FFA
C
C     MODIFY NEXT X(T) TO ALLOW FOR RIG DYNAMICS
C
      DO 20 I=1,256
      XJW(I)=CMPLX(RE(I),IM(I))
      TRY=XJW(I)*CONT(I)
      RE(I)=REAL(TRY)
      IM(I)=AIMAG(TRY)
      IF (I .EQ. 1) GO TO 20
      RE(514-I)=RE(I)
      IM(514-I)=-IM(I)
 20   CONTINUE
      ISIGN=+1
      CALL FFA
C
C     TEST FOR SATURATION AND COUNTERACT BY REDUCING GAIN ON ALL FREQS.
C
      SIG=0.0
      DO 18 I=1,512
 18   IF (ABS(RE(I)) .GT. SIG) SIG=ABS(RE(I))
      IF (SIG .LT. SIGMAX) GO TO 17
```

```
      IF (ITRAP .EQ. 1) GO TO 17
      DO 22 I=1,256
      PXX(I)=0.0
      PXY(I)=CMPLX(0.0,0.0)
      RE(I)=RE(I)*SIGMAX/SIG
      RE(256+I)=RE(256+I)*SIGMAX/SIG
 22   CONT(I)=CONT(I)*SIGMAX/SIG
      COST=0.0
      NCNT=0
      CORRECT=CORRECT*0.5
 17   CONTINUE
C
C     SET UP NEXT SET OF DRIVER SIGNALS
C
      DO 16 I=1,512
      X(KPT+I)=RE(I)
16    CONTINUE
      IWAIT=0
      RETURN
      END
```

```
C
C
C
      SUBROUTINE RANDUM
C
C
C
C     PRBS GENERATOR WITH MAX. 24 BIT REGISTER
C     GENERATES 512 RANDOM NOS. PUTS RESULTS IN RE(1-512)
C
C
      COMMON RE(1024),IM(1024),N,M,ISIGN,FCTR
         COMMON /SET3/IREG,PRBS(24),NPRBS
      REAL IM
         CONTINUE
S        LW,9     IREG
S        LI,2     256
S        LI,1     0
S 2      LW,8     9
S        SLS,8    17
S        EOR,8    9
S        SLS,9    1
S        CW,8     =X'400000'
S        BAZ      $+2
S        OR,9     =1
S        LW,3     NPRBS
S        LI,8     1
S        LI,6     0
S 1      CW,8     9
S        BAZ      $+3
S        FAS,6    PRBS-1,3
S        B        $+2
S        FSS,6    PRBS-1,3
S        SLS,8    1
S        BDR,3    1S
S        STW,6    RE,1
S        AI,1     1
```

```
S           STW,6       RE,1
S           AI,1        1
S           BDR,2       2S
S           STW,9       IREG
            RETURN
            END
C
C
C
      SUBROUTINE ENDTEST

C
C     OUTPUT & PLOT THE SIGNAL & FREQUENCY RESPONSE CHARACTERISTICS AS
C     ACHIEVED AT END OF RUN
C
C
      COMMON /SET1/X(1024),Y(1024),XJW(256),XOJW(256),YJW(256),PXY(256),
     &PXX(256)
      COMMON /SET2/TF(256),CONT(256)
      COMMON /SET4/KPT,NMOD,KS,IOPEN,GAMP,NSMOOTH,ICLOCK,NEST
      COMMON /SET5/COST,PHASE,SIGMAX,NCNT,CORRECT,CSTMIN,ITRAP,NLIM
     &,COST1
      COMPLEX TF,CONT
      COMPLEX XJW,XOJW,YJW,PXY
      WRITE(108,6)
 6    FORMAT(10X,14HTEST COMPLETED)
      CALL HOME
      CALL ERASE
      J=-1
      CALL RDNL(10,'*STOP*  !!!',J,K)
      CALL ERASE
      TMAX=0.0
      PXMAX=0.0
      DO 1 I=1,256
      IF (CABS(TF(I)) .GT. TMAX) TMAX=CABS(TF(I))
 1    IF (PXX(I) .GT. PXMAX) PXMAX=PXX(I)
C
```

```
C       PLOT AXES
C
        CALL TPLOT(0,1000,300)
        CALL TPLOT(-1,600,300)
        CALL TPLOT(0,600,500)
        CALL TPLOT(-1,600,100)
        CALL TPLOT(0,500,100)
        CALL TPLOT(-1,100,100)
        CALL TPLOT(-1,100,500)
        ICLOCK=ICLOCK/2
        FPLOT=500.0/ICLOCK
        XINC=400.0/255.0
C
C       PLOT ACHIEVED OVERALL FREQ. RESPONSE.
C
        DO 2 I=1,256
        XPLOT=100.0+(I-1)*XINC
        YPLOT=100.0+CABS(TF(I))*400.0/TMAX
 2      CALL TPLOT(-1,XPLOT,YPLOT)
C
C       LABEL AXES
C
        CALL TPLOT(0,420,75)
        CALL WT(FPLOT)
        CALL TPLOT(0,600,300)
        DO 3 I=1,256
        XPLOT=600.0+(I-1)*XINC
        THETA=0.0
        IF (CABS(TF(I)) .GT. 0.0) THETA=ATAN2(AIMAG(TF(I)),REAL(TF(I)))
        YPLOT=300.0+THETA*200.0/3.14159
 3      CALL TPLOT(-1,XPLOT,YPLOT)
        CALL TPLOT(0,600,300)
C
C       PLOT OPTIMUM TIME DELAY PHASE CHARACTERISTICS.
C
        DO 5 I=1,256
        XPLOT=600.0+XINC*(I-1)
```

```
      THETA=PHASE*(I-1)
      IF (THETA .GT. 3.14159) THETA=THETA-6.2831854
      IF (THETA .LT. -3.14159) THETA=THETA+6.2831854
      YPLOT=300.0+THETA*200.0/3.14159
 5    CALL TPLOT(-1,XPLOT,YPLOT)
      CALL TPLOT(0,920,275)
      CALL WT(FPLOT)
      CALL TPLOT(0,520,475)
      CALL WT(4,'+180')
      CALL TPLOT(0,520,100)
      CALL WT(4,'-180')
      CALL TPLOT(0,100,100)
C
C     PLOT INPUT POWER SPECTRUM
C
      DO 4 I=1,256
      XPLOT=100.0+XINC*(I-1)
      YPLOT=100.0+PXX(I)*400.0/PXMAX
 4    CALL TPLOT(-1,XPLOT,YPLOT)
      CALL TPLOT(0,150,520)
      CALL WT(9,'AMPLITUDE')
      CALL TPLOT(0,650,520)
      CALL WT(11,'PHASE (DEG)')
C
C     OUTPUT RUN DATA TO V.D.U.
C
      CALL TPLOT(0,250,570)
      CALL WT(48,'RIG MEASURED TRANSFER FN AND AUTO-SPECTRUM')
      CALL HOME
      CALL WTNL(27,'     **RUN SPECIFICATIONS**')
      CALL WT(8,'TFMAX = ',TMAX)
      CALL WT(14,'     PXXMAX = ',PXMAX)
      CALL WTNL(23,'MIN ERROR COST = ',CSTMIN)
      FPLOT=FPLOT*2.0
      CALL WT(21,'SAMPLING FREQ (HZ) = ',FPLOT)
      CALL WTNL(31,'     NO OF PTS FOR SMOOTHING = ',NSMOOTH)
      SECS=512.0*NMOD/FPLOT
```

```
      CALL WT(33,'CONTROLLER UPDATE PERIOD(SECS) = ',SECS)
      J=ABS(6.2831854/PHASE)
      IF (PHASE .EQ. 0.0) J=2**30
      TDEL=512.0/(FPLOT*J)
      CALL WTNL(27,'  SYSTEM TIME DELAY(SECS) =',TDEL)
C
C     FACILITY FOR USER GRAPH LABELLING
C     RE-RUN FROM BEGINNING.
C
      CALL LABEL1
      RETURN
      END
```

HUMAN OPERATOR

TRACKING TASKS

AUTHOR : P. W. DAVALL

LANGUAGE : FORTRAN IV/MACRO-SYMBOL

```
      SUBROUTINE INIT
C
C
C
C     THIS PROGRAM DRIVES A SPOT ON THE C.R.T. DISPLAY & MONITORS
C     A HUMAN OPERATOR'S RESPONSE IN TRACKING THIS SPOT. THE LIGHT
C     SPOT MUST BE KEPT IN THE CENTRE OF THE SCREEN FOR GOOD TRACKING
C     CHARACTERISTICS.
C
C
C
      DIMENSION FXT(2),VOX(2),VOY(2),AR(8)
      INTEGER STOPIO/8Z0E040005/
      NSAMP=1000000
S     CAL1,5  STOPIO
      CALL COCINIT(2,1S)
      CALL HOME
      CALL ERASE
C
C     INITIALISE & CHECK ANALOGUE INPUT/OUTPUT PATCH IS CORRECT
C
      I=-1
      CALL RDNL(125,'PATCH CHECK(OUTPUT 1 =XERR(OUTPUT 2 =YERR(INPUT 3 =
     &XOUT(INPUT 4 =YOUT(INPUT 5 =STOP CONTROL(INPUT 6 =EXT XIN(INPUT 7
     &=EXT YIN',I,J)
      IRPT=8Z40404040
 1    CALL HOME
      XIN=0.0
      YIN=0.0
      PIE2=6.2831854
      TR=6.0/700.0
      DO 10 I=1,2
      VOX(I)=0.0
      VOY(I)=0.0
 10   CONTINUE
      CALL ERASE
C
```

```
C      DECIDE MODE OF DRIVER SIGNAL -
C            A) RANDOM GENERATION OF TRACKING SIGNAL IN TIME.
C            B)PERIODIC GENERATION OF TRACKING SIGNAL.
C
       CALL RDNL(50,'TYPE 1 FOR PERIODIC PT CHANGE(2 FOR RANDOM MODE = ',
      &ITYPE)
       IF (ITYPE .EQ. 1) CALL RDNL(32,'TIME CONSTANT FOR POINT CHANGE = '
      &,TIME)
       IF (ITYPE .EQ. 1) NEWNO=TIME/TR
       IF (ITYPE .EQ. 1) GO TO 2
       ISET=69
C
C      SET UP FREQ. BAND FOR RANDOM TIME GENERATION OF SIGNAL.
C
       CALL RANDOM(ISET,ISET,RAND)
       CALL RDNL(22,'LOW FREQ TIME CONST = ',T1)
       CALL RDNL(23,'HIGH FREQ TIME CONST = ',T2)
       TIME=T2+(T1-T2)*RAND
       NEWNO=TIME/TR
C
C      TEST IF REPEAT OF PREVIOUS SIGNAL GENERATOR CHARACTERISTICS IS REQUIRED.
C
 2     IF (IRPT .EQ. 8ZE8404040) GO TO 101
C
C      GENERATE X-SIGNAL CHARACTERISTICS
C
       CALL GSET
       CALL WTNL(28,'**X-SIGNAL CHARACTERISTICS**')
       CALL GENERATOR(IFX,AMPX,PHASX,NX)
       XINC=PIE2/NX
C
C      GENERATE Y-SIGNAL CHARACTERISTICS.
C
       CALL WTNL(28,'**Y-SIGNAL CHARACTERISTICS**')
       CALL GENERATOR(IFY,AMPY,PHASY,NY)
       YINC=PIE2/NY
C
```

```
C      SAMPLE INITIAL START POSN. & SET UP TEST.
C
 101   CALL JOYSAMP(XV,YV)
       CALL FBACK(V0X,V0Y,FX,FY,XV,YV,XIN,YIN,XFBACK,YFBACK)
       CALL RDAC(1,FX,2,FY)
       I=-1
C
C      OPEN MAG TAPE FILE IN DATA ANALYSIS FORMAT.
C
       CALL RDNL(27,'DO YOU WANT TO OPEN FILE : ',I,IFILE)
       IF (IFILE .NE. 8ZE8404040) GO TO 200
C
C      TEST WHETHER TEST IS 1/2 DIMENSIONAL
C      OPEN FILE
C
       CALL RDNL(47,'TYPE 1 =X-SAMPLES  2 =Y-SAMPLES  3 =X AND Y  : ',NOU
      &T)
       CALL FILEHEAD(NSAMP)
 200    I=-1
C
C      START TEST
C
       CALL RDNL(32,'(TEST SET UP INDICATE TO PROCEED',I,ICONT)
       JSAMP=0
       ICNT=0
  4    CONTINUE
C
C      DROP OUT OF INTERRUPT LEVEL TO SET SAMPLE TIME.
C
  8    IST=0
       CALL CWRITE(2,0,0,1,IST,5Z20069)
       CALL CHECK(2,IMODE,ISTAT,IBC)
       IF (IAND(ISTAT,2) .NE. 2) GO TO 8
       CALL WAIT
       JSAMP=JSAMP+1
       IF (JSAMP .LT. NSAMP) GO TO 102
C
```

```
C       OUTPUT RUN DATA ON MAG TAPE.
C
        AR(1)=XIN
        AR(2)=XV
        AR(3)=XFBACK
        AR(4)=FX
        AR(5)=YIN
        AR(6)=YV
        AR(7)=YFBACK
        AR(8)=FY
        JSAMP=0
        IF (IFILE .NE. 8ZE8404040) GO TO 102
        IF (NOUT .NE. 2) CALL MOUTPUT(AR)
        IF (NOUT .EQ. 2) CALL MOUTPUT(AR(5))
  102   CONTINUE
        ICNT=ICNT+1
        IF (ICNT .LT. NEWNO) GO TO 6
        ICNT=0
        PHASY=PHASY+YINC
        IF (PHASY .GT. PIE2) PHASY=PHASY-PIE2
        PHASX=PHASX+XINC
        IF (PHASX .GT. PIE2) PHASX=PHASX-PIE2
C
C       GENERATE NEXT TIME SAMPLE OF X & Y SIGNALS.
C       1) SINEWAVE  2)SQUARE WAVE  3) SAW-TOOTH  4)RANDOM  5)EXTERNAL DRIVER.
C
        GO TO (20,21,22,23,15),IFX
   20    XP=RANDO(AMPX,XIN)
        XP=XP-XIN
        GO TO 15
   21   XIN=SINE(AMPX,PHASX)
        GO TO 15
   22   XIN=SQUARE(AMPX,PHASX)
        GO TO 15
   23   XIN=SAW(AMPX,PHASX)
   15   GO TO (24,25,26,27,5),IFY
   24    YP=RANDO(AMPY,YIN)
```

```
      YP=YP-YIN
      GO TO 7
25    YIN=SINE(AMPY,PHASY)
      GO TO 7
26    YIN=SQUARE(AMPY,PHASY)
      GO TO 7
27    YIN=SAW(AMPY,PHASY)
7     IF (ITYPE .EQ. 1) GO TO 5
      CALL RANDOM(ISET,ISET,RAND)
      TIME=T2+(T1-T2)*RAND
      NEWNO=TIME/TR
5     IF (IFX .EQ. 1) XP=XP/(NEWNO-1)
      IF (IFY .EQ. 1) YP=YP/(NEWNO-1)
6     IF (IFX .EQ. 1) XIN=XIN+XP
      IF (IFY .EQ. 1) YIN=YIN+YP
      IF (IFX .EQ. 5 .OR. IFY .EQ. 5) CALL RADCS(2,EXT,10.0,6)
      IF (IFX .EQ. 5) XIN=EXT(1)
      IF (IFY .EQ. 5) YIN=EXT(2)
C
C     SAMPLE OPERATOR RESPONSES
C
      CALL JOYSAMP(XV,YV)
C
C     TEST FOR STOP ACTION
C
      IF (XV .GT. 50.0) GO TO 1000
      IF (NOUT .EQ. 2)XV=XIN
      IF(NOUT.EQ. 1) YV=YIN
C
C     GENERATE ERROR SIGNALS IN X & Y
C
      CALL FBACK(VOX,VOY,FX,FY,XV,YV,XIN,YIN,XFBACK,YFBACK)
      FMS=FY*3.0/9.5+4.0
C
C     OUTPUT ERROR SIGNALS TO C.R.T.
C
      CALL RDAC(1,FX,2,FY,3,FMS)
```

```
      GØ TØ 4
 1000 CALL HØME
      CALL ERASE
C
C     CLØSE DATA FILE
C     REPEAT TEST
C
      IF (IFILE .EQ. 8ZE8404040) CALL WTNL(12,'CLØSING FILE')
      IF (IFILE .EQ. 8ZE8404040) CALL CLØSEFIL
      I=-1
      CALL RDNL(65,'DØ YØU WANT TØ REPEAT TEST WITH DIFFERENT TIME CHARA
     &CTERISTICS = ',I,IRPT)
      GØ TØ 1
      RETURN
      END
```

```
C
C
C
      SUBROUTINE FILEHEAD(NSAMP)
C
C
C     THIS SUBROUTINE SETS UP THE HEADER OF A DATA ANALYSIS FILE ON MAG
C     TAPE UNIT ZERO
C
C
      COMMON /HEADER/CHAN
      DIMENSION RCHAN(90)
      INTEGER CHAN(90)
      EQUIVALENCE (CHAN,RCHAN)
      I=-1
 CALL RDNL(45,'DO YOU WANT TO USE THE PREVIOUS FILE AGAIN : ',I,ISK
&FIL)
 CALL HOME
 CALL ERASE
 IF (ISKFIL .EQ. 8ZE8404040) GO TO 103
 J=-8
 CALL RDNL(28,'**FILE-HEADER(  FILE NAME : ',J,CHAN(1))
 CALL RDNL(28,'NO OF DEPENDENT VARIABLES = ',NOFD)
 CHAN(3)=NOFD
 CHAN(6)=1
 CALL WTNL(35,'(INDEPENDENT VARIABLE SPECIFICATION')
 J=-8
 CALL RD(7,'NAME : ',J,CHAN(65))
 J=-8
 CALL RDNL(13,'     UNITS : ',J,CHAN(67))
 CALL RD(17,'INCREMENT STEP = ',RCHAN(69))
 CALL RDNL(17,'     MIN VALUE = ',RCHAN(70))
 CALL WTNL(80,'DATA AVAILABLE :(   XIN   XOUT   XFBACK   XERROR(
&YIN   YOUT   YFBACK   YERROR')
 CALL WTNL(47,'((CHANNEL NO     NAME          UNITS        SCALE')
 IST=4
 DO 1 I=1,NOFD
```

```
      IST=IST+6
      CALL WT(2,'   ',I)
      CALL WTSP(10)
      IBC=-8
      CALL RD(IBC,CHAN(IST+1))
      ISP=13-IBC
      CALL WTSP(ISP)
      IBC=-8
      CALL RD(IBC,CHAN(IST+3))
      ISP=12-IBC
      CALL WTSP(ISP)
1     CALL RDNL(RCHAN(IST+5))
      IBC=-80
      CALL RD(12,'((COMMENT : ',IBC,CHAN(71))
      CALL WTNL(13,'OPENING FILE')
      CALL ERASE
      CALL HOME
      TR=6.0/700.0
      NSAMP=RCHAN(69)/TR
      IF (NSAMP .LT. 1) NSAMP=1
      RCHAN(69)=NSAMP*TR
103   CONTINUE
      CALL OPENFIL(CHAN)
      RETURN
      END
```

```
C
C
C
      SUBROUTINE WTSP(N)
C
C     WRITES SPACES TO THE V.D.U.
C
      IF (N .LE. 0) RETURN
      DO 1 I=1,N
    1 CALL WT(1,' ')
      RETURN
      END
```

```
C
C
C
      SUBROUTINE GENERATOR(IF,AMP,PHASE,NPTS)
C
C     CHOOSE TRACKING SIGNAL CHARACTERISTICS AND INITIALISE ACCORDINGLY.
C
      CALL RDNL(97,'CHOOSE GENERATING FN(1 = RANDOM(2 = SINEWAVE(3 = SQU
     &AREWAVE(4 = SAWTOOTH(5 = EXTERNAL  TYPE IN = ',IF)
      IF (IF .EQ. 5) RETURN
      CALL RDNL(16,'MAX AMPLITUDE = ',AMP)
      IF (IF .EQ. 1) RETURN
      CALL RDNL(29,'INITIAL PHASE OF GENERATOR = ',PHASE)
      CALL RDNL(22,'NO OF PTS PER CYCLE = ',NPTS)
      RETURN
      END
```

```
C
C
C
      SUBROUTINE GSET
      COMMON GAIN,DGAIN,PGAIN,PHASE
      CALL WTNL(31,'**CONTROLLER CHARACTERISTICS**(')
      CALL RDNL(17,'ROTATION ANGLE = ',PHASE)
      CALL RDNL(17,'OPEN LOOP GAIN = ',GAIN)
      CALL RDNL(12,'DIFF GAIN = ',DGAIN)
      CALL RDNL(12,'PROP GAIN = ',PGAIN)
      RETURN
      END
```

```
C
C
C
      SUBROUTINE FBACK(I0X,I0Y,FX,FY,IX,IY,XIN,YIN,XFBACK,YFBACK)
C
C     GENERATES FEEDBACK & ERROR SIGNALS USING SPECIFIED CONTROLLER
C     IN FEEDBACK LOOP.
C
      COMMON GAIN,DGAIN,PGAIN,PHASE
      REAL I0X,I0Y,IX,IY
      DIMENSION I0X(2),I0Y(2)
      I0X(1)=I0X(2)
      I0Y(1)=I0Y(2)
      I0X(2)=IX
      I0Y(2)=IY
      FX=I0X(2)*PGAIN
      FY=I0Y(2)*PGAIN
      DX=(I0X(2)-I0X(1))
      DY=(I0Y(2)-I0Y(1))
      FX=FX+DX*DGAIN
      FY=FY+DY*DGAIN
      XFBACK=FX
      YFBACK=FY
      FX=(XIN-FX)
      FY=(YIN-FY)
      FM0D=SQRT(FX**2+FY**2)
      FM0D=FM0D*GAIN
      THETA=0.0
      IF (FX .EQ. 0.0 .AND. FY .EQ. 0.0) G0 T0 1
      THETA=ATAN2(FY,FX)
1     CONTINUE
      THETA=THETA+PHASE
      FX=FM0D*C0S(THETA)
      FY=FM0D*SIN(THETA)
      IF (ABS(FX) .GT. 9.5) FX=SIGN(9.5,FX)
      IF (ABS(FY) .GT. 9.5) FY=SIGN(9.5,FY)
      RETURN
```

```
C
C
C
      SUBROUTINE RANDOM(IX,IY,YFL)
C
C     GENERATES A RANDOM NO. IN RANGE MOD(X) <1.0
C
      IY=IX*65539
      IF (IY)5,6,6
    5 IY=IY+2147483647+1
    6 YFL=IY
      YFL=YFL*.4656613E-9
      END
```

```
C
C
C
      SUBROUTINE JOYSAMP(XV,YV)
C
C     SAMPLES OUTPUT FROM TRACKER JOYSTICK.
C
      DIMENSION SAMP(3)
      DATA XMAX,YMAX/3.75,4.25/
      CALL RADCS(3,SAMP,10.0,3)
      XV=(SAMP(1)*10.0)/XMAX
      YV=(SAMP(2)*10.0)/YMAX
      IF (SAMP(3) .GT. 6.0) XV=100.0
      RETURN
      END
```

```
      FUNCTION SINE(A,PHASE)
C     SINEWAVE GENERATOR
      SINE=A*SIN(PHASE)
      RETURN
      END
```

```
C
      FUNCTION SQUARE(A,PHASE)
C     SQUARE=WAVE GENERATOR
      B=SIN(PHASE)
      IF (B .GT. 0.0) SQUARE=A
      IF (B .LE. 0.0) SQUARE=-A
      RETURN
      END
```

```
C
      FUNCTION SAW(A,PHASE)
C     SAW=TOOTH GENERATOR
      IQ=PHASE/1.575796
      IF (IQ .EQ. 0) SAW=A*PHASE/1.575796
      IF (IQ .EQ. 1) SAW=A*(3.1415926-PHASE)/1.575796
      IF (IQ .EQ. 2) SAW=-A*(PHASE-3.1415926)/1.575796
      IF (IQ .EQ. 3) SAW=-A*(6.2831854-PHASE)/1.575796
      RETURN
      END
```

```
C
      FUNCTION RANDU(A,XPAST)
C     RANDOM GENERATOR
      DATA ISET/13/
      CALL RANDOM(ISET,ISET,RAND)
      FSTEP=2.0*A*(RAND-0.5)
      IF (ABS(XPAST+FSTEP) .GT. 9.5) FSTEP=-FSTEP
      RANDU=XPAST+FSTEP
      END
```

MODELLING HUMAN

OPERATOR RESPONSE

AUTHOR : P. W. DAVALL

LANGUAGE : FORTRAN IV/MACRO-SYMBOL

```
C
C
C
      SUBROUTINE MP
C
C
C     THIS PROGRAM TAKES UPTO A 10 PARAMETER HUMAN OPERATOR MODEL &
C     OPTIMISES THESE PARAMETERS TO MEASURED OPERATOR FREQ. RESPONSE
C     MEASUREMENTS IN OPEN-LOOP & CLOSED-LOOP MODES. THE RESPONSE DATA
C     IS FED IN ON PAPER TAPE. THE ERROR FN. WHICH THE POWELL HILLCLIMB
C     ROUTINE USES TRIES TO MINIMISE THE INTEGRAL ERROR (BETWEEN MODEL
C     & MEASURED DATA) SQUARED OVER THE REQUIRED FREQ. RANGE.
C
C
      COMMON /REF/FREF(100)/LIMITS/XMAX(10),XMIN(10)/FLIMIT/NPTS,WRES
      COMMON /HELP/IEND
      COMMON /REF1/FREF1(100)
      COMPLEX FREF
      COMPLEX FREF1
      DIMENSION X(10),E(10),RIN(200)
      DIMENSION RIN1(200)
      EQUIVALENCE (RIN,FREF),(RIN1,FREF1)
      CALL COCINIT(2,1S)
 1    CALL HOME
      CALL ERASE
      IEND=0
C
C     INPUT RUN-TIME DATA
C
      CALL DINPUT(N,NPTS,X,XMAX,XMIN,RIN,RIN1,WRES,E,ESCALE,IPRINT,ICON,
     &MAXIT)
C
C     PERFORM HILLCLIMB
C
      CALL VA04A(X,E,N,F,ESCALE,IPRINT,ICON,MAXIT)
C
C     DISPLAY FREQ. RESPONSE MODEL RESULTS.
```

```
C
      CALL DOUTPUT(N,X,F)
      GO TO 1
      RETURN
      END
```

```
C
C
C
      SUBROUTINE DOUTPUT(N,X,F)
      COMMON /REF/FREF(100)/FLIMIT/NPTS,WRES
      COMMON /FBACK/HT
      COMMON /NORM/FNVAR
      COMMON /REF1/FREF1(100)
      COMPLEX FREF,GVAL,T1,T2,T3,T4,T5
      COMPLEX FREF1
      DIMENSION X(10),HREF(200)
      F=F/FNVAR
      IRT=0
 10   CONTINUE
      CALL HOME
      CALL ERASE
C
C     OUTPUT NUMBER OF PARAMETERS USED IN HILLCLIMB + MIN ERROR FOUND
C     OUTPUT MODEL TYPE BEING DISPLAYED
C
      CALL WT(26,'(DIMENSION OF HILLCLIMB = ',N)
      CALL WTNL(29,'        MINIMUM ERROR FOUND = ',F)
      DO 4 I=1,N
      IF (I .EQ. 4) CALL WTNL
      IF (I .EQ. 7) CALL WTNL
      CALL WT(2,'X(',I)
      CALL WT(4,') = ',X(I))
      CALL WT(5,'      ')
 4    CONTINUE
      IF (HT .EQ. 0.0) CALL WTNL(16,'(      OPEN LOOP')
      IF (HT .EQ. 1.0) CALL WTNL(18,'(      CLOSED LOOP')
C
C     DRAW AXES
C
      CALL TPLOT(0,100,500)
      CALL TPLOT(-1,100,100)
      CALL TPLOT(-1,600,100)
```

```
      CALL TPLOT(0,1000,300)
      CALL TPLOT(-1,650,300)
      CALL TPLOT(0,650,150)
      CALL TPLOT(-1,650,450)
      CALL TPLOT(0,700,475)
      CALL WT(5,'PHASE')
      CALL TPLOT(0,150,525)
      CALL WT(9,'AMPLITUDE')
      FREQ=(NPTS-1)*WRES/6.2831853
      CALL TPLOT(0,510,70)
      CALL WT(FREQ)
      CALL TPLOT(0,910,270)
      CALL WT(FREQ)
      PMAX=0.0
      DO 1 I=2,NPTS
      PREF=CABS(FREF(I))
      IF (HT .EQ. 0.0) PREF=CABS(FREF1(I))
      IF (PREF .GT. PMAX) PMAX=PREF
      FREQ=(I-1)*WRES
C
C     CALCULATE MODEL VALUE AT FREQUENCY  'FREQ'
C
      CALL CONTROL(GVAL,X,FREQ)
      GVAL=GVAL/(1.0+HT*GVAL)
      PREF=CABS(GVAL)
      HREF(I)=PREF
      HREF(I+NPTS)=0.0
      IF (PREF .NE. 0.0) HREF(I+NPTS)=ATAN2(AIMAG(GVAL),REAL(GVAL))
    1 IF (PREF .GT. PMAX) PMAX=PREF
      CALL TPLOT(0,10,490)
      CALL WT(PMAX)
      CALL TPLOT(0,100,100)
      XINC=500.0/(NPTS-1)
C
C     DRAW MODEL & MEASURED CHARACTERISTICS
C
      DO 2 I=2,NPTS
```

```
      PREF=CABS(FREF(I))
      IF (HT .EQ. 0.0) PREF=CABS(FREF1(I))
      XPL=XINC*(I-1)+96.0
      YPL=400.0*PREF/PMAX+94.0
      CALL TPLOT(0,XPL,YPL)
      CALL WT(1,'X')
      YPL=400.0*HREF(I)/PMAX+94.0
      CALL TPLOT(0,XPL,YPL)
2     CALL WT(1,'O')
      XINC=350.0/(NPTS-1)
      CALL TPLOT(0,650,300)
      DO 3 I=2,NPTS
      XPL=XINC*(I-1)+646.0
      YPL=HREF(I+NPTS)*150.0/3.1415927+294.0
      CALL TPLOT(0,XPL,YPL)
      CALL WT(1,'O')
      PREF=CABS(FREF(I))
      IF (HT .EQ. 0.0) PREF=CABS(FREF1(I))
      PHASE=0.0
      IF (HT .EQ. 1.0 .AND. PREF .NE. 0.0) PHASE=ATAN2(AIMAG(FREF(I)),
     &REAL(FREF(I)))
      IF (HT.EQ. 0.0 .AND. PREF .NE. 0.0) PHASE=ATAN2(AIMAG(FREF1(I)),
     &REAL(FREF1(I)))
      YPL=PHASE*150.0/3.1415927+294.0
      CALL TPLOT(0,XPL,YPL)
3     CALL WT(1,'X')
      CALL LABEL1
      IF (HT .EQ. 0.0) IRT=1
      HT=0.0
C
C     REPEAT FOR CLOSED-LOOP MODEL
C
      IF (IRT .NE. 1) GO TO 10
      HT=1.0
      RETURN
      END
```

```
C
C
C
      SUBROUTINE DINPUT(N,NPTS,X,XMAX,XMIN,RIN,RIN1,WRES,E,ESCALE,IPRINT
     &,ICON,MAXIT)
C
C     THIS SUBROUTINE READS IN -
C        N: DIMENSION OF HILLCLIMB.
C        NPTS : THE NO. OF FN. PTS. FOR MATCHING.
C        X(1,N) :THE START VALUES FOR THE PARAMETERS.
C        XMAX : MAX PARAMETER VALUES
C        XMIN : MIN PARAMETER VALUES
C        THE MAX NO OF ITERATIONS 'MAXIT'.  THE MIN ERROR CHANGE 'ESCALE' BELOW
C        WHICH A NEW DIRECTION IN THE HILLCLIMB IS ASSUMED.
C
C
      COMMON /FBACK/HT/HEADER/HEAD
      COMMON /NORM/FNVAR
      INTEGER HEAD(15)
      DIMENSION RHEAD(15)
      DIMENSION X(10),E(10),XMAX(10),XMIN(10),RIN(200)
      DIMENSION RIN1(200)
      EQUIVALENCE (HEAD,RHEAD)
      CALL HOME
      CALL ERASE
      NSET=N
      CALL RDNL(25,'DIMENSION OF HILLCLIMB = ',N)
      IF (N .EQ. 0) N=NSET
      IF (N .EQ. 10) GO TO 51
      L=N+1
      DO 101 I=L,10
      X(I)=0.0
      XMAX(I)=0.0
      XMIN(I)=0.0
      E(I)=0.0
101   CONTINUE
51    CONTINUE
```

```
      CALL WTNL(15,'SET START PØINT')
      CALL WTNL(45,'NØ       START       MAX       MIN       ACCURACY')
      DØ 1 I=1,N
      CALL WT(I)
      CALL WT(5,'      ')
      IBC=8
      RSET=X(I)
      CALL RD(IBC,X(I))
      IF (IBC .FQ. 0) X(I)=RSET
      ISKP=11-IBC
      CALL WT(ISKP,'            ')
      IBC=8
      RSET=XMAX(I)
      CALL RD(IBC,XMAX(I))
      IF (IBC .EQ. 0) XMAX(I)=RSET
      ISKP=9-IBC
      CALL WT(ISKP,'            ')
      IBC=8
      RSET=XMIN(I)
      CALL RD(IBC,XMIN(I))
      IF (IBC .EQ. 0) XMIN(I)=RSET
      ISKP=9-IBC
      CALL WT(ISKP,'            ')
      IBC=8
      RSET=E(I)
      CALL RDNL(IBC,E(I))
      IF (IBC .EQ. 0) E(I)=RSET
1     CØNTINUE
55    CONTINUE
      HEAD(13)=0
      CALL HØME
      CALL ERASE
      J=-1
      CALL RDNL(10,'REPEAT FN?',J,IRPT)
      IF (IRPT .EQ. 8ZE8404040) GØ TØ 50
      CALL RDNL(27,'DEVICE NØ FØR DATA INPUT = ',IDV)
      IF (IDV .NE. 1) GØ TØ 55
```

```
      CALL WTNL(16,'PAPER TAPE INPUT')
      CALL BUFFERIN(1,1,HEAD,15,IST)
      CALL WT(12,'FILE NAME : ')
      CALL WTNL(8,HEAD(1))
      NPTS=HEAD(11)
      WRES=RHEAD(14)*6.2831853/(NPTS-1)
      GAINMOD=0.0
      PHASCOST=0.0
      DO 54 I=1,NPTS
      J=I*2-1
      CALL BUFFERIN(1,1,RIN(J),2,IST)
      PHASE=RIN(J+1)
      IF (I .NE. 1) GAINMOD=GAINMOD+ABS(RIN(J)-1.0)
      IF (I .NE. 1) PHASCOST=PHASCOST+ABS(PHASE)
      RIN(J+1)=RIN(J)*SIN(PHASE)
      RIN(J)=RIN(J)*COS(PHASE)
   54 CONTINUE
      GAINMOD=GAINMOD/(NPTS-1.0)
      PHASCOST=PHASCOST*180.0/(3.14159*(NPTS-1.0))
      CALL WT(9,'MODCOST =',GAINMOD)
      CALL WTNL(13,'PHASE COST = ',PHASCOST)
      IF (HEAD(13) .EQ. 8ZE8404040) GO TO 55
      CALL WT(7,'NPTS = ',NPTS)
      CALL WTNL(12,'      FMAX = ',RHEAD(14))
      CALL WT(10,'NSMOOTH = ',RHEAD(15))
      CALL WTNL(19,'      NO OF BLOCKS = ',HEAD(12))
      IBC=-1
      CALL BUFFERIN(1,1,HEAD,15,IST)
      DO 60 I=1,NPTS
      J=I*2-1
      CALL BUFFERIN(1,1,RIN1(J),2,IST)
      PHASE=RIN1(J+1)
      RIN1(J+1)=RIN1(J)*SIN(PHASE)
      RIN1(J)=RIN1(J)*COS(PHASE)
   60 CONTINUE
      CALL RDNL(2,'!!',IBC,J)
      CALL HOME
```

```
      CALL ERASE
50    CONTINUE
      HT=1.0
      CALL RDNL(23,'MAX STEP SCALE FACTOR = ',ESCALE)
      CALL RDNL(95,'PRINT CONTROL(0= NO PRINTING(1= PRINT AFTER EVERY LI
     &NE SEARCH(2= PRINT AFTER EVERY ITERATION = ',IPRINT)
      I=-1
      CALL RDNL(32,'DO YOU WANT CONVERGENCE CHECK : ',I,ICON)
      IF (ICON .EQ. 8ZE8404040) ICON=2
      IF (ICON .NE. 2) ICON=1
      CALL RDNL(23,'MAX NO OF ITERATIONS = ',MAXIT)
      FNVAR=0.0
      DO 57 I=2,NPTS
      J=I*2-1
      FNVAR=FNVAR+RIN1(J)**2+RIN1(J+1)**2
57    FNVAR=FNVAR+RIN(J)**2+RIN(J+1)**2
      RETURN
      END
```

```
C
C
C
      SUBROUTINE VA04A (X,E,N,F,ESCALE,IPRINT,ICON,MAXIT)                    VA04A010
CVA04A    MINIMISATION ROUTINE                                               VA04A000
C                                                                            VA04A001
C                                                                            VA04A002
C  ***************************************************************           VA04A003
C                                                                            VA04A004
C     C-E-I-R  MATHEMATICAL SERVICES DIVISION PROGRAM LIBRARY.               VA04A005
C                                                                            VA04A006
C  ***************************************************************           VA04A007
C                                                                            VA04A008
C                                                                            VA04A009
C                                                                            VA04A011
C                                                                            VA04A012
C  ***************************************************************           VA04A013
C                                                                            VA04A014
C                                                                            VA04A015
C     MINIMISATION OF A FUNCTION OF SEVERAL VARIABLES.                       VA04A016
C                                                                            VA04A017
C     METHOD AND PROGRAM DUE TO M.J.D.POWELL.                                VA04A018
C     SEE THE COMPUTER JOURNAL, VOL. 7, NO. 2, JULY 1964, PAGE 155,          VA04A019
C     FOR A DESCRIPTION.                                                     VA04A020
C                                                                            VA04A021
C                                                                            VA04A022
C  ***************************************************************           VA04A023
C                                                                            VA04A024
C                                                                            VA04A025
C     ARGUMENTS IN CALLING SEQUENCE -                                        VA04A026
C                                                                            VA04A027
C     X(I)    COORDINATES. INPUT AS APPROXIMATION, OUTPUT AS OPTIMUM         VA04A028
C             VALUE TO REQUIRED ACCURACY.                                    VA04A029
C     E(I)    ABSOLUTE ACCURACY REQUIRED IN X(I).                            VA04A030
C     N       NUMBER OF VARIABLES.                                           VA04A031
C     F       OUTPUT AS THE MINIMUM VALUE OF THE FUNTION                     VA04A032
C     ESCALE LIMITS THE MAXIMUM CHANGE IN THE VARIABLES AT A SINGLE          VA04A033
```

```
C            STEP. X(I) WILL NOT BE CHANGED BY MORE THAN ESCALE*E(I).      VA04A034
C      IPRINT CONTROLS PRINTING (OFF-LINE). IF ZERO, NO PRINTING. IF       VA04A035
C             ONE, VARIABLES AND FUNCTION PRINTED AFTER EVERY SEARCH       VA04A036
C             ALONG A LINE. IF TWO, THEY ARE PRINTED AFTER EVERY           VA04A037
C             ITERATION, I.E. (N+1) SEARCHES ALONG A LINE.                 VA04A038
C      ICON   MUST BE SET TO 1 OR 2. IF 2, WHEN ITERATION COMPLETE         VA04A039
C             ROUTINE DISPLACES RESULTANT POINT BY TEN TIMES THE           VA04A040
C             REQUIRED ACCURACY AND USES THIS AS INITIAL POINT FOR         VA04A041
C             RE-ITERATION. RESULTS OF BOTH ARE THEN COMPARED AS A         VA04A042
C             CHECK ON CONVERGENCE.                                        VA04A043
C      MAXIT  THE MAXIMUM NUMBER OF ITERATIONS ALLOWED. ROUTINE IS         VA04A044
C             LEFT WHEN THIS NUMBER IS REACHED.                            VA04A045
C                                                                          VA04A046
C                                                                          VA04A047
C  ********************************************************************    VA04A048
C                                                                          VA04A049
C                                                                          VA04A050
C     SUBROUTINE NECESSARY - CALCFX (N,X,F)                                VA04A051
C         N IS AS ABOVE, X(I),...X(N) ARE THE CURRENT VALUES OF THE        VA04A052
C         VARIABLES.  CALCFX MUST SET F TO THE CORRESPONDING VALUE OF      VA04A053
C         THE FUNCTION TO BE MINMINIMISED.                                 VA04A054
C                                                                          VA04A055
C                                                                          VA04A056
C  ********************************************************************    VA04A057
C                                                                          VA04A058
C                                                                          VA04A059
C                                                                          VA04A060
C                                                                          VA04A061
C                                                                          VA04A062
C  ********************************************************************    VA04A063
C                                                                          VA04A064
C                                                                          VA04A065
      COMMON W                                                             VA04A066
C                                                                          VA04A067
C                                                                          VA04A069
C     W IS A WORKING STORAGE AREA OF N+3 VECTORS Y0,Y1,...YN+2, EACH       VA04A070
C                       OF LENGTH N.                                       VA04A071
```

```
C                                                                       VA04A072
C     YO(J)  THE GREATEST STEP MOVEMENT ALLOWED IN THE J-TH SEARCH.     VA04A073
C     Y1   )                                                            VA04A074
C     Y2   )                                                            VA04A075
C     ..   )  DIRECTIONS OF SEARCH.                                     VA04A076
C     ..   )                                                            VA04A077
C     YN   )                                                            VA04A078
C     YN+1   INITIAL POINT OF ITERATIVE CYCLE.  ALSO, VECTOR JOINING    VA04A079
C              INITIAL POINT TO FINAL POINT.                            VA04A080
C     YN+2   FINAL POINT REACHED BEFORE DISPLACEMENT WHEN SECOND        VA04A081
C              CONVERGENCE CRITERION IS USED (I.E. ICON = 2).           VA04A082
C                                                                       VA04A083
C                                                                       VA04A084
C     ------------------------------------------------------------      VA04A085
C                                                                       VA04A086
C     DICTIONARY OF OTHER SYMBOLS                                       VA04A087
C                                                                       VA04A088
C *** INDICES ***                                                       VA04A089
C                                                                       VA04A090
C     ILINE  INDEX OF CURRENT DIRECTION.                                VA04A091
C     IDIRN  ADDRESS OF FIRST COMPONENT OF ONE OF Y1,Y2,...YN.          VA04A092
C     IXP    ADDRESS OF A COMPONENT OF YN+1.                            VA04A093
C     JIL    DIRECTION TO BE CHANGED.                                   VA04A094
C     JJ     N(N+1).                                                    VA04A095
C     JJJ    N(N+2).                                                    VA04A096
C     K      CURRENT INDEX FOR W-BLOCK.                                 VA04A097
C                                                                       VA04A098
C *** SCALARS ***                                                       VA04A099
C                                                                       VA04A100
C     F      CURRENT VALUE OF FUNCTION.                                 VA04A101
C     FA   )                                                            VA04A102
C     FB   )  VALUES USED IN PREDICTION OF MINIMUM.                     VA04A103
C     FC   )                                                            VA04A104
C     FI     CURRENT MINIMUM VALUE.                                     VA04A105
C     FP     VALUE AT START OF ITERATIVE CYCLE.                         VA04A106
C     FHOLD  VALUE AT END OF ITERATIVE CYCLE.                           VA04A107
C     FPREV  VALUE AT END OF PREVIOUS SEARCH.                           VA04A108
```

```
C      FKEEP  VALUE HELD BEFORE DISPLACEMENT WHEN THE SECOND                  VA04A109
C                  CONVERGENCE CRITERION IS USED.                            VA04A110
C      SUM    DIFFERENCE BETWEEN INITIAL AND FINAL VALUES OF F               VA04A111
C                  DURING A SEARCH.                                          VA04A112
C      D      PARAMETER ALONG CURRENT DIRECTION.                             VA04A113
C      DA   )                                                                VA04A114
C      DB   )  PARAMETERS USED IN PREDICTING A MINIMUM.                      VA04A115
C      DC   )                                                                VA04A116
C      DL     PREVIOUS VALUE OF PARAMETER.                                   VA04A117
C      DI     VALUE OF PARAMETER AT CURRENT MINIMUM.                         VA04A118
C      DD     INCREMENT IN PARAMETER, D=DI.                                  VA04A119
C      DDMAX  CURRENT GREATEST ALLOWED VALUE OF DD.                          VA04A120
C      DMAX   ABSOLUTE GREATEST ALLOWED VALUE OF DD.                         VA04A121
C      DACC   SMALLEST ALLOWED INCREMENT IN D.                               VA04A122
C      DDMAG                                                                 VA04A123
C      DMAG   INITIAL VALUE OF PARAMETER D.                                  VA04A124
C      SCER   SUCH THAT DACC = SCER*DMAX.                                    VA04A125
C      AAA    MAX(YI(J)/E(J) FOR ALL J AND GIVEN I.                          VA04A126
C                                                                            VA04A127
C *** COUNTERS AND SWITCHES ***                                              VA04A128
C                                                                            VA04A129
C      ITERC  NUMBER OF ITERATIVE CYCLES COMPLETED.                          VA04A130
C      NFCC   NUMBER OF FUNCTION EVALUATIONS (UPDATED EVERY TIME             VA04A131
C                  CALCFX IS CALLED).                                        VA04A132
C      ITONE  =1  SEARCH DIRECTION AS PART OF ITERATIVE CYCLE.               VA04A133
C             =2 AT END OF SEARCH IN NEWLY-FORMED DIRECTION.                 VA04A134
C             =3 AT BEGINNING OF SEARCH IN NEWLY-FORMED DIRECTION.           VA04A135
C      ISGRAD =1  (WITH ITONE=1) FOR DIRECTIONS USED BEFORE.                 VA04A136
C             =2  (WITH ITONE=1) FOR INITIAL DIRECTIONS.                     VA04A137
C      IND )  BOTH SET EQUAL TO ONE THROUGHOUT IF ICON=1.  WHEN ICON=2       VA04A138
C      INN )       IND=1,2 AND INN=1,2 SELECT VARIOUS PATHS AFTER            VA04A139
C                  DISPLACEMENT.                                             VA04A140
C      IS     =1,2,3,4,5,6  DEFINES TYPE OF OUTPUT TO AREA OF PROGRAM        VA04A141
C                  WHICH RESETS X AND F (EFN 58).                            VA04A142
C                                                                            VA04A143
C  ************************************************************************  VA04A144
C                                                                            VA04A145
```

```
C                                                                       VA04A146
C   *****  HERE WE GO . . .                                             VA04A147
C                                                                       VA04A148
C                                          * INITIALISE                 VA04A149
C                                                                       VA04A150
      COMMON /HELP/IEND
      COMMON /LIMITS/XMAX(10),XMIN(10)
      DIMENSION W(130),X(10),E(10)
      DOMAG=0.1*ESCALE                                                  VA04A151
      SCER=0.05/ESCALE                                                  VA04A152
      JJ=N*N+N                                                          VA04A153
      JJJ=JJ+N                                                          VA04A154
      K=N+1                                                             VA04A155
      NFCC=1                                                            VA04A156
      IND=1                                                             VA04A157
      INN=1                                                             VA04A158
      DO 1 I=1,N                                                        VA04A159
      DO 2 J=1,N                                                        VA04A160
      W(K)=0.                                                           VA04A161
      IF(I-J)4,3,4                                                      VA04A162
    3 W(K)=ABS (E(I))                                                   VA04A163
      W(I)=ESCALE                                                       VA04A164
    4 K=K+1                                                             VA04A165
    2 CONTINUE                                                          VA04A166
    1 CONTINUE                                                          VA04A167
      ITERC=1                                                           VA04A168
      ISGRAD=2                                                          VA04A169
      CALL CALCFX(N,X,F)                                                VA04A170
      FKEEP=ABS (F)+ABS (F)                                             VA04A171
C                                        * PREPARE ITERATIVE CYCLE      VA04A172
    5 ITONE=1                                                           VA04A173
      FP=F                                                              VA04A174
      SUM=0.                                                            VA04A175
      IXP=JJ                                                            VA04A176
      DO 6 I=1,N                                                        VA04A177
      IXP=IXP+1                                                         VA04A178
      W(IXP)=X(I)                                                       VA04A179
```

```
    6 CONTINUE
      IDIRN=N+1
      ILINE=1
C                                     * PREPARE SEARCH ALONG ILINE
    7 DMAX=W(ILINE)
      DACC=DMAX*SCER
      DMAG=AMIN1 (DDMAG,0.1*DMAX)
      DMAG=AMAX1(DMAG,20.*DAGG)
      DDMAX=10.*DMAG
      GO TO (70,70,71),ITONE
   70 DL=0.
      D=DMAG
      FPREV=F
      IS=5
      FA=F
      DA=DL
    8 DD=D-DL
      DL=D
   58 K=IDIRN
      DO 9 I=1,N
      X(I)=X(I)+DD*W(K)
      K=K+1
    9 CONTINUE
      CALL CALCFX(N,X,F)
      IF (IEND .EQ. 1) RETURN
      NFCC=NFCC+1
      GO TO (10,11,12,13,14,96),IS
   14 IF(F-FA)15,16,24
   16 IF (ABS (D)-DMAX) 17,17,18
   17 D=D+D
      GO TO 8
   18 CALL WTNL(38,'MAXIMUM CHANGE DOES NOT ALTER FUNCTION')
      GO TO 20
   15 FB=F
      DB=D
      GO TO 21
   24 FB=FA
```

```
   DB=DA                                                                VA04A217
   FA=F                                                                 VA04A218
   DA=D                                                                 VA04A219
21 GO TO (83,23),ISGRAD                                                 VA04A220
23 D=DB+DB-DA                                                           VA04A221
   IS=1                                                                 VA04A222
   GO TO 8                                                              VA04A223
83 D=0.5*(DA+DB-(FA-FB)/(DA-DB))                                        VA04A224
   IS=4                                                                 VA04A225
   IF((DA-D)*(D-DB))25,8,8                                              VA04A226
25 IS=1                                                                 VA04A227
   IF(ABS (D-DB)-DDMAX)8,8,26                                           VA64A228
26 D=DB+SIGN (DDMAX,DB-DA)                                              VA04A229
   IS=1                                                                 VA04A230
   DDMAX=DDMAX+DDMAX                                                    VA04A231
   DDMAG=DDMAG+DDMAG                                                    VA04A232
   IF(DDMAX-DMAX)8,8,27                                                 VA04A233
27 DDMAX=DMAX                                                           VA04A234
   GO TO 8                                                              VA04A235
13 IF(F-FA)28,23,23                                                     VA04A236
28 FC=FB                                                                VA04A237
   DC=DB                                                                VA04A238
29 FB=F                                                                 VA04A239
   DB=D                                                                 VA04A240
   GO TO 30                                                             VA04A241
12 IF(F-FB)28,28,31                                                     VA04A242
31 FA=F                                                                 VA04A243
   DA=D                                                                 VA04A244
   GO TO 30                                                             VA04A245
11 IF(F-FB)32,10,10                                                     VA04A246
32 FA=FB                                                                VA04A247
   DA=DB                                                                VA04A248
   GO TO 29                                                             VA04A249
71 DL=1.                                                                VA04A250
   DDMAX=5.                                                             VA04A251
   FA=FP                                                                VA04A252
   DA=-1.                                                               VA04A253
```

```
      FB=FHOLD                                                          VA04A254
      DB=0.                                                             VA04A255
      D=1.                                                              VA04A256
   10 FC=F                                                              VA04A257
      DC=D                                                              VA04A258
C                                    * SEARCH ILINE FOR A MINIMUM       VA04A259
   30 A=(DB-DC)*(FA-FC)                                                 VA04A260
      B=(DC-DA)*(FB-FC)                                                 VA04A261
      IF((A+B)*(DA-DC))33,33,34                                         VA04A262
   33 FA=FB                                                             VA04A263
      DA=DB                                                             VA04A264
      FB=FC                                                             VA04A265
      DB=DC                                                             VA04A266
      GO TO 26                                                          VA04A267
   34 D=0.5*(A*(DB+DC)+B*(DA+DC))/(A+B)                                 VA04A268
      DI=DB                                                             VA04A269
      FI=FB                                                             VA04A270
      IF(FB-FC)44,44,43                                                 VA04A271
   43 DI=DC                                                             VA04A272
      FI=FC                                                             VA04A273
   44 GO TO (86,86,85),ITONE                                            VA04A274
   85 ITONE=2                                                           VA04A275
      GO TO 45                                                          VA04A276
   86 IF (ABS (D-DI)-DACC) 41,41,93                                     VA04A277
   93 IF (ABS (D-DI)-0.03*ABS (D)) 41,41,45                             VA04A278
   45 IF ((DA-DC)*(DC-D)) 47,46,46                                      VA04A279
   46 FA=FB                                                             VA04A280
      DA=DB                                                             VA04A281
      FB=FC                                                             VA04A282
      DB=DC                                                             VA04A283
      GO TO 25                                                          VA04A284
   47 IS=2                                                              VA04A285
      IF ((DB-D)*(D-DC)) 48,8,8                                         VA04A286
   48 IS=3                                                              VA04A287
      GO TO 8                                                           VA04A288
   41 F=FI                                                              VA04A289
      D=DI-DL                                                           VA04A290
```

```
      DD=SQRT((DC-DB)*(DC-DA)*(DA-DB)/(A+B))                          VA04A291
      DO 49 I=1,N                                                     VA04A292
      X(I)=X(I)+D*W(IDIRN)                                            VA04A293
      W(IDIRN)=DD*W(IDIRN)                                            VA04A294
      IDIRN=IDIRN+1                                                   VA04A295
   49 CONTINUE                                                        VA04A296
      W(ILINE)=W(ILINE)/DD                                            VA04A297
      ILINE=ILINE+1                                                   VA04A298
C                              (OPTIONAL PRINT-OUT OF PRESENT RESULTS) VA04A299
      IF(IPRINT-1)51,50,51                                            VA04A300
   50 CALL HOME
      CALL ERASE
      CALL WT(21,'((ITERATION CYCLE NO ',ITERC)
      CALL WT(22,'     NO OF FN CALLS = ',NFCC)
      CALL WTNL(16,'      FN VALUE = ',F)
      CALL WTNL
      DO 52 I=1,N
      IF (I .EQ. 4) CALL WTNL
      IF (I .EQ. 7) CALL WTNL
   52 CALL WT(6,'     X(',I,4,') = ',X(I))
      CALL WTNL
      ME=-1
      CALL RD(ME,MC)
      GO TO(51,53),IPRINT                                             VA04A304
C                              (ITONE IS 2 FOR NEW DIRECTION)          VA04A305
   51 CALL WT(1,'X')
      GO TO (55,38),ITONE
C                                                                     VA04A307
C                                    * UPDATE DIRECTION TO BE         VA04A308
C                                          REPLACED                   VA04A309
   55 IF (FPREV-F-SUM) 94,95,95                                       VA04A310
   95 SUM=PREV-F                                                      VA04A311
      JIL=ILINE                                                       VA04A312
C                              (ARE ALL DIRECTIONS USED)               VA04A313
   94 IF (IDIRN-JJ) 7,7,84                                            VA04A314
   84 GO TO (92,72),IND                                               VA04A315
C                                    * SET NEW DIRECTION              VA04A316
```

```
      DD=SQRT((DC-DB)*(DC-DA)*(DA-DB)/(A+B))                          VA04A291
      DO 49 I=1,N                                                     VA04A292
      X(I)=X(I)+D*W(IDIRN)                                            VA04A293
      W(IDIRN)=DD*W(IDIRN)                                            VA04A294
      IDIRN=IDIRN+1                                                   VA04A295
   49 CONTINUE                                                        VA04A296
      W(ILINE)=W(ILINE)/DD                                            VA04A297
      ILINE=ILINE+1                                                   VA04A298
C                              (OPTIONAL PRINT-OUT OF PRESENT RESULTS) VA04A299
      IF(IPRINT-1)51,50,51                                            VA04A300
   50 CALL HOME
      CALL ERASE
      CALL WT(21,'((ITERATION CYCLE NO ',ITERC)
      CALL WT(22,'     NO OF FN CALLS = ',NFCC)
      CALL WTNL(16,'      FN VALUE = ',F)
      CALL WTNL
      DO 52 I=1,N
      IF (I .EQ. 4) CALL WTNL
      IF (I .EQ. 7) CALL WTNL
   52 CALL WT(6,'     X(',I,4,') = ',X(I))
      CALL WTNL
      ME=-1
      CALL RD(ME,MC)
      GO TO(51,53),IPRINT                                             VA04A304
C                              (ITONE IS 2 FOR NEW DIRECTION)          VA04A305
   51 CALL WT(1,'X')
      GO TO (55,38),ITONE
C                                                                     VA04A307
C                                    * UPDATE DIRECTION TO BE         VA04A308
C                                          REPLACED                   VA04A309
   55 IF (FPREV-F-SUM) 94,95,95                                       VA04A310
   95 SUM=PREV-F                                                      VA04A311
      JIL=ILINE                                                       VA04A312
C                              (ARE ALL DIRECTIONS USED)               VA04A313
   94 IF (IDIRN-JJ) 7,7,84                                            VA04A314
   84 GO TO (92,72),IND                                               VA04A315
C                                    * SET NEW DIRECTION              VA04A316
```

```
   92 FHOLD=F                                                                  VA04A317
      IS=6                                                                     VA04A318
      IXP=JJ                                                                   VA04A319
      DO 59 I=1,N                                                              VA04A320
      IXP=IXP+1                                                                VA04A321
      W(IXP)=X(I)-W(IXP)                                                       VA64A322
   59 CONTINUE                                                                 VA04A323
      DD=1.                                                                    VA04A324
      GO TO 58                                                                 VA04A325
C                                          * TEST IF JIL-TH DIRECTION IS        VA04A326
C                                              TO BE REPLACED                   VA04A327
   96 GO TO (112,87),IND                                                       VA04A328
  112 IF (FP-F) 37,91,91                                                       VA04A329
   91 D=2.*(FP*F-2.*FHOLD)/(FP-F)**2                                           VA04A330
      IF (D*(FP-FHOLD-SUM)**2-SUM) 87,37,37                                    VA04A331
C                                          * YES - REPLACE JIL-TH               VA04A332
C                                              DIRECTION                        VA04A333
   87 J=JIL*N+1                                                                VA04A334
      IF (J-JJ) 60,60,61                                                       VA04A335
   60 DO 62 I=J,JJ                                                             VA04A336
      K=I-N                                                                    VA04A337
      W(K)=W(I)                                                                VA04A338
   62 CONTINUE                                                                 VA04A339
      DO 97 I=JIL,N                                                            VA04A340
      W(I-1)=W(I)                                                              VA04A341
   97 CONTINUE                                                                 VA04A342
   61 IDIRN=IDIRN-N                                                            VA04A343
      ITONE=3                                                                  VA04A344
      K=IDIRN                                                                  VA04A345
      IXP=JJ                                                                   VA04A346
      AAA=0.                                                                   VA04A347
      DO 65 I=1,N                                                              VA04A348
      IXP=IXP+1                                                                VA04A349
      W(K)=W(IXP)                                                              VA04A350
      IF (AAA-ABS (W(K)/E(I))) 66,67,67                                        VA04A351
   66 AAA=ABS (W(K)/E(I))                                                      VA04A352
   67 K=K+1                                                                    VA04A353
```

```
   65 CONTINUE                                                          VA04A354
      DOMAG=1.                                                          VA04A355
      W(N)=ESCALE/AAA                                                   VA04A356
      ILINE=N                                                           VA04A357
      GO TO 7                                                           VA04A358
C                                        * NO - RESTORE END-POINT       VA04A359
   37 IXP=JJ                                                            VA04A360
      AAA=0.                                                            VA04A361
      F=FHOLD                                                           VA04A362
      DO 99 I=1,N                                                       VA04A363
      IXP=IXP+1                                                         VA04A364
      X(I)=X(I)-W(IXP)                                                  VA04A365
      IF (AAA*ABS (E(I))-ABS (W(IXP))) 98,99,99                         VA04A366
   98 AAA=ABS (W(IXP)/E(I))                                             VA04A367
   99 CONTINUE                                                          VA04A368
      GO TO 72                                                          VA04A369
C                              (NEWLY-FORMED DIRECTION)                 VA04A370
   38 AAA=AAA*(1.+DI)                                                   VA04A371
      GO TO (72,106),IND                                                VA04A372
C                                                                       VA04A373
   72 IF (IPRINT-2) 53,50,50                                            VA04A374
   53 GO TO (109,88),IND                                                VA04A375
C                                                                       VA04A376
  109 IF (AAA-0.1) 89,89,76                                             VA04A377
C                                                                       VA04A378
C                                                                       VA04A379
   89 GO TO (20,116),ICON                                               VA04A380
C                                                                       VA04A381
  116 IND=2                                                             VA04A382
C                                                                       VA04A383
      GO TO (100,101),INN                                               VA04A384
C                                                                       VA04A385
  100 INN=2                                                             VA04A386
      K=JJJ                                                             VA04A387
      DO 102 I=1,N                                                      VA04A388
      K=K+1                                                             VA04A389
      W(K)=X(I)                                                         VA04A390
```

* OPTIONAL PRINT-OUT

* IS ACCURACY SATISFIED

* YES - IS SECOND CONVERGENCE CRITERION REQUIRED

* YES

* IS SECOND MINIMUM COMPUTED

* NO - DISPLACE FIRST MINIMUM

```
      X(I)=X(I)+10.*E(I)                                                    VA04A391
      IF (X(I) .GE. XMAX(I)) X(I)=XMAX(I)-E(I)*ESCALE/2.0
      IF (X(I) .LE. XMIN(I)) X(I)=XMIN(I)+E(I)*ESCALE/2.0
  102 CONTINUE                                                              VA04A392
      FKEEP=F                                                               VA04A393
      CALL CALCFX (N,X,F)                                                   VA04A394
      NFCC=NFCC+1                                                           VA04A395
      DDMAG=0.                                                              VA04A396
      GO TO 108                                                             VA04A397
C                                       * TEST FOR NO DECREASE IN F         VA04A398
   76 IF (F-FP) 35,78,78                                                    VA04A399
 78     CALL WTNL(31,'ACCURACY LIMITED BY ERRORS IN F')
      GO TO 20                                                              VA04A402
   88 IND=1                                                                 VA04A403
C                                       * RESET STEP LENGTH                 VA04A404
   35 DDMAG=0.4*SQRT (FP-F)                                                 VA04A405
      ISGRAD=1                                                              VA04A406
  108 ITERC=ITERC+1                                                         VA04A407
C                                       * TEST IF NUMBER OF ITERATIONS      VA04A408
C                                             ENOUGH                      VA04A409
      IF (ITERC-MAXIT) 5,5,81                                               VA04A410
C                                       * YES                               VAC4A411
 81   CALL WTNL(23,'ITERATIONS COMPLETED = ',MAXIT)
      IF (F-FKEEP) 20,20,110                                                VA04A414
  110 F=FKEEP                                                               VA04A415
      DO 111 I=1,N                                                          VA04A416
      JJJ=JJJ+1                                                             VA04A417
      X(I)=W(JJJ)                                                           VA04A418
  111 CONTINUE                                                              VA04A419
      GO TO 20                                                              VA04A420
C                                       * SECOND MINIMUM HAS BEEN           VA04A421
C                                         COMPUTED - NOW COMPARE            VA04A422
C                                             WITH FIRST                    VA04A423
  101 JIL=1                                                                 VA04A424
      FP=FKEEP                                                              VA04A425
      IF (F-FKEEP) 105,78,104                                               VA04A426
  104 JIL=2                                                                 VA04A427
```

```
      FP=F                                                          VA04A428
      F=FKLEP                                                       VA04A429
  105 IXP=JJ                                                        VA04A430
      D0 113 I=1,N                                                  VA04A431
      IXP=IXP+1                                                     VA04A432
      K=IXP+N                                                       VA04A433
      G0 T0 (114,115),JIL                                           VA04A434
  114 W(IXP)=W(K)                                                   VA04A435
      G0 T0 113                                                     VA04A436
  115 W(IXP)=X(I)                                                   VA04A437
      X(I)=W(K)                                                     VA04A438
  113 C0NTINUE                                                      VA04A439
      JIL=2                                                         VA04A440
      G0 T0 92                                                      VA04A441
C                                     * IS ACCURACY SATISFIED       VA04A442
  106 IF (AAA-0.1) 20,20,107                                        VA04A443
   20 RETURN                                                        VA04A444
C                                     * N0                          VA04A445
C                                     * S0 G0 AND RESET STEP-LENGTH VA04A446
  107 INN=1                                                         VA04A447
      G0 T0 35                                                      VA04A448
      RETURN
      END                                                           VA04A449
```

```
C
C
C
      SUBROUTINE CALCFX(N,X,F)
C
C        CALCULATE ERROR FN. VALUE WITH N PARAMETER VALUES X & PUT RESULT
C     IF F
C
      COMMON /REF/FREF(100)/LIMITS/XMAX(10),XMIN(10)/FLIMIT/NPTS,WRES
      COMMON /FBACK/HT
      COMMON /REF1/FREF1(100)
      COMPLEX FREF1
      COMPLEX T1,T2,T3,T4,T5,GVAL,FREF,E
      DIMENSION X(10)
      G=-1.0
C
C     TEST FOR PARAMETERS GOING OUTSIDE LIMITS.
C
      DO 1 I=1,N
      IF (X(I) .GT. XMAX(I)) G=F+(X(I)-XMAX(I))*F
 1    IF (X(I) .LT. XMIN(I)) G=F+(XMIN(I)-X(I))*F
      IF (G .GT. F) F=G
      IF (G .NE. -1.0) RETURN
C
C     FIND INTEGRAL ERROR SQUARED BETWEEN MEASURED & MODELLED OPEN-LOOP
C     FREQ RESPONSE + CLOSED LOOP FREQ RESPONSE.
C     THE IDEA IS TO MINIMISE THE SUM OF THESE TWO
C
      F=0.0
      DO 2 I=2,NPTS
      W=(I-1)*WRES
      CALL CONTROL(GVAL,X,W)
      T1=FREF1(I)-GVAL
      F=F+REAL(T1)**2+AIMAG(T1)**2
      GVAL=GVAL/(1.0+HT*GVAL)
      E=FREF(I)-GVAL
 2    F=F+REAL(E)**2+AIMAG(E)**2
```

```
      RETURN
      END
```

```
C
C
C
      SUBROUTINE CONTROL(GVAL,X,W)
C
C     GENERATE MODEL FN VALUES FOR HUMAN OPERATOR IN OPEN LOOP FROM 6 X VALUES
C           1=GAIN
C           2=TIME DELAY
C           3=INTEGRATOR IMPURITY
C           4=MUSCLE TIME LAG
C           5=VELOCITY LEAD
C           6=PHYSIOLOGICAL LAG FOR STABILITY
C
C
      DIMENSION X(10)
      COMPLEX GVAL,A,B,C,D,E,F
      G=X(1)
      A=CMPLX(COS(W*X(2)),-SIN(W*X(2)))
      B=CMPLX(X(3),W)
      C=CMPLX(1.0,W*X(4))
      D=CMPLX(1.0,W*0.04)
      E=CMPLX(1.0-(W**2)*X(6),W*X(5))
      GVAL=(G*A*E)/(B*C*D)
      RETURN
      END
```

FAST FOURIER PROGRAM

AUTHOR : P. N. DAVALL

LANGUAGE : FORTRAN IV/MACRO-SYMBOL

```
      SUBROUTINE FFA
C
C
C         FAST FOURIER ALGORITHM.
C         FORWARD TRANSFORM       ISIGN=-1
C         (IMAGINARY DATA PTS) AND PUTS N COMPLEX COEFFS IN ASCENDING FREQ ORDER
C         BACK INTO REAL AND IMAGINARY DATA ARRAYS.
C         THE LAST N/2 PTS ARE THE ALIASED PAIRS OF THE PREVIOUS N/2 PTS.
C         FOR THE INVERSE TRANSFORM ISIGN=+1,AND DATA IS LOADED AS FOR
C         FORWARD TRANSFORM WITH ALIASED PAIRS IN LAST N/2 PLACES.
C         TIME FOR 512 PTS TRANSFORM = 0.25 SECS ON SIGMA 5
C
C
      DIMENSION FCOS(129)
      COMMON RE(1024),IM(1024),N,M,ISIGN,FCOS,FCTR,AR(8,512)
      REAL IM
      DOUBLE PRECISION ONEONE
      DATA ONEONE/9Z100000001/
      N2=N/2
      N4=N2/2
      NP=N4+1
      NB=N
      NC=0
      ND=NB
      J2=1
      N2J=NB
      NX=N2+1
      DO 3 J=1,M
      NI=J2
      N2J=N2J/2
      J2=J2+J2
      IN2J=-N2J
      DO 2 I=1,NI
      IN2J=IN2J+N2J
     S      LW,5       IN2J
     S      AI,5       1
     S      LW,9       IN2J
```

```
S           CW,9        N4
S           BL          4S
S           SW,9        NX
S           LCW,5       9
S4          LW,9        FC0S-1,5
S           STW,9       W1
        IF (IN2J .GT. N4) W1=-W1
S           LW,7        N4
S           AI,7        2
S           SW,7        5
S           LW,9        FC0S-1,7
S           MW,9        ISIGN
S           STW,9       W2
S           LW,6        IN2J
S           AW,6        N8
S           LW,4        IN2J
S           SLS,4       1
S           AW,4        NC
S           LW,7        4
S           AW,7        N2J
S           LW,5        6
S           AW,5        N2
S           LW,1        N2J
S1          AD,4        0NE0NE
S           AD,6        0NE0NE
S           LW,8        W1
S           FMS,8       RE-1,7
S           LW,10       W2
S           FMS,10      IM-1,7
S           FSS,8       10
S           LW,9        W1
S           FMS,9       IM-1,7
S           LW,10       W2
S           FMS,10      RE-1,7
S           FAS,9       10
S           LW,10       RE-1,4
S           LW,12       10
```

```
S           FAS,10      8
S           STW,10      RE-1,6
S           LW,11       IM-1,4
S           LW,13       11
S           FAS,11      9
S           STW,11      IM-1,6
S           FSS,12      8
S           STW,12      RE-1,5
S           FSS,13      9
S           STW,13      IM-1,5
S           BDR,1       1S
  2         CONTINUE
          NB=NC
          NC=ND
  3       ND=NB
C
C
C           TRANSFER DATA TO OUTPUT REGISTER AND NORMALISE IF REQUIRED.
C
          IAR=0
          IF (NB .EQ. 0) IAR=N
          IF (ISIGN .GT. 0) FCTR=1.0
          DO 5 I=1,N
          J=I+IAR
          RE(I)=RE(J)/FCTR
  5       IM(I)=IM(J)/FCTR
          RETURN
          END
```